Report No. FHWA-RD-79-84

PB80106289

REDUCTION OF ADVERSE AERODYNAMIC EFFECTS OF LARGE TRUCKS

Vol. I. Technical Report
September 1978
Interim Report

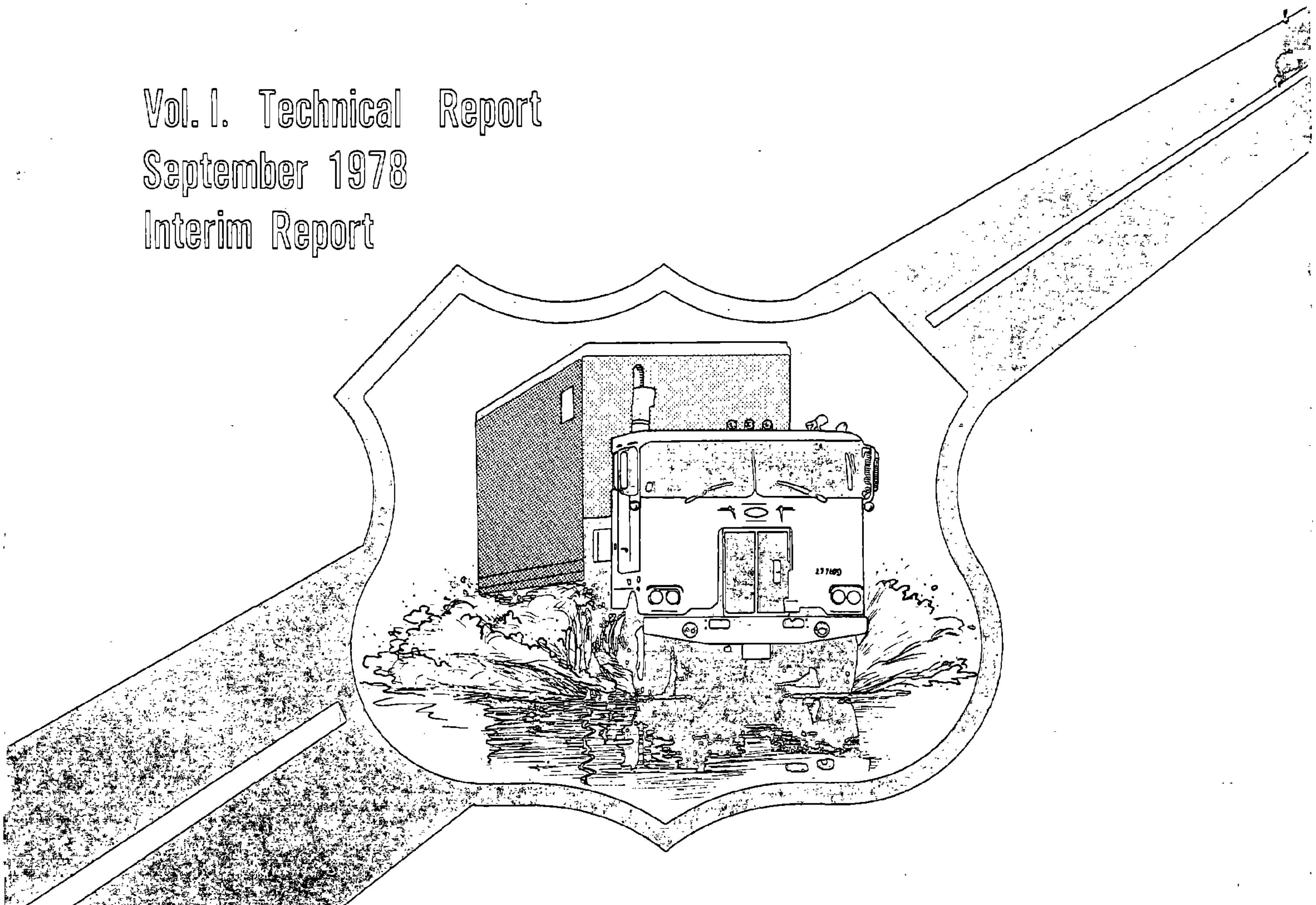

Document is available to the public through the National Technical Information Service, Springfield, Virginia 22161

Prepared for
FEDERAL HIGHWAY ADMINISTRATION
Offices of Research & Development
Environmental Design & Control Division
Washington, D.C. 20590

FOREWORD

This report documents the first phase of a study to develop and evaluate methods for minimizing adverse aerodynamic effects caused by large trucks on adjacent vehicles. The second phase will subsequently involve a limited over the road field evaluation. The report will be of interest to researchers concerned with the aerodynamic phenomena of splash, spray and truck-induced aerodynamic disturbances and motor vehicle administrators concerned with methods of remedying these aerodynamic effects.

This study is a part of Project 1U, "Safety Aspects of Increased Size and Weight of Heavy Vehicles" of the Federally Coordinated Program (FCP) of Research and Development. The project manager is Michael D. Freitas and the contract manager is George B. Pilkington II.

A limited number of copies of this report are available for official use from the Environmental Design and Control Division, HRS-41, Office of Research, Federal Highway Administration, 20590. Additional copies are available from the National Technical Information Service, (NTIS) Springfield, Virginia, 22161 a small cost will be made by NTIS.

D. Solomon
for Charles F. Scheffey
Director, Office of Research
Federal Highway Administration

NOTICE

Technical Report Documentation Page

1. Report No.	2. Government Accession No.	3. Recipient's Catalog No.
FHWA-RD-79-84		PB 80 106289

4. Title and Subtitle	5. Report Date
REDUCTION OF ADVERSE AERODYNAMIC EFFECTS OF LARGE TRUCKS Volume I: Technical Report	September 1978
	6. Performing Organization Code
	8. Performing Organization Report No.
7. Author(s) David H. Weir, Jay F. Strange, Robert K. Heffley	TR-1093-1
9. Performing Organization Name and Address Systems Technology, Inc. 13766 South Hawthorne Boulevard Hawthorne, California 90250	10. Work Unit No. (TRAIS)
	11. Contract or Grant No. DOT-FH-11-9165
	13. Type of Report and Period Covered Interim Report; November 1976 to September 1978
12. Sponsoring Agency Name and Address Federal Highway Administration U.S. Department of Transportation Washington, D.C. 20590 Environmental Design and Control Division	14. Sponsoring Agency Code E0412

15. Supplementary Notes

Contract Manager: George B. Pilkington II, HRS-41

16. Abstract

The overall objective of this study has been to develop methods of minimizing three aerodynamic-related phenomena: truck-induced aerodynamic disturbances, splash, and spray. An analytical methodology has been developed and used to characterize aerodynamic flow, truck splash and spray generation and propagation, adjacent driver visibility factors, the performance of the disturbed adjacent driver/vehicle system, and benefit/cost comparisons. These same factors have been studied in a series of driving simulator, wind tunnel, and full scale tests and experiments. Attention in the experiments and analyses has focused on understanding the phenomena, as well as on identifying and developing devices, techniques, and procedures for minimizing these aerodynamic effects. Several truck mounted devices and prototype concepts are identified which have the potential to alleviate the adverse effects of splash and spray in a cost-effective way. These include collector flaps, simple fenders, and aerodynamic panels and devices near the tractor, under the truck, and around the wheels. Non-vehicle means of alleviation are considered, as well.

17. Key Words	18. Distribution Statement
Trucks, splash and spray, truck operations, aerodynamics, driver performance, drag, cost-benefit	Document is available to the U.S. public through the National Technical Information Service, Springfield, Virginia 22161.

19. Security Classif. (of this report)	20. Security Classif. (of this page)	21. No. of Pages	22. Price
Unclassified	Unclassified		417-A01

Form DOT F 1700.7 (8-72) Reproduction of completed page authorized

PREFACE

This report documents the first phase of a study to develop methods to minimize the adverse aerodynamic and splash and spray effects caused by large trucks on the highway. This phase occupied 20 months and included analyses, laboratory experiments, wind tunnel tests, and full scale tests with trucks and devices. The second phase, to be accomplished subsequently, involves a limited over the road field evaluation.

The program was accomplished for the Environmental Design and Control Division, Office of Research, Federal Highway Administration, under Contract DOT-FH-11-9165. The FHWA Contract Technical Manager was George B. Pilkington II. The STI Principal Investigator was David H. Weir, and the Technical Director was Irving L. Ashkenas.

This program has been a highly interdisciplinary effort involving a wide range of technical skills and a relatively large number of people. In order to complement our capabilities, Systems Technology, Inc. (STI) has used three subcontractors in the accomplishment of this program, i.e.:

- AeroVironment, Inc., in Pasadena, California, with Co-Principal Investigator Peter B. S. Lissaman.
- Western Highway Institute in San Bruno, California, with Project Engineer Thurman S. Sherard.
- Alan M. Voorhees and Assoc., Inc., in McLean, Virginia, with Project Engineer William A. Stimpson.

Results of their work have been summarized in this report for completeness. In addition, details of the AeroVironment, Inc., and Alan M. Voorhees and Assoc., Inc., technical activities and results have been reported under separate cover.

The full scale aerodynamic and splash and spray tests were accomplished at the Firestone Test Center in Fort Stockton, Texas, under the auspices of Western Highway Institute. The support and cooperation of the Firestone Test Center personnel was greatly appreciated, including, in particular, that of William B. Straub, Richard Vannoy, and Larry Crowell. Western Highway Institute committee members, personnel, and affiliates who comprised the test task force included T. R. Swennes, D. A. Clendenen, G. F. Cantlay, G. Ketchum, H. Reed, W. Reddaway, F. Roberts, E. Schepp, J. R. D'Amico, J. Rodgers, W. Gibson, D. Fortune, J. Gaussoin, D. Glasenapp, D. Zielinski, W. French, L. Larson, and J. Noble.

Also contributing substantially to the success of the experimental program were those who assisted in preparation of the models and providing equipment for the full scale tests. These include Globe Fabricators who provided design data for the Feedliner semitrailer, and Freuhauf Corporation who assisted with details of the tanker semitrailer. The wind tunnel models were built by Raines Engineering Co. in Anaheim, California. Particular thanks are due to GMC Truck and Coach Division, Freightliner Corporation, International Harvester Corporation, East Texas Motor Freight Lines, Yellow Freight System, Frozen Food Express, Bill James Trucking, and Whitfield Associated Transport for providing tractors, semitrailers, and other support for the full scale splash and spray tests.

The driving simulator investigation was accomplished under the direction of R. Wade Allen of STI. He was supported in this effort by Jeffrey Hogge and James Nagy, also of STI.

Significant contributions were made by a number of other STI staff members. Contributing to the initial planning were Henry Jex, John Zellner, Walter Johnson, and Arthur Blauvelt. Playing key roles in preparing for and accomplishing the full scale tests were Ronald Fifer and Richard Klein, with support from David Thomas and Larry Ingersoll. Participating in the data analysis and interpretation were David Mitchell and Gloria Benis. The authors are also indebted to the STI Production Staff for their care and diligence in preparing this report for publication.

Significant contributions to the AVI aerodynamic effort were made by Robert L. Radkey and Bart Hibbs.

Significant contributions to the AMV cost-effectiveness effort were made by Steven R. Shapiro and Marilyn Johnson.

TABLE OF CONTENTS

		Page
I.	INTRODUCTION	1
	A. Objectives	1
	B. Elements of the Technical Approach	1
	C. Project Team Organization	3
	D. Overview of the Interim Report	4
II.	ELEMENTS OF THE PROBLEM	6
	A. Discussion of the Issues	6
	B. Situational Parameters and Conditions	9
	C. Findings of Prior Studies	11
	D. Non-Vehicle Alleviation Techniques	23
	E. Selection of Example Test Vehicle	32
III.	PRELIMINARY ANALYSES AND EXPERIMENTS	36
	A. Generation of Splash and Spray	37
	B. Dispersion of Splash and Spray	55
	C. Driver/Vehicle System Properties	67
	D. Driving Simulator Tests	83
IV.	CANDIDATE DEVICES FOR MINIMIZING ADVERSE EFFECTS	103
	A. Categories of Devices	103
	B. Devices to Reduce Drag	104
	C. Aerodynamic Devices for Splash and Spray	110
	D. Collector Devices for Splash and Spray	115
	E. Device Characteristics as Prototypes	121
V.	AERODYNAMIC TESTS AND RESULTS	127
	A. Wind Tunnel Facilities, Models, and Test Procedures	128
	B. Aerodynamic Flow Around Trucks	150
	C. Truck Force and Moment Data	165
	D. Adjacent Car Force and Moment Data	180
VI.	SPLASH AND SPRAY TESTS AND RESULTS	206
	A. Splash and Spray Test Procedures	208
	B. Basic Truck Results	222

Page

VI. SPLASH AND SPRAY TESTS AND RESULTS (Continued)

C. Correlations Between the Measures 242

D. Visibility Values for Various Truck Configurations . . . 260

E. The Effect of Alleviation Devices on Visibility 260

VII. COST-EFFECTIVENESS ANALYSIS 286

A. Overview of C-E Approach 287

B. Cost-Effectiveness Program 290

C. Fuel Consumption Program 293

D. Input Data and Scenarios 299

E. Cost-Effectiveness Findings 307

VIII. CONCLUSIONS AND RECOMMENDATIONS 333

A. Aerodynamic Effects 333

B. Splash and Spray Effects 338

C. Performance of Adjacent Driver/Vehicle 341

D. Cost-Effectiveness 345

REFERENCES 354

LIST OF FIGURES

		Page
1.	Examples of Splash and Spray Suppression Devices from Past Tests	19
2.	Primary Splash and Spray Generation Mechanisms for a Single Wheel	39
3.	Averaged Spray Distributions for Theoretical Tread Throw	43
4.	Tread Nomenclature for Single Wheel Model	47
5.	Simple Single Wheel Model Distribution of Water Mass Flow	48
6.	Comparison of Droplet Size Distributions for Single Wheel Sprays	48
7.	Single Wheel Droplet Size Distributions, Mass Distributions, and Calculated Concentrations	51
8.	Collector Measured Average Mass Flow at Various Positions Along 2 Axle COE Plus Triple 27 ft Van Configuration	54
9.	Division of Incident Water Into Single Wheel Streams and Formation of Interference Sprays Including Impactions	56
10.	Basic Pasquill-Gifford Dispersion Relations	58
11.	Plume Behavior for a Single Source	59
12.	Spray Source Locations Used in Dispersion Analysis, 3 Axle COE Plus 40 ft Van	62
13.	3 Axle COE Plus 40 ft Van, x-Plane Concentrations	63
14.	3 Axle COE Plus 40 ft Van, x-Plane Isopleths	64
15.	3 Axle COE Plus 40 ft Van, z-Plane Concentrations	65
16.	3 Axle COE Plus 40 ft Van, z-Plane Isopleths	66
17.	Typical Truck-Car Disturbance Situations	67
18.	Driver/Vehicle System Concept	71
19.	Effective Open-Loop Driver/Vehicle System Describing Functions for 16 Ss, 1974 Nova in Wind Regulation Maneuver	74

		Page
20.	Typical Aerodynamic Disturbance Data for Station Wagon Disturbed by Truck or Bus	76
21.	Comparison of Results for Station Wagon	77
22.	Effect of Disturbed Vehicle Properties on Gust	79
23.	Effect of Crosswind Angle on Driver/Vehicle Lane Keeping Performance	81
24.	Example Visibility Conditions	85
25.	Cloud Density Distribution Simulation Scheme	86
26.	Typical Driving Simulator Data (Ensemble Average Over 4 Runs)	89
27.	Comparison of Visibility Measures and Aerodynamic Disturbance at a 2.2 m/s Overtaking Speed for Various Cloud Conditions	91
28.	Variation in Steering Response with Visibility and Aerodynamic Disturbance Conditions	95
29.	Variation in Yaw Velocity with Visibility and Aerodynamic Disturbance Conditions	96
30.	Variation in Lateral Acceleration with Visibility and Aerodynamic Disturbance Conditions	97
31.	Variation in Lateral Lane Deviations with Visibility and Aerodynamic Disturbance Conditions	98
32.	Driver "Accident Risk" Ratings for Various Visibility and Aerodynamic Disturbance Conditions	100
33.	Driver "Task Difficulty" Ratings for Various Visibility and Aerodynamic Disturbance Conditions	101
34.	Cab Mounted Drag Shields	105
35.	Underbody Baffle Plus Splitter Panel Concept	109
36.	Gap Filler Panel Concept for Full Scale Tests	111
37.	Partial Gap Panel Concept for Full Scale Tests	111
38.	End Plates for Partial Gap Panel	112
39.	Angled Side Vane Concept, Side View	113

		Page
40.	Angled Side Vane Concept, Plan View	113
41.	Sketch of European Fender	116
42.	Sketch of Quarter Fenders on Tractor	116
43.	Sketch of Roberts Fender on Semitrailer	118
44.	Sketch of Reddaway Fender	119
45.	GALCIT Tunnel Setup with Basic Truck and Tufts	129
46.	Northrop Test Setup	131
47.	Three Axle COE Plus 40 ft Van Model	133
48.	Three Axle COE Plus Dry Cargo Tanker Model	133
49.	Three Axle COE Plus Flatbed Model	134
50.	Three Axle COE Plus Liquid Cargo Tanker Model	134
51.	Three Axle CBE Plus 40 ft Van Model	135
52.	Three Axle CBE Plus Dry Cargo Tanker Model	135
53.	Two Axle COE Plus 27 ft Van Model	136
54.	Two Axle COE Plus 27 ft Van Plus 40 ft Van Trailer Model . .	136
55.	Vertical Gap Splitter Panel	140
56.	Horizontal Gap Bottom Plate	140
57.	Cab-Mounted Drag Shield	141
58.	Dam Under Front Bumper	141
59.	Gap Filler Block	142
60.	Lateral Lips on Van Upper Edge	142
61.	Angled Side Vanes Around Tractor Wheels	143
62.	Longitudinal Underbody Baffle	143
63.	Full Fenders over Tractor Tandems	144
64.	Horizontal Flow Deflector Foil	144

Page

65. 1972 Chevrolet Station Wagon Model 145

66. Typical Relative Car-Truck Locations Tested at Northrop . . . 148

67. Velocity Components Projected on x-y Plane 153

68. Iso-Pressure Contours 155

69. Typical Tuft Photograph, 3 Axle COE Plus 40 ft (12.2 m) Van, $\psi_W = -20$ deg 160

70. Streamlines and Turbulence, Basic Truck Configuration 161

71. Wake Velocities from Full Scale Anemometers, 3 Axle COE Plus 40 ft Van 163

72. Summary of Full Scale Ground Aneometer Data 164

73. Assumed Variation in Effective Cross Sectional Area with Relative Wind Angle 176

74. Comparison of Side Force Coefficients, Zero Crosswind 182

75. Adjacent Car-Alone Lateral-Directional Data 184

76. Aerodynamic Disturbance with Basic Truck 186

77. Aerodynamic Disturbance with 3 Axle COE Plus Flatbed 188

78. Aerodynamic Disturbance with 3 Axle COE Plus Liquid Cargo Tanker 189

79. Aerodynamic Disturbance with 3 Axle COE Plus 40 ft Van 191

80. Aerodynamic Disturbance with 2 Axle COE Plus 27 ft Van 192

81. Aerodynamic Disturbance with 2 Axle COE Plus Double 27 ft Vans 193

82. Aerodynamic Disturbance with 3 Axle CBE Plus Dry Cargo Tanker 195

83. Aerodynamic Disturbance with Drag Shield 197

84. Aerodynamic Disturbance with Full Fenders on Tractor Tandems 199

85. Aerodynamic Disturbance with Longitudinal Underbody Baffle 200

86. Aerodynamic Disturbance with Horizontal Gap Bottom Plate 202

Page

87. Aerodynamic Disturbance with Vertical Gap Splitter Panel 203

88. Aerodynamic Disturbance with Angled Side Vanes 204

89. Firestone Test Center Track 208

90. Detail of Wet Test Area 210

91. Track Instrumentation for Truck-Alone Tests 212

92. WHI Test Observer's Report Form 215

93. Driver Rating Form 217

94. Example of Truck-Alone, Track Data Sheet 223

95. Example of Adjacent Car Data Sheet 224

96. Effect of Semitrailer Load on Visibility Measures 227

97. Effect of Truck Speed on Visibility Measures 228

98. Effect of Truck Speed on Opaque Splash and Spray Cloud Areas 229

99. Basis for Truck Lane Position Scaling Factor 231

100a. Ambient Wind Angle Scaling Curve, Southbound 233

100b. Ambient Wind Angle Scaling Curve, Southbound 234

101a. Ambient Wind Angle Scaling Curve, Northbound 235

101b. Ambient Wind Angle Scaling Curve, Northbound 236

102. Flow Chart of Visibility Scaling Procedure 239

103. Correlation of Laser Raw Data, Downwind 244

104. Correlation of Photometer and Laser Raw Data, Downwind 245

105. Correlation of Laser Raw Data, Upwind 246

106. Correlation of Photometer and Laser Raw Data, Upwind 247

107. Correlation of Observer Rating from Ahead and Visibility, Laser at 2 ft 249

108. Correlation of Observer Rating from Behind and Visibility, Laser at 2 ft 250

Page

109. Correlation of Observer Rating from Ahead and Visibility, Laser at 6 ft 251

110. Correlation of Observer Rating from Behind and Visibility, Laser at 6 ft 252

111. Correlation of Observer Rating from Ahead and Visibility, Photometer 253

112. Correlation of Observer Rating from Behind and Visibility, Photometer 254

113. Relation Between Task Difficulty Rating and Visibility . . . 256

114. Relation Between Accident Risk Rating and Visibility 257

115. Relation Between Path Performance and Visibility 259

116. Relation Between Task Difficulty Rating and Path Performance 261

117. Relation Between Accident Risk Rating and Path Performance 262

118. Effect of Semitrailer Type on Raw Visibility Measures, COE 264

119. Effect of Semitrailer Type on Raw Visibility Measures, CBE 265

120. Effect of Semitrailer Type on Scaled Visibility Values, COE 267

121. Effect of Semitrailer Type on Scaled Visibility Values, CBE 268

122. Comparison of Raw Visibility Measures for Reddaway Fenders and Basic Truck 272

123. Comparison of Raw Visibility Measures for Angled Side Vanes and Basic Truck 273

124. Comparison of Raw Visibility Measures for Gap Filler Panels and Basic Truck 275

125. Comparison of Scaled Visibility Values for Reddaway Fenders and Basic Truck 278

126. Comparison of Scaled Visibility Values for Partial Gap Panels and Basic Truck 279

Page

127. Comparison of Scaled Visibility Values for Angled Side Vanes and Basic Truck 280

128. Comparison of Scaled Visibility Values for Gap Filler Panels and Basic Truck 282

129. Effect of Scaling Procedures on Visibility Margins 283

130. Macro Flow Chart of TRKSIM Program 291

131. Flow Chart of CONSUM Program 295

132. Selected "Real World" Circuits 309

133. Relative Cost-Effectiveness by B/(C + 4) Ratio 314

134. Air Resistance Horsepower Versus Absolute Wind Angle 318

135. Average Marginal Visibility over 17 Prototypical Wind Conditions 319

136. Total Operating Cost as a Function of Fleet Size 322

LIST OF TABLES

		Page
1.	Splash and Spray Suppression Devices and Results of Past Tests	17
2.	Summary of Selected Past Tests	21
3.	Summary of Devices	122
4.	Estimated Costs for Selected Prototype Devices	125
5.	Mean Wake and Turbulence Velocities	166
6.	Drag Values for Various Truck Configurations	168
7.	Drag Coefficient Breakdown for Multiple Trailer Configurations	171
8.	Drag Values for Variations in Basic Truck Configuration	172
9.	Drag Values for Basic Truck with Device	174
10.	Nominal Drag Increments for Various Devices	175
11.	Lateral-Directional Coefficients for Various Truck Configurations	179
12.	Summary of Splash and Spray Tests — June 1977	220
13.	Summary of Visibility Values for Various Truck Configurations	269
14.	Summary of Raw Visibility Measures for Various Devices, Downwind Conditions, Laser at 2 ft	276
15.	Summary of Scaled Visibility Margins for Various Devices	284
16.	Percentage Improvements in Fuel Economy for MO System	297
17.	Performance Characteristics	300
18.	Summary of Economic Characteristics for Input to C-E Analysis	302
19.	Key Physical Characteristics of Prototypical Operating Scenarios	305
20.	Geographic Variations Among Selected "Real World" Operating Scenarios	308

		Page
21.	Matrix of Economic Conditions	310
22.	Average Benefit/Cost Rankings for Differing Economic Assumptions	311
23.	Average Values of $B/(C+4)$ for Differing Economic Assumptions	313
24.	Marginal Visibility for Prototypical Wind Conditions	316
25.	Approximate Range of System Benefits and Associated Costs	321
26.	Average Capital Costs	323
27.	Capital Cost as a Ranking Criterion	324
28.	Daily Marginal Cost Components as a Function of Ambient Wind for 9 Most Cost-Effective Systems	326
29.	Daily Marginal Cost Components for Empty Truck as a Function of Terrain for 9 Most Cost-Effective Systems	326
30.	Daily Marginal Cost Components for Weighted Out Truck as a Function of Terrain for Nine Most Cost-Effective Systems	327
31.	Percentage Improvements in Fuel Economy for 9 Most Cost-Effective Systems	328
32.	Fuel Savings as a Ranking Criterion	329
33.	Illustrative Results for "Real World" Scenarios	330

NOMENCLATURE

a	Tread groove width
a_y	Lateral acceleration
A	Vehicle frontal area
A_{EFF}	Effective frontal area
b	Tread groove depth
c	Spray mass concentration
C_D	Aerodynamic drag coefficient
ΔC_D	Change in aerodynamic drag coefficient
C_{D_B}	Base drag
C_{D_F}	Friction drag
C_{D_G}	Gap interference drag
C_{D_I}	Induced drag
C_{D_P}	Form drag
C_{f_B}	Forebody friction drag
C_ℓ	Aerodynamic roll moment coefficient
$C_{\ell_{\psi_W}}$	Aerodynamic roll moment derivative
C_L	Aerodynamic lift coefficient
C_m	Aerodynamic pitch moment coefficient
C_n	Aerodynamic yaw moment coefficient
ΔC_n	Change in aerodynamic yaw moment coefficient
$C_{n_{\psi_W}}$	Aerodynamic yaw moment derivative
C_p	Pressure coefficient
C_y	Aerodynamic side force coefficient
$C_{y_{\psi_W}}$	Aerodynamic side force derivative

d	Droplet diameter
e	Base of Naperian logarithm
G_b^a	Transfer function relating input b to response a
G_s	Steering ratio
h	Road water depth
j	$\sqrt{-1}$
K_1	Wake mean flow velocity component
K_2	Turbulence velocity constant
ℓ	Vehicle wheelbase
L	Aerodynamic roll moment
L_c	Length of simulated spray cloud
n	Driver remnant
n_t	Number of tire grooves
N	Aerodynamic yaw moment
N_b^a	Numerator of transfer function G_b^a
q	Dynamic pressure
Q_o	Initial mass flow
r	Yawing velocity or heading rate
R	Maximum reduction in light transmitted through spray cloud
R_t	Radius of tire
S	Surface tension
t	Vehicle track
T	Data segment or run length
u,v,w	Flow velocity components along x,y,z
U	Forward velocity
U_c	Velocity of adjacent car along roadway

U_T	Velocity of truck along roadway
U_o	Forward speed of adjacent car
U_1	Mean wake flow velocity
U_∞	Free stream velocity
v	Wake flow velocity
v_o	Truck airspeed component in direction of travel
V	Visibility value or measure
V_d	Velocity of droplet at a point along its trajectory
V_I	Initial injection velocity of droplet stream
V_T	Velocity of flow turbulence component
V_0	Visibility measure with no ambient wind
V_5	Visibility measure with 5 mph (2 m/s) ambient wind
$\dot{w}_{total}$	Total water flow rate in path of tire
$\dot{w}_{tread}$	Flow rate of water picked up in tread grooves
$\dot{w}_{wave}$	Flow rate of displaced water
W	Width of tire contact patch
$\measuredangle W$	Angle of ambient wind
$\|W\|$	Magnitude of ambient wind
$\measuredangle WV$	Angle of relative wind with respect to vehicle centerline
$\|WV\|$	Magnitude of relative wind
x,y,z	Coordinate system for spray dispersion analysis
x_B	Distance relative to front of bus along roadway
x_T	Distance relative to front of truck along roadway
y_c	Desired or commanded roadway path
y_I	Lateral lane deviation or position
$\hat{y}_I$	Peak lateral deviation

y_T	Lateral distance relative to truck centerline
Y	Aerodynamic side force
Y_c	Effective vehicle dynamics transfer function
Y_p	Driver describing function
Y_p^*	Effective driver describing function
Y_{vg}	Lateral acceleration per unit crosswind
Y_y	Driver describing function for lateral deviation response
Y_ψ	Driver describing function for heading response
α	Spray angle for water thrown from tire
δ	Depth of water film on tire
δ_{sw}	Steering wheel angle
δ_w	Steer angle
$\overline{\delta_o}$	Mean initial steering wheel angle
η	Aerodynamic disturbance
ρ	Density, simulated spray density
σ_y	Turbulence scale length along y axis
σ_z	Turbulence scale length along z axis
τ	Effective time delay
φ_M	System phase margin
ψ	Heading angle
ψ_W	Relative crosswind angle
ω	Angular frequency
ω_c	System crossover frequency
Ω	Angular velocity of tire

Special Symbols

$(\hat{\ })$	Peak value
$(\vec{\ })$	Vector
$(\bar{\ })$	Mean
$(\overline{\ }^{2})$	Mean square

SECTION I

INTRODUCTION

A. OBJECTIVES

The overall objective of the program (Ref. 1)* has been to develop methods of minimizing the adverse effects of three aerodynamic related phenomena: vehicle-induced air force disturbances, splash, and spray. Such development has been effected through a combination of state of the art review and assessment, analytical techniques, laboratory and model scale experiments, full scale tests, and cost effectiveness evaluation. The entire process and the study have been aimed toward the development of optimum and feasible methods of minimizing the adverse aerodynamic disturbance, splash, and spray phenomena associated with trucks.

The emphasis has been on devices fixed to trucks which can improve the air flow properties around the truck and reduce the formation and propagation of splash and spray as experienced by adjacent motorists. Such devices have been conceptualized, developed as prototypes, tested under controlled full scale conditions, and assessed with respect to cost/benefit. Non-vehicle means of minimizing the adverse effects of the three phenomena have been considered, also, to the extent that results and interpretations were available.

B. ELEMENTS OF THE TECHNICAL APPROACH

The overall technical approach used in this program has included the following activities:

- Work plan preparation and literature search
- Analyses
- Preliminary experiments with a driving simulator
- Model scale wind tunnel experiments

---

*Reference numbers refer to list at the end of the main text.

- Full scale laboratory tests with a single wheel
- Aerodynamic field tests
- Splash and spray field tests
- Cost-effectiveness analyses
- Over-the-road evaluations
- Reporting

All but the over-the-road evaluations comprised Phase 1 of the program effort, and are the subject of this Interim Report.

Those aspects of the analytical and experimental approach related to aerodynamic flow and driver/vehicle performance were patterned after earlier STI work (Refs. 2 and 3) on truck and bus aerodynamic disturbances. These efforts developed and verified methodology and criteria for quantifying the performance of a car in the influence of such aerodynamic interference effects. This earlier work proceeded through a series of laboratory experiments, driver/vehicle analyses, and full scale validation to arrive at this way of judging the aerodynamic disturbance hazard due to a truck or bus. In this respect it served as a useful prototype for the current program, and the methods and criteria for aerodynamic-interference effects are basically applicable to the total picture including splash and spray. Thus, rather than separately analyzing induced-aerodynamic, splash, and spray effects and possibly weighting each to arrive at some artificial figure of merit, the aim has been to judge their integrated and combined effect in the context of composite measures considering such things as visibility, subjective ratings, and path deviations of the adjacent car/driver.

To accomplish the objectives of this program, additional methodology was needed beyond that already developed for only aerodynamic-interference inputs, i.e., it was necessary to establish:

- The quantitative effects of degraded visibility under various conditions and situations on driver behavior
- A better understanding of the physics of splash and spray formation and propagation

- The connections between splash/spray characterization — patterns, densities, drop sizes, etc. — and visibility
- Methods for relating visibility and driver behavior to the cost of devices, in a cost-benefit sense

To round out the needed methodology, the methods and procedures required to devise and select optimum arrangements needed development, i.e., the estimation of aerodynamic and splash/spray effects from truck or alleviating device properties.

Overall, the approach taken allowed us to consider aerodynamic, splash, and spray details with quantitative precision; while at the same time focusing our main effort on the properties of complete trucks under real world, full scale conditions. Further discussion of the issues involved in this problem of aerodynamics, splash, and spray is presented in Section II; and the associated technical approaches are detailed throughout the report.

C. PROJECT TEAM ORGANIZATION

This program has been a highly interdisciplinary effort involving a wide range of technical skills. In order to complement our capabilities, Systems Technology, Inc. (STI) has used three subcontractors in the accomplishment of this program, i.e.:

- AeroVironment, Inc. (AVI) for their expertise in aerodynamic flow modeling, spray formation and propagation, and their general experience in vehicle-related aerodynamic testing
- Western Highway Institute (WHI) for their background in splash and spray alleviation and testing, truck operations, and safety and highway engineering in general
- Alan M. Voorhees and Associates, Inc. (AMV) for the cost-effectiveness analyses and their special expertise in the areas of engineering economics and operations research

Descriptions and results of each of their activities have been incorporated into this document to make it complete and self contained, and their special contributions are identified where appropriate. In addition, separate detailed technical reports have been prepared by AVI and AMV to document their efforts and results, Refs. 4 and 5, respectively.

The full scale aerodynamic and splash and spray tests were accomplished at the Firestone Test Center in Fort Stockton, Texas, under the auspices of Western Highway Institute. The model scale wind tunnel tests were accomplished at the GALCIT and Northrop Aircraft subsonic tunnels under the direction of STI.

D. OVERVIEW OF THE INTERIM REPORT

The next section of this report extends the introduction with a discussion of the problem of truck generated aerodynamic, splash, and spray disturbances. It includes summaries of pertinent prior work, non-vehicle alleviation techniques, and considerations in the selection of the example test vehicles.

Results of analyses and laboratory experiments which helped guide the wind tunnel and full scale tests and data interpretation are given in Section III. Truck mounted alleviation devices studied in the wind tunnel and full scale tests are described in Section IV. Although in some ways these devices resulted from said tests, they are characterized early in the report to help the reader interpret the procedures and results.

The aerodynamic tests are summarized, and the results are presented, in Section V. Topics include air flow around the truck and in the wake, truck drag, and forces and moments on the adjacent car — all as a function of truck type, devices, ambient wind, and other situational parameters. Note that the detailed AVI technical report (Ref. 4) complements this section in the area of flow modeling.

The splash and spray tests are summarized, along with the data and interpretation, in Section VI. Although a variety of subjective and objective measures are helpful to quantify splash and spray, visibility measures from a track-mounted laser are used to compare different truck types and configurations, and to quantify the alleviating properties of the various devices.

The cost-effectiveness analysis and results are given in Section VII. Here the AMV technical report (Ref. 5) provides supporting detail and backup data, but the essential results and descriptions are given in Section VII.

The conclusions and recommendations are given in Section VIII. Implications for Phase 2 are noted, also.

Further details of the splash and spray data are given in Volume II of this report.

SECTION II

ELEMENTS OF THE PROBLEM

This section begins with a discussion of the nature of the total problem of aerodynamics, splash, and spray associated with truck operations under adverse weather conditions. This includes a description of the assumed scenario on the highway, with its driver, vehicle, and disturbance elements. Though general in content, the aim is to provide a framework within which to view the detailed analyses, experiments, and results presented in subsequent sections.

The next article lists the important parameters and variables of the aerodynamics, splash, and spray situation. This is followed by a review of prior research to understand the splash and spray problem and develop means of alleviation. Next is a discussion of non-vehicle means, i.e., ways of reducing or avoiding the adverse aerodynamic and visibility effects other than by devices affixed to the truck.

This section concludes with a discussion of the basis for selecting the tractor/trailer trucks used as examples for purposes of analysis and testing.

A. DISCUSSION OF THE ISSUES

Movement of a truck along the roadway under wet weather conditions can affect and disturb the adjacent motorist in several ways. The air flow around the truck and in the wake can cause force and moment disturbances on the car, particularly when the car is close to the truck or when the ambient wind is such that the car is downwind. The splash and spray in the air can obscure or block the driver's vision, and larger droplets striking the windshield can further obstruct vision and increase the requirements on the wipers.

When the motorist initially overtakes the truck, his view alongside of and forward of the truck may be blocked, even though he is still operating in relatively clear air. Perceiving risk, he may choose not to pass; because the presence of other traffic, obstacles in the lane, and even the geometry of the roadway ahead are not clear. If he follows the truck at a safe distance other overtaking drivers may be balked, and they may take excessive risks in their urge to maintain their operating speed. Once a motorist begins to pass the truck and moves alongside, he becomes enveloped in the spray cloud which obscures vision ahead and to the side to a degree dependent upon many situational factors. In addition, intermittent splash may strike the windshield if there is puddling or uneven wetting of the roadway surface in the path of the truck. As the car moves abreast of the front of the truck, visibility clears. In each of these phases of overtaking and passing, as noted above, there can be added buffeting of the car due to the air flow around the truck.

When a truck overtakes and passes a car, similar aerodynamic and visual disturbances occur. In addition, there may be an element of surprise, which can increase the driver's workload and further increase the perceived risk and potential hazard.

For introductory purposes, the phenomena of splash and spray can be described in simple terms. Splash tends to be relatively large droplets which move in ballistic trajectories. Spray is composed of the smaller droplets, which, as an aerosol, tend to be suspended in the air and move with the air flow. Formation of spray requires a source of water, such as a stream of splash or a wet surface, plus a relatively high velocity flow of air which helps break the droplets down to a very small size. Typically, spray is formed when a stream of water or large droplets strikes a hard or smooth surface, in the presence of a high velocity air flow. It is fundamental, then, that spray can be alleviated by modifying or removing one or more of these three elements: the water, the surface, or the high velocity air. The physics of splash and spray formation and propagation are discussed in much greater detail in Section III and Ref. 4.

Operation of the truck is also influenced by its configuration and the ambient wind. A primary factor is the truck drag which has a direct effect on fuel economy, and it can be either increased or decreased by the presence of devices. The various splash and spray devices can also influence the cost of maintenance, and they can complicate line operations, e.g., due to brake heating, or when there is a need to install and remove chains. Such factors are also addressed in some detail in Sections IV and VII.

Obviously, the ideal device or other solution to the problem would be one which reduced splash and spray, decreased truck drag, decreased the aerodynamic disturbance of the adjacent car, involved no initial or recurring costs, and had no adverse effects on truck operations. As will be shown in later sections, some combinations of devices have the potential of reducing splash and spray and truck drag, but they all have some cost associated with them (which can be offset by fuel savings in some cases).

Included in the devices of primary interest in this study are those that alter the aerodynamic flow in the vicinity of the truck. These would tend to suppress the formation and propagation of splash and spray, to reduce the overall aerodynamic disturbance to adjacent vehicles, and perhaps to reduce the associated truck drag as well. The other main class of device includes those that collect the splash and spray or prohibit its formation. In summary, the conceivable methods of minimizing adverse aerodynamic effects involve:

- Alterations in truck or adjacent vehicle operating procedures (e.g., training, speed reduction, lane selection), or roadway modifications

- Changes in the basic truck configuration to reduce deleterious air flow and spray generation characteristics

- Incorporation of add-on devices to inhibit or collect splash and spray, or to reduce aerodynamic drag and splash and spray, while having a beneficial effect on disturbing aerodynamic forces

The first method, non-vehicle techniques, is discussed in Article D, below. While such alleviation possibilities have not been excluded entirely, our principal focus has been on devices fixed to the truck. Our approach to such devices and their properties are presented in Section IV, and the associated experimental results and consequences are detailed in Sections V through VIII. Some additional discussion of the aerodynamic effects on the adjacent car of changing the truck shape is given in Article C, below, based on prior STI/FHWA work. The results of prior efforts to conceive and develop truck mounted devices to suppress splash and spray are also given in Article C.

B. SITUATIONAL PARAMETERS AND CONDITIONS

There are a variety of truck-centered and situational parameters which determine the nature and magnitude of the disturbance caused by aerodynamic and splash and spray effects. A listing of these factors helps to define what splash and spray involves and it provides further dimension to the problem.

1. Truck-Centered Parameters

Parameters which are truck-centered include the following:

- Truck shape and configuration, including number of axles and length
- Underbody detail
- Truck-mounted devices
- Tire tread depth
- Forward speed
- Load

In this program, a variety of truck configurations has been considered (see Article E, below). Although doubles and triples were studied, attention has focused on 5 axle tractor plus semitrailer rigs. Variations in underbody detail were present in the test vehicles and were included in the wind tunnel tests. A large number of truck-mounted devices has been studied, of course, since their definition and assessment was the main point of the project. Tire tread depth effects were considered in the single wheel laboratory experiments, but the vehicles in the full scale splash and spray tests all had new or near new tire tread depth levels (e.g., greater than 9 mm, on the whole). Speeds of 50 and 60 mph (80 and 97 km/h) were used, and the effects of variations in GVWT were studied with the basic truck, 3 axle COE plus 40 ft (12.2 m) van.

2. Other Situational Parameters

Non-truck parameters which are important to defining the disturbance conditions include:

- Pavement texture and geometries
- Water depth
- Magnitude and direction of the ambient wind
- Ambient light and visibility

The full scale splash and spray tests of this project involved one pavement texture and a flat, straight test section with a cross slope of about 1 percent for drainage. The ambient wind varied, of course, over the whole test period, but it tended to remain fairly constant for periods on the order of an hour. The current tests were run in the daylight with bright sunshine conditions, for the most part.

Other parameters which comprise the test conditions center on the adjacent car, and they include:

- Aerodynamic and handling properties
- Driver field of view (windscreen framing properties)
- Forward speed, and speed relative to the truck
- Driver skill and perceptual factors

The example adjacent car in the experiments reported here was a full sized Chevrolet station wagon, vintage 1973. Aside from being representative, it had been studied extensively in prior wind tunnel and full scale experiments, as will be described. The drivers were all males, 25-40 years old, with no impairment and average to above average skill, as discussed in Article VI.A.

As can be seen, there are many factors which affect aerodynamic, splash, and spray disturbances. Prior studies have considered many of these in some detail, including many of the truck-centered parameters, pavement texture, water depth, and the aerodynamics and handling of the adjacent car. Where possible, this program has tried to use and build on prior findings, and to concentrate on the effects of truck configuration and the potential benefits of truck-mounted devices.

3. Concept of a Basic Case

This focus on the truck has lead to the concept of a "basic case," and the study of variations thereto. Briefly, the basic case includes:

- 3 axle COE tractor plus 40 ft (12.2 m) van (3S2)
- No devices
- Near new tread depth
- Forward speed of 60 mph (97 km/h)
- Empty (no load)
- Water depth of about 0.055 in. (1.4 mm)
- Daylight
- Typical station wagon as adjacent car

This basic case and the truck variations studied are described more specifically in subsequent sections.

C. FINDINGS OF PRIOR STUDIES

This program has endeavored to extend the state of knowledge and identify solutions to the disturbance problems described above. Hence, considerable attention has been paid to prior results. In this article some of those prior results and activities are reviewed, in order to provide a basis for the new results given in later sections.

1. Studies of Truck-Car Aerodynamic Disturbance

A prior FHWA-funded study by STI (Refs. 2 and 6) provides quantification of the nature and magnitude of the effect of truck-induced aerodynamic disturbances on a passenger car. The results are expressed in terms of overall car/driver safety performance, with the emphasis on steering control and side to side deviations in the car's path along the roadway in the vicinity of the truck. The basic situations studied involve a station wagon and a tractor/semitrailer, a two lane road, overtaking and passing and car-truck oncoming. Within this framework the following parameters were varied: truck width and shape, lateral separation and lane width, ambient wind magnitude and direction, car-truck speeds, car handling properties, and driver skill and alertness. Specific attention was given to the potential effects of increasing truck width from 96 to 102 inches (2.44 to 2.59 m). The study comprised full scale experiments, wind tunnel tests, and combined car/driver/disturbance analyses. As discussed below, the results were interpreted in terms of possible actions and remedial implications in the areas of roadway design, truck size and configuration, and car/driver dynamics and control characteristics.

a. Truck Configuration Effects

With no ambient wind or only a headwind, the main disturbance comes from the bow wave near the front of the truck. Streamlining the front of the tractor was found to reduce the disturbance magnitude somewhat, as can increased ground clearance under the tractor. Headwinds tend to magnify the bow wave disturbance. With a crosswind the bow wave disturbance component is still there, but the other crosswind-related disturbance effects are much larger when the car is passing downwind.

The truck wake was found to have a substantial disturbance effect, especially in crosswinds with the car downwind. Drop bed trailers and vans that allow less flow under the truck caused larger car/driver disturbances and deviations in a crosswind, with the car passing on the downwind side. Variations in the size of the gap between tractor and trailer did not affect the disturbance in ways important to performance, because the corresponding gap flow is generally above the level of the car, and the perturbation is rapid relative to the response of the passing car. With the car on the upwind side of the truck, the wake blows the other way, and the disturbance is generally very small.

Increasing truck width can increase the disturbance and affect car/driver performance. With a large crosswind the width effect is relatively small, compared to the basic crosswind effect. With no wind or headwinds only, the incremental width effects are a greater percentage of the basic bow wave disturbance. In the more critical speed regime, a 6 inch (150 mm) overall width increase caused about a 5 percent increase in lateral deviation of the car, which is about double the percentage increase associated with a 3 inch (76 mm) reduction in the side to side clearance of car and truck. Preliminary experiments in Ref. 2 showed that the bow wave disturbance effect of a 6 inch (150 mm) overall width increase can probably be largely offset by suitable rounding and streamlining of an otherwise blunt tractor front.

Preliminary investigations of truck length effects were accomplished by extrapolating the then existing data to a double bottom truck configuration with two 27 ft trailers instead of one 40 footer. The same tractor was used and the overall length increased by about 10 ft (3 m). The analyses suggested no difference would occur in the no crosswind case, because the bow wave is unchanged and it dominates the disturbance. The crosswind effects were about the same also, because the flow between the trailers appeared to offset the effect of increased vehicle length. Generally, the more porous the truck/trailer configuration to a crosswind (flow under and through the rig) the less the disturbance to a vehicle passing on the downwind side.

b. Operational Effects

From the standpoint of the highway designer and traffic engineer, the important variables in the truck disturbance situation were found to be:

- Ambient winds on the roadway
- Lateral separation of the vehicles
- Absolute speed of the vehicles
- Relative (overtaking) speed of the vehicles
- Driver alertness

Specific numerical results, boundaries, and criteria are presented in Refs. 2 and 6, and some of the implications are discussed below.

The ambient wind plus the vehicle's ground speed combine to produce a net airspeed. Since this is an aerodynamic phenomenon the dynamic pressure of this airspeed scales the intensity of the disturbance, as the square of the airspeed for a single vehicle or as the product of the respective car and truck airspeeds in the disturbance situation. Hence, it is always desirable to reduce the net airspeed by reducing vehicle speed or ambient headwind or both. In terrain with prevailing headwinds, the route and roadway layout should be designed to reduce their effect where feasible.

More lateral separation of the vehicles can be achieved in windy regions by increasing lane widths and medians. Another possibility suggested was to separate truck lanes from other vehicle lanes by an auxiliary median (or lane closed to traffic under extreme wind conditions). With no crosswinds, a small increase in lateral separation will offset truck width increase (and other configuration) effects, as noted above. With strong crosswinds, however, the truck wake disturbance persists some distance downwind from the truck and simply increasing separation is less effective.

The Ref. 2 study showed that the disturbance effects are generally more critical when car and truck are proceeding in the same direction. With no crosswind, the bow wave disturbance from an oncoming truck causes a relatively small disturbance because of its very short duration, and adequate lateral separation (via lane width or median) will provide sufficient alleviation. With a crosswind, the wake blowing from the oncoming truck towards the car can provide a large disturbance input. The resulting effect on performance was estimated to be of the same order as that for the same direction of travel case, but specific measures were not made.

Higher relative overtaking speeds (same direction) generally caused less disturbance of the car, because the encounter duration was shorter and the car inertia tends to attenuate rapidly changing forces and moments. Hence, reduced truck speeds were suggested to provide additional alleviation under adverse conditions.

Certain types of vehicles such as small vans, cars towing trailers, and camper combinations serve to provide the more critical cases from the standpoint of highway design and operation. They are more susceptible to aerodynamic disturbances. They have poorer handling response once disturbed. They tend to have lower speeds relative to the disturbing trucks, and they tend to operate in the right lanes on multilane highways in closer proximity to the trucks. The criticality of these adjacent vehicles to aerodynamic disturbances has been confirmed in an FHWA-funded study which considered a variety of vehicles exposed to the disturbance caused by an intercity bus (Ref. 3).

An alerted driver, familiar with potential truck disturbances, was found to be important to safe operation in the more critical situations. Since the intensity of the disturbance varies significantly with the conditions, the driver cannot always anticipate a disturbance situation when overtaking a truck or other large vehicle. As a result, he should expect it alongside a truck in a crosswind and at the front of a truck with a headwind. Conservatively, the driver should always expect it and be prepared to react and then counterreact as the disturbance decreases. The poorer driver (e.g., with a longer time delay) or one who is unfamiliar with his vehicle may have more difficulty. Defensively, it can help for the driver to increase his overtaking speed to have a 10 mph (16 km/h) or more headway advantage. He should move towards the edge of the lane away from the truck when the wake is blowing towards his car. With no crosswind, he should stay in the middle of his lane to avoid being pushed beyond the lane edge by the bow wave. Suitable warning signs for the driver in areas with prevailing winds, training, and publicity were suggested as potential means of alleviation, also.

Suggested guidelines for operation by the truck driver are given in Ref. 2. He should move toward the side of the lane away from passing vehicles and other traffic, when there are no vehicles or pedestrians on the shoulder. He should be alert for a passing car that may experience difficulty. In the same vein, he should recognize that when his truck overtakes a slower vehicle it may cause an unexpected disturbance of the overtaken vehicle and its driver. As noted, the analyses and experiments (and some corroborative accident data) show that this latter situation can be particularly critical when a truck overtakes a car towing a travel trailer.

2. Studies of Devices to Reduce Drag and Splash and Spray

Recent literature is rife with studies of add-on devices intended to reduce either aerodynamic drag or splash and spray (for example, Refs. 7-24). Although there can be some interaction between these two types of device, work to date has not usually recognized that possibility, and the literature treats them separately for the most part.

a. Drag Reduction Devices

Historically, the search for better fuel economy has lead to the development and use of truck-mounted devices designed to reduce drag, and interest has intensified in recent times. Most commonly, these take the form of solid or porous shields mounted on the tractor. Fairings on the leading edge of the semitrailer have also been used, including rounding the leading edges. Other, more radical approaches have included fairings across the gap, streamlined tractors, and streamlining the combination tractor/semitrailer as a unit. These approaches are typified by the devices and methods studied in Refs. 7 and 13-24. As discussed in Section IV, tractor mounted drag shields figure prominently in our approach to cost-effective solutions to the truck-induced aerodynamic and visibility disturbance problem.

To the extent that drag devices inhibit the crosswind air flow down and through the gap, they could decrease disturbance outflow in that region, also. Past attempts to reshape the semitrailer fore- and upper-body streamlines have not generally resulted in significant changes in aerodynamic disturbance generation patterns. Drag reduction devices which affect the underbody air flow, on the other hand, could be expected to change the crosswind disturbance patterns to some extent, since the car is low relative to the truck.

b. Splash and Spray Suppression Devices

A wide variety of direct splash and spray suppression devices has been designed, developed, and tested. These have shown varying levels of effectiveness (in past tests) and applicability in alleviating truck induced splash and spray. Table 1 lists typical examples of these devices, which are grouped into five descriptive categories, i.e.,

- Conventional fenders and mudflaps
- Spray protector skirts
- Water collector fenders
- Air and water deflectors
- Other suppression devices and techniques

Some of these devices from past tests are sketched in Fig. 1.

TABLE 1. SPLASH AND SPRAY SUPPRESSION DEVICES AND RESULTS OF PAST TESTS

DEVICE	FUNCTIONING PRINCIPLE	ADVANTAGES	DISADVANTAGES	REFERENCES
Conventional fenders	Has "lip" to reduce outward splash and spray	Upward splash containment	Not effective; tends to atomize upward splash	12
Mudflaps	Flexible shield behind wheel blocks rearward splash	Effective at low speed; low cost	Not effective at high speed; atomizes splash and can produce additional spray	12, 25
Spray protector skirts				
DOT spray protector and louvred	Envelopment of wheels	Effective for upper tire splash and spray	No effect on rearward splash; can cause serious brake and tire heating	11, 12
Koneta skirt	Containment of upper wheel splash and spray	Airstream "fencing" reduces underbody turbulence, ventilates brakes	Not effective (only 2 percent overall reduction in spray)	26
Dunlop, AG (Germany), fender with skirt/lip extensions	Molded rubber fender contains splash and spray	Reduces side spray	Drops water back into wheel path; not too effective for rearward splash; possible brake heating	11
Water collector fenders				
Roberts fender and modifications	Slotted and corrugated inner fender converts spray to droplets, drains away from wheel	Reduces side spray; 2-6 percent overall spray reduction; little brake heating	Rejected water is dropped back into wheel path; has little effect on rearward splash; can clog with ice, slush, etc.	11, 26
Reddaway fender	"Astroturf"-type material used to entrap and absorb spray	9-10 percent overall spray reduction; little brake heating	Collected water is dropped back into wheel path; can clog with ice, mud, etc.	26
PABS fender	Perforated/corrugated lower fender converts spray to droplets, drains toward center of vehicle	15-20 percent overall spray reduction	Inadequate drainage capacity; can clog with ice, etc.	11, 26
Oregon Division of Highways suppression fender	Perforated metal collector, with air deflection vanes	Reduced side spray	Not effective for rearward splash and spray	11

(Continued on next page)

TABLE 1. (Concluded)

DEVICE	FUNCTIONING PRINCIPLE	ADVANTAGE	DISADVANTAGES	REFERENCES
Air and water deflectors				
Gaussoin deflector	Flexible shield in front of wheel deflects air/water around wheels, reduces turbulence	Reduces side spray; will not clog, etc. etc.; low cost	Not effective for rewarward splash and spray	11
Scoop-type airstream direction	Forced air currents redirect flow toward center of vehicle	Effect increases with vehicle speed	Insufficient flow rate/force; susceptible to clogging; poor for downwind travel	12
Other suppression devices				
Chined tires	Sidewall ridge deflects side splash downward	Reduces side splash; keeps splash at low angles	Not effective for rearward splash; not durable; tire balance problems	12
Scrubbers, wipers	Brushes remove water from tire tread	Reduces rearward splash	Lack of durability; clogging problems	12
Air compressor and blower flow deflector	Forced air redirects air and water toward center of vehicle	Independent of speed, wind, clogging problems; maximum control of airstream	High initial and operating costs; not adequately developed	12
Vehicle configuration changes	Relocation of fuel tanks, stirrups, other components; lowered body; altered aerodynamics; reduced tire size	May improve splash and spray suppression	May compromise other subsystem performance; cost; size regulations	11, 12

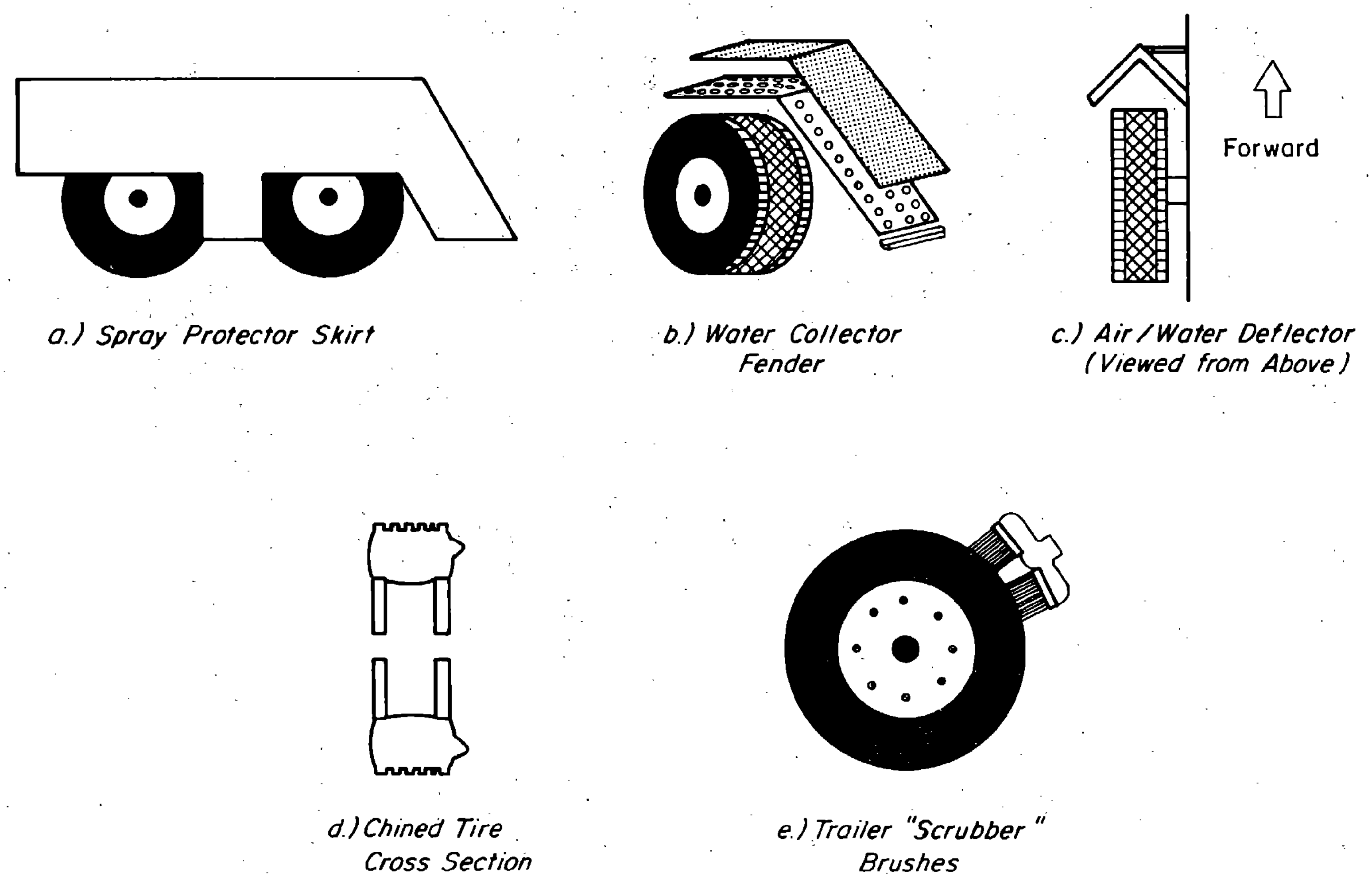

Figure 1. Examples of Splash and Spray Suppression Devices from Past Tests

Conventional fenders and mudflaps, though somewhat effective in reducing low-speed splashing of water, mud, slush, etc., typically "atomize" impinging water droplets at highway speeds, thus leading to and amplifying the formation of spray. They can also generate substantial side spray. In particular, mudguards have been researched by several states and European nations (e.g., Refs. 12 and 25) along lines of "required equipment" legislation and have been found to be of only limited (low-speed) benefit.

More recently, specialized devices designed specifically for splash and spray suppression have undergone comprehensive testing, e.g., Western Highway Institute tests at Portland, Oregon (1971), at Fort Stockton, Texas (1972), and (with SWRI participation) at Madras, Oregon (1974). Results of these tests are reviewed in Refs. 11 and 26, and the sequence is summarized in Table 2. The initial Oregon tests were aimed at evaluating the DOT fender proposed at that time (see Fig. 1a). The Fort Stockton tests in July 1972 considered 11 truck types, but there were problems with the laser transmissometer. These problems were resolved in the Corvallis tests, and the laser methodology was used successfully in the present program (see Section VI). The Hondo tests gave useful data on the effects of load, water depth, and tire wear, allowing variation in these parameters to be de-emphasized in the current study. The Madras tests provide useful comparative information regarding suppression devices, eliminating some from further consideration.

In general, most of the devices tested in the past have shown improved splash and spray suppression to varying degrees, as compared to the base vehicle; none, however, provided the desired overall level of effectiveness. The DOT spray protection skirts, for example (Fig. 1a), achieve maximum spray suppression via envelopment of the rotating wheels, but at the expense of poor brake and tire ventilation. Also, typical of most of the suppression devices, the skirt can reduce sideward spray but in doing so it drops the deflected water back into the wheel path, increasing the intensity of rearward-directed splash. This rearward splash is often directed at rear wheels or other exposed components which regenerate atomized spray.

Water collector fenders (e.g., the PABS in Fig. 1b) alleviate this problem somewhat by allowing the deflected water to pass through a perforated lower fender, whence it is collected and channeled away from the wheel path.

TABLE 2. SUMMARY OF SELECTED PAST TESTS

LOCATION	ORGANI-ZATION	DATE	PURPOSE	MEASURES	REFER-ENCE
Oregon	WHI, et al.	March 1971	Braking, DOT fenders		
Oregon	WHI, et al.	August 1971	Braking, DOT fenders		
Fort Stockton	WHI, et al.	July 1972	Various truck types (11)	Laser transmissometer Observer ratings (1-5) Light intensity meter	11
Hondo	NHTSA, SWRI	Summer 1972	Tires, load, surface, water depth	Photometer	11
Corvallis	WHI, et al.	March 1973	Instrumentation development	Lasers worked Chase cars	
Madras	WHI, SWRI	July 1974	Devices	Lasers Photographic densi-tometer	26

The Roberts fender is similar. This type of device showed relative good performance in prior studies (up to 20 percent reduction in overall splash and spray). The principle involved is sound, i.e., collect the spray and prevent its transport into the airstream or its redeposit in front of following wheels, but inadequate drainage and ice and mud clogging problems limited its immediate applicability. The Madras tests also showed the Reddaway fender to be potentially effective, and this has carried over into this program.

Another device approach uses deflectors to modify the flow of air and water beneath the vehicle (e.g., Fig. 1c). The general objective is to redirect the spray, by means of suction or blowing, toward the center of the vehicle. Though only limited testing has occurred in the past, the results suggest that this type of device holds development potential. Another concept uses an air compressor to induce redirection of water/airstreams, though it is apparent that the practical and cost-benefit aspects of such a device may not be advantageous. Other suppression possibilities include the use of chined tires (Fig. 1d), tire scrubbers/wipers (Fig. 1e), and changes in vehicle configuration (i.e., locations of components, underbody streamlining, lowering of chassis). There is some evidence in the results reported in Ref. 73 that increased bus ground clearance confines roadway dust (and spray, by inference) to below eye level heights, improving visibility. Each of these ideas has a splash and spray reduction potential, but there are other performance and cost-benefit tradeoffs.

c. Implications of the Prior Work

In considering the selection and development of the most advantageous suppression device, past efforts have recognized the need to consider the specific splash and spray patterns and interactions of different tractor and semitrailer combinations (e.g., Ref. 11). In general, vehicle-to-vehicle differences in spray generation, as well as cost-benefit tradeoffs encountered across the range of anti-disturbance and anti-spray devices, must be considered in seeking an overall solution to the problem.

In view of the past results described above, several ideas appeared promising at the outset of this project. These included testing of air deflector devices near the front wheels, use of Astroturf material around and behind wheels (Reddaway fenders), and placement of other devices to direct large scale air currents down and toward the vehicle centerline. Other promising possibilities included:

- Devices which inhibit air flow down the gap behind the tractor
- Larger mudflaps, extending to the ground
- Vertical plate, like a mudflap, between the tandem wheels
- Astroturf or other collector between the wheels
- Wider fenders, allowing more air flow around the tires and brakes
- Movement of the fuel tanks, so that they are not directly behind the front wheels

Approaches which have not been successful prior to now have included wheel skirt devices, but there was not sufficient data to rule them out, completely.

As noted above, drag reducing devices such as tractor mounted shields have demonstrated cost advantages, and their possible influence on splash and spray further suggested that they be considered in our planning.

Regarding instrumentation, the prior work showed that lasers and photometers could be used to quantify spray in a repeatable way. Densitometer measures, from photographs with suitable backgrounds, also have a potential role. Color and black and white photos provide a useful data record and basis for comparison, also. Observer ratings have been extensively used in past tests, and this together with their use as a subjective measure of what the eye perceives, makes them an important part of the splash and spray assessment process.

D. NON-VEHICLE ALLEVIATION TECHNIQUES

As stated, the emphasis in this study has been on alleviating devices fixed to the truck and other truck-centered means. At the same time attention has been paid to non-vehicle issues where convenient. Some initial discussion in this regard was presented in Article C.1.b, above, and further comments are given below, based on material developed by subcontractor AMV.

1. Driver Training

Several levels of educational plans could be appropriate, in order to account for differing types of involvement in vehicle-to-vehicle aerodynamic interactions. In decreasing order of likely effectiveness, the plans might be addressed to driver groups operating the following types of vehicles:

- Line-haul tractor/trailer combinations
- Single unit service vans
- Private automobiles

For the trucks, drivers could be instructed in special operating controls or procedures to ameliorate adverse aerodynamic effects. Also, driving traits which can contribute to unsafe reactions by other drivers would be identified and discouraged. For instance, the passing of slow vehicles by a loaded truck, on a long grade with a very small speed differential, often causes long following queues to form. Under wet pavement conditions, such queues contribute to reduced visibility, result in gap sizes unsafe for emergency stopping, and may encourage hazardous passing maneuvers by drivers of more responsive passenger cars.

While fleet tractor/semitrailer drivers could receive appropriate supplemental training through their employer, many independent truckers could not. Perhaps the union could participate in a safety-oriented educational effort. Whatever the possible training implementation problems, the desired driver knowledge or performance could certainly be tested by expanding current qualifying examinations to give greater emphasis to driving techniques which reduce the adverse effects of concern here.

Many of the smaller van-type trucks are operated in fleets (e.g., telephone and gas companies), and there appears to be a good potential for more rigorous driver training and testing. Such training could cover the operation of this vehicle as a producer of adverse effects (with respect to subcompact automobiles), as well as an impactee in interactions with larger trucks. As a result of their aerodynamic properties and volume-to-weight ratio, two-axle vans can be more susceptible to aerodynamic force effects.

With the assistance of improved driver training and handbooks, following and passing maneuvers could be more fully defined to account for the effects of splash and spray. Applying the findings of past and present research, for example, better wet weather passing behavior might be discussed by addressing such questions as:

- How fast should one travel to pass a large truck which is emitting splash and spray? What is the safety trade-off between minimizing the time during which visibility is obscured by spray and increasing the probability of an accident or violation due to higher speed?

- When should the windshield washer or high-speed wipers be used? If their operation requires one hand to be removed from the steering wheel, is the improvement in visibility worth the increased psychomotor workload at a possibly critical time?

In addition to developing reasonable answers for such questions, the general driver training approach to alleviating the adverse aerodynamic effects of large trucks must overcome at least two other implementation problems. One involves the importance of performance standards in the public driver licensing process. Unfortunately, it would not be practicable to include a wet weather truck-passing situation in very many actual road tests; only a background understanding of the subject could be checked in the licensing examination.

The other training implementation problem involves the general inadequacy of current driver handbooks. In reviewing those of seven geographically scattered states (Florida, Maryland, Massachusetts, Michigan, Texas, Vermont, and Virginia), it was learned that none recognizes splash and spray from trucks as a wet weather driving problem. Wet pavements and adverse visibility conditions are briefly mentioned as potentially hazardous situations, but only because of possible skidding and stopping-distance problems. If some experienced drivers do in fact perceive a splash and spray problem, the value of their experience is certainly not being conveyed to the authors of the handbooks or to the many new drivers whose training courses often revolve around the handbooks.

2. Operational Controls and Regulations

This category of countermeasure includes all traffic control mechanisms, whether implemented through signing or via unposted operational rule. Most of the rather few applications to date have dealt with speed and lane restrictions for large vehicles, were instituted prior to the 55 mph (89 km/h) speed limit, and have not been comprehensively evaluated with regard to traffic flow, safety, or economic effects. Due to the largely untested nature of the various operational controls and regulations which might reduce or ameliorate the adverse aerodynamic effects of large trucks, much of the following discussion is conceptual in nature.

a. Speed Controls

Prior results have shown that splash and spray are substantially reduced by moderate decreases in speed. Controls could be adopted for just large trucks or for all vehicles in the traffic stream, and they could be either continuous or based on weather conditions. Relatively little is known about the degree of enforceability associated with each of these regulatory combinations. One would expect, however, that a system based on conditions and applicable to all vehicles would be most believable and equitable, and hence most enforceable. Under current commercial trucking economics, a continuous regulation applying only to large trucks would probably be least enforceable.

Regardless of specific policy, there would be additional costs for enforcement, the control devices required, and the longer travel times which would accrue. If the policy applied only to one class of vehicle, the increase in traffic stream speed variance could result in higher accident costs as well. At least partially offsetting these cost increases would be potential savings in visibility-related accidents, fuel consumption, and other operating costs. If the speed regulation applied to all vehicles, the severity (if not frequency) of accidents would be less, with a concomitant reduction in accident costs.

b. Lane-Usage Controls

There are at least two conceivable lane-usage controls. The first would require that large trucks on multilane highways be operated in the leeward lane under crosswind conditions. This would allow the drivers of faster vehicles to pass in the windward lane under better visibility conditions. Unfortunately, this concept could be: difficult to implement, hard to enforce, a source of hazardous perturbations in the normal traffic flow, and a disbenefit to oncoming vehicles under some conditions (i.e., where the leeward lane is on the left and there is little or no median strip). Despite these drawbacks, the method has been adopted successfully in Sweden (Ref. 27) and Canada on a limited basis.

Another type of lane-usage regulation could take the form of sign-reinforced driver training which would encourage truck drivers to operate to the right of the lane centerline. As discussed previously, this would tend to reduce both aerodynamic and visibility disturbances. However, structural damage to the pavement edge and shoulder treatment will occur earlier if heavy loads are consistently applied further to the right. A raveled pavement and worn edgeline would seem to detract from safety as much as degraded visibility during the passing maneuver.

c. Warning Signs and Other Traffic Advisories

Where and when unusually heavy rainfall, strong winds, or hazardous combinations of rainfall and wind can be identified on a long-term or short-term basis, it may be desirable to provide special warning signs or traffic advisories. Such special guidance could remind drivers of speed versus hydroplaning relationships, safe following distances, and procedures to follow during the truck passing maneuver to alleviate the adverse aerodynamic effects.

The key implementation difficulty would be in making the messages sufficiently concise and believable. Variable-message signing would be the most effective technique, especially if supplemented by radio advisories. Such signing could be expensive, and general radio advisories might have to be used under more extreme environmental conditions. Despite these drawbacks, signs and other wind indicators have been successfully deployed in parts of Europe.

d. Improved Roadway Delineation

Any operational measure which increases the driver's feeling of security as to his placement and trajectory on the highway should be of value during vehicle-to-vehicle aerodynamic interactions. Stronger roadway delineation enhances this feeling of security. For instance, the use of bold paint striping, raised pavement markers, and shoulder treatments of contrasting texture and/or color would provide additional guidance under adverse conditions. This would be valuable for both day and nighttime driving conditions, and be especially important during those moments when forward visibility may be sharply restricted by splash and spray. Improved "far" delineation, such as retroreflective raised pavement markers and post-mounted delineators, could also be of great assistance to the driver under wet nighttime conditions, when other types of delineation are largely obscured and the adverse visibility effects of truck-produced splash and spray are most critical.

e. Highway Maintenance Procedures

This category of countermeasure includes such items as the frequent cleaning of drainage inlets, the plowing of snow further back on the shoulder to promote drainage, and the extent to which chemicals or sand are applied to slippery pavements (which may increase the opacity of truck spray on the windshield). Certainly improved pavement draining would be beneficial to operational efficiency and safety in general; however, the question of skid resistance versus spray opacity probably favors the former. One other factor, the amount of pruning done to roadside vegetation, should be mentioned for completeness, although it is unlikely to have any significant effect on crosswind characteristics under most conditions.

3. Highway Design Changes

This last major category of non-vehicle countermeasures ranges in scale from pavement surface modifications to basic questions of route location and orientation. The various candidate design changes are discussed below in probable order of increasing impact upon the highway planning and design process.

a. Improved Roadway Drainage System

One of the most popular techniques for improving roadway drainage, to reduce hydroplaning and skidding accidents, is pavement grooving. A little acknowledged byproduct is the likely decrease in the supply of water available for splash and spray generation (assuming that water accumulation in the grooves is not pulled out by passing tires). While seemingly a rather effective wet-weather safety measure, pavement grooving is not without its disadvantages. Perhaps most significant is the high cost of installation. Also, grooving may result in steering disturbances and passenger discomfort for certain combinations of vehicle suspension system and tire design.

Another important method of improving pavement drainage is to construct pavements having steeper cross slopes. Design standards in the last fifteen years have called for flatter pavement. However, several factors now suggest that they may need to be re-examined, for example:

- The contribution of pavement surface water to hydroplaning and vehicle splash and spray is being viewed with increasing concern.
- Several successful steps taken to improve longitudinal skid resistance should also offset the sideslipping potential attributed to higher crown. These steps include better tire design, grooved pavement, fast-draining paved shoulders, and chemical de-icing.
- The combination in newer designs of straighter horizontal alignments, greater sight distances, generous lane widths, and stronger roadside delineation should lessen the probability of shoulder encroachment under any pavement surface conditions.

Other drainage improvements might include the use of open graded asphalt friction courses, smoother and more steeply sloped shoulders, higher capacity gutters, and larger and more frequently spaced curbside drainage inlets. A basic objective throughout a highway design review should be to minimize both the source of splash and spray and the potential for introducing new hazards in the reconfigured roadway environment.

b. Introduction of Wind Barriers

The berms, walls, and fences installed with increasing frequency as traffic noise attenuators also serve to some degree in blocking crosswinds which accentuate the adverse aerodynamic effects of large trucks. Just how effective these barriers are in fulfilling this secondary function remains to be determined. Height limitations based on aesthetic considerations comprise the primary technical constraint, while some care must be taken not to end the barriers suddenly and causing a sharp wind gradient. The construction and maintenance costs for continuous barriers probably would be difficult to justify if noise were not also considered a substantial impact which had to be alleviated. An alternative to artificial construction is to use trees and other planting along the roadside.

A more limited use of barriers would be at open locations where crosswinds are especially severe or unexpected. A high fill section following a deep cut section is a possible example. Drivers in such terrain may already have their workload increased by grade climbing, visibility, or passing problems. If a motorist enters the fill section in the shadow of a large truck and is exposed to a sudden onset of crosswinds upon completing his pass, a hazardous situation could result. The presence of the shoulder or the upslope of the fill may provide an opportunity for mounting and protecting some sort of windbreak.

A third application of wind barriers would be on bridges. Either the bridge rail could be heightened and solidified or fencing could be installed on the outer side of the vehicle or pedestrian barrier. In some cases, cyclone fencing already exists and need only be equipped with some sort of lightweight sheeting or slats. The primary disadvantage would again be the likelihood of poor aesthetics. If the bridge were unusually narrow, high opaque sides could also constrict traffic flow, due in part to perceptual narrowing.

Finally, a fourth possible location for wind barrier installation would be on tunnel approaches. Here the focus would be on providing a transition from a completely controlled state (insofar as natural winds are concerned) to an uncontrolled state. This transition problem is somewhat similar to that of acclimating a driver to the change in light level experienced in entering and departing a tunnel. Not only should the prospective barrier vary gradually in its porosity to crosswinds, but the full pavement wetness should probably be reintroduced prior to the driver reaching the point where he is completely unshielded from crosswinds.

c. Use of Wider Lanes

As previously indicated, wider lanes would allow greater lateral separation between passing vehicles, the same type of benefit sought with the suggestion that truck drivers operate to the right of centerline. With 13 or 14 foot (4.0 or 4.3 m) lanes, however, greater separation could be obtained without necessarily disturbing the centrality of lateral placement. Studies have shown that increasing lane widths beyond 11 ft (3.4 m) can result in an increase in accident rates. Another disadvantage of increased lane width would be the construction cost increase associated with the use of wider pavements.

d. Route Location and Orientation

Although many other more important issues of highway economics, access, and aesthetics may be decisive, prevailing winds might also be considered in selecting the route for a new highway. That route alternative minimizing the time during which drivers must travel with significant crosswinds would be preferred if all other factors were equal. However, it is unlikely that they ever will be.

E. SELECTION OF EXAMPLE TEST VEHICLES

To carry out the experiments and analyses of the research, it was necessary to select example vehicles to represent the disturbing truck and the disturbed adjacent car. The considerations involved in this selection process, and the results, are described in this article.

The main factors in vehicle selection, especially with regard to the trucks, included a desire that they include examples which were:

- Representative of over the road commercial vehicles
- Typical, in the sense of their disturbance generation and interaction with the adjacent car
- Critical, in the same sense
- Relatable to past applied research studies
- Pertinent to possible future trends in truck configurations

For tying in with prior studies, it was useful to use a truck example for which wind tunnel and full scale data and analyses existed, and for which a suitable wind tunnel model was available. That was feasible and selection of suitable examples presented no difficulties. For each vehicle, truck and adjacent car, we consider a "basic case" plus variations thereto. The vehicles are described in more specific detail (dimensions, etc.) in Sections V and VI. Metric equivalents are shown there, also.

1. Example Trucks

A variety of example trucks was included in the wind tunnel and full scale tests. This included a 3 axle COE tractor plus 40 ft (12.2 m) van semitrailer as the basic case, plus variations in both the tractor and semitrailer configuration — as discussed below.

a. Basic Truck, COE Plus 40 ft Van

The reference or basic truck used was a 3 axle cab over engine (COE) tractor plus a 40 ft (12.2 m) tandem axle dry cargo van. Western Highway

Institute data indicate that it is representative of about 80 percent of the rigs* in over the road operations. Past results taken together suggest that it is among the worst configurations for splash and spray generation, and it can also cause strong aerodynamic disturbances because of its size. It is one of the more difficult rigs upon which to mount fenders, because of the limited clearance around the tractor duals and the fact that the van dimensions extend to the legal limit, in general.

From a research standpoint, past disturbance data and results are most extensive for this configuration (e.g., Refs. 2, 6, 29-31). In addition, a suitable high quality variable configuration wind tunnel model was available from past STI/FHWA studies (Refs. 2 and 29).

b. Variations on the Semitrailer

Three additional semitrailer configurations were selected as variations on the basic truck for analytical and experimental study. They are:

- Liquid cargo tanker; elliptical cross section, 9200 gal (34,800 litre) capacity, tandem axle
- Dry cargo tanker, "Feedliner," tandem axle
- Flatbed, tandem axle

The liquid cargo tanker provides a significant variation in truck shape, particularly on the underside and around the wheels. It has a different potential for mounting fenders and deflectors than does the 40 ft van, and current design practice bears this out.

The dry cargo tanker is a type commonly used to haul livestock food in rural regions. As the figure in Section V shows, it has high sides sloping inward around the bottom, and it represents one potentially critical case in terms of shape and wheel exposure.

The flatbed represents an aerodynamic variation, also. The underbody is similar to the 40 ft van, while the upper shape is different.

*This includes the recent trend towards 45 ft (13.7 m) vans, which represent a very minor variation on the basic truck for purposes of this study.

c. Variations on the Tractor

The two tractor versions used were the COE of the basic truck and the cab behind engine (CBE) or "conventional" configuration. In the models and full scale examples, the 3 axle COEs and CBEs had the same chassis with different cabs.

The resulting change in shape was expected to affect the drag, and the change in the air flow could influence the formation and propagation of splash and spray. Compared to the COE, the CBE also has a shorter gap between the tractor and semitrailer face, for a given chassis wheelbase.

d. Other Truck Variations

Another truck version selected for model and full scale study was a 2 axle COE tractor plus a 27 ft (8.2 m) van (single axle). Such COEs generally have a short cab dimension. That coupled with a typically small gap leads to a potentially important shape change relative to the basic truck. Hence, the reduced number of axles and the shorter gap were both expected to affect the splash and spray characteristics.

Further variations on this theme included:

- 2 axle COE + double 27 ft vans
- 2 axle COE + triple 27 ft vans

These provide a length variation of some interest. The "doubles" rigs are fairly common, while triples have been proposed as a future trend, and are in operation in some of the Rocky Mountain states.

2. Adjacent Car

The example adjacent car selected was a full size Chevrolet station wagon, vintage 1973. This car was representative of U.S. practice at the time the project was started. Aerodynamically, it is relatively insensitive to crosswinds and other disturbances (based on work in Refs. 2, 3, and 29). Its handling properties are about average. The car was available for full scale tests and it could be instrumented fairly readily.

As the example adjacent car, the Chevrolet station wagon ties in well with prior work. It has been used in past disturbance studies (Refs. 2, 3, and 6), and results and data quantifying its aerodynamics, handling dynamics, and disturbance properties are available as a consequence. This provided a useful input to the analyses and simulation of this program, saving time and cost. A wind tunnel model was also available from the prior STI/FHWA work.

Despite the selection of one adjacent car example, we have a good understanding of the effects of varying adjacent car properties. For instance, in past FHWA-funded aerodynamic studies (Refs. 3 and 29) we have considered the truck/bus-car disturbance properties of

- Station wagon plus trailer
- Chevrolet sedan
- Datsun 510 subcompact
- VW station wagon (microbus)
- Pickup truck plus camper

In each case, the aerodynamic and handling properties have been quantified analytically and experimentally. In addition, current NHTSA-funded work at STI (Ref. 32) is extending our knowledge of the aerodynamics and response properties of passenger vehicles. As a result, we can draw conclusions about the effects of varying adjacent car properties, as a function of the truck and situational characteristics, without necessarily using a range of cars in an additional test program.

SECTION III

PRELIMINARY ANALYSES AND EXPERIMENTS

Several analytical and experimental activities were undertaken during the early stages of the program in order to

- Better define the nature of the aerodynamic and splash and spray effects of trucks and their relation to the behavior of the adjacent motorist
- Help identify potential methods and devices for alleviating said adverse effects
- Guide planning for the more elaborate wind tunnel and full scale tests.

These analytical and experimental activities and their results are summarized in this section.

Described first are the generation and dispersion of splash and spray, in Articles A and B, respectively. This work is condensed directly from the AeroVironment report, Ref. 4. As discussed in Article A, and Section II, above, the mechanism by which water droplet clouds are formed in the vicinity of a vehicle traveling along a wet road involves a complicated interaction of aero-hydrodynamics. The primary mechanism of the process is that in which the wheel and tire pick up water from the road surface film, or displace it in the form of side and forward splashes. This water contains both large and small droplets which may be broken into smaller droplets by impaction with solid surfaces or by its velocity induced interaction with the air flow. This process of formation of fine droplet mists is called spray generation.

This spray, which is concentrated near the wheels and fenders, is then convected by the local air flow and dispersed by the turbulence in the air flow to form the spray clouds which move with the vehicle. As described in Article B, this is called the dispersion process. It is obvious that this dispersion cannot be predicted unless the details of the air flow in the vicinity of the spray generation centers are known. Thus, an additional important link in understanding these mechanisms involves estimating the aerodynamic flow field, and additional material related to the air flow around the trucks is given in Section V. Knowing the air flow and associated turbulence, then the dispersion along any stream tube may be determined using techniques which have been developed in air quality and plume modeling. The basic idea of this procedure is to consider the history of a puff or cloudlet of drops following a stream tube. It is convected at the speed of the mean flow, while the stream tube's scale, or radius, increases as a function of the local turbulence. Additional factors such as the influence of the ground plane and the truck side, as well as the fallout under gravity, can be taken into account. Then a computer program can be developed to calculate droplet concentrations for any position in the field.

Analytical methods have been used at STI to quantify and interpret the response and performance of the driver/vehicle system in the vicinity of the truck, and the basis for this work is discussed in Article C. Preliminary studies of driver behavior in truck splash and spray encounters were accomplished in the STI Driving Simulator, and these are described in Article D.

A. GENERATION OF SPLASH AND SPRAY

The droplet clouds which cause splash and spray visibility effects are created largely by the ejection of road surface water into the air by the vehicle tires, and by the subsequent breakup of a portion of the drops due to impaction on nearby tires and parts of the vehicle body. Summarizing the AeroVironment work, Ref. 4, this article discusses the mechanisms of splash and spray generation operative for a single wheel and then discusses the more complicated mechanisms at work for multiple wheel sets and for wheels ejecting droplet streams onto impaction surfaces. The basic results of previous work are first discussed and then some simple models developed by AeroVironment are described. The analytical model is then compared with the spray data obtained from the single wheel tests and the full scale track tests.

1. Overview of Splash and Spray Mechanisms

The four primary mechanisms for water ejection by a tire are bow and side splash waves, tread pickup, and capillary adhesion. These mechanisms are illustrated in Fig. 2. All four are functions of tire speed, road water depth, and tire design. Of the total water film in the tire path, part is passed through the tread grooves and the remainder is displaced ahead of the tire in a bow wave and to either side of the tire in side waves. The droplets in the bow and side waves are relatively large in size and these droplet streams are usually categorized as splash. The side waves are created by displacement of the road water toward the sides of the tire. Although the volume of water thrown can be large, side waves do not usually constitute a severe problem, because the splash travels in relatively low trajectories outboard from the truck or impacts on the truck underframe and is returned to the road.

The water that is passed through the tread grooves is ejected into the air immediately as tread pickup or is retained on the tire as a thin film in capillary adhesion. The capillary film is stripped from the tire by the incoming airstream. This phenomenon is quite variable and depends on the wind speed and how well the tire is shielded from the wind. The droplets in the tread pickup stream are distributed in size from small (less than 1 mm) to reasonably large (3 to 5 mm), but the stream is not characterized by large droplets as are the bow and side wave streams. Most of the drops thrown by the treads travel in low trajectories, but some are ejected high enough to degrade visibility. A greater contribution is created by the impaction of tread-thrown droplets on following tires, or on parts of the truck body such as the gas tanks, fender wells, mud flaps, or frames. These impacting droplets break up into clouds of fine droplets (much less than 1 mm) which are carried away from the truck at sufficient height and in sufficient concentrations to cause a considerable reduction in visibility.

Water held in the thin capillary adhesion film is stripped off near the top of the tire by the incoming airstream and forms a cloud of fine droplets. This spray cloud can have a major effect on visibility, because it forms in the wheel wells or in the space between the tire and the

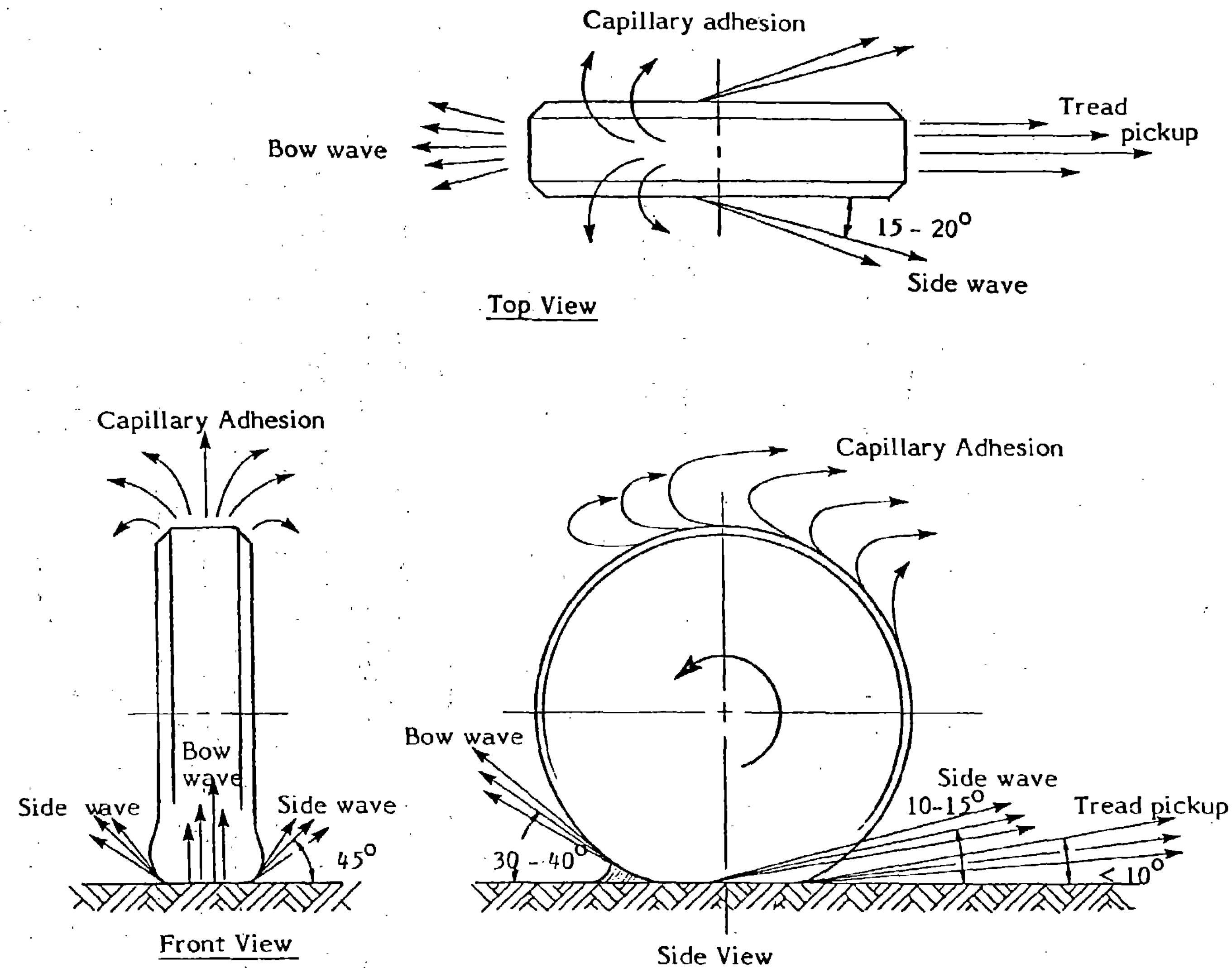

Figure 2. Primary Splash and Spray Generation Mechanisms for a Single Wheel

underbody of the trailer and is ejected outboard from these regions to nearby low pressure regions in the flow field, at approximately the windshield height of a passing car. The capillary adhesion spray and the tread-throw impaction spray constitute the major components.

2. Effect of Operational and Tire Factors

For water depths greater than about 3 mm the tread grooves are filled, and excess water in the tire path is displaced into the bow and side waves. This phenomenon is readily observed when a tire passes through a puddle, sending up a large splash. Under conditions of deep water and high speed, severe bow and side wave splash streams can result. It has been noted that at a given speed the size of the droplets ejected by a tire increases as the water depth increases (Ref. 25). Further discussion of the effect of operational and tire factors on droplet size is given in Ref. 4.

Speed of the tire through the water is a major factor in splash and spray generation. Maycock (Ref. 25) showed that the overall spray water density measured 30 ft (9.2 m) behind a test truck increased in proportion to the 2.8 power of the vehicle speed, with the best fit for speeds between 45 mph (20 m/s) and 75 mph (33 m/s). Very little spray was measured at speeds below 30 mph (13 m/s). Since the amount of water encountered by the adjacent vehicle is equal to the spray density times the vehicle velocity, the visibility effect could increase in proportion to as much as the 3.8 power of the velocity. Maycock also noted that the length of the spray cloud trailing the vehicle was proportional to the velocity squared. It has been observed that wave splash is thrown farther laterally and vertically as vehicle speed increases and that droplet size is strongly affected by increasing speed. Maycock indicated that below 13 m/s water is ejected principally in tread throw and waves as large droplets which do not break up into spray and fall back to the ground, where they are extinguished (no rebound). However, as speed increases, more water is ejected as fine spray, until at speed of 33 m/s most of the water thrown is in a fine spray and very little falls to the ground as large drops. These results are configuration dependent and cannot be readily generalized, but they do lead to the overwhelming conclusion that increasing speed increases every aspect of splash and spray. The effect of truck speed on spray-related visibility is further detailed in Section VI, based on the data obtained in this program.

For water depths less than about 3 mm tread design affects the amount of water picked up by the grooves rather than displaced in splash waves. As the groove volume increases, more water passes through the grooves and less is displaced in splash. For water depths greater than about 3 mm, even in well profiled tires, all the drainage grooves are filled and all the excess water in the path of the tire must be displaced in waves. If the tire is smooth (zero tread groove volume), water is still thrown like tread pickup, but it is thrown off the tire much nearer the sidewalls than the center of the tire face. The droplets thrown by smooth or worn tires in general appear to be smaller than those thrown by treaded tires, but this is not substantiated by direct measurements reported in the literature. Kamm and Wray (Ref. 9) reported in a series of tests on tires with different tread designs that the actual tread design has no marked effect on spray. This tends to support the idea that tread groove volume is the important parameter.

Since the volume of water ejected into the air is directly related to the width of the tire, this aspect of tire design greatly affects the splash and spray generated. The shape of the tire footprint and the details of the shape at the tread face and sidewall juncture can influence the angles at which splash waves leave the tire, although there is insufficient research available to determine this effect quantitatively. An extreme example is the addition of chines to suppress side wave splash on aircraft tires.

3. Spray Generation by Tread Pickup and Capillary Adhesion

The mechanisms of spray generation by tread pickup and capillary adhesion are considered together, because they are closely related phenomena. Braun (Ref. 33) indicates that at low speeds a tire forms a circulating water ring in which water is carried in a film adhering to the groove surfaces or tire face over the top of the tire and back to the roadway. As the wheel speed increases, the centrifugal forces overcome the adhesion forces and tangential sprays result, forming the tread pickup spray.

Because of the high accelerations experienced as the individual tread lugs and groove elements move away from the contact surface in a progressing cycloid, most of the water will be discharged from the tire almost immediately. Consequently, an observer moving with the tire sees a spray with the greatest concentrations near the ground, leaving the tire below 10 deg of arc, as shown in Fig. 2. The thin film remaining on the tire continues to be shed in decreasing amounts, possibly due to increasing resistance forces along the groove faces as the film thins. Finally, near the top of the tire the incoming air stream creates a surface shear strong enough to strip the capillary film in a spray of very fine droplets.

A theoretical treatment of the tread pickup phenomena including the consideration of a number of possible mechanisms has been made in Ref. 4. Some interesting results have been obtained which contain the correct physical character of the observed phenomena using ordinary continuum, fluid mechanics concepts and some simplifying assumptions.

a. Tread Pickup Models

Each of the various tread throw models tried started with a different set of assumptions for the throw mechanism. Each assumed that the tire tread starts flat on the ground with zero velocity. A tread point starts accelerating upward at a uniform rate, and the water in the tread grooves is assumed to start at rest. Details of these modeling approaches are given in Ref. 4. The gist of one of them is summarized as follows. It assumes that the water starts as a thin film on the sides of the tire groove. As the tread and groove accelerate upwards, the water film is assumed to take on a parabolic velocity distribution similar to that of flow in a narrow channel. Droplets are assumed to be produced when the water leaves the groove, and their velocity is assumed to be equal to the average exit velocity of the water. The principles of this model are shown in Fig. 3. It should be noted that the outermost layer of the thin film on the groove face does not accelerate with respect to the road. Figure 3 shows the spray distribution as a function of angle. The numbers in the Fig. 3 example show how the mass of water carried in a film 1 mm thick, on a unit of groove face 10 mm wide and of specified depth, is thrown per degree

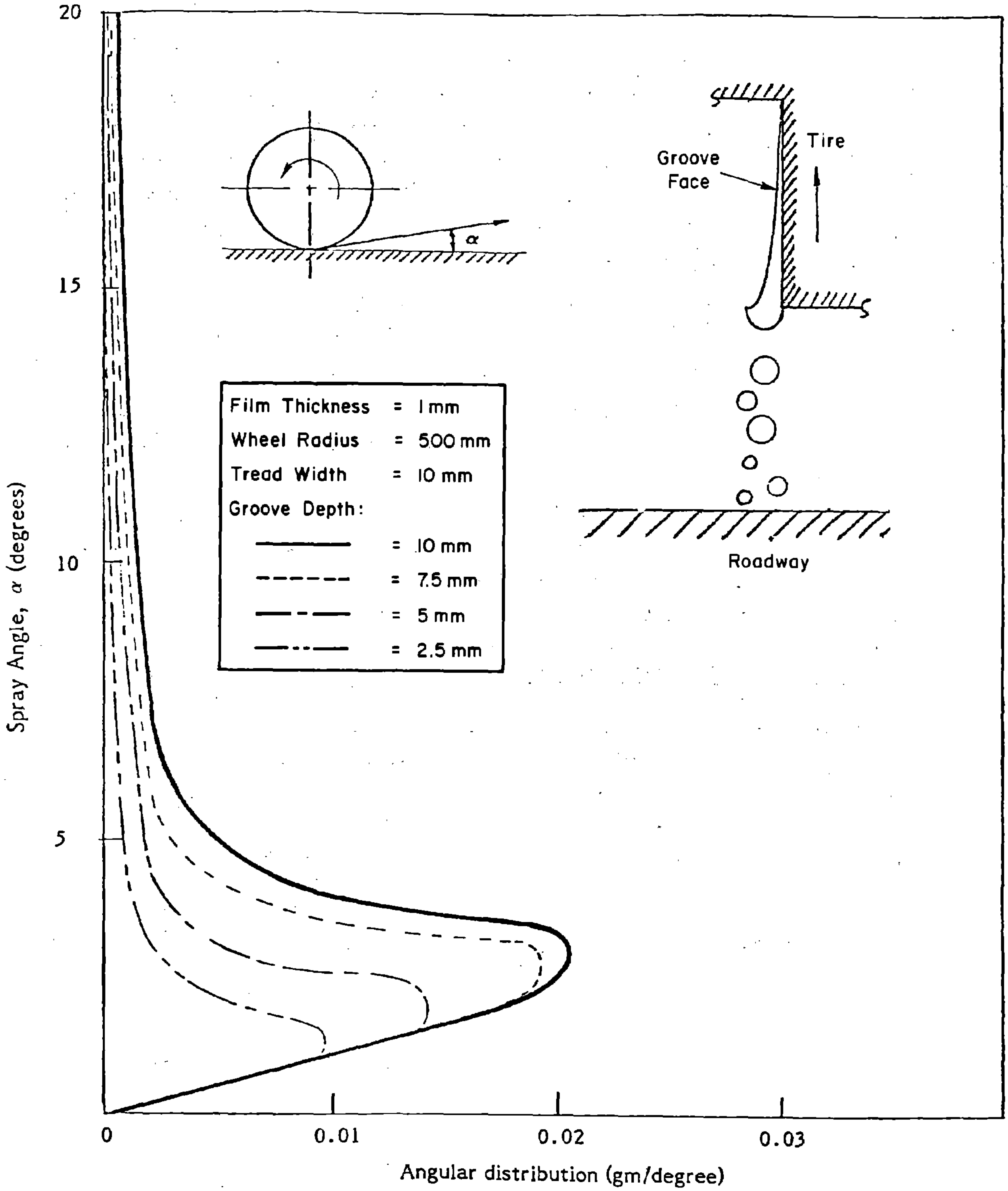

Figure 3. Averaged Spray Distributions for Theoretical Tread Throw

of angle measured from the tire contact point. Figure 3 shows the spray distribution after the curve has been averaged to estimate the true spray pattern in the real world. Variations in groove depth and film thickness tend to distribute the thrown water through a set of angles which can be averaged to give a smooth and more realistic distribution. In this process, the peak of the distribution was arbitrarily reduced to 60 percent of the theoretical value and the total concentration was conserved (area under the curve was held constant). These curves give the spray distribution created by the single groove face 10 mm deep and 10 mm wide.

As the film gets thicker, the amount of water thrown at any one angle increases proportionally but the shape of the curve does not change. Increasing depth of the groove will cause the curve to be stretched upward to higher angles, and the total amount of water thrown by the tread element will increase. Changing the speed of the tire will not change the curve for a single element. Increasing the wheel diameter stretches the curve to greater angles. More detail on behavior of the model and the complete analytical development of the model are contained in Ref. 4.

b. Capillary Adhesion Film Estimates

Three separate estimates have been made of the thickness of the capillary adhesion film. As detailed in Ref. 4, these have considered: 1) only surface tension and tire curvature; 2) the remaining depth of the water layer thrown from the treads; and 3) the size of individual surface adhering drops which, if closely packed, could be considered a surface film.

Considering only surface tension and tire curvature, the film depth, δ, can be expressed as

$$\delta = \frac{S}{\rho} \frac{1}{(\Omega R_t)^2}$$

where, in cgs units,

S = Surface tension of water, 70 dynes/cm

ρ = Density of water, 1 gm/cm^3

Ω = Angular velocity of tire, rad/sec

R_t = Radius of tire, cm

Using an estimate of 2500 cm/sec for ΩR_t, a film depth of 1.1×10^{-5} cm is calculated, which appears quite small in comparison to the amount of water initially retained in the tread groove, which is on the order of 10 mm.

Using the tread throw model described in Item a, above, and recognizing the inaccuracy of the model at high angles of throw, a film depth was calculated which corresponds to the position at the top of the tire. The film depth was taken to be the remaining depth of the water initially picked up by the tread groove surfaces after enough time has elapsed for one-half revolution of the tire. The estimated depth based on a 1 mm film adhering to a 10 mm deep tread groove, 6 mm wide, is 5 μm, which is considerably larger than the estimate in the previous paragraph.

The third estimate was made based on the volume of water contained in a film composed of closely packed individual droplets adhering to the tire face. For hexagonal packing, which represents an upper limit to this physical situation, a film depth of 0.2 mm was calculated.

These estimates are widely divergent, but they do suggest upper and lower bounds on the amount of water retained in the capillary adhesion film near the top of the tire. If a median order of magnitude is assumed, the film thickness could be on the order of 0.1 mm. Assuming that the entire volume of the capillary adhesion film is stripped by the air stream, Ref. 4 shows that roughly one percent of the water picked up by the treads is put into the air as capillary adhesion spray.

4. Splash Generation by Displacement Waves

Consideration of the displacement waves originating from a rolling tire indicates that only a very detailed analysis of water jet interaction, complete with tire geometry details, would be adequate to derive useful predictive results concerning this phenomenon. Trott (Ref. 34) gives a good qualitative description of the bow and side wave mechanisms; and other authors, notably Braun (Ref. 33), Maycock (Ref. 25), and Kamm (Ref. 9), describe the effect of road water depth, tire speed, tire inflation pressure, and tire design on displacement waves.

The basic wave geometry is shown in Fig. 2. As noted earlier, when the road water depth is less than 3 mm, some of the water in the path of the tire is picked up in the tread grooves and the remainder is displaced to the sides and ahead of the tire in the side and bow waves. When the water depth is greater than 3 mm the tread grooves are filled and all the remaining water is displaced in waves. Little is known about how the water is distributed between the bow and side waves, but qualitative observations suggest that for well-treaded tires operating in less than 3 mm of water, most of the splash is thrown in the side waves.

The effect of speed on splash waves is also not well understood. While the general spray volume increases proportional to speed to the 2.8 power, the contribution of the side and bow waves to the spray volume may be quite low because the side waves lie along low trajectories. In the lower limit, the increase in wave splash volume must at least be proportional to the vehicle speed because more pavement will be swept per unit time as the speed increases. Observations also suggest that droplet size from the splash waves decreases as velocity increases. There is, however, no cohesive theory to explain this phenomenon quantitatively.

5. Simple Single Wheel Model

Based primarily on these qualitative results, a simple model has been constructed to describe splash and spray generation by a single wheel. The model maintains the continuity of mass in that all water in the path of the tire is accounted for in the splash and spray streams. Where possible, the results of more sophisticated models have been incorporated in this model.

The underlying assumption of the model is that the tire grooves are filled when the water depth on the road reaches 3 mm. The total water in the path of the tire per second, $\dot{w}_{total}$, is divided into the water per second displaced in waves, $\dot{w}_{wave}$, and the water per second picked up in the tread grooves, $\dot{w}_{tread}$. The distribution of $\dot{w}_{wave}$ between the bow and side waves is an estimate based on observations of truck tires operating at 25 m/s. The distribution of $\dot{w}_{tread}$ between the tread throw spray and the capillary adhesion spray is an estimate based on calculations of the depth of the capillary adhesion film. Tire tread pattern details are easily included because the volume of the grooves appears to be the most important parameter.

Based on the detail in Ref. 4, these simple model components are given by:

Total volume of water in path of tire per second:	$\dot{w}_{total} = UhW$
Volume of water picked up in treads per second assuming the treads are full when h = 3 mm and h ≤ 3 mm:	$\dot{w}_{tread} = \frac{h}{3} Un_t ab$
Volume of water picked up in treads per second when h ≥ 3 mm:	$\dot{w}_{tread} = Un_t ab$
Volume of water displaced by bow and side waves:	$\dot{w}_{wave} = \dot{w}_{total} - \dot{w}_{tread}$

The terms and dimensions are defined in Fig. 4. Because no accurate theory or data exist on the distribution of water between the tread pickup, bow wave and side waves, it has been arbitrarily assumed that the bow wave is 10 percent of the wave displacement, while each side accounts for 45 percent. In addition, the capillary adhesion has been assumed to be about 1 percent of the tread pickup, based on the previously described models. The resulting allocation is depicted in Fig. 5.

Estimated droplet size distributions are shown in Fig. 6. These are estimates but contain the essential character of the various droplet streams and are supported by data taken in the single wheel experiments and full scale experiments conducted as a part of this program.

a = tread groove width
b = tread groove depth
n_t = number of grooves
U = tire velocity
h = road water depth
W = tire width at road contact

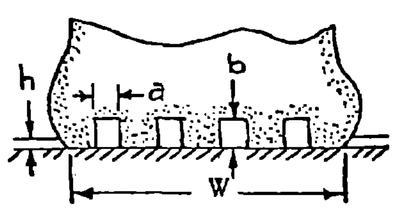

Figure 4. Tread Nomenclature for Single Wheel Model

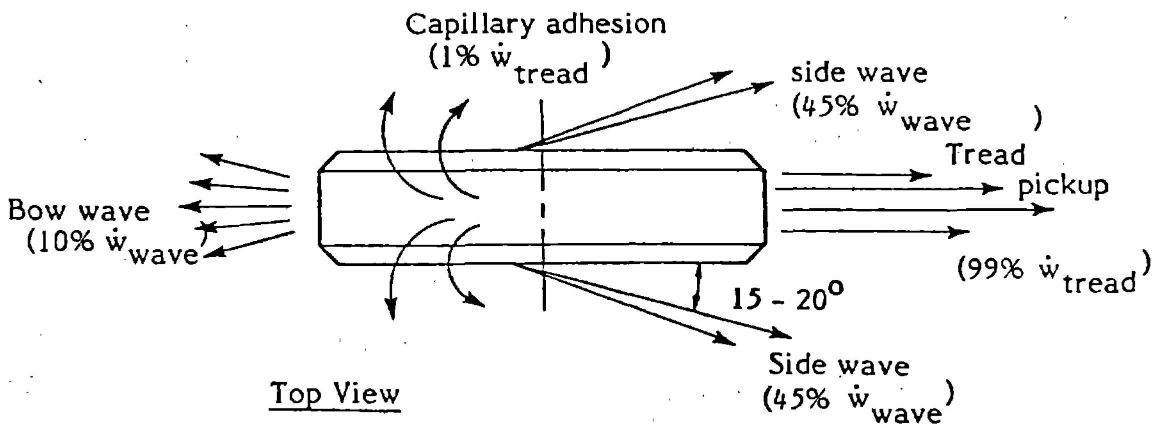

Figure 5: Simple Single Wheel Model Distribution of Water Mass Flow

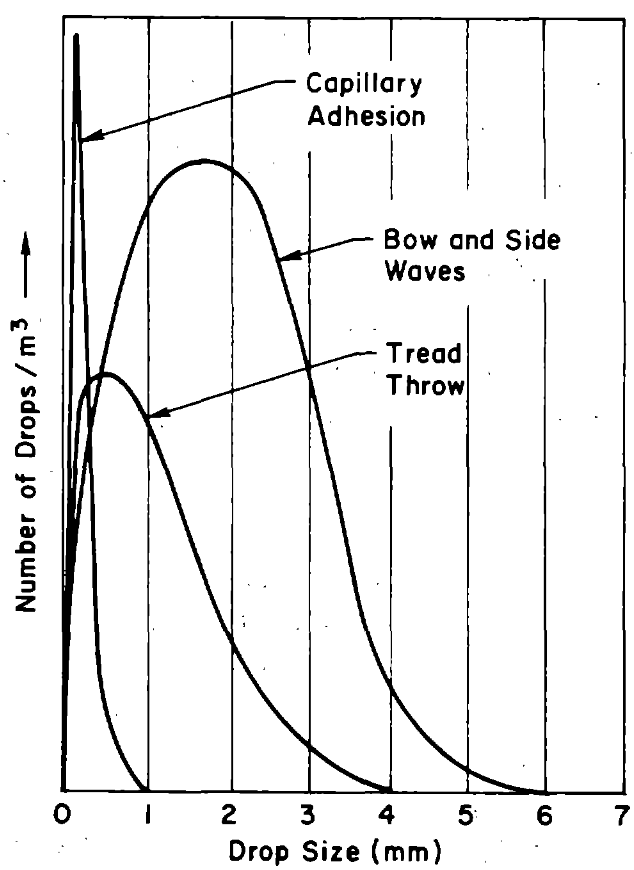

Figure 6. Comparison of Droplet Size Distributions for Single Wheel Sprays

6. Analysis of Single Wheel Tests

Tests were run by AeroVironment, Inc., at Camarillo County Airport near Oxnard, California, to provide data on the mechanisms of splash and spray generation by single wheel and dual adjacent wheel configurations. Test runs were made with light and heavy loads, normal and smooth (taped) treads, varying speeds, and numerous auxiliary devices such as aft-mounted plain and astroturf-covered flaps. The test setup, data, and results are presented in more detail in Ref. 4. This section summarizes the more pertinent results.

For these tests, quantitative measures of both spray density and droplet size were taken for a number of configurations. Spray density was measured by an array of water collector tubes positioned about 110 cm behind the wheel center, and droplet sizes were measured using a droplet sizer developed by AVI for these tests. The droplet sizer passes a porous screen coated with powdered sugar past an orifice through which droplets are flowing. The droplets leave distinct patterns in the sugar, and the pattern images are correlated to actual droplet size by a calibration curve. Average spray density can also be deduced from the droplet screens.

a. Single Wheel Collector Results

Results in Ref. 4 from the collector measures show approximately Gaussian spray density distributions across the tire face, and intensity increasing considerably toward the ground. The heavy tire produced considerably more spray than the light tires, except at the high throw angles where the smooth tire produced more spray than the normally treaded tires.

The reason why the heavily loaded tire produced much more spray cannot be fully explained by the simple single wheel theory since the tread volume was not appreciably increased. It is more likely that the lightly loaded tires were partially hydroplaning, because a low inflation pressure was used to maintain a tire shape closer to that of the loaded cross section.

The collector data were used to estimate the total mass of water thrown by the treads per second. Because the bottom collectors were positioned at a throw angle of approximately 13 deg, they missed the major portion of the tread throw stream which was later shown to lie below 10 deg. Consequently, the collector data were extrapolated to the lower angles. In the throw angle region where data were obtained, the results are in reasonable agreement with the corresponding (for tread depth) analytical values in Fig. 3.

The single wheel test results indicate several things. First, the simple model is reasonably accurate in accounting for the tread throw volume for well defined cases where the tire footprint is in uniform contact with the ground. For heavily loaded or nearly smooth tires, the simple model does not account for observed results. In the case of the heavy tire, this may be due to deformations at the tire face which increase the effective tread volume. Second, the tread throw model summarized in Article 3, above, appears to overpredict the low angle spray density, at least as applied to the extrapolation of the collector data.

b. Single Wheel Droplet Sizer Results

Data were obtained for specimen droplet sizer screens mounted at various locations behind the wheel. Of particular interest are Runs 2, 5, 33, and 34. For Runs 2 and 33, the sizer was positioned nearly on the tire centerline 50 in. (1.27 m) aft of the tire center and 31 in. (0.79 m) above the ground. For Runs 5 and 34, the sizer was similarly positioned only 10.5 in. (0.27 m) farther outboard. The run numbers are those of Ref. 4.

An analysis of these screens is shown in Fig. 7. Droplets were counted and categorized according to size using a calibration curve to determine the actual size from the image size. The distributions shown in Fig. 7 give a good picture of the droplets in the tread throw stream from the lightly loaded and heavily loaded tires. They also show that very little spray exists away from the main tread throw stream. It is particularly interesting to note the shift in the centerline distributions towards larger droplets for the heavily loaded tire. Overall, the heavily loaded single and dual adjacent tires produced much more spray than the other configurations. Most of the screens located outside of the main droplet streams showed very low concentrations. The astroturf-covered aft flap resulted in a considerable reduction in spray concentration further aft.

In order to quantify these results and relate them to the collector data, spray concentrations were determined assuming the passage of spray

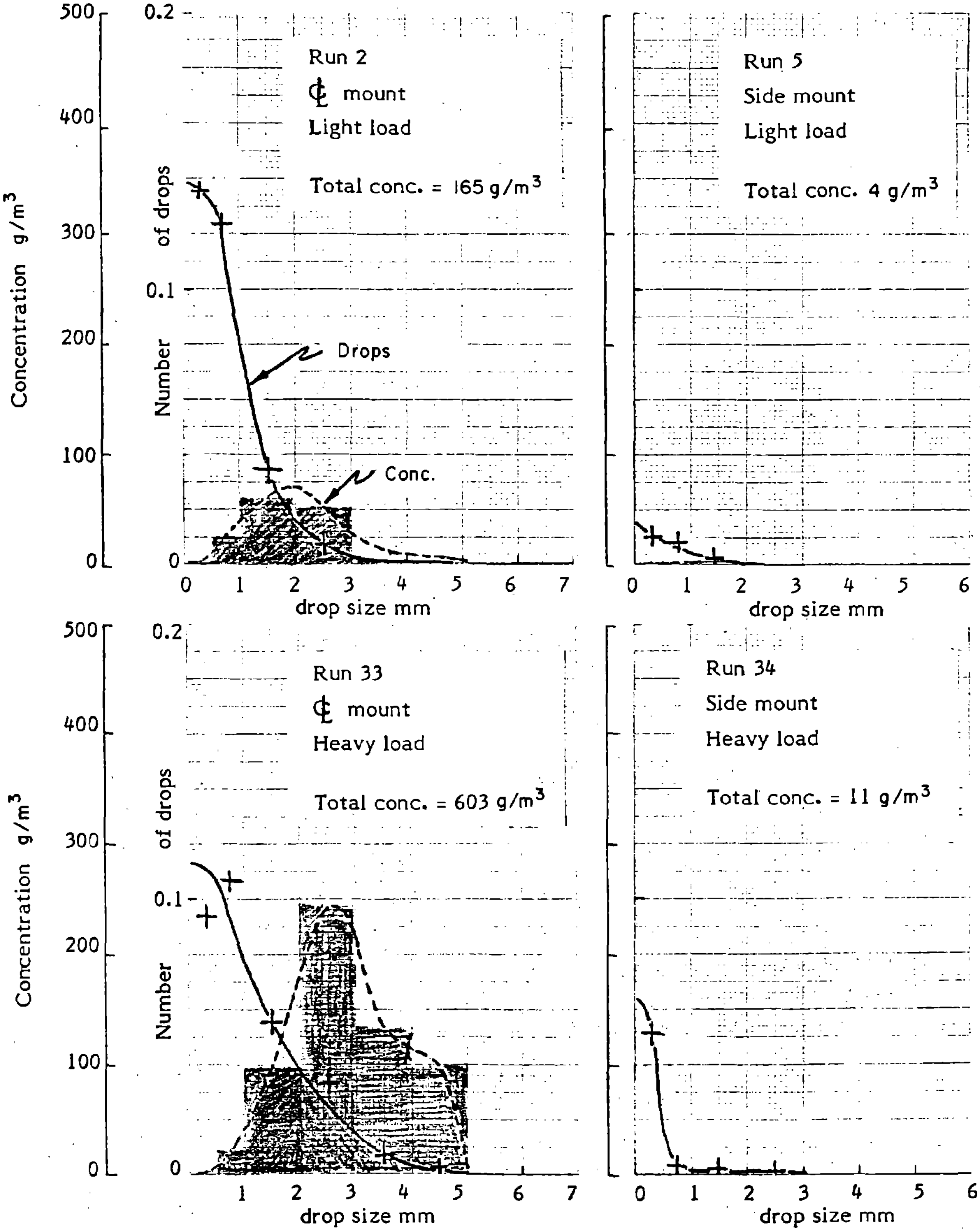

Figure 7. Single Wheel Droplet Size Distributions, Mass Distributions, and Calculated Concentrations (Ref. 4)

through the sizer orifice at freestream velocity, as detailed in Ref. 4. The calculated spray concentrations from the screens, shown in Fig. 7, were found to be greater than those calculated from the droplet collector measurements. The collector concentrations are considered to be more representative of average spray proportions than the screen concentrations for several reasons. The collectors are essentially integrating devices that collect water over a reasonably large time interval and thus provide a good average of the spray. The droplet screens are virtually instantaneous samplers which record events taken over a very short time interval. The spray cloud is an unsteady, turbulent, fluctuating distribution with the characteristic peak/mean ratio of turbulent plumes. Moreover, the reduced screen data are biased by the selection for reduction of screens containing only rather extensive droplet signatures, so that good droplet spectra readings can be obtained. In retrospect, the samples indicating very low droplet concentrations were not reduced, but evidently contribute to mean levels. Meander, scatter, and variance levels are not known for this spray situation, but it is noted that for plumes, peak/mean concentration ratios of the order of 3-5 can occur.

8. Multiple Wheel Set Spray Generation Model

The generation of splash and spray by multiple wheel sets can now be considered to complete this article, and to provide the input for the multiple discrete source dispersion model presented in Article B, below.

The multiple wheel set spray model uses the simple single wheel model as its basis and considers mechanisms of surface water removal, surface water replenishment, multiple wheel interference spray generation, and droplet impaction to construct quantitative representations of multiple wheel set configurations. Observations of successive wheel sets in the full scale data indicate that the spray diminishes for following sets. For the typical 3 axle COE plus 40 ft (12.2 m) van, most of the spray cloud appears to be generated by the front wheels and the drive tandems, with considerably less generated by the semitrailer tandems. Figure 8 gives a quantitative measure of this phenomenon as reduced from the full scale droplet collector data for the 2 axle COE tractor with three 27 ft

(8.2 m) trailers. It is readily seen that the spray is reduced for successive wheel sets.

Starting with the simple single wheel model, it is assumed that each tire throws or displaces only 85 percent of the water in its path. For typical truck configurations, the front wheel track lies approximately 3 in. (76 mm) outboard of the center of the dual wheels. Consequently, the drive tandem duals receive surface water which is nearly undisturbed by the front wheels. Succeeding tire sets follow along the same track as the drive set. If the 85 percent assumption is used, then the rear wheels of the third 27 ft van shown in Fig. 8 would pick up less than 0.0001 as much water as the drive wheels. Clearly this is not the case. Water must be replenished in the path of following wheel sets. It is not known precisely how this happens, but several mechanisms are quite probable. Some of the water thrown by leading wheel sets returns to the ground in the path of following wheels. This is true also for runoff from the wetted underside of the tractor and semitrailer. And, each cleared path through the water will begin to fill up again as water migrates inward from the sides of the cleared track. For water film depths on the order of 1 mm, this process is slow in comparison with passage of the truck and little replenishment results. This is substantiated by the observation of wheel tracks that persist many truck lengths downstream of the truck.

Using the models and the full scale collector results, a water pickup schedule for the complete 3 axle COE plus 40 ft van rig is developed in Ref. 4. Some assumptions have been made about water replenishment to give reasonable correspondence to the results shown in Fig. 8. For the front wheel, 5 percent replenishment is assumed to cover return water from the front wheel tread pickup plus water dripping back to the roadway from the front wheel well. For the drive tandem duals, 5 percent replenishment is assumed due to the first dual tread throw impaction on the second dual. Prior to the trailer tandem duals, 20 percent of the pre-drive-tandem water is assumed returned to the road. This is made up by drive tandem tread throw and roostertail contributions which fall in the path of the rear wheels. And, after the first trailer tandem, 5 percent replenishment is assumed again. Total water remaining in the tracks of the tandem wheels is less than 1 percent of the original water on the road.

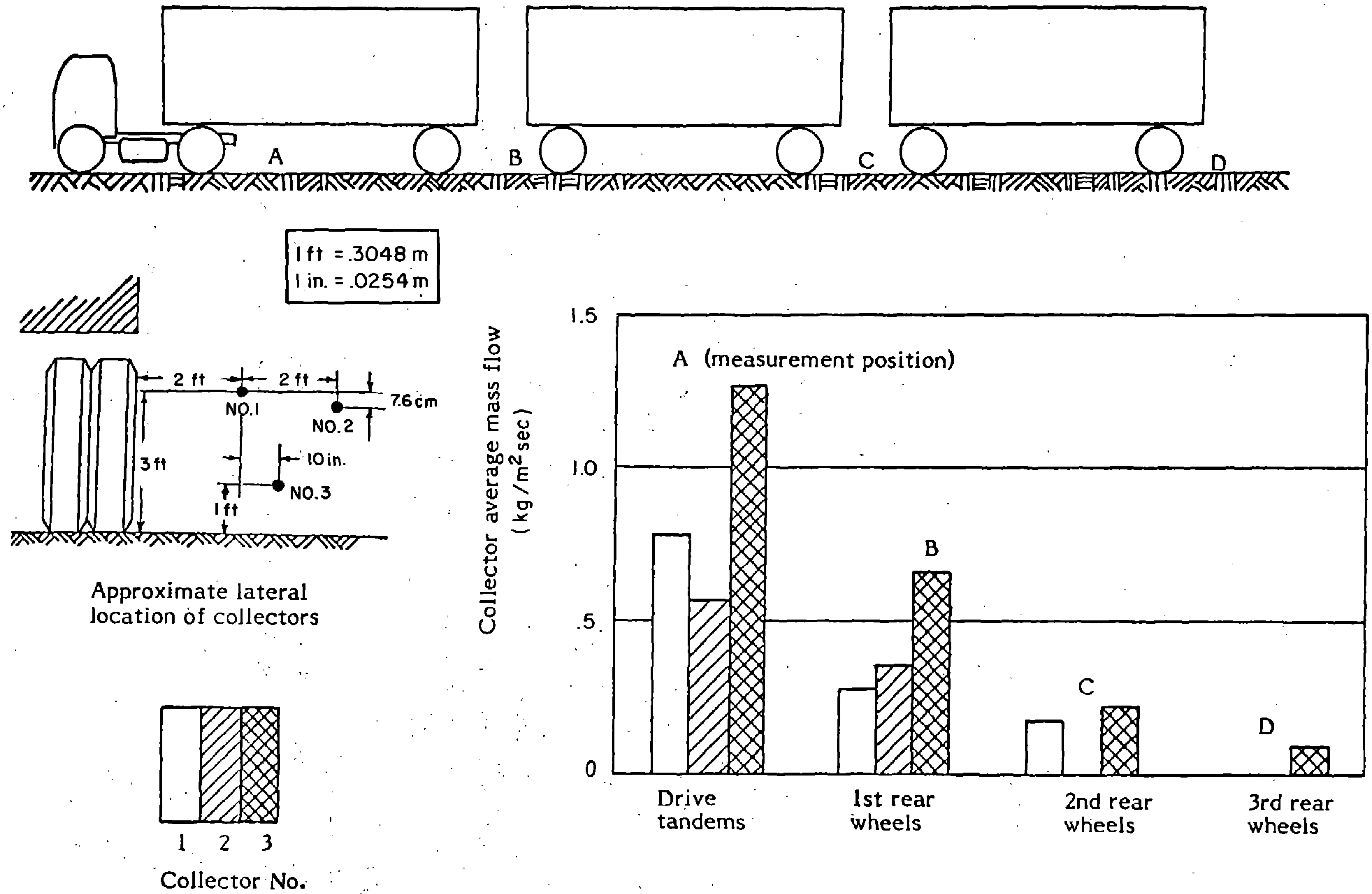

Figure 8. Collector Measured Average Mass Flow at Various Positions Along 2 Axle COE Plus Triple 27 ft Van Configuration

To complete the multiple wheel set model, the total spray generated by each wheel was divided up into wave and tread throw components, and configuration-dependent phenomena such as spray impaction on the gas tanks were treated. The breakup of the various sprays is illustrated in Fig. 9. Amounts of spray reflected upon impaction and combining to form interference sprays are estimates chosen to be consistent with the observations and data presented here and in Ref. 4. These spray stream mass flows form the basis for choosing source strengths for the spray dispersion computer model. The numbers are slightly different for those runs because the additional small increments of overlap between the front tire and following tandems have been taken into account.

B. DISPERSION OF SPLASH AND SPRAY

This article summarizes the analytical model developed by AeroVironment, Inc., which computes the spray field concentration distribution near the truck. First, the basic dispersion model for a source emitting particle of a given size in a turbulent flow is discussed. Then a full computer model integrating all the sources on an arbitrary truck configuration is described. Finally, examples of the computer-generated concentrations of the spray fields are shown, together with a comparison with field data obtained from the full scale tests. The material presented here is based on the detail in Ref. 4.

The analysis of the dispersion of water droplet sprays in the fully separated truck wake is a difficult problem at best. Droplet streams containing different size droplets are introduced from multiple sources into an extremely complex flow field. Rational dispersion analysis using the well established Pasquill-Gifford diffusion relations can be applied to this problem, but appropriate mean and turbulence velocities must be determined and spray sources must be adequately categorized to do so.

In addition, the dispersion model must contain enough structure to satisfy the basic physics of the phenomena. For instance, droplet streams are injected into the flow field with velocities which are different in magnitude and direction from the mean flow velocity. But, the airstream acts on these droplets and eventually they are carried downstream at the

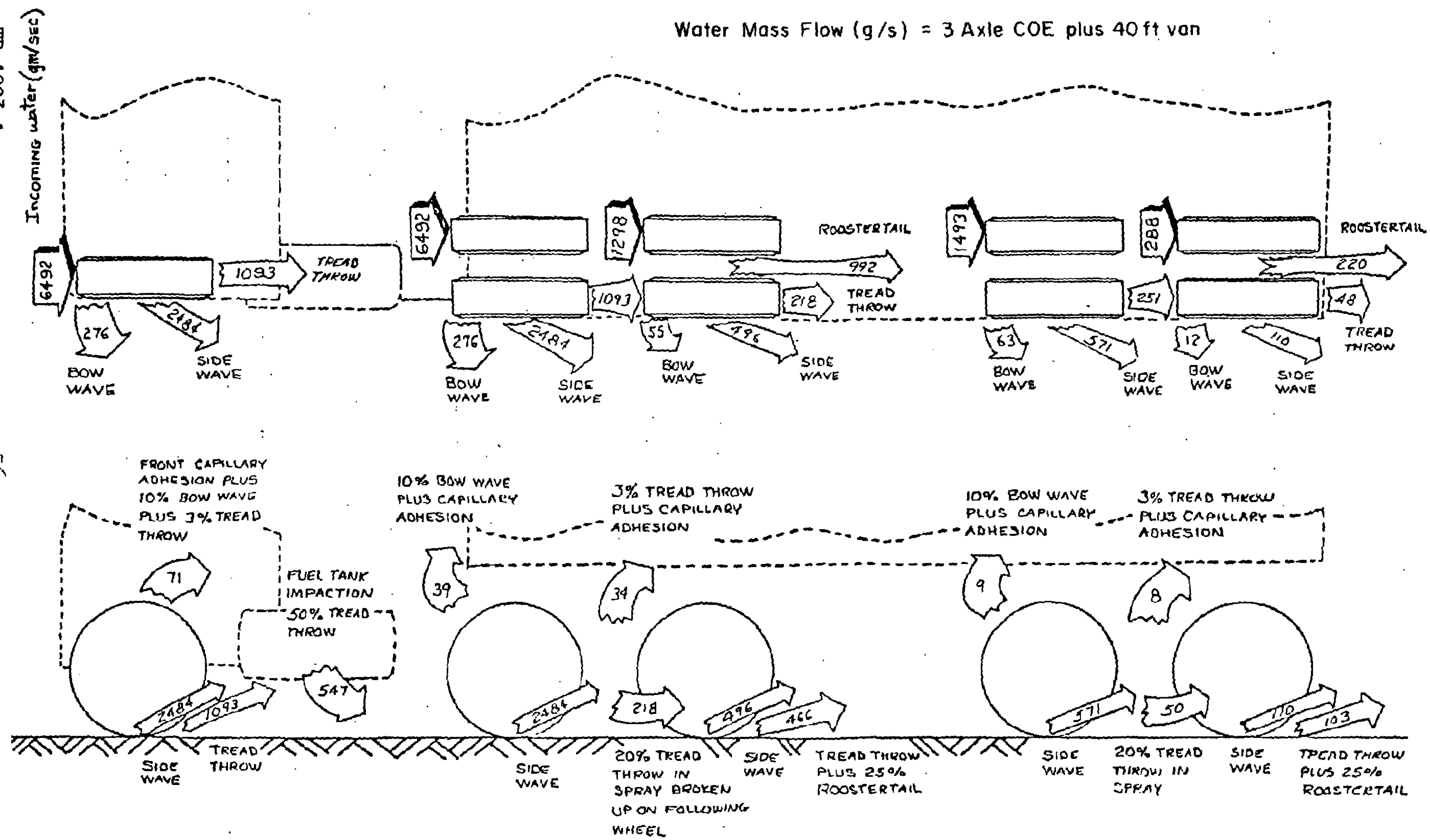

Figure 9. Division of Incident Water Into Single Wheel Streams (Top) and Formation of Interference Sprays Including Impactions (Bottom)

mean velocity. Additionally, droplets fall under gravitational force until they are extinguished upon contact with the ground, or are suspended aloft by strong turbulence until they disperse to very small concetrations. Consequently, a model should satisfy the near-field condition of initial droplet injection velocity, satisfy the far-field condition of alignment with the mean flow, and contain mechanisms for droplet fall under gravitational force and eventual dispersion to infinitely small concentrations. The model presented in Ref. 4 for this analysis fulfills these requirements and permits consideration of the rebound of droplets off the side of the truck. Yet, the model is simple enough that the intricate details of the near wake do not have to be known, which is appropriate because those flows are much too complicated for detailed analysis and only regional mean and turbulence velocities have been determined experimentally.

1. Use of the Gaussian Plume to Model Spray Dispersion

Classical diffusion analysis of plumes as pioneered by Pasquill (Ref. 35) and Gifford (Ref. 36) holds that they disperse with a Gaussian cross stream concentration distribution and expand linearly with downstream distance. The Pasquill-Gifford equation

$$c(x,y,z) = \frac{Q_o}{U_1} \frac{1}{2\pi\sigma_y\sigma_z} \exp\left[-\frac{1}{2}\left(\frac{y}{\sigma_y}\right)^2 - \frac{1}{2}\left(\frac{z}{\sigma_z}\right)^2\right]$$

where c is the concentration and Q is the initial mass flow. The mechanism of dispersion is the lateral transport of small particles by turbulent eddies in the flow field. These eddies are characterized by a turbulence velocity which acts in all directions and defines the extent of lateral dispersion as shown schematically in Fig. 10.

This approach can be applied directly to the problem of a fine droplet spray introduced into a uniform flow field; however, when large droplets are considered and/or droplets are injected into the flow field with some initial velocity different from that of the mean flow, the approach has to be modified. In that case, the acceleration of the droplet depends on the size of the droplet and the aerodynamic drag force which is related to the net velocity by an aerodynamic drag law. Using the reference frame of the

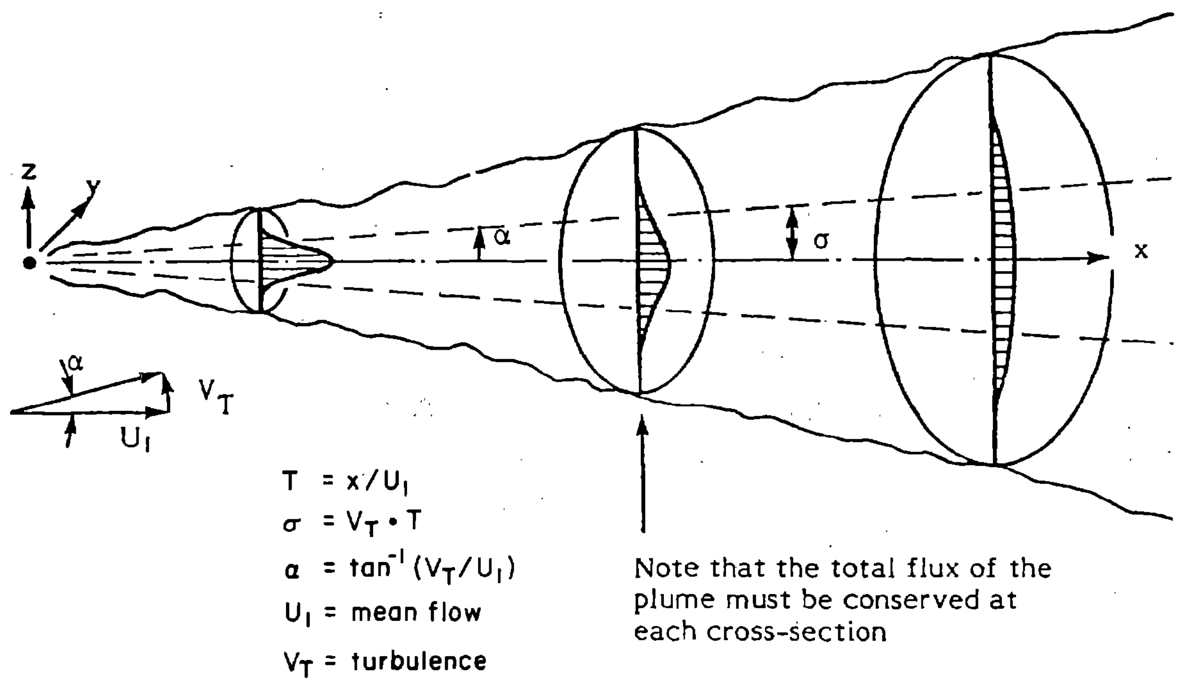

Figure 10. Basic Pasquill-Gifford Dispersion Relations

droplet, a differential equation can be written which, when integrated, will give the droplet's velocity and position as a function of time as the particle accelerates. Knowing these quantities, the actual trajectory and velocity can be determined.

If all droplets in a given spray stream are assumed to be of the same size, then dispersion of this stream can be modeled using the Pasquill-Gifford equation by assuming the trajectory of a single drop to be the centerline of a dispersion plume. Another simplifying assumption is that concentrations are Gaussian normal to the mean flow field streamlines rather than normal to the plume centerline. This greatly reduces the computational complexity of the model. As described in Ref. 4, the effect of gravity on the droplets can be accounted for by assuming that the vertical component of the final freestream velocity is the terminal full speed of the droplets. This approach works rather well, and if the velocity difference between initial and final velocities is several times greater than the terminal fall speed, the effect of gravity is very small and an acceptably accurate trajectory in the vertical plane is achieved.

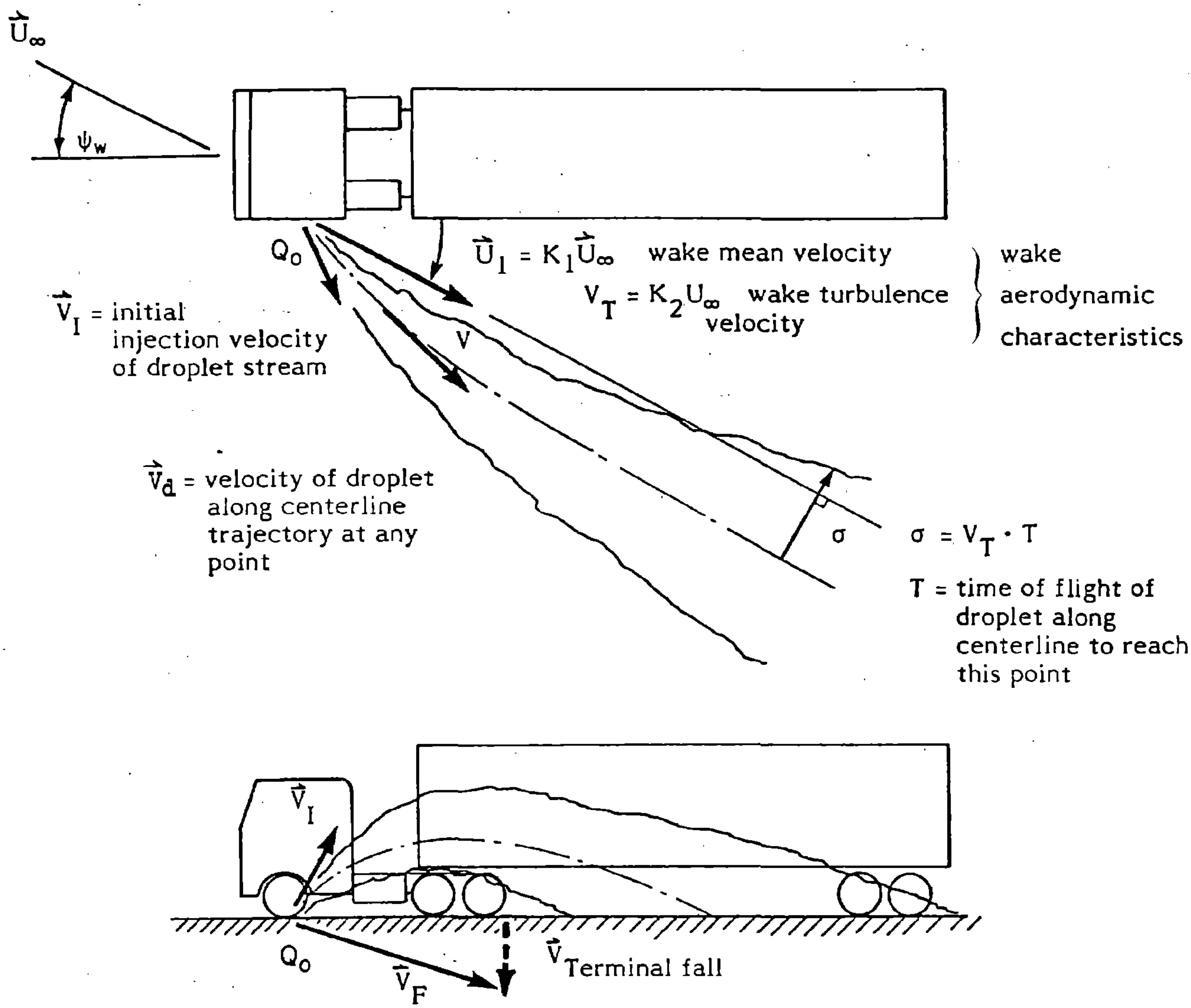

Figure 11. Plume Behavior for a Single Source

The resulting model gives reasonable droplet behavior and dispersion spray stream treated as dispersing plumes, illustrated in Fig. 11. Knowing only the initial spray mass flow (g/s), the droplet size, the initial injection velocity ($\vec{V}_I$), the relative wind angle (ψ_W), the wake mean velocity ($\vec{U}_1$), and the wake turbulence velocity ($\vec{V}_T$), the concentration of water (g/m^3) due to a single source can be determined at any point in space. The development of the appropriate equations is contained in Ref. 4.

2. Discrete Source Model of Complete Configurations

The total water concentration at a point in space due to a number of discrete spray plume sources can be calculated. The various spray streams of a single wheel, a multiple wheel set, or a complete truck configuration can be represented. The model generates detailed concentration plots and isopleth plots of the truck splash and spray. A complete description of the model is contained in Appendix G of Ref. 4.

The model requires the following inputs for each case

- Freestream velocity, U_∞
- Relative wind angle, ψ_W

and the following inputs for each source

- Source water mass flow, Q_o
- Wake mean flow velocity constant, K_1
- Turbulence velocity constant, K_2
- x, y, z components of source initial velocity vector, $V\Phi_x$, $V\Phi_y$, $V\Phi_z$
- x, y, z coordinates of source location, x_{p_o}, y_{p_o}, z_{p_o}
- Droplet diameter for this source, d
- Initial spray plume width at the source, σ_o

The output is in the form of concentration plots or isopleth plots in a specified x, y, or z plane. A basic rectangular image is included to mark the location of the truck and each source is marked with a letter of the alphabet in the order in which they are input.

a. <u>3 Axle COE Plus 40 ft Van Example Results</u>

One configuration studied in detail was the 3 axle COE plus 40 ft van. Source descriptions and inputs are presented in Ref. 4. Source inputs were developed using the splash and spray generation model described in Article A.8, above. Source strengths are not exactly the same as those shown in Fig. 9, because the slight amount of tire overlap between the front tire and the tandems was included in the analysis. In any case, spray source mass flows and initial velocities were estimates, since no accurate supporting data exist regarding their breakdown. The corresponding source locations are shown in Fig. 12. Source initial velocities and σ_O's were chosen to correspond to observed spray plume initial directions and diameter. Droplet sizes were chosen based on the experimental results on droplet size discussed in Article A.6. Constants K_1 and K_2 were chosen based on the wind tunnel and ground based anemometer data.

Figure 13 shows the spray concentrations in g/m^3 for the basic truck at $\psi_W = 0°$ as viewed in the x-plane just aft of the tractor tandems. Figure 14 shows spray isopleths for the x-plane views also, taken just behind the drive tandems at $\psi_W = 0°$. This figure gives a more graphic view of the extent of the spray alongside the truck. Figure 15 shows spray concentrations viewed in the z-plane at a height of 1 m above the ground for $\psi_W = 0°$. The height was chosen to be close to windshield height for a passing car and low enough to capture the main truck spray plumes. Corresponding isopleths are presented in Fig. 16. These figures highlight the regions of maximum spray density. Similar figures given in Ref. 4 show the leeward drift of the spray cloud with increasing yaw angle. Another example series given there illustrates the effect of reducing source strength (e.g., by Reddaway fenders) and modifying the aerodynamics via a cab-mounted drag shield.

In general, these analytical results are in good agreement with the spray-related visibility measures obtained during the June and November, 1977, full scale tests. This can be seen in the checkerboard photographs on the individual data sheets in Appendix B. It is also evident in comparisons shown in Ref. 4, based on the same Appendix B data.

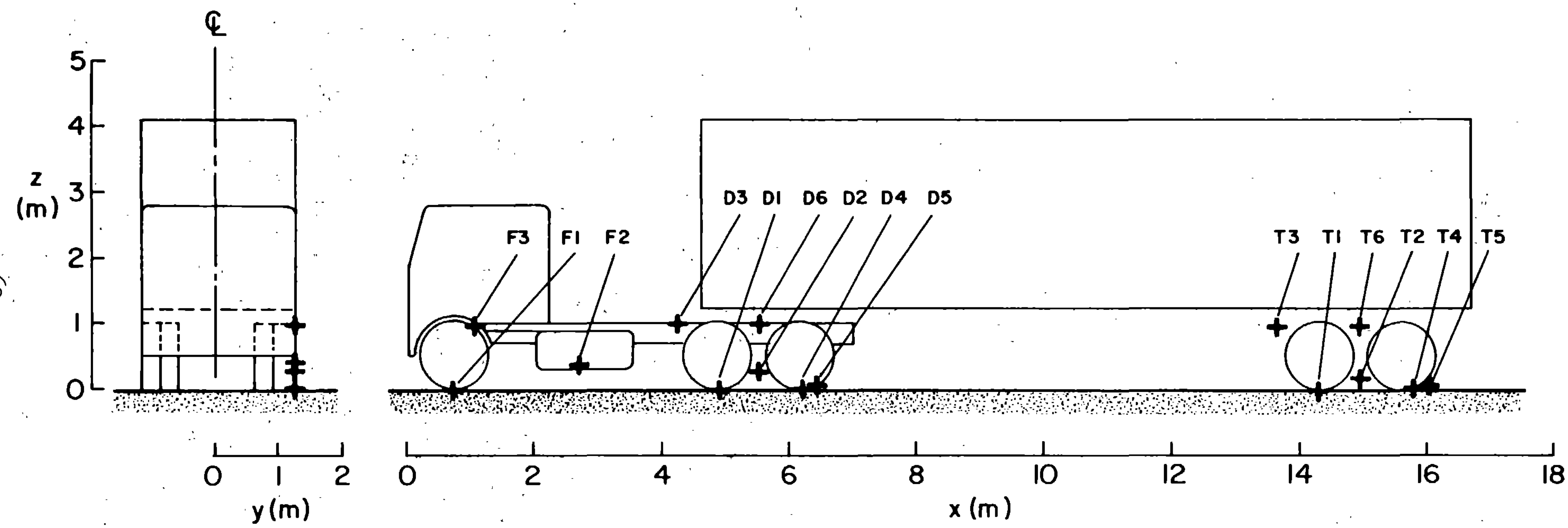

Figure 12. Spray Source Locations Used in Dispersion Analysis, 3 Axle COE Plus 40 ft Van

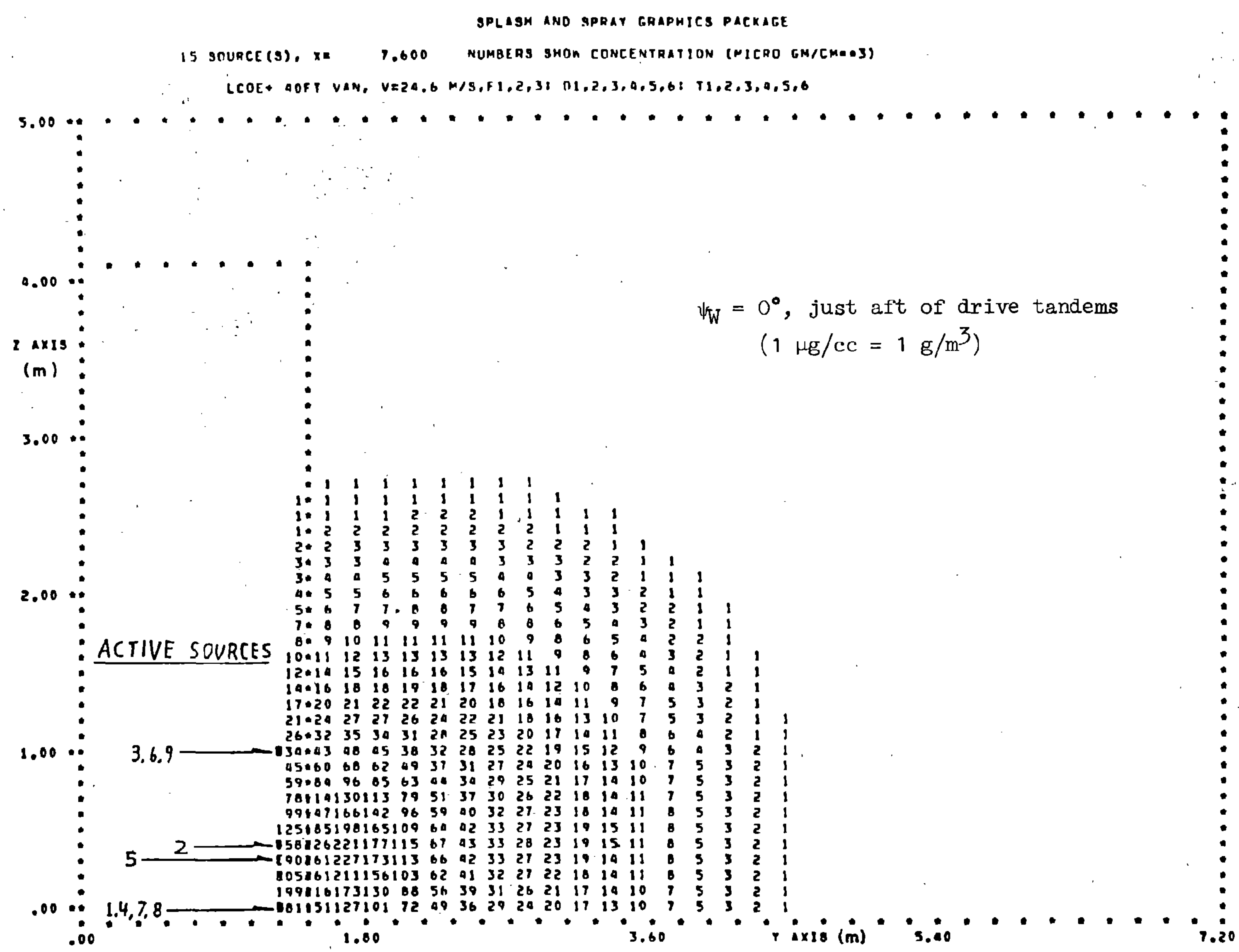

Figure 13. 3 Axle COE Plus 40 ft Van, x-Plane Concentrations

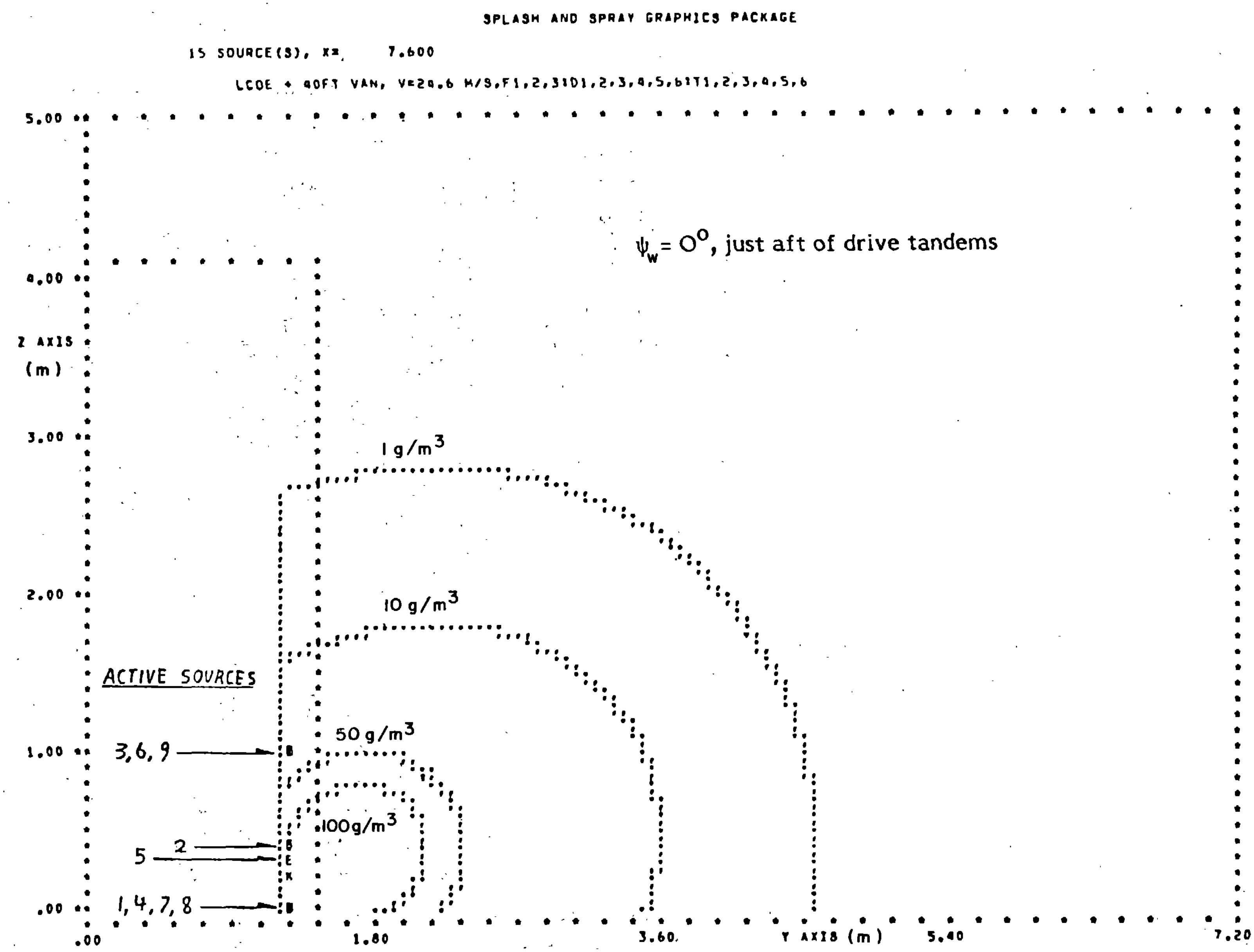

Figure 14. 3 Axle COE Plus 40 ft Van, x-Plane Isopleths

SPLASH AND SPRAY GRAPHICS PACKAGE

15 SOURCE(S), Z= 1.000 NUMBERS SHOW CONCENTRATION (MICRO GM/CM**3)

LCOE + 40FT VAN, V=24.6M/S,F1,2,3;D1,2,3,4,5,6;T1,2,3,4,5,6

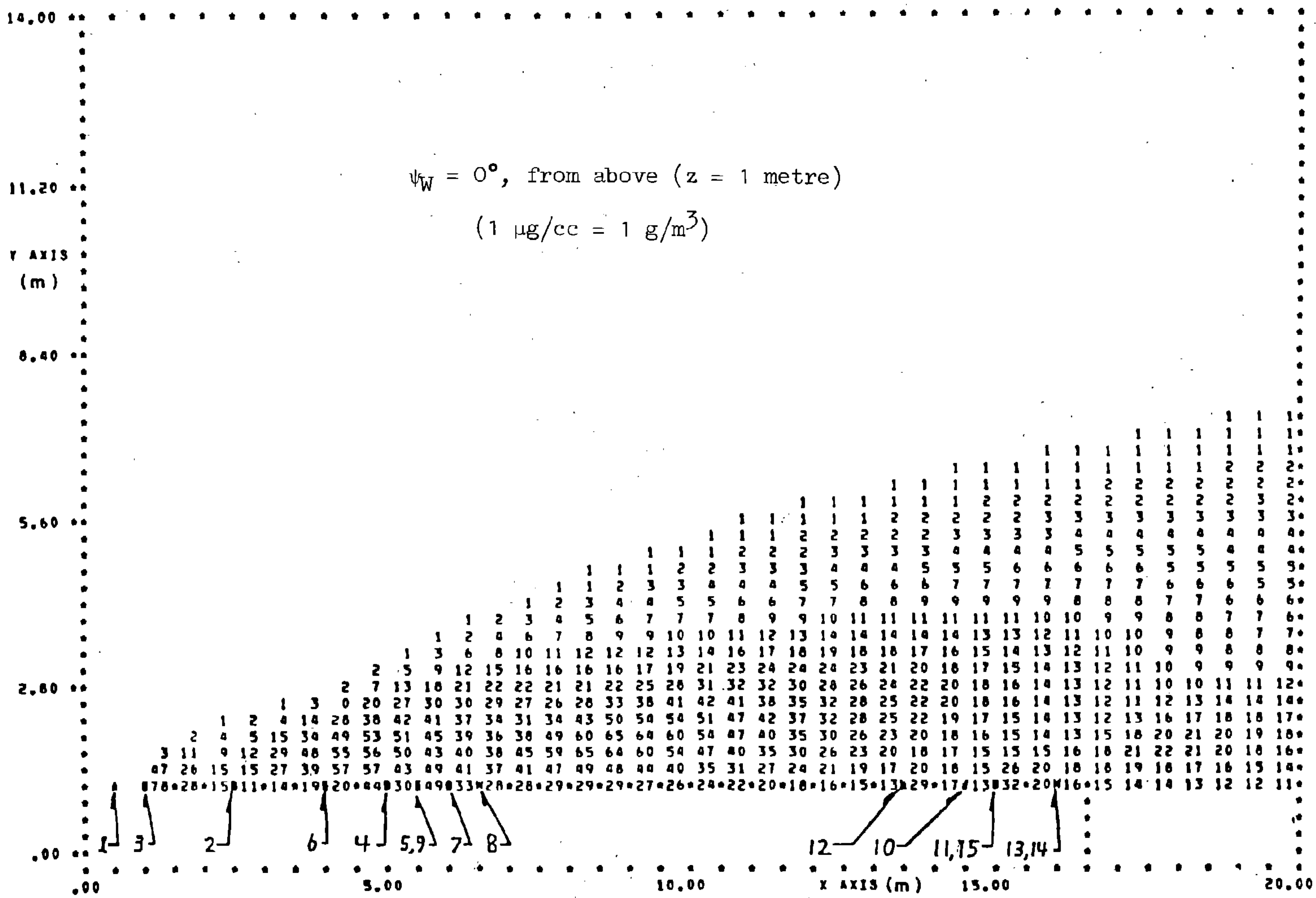

Figure 15. 3 Axle COE Plus 40 ft Van, z-Plane Concentrations

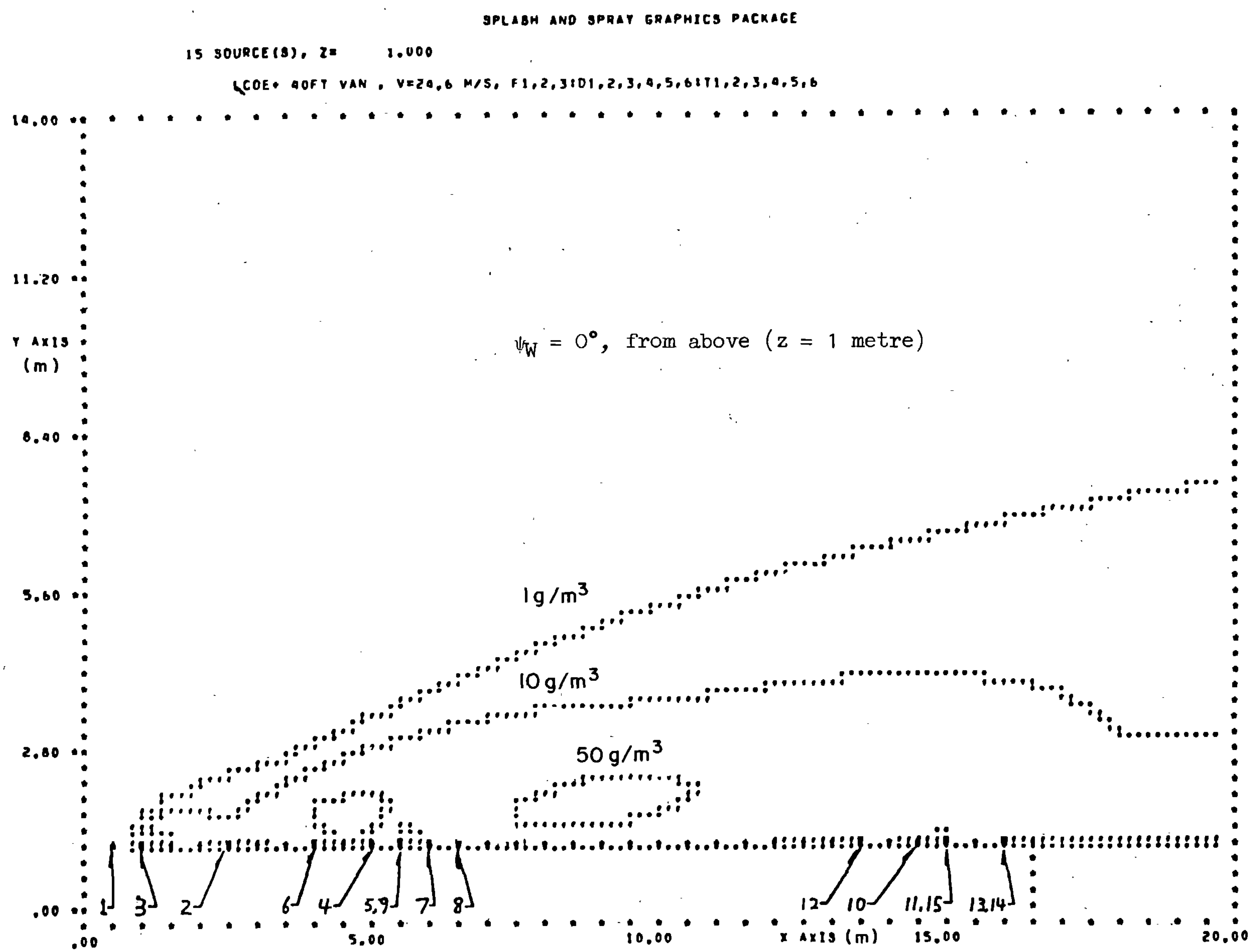

Figure 16. 3 Axle COE Plus 40 ft Van, z-Plane Isopleths

C. DRIVER/VEHICLE SYSTEM PROPERTIES

Aerodynamic and visibility disturbances in the vicinity of a truck can degrade the path performance of an adjacent car and cause corresponding reductions in safety. Analytical procedures have been developed for investigating the effect of such disturbances on the driver/vehicle system, and they are summarized here. Additional background material on driver/vehicle models, analysis, and their applications are given in Refs. 2, 3, 6, and 37-45, for example.

1. Disturbance Situation and Driver Task

The geometry of aerodynamic disturbance situations is shown in Fig. 17. The car (disturbed vehicle) is shown on the left of the truck, either overtaking it or being overtaken by it. Positive lateral path deviations (y_I) move the car toward the right (and toward the truck). The driver's task is to stay in the center of his lane and avoid drifts in lane position. To

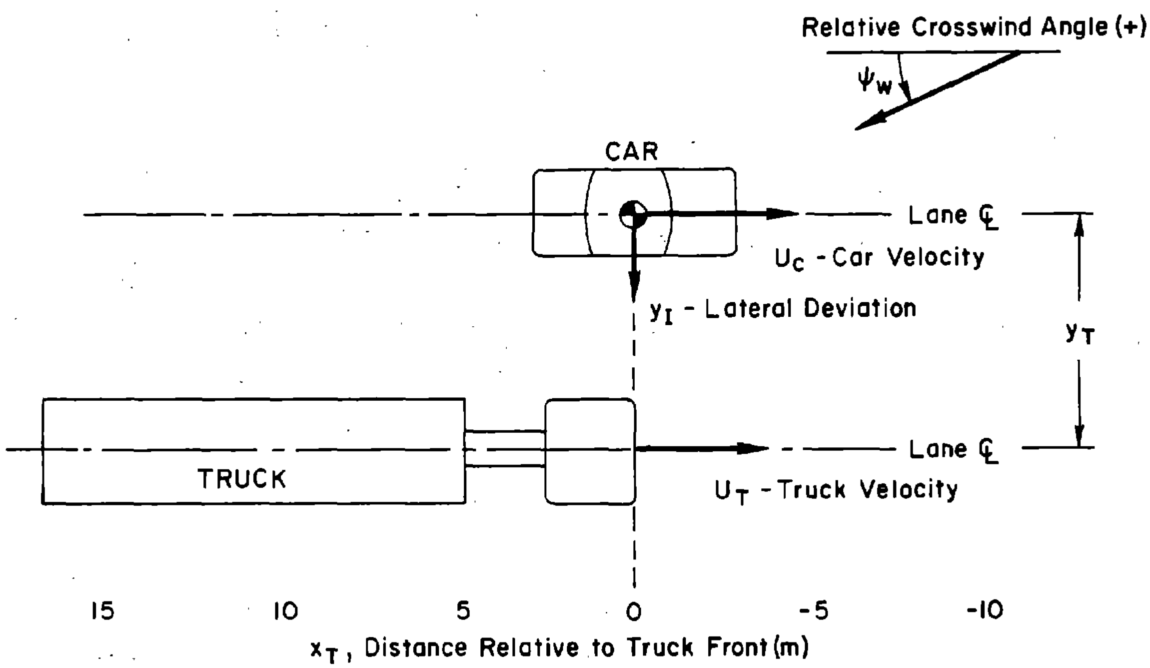

Figure 17. Typical Truck-Car Disturbance Situation

accomplish this, he makes steering corrections, based on perceived motions of his vehicle, to minimize the lateral deviations caused by the disturbance. One convenient performance measure is the peak lateral deviation from the lane centerline due to the disturbance ($\hat{y}_I$).

The truck creates a turbulent wake that propagates downwind. A positive relative crosswind is one that causes the wake from the truck to blow away from the lane the car is in, and conversely. The crosswind angle (ψ_W) is measured relative to a sensor on the moving truck, and it reflects a combination of the ambient wind (relative to the ground) and vehicle motion. Zero crosswind refers to the case with no relative crosswind angle, although a headwind or tailwind may be present. Because the vehicles are symmetrical, the results are equally applicable to the case with the car on the right. If the car and truck are traveling along their respective lane centerlines, the centerline separation equals the lane width.

2. Basic Driver/Vehicle Model

The dynamic model for driver/vehicle response and performance is based on an empirical theory of manual control that takes into account:

- Guidance and control requirements related to stability and path following, and
- Driver requirements related to human characteristics

The driver responds to stimuli from the full visual field. The current driver control model is based on human response data obtained in a variety of vehicular control tasks, including driving. The basic manual control theory is presented in Refs. 39 and 42, for example. Specializations to driver control have been described in detail (e.g., Refs. 37 and 43-45) and are reviewed briefly below.

To set up the driver/vehicle system dynamic model, the vehicle properties are readily defined using linear or nonlinear differential equations of motion. One derivation and summary is given in Ref. 46 for passenger automobiles. There, directional properties pertinent to steering control are modeled using linear equations in three degrees of freedom: lateral velocity, yawing velocity, and body roll angle. The equations of vehicle motion and steer angle response functions have been quantified, subsequently, by using chassis and tire data and verified in full scale tests (e.g., Refs. 3, 43, 45, and elsewhere). More complete models abound in the literature, among the best of which are the HVOSM model developed by FHWA (Ref. 47) and the APL-JHU HVHP model developed by NHTSA (Ref. 48).

To model the driver we rely on a nonlinear approach in which the driver's control behavior is characterized by an input-dependent describing function(s) plus remnant representation. The describing functions represent the driver's action in reducing errors in lane position, vehicle heading, etc., whereas the remnant amounts to a kind of driver-induced noise. As the operative element in the system, the driver adapts his dynamic characteristics (describing functions) so as to satisfy the key guidance and control requirements for the driver/vehicle system. Stated verbally, the guidance and control requirements for lane position control are:

- To establish and maintain the automobile on the specified path
- To reduce path errors to zero in a stable, well damped, and rapidly responding manner
- To establish an equilibrium driving condition
- To maintain the established path in the presence of disturbances such as gusts, crosswinds, and roadway disturbances

These requirements relate primarily to the relatively low-frequency path modes of the driver/vehicle system. To satisfy them, "outer" control loops which involve the feedback of vehicle motion quantities such as lateral position in the lane must be set up or "mechanized" by and through the driver. However, with only this control acting the system may not be stable, well-damped, and rapidly responding in transient operations. To provide this, equalization using feedback of additional vehicle motion quantities is ordinarily required, as discussed below.

a. Driver Describing Function

Driver closed-loop steering response can be modeled by describing functions with parameters that depend on the system and situation, rules that tell how to adjust the parameters, and an additive remnant.

Remnant is the part of the driver control output that is not linearly correlated with the input, and it can be modeled as a random noise added to that output. Its main source seems to be nonstationary behavior. Some evidence of remnant is seen in the steer angle and yaw velocity of the full scale data shown subsequently. Generally, it can be neglected when differences in performance due to changes in the vehicle, roadway geometry, disturbance situation, and so on are analyzed.

The rationale of driver equalization can be expressed most simply by using an approximate crossover model (Ref. 42), which states that the driver adjusts his describing function (Y_p) in each loop such that the open-loop function, made up of the effective vehicle dynamics (Y_c) and the driver, in the vicinity of the gain crossover frequency for that loop has the following approximate form:

$$Y_p Y_c \doteq \frac{\omega_c e^{-j\omega\tau}}{j\omega} \qquad (1)$$

The crossover frequency (ω_c) in Eq. 1 is a key parameter. It corresponds to the "bandwidth" of the closed-loop driver/vehicle system, and its magnitude determines the quality of control and system responsiveness. The crossover frequency is adjusted by the driver for a given situation based on the vehicle's handling properties, the driver's skill level, and the nature of the inputs and the perceptual situation. The time delay (τ) in Eq. 1 includes neuromuscular dynamics as well as any high-frequency vehicle lags. In multiloop situations the controlled element dynamics will include the effects of all the inner loops closed. Experimental values of the parameters in Eq. 1 and the basic adjustment rules are reported in the references listed above, for various situations and tasks.

b. Driver/Vehicle System Structure

Multiloop control involving more than one feedback stimulus is needed to satisfy the guidance, control, and driver requirements. The system shown in Fig. 18 is representative for the steering control task of interest and the typical passenger cars. This system has a primary feedback loop for functions of vehicle heading angle plus an outer loop for functions of lateral deviation. In the model these feedback cues are operated on by the driver's describing functions to produce steer angle corrections.

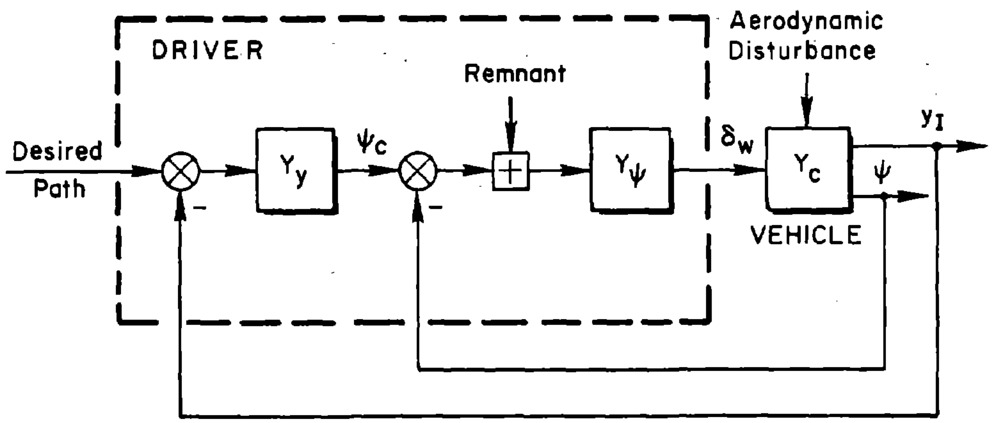

Figure 18. Driver/Vehicle System Concept

Y_ψ and Y_y (Fig. 18) account for the effective driver response properties. However, they are not necessarily an exact analog of the system details. As noted, driver perceptual activity may involve some attention to other cues such as yaw velocity and lateral acceleration, but the net effects of these feedbacks (if present) are embodied in Y_ψ and Y_y. Similarly, higher order dynamic properties of the vehicle can be reflected in the three-degree-of-freedom model for the range of frequencies and amplitudes important to driver control in aerodynamic disturbance regulation tasks.

The mathematics for the multiloop system in Fig. 18, and the associated response data presentations, can be simplified by expressing the behavior of the driver/vehicle system in terms of an equivalent single loop operation.

In such a single loop system the denominator of the closed loop system transfer functions will have a form in which the open loop system transfer function, G, is added to unity, i.e., $1 + G$. If an effective driver describing function is defined as Y_p^*, in the fashion shown below, then the closed loop denominator for Fig. 18 is

$$D'' = 1 + Y_\psi G_s (G_{\delta_w}^{\psi} + Y_y G_{\delta_w}^{y})$$

$$= 1 + Y_p^* G_s G_{\delta_w}^{\psi} \tag{2}$$

where G_s is the steering ratio, $G_{\delta_w}^{\psi}$ and $G_{\delta_w}^{y}$ are the respective vehicle transfer functions, and

$$Y_p^* = Y_\psi \left(1 + Y_y \frac{G_{\delta_w}^{y}}{G_{\delta_w}^{\psi}} \right)$$

$$= Y_\psi \left(1 + Y_y \frac{N_{\delta_w}^{y}}{N_{\delta_w}^{\psi}} \right) \tag{3}$$

In these equations the effective open single-loop driver/vehicle transfer function is $Y_p^* G_s G_{\delta_w}^{\psi}$. The effective driver describing function is seen to depend on the heading loop driver describing function, Y_ψ, and that for the lateral position loop, Y_y, as well as on the vehicle y and ψ transfer function numerators. This latter point is emphasized by the ratio $N_{\delta_w}^{y}/N_{\delta_w}^{\psi}$ in Eq. 3, a notation which represents the vehicle transfer function numerators specifically.

Fairly extensive data are available from recent full scale experiments (e.g., Refs. 41, and 43-45) to quantify the equivalent open loop describing function of the driver/vehicle system, $Y_p^* G_s G_{\delta_w}^{\psi}$, for aerodynamic disturbance regulation tasks. These data are for a range of passenger car dynamics, and a variety of male and female subjects. An example of this frequency response function for 8 male and 8 female subjects from the

Ref. 43 study is shown in Fig. 19. These data are for a 1974 Chevrolet Nova with a random appearing side gust-like disturbance. The key properties of such describing functions are summarized by the crossover frequency, ω_c, the phase margin, φ_M, and the slope of the amplitude ratio (see Fig. 19c for callouts of these quantities). For the female drivers, the amplitude ratio slope is almost exactly −20 dB/dec, whereas it is somewhat less (−15 dB/dec) for the males. This indicates that the women are somewhat more effective in suppressing very low frequency disturbances than the men, whereas the men showed slightly higher system bandwidths, as measured by ω_c. The phase margins were essentially the same for all. The differences noted are relatively minor, although they illustrate the small-detail resolution which the method permits.

Another key point in these data is the variability. This is indicated graphically in Fig. 19 by the $\pm 1\sigma$ hatch marks above and below the plotted average points. Also available are histograms for the describing function data points themselves and for the characterizing parameters, ω_c and φ_M. Consequently, any performance estimates made with these data can be couched in terms of population averages plus likely statistical variations.

With data such as these (or their mathematical model replacements), the denominator function D" in Eq. 2 can be considered completely known. That is, the common factor $[1/(1 + Y_p^* G_s G_{\delta_w}^{\psi})]$ present in all response quantities is easily determined from the data of Fig. 19. This leaves the numerator functions to be adjusted according to the situations which are to be characterized and analyzed.

3. Adding Aerodynamic Disturbances to the Model

The effects on lateral lane position of aerodynamic disturbances, η, can be computed for a given passenger car and aerodynamic disturbance using the equation:

$$y_I = \left[\frac{1}{1 + Y_p^* G_s G_{\delta_w}^{\psi}} \right] (G_\eta^y + Y_\psi G_s G_{\eta\delta_w}^{y\psi}) \eta \tag{4}$$

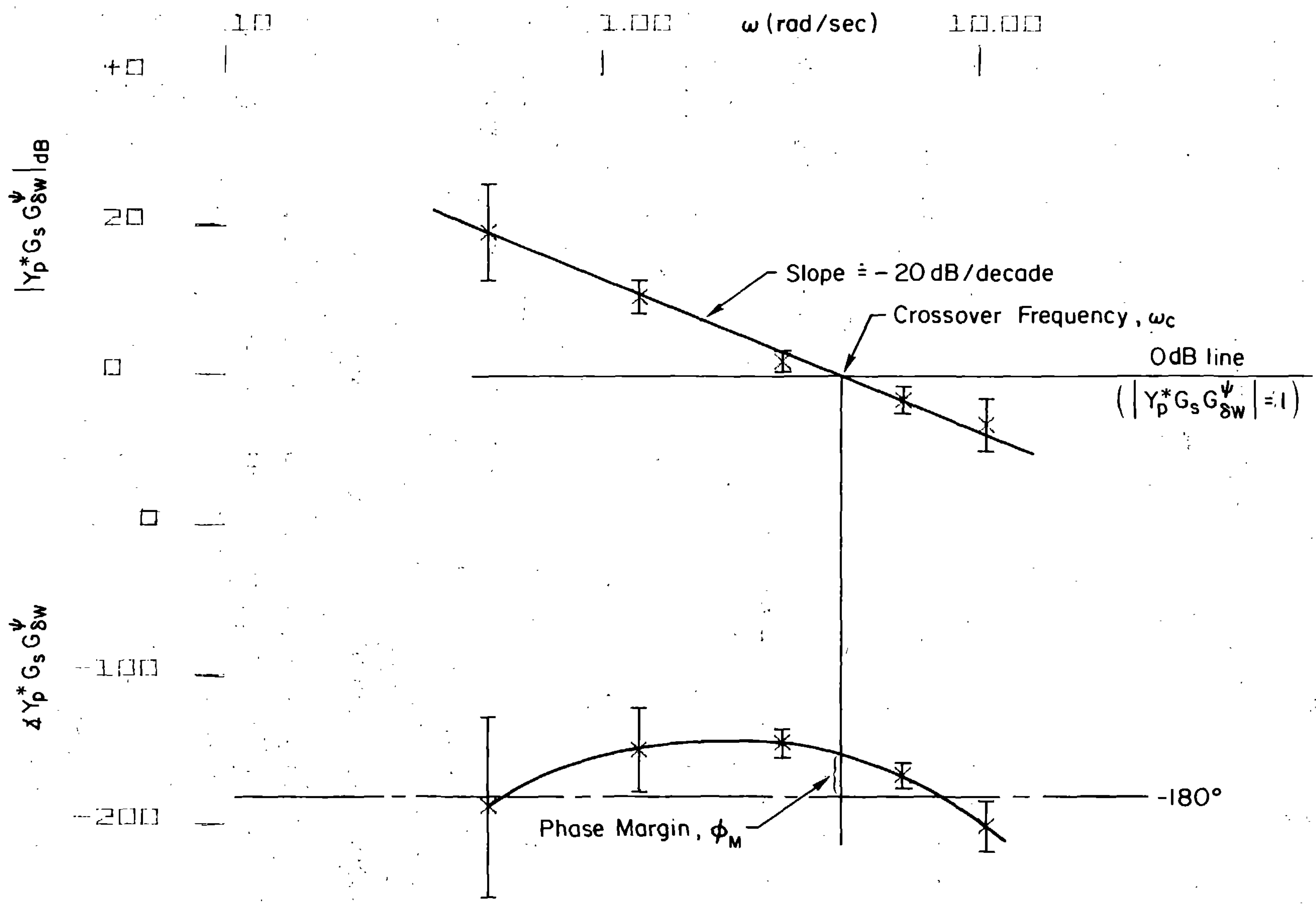

Figure 19. Effective Open-Loop Driver/Vehicle System Describing Functions for 16 Ss, 1974 Nova in Wind Regulation Maneuver (Ref. 43)

Here, the vehicle transfer function G_{η}^{y} relates the lateral position of the car alone to the disturbance η, and the coupling transfer function $G_{\eta\delta_w}^{y\psi}$ is also a vehicle-alone property. The corrective effect of the driver control action is given by the bracketed term in front. As can be appreciated from the data of Fig. 19, at frequencies less than the crossover frequency this bracketed term is a number less than unity. It thus serves to reduce the lateral deviation that the car would have if the driver were not present and active. The gust susceptibility of the car is accounted for by the G_{η}^{y} and $G_{\eta\delta_w}^{y\psi}$ transfer functions, whereas the time course and magnitude of the aerodynamic disturbance itself is given by η. When these quantities are known for a specific situation, from vehicle equations of motion and wind tunnel force and moment data, transient and steady state calculations of the lateral deviation y_I can be made.

4. Example Results for Disturbance Situations

The yaw moment and side force disturbances on an adjacent car have been quantified in past studies (see Refs. 2, 3, 6, 29 and 30) for various truck and bus shapes, using wind tunnel experiments and 1/10 scale models. The forces and moments of the disturbed car were measured for various relative crosswind angles, centerline separations, and longitudinal positions. Details of those scale model experiments are given in Ref. 29.

Example C_n and C_y disturbance coefficients are shown in Fig. 20a for a full-sized station wagon in the presence of a 3 axle COE plus 40 ft van semitrailer. These data are for zero crosswind and three centerline separations. The principal disturbance in this case results from the flow around the bluff front of the truck. Intercity bus data have a similar appearance for the zero crosswind case. Crosswind disturbance data are shown in Fig. 20b wherein the disturbed adjacent vehicle passes along the lee side of the truck or bus. In this case the main disturbance is large and of lower frequency than the zero crosswind situation, and it results from the truck or bus shadowing the relative crosswind. The data in Fig. 20b also show differences between truck and bus shape. Variations in centerline separation have less effect on the disturbance magnitude with a crosswind than they do with zero crosswind. Additional aerodynamic data for vehicle disturbance situations

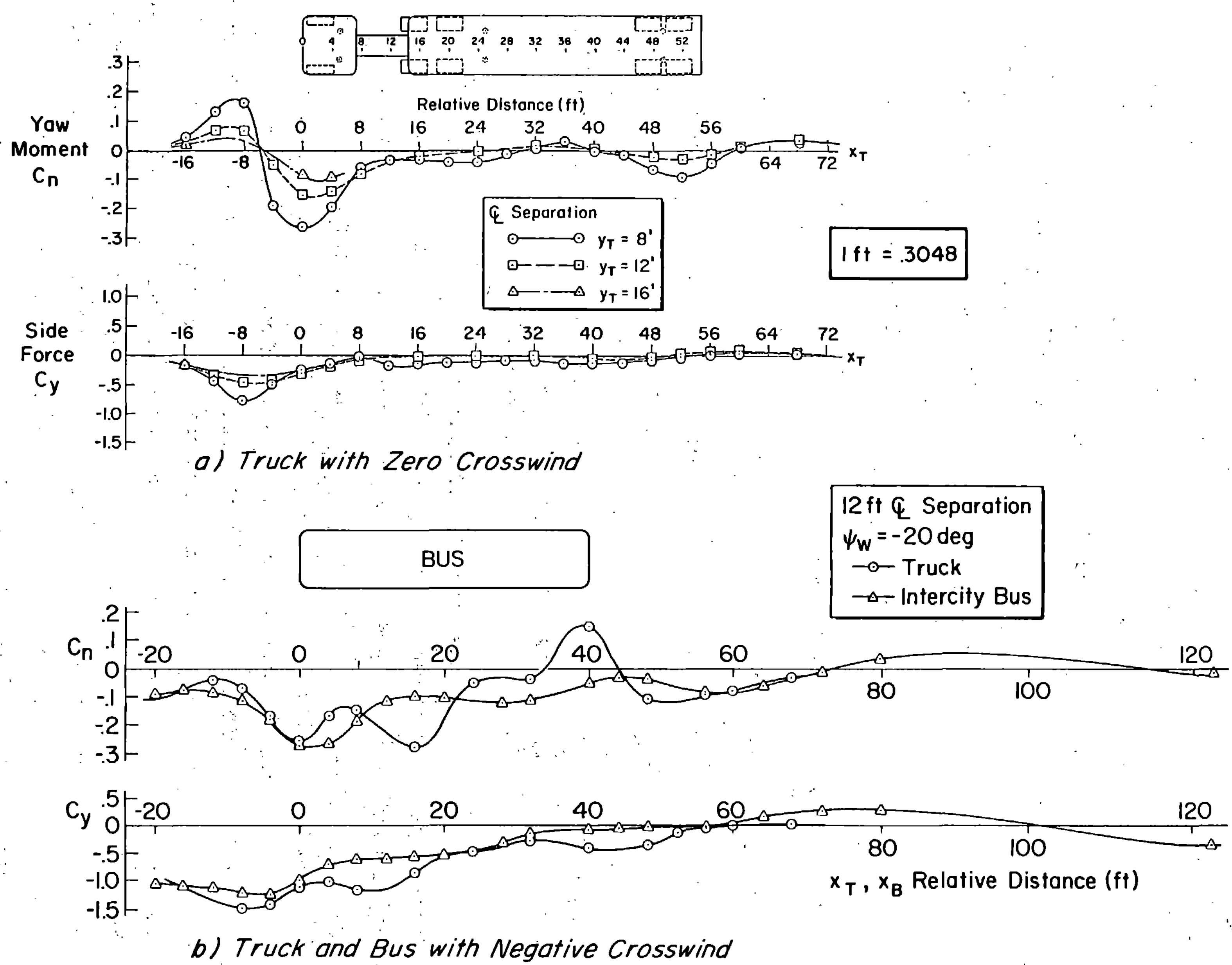

Figure 20. Typical Aerodynamic Disturbance Data for Station Wagon Disturbed by Truck or Bus

were obtained as part of the present program, and they are presented in Section V.

Driver/vehicle response and performance estimates for various situations have been computed in past studies (Refs. 2, 3, and 6) using the models and data discussed above. Simultaneous full scale tests with instrumented vehicles have been used to confirm the analytical and model results. An example comparison of analytical and full scale results is shown in Fig. 21, from Ref. 3. The aerodynamic disturbance shown was caused by the station wagon passing an intercity bus at a relative speed of 7 mph (3 m/s) with a strong crosswind. In Fig. 21, δ_W is the front wheel steer angle, r is the heading rate, and $|WV|$ and $\measuredangle WV$ are the magnitude and angle of the wind relative to the moving car. The results show good agreement, particularly in terms of

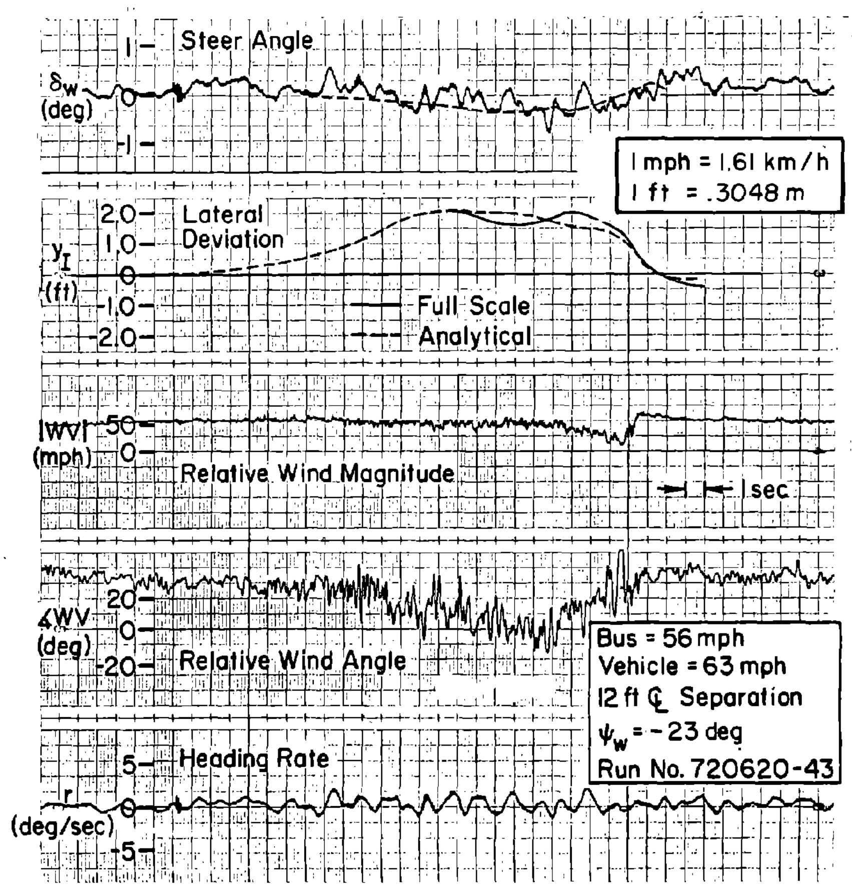

Figure 21. Comparison of Results for Station Wagon

the overall y_I. The higher frequency (3 to 10 rad/sec) oscillations in the δ_W and r data can be accounted for as remnant.

The driver/vehicle response values shown in Fig. 19 and typically used in model calculations are based on a reasonably skilled and alert driver attempting to maintain a constant path in the lane. This level of control activity and performance is sufficient for studying the effects of changing other parameters such as truck shape and ambient wind, and the results of these comparisons are insensitive to fairly wide variations in driver skill and attentiveness. In an absolute sense, however, the performance values shown could improve somewhat with a very skilled driver and degrade substantially if the adjacent driver were inexperienced or distracted.

Splash and spray aside, there are several ways to improve driver/vehicle performance in aerodynamic disturbance situations. Changing vehicle shapes reduces the magnitude of the aerodynamic disturbance. Increasing the distance between vehicles is invariably beneficial. Increasing the speed of the passing car helps by reducing exposure time and increasing the frequency content of the disturbance (which results in greater attenuation by the car's inertia). If the truck passes the car, reduction in the speed of either vehicle is generally helpful. Better car-handling dynamics and driver skill improve performance. Reducing the vehicle airspeeds and wake effects is helpful, and this will occur with no headwind (or a tailwind) and when the crosswind (if present) is such that the truck wake is not blowing across the path of the car, as previously discussed.

The effect of varying the handling and aerodynamic properties of the adjacent vehicle are shown in Fig. 22. Their aerodynamic properties are shown in Fig. 22b in terms of Y_{v_g}, the lateral acceleration per unit crosswind gust. The normalized yaw moment could be used as well. Large low-density vehicles (such as a pickup truck-camper or a utility van) are more gust-sensitive than conventional sedans. Driver/vehicle performance of these vehicles in the presence of a bus disturbance with strong negative crosswind is shown in Figs. 22a. The differences in performance generally follow the trend of the gust sensitivities, with the exception of the station wagon and station wagon towing a trailer. These perform poorly because of their aerodynamic and handling properties, as detailed in Ref. 3.

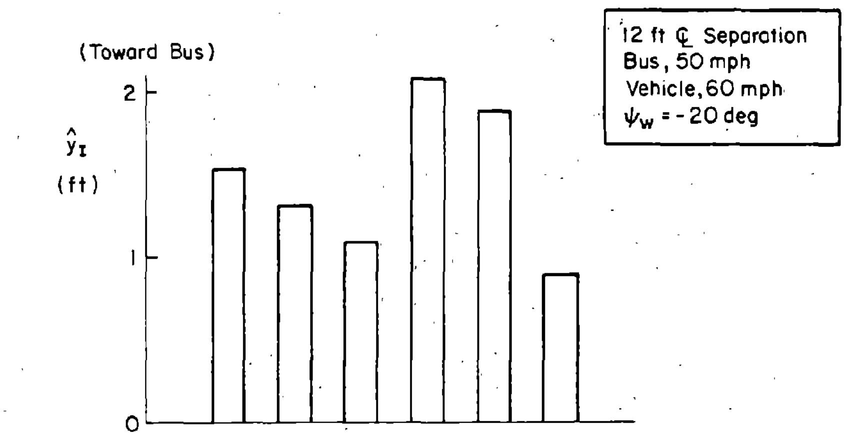

a) Peak Lateral Deviation due to Bus Disturbance

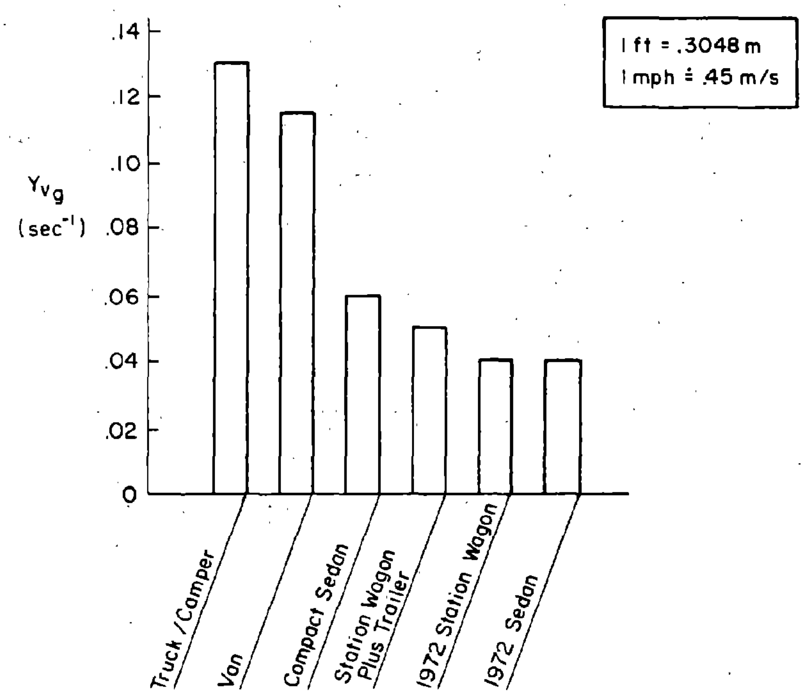

b) Crosswind Gust Sensitivity, Vehicle-Alone

Figure 22. Effect of Disturbed Vehicle Properties on Gust

The direction and magnitude of the ambient wind relative to the moving vehicles are significant parameters in vehicle disturbance situations, and there are two basic conditions:

- Zero crosswind in which the flow about the front of the truck or bus pushes the vehicle away (also representative of vehicle passing upwind of a truck or bus in a crosswind), and

- Negative crosswind (disturbed vehicle downwind) in which the wake alongside and to the rear of the truck or bus "pulls" the two vehicles together.

The variations in performance with relative wind for two nominal disturbance situations caused by a bus are shown in Fig. 23. Both positive (toward bus) and negative (away from bus) peak deviations are shown. Positive crosswind (car upwind from bus) results differ little from zero crosswind. For negative relative crosswind angles and magnitudes greater than about 5 deg, the performance decreases sharply because of the large amplitude, low frequency disturbance caused by the shadowing effect of the bus. Results for the COE plus semitrailer truck have a similar form, although the negative crosswind performance degradation transition occurs at $\psi_W \doteq -10$ deg because of the differences in shape and configuration between the bus and the truck.

Varying the speeds of both the car and the truck or bus has a substantial effect on performance. This is shown in Fig. 23 with two car speed/bus speed combinations: 60/50 and 70/65. The 70/65 case results in substantially larger path deviations by the car. At higher speeds the dynamic pressure increases, and this amplifies the level of the disturbing forces and moments. At lower relative speeds the disturbance lasts longer and changes more slowly, which tends to disturb the car more despite corrective driver steering. At higher speeds the car's handling dynamics change, it responds more gradually to driver steering corrections, and this reduces performance.

All of the example results discussed here are for the bus (or truck) and the disturbed vehicle traveling in the same direction. Oncoming vehicles present a case in which the relative speed is very high. This generally causes the aerodynamic disturbance to have a very short duration and results in a relatively small lateral deviation of the driver/vehicle system. The median on most modern highways increases separation and reduces the disturbance due to oncoming vehicles.

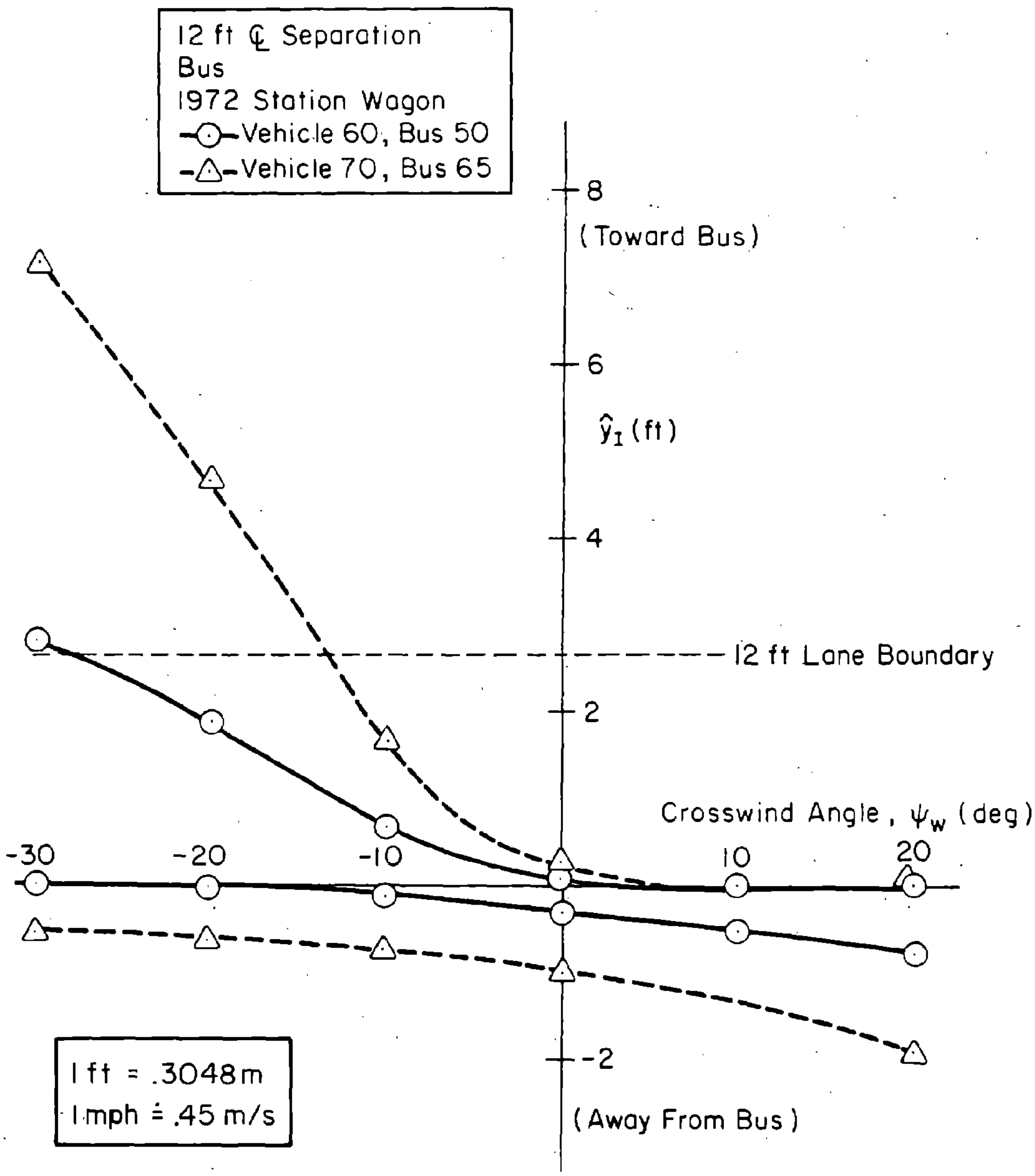

Figure 23. Effect of Crosswind Angle on Driver/Vehicle Lane Keeping Performance (Ref. 3)

5. Accounting for Visibility Effects in the Model

Splash and spray, in contrast to the aerodynamic disturbances, exert only minor or negligible forces directly on the driver/vehicle system. Their effect is more to interrupt closed loop operations by reducing or momentarily eliminating driver visual inputs. These effects can be considered in the same general framework as that introduced above, albeit as system parameter variations rather than as forcing functions to which the system responds. The modeling factors are outlined below.

To simplify this discussion we can neglect aerodynamic disturbances, and assume the forcing inputs are primarily the desired path, y_c, and driver remnant, n. The driver/vehicle system's lateral deviation will then be:

$$y_I = \left[\frac{1}{1 + Y_p^* G_s G_{\delta_w}^{\psi}}\right] Y_\psi G_s G_{\delta_w}^{y} (Y_y y_c + n) \qquad (5)$$

The effects of the splash and spray on the visual scene show up in the model as changes in the describing functions, Y_y and Y_ψ, and the remnant, n. Results of a recent study for the FHWA (Ref. 49) help relate the combined effects of adverse visibility and roadway delineation to changes in the driver/vehicle system guidance and control properties. Data were gathered in a fixed-base simulator and in a full scale car and van on the road. The results show that the major effects of a reduced visual segment appear to occur in the following order:

- Reduction of the lateral lane position gain, i.e., the describing function Y_y becomes smaller
- Increase in the driver remnant, n
- Reduction in the heading loop gain, Y_ψ becomes smaller

Physically, the reduction in lane position gain, with a lesser reduction in the heading loop, is tantamount to a reduction in sight distance of the eye point of regard. This is completely consistent with the "physically" reduced visual segment. As this is reduced, the ability to generate good closed loop path control decreases.

Remnant buildup can increase the lane position deviation in the same fashion as an increase in any other forcing function. Although the increased remnant due to adverse visibility is not well understood, it appears that more scanning is required of the driver than ordinarily takes place. To the extent that this is the explanation, the remnant must indeed go up, because scanning among various elements of the visual field for information is a well established cause for remnant (see Ref. 42).

In summary, considering these effects and Eq. 5, the lateral deviation due to visibility effects will be increased by remnant increases and by reductions in the describing function gains. The position and heading describing functions can become smaller than normal, but not necessarily together. In any event, the result would be a reduction in the effective open loop describing function Y_p^*. As this quantity decreases the closed loop system modifying term $[1/(1 + Y_p^* G_s G_{\delta_w}^{\psi})]$ increases. In fact, if $Y_p^* G_s G_{\delta_w}^{\psi}$ becomes small relative to 1, the driver/vehicle feedback control system becomes essentially open loop.

D. DRIVING SIMULATOR TESTS

A series of tests was run in the STI Driving Simulator early in the program. One purpose was to study the effects of visibility changes on driver performance, and to gain a further understanding of the important visual cues. Related to this was an interest in trying to identify spray cloud shapes and patterns which would minimize adverse visibility effects on the adjacent driver. Finally, we wanted to further develop candidate visibility and performance measures for use in the full scale splash and spray tests.

1. Simulator Setup

The test subjects were presented with a part-task simulation that provided the essential features of a truck splash and spray passing scenario. This included:

- An interactive truck image
- Visibility reduction due to a truck-related spray cloud
- Truck-induced aerodynamic force and moment disturbance to the simulated car lateral equations of motion

These features were incorporated into an extant automobile simulation (Ref. 50), which already displayed features in the ground plane such as delineation, intersections, and raised edge reflectors. The display electronics were expanded to portray an interactive truck with various spray-induced visibility reductions, as exemplified in Fig. 24. Aerodynamic forces and moments were imposed on the analog vehicle equations of motion, through the use of a minicomputer, causing the visual scene to be disturbed laterally. The truck was introduced on the simulator display, traveling at a fixed speed some distance ahead of the driver subject with prescribed spray cloud characteristics. The driver could overtake and pass the truck by controlling the speed and lateral position of the vehicle. Details are given below.

a. Visual Scene

The simulator mechanization of spray visibility reduction is illustrated in Fig. 25. It assumes a cylindrical cloud of length L_c, with an elliptical cross section density. The contrast of any element in the scene (road delineation, side of truck, etc.) is a function of both the viewing distance through the cloud and the density along the line of sight. A constant density along any given line of sight is assumed, which is determined by both the position of the driver and target element as illustrated.

Although somewhat simplified over real spray cloud conditions, this approach provides appropriate basic visibility characteristics. For example, visibility varies with the driver's lateral position relative to the truck, as well as the lateral position of all road elements. Also, visibility increases as the line of sight viewing distance through the cloud decreases due to the driver and/or visual elements emerging from the cloud. Thus, as the driver passes the truck he observes the visibility of down-the-road cues to first decrease, then increase.

a) Wide Low Cloud Obscuring Delineation

b) Narrow Tall Cloud Obscuring Truck

c) Large Cloud Obscuring Delineation and Truck

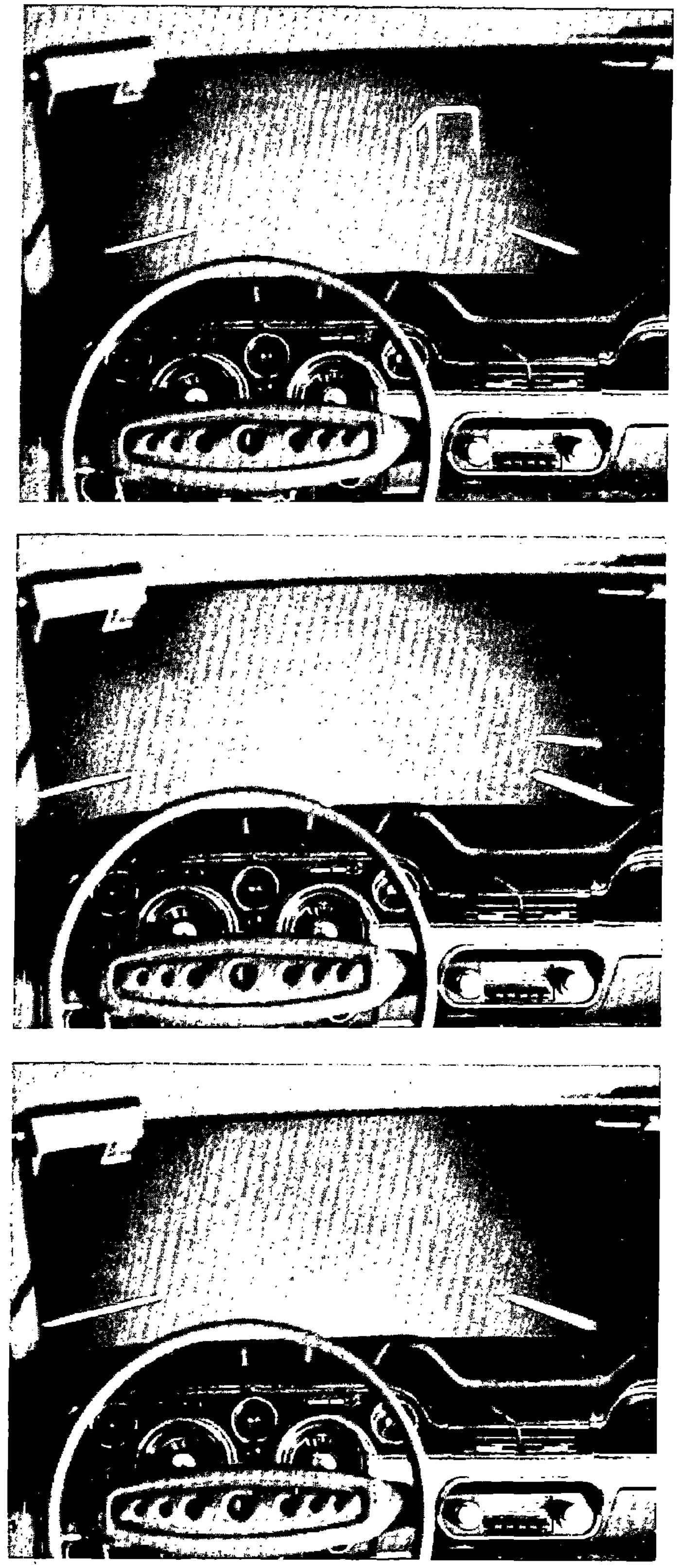

Figure 24. Example Visibility Conditions

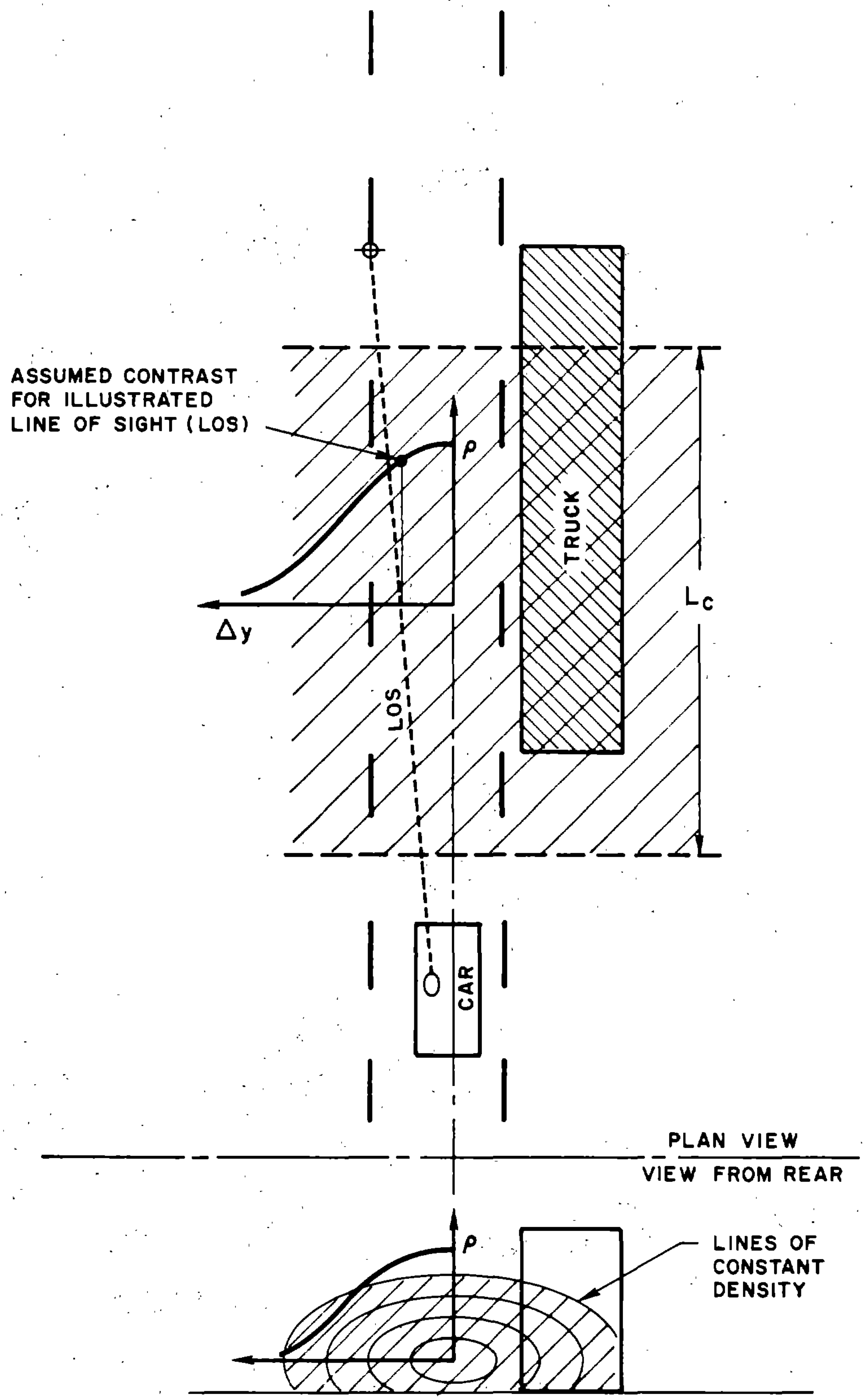

Figure 25. Cloud Density Distribution Simulation Scheme

The display circuitry was set up to allow for variation of: 1) the height and lateral position of the density ellipse; 2) the magnitude of the major and minor ellipse axes; 3) the density falloff as a function of distance from the ellipse center; and 4) the overall magnitude density of the cloud. With these variations we were able to simulate a wide range of generic cloud configurations in order to determine the consequences on performance and driver opinion of the loss of various visual cues.

b. Vehicle Dynamics and Disturbance

Linear two-degree-of-freedom equations were used to describe the basic lateral-directional (steering) equations of motion for the simulated car. Aerodynamic side force and yaw moments appropriate to a car passing a truck (see Article C, above) were provided by a minicomputer table lookup routine as a function of the relative longitudinal car/truck position displayed to the driver.

The aerodynamic disturbances used were patterned after the truck data shown in Fig. 20. They are a function of the average distance from the car to the truck, the relative wind angle, and the car and truck speed and configuration. The steady state components were deleted in the crosswind case for computational convenience. Three different disturbance levels were used in this experiment, two corresponding to a typical (1972 Chevrolet) station wagon with and without a −20 deg relative crosswind angle and a third representing a VW station wagon (bus) with the crosswind. The disturbance functions for the two crosswind conditions were derived from Ref. 2, and the vehicle differences were obtained by varying the equation of motion coefficients.

c. Measures

Driver behavior was measured using control and vehicle motion variables and subjective ratings. The variables were digitized on-line, and an algorithm was provided for taking ensemble averages over repeat runs. The mean squared value of the various variables was also integrated over a 25 sec interval. For example, in the case of the steering wheel signal, $\delta_{sw}(t)$, the integrated mean square value was given by:

$$\overline{\delta_{sw}^2} = \frac{1}{25} \int_0^{25} [\delta_{sw}(t) - \overline{\delta_o}]^2 \, dt \tag{7}$$

The $\overline{\delta_o}$ term was the average value of the first five samples (1.25 sec), used to take out any initial mean offsets. Typical simulator data illustrating the above measurements are given in Fig. 26. The time responses shown are ensemble averages over four replications, for a given driver subject and test condition. The yaw moment disturbance input is shown at the bottom of the figure. Lateral lane position provided an overall safety performance measure. Steering wheel activity was used as the measure of driver behavior. The forward speed was fixed, as if by autothrottle, at the desired value relative to the truck.

The "accident risk" and "task difficulty" rating scales used by the driver subjects were the same ones used in the subsequent full scale tests. It is shown in Section VI (Fig. 93). The subjects were formally instructed in the task, and in the rating procedure.

2. Experimental Design and Procedure

The two variables of most interest in this simulator study were visibility and aerodynamic disturbance. Relative speed and vehicle properties were also varied. Because it was a limited preliminary study, only certain combinations of visibility conditions, vehicles, and speeds were used, as discussed below.

a. Visibility

Five experimental spray cloud configurations were defined to selectively obscure various visual cues. A "narrow" cloud (N) obscured the truck, but left some delineation visible on the left-hand side. A wide cloud (W) was used to obscure only the bottom of the truck, leaving the top for visual reference but effectively obscuring all the delineation. Two different large clouds (M and L) effectively obscured both the truck and the delineation. Both large clouds were the same size, but one (M) was translated 20 ft (6 m) further to the rear of the truck than the other. Finally, the clear condition (C) provided a baseline against which to compare the various

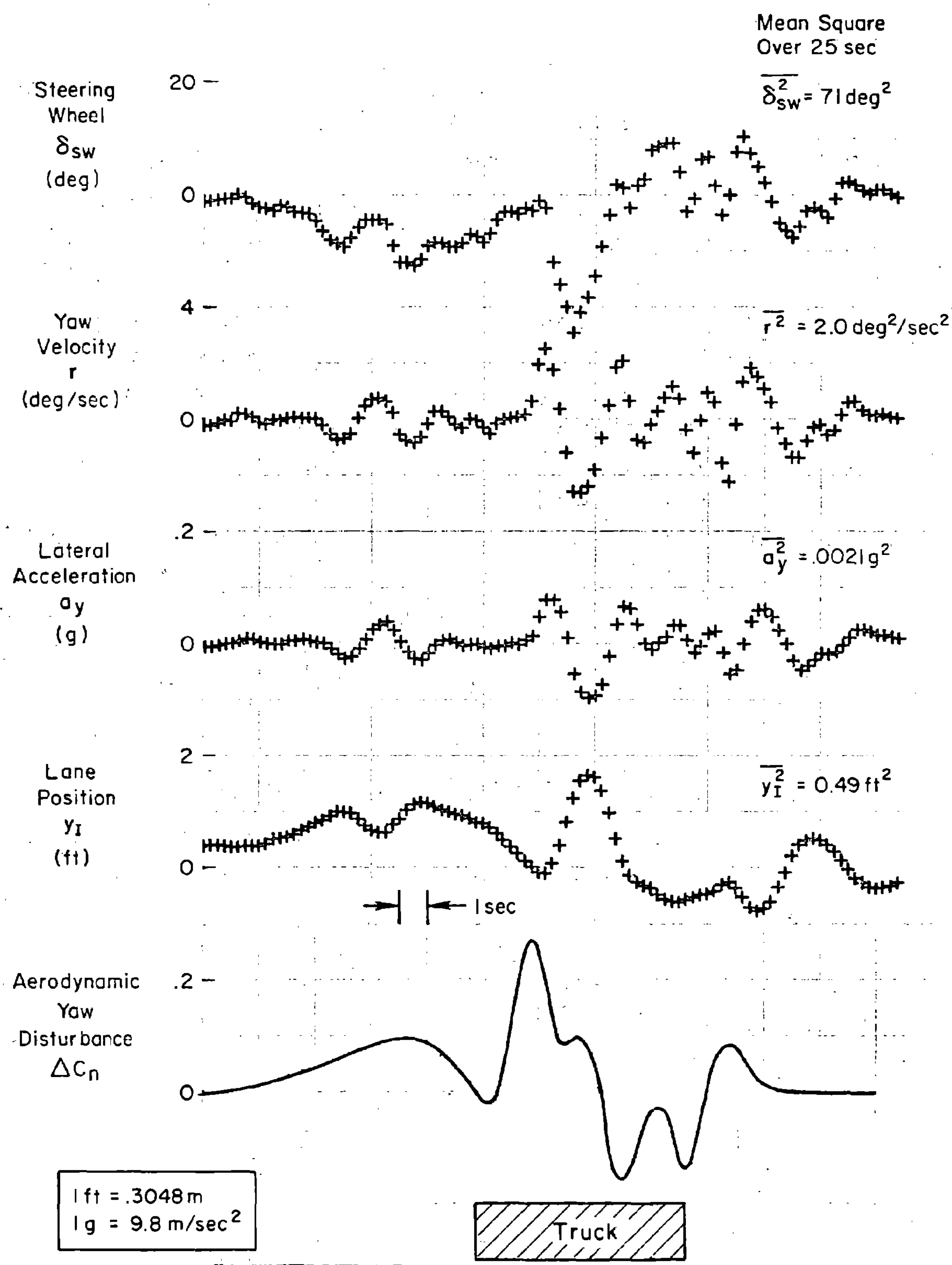

Figure 26. Typical Driving Simulator Data (Ensemble Average Over 4 Runs)

degraded situations. In each case, the visibility obscuration was a time varying effect with various cues disappearing and reappearing as the car moved past the truck through the spray cloud.

In order to quantify the visibility effect of each cloud condition, subjects were asked to indicate the point at which various visual cues were visible. The data were averaged over subjects and are summarized in Fig. 27 along with cloud dimensions and the aerodynamic yaw disturbance. Several effects are apparent from Fig. 27 which help interpretation of the performance and rating data. First, note that the back of the truck becomes visible within the clouds at a range of 45 ft (14 m), which is well in advance of the "high frequency" portion of the aerodynamic disturbance (i.e., the 10-20 sec portion). Truck and/or delineation cues are then available for the remainder of the run. In the case of the wide cloud (W) the top of the truck is always visible as the driver approaches; and for the narrow cloud (N), down-the-road delineation cues are available prior to reaching the truck and the "high frequency" disturbance region. Thus, the narrow and wide clouds may have a lesser effect on driver/vehicle system response.

b. Aerodynamic Disturbance and Speed

The magnitude of the aerodynamic disturbance was varied by varying the car/truck overtaking speed, the relative crosswind angle, and the vehicle dynamics. A larger disturbance was achieved when the relative crosswind was −20 deg. Car speed was varied to give two overtaking speeds, 5 and 10 mph (2.2 and 4.5 m/s) with the crosswind present. This variation had a combined effect on the aerodynamic disturbance. The higher speed gave a slightly higher dynamic pressure, increasing the disturbance magnitude. But, the exposure time was cut in half for the higher relative speed, and the frequency content of the time varying disturbance was doubled. On balance, the 4.5 m/s overtaking speed seemed to cause a slightly greater disturbance.

A higher level of disturbance was achieved by changing the vehicle dynamics and aerodynamics from the 1972 Chevrolet station wagon (W) to a VW bus (V). The simulated VW had somewhat slower handling response and a greater sensitivity to aerodynamic disturbance.

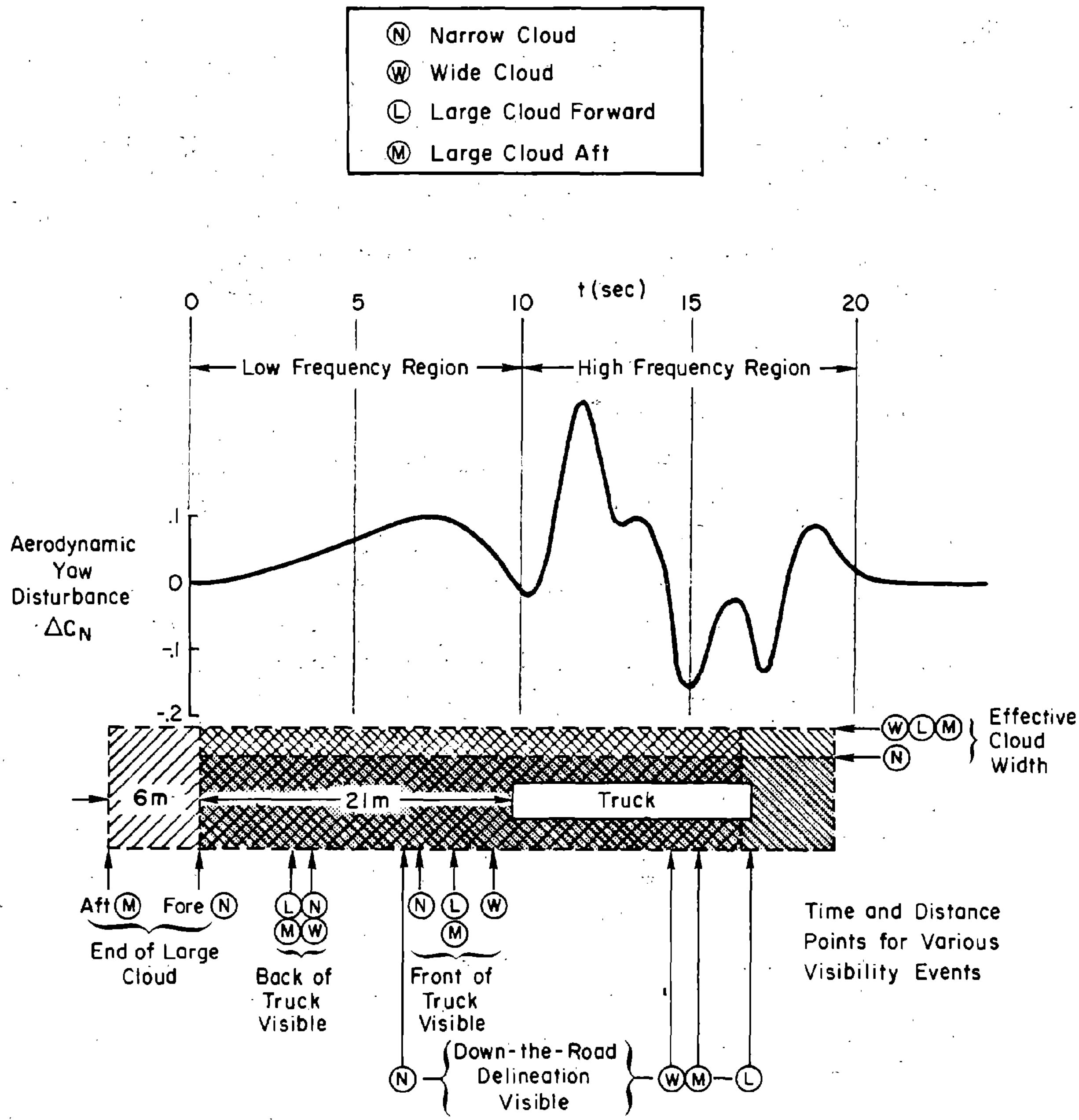

Figure 27. Comparison of Visibility Measures and Aerodynamic Disturbance at a 2.2 m/s Overtaking Speed for Various Cloud Conditions

The aerodynamic disturbance conditions were completely replicated for the large cloud visibility condition, while the visibility conditions were completely replicated for the station wagon dynamics and 5 mph (2.2 m/s) overtaking speed. Three disturbance conditions were replicated for both the clear and large cloud visibility conditions to study the interaction between disturbance and visibility. The test conditions are denoted by a code — for example, W1M means station wagon (W), at 5 mph (2.2 m/s) relative speed (1), and with the large cloud aft (M). A 10 mph (4.5 m/s) relative speed would use a code of 2.

c. Scenario and Driver Subjects

The scenario described to the subjects was that of driving on a four lane divided freeway (two lanes each way) on an overcast and rainy day. The truck speed for all conditions was fixed at 55 mph (25 m/s), so that 5 and 10 mph (2.2 and 4.5 m/s) overtaking speeds meant car speeds of 60 and 65 mph (27 and 29 m/s), respectively. In every case, the speed was fixed, to maintain a constant overtaking rate, in an effort to minimize intra- and inter-subject variability.

Four subjects were used in the formal experiments, and each experienced the same combinations of experimental variables. These drivers comprised the STI team of engineers who also drove in the full scale splash and spray tests, in order to give the maximum connection between the two program phases.

The conditions were grouped into two subsets by vehicle type — eight "wagon" conditions and two "VW" conditions. The two condition groups were presented to the subjects over three sessions. The first two sessions ran 2-3 hours each, and each included three to five wagon conditions. The two VW conditions were presented during a separate one-hour session to minimize the effects of different vehicle dynamics. Each of the two groups of conditions was presented to each subject in random order counterbalanced across subjects to minimize order effects.

The first minutes of each formal session served as a warmup. This was followed by a 15-25 minute session during which a subject typically made 8 to 9 truck passes for the given visibility and passing speed combination.

The first pass on which the condition's aerodynamic disturbance was given was treated as a warmup and was not analyzed with later passes. The aerodynamic disturbance on a given pass was one of three types. Besides the disturbance corresponding to the condition, there were two options: no disturbance, and a random gust input that produced forces and moments less than or equal to those of the aerodynamic disturbance. Both of the optional inputs were randomly interspersed in each session's runs to avoid the driver's responding to the truck-induced inputs in a programmed or anticipatory way. The average rate for the optional inputs was 3 in 10 passes (0.6 for the random gust; 2.4 for the no disturbance case). Thus, the largely unpredictable character of real-world disturbances was preserved. The no disturbance "placebo" passes also exposed any unrealistic anticipatory behavior in a subject's input.

Prior to the formal testing, each subject was trained about an hour on each of two days, before the day of the first formal session. The training timespan and regimen were individually adjusted to assure that the subject would be sufficiently accustomed to handling the simulated vehicle. Three of the four subjects had considerable prior experience in operating the driving simulator.

During preliminary analysis, one subject's data were found to be quite atypical. There were some possible overlearning trends in his data, since he had been used in preliminary testing, which may have resulted in unusual effects due to repeated exposure. This subject's data were dropped from subsequent analysis.

3. Results of the Simulator Experiments

Two kinds of measures are presented here, mean square values of the responses and subjective ratings. Each mean square value is for an ensemble of four 25 sec runs.

a. Performance Measures

Mean square values were computed for each variable in Fig. 26 over each of the four runs used to compute the ensemble traces. Several runs gave unusually high mean square values and were obviously outliers, so in each group of four measures the highest value was eliminated in the calculation. Then the average rms value of the remaining three numbers was computed. These data are plotted in Figs. 28-31.

In Fig. 28 rms steering wheel response as a function of various visibility and aerodynamic disturbance conditions is shown. It is apparent the driver steering response is a function of the aerodynamic disturbance (Fig. 28b), but is not affected by the change in visibility conditions. Note that the difference between W and V is due mainly to differences in the simulated vehicle aerodynamics and handling properties, and represents a steering gain effect.

The car's yawing velocity and lateral acceleration provide direct measures of the disturbance and the drivers' activity in attempting to correct for same, and thus might provide more sensitive measures of visibility effects. In Figs. 29 and 30 we see some evidence of visibility effects in the yaw velocity and lateral acceleration measures, but the effect is small. In Part a of each figure the motions increase somewhat as visual cues are progressively removed by the various cloud conditions. The worst condition is the large aft cloud (W1M) which is the same size as the large forward cloud (W1L) but translated 20 ft (6 m) further back behind the truck. Also, note in Figs. 29c and 30c that visibility effects seem to occur over a range of aerodynamic disturbance levels. The change between W and V, due to varying the vehicle dynamics, is not unexpected and reflects the increased aerodynamic sensitivity and slower handling response of the latter, noted before.

The primary driver/vehicle performance measure related to traffic safety is lateral lane position. In Fig. 31 rms lane position is plotted both as a function of visibility and disturbance conditions. Here we do not see any sensitivity to visibility condition, although the sensitivity to disturbance level for Vehicle V is still apparent.

It is interesting to note that lateral acceleration showed some small sensitivity to visibility, while the lane position measures did not. Lateral position is the second integral of a_y. Typically, any a_y effects which occur at higher frequencies are attenuated in the rms lane position variable.

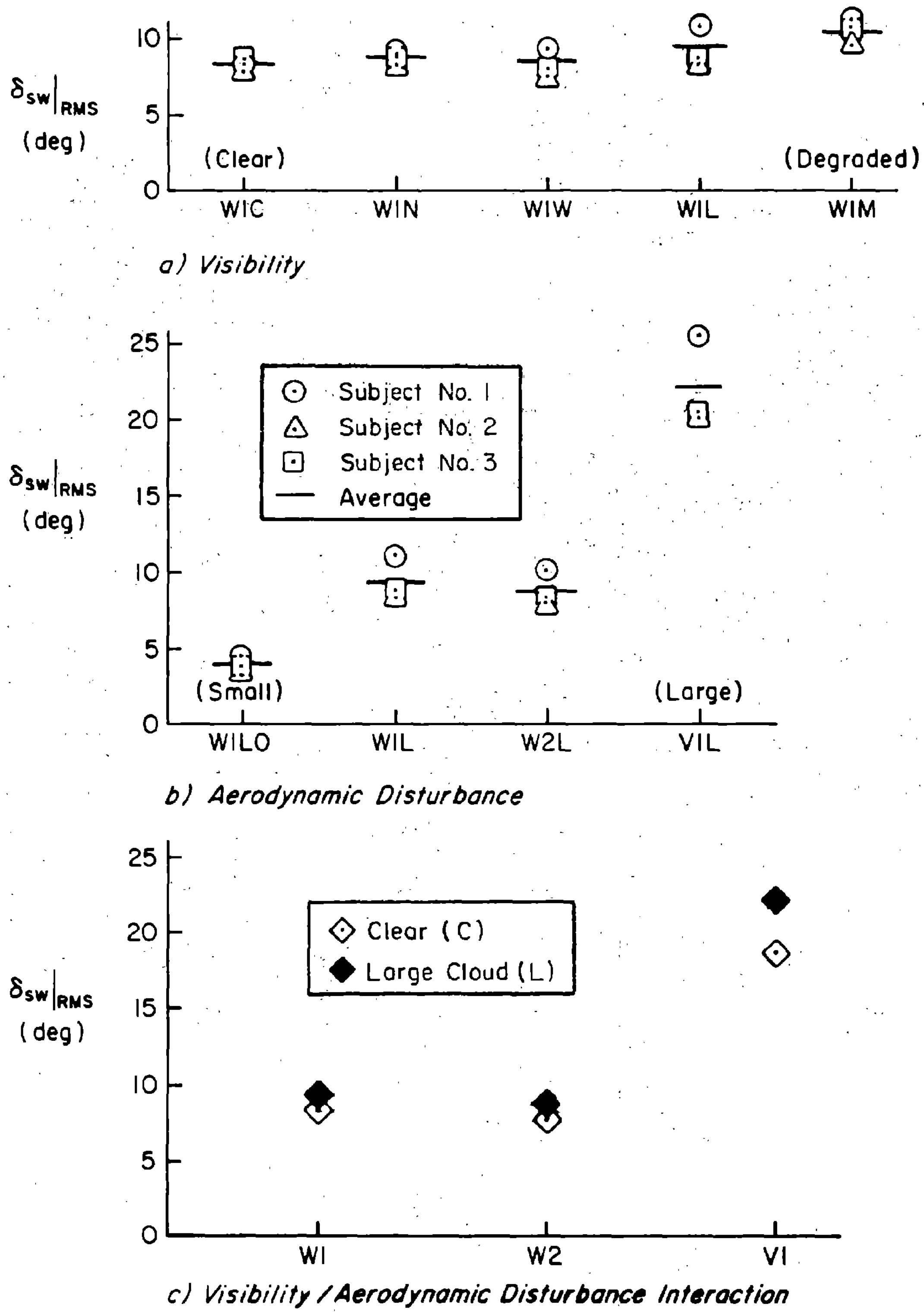

Figure 28. Variation in Steering Response with Visibility and Aerodynamic Disturbance Conditions

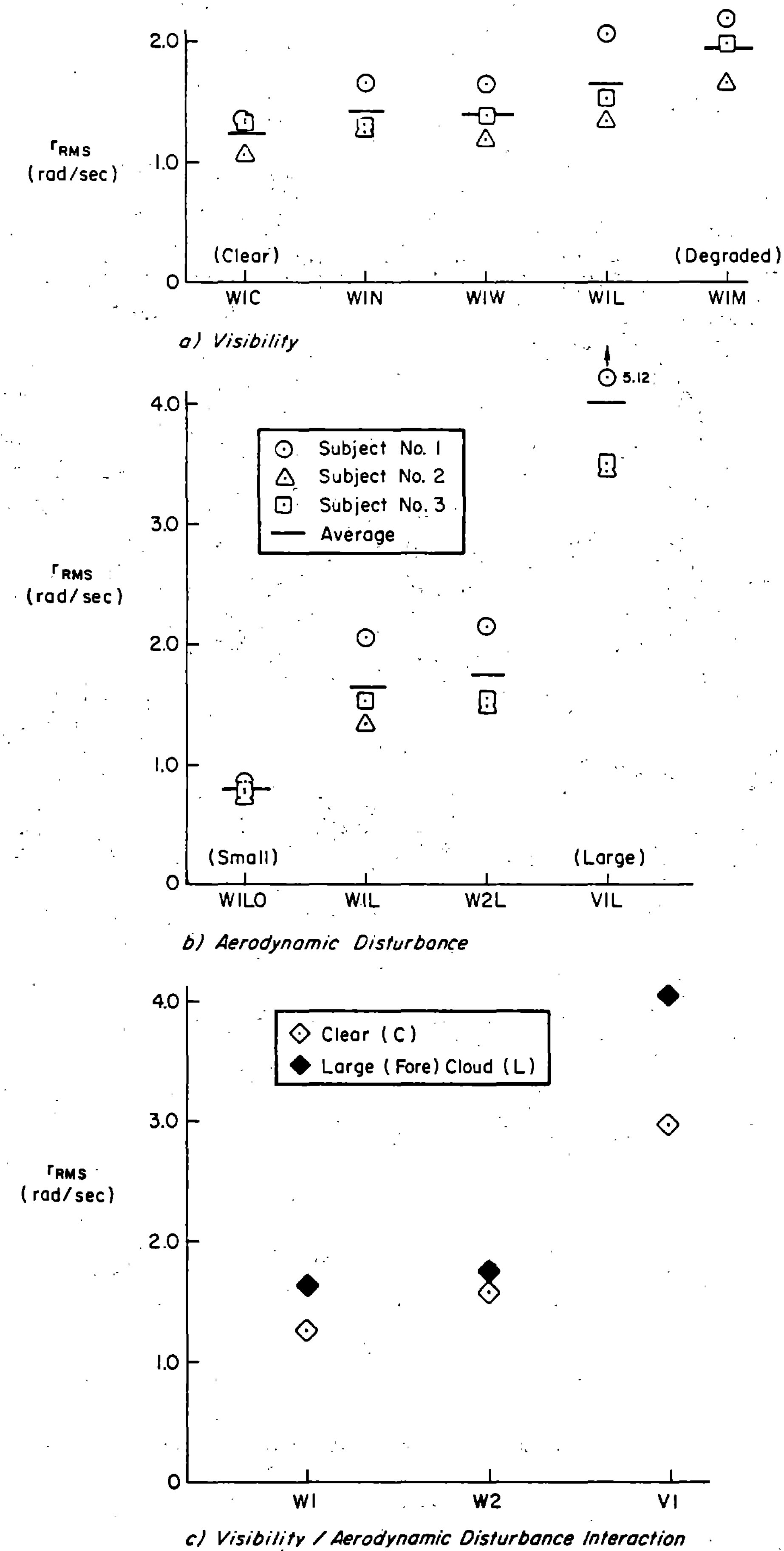

Figure 29. Variation in Yaw Velocity with Visibility and Aerodynamic Disturbance Conditions

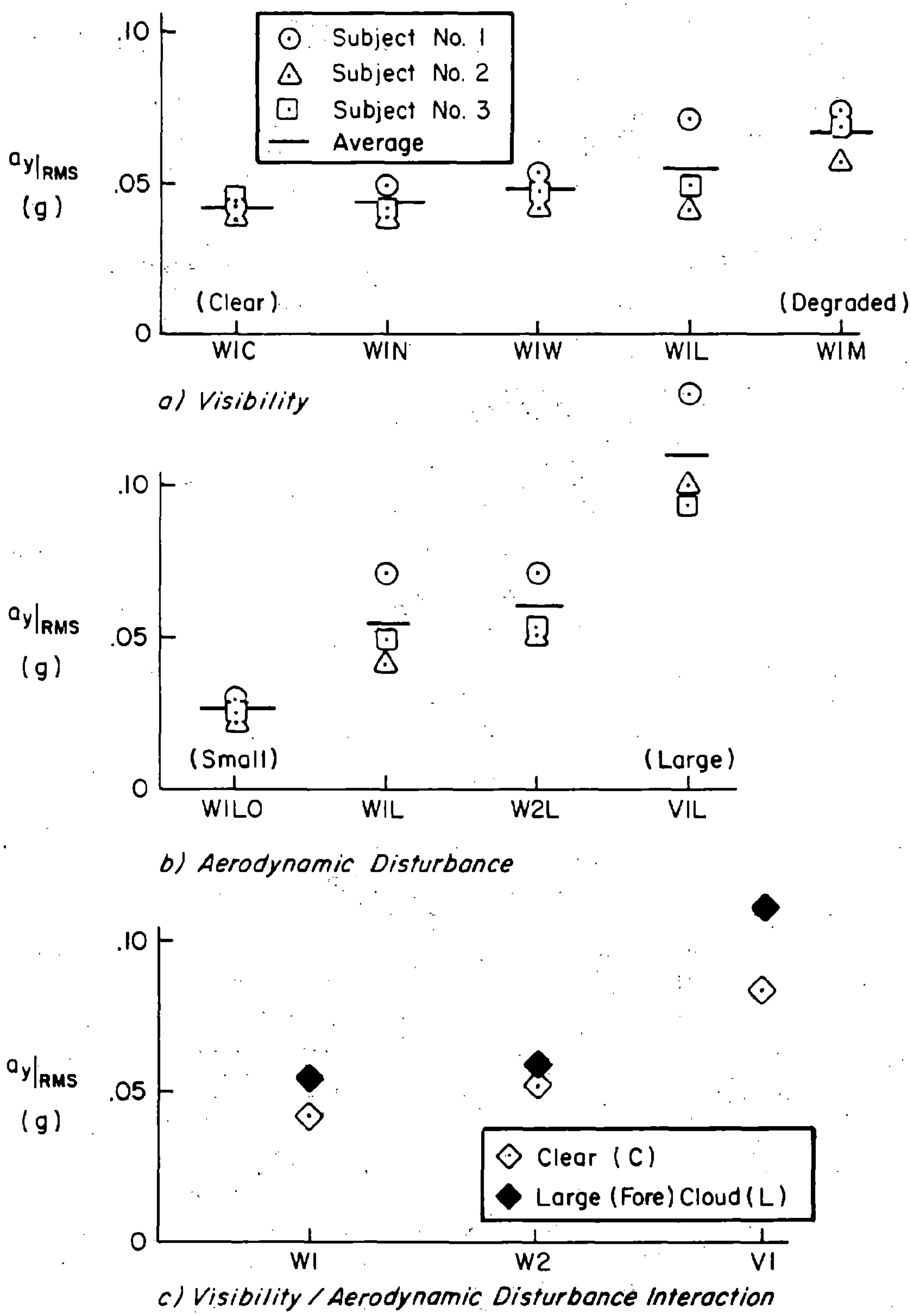

Figure 30. Variation in Lateral Acceleration with Visibility and Aerodynamic Disturbance Conditions

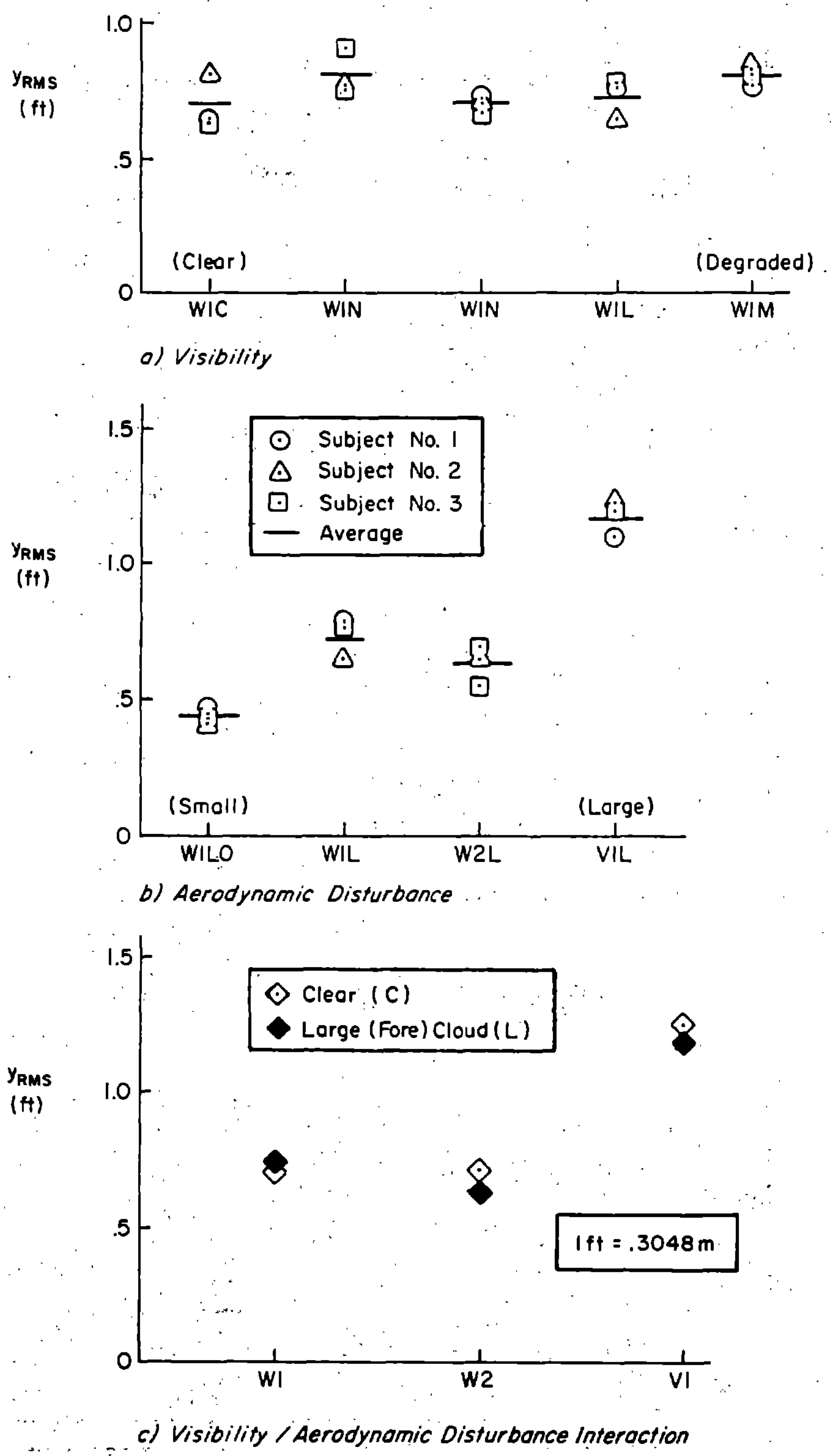

Figure 31. Variation in Lateral Lane Deviations with Visibility and Aerodynamic Disturbance Conditions

Overall, the effects of the visibility conditions tested here on driver response and performance were quite small, and a strict objective interpretation would not indicate significant safety-related performance changes. The driver opinion data given below provide for further insight into the experimental results.

b. Driver Ratings

Driver ratings were obtained from each subject on each experimental condition as noted above. The results of the "accident risk" rating averaged over subjects are illustrated in Fig. 32. Considering cloud visibility effects, only (Fig. 32a), the large aft cloud seems to cause a distinctly poorer reaction from the subjects than the remaining conditions. Ratings were quite sensitive to aerodynamic disturbance effects (Fig. 32b), and the magnitude of the aerodynamic effect seems to emphasize visibility differences as shown in Fig. 32c. "Task difficulty" rating results are plotted in Fig. 33. The results are similar to the accident risk ratings, with the possible exception of the aerodynamic disturbance variation in Fig. 33b which exhibits higher (worse) disturbance ratings for the low visibility cases than are seen in the accident risk ratings.

These driver ratings reflect the subject's impression of the relative severity of the various experimental conditions. They show a greater sensitivity than the previously discussed performance results. As would be expected, the driver's reaction seems to stem from what he perceives about the increased difficulty of the task, as opposed to significant changes in system performance measures.

c. Discussion

Referring back to the visibility measures in Fig. 27, some added understanding of these results can be obtained. First, the fact that the back of the truck became visible within the clouds at a range of 45 ft (14 m) aft, and that cues were then available for the remainder of the run, may account for some of the insensitivity of lateral lane position measures to visibility conditions. Also, the top of the truck was always visible

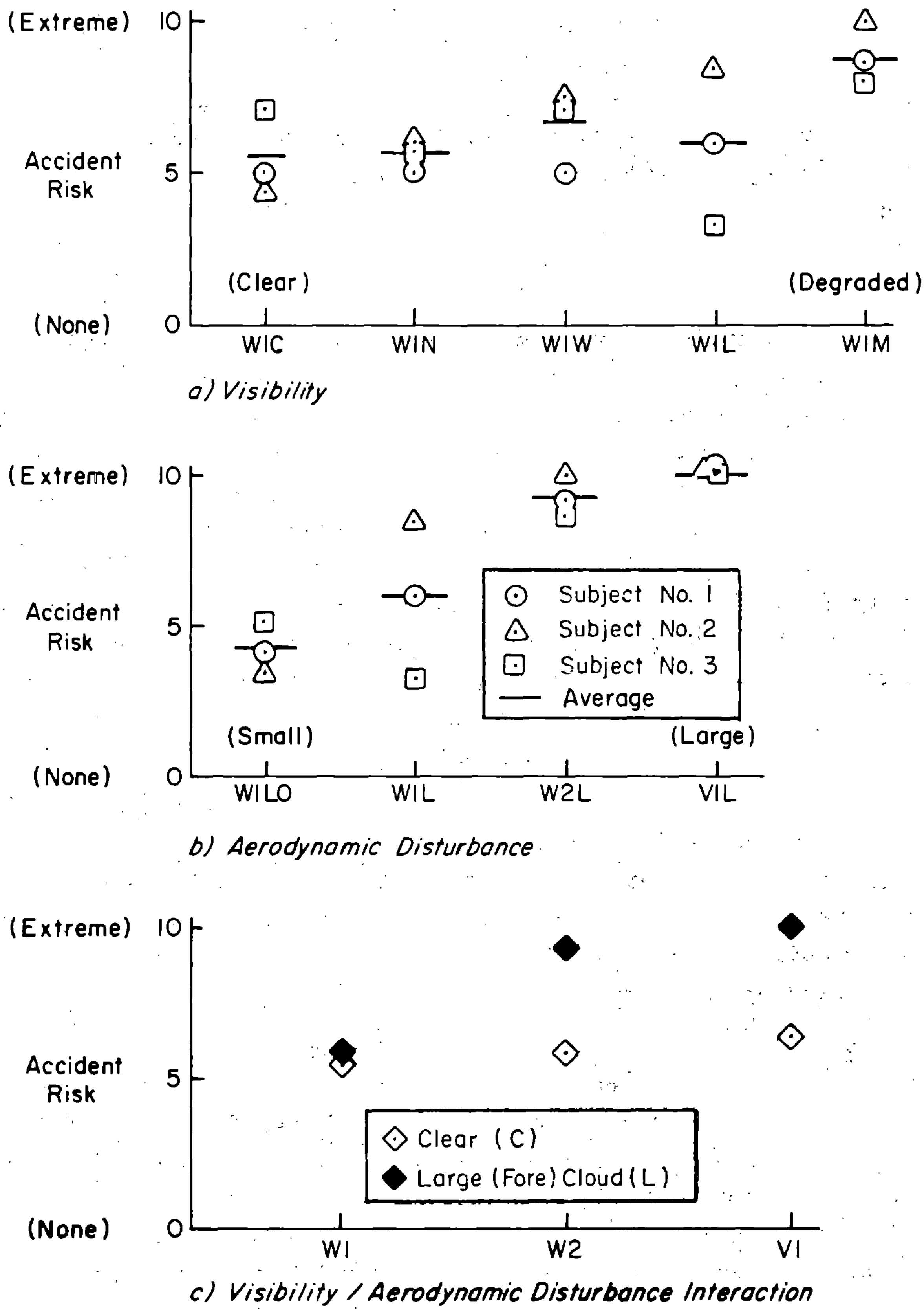

Figure 32. Driver "Accident Risk" Ratings for Various Visibility and Aerodynamic Disturbance Conditions

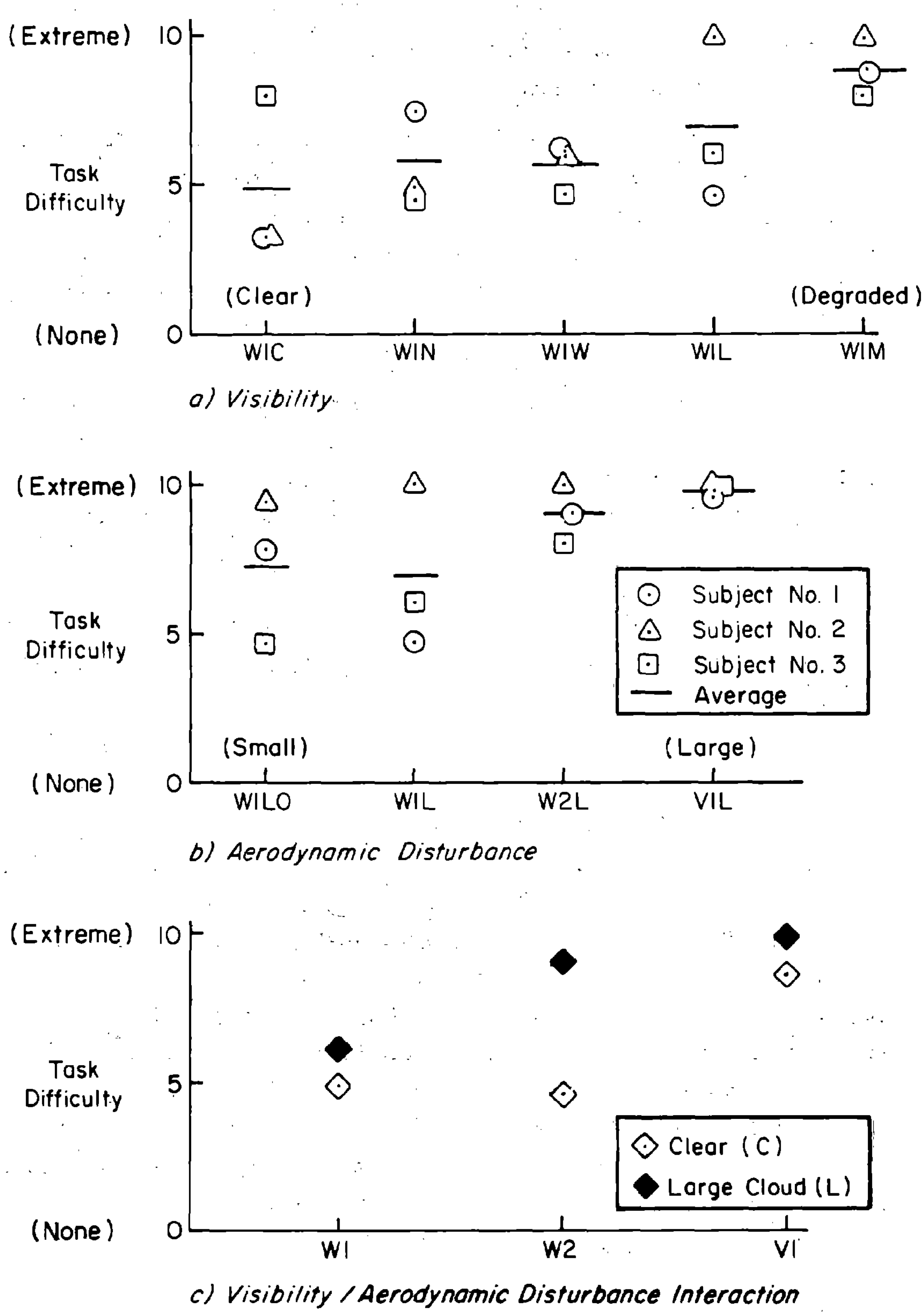

Figure 33. Driver "Task Difficulty" Ratings for Various Visibility and Aerodynamic Disturbance Conditions

with the wide cloud (W), and road delineation cues were available much of the time with the narrow cloud (N).

The visibility effect responsible for the performance and rating differences between the fore and aft positions of the large cloud warrants discussion, too. For all practical purposes the cues available to the driver would appear to be similar except for the beginning of the cloud. As shown in Fig. 27, the driver encounters the aft (M) cloud 20 ft (6 m) sooner, and at a 5 mph (2.2 m/s) overtaking speed this means his cues are degraded for about 2.7 sec longer. More to the point, if we calculate the difference between the point of cloud entry and the point where the back of the truck appears and provides additional cues, we find the following. For the forward large cloud (L) the driver travels 25 ft (8 m) or 3.4 sec at a 2.2 m/s overtaking speed, between cloud entry and first sight of the rear of the truck. For the aft cloud (M) the driver travels 45 ft (14 m) or 6.1 sec in the region of the worse cue deprivation. This is almost a factor of 2 to 1 between the two large cloud conditions. It is conceivable that the driver's opinion is degraded more for the aft cloud position because of this initial period of extended cue deprivation.

In summary, driver/vehicle system performance (lateral lane position) was not significantly impaired under any combination of conditions. Intervening performance variables including rms yawing velocity and lateral acceleration showed minor effects, and a significant influence on driver opinion was noted. Overall, the simulator results suggest that the spray cloud length behind the truck seems to have the most significant visibility effect. Means should be sought to minimize spray cloud length in the adjacent lane. Secondly, visibility effects are influenced by aerodynamic disturbance level, with higher levels giving more sensitive visibility effects. Therefore, means for reducing disturbance levels should be sought. To the extent that visibility and aerodynamic disturbance effects go hand in hand, simultaneous reduction of each should give significant improvement in driver subjective reaction.

SECTION IV

CANDIDATE DEVICES FOR MINIMIZING ADVERSE EFFECTS

To this point, the report has presented a number of background considerations, and reviewed the objectives and results of the preliminary analyses and experiments. Prior to detailing the more elaborate aerodynamic and splash and spray tests and results, this section describes the devices that were studied in model and full scale. Although, chronologically, the devices resulted in part from those experiments, it is logical to describe them in one place at the outset to avoid repetition and an unnecessary air of suspense.

As discussed in Section II, the focus in this study has been on devices fixed to over-the-road trucks, for purposes of alleviating or reducing their adverse aerodynamic and splash and spray effects on adjacent vehicles and motorists. Hence, this section concentrates on truck-mounted devices.

It begins by dividing the devices into categories for ease of description. Then the physical properties and function of each device are described, including a sketch or illustration of the prototype tested. This is followed by more detail regarding projected operational characteristics, costs, and possible disadvantages of a given concept. The cost information is used in the Section VII analyses.

A. CATEGORIES OF DEVICES

It is convenient to place the devices under consideration in three categories. The first includes devices that are directed mainly at reducing truck drag, with and without crosswinds. These devices may also reduce splash and spray because of their influence on the air flow around the truck. The second category is for aerodynamic devices which are intended to reduce spray by modifying the air flow which influences its formation and propagation. The third category includes collector devices whose purpose is to inhibit the formation of splash and spray, or contain it, at its source in the area of the wheels and the underbody structure. The latter category is, of course, more hydrodynamic in nature, while the first two are aerodynamic.

As has been noted, the aerodynamic drag of the truck and the flow perturbation are directly related — a streamlined truck giving less perturbation than a non-streamlined truck, in principle. However, drag considerations aside, near the front of the truck the air must be pushed aside by as much as 1.2 m, and this generally occurs very abruptly because practical truck design and regulations are not conducive to long tapered forebodies. In contrast, under crosswinds, the wake from the air flow direction is the important consideration — with less emphasis on the front of the truck. With regard to the disturbance created, considerations of practicality and diverse wind conditions indicate that practical basic truck streamlining generally will have little effect on the critical flow field about an adjacent vehicle. This was shown in Ref. 2 where the adjacent car disturbance results for a tractor nose and trailer forebody modification were nearly the same as for the unmodified truck.

B. DEVICES TO REDUCE DRAG

The devices studied in this category include cab (tractor) mounted drag shields, rounded corners on the semitrailer leading edges, dam below the bumper on the tractor, lateral lips on the semitrailer, longitudinal baffle under the semitrailer, and vertical splitter panel in the gap. While the first four focused on drag, the latter two were also expected to reduce spray, as well. These devices are detailed below.

1. Drag Shield Mounted on the Cab

As discussed in Section II, drag shields have received intensive study and they are widely used on over-the-road trucks at this time. They were included in this study for completeness, and in order that we would be considering configurations representative of current and future practice. It was also expected that they would complement other devices for alleviating splash and spray.

Two drag shields were used, the AeroVironment Aeroboost III and Uniroyal Air Shield No. 9037. They are sketched in Fig. 34, and a photo of the wind

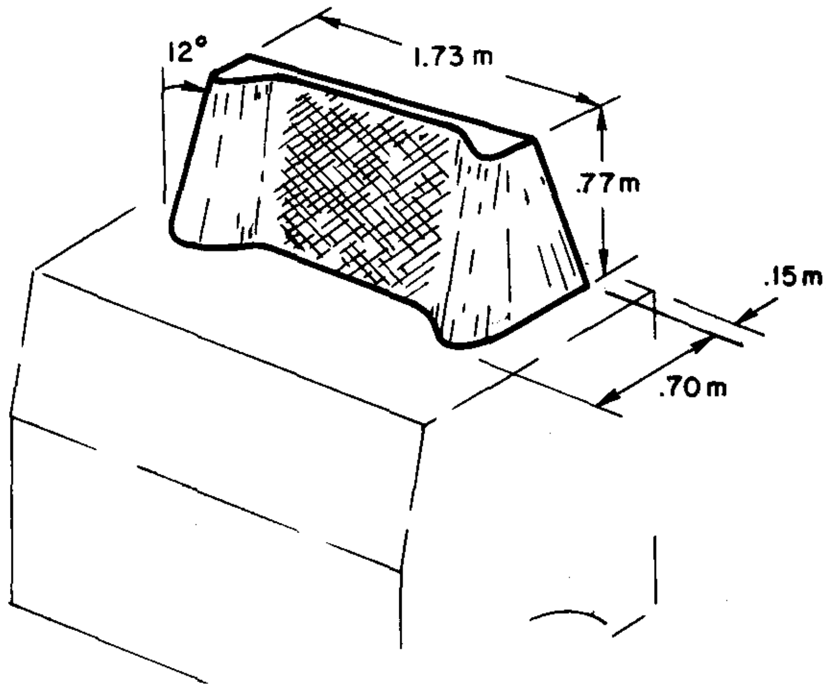

a) Aeroboost III

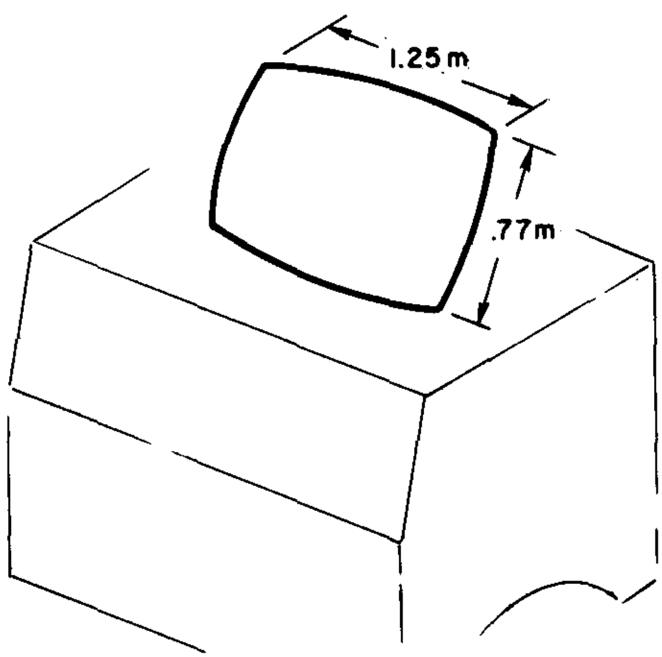

b) Uniroyal Air Shield No. 9037

Figure 34. Cab Mounted Drag Shields

tunnel model of the Aeroboost is given in Fig. 57, in Section V. The latter design features rounded edges and a porous face, intended to enhance its drag reducing properties in a crosswind. The Uniroyal has a more typical appearing curved plate shape. It was tilted back at a nominal angle of about 25 deg from the vertical.

The Aeroboost design was used in the wind tunnel tests, and in both series of full scale tests at Fort Stockton. The Uniroyal was also used in the second Fort Stockton series. Our results, and that in the literature, indicate that the functional properties of the two versions are about the same, insofar as the level of detail of this program is concerned. As a consequence, we do not distinguish between the two designs in the results of Sections V through VII.

The drag shield functions by smoothing the transition of air from over the top of the tractor towards the face of the semitrailer. Studies have shown that it is positioned properly when the flow streamline from the top of the shield (e.g., from a flow visualization test) just intersects the upper edge of the semitrailer. This is achieved by adjusting the fore and aft location of the shield, and by setting it at an angle sloping to the rear in the case of the Uniroyal type. Among other things, the drag shield reduces the amount of air flowing down in the gap, and striking the leading portion of the tractor duals. As a result it can influence the formation and propagation of spray, as demonstrated subsequently.

Drag shields can be installed on virtually any type of truck. They are most effective when the semitrailer face (or other truck body) rises considerably above the top of the cab. They are also more effective when the gap between the back of the tractor and the front of the semitrailer is relatively short.

2. Rounded Corners on the Semitrailer

Another proven method of reducing truck drag is to round the vertical leading edges of the van-type semitrailer, although it is not as effective as the cab mounted drag shield. A modest range of corner radii was studied in the wind tunnel tests, described in Section V. Although drag reduction is their main purpose, we also tried to determine whether there was any measurable change in the air flow which might influence spray formation and propagation.

The vertical leading edge radii studied in the wind tunnel were

- Square
- 12 in. (0.305 m)
- 24 in. (0.61 m)

with the basic truck. The standard corner radius was 12 in. (0.305 m), and that was used in the other wind tunnel tests with the 40 ft van.

This type of modification is limited to relatively boxy van-type trucks. Its main disadvantage is the reduction in cubic cargo capacity as the corner radii increase.

3. Dam Below the Tractor Bumper

Aerodynamic work with passenger cars suggested that a dam below the front bumper, to block the air flow under the COE tractor, might reduce the drag. This modification was tried on the basic truck in the wind tunnel tests, and a photo of the device is given in Section V (Fig. 58).

It proved unsuccessful, as the drag went up, and the aerodynamic disturbance of the adjacent car, near the front of the truck, was increased. This is undoubtedly due to the truck being relatively tall and having large ground clearance, whereas automobiles have a low profile and some of the displaced air can flow readily over the top.

4. Lateral Lips on the Semitrailer

Rounded lips or moldings were placed around the upper edge of the basic truck semitrailer across the front and along the sides. The intent was to reduce the drag in crosswind conditions, and it was moderately successful. Details and a photograph of the wind tunnel model of this device are given in Section V.

On a standard sized truck, this modification exceeds the current width limits. As with the rounded corners, described above, it is only pertinent for boxy, van-like vehicles with vertical sides.

5. Longitudinal Baffle Under the Semitrailer

A vertical panel was placed under the van semitrailer, down the underbody centerline from behind the fifth wheel to the rear axle. In full scale, the panel dropped from the underside of the floor down to about 6 in. (.15 m) from the roadway surface. In the model, the baffle ran the full length of the truck, including under the tractor. This baffle serves to inhibit the air flow under the truck in the crosswind condition. In so doing, it reduces both the truck drag and the splash and spray in the crosswind, as detailed in Sections V and VI. As shown in Ref. 2, the aerodynamic masking effect created thereby will increase the force and moment disturbance of an adjacent car downwind. The longitudinal baffle has no effect in still air, or with only a headwind, due to its symmetrical location on the centerline. To augment its splash and spray suppression properties, the longitudinal baffle could be covered with the grass-like material used in the Reddaway fenders, as discussed subsequently.

In the wind tunnel tests, this baffle was represented by a vertical metal panel under the truck model, as detailed in Section V. For the full scale tests, it was mocked up from plywood panels rigidly attached to the semitrailer underbody (see Section VI). This type of modification is pertinent to most truck configurations. Some semitrailers, such as drop beds and dry cargo tankers, are designed with reduced clearance which tends to have the same effect. Aside from the possible increase in the adjacent car disturbance noted above, the main disadvantages of this device seem to be its vulnerability to damage, reduced payload, and the need to maintain the desired ground clearance as the semitrailer load varies. The longitudinal baffle was also tested in conjunction with the gap splitter panel, described below.

6. Splitter Panel in the Gap

A vertical panel was placed in the gap, along the truck centerline, between the tractor and the semitrailer. In the wind tunnel it extended from the bottom of the van to the level of the tractor cab roof. In the full scale tests it extended from the bottom of the van to 8 ft (2.44 m) from the bottom, and it was attached to the back of the drag shield at the top front. Such a baffle tends to block the lateral flow through the gap in a crosswind. Although originally intended as a spray alleviation device, it also helps reduce the drag in a crosswind, particularly in combination with the longitudinal baffle, as detailed in later sections. Because it is higher up, and extends for a shorter distance along the truck, the gap splitter panel has less adverse effect on the aerodynamic disturbance of the adjacent car (as illustrated by the rectangular-block-in-the-gap data of Ref. 2). The splitter panel only influences the crosswind case, due to its symmetrical location on the truck centerline.

The splitter panel plus longitudinal baffle concept is sketched in Fig. 35. In the wind tunnel experiments, the splitter panel was represented by a vertical metal panel fixed in the gap, as detailed in Section V. For the full scale tests it was mocked up using a heavy, 22 oz (750 g/m^2), vinyl coated nylon tarpaulin, restrained by nylon cords and shock cords, to a metal framework flush mounted to the face of the semitrailer. The latter allowed easy hookup when the tractor was attached to the semitrailer, and permitted the rig to articulate and flex vertically.

The gap splitter panel principle could be adapted to virtually any tractor/semitrailer combination. By using a flexible material it can be configured so as not to interfere with air hoses and accessories, and yet accomplish its aerodynamic function. It is vulnerable to damage, and it could interfere with driver movement through the gap area. On the other hand, it need only be deployed during periods of inclement weather.

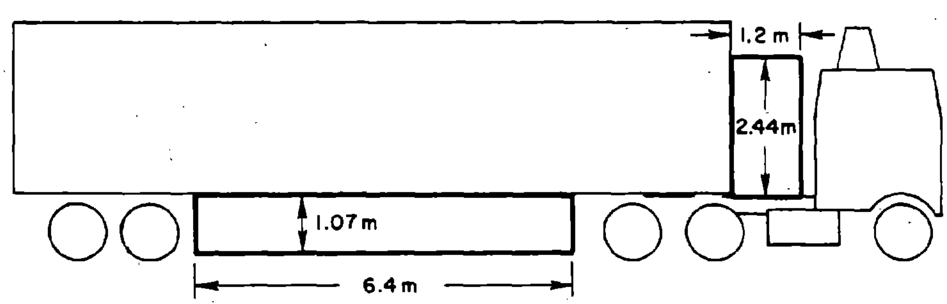

Figure 35. Underbody Baffle Plus Splitter Panel Concept

C. AERODYNAMIC DEVICES FOR SPLASH AND SPRAY

Devices studied which were intended to alleviate splash and spray by modifying the air flow around the truck include gap filler panel, partial gap panel, angled side vanes, and deflector foil mounted on the rear of the semitrailer. In addition, as noted above, the drag shield, longitudinal baffle, and gap splitter panel also contributed to the measured reductions in splash and spray. The three additional devices, noted first, are detailed below.

1. Filler Panel in the Gap

A flexible, nominally horizontal panel was placed in the gap between the tractor and semitrailer. It extended laterally the full width of the truck (van). The purpose of such a panel is to block the air flowing down in the gap, and to keep said flow from striking the tractor duals and contributing to the formation of spray. To some extent the gap panel is an alternative to a properly set drag shield for this purpose, since the latter also reduces the down flow in the gap. Because of its location just above the tractor frame and wheel area, its potential effectiveness is not reduced by the presence of a crosswind component. Since it serves to close the bottom of the gap, and cover the portion of the tractor wheels which are normally exposed, the concept is applicable to most trucks.

For the full scale tests the gap filler panel was mocked up using a heavy, vinyl coated nylon tarp. It was mounted at two different angles, as shown in Fig. 36. The tarp was rigidly attached to a metal framework on the face of the semitrailer, and connected to the back of the tractor by shock cords. This permitted the truck to articulate and flex vertically, and allowed the panel to work around the air hose mounts and other accessories.

As with the gap splitter panel, its main disadvantages would appear to be vulnerability to damage and interference with driver access to the gap area, yet it only needs to be deployed in wet weather.

In the wind tunnel, a horizontal metal plate was used, mounted above the frame rails, as detailed in Section V, in order to close off the bottom of the gap.

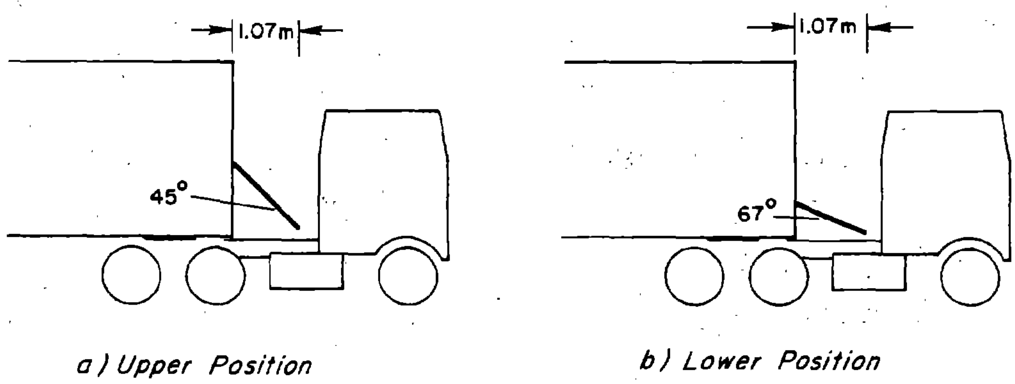

Figure 36. Gap Filler Panel Concept for Full Scale Tests

2. Partial Panel in the Gap

As a variation on the gap panel described above, a rigid panel was attached to the face of the semitrailer, extending at an angle part way across the gap. The bottom of the panel was even with the bottom of the semitrailer. Again, the purpose was to stop the air flow down in the gap from hitting the wheel area. The full scale test configuration is shown in Fig. 37. The prototype mockup was made from plywood fastened to a supporting metal framework. In practice, this panel might be fabricated from sheet aluminum, as part of the semitrailer structure.

The basic partial panel extended the width of the semitrailer. Two variations were tested, also, involving straight and angled end plates. These are sketched in Fig. 38. Their effectiveness against spray is detailed in Section VI. These end plates extended beyond the current width limit.

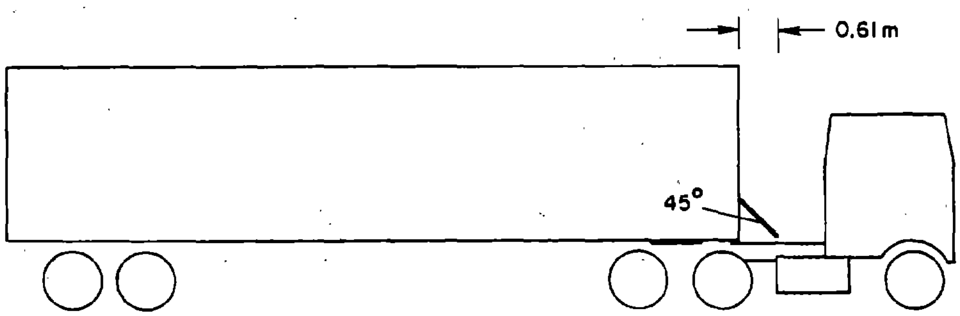

Figure 37. Partial Gap Panel Concept for Full Scale Tests

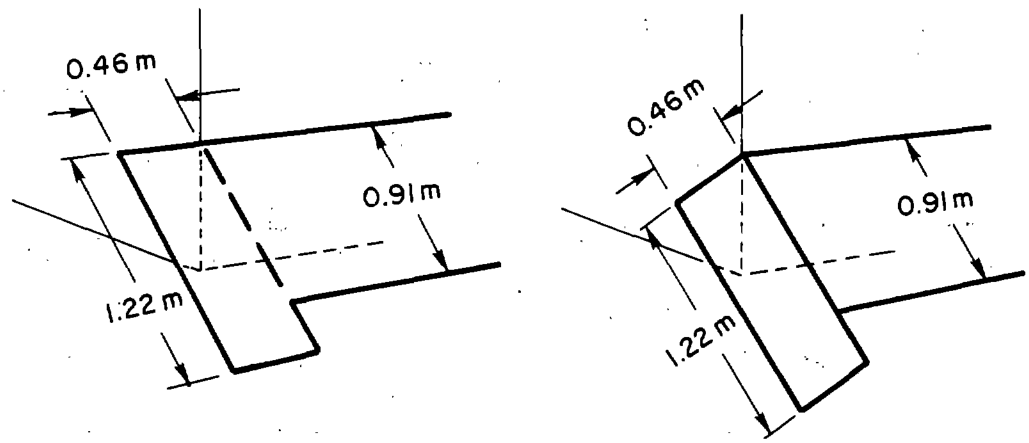

a) Straight *b) Angled at 45 deg*

Figure 38. End Plates for Partial Gap Panel

The partial gap panel is most pertinent to boxy, van-like semitrailers with their flat front face. Since it is a rigid, cantilevered structure, its size is limited by considerations of articulation, vertical flexing, and clearance of accessories. Such a design should be more durable than the tarp-like gap filler panel, and it would give better driver access to the area behind the cab. It is always in place and there is no need to deploy it.

3. Angled Side Vanes Around the Wheels

Vanes were installed ahead of and behind the tractor and semitrailer wheels on the basic truck. The objective of this device was to draw air in and around the wheels toward the center of the truck, thereby carrying the spray under the truck and away from the adjacent car. The vanes were 4 ft (1.22 m) high on the steered axle and 3.5 ft (1.07 m) high elsewhere, mounted vertically, with about 6 in. (0.15 m) roadway clearance at the bottom. The side view is drawn in Fig. 39 for the basic layout.

The plan view arrangement used in the initial full scale tests with the basic layout is shown in Fig. 40a. By contrast, the basic wind tunnel configuration included vanes ahead of the steered axle, but none ahead of the semitrailer tandems. A photograph of the wind tunnel model is given in Fig. 61 of Section V.

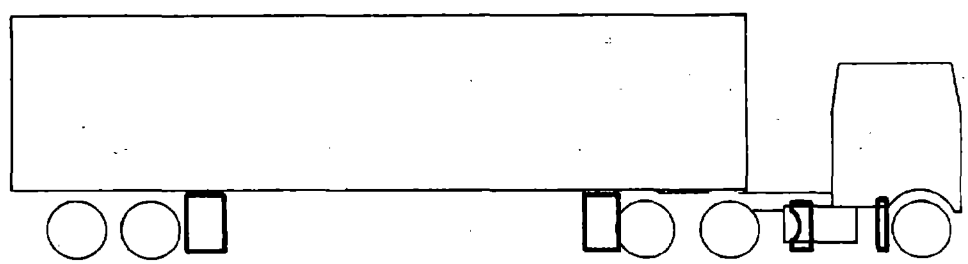

Figure 39. Angled Side Vane Concept, Side View

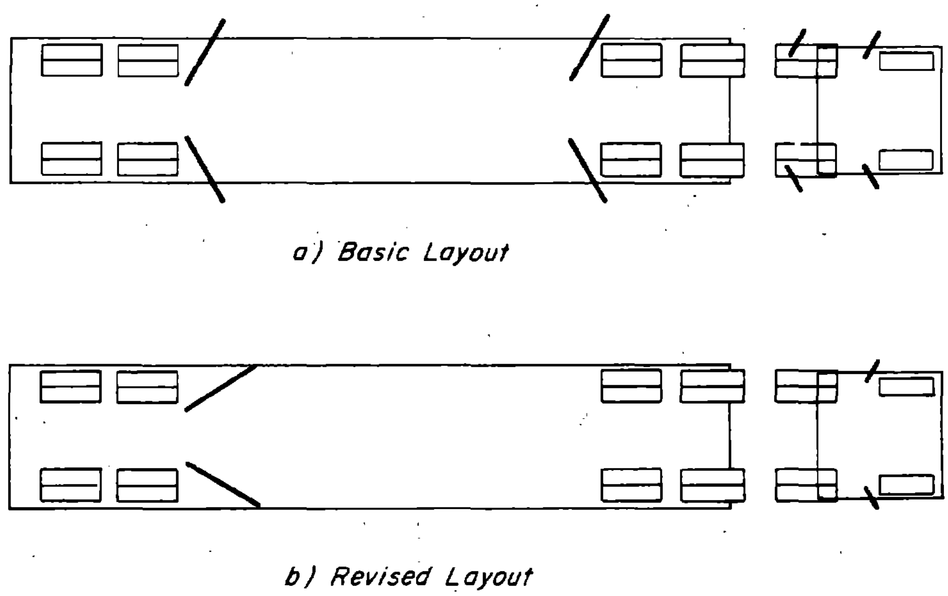

Figure 40. Angled Side Vane Concept, Plan View

In the initial basic layout, the vanes were set to protrude beyond the current legal width of the truck, in order to enhance their effectiveness in ducting the air flow. During the full scale tests several different sets of vanes and vane angles were used in an effort to optimize the spray alleviation performance. The final configuration is that shown in Fig. 40b. It features a more acute semitrailer vane angle relative to the centerline, and the end of the semitrailer vanes were set so as not to extend beyond the legal width limit. The splash and spray suppression properties of these vanes could be further enhanced by covering the faces with the grass-like material used in the Reddaway-type fender, discussed later.

In the wind tunnel the vanes were machined from aluminum and fitted to the truck model. The full scale test mockups were made of plywood. They were mounted against the underside of the semitrailer, and around the tractor wheels, and restrained from deflecting in the airstream by lightweight braided wires.

The vanes appear to be best suited to the van semitrailer with its flat bottom and relatively open underside, fairly high off the ground. This provides a pathway for the air, allowing it to flow in around the sides and out the rear of the truck. Their main disadvantages would include the added weight (reduction in payload), and possibly vulnerability; however, the latter should be no worse than that for conventional mudflaps, since they approximate an enlarged and reoriented version of the standard device.

4. Deflector Foil on the Rear of the Semitrailer

For the wind tunnel tests, an air foil was placed horizontally across the top rear of the semitrailer van. A photo of the device is shown in Fig. 64 of Section V, and it looked somewhat like a spoiler or the raised rear "wing" on a racing car. The idea of this device was to deflect air down at the rear of the truck, into the stagnation region at the base. This body of "still air" moving along with the truck is an area where spray can collect and intensify, and the hope was that the deflected air would tend to disperse it.

The device was not tested in full scale, due mainly to the fact that it increased the truck height substantially beyond the legal limit. Also, mounting the prototype would have required considerable modification to the semitrailer van.

The wind tunnel results showed that it did deflect the air, somewhat, with a small drag penalty (see Section V).

D. COLLECTOR DEVICES FOR SPLASH AND SPRAY

Devices studied which were intended to alleviate splash and spray by collecting and containing the droplets include the European fender, the Roberts fender, the Reddaway fender, and the "fuzzy truck" underbody. These four devices are described below. In addition, the longitudinal baffle and angled side vanes, described in previous articles, tend to collect splash and spray, particularly when coated with a mat-like material such as that used in the Reddaway fender.

As discussed in Section II, numerous fenders and other devices for suppressing splash and spray have been proposed, and some of these had been tested in prior studies. In the planning stage all the devices tested in prior WHI and SWRI tests (see Table 1 in Sec. II) were considered as potential candidates. The ones tested here were selected for combinations of several reasons including: prior results to demonstrate their potential for alleviation, lack of significant or inherent deficiencies, practicality, and availability of a working prototype set for test purposes. In some cases (e.g., the Roberts fender) several similar devices were available, and a representative example was chosen.

1. European Fender

A set of the molded rubber European-type fenders manufactured by Dunlop was included in the second Ft. Stockton test series. This provided an example of a currently legislated device for comparison purposes, and it gave a reference point from prior European research which lead to that design and associated requirements for its use.

An example of such a fender is sketched in Fig. 41. Fender Code PF-2071 was used. They cover both wheels in the dual pair, and they are long enough to cover a tandem set. In the November tests, they were attached to the underside of the van semitrailer of the basic truck (above the outside wheels) over the tandem duals at the rear, only.

Two sets of "quarter fenders" were mounted about the tractor tandem duals as sketched in Fig. 42. These were mounted on rods attached to the frame rails.

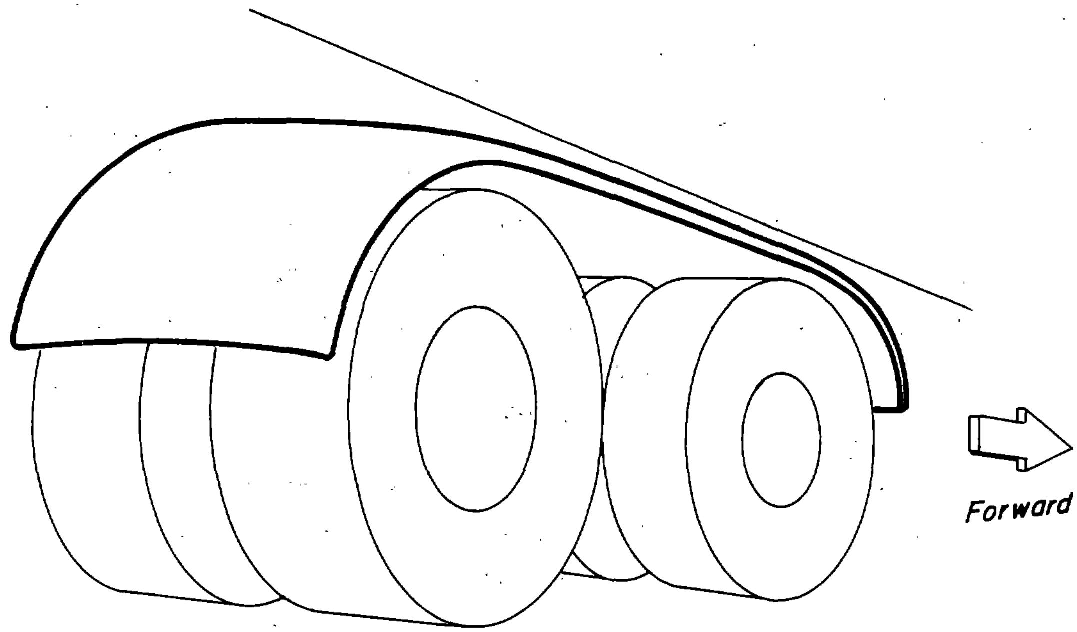

Figure 41. Sketch of European Fender (PF-2071)

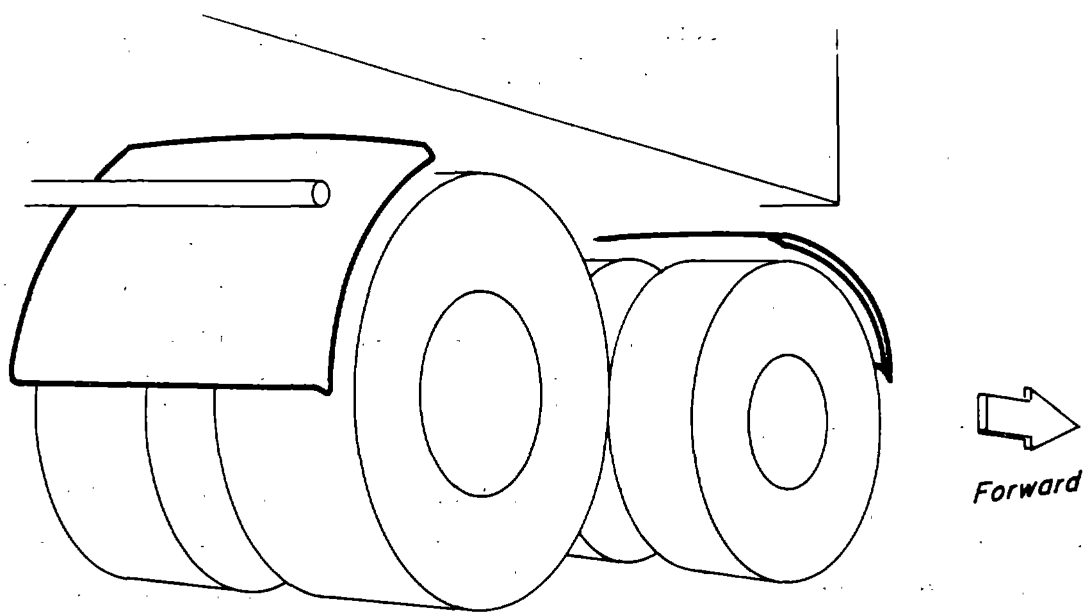

Figure 42. Sketch of Quarter Fenders on Tractor

The lips along the inside and outside edge, and the overhangs at the front and rear, of the PF-2071 are designed to trap the splash and spray from around the tires and the underside of the van. The overhang at the rear covers the rear tire from behind and avoids the need for a standard mudflap.

The fenders are relatively lightweight, yet rugged, because of their rubber composition design. The lips along the inside and outside edge only extend down about 80 mm, and this may limit their effectiveness in trapping the side spray from the top of the tires. This will also vary with normal load and suspension deflection. In addition, the water "collected" on the underside of the fender drips back onto the tire, recycling into that spray source.

These fenders appear to be adaptable to most trucks, requiring only a supporting surface or structure for mounting.

2. Roberts Fender

A set of Roberts fenders was installed on the basic truck for the full scale splash and spray tests. As described in Section II, these fenders have a corrugated and slotted inner liner which collects the splash and spray droplets and drains the water to the roadway inside the wheel.

The Roberts fender is sketched in Fig. 43. The water collects between the inner and outer liner, and runs down to the trough. The fenders were mounted to the underside of the semitrailer (for the rear tandem duals), and to lateral supports attached to the tractor frame rails for the tractor tandem duals. They were also placed inside the fender wells over the front wheels. They sit close to the tire, yet past experiments have shown little tendency for the tires and brakes to overheat. There are no lips at the edges so any side spray between the wheels and fenders can escape freely — which is generally undesirable.

The fenders are lightweight. The prototype version tested seemed relatively fragile, due perhaps to the temporary and jury-rigged nature of the test installation. These fenders are reported to be susceptible to clogging by mud, slush, and ice (under very adverse conditions). They

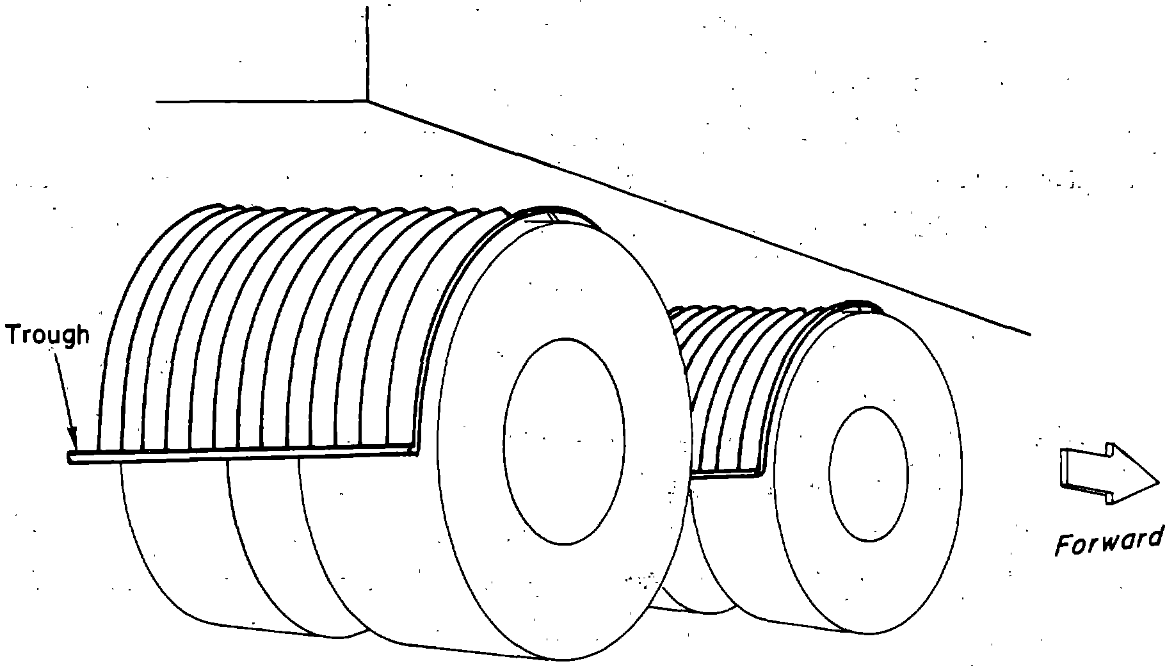

Figure 43. Sketch of Roberts Fender on Semitrailer

would also interfere with the use of tire chains because of their proximity to the tire.

The Roberts fenders are not well suited to installation on the 40 ft van semitrailer configuration, because there is little clearance between the top of the tire and the bottom of the box, particularly when loaded. They install more readily, and reportedly work better, on more open truck designs, such as liquid cargo tankers.

3. Reddaway Fender

Several variations on the Reddaway-type fender were studied in the full scale tests. These were based on the Spray Guard version of the Reddaway fender, manufactured by Monsanto Plastics and Resins Co. The basic material of this fender is an astroturf-like plastic "grass" material bonded to a hard plastic backing. This grass material collects and contains the splash and spray around the wheels, and it runs down through the grass and drips off the bottom onto the roadway.

The complete form of the Monsanto version of the Reddaway fender system is sketched in Fig. 44. There is a rear flap, similar in size and

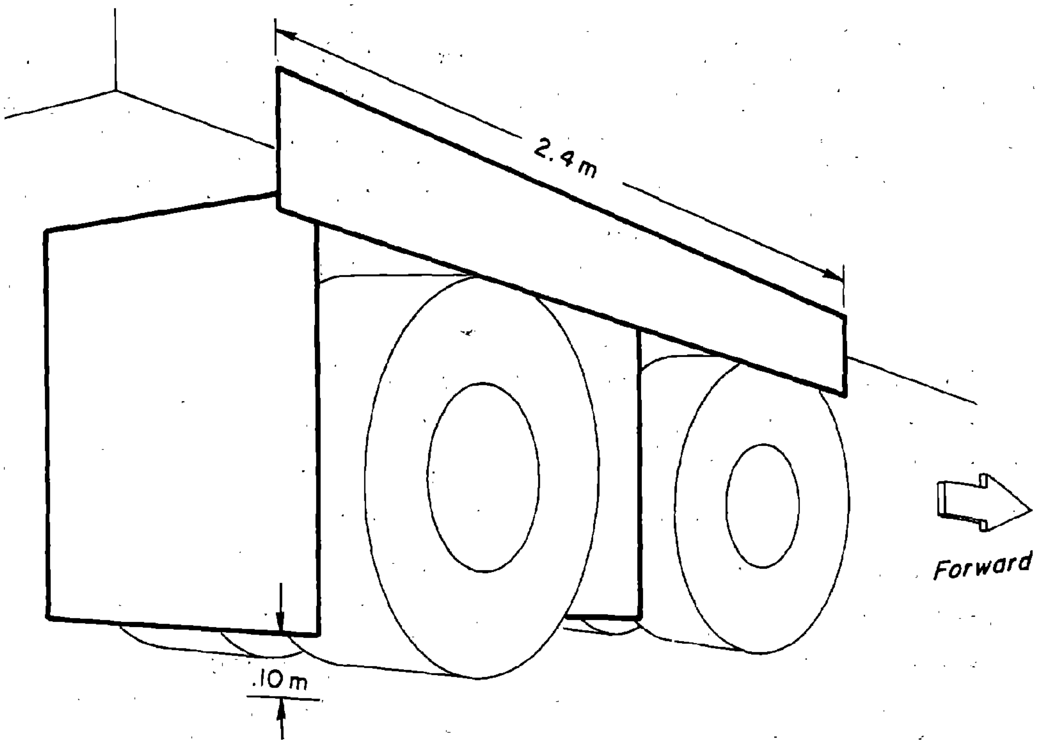

Figure 44. Sketch of Reddaway Fender

location to a conventional mudflap; a double-sided flap between the tandems; and a side flap which extends down over the outside upper edge of the wheels. The ground clearance of the vertical flaps was about 10 cm. As shown, the fenders attach to the semitrailer for both the tractor and semitrailer tandem duals. The grass-like liner is on the inside of these flaps, facing the tires. One variation tested had the double-sided flap between the tandems deleted, as discussed in Article E, subsequently. In that case, it may be desirable to extend the side flap downwards, in the area between the tandems, perhaps as a triangular-shaped extension.

The fenders are relatively light in weight. They can be mounted securely to the box-like van bodies. Their plastic and resin laminate construction makes them relatively rugged. Experience of the Oregon State Highway Department indicates that they can have a relatively long life (e.g., 5-10 years) and that they are not particularly susceptible to clogging by ice, snow, and slush. They are flexible, and bend out of the way — the side flap can be lifted up — so that the tires can be accessed for installation of chains, maintenance, and tire checking.

The Reddaway fenders appear to be best suited for installation on the 40 ft van semitrailer, or other configuration which allows a convenient support from which to hang the flaps. This contrasts with the Roberts fenders, for example, which are more rigid and are better suited to cantilevered and point mounting.

4. Fuzzy Truck

The three collector devices discussed above have been commercially developed and used over the road, including the Roberts fender on a limited basis. The fuzzy truck, on the other hand, was suggested as a result of the preliminary analyses and experiments on this program.

The fuzzy truck concept recognizes the collection and suppression properties of the grass-like material used in the Reddaway design. Instead of putting it on flaps, the idea is to attach it directly to the truck chassis and structure in the vicinity of the tandem duals. This includes the fuel tanks, frame, and stirrups on the tractor, the underside of the semitrailer, the landing gear and other structures in that area. The mudflaps can be replaced by fuzzy Reddaway-type flaps. This approach works on the principle that much of the spray is formed when the splash and spray from the wheels strikes the underbody and chassis of the truck, in the presence of relatively high velocity air. By having mat-like collector surfaces in these areas, this secondary spray formation could be inhibited and the water could run down through the grass and drip on the roadway. The material directly above the wheels would tend to offset the need for a side flap to contain the characteristic side spray from that area.

This collector concept is fairly lightweight. For purpose of our tests, the prototype was mocked up by spreading and attaching panels of the grass-like material (manufactured by Monsanto) over the underbody areas described above. One production concept would be to attach the "fuzz" directly to the surface, for example in the way that undercoat is sprayed on vehicles. In other words, it could be applied as a sticky undercoat, sprayed on, and then covered by suitable flocking material. This approach would have the advantage that it could be patched or replenished, periodically, as needed. In addition, it does not add any flaps or panels (other than the standard mudflaps) to interfere with access to the wheels, cooling air flow, etc.; and it does not modify the basic appearance or shape of the truck, which seems to be an important factor in obtaining driver or owner/operator acceptance of an alleviation device.

The fuzzy truck idea would appear to have general applicability to all types of trucks, since it does not require mounting points, bracketry, etc.

E. DEVICE CHARACTERISTICS AS PROTOTYPES

To support the cost-effectiveness analyses in Section VII, further description of the devices is needed related to cost and operational service properties. Estimates for these values have been made, and they are presented below. For the Reddaway-type fender, cost and service estimates are available from Monsanto which correspond to volume production lots. For the other devices, the estimates apply more to the fabrication and operational testing of pre-production prototypes.

As discussed previously, some of the devices were used in combination, and two or more variations of nearly every device were tested and analyzed. Accordingly, these variations are defined in Table 3. Then, the basis for the prototype cost information is discussed.

1. Summary of Device Variations

The aerodynamic and splash and spray devices, and variations thereto, are summarized in Table 3. Most of these were tested in the second Ft. Stockton test series. They have all been subjected to comparative analysis. In each case, the device or modification is to the basic truck, consisting of a 3 axle COE tractor plus a 40 ft van semitrailer. It is denoted by T1 in subsequent data tables and run logs.

Four versions of the angled side vanes are listed in Table 3, including the basic and revised vane layouts from Figs. 40a and 40b, V1 and V4, respectively. Configurations V2 through V4 have the drag shield added. V3 is an intermediate version, with the vanes behind the tractor tandems deleted from the basic configuration.

TABLE 3. SUMMARY OF DEVICES

Drag shield		
	D1	Drag shield
Longitudinal baffle		
	L1	Longitudinal baffle + gap splitter panel + drag shield
	L2	Longitudinal baffle + gap splitter panel
	L3	Longitudinal baffle
	L4	Longitudinal baffle + drag shield
Gap filler panel		
	G1	Gap filler panel in upper position
	G2	Gap filler panel in lower position
Partial gap panel		
	P1	Partial gap panel
	P2	Partial gap panel + straight end plates
	P3	Partial gap panel + angled end plates
Angled side vanes		
	V1	Angled side vanes (basic layout)
	V2	Angled side vanes (V1) + drag shield
	V3	Like V2, less vanes behind tractor tandems
	V4	Like V3, less tank vanes and with trailer vane angles reset
European fender		
	E1	European fender with grass-like liner
	E2	European fender (basic)
Roberts fender		
	R1	Roberts fender
	R2	Roberts fender + drag shield
Reddaway fender		
	M0	Reddaway fender system + drag shield
	M1	Reddaway fender system
	M2	Like M1, less flaps between the tandems
	M3	Like M1, grass forward only
	M4	Like M2, less side flaps
	M5	Like M4, less rear flaps on tractor
	M6	Like M2 + drag shield + longitudinal baffle
	M7	Like M2 + drag shield
Fuzzy truck		
	F1	Fuzzy truck
	F2	Fuzzy truck + drag shield
	F3	Like F2 + longitudinal baffle

The European fender was tested in its basic version (E2), and with the Reddaway-type material lining the inside. The latter was provided by Monsanto, and was the same as the material used to mock up the fuzzy truck.

The complete Reddaway fender system (M1) is that sketched in Fig. 44. Adding the drag shield was generally helpful for any version (viz., M0, M6, and M7). Versions M2 and M3 involve variations in the flap between the tandems, M3 having the grass-like material on the forward facing side only. Although not tested in full scale, configurations M6 and M7 were hybridized from the data and included in the cost-effectiveness analysis.

The fuzzy truck configuration, F3, also evolved during the data interpretation and analysis phases, when it became evident that their attributes were complementary.

2. Cost Estimates

Monsanto has provided preliminary estimates for the costs and installation of the Reddaway-type fender. In large commercial quantities they would expect the price range of the Spray Guard components to be in the ranges:

Single sided flap	\$1.25-1.75/ft^2 (\$0.13-0.19/m^2)
Double sided flap	\$2.75-3.25/ft^2 (\$0.29-0.35/m^2)
Grass material, 1 m × 15 m	\$0.75-0.85/ft^2 (\$0.08-0.10/m^2)

The single sided flap stock would be used for the front, rear, and side flaps around the tandem duals. The double sided flap is intended to go between the duals, if used, as discussed above. The grass-like material was used to create the fuzzy truck as a prototype, and it could be used to coat the longitudinal baffle, angled side vanes, etc.

Estimates by Monsanto for installation (in manhours per pair) of the Reddaway components are as follows:

Replace current trailer back flaps	1
Replace current tractor back flaps	1
Install side skirts	1.5
Install tandem flaps	1.8
Install steering flap	1.5-2.5

Equipping more than one truck is estimated to reduce these costs 25-35 percent. These estimates are based upon their experience at the second Ft. Stockton tests and equipping trucks for field testing during the first part of 1978.

Preliminary estimates of the costs of prototype version of the other combinations of devices studied have been made, and these are summarized in Table 4. The drag shield is, of course, a production item. Fabrication costs of the other devices would be expected to reduce somewhat, in going from prototype to production lots. In each case, the salvage value has been assumed to be zero. The drag shield is assumed to last 10 years with no salvage value, i.e., a cost of $41/year. The cost per man-hour of installation and maintenance has been assumed to be $15 in Table 4, and recurrent and replacement costs have not been discounted to present (initial) value. The computed cost per year is shown in the last column for comparison purposes.

The device codes were defined in Table 3. The longitudinal baffle, L3, is a series of panels, under the semitrailer, assumed to be made of double-sided (and backed) Spray Guard material. L2 consists of L3 and G1, where the latter is a vertical tarp in the gap. Configuration L1 consists of L2 plus the drag shield. The service lives of L1 and L2 are assumed to be limited primarily by the life of the tarp panel in the gap. The cost of L2 was obtained by adding 1/5 or the life cost of L3 to the fabrication cost of G1, and then showing the other costs of G1. Similarly, L1 costs are obtained from L2 costs, with 1/10 the life cost of the drag shield added to the fabrication cost. The maintenance costs of the longitudinal baffle are assumed to involve mainly cleaning the grass and repairing tears.

The partial gap panel is assumed to be a rigid aluminum panel attached to the face of the semitrailer with suitable mounting bracketry. The shape is assumed to not affect the cost. The service life is expected to be limited by wear and tear.

The gap filler panel is made of heavy fabric or tarpaulin. G1 and G2 denote different angles relative to the horizontal. The tarp is assumed to be retractable to the face of the semitrailer, much like a window shade, and hooks are required on the tractor. A nonretractable version would have a slightly lower initial cost, but it would be more vulnerable to damage during

TABLE 4. ESTIMATED COSTS FOR SELECTED PROTOTYPE DEVICES

DEVICE		EST. SERVICE LIFE (YRS)	FAB. COST ($)	INSTAL-LATION (MAN-HRS)	MAINTENANCE NO. OF ACTIONS	MAINTENANCE MAN-HRS. EACH	LIFE COST ($)	COST PER YR. ($)	REMARKS
Drag shield		10	350	4	0		410	41	Adjustable
Partial gap panel	P1	5	170	4	0		230	46	Aluminum
	P2	5	170	4	0		230	46	Aluminum
	P3	5	170	4	0		230	46	Aluminum
Gap filler panel	G1	1	170	3	4	2	335	335	Tarp
	G2	1	170	3	4	2	335	335	Tarp
Longitudinal baffle	L1	1	417	3	4	2	582	335	
	L2	1	376	3	4	2	541	335	
	L3	5	310	8	20	2	1030	206	Grass panels
Angled side vanes	V1	5	525	8	20	1	945	189	
	V2	5	730	8	20	1	1150	230	
	V3	5	555	6	20	1	945	189	
	V4	5	468	4	20	1	828	166	
Fuzzy truck	F1	5	285	4	20	1	645	129	Grass
	F2	5	490	4	20	1	850	170	Grass

hookup and storage. Also, it cannot be stowed as conveniently during periods of good weather. Service and maintenance would involve such things as tears and cleaning the retractor mechanism.

The angled side vanes are envisioned to be rigid panels faced with the grass-like material. As summarized in Table 3, V1 is the basic set of angled side vanes at all wheels. V2 adds the drag shield. V3 deletes the vanes behind the tractor tandems and the result is assumed to cost 2/3 of V1 plus the drag shield. V4 deletes the tank vanes, and costs 1/2 of V1 plus the drag shield. Maintenance is expected to involve mainly cleaning and repairing the grass.

The fuzzy truck configurations are described in Table 3, also; F2 includes the drag shield. Maintenance is expected to involve cleaning and repair of tears or replacement of a coating applied to the chassis and structure.

SECTION V

AERODYNAMIC TESTS AND RESULTS

The purpose of the wind tunnel tests was to provide the basic aerodynamic flow and force and moment data for use in other phases of the program. Specifically, the wind tunnel tests:

- Described and measured wake flow details and obtained limited pressure data for use in disturbance and splash and spray propagation analyses
- Looked at the effect on air flow and disturbances of selected remedial devices
- Measured forces and moments on trucks, with and without devices
- Provided additional disturbance measures on an adjacent vehicle for a variety of truck configurations

The general approach was to make selected measurements, guided by existing data and our experience in similar previous studies (i.e., Refs. 2, 3, 29, and 31). The cost of wind tunnel proparation and testing precluded a blanket approach with an all-inclusive, systematic test matrix. Maximum use was made of existing wind tunnel models and hardware.

The wind tunnel tests were made in two separate series, each involving a different facility. The initial series of experiments was carried out at the California Institute of Technology, GALCIT, 10 ft (3.1 m) diameter wind tunnel. This involved force and moment measurements on several truck configurations and a corresponding series of flow visualization measurements. The second set of tests was conducted at the Northrop 7 × 10 ft (2.1 × 3.1 m) Low Speed Wind Tunnel. This included truck plus adjacent disturbed vehicle tests plus some additional flow visualization experiments.

The first article in this section describes the wind tunnel facilities, models, and test procedures. This is followed by a description of the air flow data and example results. Article C summarizes the truck drag measures, used later in the cost-effectiveness analyses of Section VII. The last article presents data to show the forces and moments on the adjacent car for various truck configurations.

A. WIND TUNNEL FACILITIES, MODELS, AND TEST PROCEDURES

The features of the wind tunnels and models are described below. Test procedures are also treated.

1. GALCIT and Northrop Wind Tunnels

The GALCIT wind tunnel has a 10 ft (3.05 m) diameter cross-section in which a ground plane is mounted. An external strain gauge balance is located directly beneath a yaw table centered in the ground plane. The yaw table is 64 in. (1.6 m) in diameter, and it can be rotated to simulate crosswinds. The general planview is shown in Fig. 45, and additional detail is shown subsequently in Figs. 58-61.

Flow visualization measures were obtained at GALCIT by photographing tufts of yarn attached to the truck surface, and to an array of 40 vertical posts placed on the left (looking forward), in either a forward or aft longitudinal position. These tuft array positions are shown in Fig. 45. In certain cases, posts with tufts were attached to the front and rear faces of the semitrailer. These posts and tufts are also shown, subsequently, in the photographs of Figs. 58-61. Runs were also made using the basic truck, consisting of a three-axle cabover engine (COE) plus a 40 ft (12.2 m) van, with static pressure ports on the sides of the van, and 3 pitot-static pressure probes situated at different vertical heights and located at seven different points to the left of the truck. The locations of these pressure ports and probes are shown in Figs. 3-5 and 3-6 of Ref. 4 (Vol. 1). The model is described, subsequently.

The Northrop wind tunnel has a 7 × 10 ft (2.1 × 3.1 m) rectangular cross section. It features a relatively long test section, approximately 20 ft (6.1 m) long, and a full width yaw table, 10 ft (3.1 m) in diameter, mounted in the tunnel floor. The test setup involved mounting a six component strain gauge balance internal to a 1972 Chevrolet station wagon model (described subsequently). The balance was mounted to the base (underbody) of the car and to a support pedestal, then the car body was fitted over the balance and attached to the base. This assembly was attached through the support pedestal to special floor plates placed in the tunnel yaw table. Two different

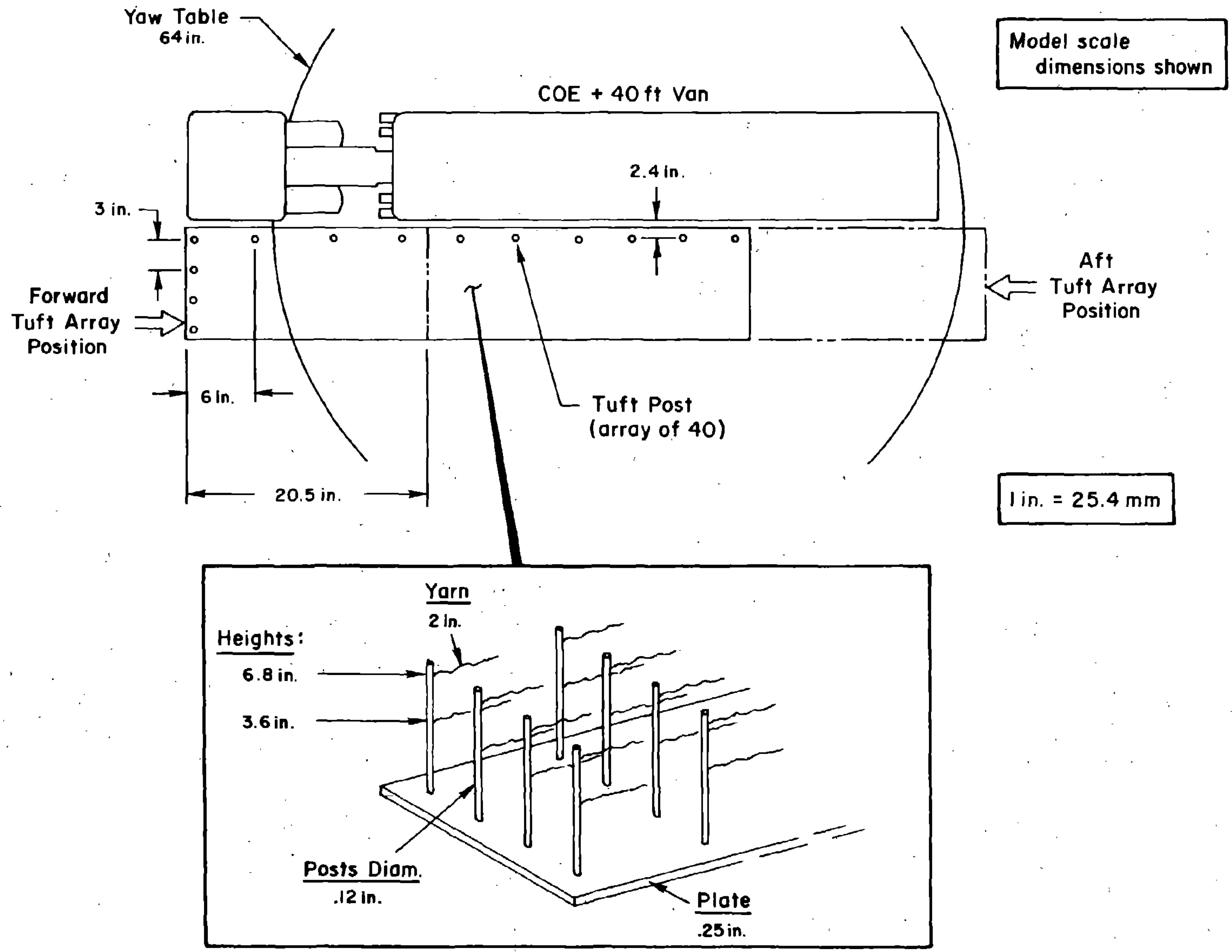

Figure 45. GALCIT Tunnel Setup with Basic Truck and Tufts

longitudinal positions on the floor plates, forward and aft, were used for mounting the car. Various truck configurations were bolted, via support pedestals, to the floor plates to the right of the car. A pattern of holes on the floor plates allowed the truck to be mounted at various points, longitudinally, so as to vary the relative car-truck positions. A truck centerline to car centerline separation of 12 ft (3.66 m) full scale was used for all runs. This entire setup rotated with the yaw table through a large range of relative wind angles. The layout provided sufficient area to conduct the adjacent car-truck tests. The same test arrangement was used in prior studies (Refs. 2, 3, and 29). The overall setup is shown in Fig. 46.

Two flow angularity probes were mounted at Northrop: one directly in front of the car, at 3.4 in. (86 mm) above the floor plates; and another to the right of the trucks with probe tip symmetric with the car mid-wheelbase, at 3.4 in. (86 mm) above the yaw table. These probes were moved, correspondingly, as the car was moved.

2. Truck Models

A variety of truck model configurations were at GALCIT and Northrop. The basic configuration was a 3 axle COE plus 40 ft van. This model was already in existence at the outset of the project, and it had been fabricated in connection with prior FHWA-funded research at STI (Refs. 2 and 29). The devices were mounted on this base configuration. It was also modified to accept other semitrailer body shapes, and a CBE (conventional) tractor body. An additional short truck model was fabricated also. The models were all 1/10 scale replicas of existing vehicles. They are described below.

Models of the following full scale trucks were used in the wind tunnel tests:

- 3 axle COE plus 40 ft (12.2 m) van semitrailer
- 3 axle COE plus dry cargo tanker semitrailer
- 3 axle COE plus flat bed semitrailer
- 3 axle COE plus liquid cargo tanker semitrailer

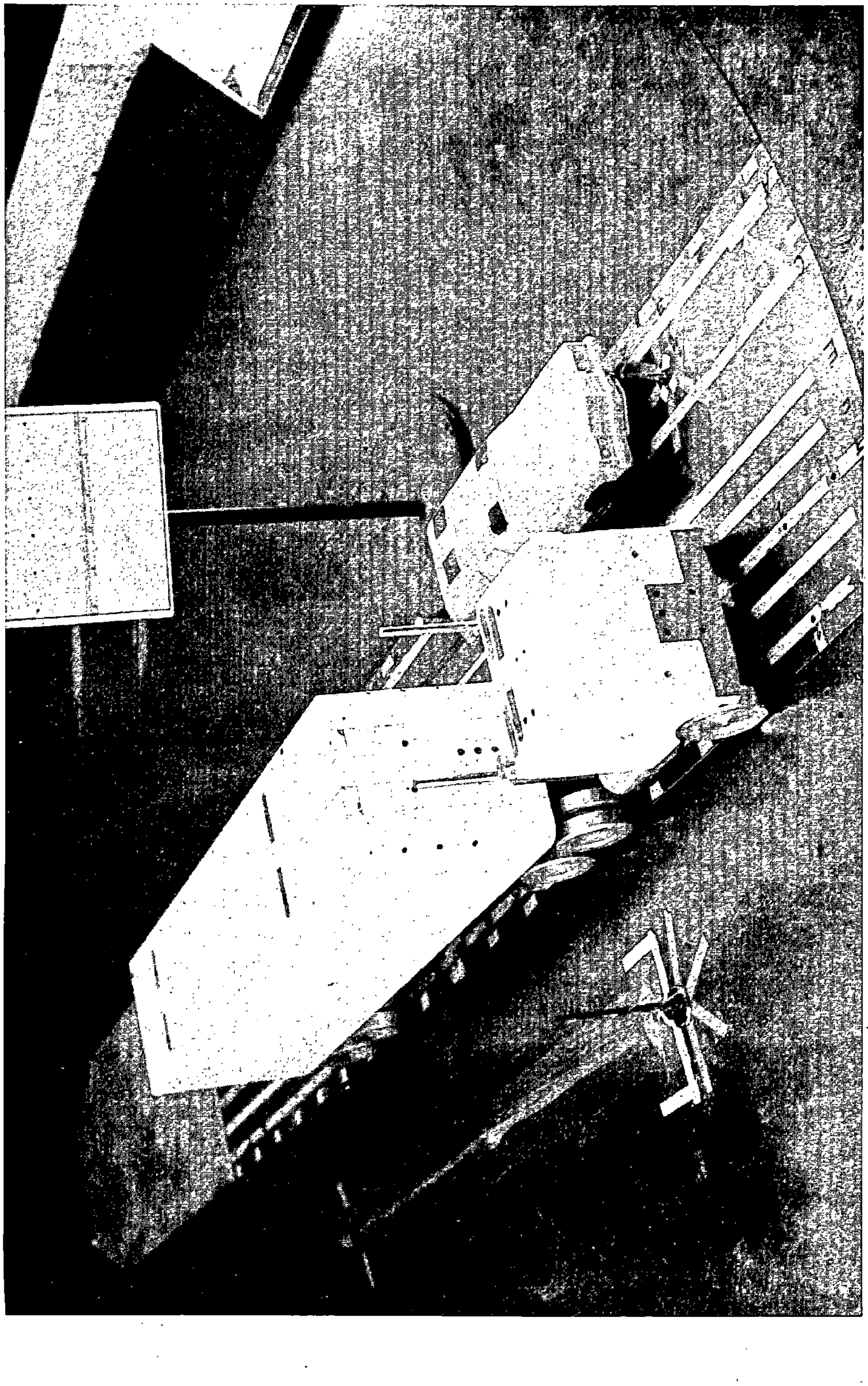

Figure 46. Northrop Test Setup

- 3 axle CBE plus 40 ft (12.2 m) van semitrailer
- 3 axle CBE plus dry cargo tanker semitrailer
- 2 axle COE plus 27 ft (8.2 m) van semitrailer
- 2 axle COE plus 27 ft (8.2 m) van semitrailer plus 40 ft (12.2 m) van trailer

All models but the basic configuration were fabricated as part of this program. The last configuration listed was used to simulate a doubles configuration, with respect to the air flow around the leading semitrailer (at Northrop).

Drawings of the truck models listed are given in Figs. 47-54. The dimensions shown on the figures are in inches (millimetres) in model scale, except for the reference frontal area (A) which is square feet (also model scale). The reference frontal area includes both the tractor and semitrailer outlines. The wheelbase is ℓ and the track is t. The wheelbase is measured from the forward (steered) tractor axle to midway between the semitrailer tandems, or to the axle of a single axle semitrailer. The track is the lateral separation of the midpoints of the outer semitrailer wheels. A complete set of mounting pedestals is shown for each model, although not all were used in the GALCIT tests. Not shown are tractor and semitrailer rear wheel mudflaps that were included. The end view outlines are intended to show the nominal semitrailer cross-section and not the forward detail.

The three axle COE and CBE tractors modeled were of long wheelbase, 187 in. (4.75 m) full scale, patterned after Peterbilt models 352-86 and 359-19, respectively. The three axle COE was based on an existing model (Refs. 2 and 29) which consisted of a wooden cab shell bolted to a metal backbone. The cab included a bumper and window detail. Wheels with axles and mudflaps, fuel tanks, and different fifth wheels attached to the backbone. Rearview mirrors, exhaust stacks, a removable bumper and grill, and a top of cab air cleaner were added for the current program. The CBE also consisted of a wooden cab shell which bolted in place of the COE to the same backbone. As such it incorporated the same wheels with axles and mudflaps, fuel tanks, and fifth wheels. The windshield, hood, headlights, bumper, grill, and wheel fenders were detailed. Rearview mirrors, exhaust stacks,

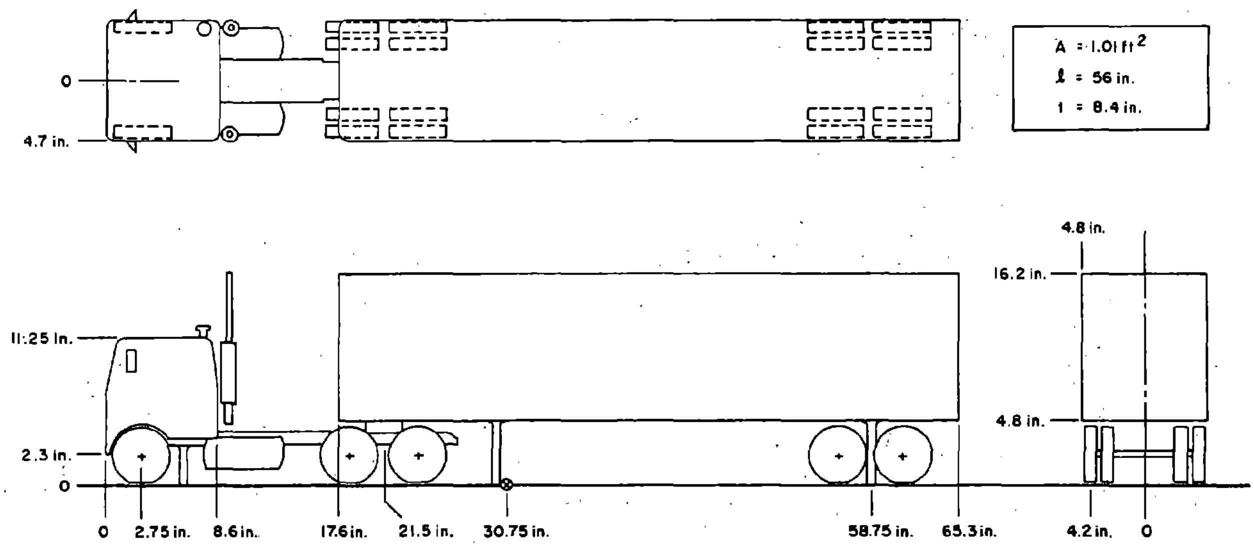

Figure 47. Three Axle COE Plus 40 ft Van Model

1 in. = 25.4 mm

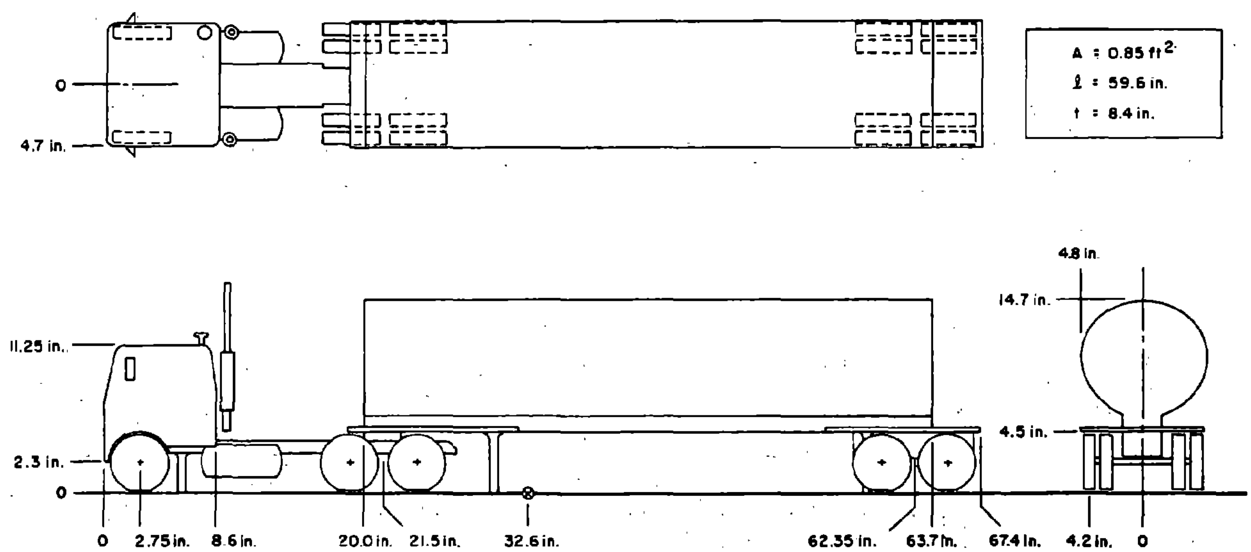

Figure 48. Three Axle COE Plus Dry Cargo Tanker Model

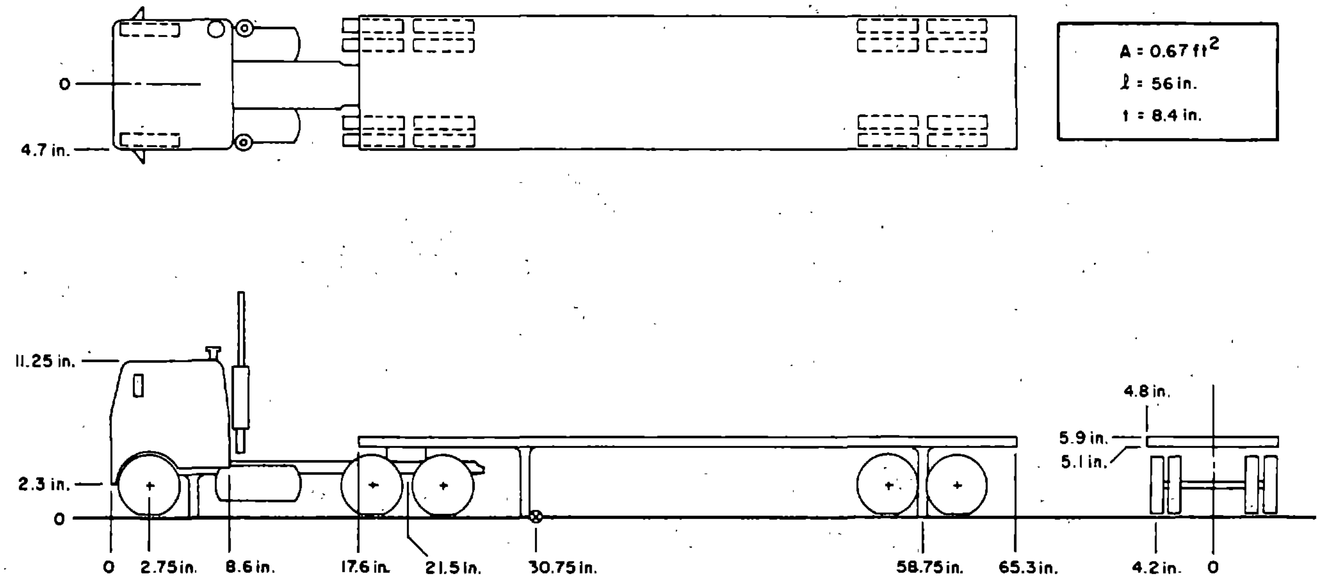

Figure 49. Three Axle COE Plus Flatbed Model

1 in. = 25.4 mm

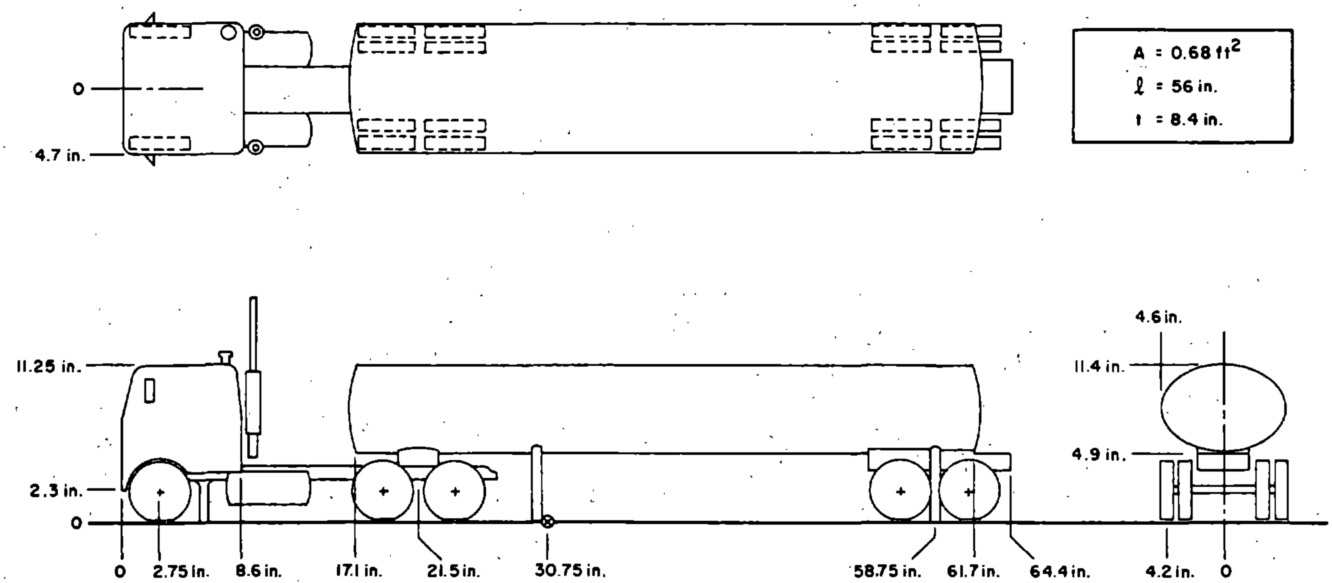

Figure 50. Three Axle COE Plus Liquid Cargo Tanker Model

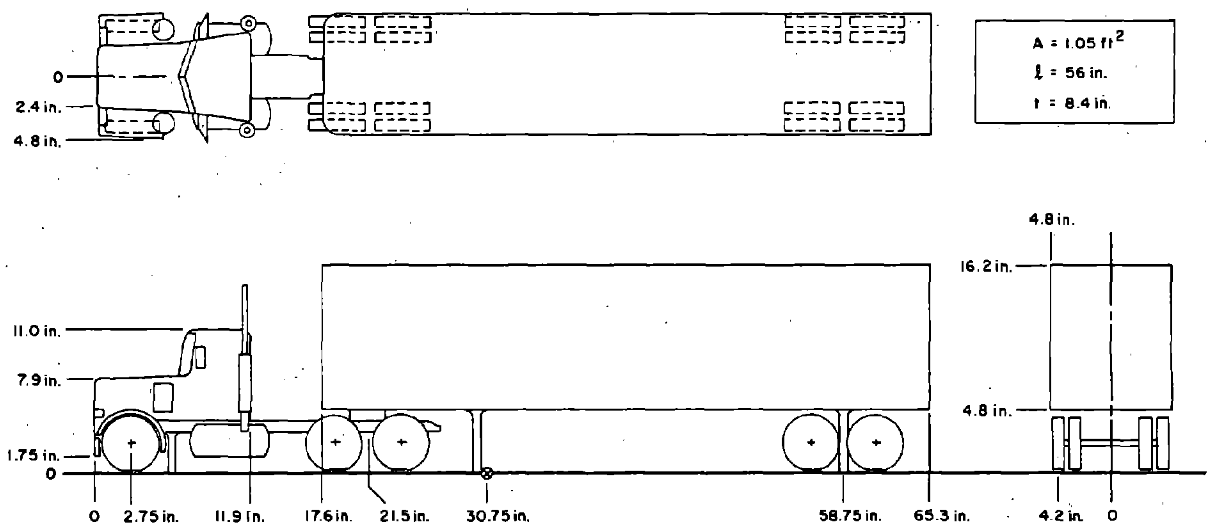

Figure 51. Three Axle CBE Plus 40 ft Van Model

1 in. = 25.4 mm

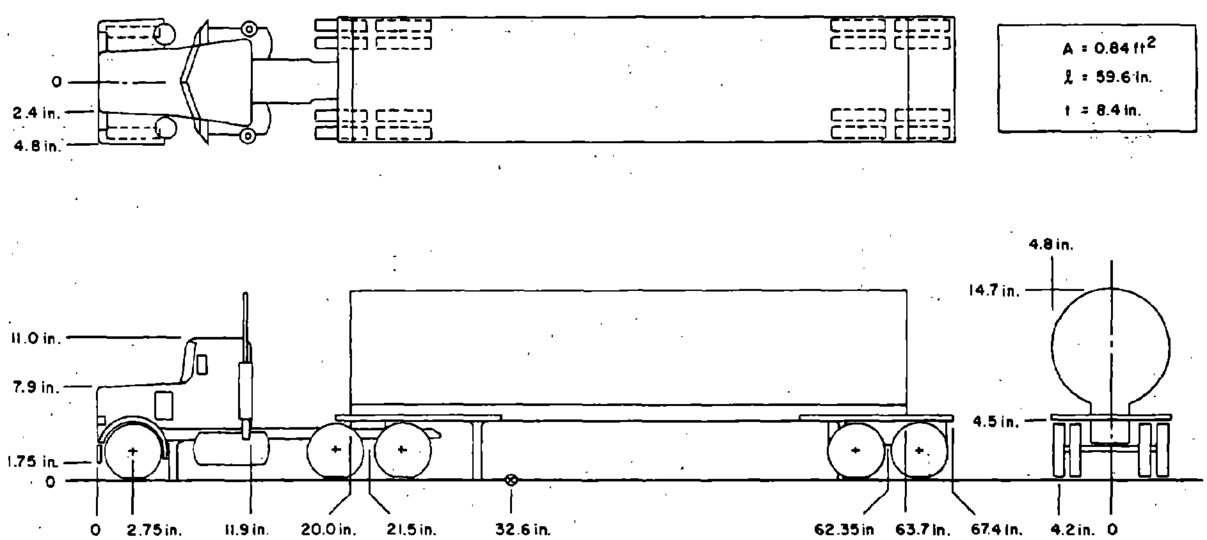

Figure 52. Three Axle CBE Plus Dry Cargo Tanker Model

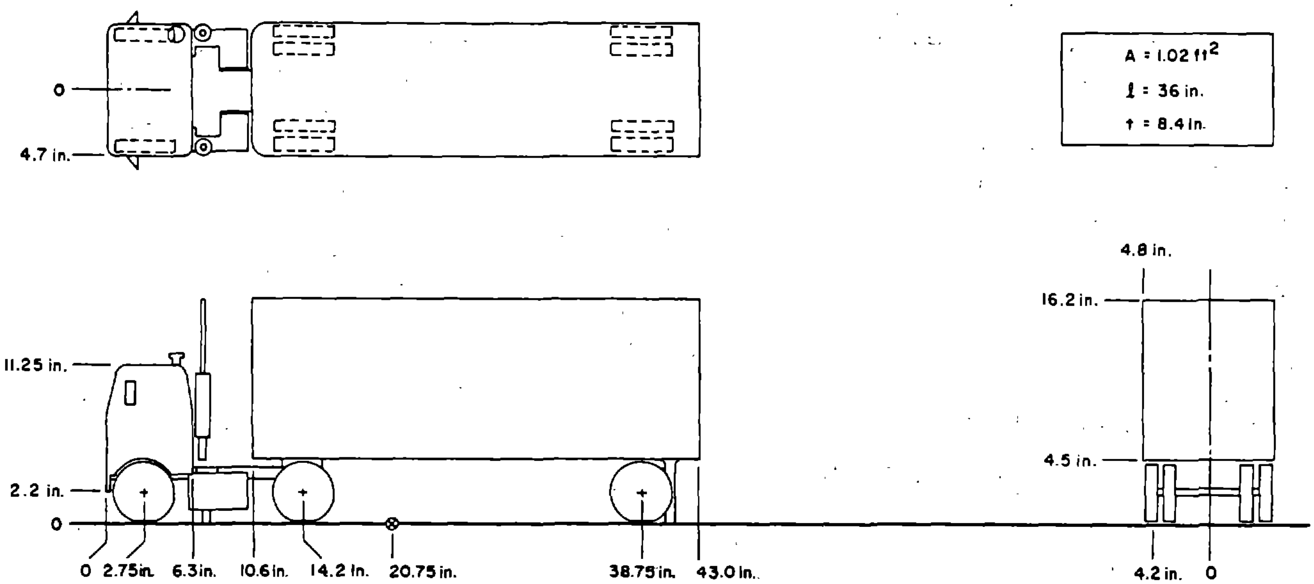

Figure 53. Two Axle COE Plus 27 ft Van Model

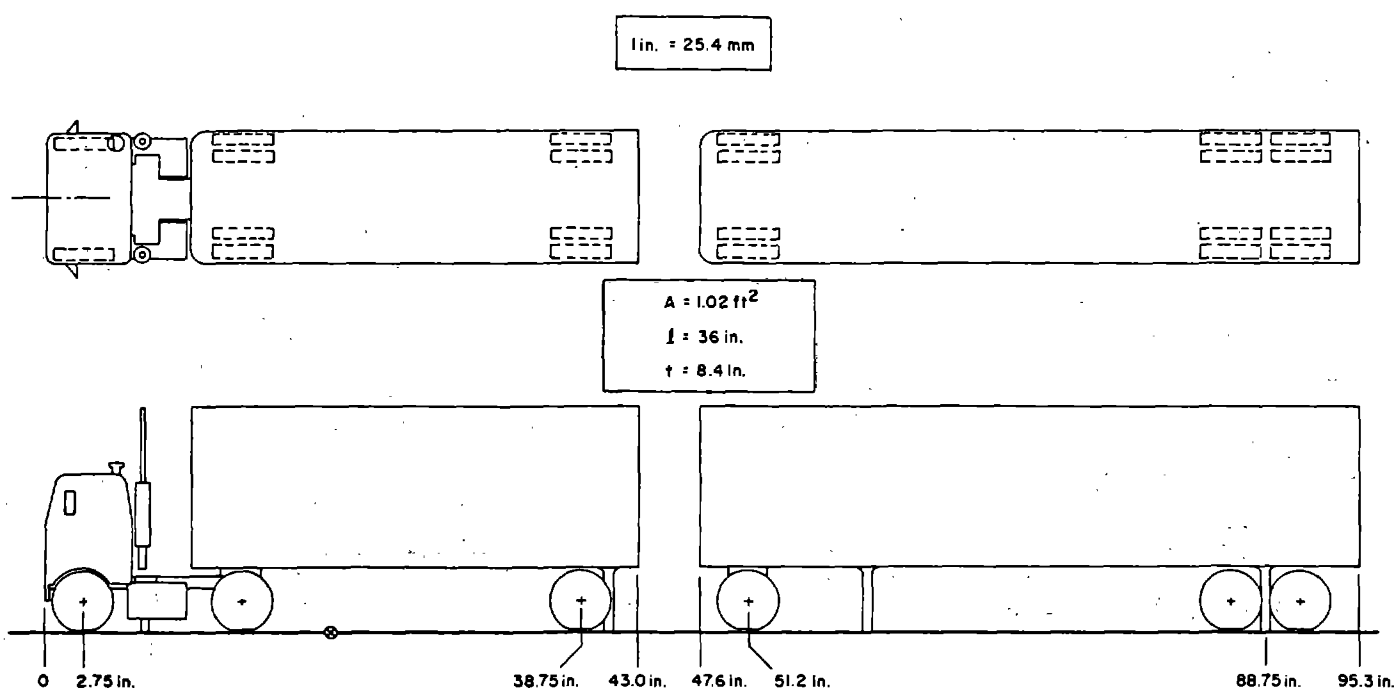

Figure 54. Two Axle COE Plus 27 ft Van Plus 40 ft Van Trailer Model

air cleaner, and blower were included. A photo of the basic truck (with drag shield) is given in Fig. 57, subsequently.

The existing 40 ft van model was a typical dry freight tandem axle box design. Its full scale equivalent was 8 ft (2.4 m) wide and 13.5 ft (4.1 m) high, with 12 in. (0.3 m) radii vertical leading edges. It consisted of a wooden shell mounted to the same metal backbone. Wheels and axles attached to the backbone. Modifications for these tests included fixing the width at 8 ft (2.4 m), where it had been variable. Leading vertical corners of different radii were provided, and static pressure ports were included on the left side, the front, back, and the bottom.

The dry cargo tanker model was patterned after a 36 ft (11 m) Feedliner, Model RGM. Its wooden body attached to a metal base plate at either end. Tandem wheels with axles and mudflaps were mounted to the rear base plate. The loading and unloading belts and apparatus were not included. They are located at the rear of the actual RGM semitrailer, and they would have involved more intricate model work than their expected effect on the flow field and the adjacent car force and moment warranted. Note that Feedliner Model RDM, which was tested full scale, see Sections II and VI, differed from Model RGM in having its loading and unloading apparatus located along the lower left side of the semitrailer. However, this difference was not considered significant in terms of relating the full scale and wind tunnel data for purposes of this program.

The 40 ft flatbed model was fabricated from a suitably sized metal plate to which tandem wheels with axles and mudflaps were bolted.

The liquid cargo tanker was a 1/10 scale replica of a 9200 gal (34,800 L) Fruehauf, Model TAG-F2-ESF 9200. It consisted of a large upper and a smaller bottom shell, each of which is attached to the metal backbone, completely enclosing it. Two shaped end plates attached to this assembly. The 40 ft van backbone was used. Tandem wheels with axles and mudflaps bolted to the backbone through the bottom shell.

The two axle COE and 27 ft (8.2 m) van models were designed and built in the same way as the three axle COE and 40 ft van described above. Each consisted of a wooden body shell attached to a metal backbone. The short wheelbase, 114 in. (2.90 m) full scale, two axle COE was patterned after a

Peterbilt Model 282-63. It included the same features as the three axle COE. The 27 ft van modeled had a single axle with dual wheels and mudflaps, and fixed, 12 in. (0.3 m) radius, vertical leading edges. This truck model was designed to stand alone, having no parts in common with the other models.

The truck models were mounted, via four pedestals through the ground board, to the GALCIT balance mechanism. Six pedestals were used at Northrop, as illustrated subsequently in Fig. 62. The basic four pedestals bolted directly to the particular truck's backbone, or base plates for the dry cargo tanker, so as to keep all wheels from touching the ground plane. This was necessary to prevent wheel contact forces from affecting the balance measures. Two pedestals attached to the tractor backbone and two to the semitrailer backbone in the case of the two axle COE and 27 ft van. Each configuration required its own set of pedestals.

Of the truck models listed at the beginning of this article, all but the

- 3 axle CBE plus dry cargo tanker semitrailer, and
- 2 axle COE plus 27 ft (8.2 m) van semitrailer plus 40 ft van (12.2 m) van trailer

were run at GALCIT. At Northrop, all were run but the

- 3 axle COE plus dry cargo tanker semitrailer.

The 3 axle CBE version was selected over the COE in the adjacent car tests, because the CBE provided a more realistic tractor to semitrailer gap size.

3. Models of Devices

A variety of devices was tested in the wind tunnel, as add-ons and modifications to the basic truck configuration. The devices were designed to either alleviate splash and spray, or to reduce the drag of the truck. The former were run in the wind tunnel to assess their effect on the air flow around the truck, and any influence they might have on the force and moment disturbance of the adjacent car.

The following devices and modifications to the basic truck configuration were modeled and run:

- Vertical gap splitter panel between tractor and semitrailer

- Horizontal gap bottom plate between tractor and semitrailer

- Cab-mounted drag shield, approximately 70 percent porous

- Dam under the 3 axle COE front bumper

- Vertical leading edges on semitrailer with 24 in. (0.61 m) radii, full scale

- Vertical leading edges on semitrailer with square corners

- Gap filler block, to extend van semitrailer forward about 5 ft (1.5 m), full scale. It had 6 in. (0.15 m) radii vertical leading edges, full scale.

- Lateral lips on van upper edge, across the front and down the sides

- Angled side vanes ahead of and behind the tractor wheels, angled at 60 deg to the truck longitudinal centerline

- Longitudinal underbody baffle hanging vertically beneath the entire truck, approximately on the centerline

- Full fenders over the tractor tandem wheels

- Horizontal flow deflector foil placed on the top rear of the van

These devices are illustrated in the photographs of Figs. 55-64, with the exception of the vertical leading edges. Their design and function are described in Section IV. Note that the vanes just behind the steered wheels in Fig. 61 were run at GALCIT but not at Northrop. In addition, a run was made with wheel mudflaps removed on the basic configuration.

The devices listed above were run at GALCIT, to study air flow and to obtain the configuration drag properties. In addition, the drag shield was run at GALCIT on the 3 axle CBE plus 40 ft van with porosities of approximately 70 and 50 percent, as well as fully blocked (nonporous). The devices

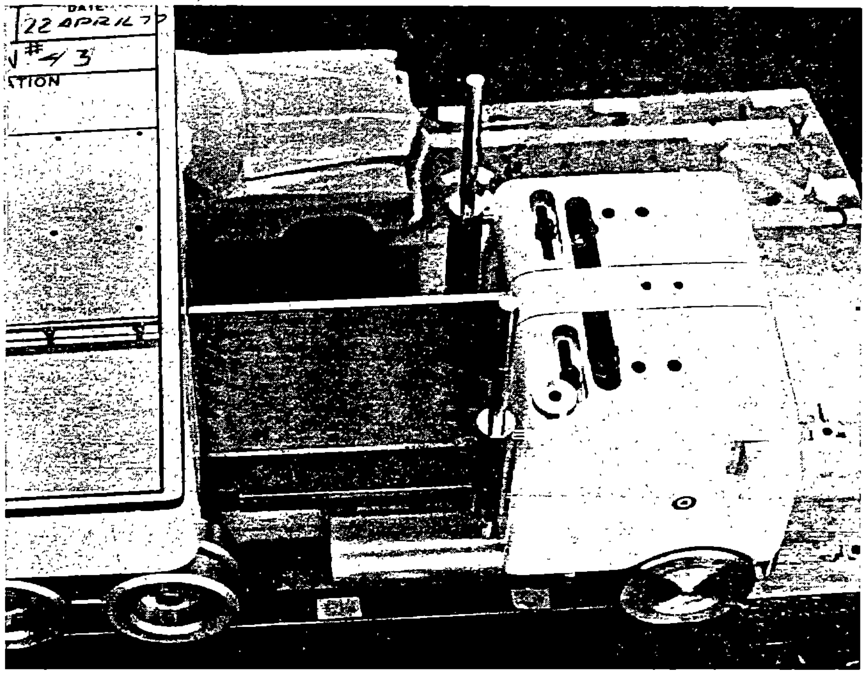

Figure 55. Vertical Gap Splitter Panel

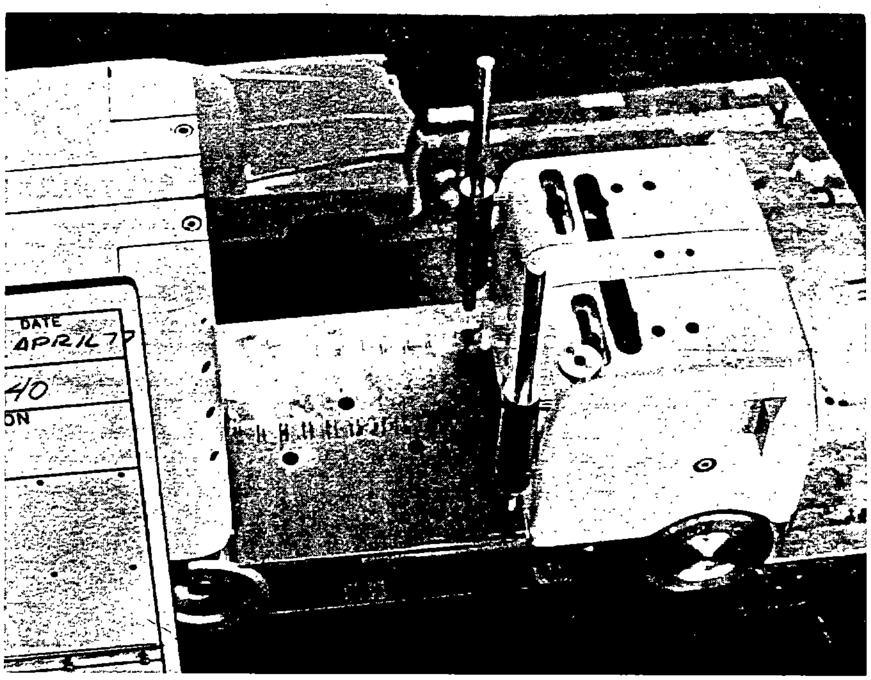

Figure 56. Horizontal Gap Bottom Plate

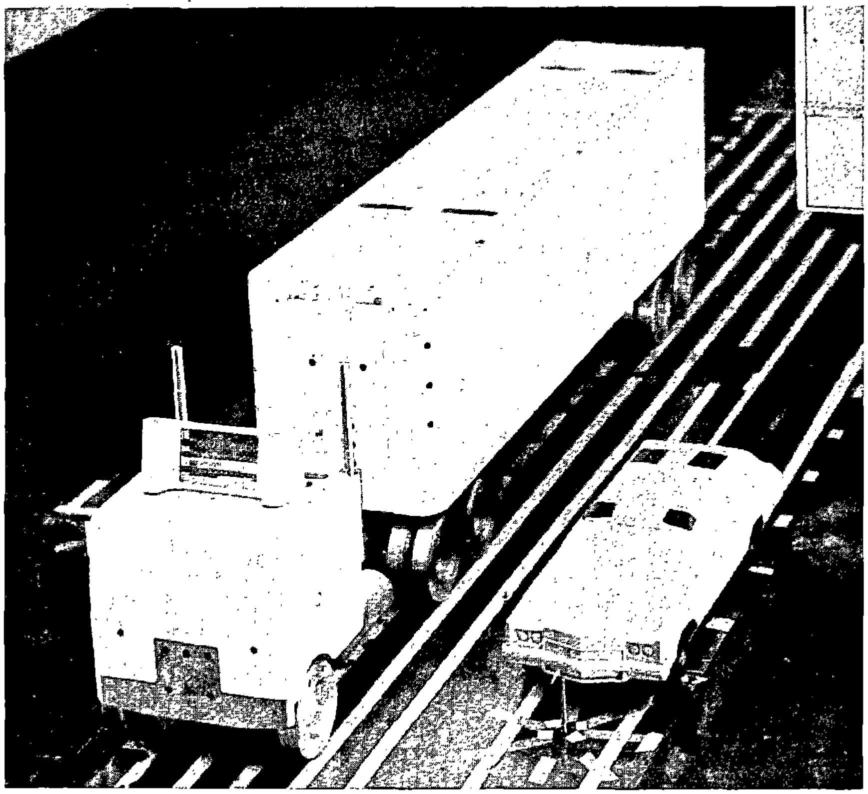

Figure 57. Cab-Mounted Drag Shield

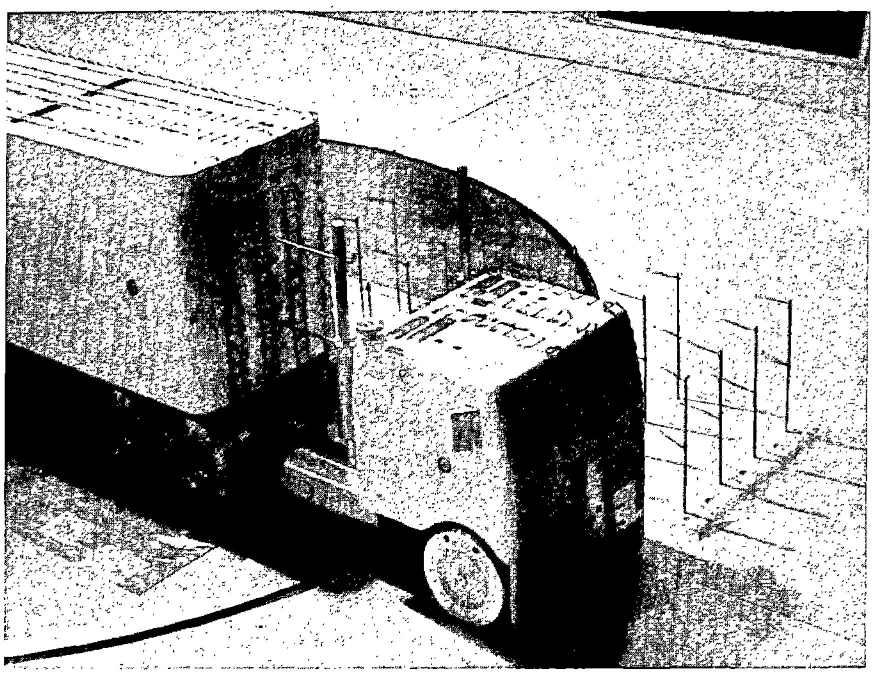

Figure 58. Dam Under Front Bumper

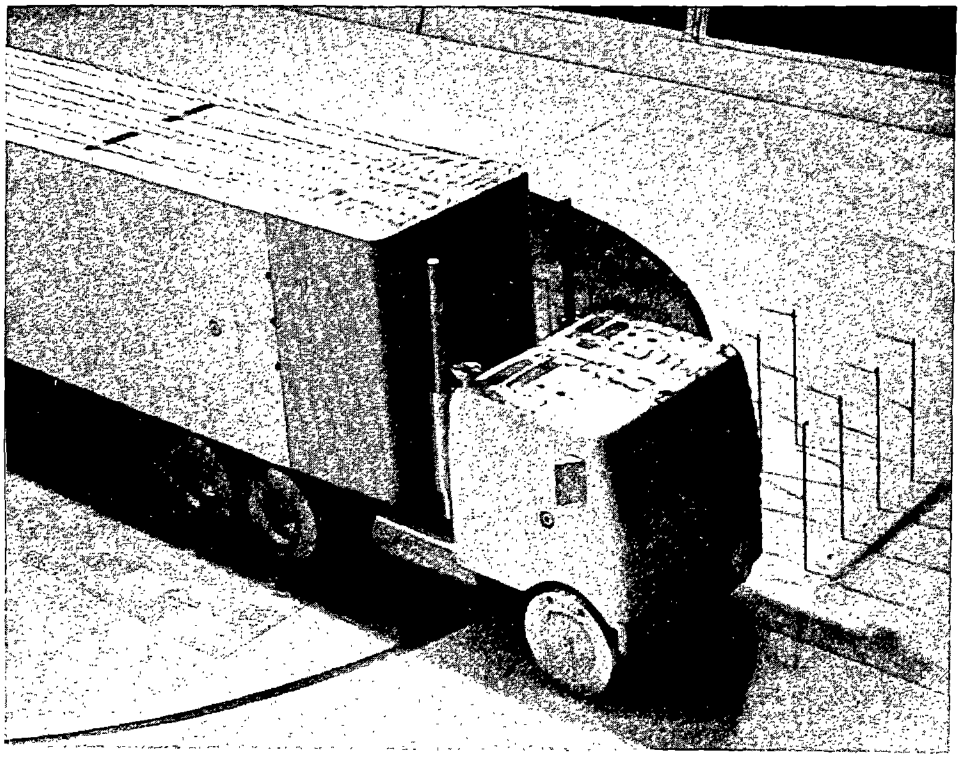

Figure 59. Gap Filler Block

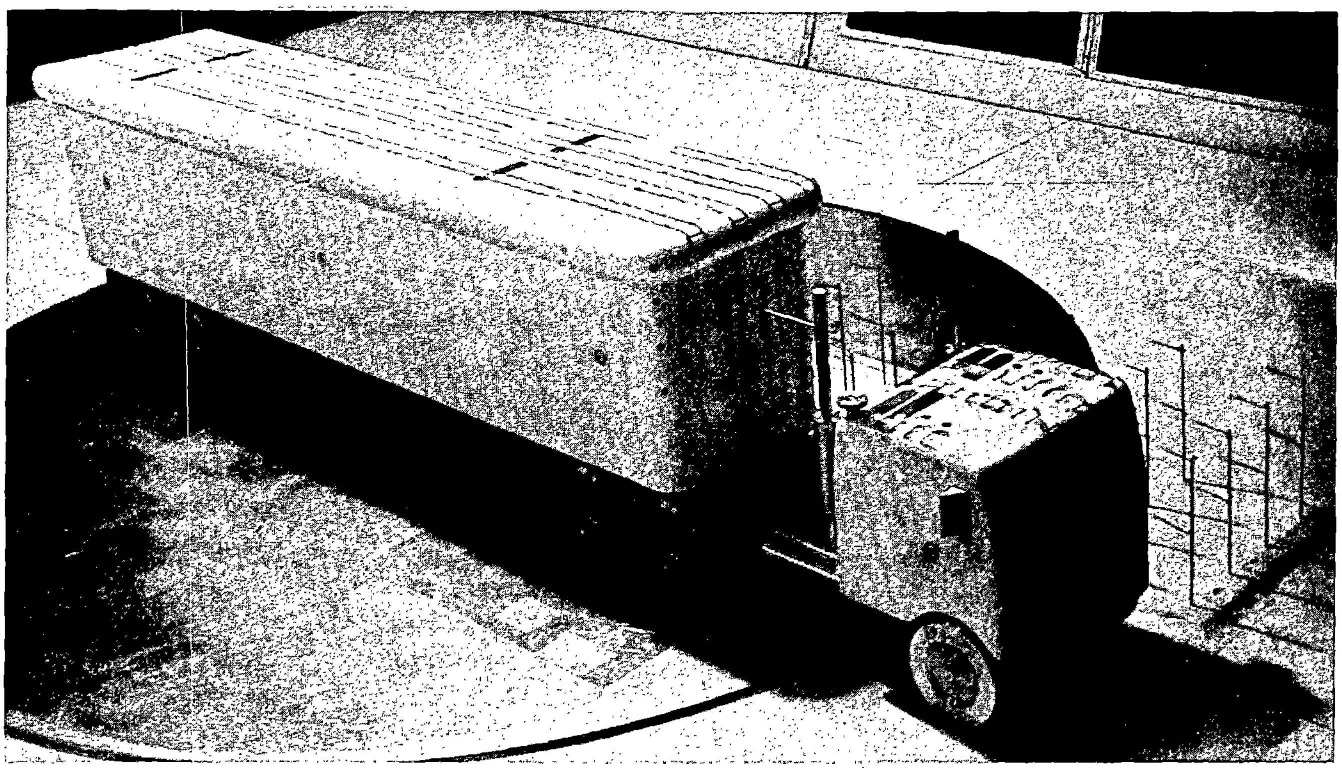

Figure 60. Lateral Lips on Van Upper Edge

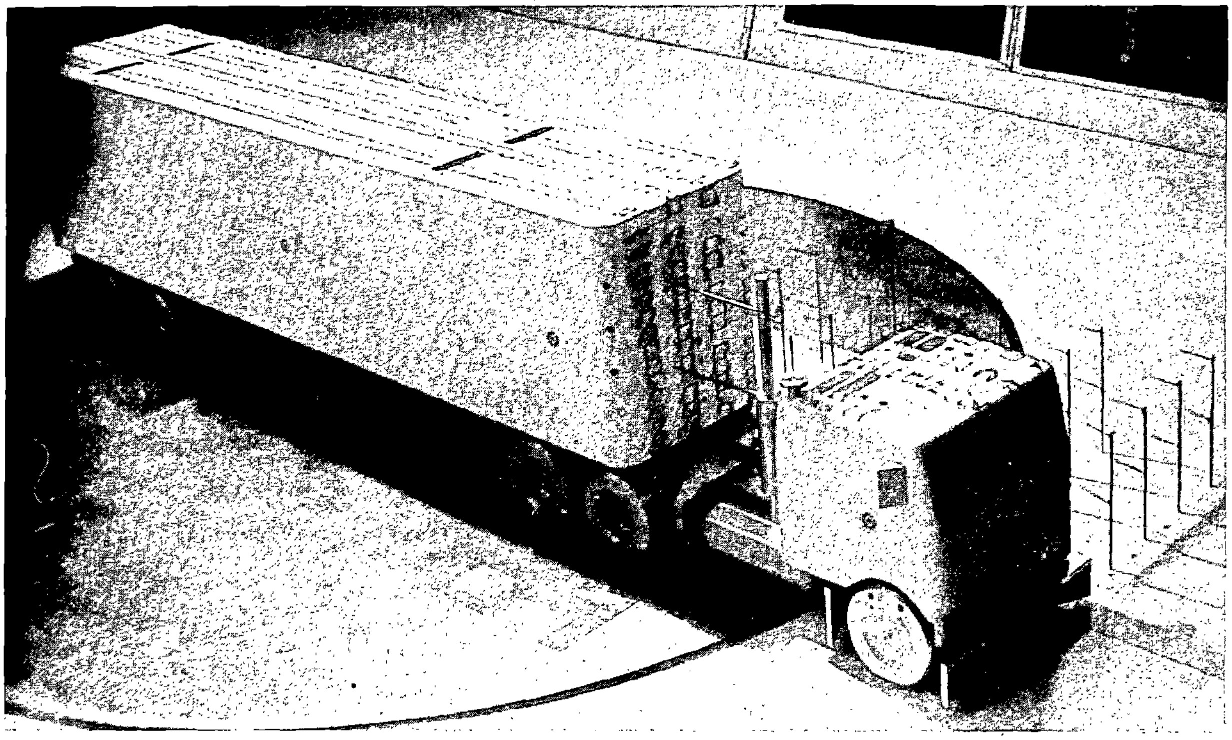

Figure 61. Angled Side Vanes Around Tractor Wheels

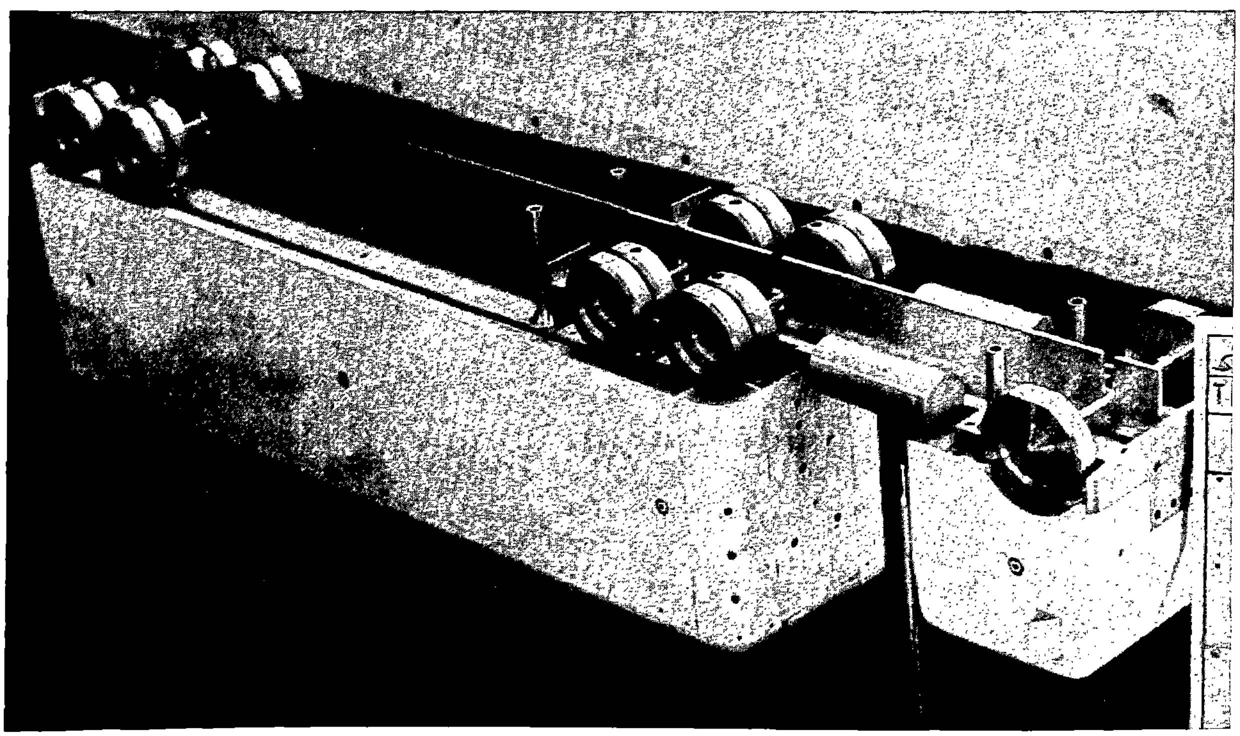

Figure 62. Longitudinal Underbody Baffle

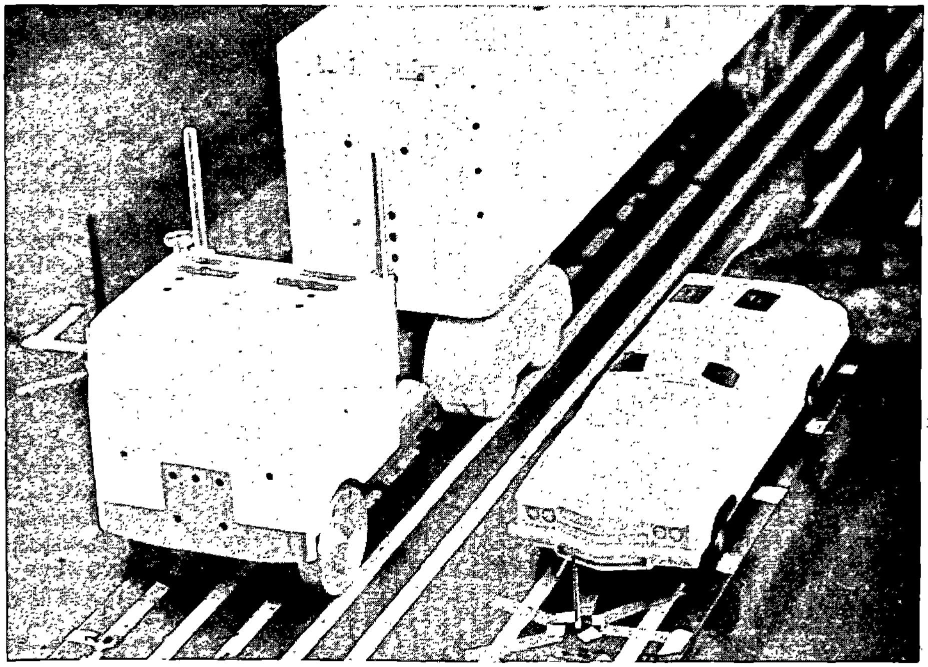

Figure 63. Full Fenders Over Tractor Tandems

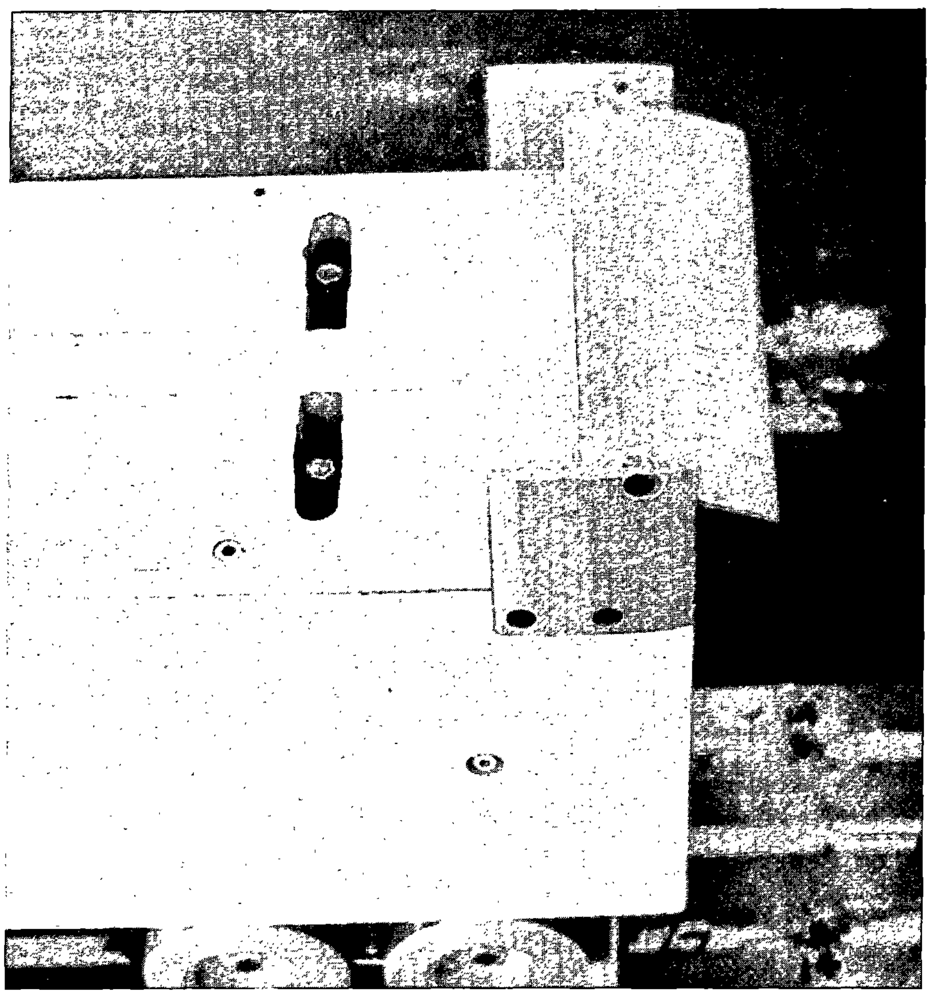

Figure 64. Horizontal Flow Deflector Foil

listed above were also run in the adjacent car tests at Northrop, with the exception of the

- Dam under the 3 axle COE front bumper
- Gap filler block
- Lateral lips on van upper edge

At Northrop the drag shield porosity was set at about 50 percent, and it was also run on the 3 axle CBE plus 40 ft van against the adjacent car.

4. Adjacent Car Model

The adjacent car model used at Northrop was a 1/10 scale replica of a 1972 Chevrolet station wagon. It was originally fabricated in connection with the test program reported in Refs. 3 and 29. It is illustrated in Figs. 46, 57, and 63. The body contours were carefully matched to full scale, and the rain gutters around the side windows were modeled and the windows were inset. Sufficient underbody detail was included to give a generally equivalent roughness to the underside of the vehicle. Radiator flow was not provided; however, past experiments (e.g., White, Ref. 51) have shown that this has little effect on the lateral-directional aerodynamic data, which have been shown to be of most importance in the truck-car aerodynamic disturbance problem. Front and side view drawings of this model are shown in Fig. 65. The reference frontal area, wheelbase, and track are

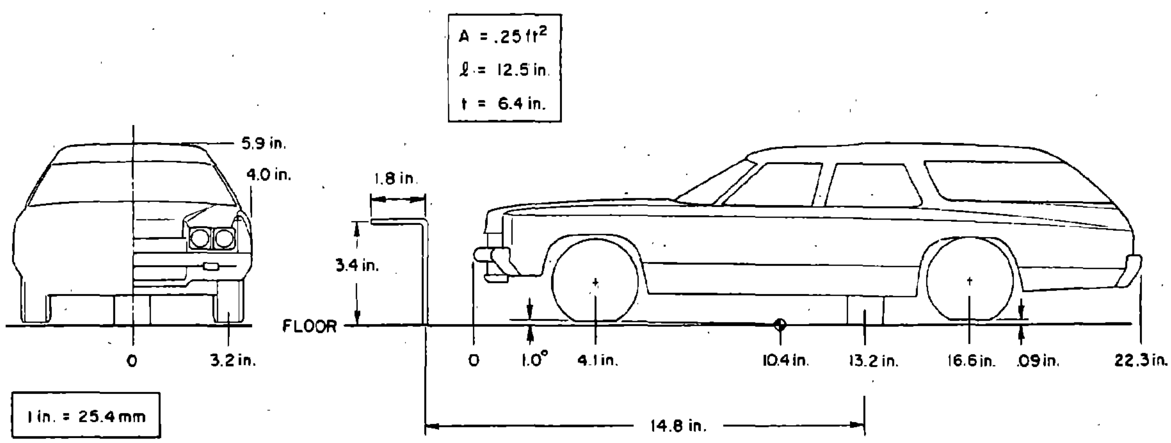

Figure 65. 1972 Chevrolet Station Wagon Model

defined in a way which corresponds to that of the truck model in Fig. 47. The model consisted of a mahogany body shell mated to an aluminum baseplate. The baseplate held wheels and underbody structure as well as the balance block. The balance was attached to the model via the balance block and to the tunnel floor by a 1.2 in. (30.5 mm) diameter vertical strut.

Aerodynamic measurements were made using a 1.25 in. (32 mm) diameter Task Mk V balance. The balance center was located close to the estimated aerodynamic center of the vehicle, in order to minimize aerodynamic moment measurement error. The dynamic range for side force and yaw moment measures were ±550 lb (2447 N) and ±1170 in.-lb (132.2 N·m), respectively.

Flow probes were located just ahead of the station wagon and to the right of the trucks, as shown in Fig. 46. They were a five port design to measure flow direction and magnitude, similar to those used in previous STI wind tunnel tests (Refs. 2, 3, and 29). The base of the probe in front of the car was mounted flush with the floor plates. The probe to the right of the truck was mounted on a small rounded edge base which attached to the tunnel floor.

5. Test Procedures and Conditions

The test conditions and procedures used at the two facilities differed somewhat, due to their physical properties and to the differences in the test objectives.

a. GALCIT Conditions

The GALCIT tests were run at a tunnel dynamic pressure (q) of 60 psf (414 kPa), which provided a Reynolds number of 1.4×10^6 per foot (0.43×10^6 per metre). Based on the truck model wheelbase, this resulted in an effective Reynolds number of about 6.5×10^6 for the trucks. This is about one-fourth of full scale (at 55 mph, 25 m/s) and well above the critical transition value. This was adequate for the relatively large models used in these tests.

Force and moment and flow visualization (tuft) measurements were taken simultaneously. Calibration and pressure measures were taken separately.

Data for all the truck force and moment and flow visualization runs were taken at 0 deg and −20 deg relative crosswind (yaw) angles, except as noted below. Negative angles corresponded to having the left side of the truck downwind (the models are symmetrical left and right). For other runs data were taken at the yaw angles indicated in the following.

Initially, the basic truck was mounted and run without tufts or pressure probes, to check the test setup and obtain baseline data. Data were taken at relative crosswind angles of 0, −20, −10, 0, and +10 deg. The test sequence was then repeated for this truck with the tufts in place. Next, the various devices were added and run with tufts, one at a time. Then, the 3 axle CBE plus 40 ft van was run with tufts. The drag shield was placed on this configuration and run at 0 deg only (for the three different shield porosities). Following that, the pressure measurement runs with the basic truck (without tufts) were made at 0 and −20 deg. The pressure probes were calibrated, with truck removed, at −30, −20, −10, and 0 deg yaw. Finally, the other truck types were run with tufts.

b. <u>Northrop Conditions</u>

The adjacent car runs at Northrop were made at a tunnel dynamic pressure (q) of 140 psf (965 kPa), which gave a Reynolds number of approximately 2.2×10^6 per foot (0.67×10^6 per metre). Based on the 1972 station wagon model wheelbase of 12.5 in. (0.32 m), this provided an effective Reynolds number of approximately 2.3×10^6. This is about 40 percent of full scale (at 55 mph), and this Reynolds number is about a factor of 4 above the critical value where the flow transitions from laminar to turbulent in the full scale case. It represents an optimum compromise of model scale and wind tunnel flow velocity. Two runs each were made at 60 psf (414 kPa) and 100 psf (689 kPa), to confirm the very small effect of varying Reynolds number.

All flow visualization (tuft) runs were made at 60 psf (414 kPa) to correspond to the GALCIT conditions.

Data were recorded primarily at yaw table angles (relative crosswind angles) of 0, +25, +20, +15, +10, +5, 0, −5, −10, −15, −20, −25, and 0 deg.

Again, negative yaw angles corresponded to the left side of the truck downwind (car downwind of truck). For flow angularity probe calibrations additional yaw angles were run. For tuft runs, only 0 and −20 deg were run.

Runs at the start of the test series were for flow angularity probe calibrations. Then the car was run alone in the forward mount position, to gather baseline data to compare with previous results (e.g., Refs. 3 and 29). Next, the basic truck was installed beside the car and run at several relative car-truck positions along the forward part of the truck. This setup is illustrated in Figs. 57 and 63. Similar runs were made with this truck with the add-on devices installed, one at a time. The CBE plus 40 ft van was installed alongside the car next, and run at several relative car-truck positions along the forward part of the truck, both with and without the drag shield. The other truck types were run in a similar manner. The car was then moved to the aft mount position and run alone, to gather baseline data at that location. The basic truck was then added to obtain relative car-truck positions in the aft area. The various truck types and devices which were expected to alter the flow in the aft region of the basic truck were run after that. Finally, tuft runs were made on the CBE plus dry cargo tanker and in the gap region between the 27 ft van and 40 ft van with two axle COE tractor (simulated double bottom configuration). Typical relative car-truck positions for the various basic truck configurations are summarized in Fig. 66.

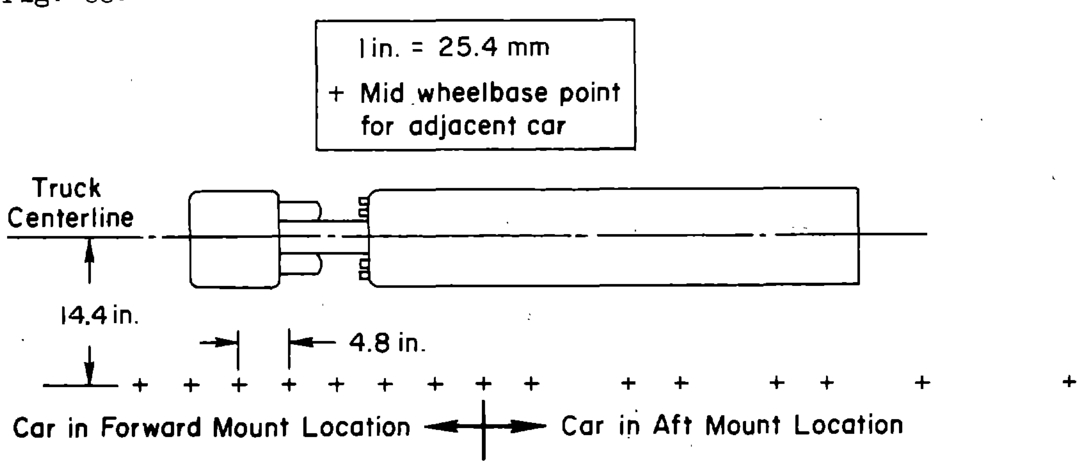

Figure 66. Typical Relative Car-Truck Locations Tested at Northrop

c. Other Test Considerations

Ground vehicle aerodynamic problems always involve boundary layer considerations. The full scale, real world boundary layer varies with terrain and wind conditions, and it may differ in turn from model scale boundary layer properties. Because of this variation, it is important to know whether changing the boundary layer shape or thickness has a significant effect on the resulting aerodynamic forces and moments. Prior research has indicated, in general, that the boundary layer can have some effect on longitudinal measures (pitch moment, lift, and drag) and a lesser effect on lateral-directional measures (side force, yaw moment, and roll moment). The former is pertinent to the truck drag measures, while the latter relates to the forces and moments on the adjacent car.

A prior series of experiments was conducted at GALCIT by STI (Refs. 3 and 29) to assess the effect of varying the boundary layer thickness on the force and moment measures on a 1/10 scale 1970 Chevrolet station wagon model. The displacement thickness (δ^*) was varied from 0.09 in. (2.3 mm) to 0.35 in. (8.9 mm). These correspond to the nominal boundary layer on the Northrop tunnel floor, and the GALCIT ground board value, respectively. The lateral-directional measures were virtually unchanged (Ref. 29). These findings are consistent with those in the literature. In comparing wind tunnel and full scale results, for example, Carr (Ref. 63) reported that side force and yawing moment coefficients of road vehicles measured in wind tunnels are slightly higher, but within 5 percent of the full scale coefficients.

In these boundary layer experiments, the drag on the car model (similar to that in Fig. 65, but a 1970 year model) decreased about 10 percent with the thicker value of δ^*. For the truck tests at GALCIT with a q of 60 psf (414 kPa), however, the displacement thickness varied from about 0.09 to 0.17 in. (2.3 to 4.3 mm) across the yaw table. The ratio of this free-test-section thickness to the minimum underbody clearance was about 4 percent for the truck models. This is less than the maximum value of 6 percent recommended in Ref. 52 for obtaining valid drag data. To confirm these criteria, the truck drag measures obtained during this program were checked, subsequently, against values reported in the literature for similar configurations and variations thereto. This correlation effort, and some resulting data adjustments, are discussed in Article C, below.

Radiator flow can influence pitch and lift, but its effect on the lateral-directional measures is small (e.g., Ref. 51). The effect on drag for passenger cars is usually less than 5 percent (e.g., Ref. 53), and its influence on large commercial vehicles should be even less. Similarly, wheel rotation effects have been found to be small for passenger vehicles (e.g., Refs. 7 and 53). It can be important for open-wheeled vehicles such as formula race cars, where the wheel frontal area is a large fraction of the total. Its effect on tractor plus semitrailer trucks has not been determined to our knowledge; but it is presumably negligible because the wheels are a small fraction of the vehicle area, and they are immersed in separated and turbulent flow regions for the most part. Neither radiator flow nor wheel rotation was included in these tests.

In general, and in spite of significant differences in scale, it has been found that carefully conducted wind tunnel tests can give virtually the same aerodynamic coefficients as occur in full scale. For tractor-semitrailer rigs there are occasional small discrepancies in drag coefficient, due to such things as poor representation of the ground plane, as discussed by Lissaman (Ref. 19). However, with sufficiently large models the wind tunnel drag data are in general agreement with full scale testing as reported, e.g., in Ref. 64.

B. AERODYNAMIC FLOW AROUND TRUCKS

The flow fields in the vicinity of large trucks constitute a complicated fluid mechanical process. Various features of this flow are described in the following article. First, the nature of the flow structure is described. Some of the pertinent findings of prior wind tunnel testing are then described, as well as the nature of the turbulence in the separated wake and the effects of yawed flow and of aerodynamic drag reduction devices. This is followed by a description of the major aerodynamic flow results obtained from the current program, including both the wind tunnel testing and the full scale experiments.

The results presented in this article are largely the findings of AeroVironment, Inc. (AVI). Additional details are presented in their source document, Ref. 4. The wind tunnel tests and data reduction were accomplished by STI with the assistance of AVI. The full scale tests were conducted by STI and WHI, with AVI performing the air flow experiments and measures.

1. Nature of the Flow and Background

A large highway truck behaves aerodynamically like a bluff body. Current vehicle models do not pay much attention to aerodynamic streamlining, and design considerations of strength, structural simplicity, mechanical convenience and maximum payload volume dominate the basic shape. In addition, various highway regulations relating to maximum width, height, and length of vehicles lead to the rectangular box shape which maximizes volume.

The truck is exposed to a complicated external aerodynamic field consisting not only of the relative flow created by the motion of the rig, but also the flow associated with ambient winds. These natural winds consist of a non-uniform flow field increasing in magnitude with height, and generally non-uniform in turbulence, with large longitudinal and lateral non-uniformities associated with gusts and shifts in wind direction. Because of the bluff nature of the truck body, and the numerous hard edges and mechanical protrusions, as well as the presence of cross-flows due to wind, the flow associated with these vehicles always contains major volumes of separated flow in the wake of the separated regions.

Our interest relates to the diffusion and dispersion of spray generated by the vehicle, and to the aerodynamic forces and moments on an adjacent car due to the flow field and its variations. With regard to spray, a principal concern is with the flow fields downwind of the various wheel sets, which serve as generators of splash and spray. In principle we wish to define the mean flow speed and directions and the general turbulence levels for stream tubes emanating from these generation regions and progressing downstream. On the other hand, rather than try to deduce the force and moments on the adjacent car from the flow field, we have measured them directly (as described in Articles A and D).

It must be borne in mind that, although tractor and semitrailer rigs differ substantially in their detailed features, their basic geometries are substantially similar, so that similar wake fields may be expected. Further, note that the intense turbulence in the separated regions imposes a type of coherence at a certain scale. In a sense, while the wakes of different vehicles all differ, within certain levels of accuracy they are all the same for a given class of vehicle. The study and analysis of the aerodynamic flow fields of trucks is a complex subject, and extensive research exists. This discussion is necessarily limited to those features of the aerodynamics which affect the dispersion of splash and spray generated by the wheels.

A prior study of particular pertinence here was accomplished by STI for FHWA (Ref. 31). In it, flow field properties were measured at various locations in the vicinity of a tractor/semitrailer truck. The results were shown as three-dimensional flow vectors, and as dynamic pressure estimates. The flow velocity vector at a given point was expressed via three normalized, orthogonal components (u/U_∞, v/U_∞, and w/U_∞) in an x, y, z coordinate system. The components were projected on a horizontal (x, y) plane to obtain a vector field. Example results are shown in Fig. 67 for the no crosswind and −20 deg relative crosswind angle cases. The vectors shown are the normalized components, u/U_∞ and v/U_∞, measured at a height 36 in. (0.91 m) above ground, full scale. The tail of each vector is to the left, and the left end corresponds to the probe location. The truck model was the same as the basic configuration used in the present program and the measures were made at Northrop.

The no crosswind data in Fig. 67a show an increase in flow angularity and magnitude around the tractor. This correlates with the disturbing forces and moments experienced by an adjacent vehicle. The data also show some outward flow angularity alongside the semitrailer, and this may be anomalous. Some flow convergence is seen at the rear of the semitrailer. The well defined wake directly behind the truck comprises turbulent air whose mean component was too small to be recorded accurately. The −20 deg relative crosswind data in Fig. 67b show much greater flow disturbance due to the truck. The angularity is increased at the front of the tractor.

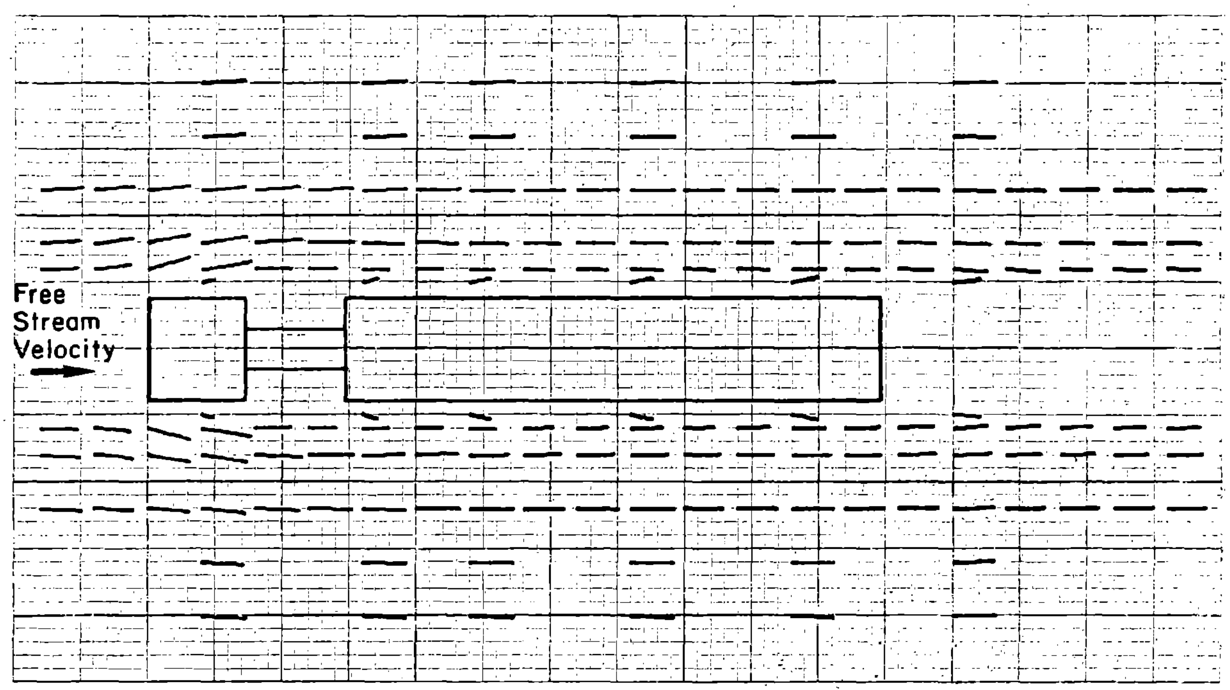

a) No Crosswind

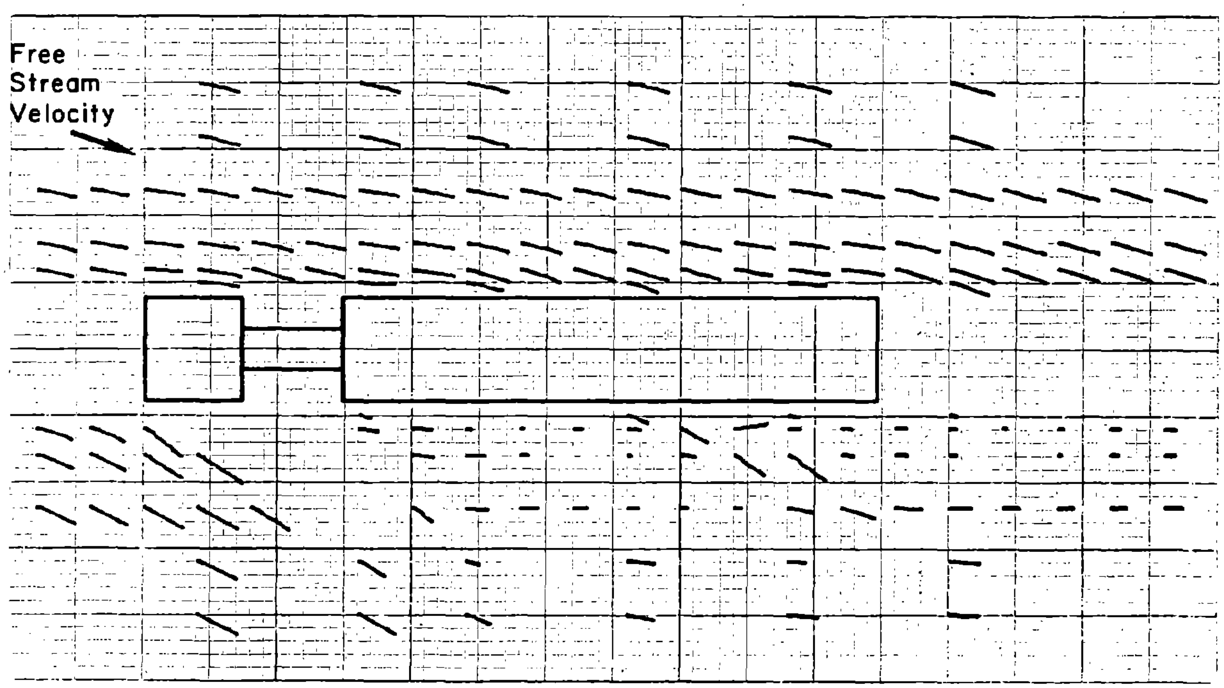

b) -20 deg Relative Crosswind

Figure 67. Velocity Components Projected on x-y Plane, 36 in. (0.91 m) Probe Height (From Ref. 31)

Downwind of the tractor (and the gap aft of the tractor) the flow was too turbulent to obtain reliable steady flow measures with the probes used. Farther back on the downwind side the flow was also disturbed, and the data show a large reduction in relative magnitude (except for the region where there is substantial flow under the trailer). Increased flow angularity due to flow under the trailer is also seen on the upwind side. The large changes in magnitude and angularity on the downwind side correlate well with the relatively large force and moment disturbances experienced by a passing vehicle.

Measures of the pressure at given points in the flow field were also made in the Ref. 31 study. These were obtained from a combination of the static pressure and the dynamic pressure, which is proportional to the square of the local flow velocity. Such total pressure estimates are reported in Ref. 31 for two truck widths, three probe heights, 0 and −20 deg crosswind, and various x and y locations. Contours of constant total pressure (isobars) are shown in Fig. 68a for the zero crosswind case. The values shown are estimates (in psi) for a 36 in. (full scale) probe height. At 60 mph (27 m/s) the free stream stagnation pressure was 14.764 psi (101.79 kPa). Isobars for the −20 deg relative crosswind case are shown in Fig. 68b. The values shown are for a 36 in. (.91 m) probe height, and the same free stream stagnation pressure. The contours in the crosswind case tend to indicate the regions of laminar and turbulent flow, the former occurring around the front of the tractor and ahead of the rear duals on the downwind side. The pressure contours in Fig. 68 did not correlate in any clear way with the dominant peaks and variations in the corresponding force and moment data (i.e., Refs. 2 and 29). They may be pertinent to the interpretation of spray propagation patterns, however.

The Ref. 31 flow measures adjacent to the truck identified a boundary layer on the trailer extending about 1 to 1.5 ft (.3-.45 m) from its surface The boundary layer also propagates aft of the wheels in the zero crosswind case, to give an effective boundary layer below the side of the trailer. It was difficult to obtain meaningful angularity measures within the truck surface boundary layer, as the differential pressures simply reflected the flow gradient.

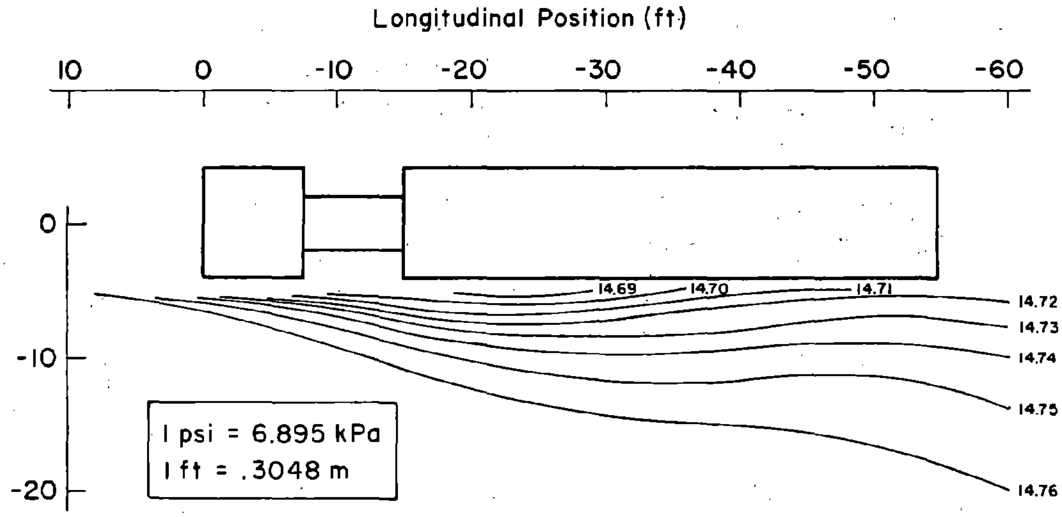

a) No Crosswind

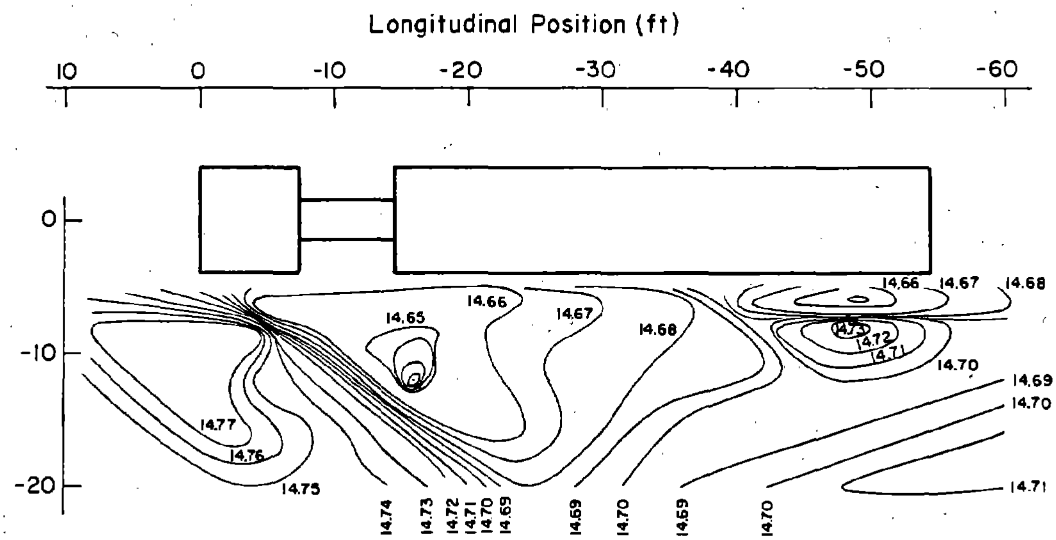

b) -20 deg Relative Crosswind

Figure 68. Iso-Pressure Contours (From Ref. 31)

In general, the wake region aft of the truck in the zero crosswind case comprises turbulent air with small average velocity magnitude. The wake downwind in the crosswind case is composed of alternating regions of fairly uniform large amplitude crossflow (e.g., under the trailer), and regions of lower amplitude turbulent flow. Traversal of these alternating regions, as well as changes in the flow angularity, cause the large changes in the forces and moments which can disturb an adjacent vehicle.

2. Flow Field Modeling

Improved understanding of fluid mechanics and modern computers have made it possible to calculate the flow fields about some bodies with good accuracy. This is not the case, however, for the flow fields about the bulky shapes that characterize road vehicles (e.g., Ref. 54). For this reason, it is current practice to determine the detail flow fields of trucks by wind tunnel modeling.

Recent discussions on the numerical modeling of blunt-body flows are contained in Ref. 54, which concludes that no rational analytical methods to determine flow fields of these vehicles exist, and that even the most advanced numerical techniques will require considerably more development before they can be of even approximate validity. The pertinent issues and limitations are detailed in Ref. 4. On the other hand, in wind tunnels a good representation of the separated flow can be obtained, although there may sometimes be questions raised about scale effect, as it relates to Reynolds number and separation phenomena, as well as to ground plane effects. A discussion of the determination of flow fields by wind tunnel modeling and a classification of the general effects of different truck geometrical features are given in Ref. 55.

Most semitrailers are approximately rectangular and of relatively the same proportions and scales. For zero crosswind there is always a typical subsonic base separation region at the rear face. Whether the flow is separated on the longitudinal sides depends upon the length of the trailer, and on the details of the corners of the front face, as well as whether devices have been installed on the tractor or semitrailer.

The base pressure is approximately constant with a pressure coefficient of between −0.2 and −0.3. It is a matter of interest that differences in gap between the tractor and semitrailer, and even removing the tractor completely (in a wind tunnel test), have a rather minor effect on the semitrailer base pressure. The rear wake flow behind the base appears normally to consist of a recirculating cell of approximately hemispherical shape, like a half bubble attached to the base. No turbulence measurements in this cell are available.

The flow at the front end of the truck varies somewhat depending upon the design of the tractor. A significant flow aspect from the point of view of splash and spray is the pronounced downward flow through the gap between the tractor and trailer. This flow appears to increase with increase in gap distance (Ref. 55), based on smoke visualization measurements and from observations that the drag of the total rig increases as the gap is increased. Drag reducing shields mounted on the semitrailer roof significantly alter this flow. These can apparently eliminate the downward vertical flow if the shield is appropriately sized for the proportions of both the gap and the step height. The latter is defined as the difference in height between the tractor and semitrailer roofs.

At zero crosswind there is always a separated region behind the semitrailer and in the gap, but normally the flow, more than about half a body width away at the sides, is smooth, parallel to the distant flow and at about the same speed, as illustrated in Fig. 67.

If we now consider the flow streamlines for the case of a crosswind, a distinctly different situation occurs. At angles exceeding about a 10 deg relative crosswind (yaw) angle there is massive separation not only at the base and behind the tractor but also on the lee sides of both the tractor and the semitrailer. This can be observed vividly in flow visualization photographs presented by Cooper in a discussion appended to Ref. 55. The complicated nature of this flow can be further observed in the surface flow patterns presented in Ref. 56, and in the STI (Ref. 31) flow field surveys discussed above.

Although the flow is very complicated, and specific details will vary for different geometries, the important result is that in all cases near the wheels, on the lee side there is a major volume of separated flow. Major variables which may be expected to change this significantly include the size of the gap and any gap sealing devices, the rounding of the side edges of the semitrailer, the effects of a drag reducing shield on the tractor, and the effect of the underbody baffle. Removing the gap, either by moving the tractor close to the semitrailer face, or by adding a vertical plate as a gap sealer, does not greatly affect the large turbulent separated area in the lee of the semitrailer. Presumably this is because of the strong three-dimensional effects on the separated flow moving over the top and bottom of the rig.

Both the mean and turbulent components of the flow field are pertinent from a modeling standpoint. For the zero crosswind case, it appears that, in the vicinity of the trailer sides, the flow is smooth, almost parallel to the distant flow, with a small perturbation in speed associated with the displacement of the semitrailer. For the case with a relative crosswind angle, the lee side of the semitrailer is separated, and the general flow is approximately in the free stream direction, but with significant turbulence. This type of flow is characteristic of a separated wake, where the mean velocity is reduced and the turbulence component is high. Measured values for these quantities are given subsequently. In general, the mean velocity varies from about 50 to 80 percent of the free stream flow, with the mean turbulence velocity at about 10 percent of the free stream speed. For the determination of spray dispersion it is only necessary to know the mean streamlines and stream velocities for stream tubes emanating from the spray generation centers at the wheels and the turbulence in the vicinity of these stream tubes (see Section III.B).

3. Wind Tunnel Test Results

As described in Article A, a variety of truck models was tested at GALCIT. The flow field was mapped using tufts on posts, and fastened to the models. Results for all the configurations are given in Ref. 4. They are illustrated below for the basic configuration, 3 axle COE plus 40 ft (12.2 m) van.

An actual tuft photograph is shown in Fig. 69 for the basic truck at a relative crosswind angle of −20 deg. Plots of streamlines and turbulence are shown in Fig. 70 for the no crosswind and −20 deg relative crosswind cases. The streamlines shown are analogous to the flow vector components plotted in Fig. 67 from Ref. 31. Shown in Fig. 70 are the streamlines and turbulence maps of the flow around the truck constructed from the tuft patterns, as well as the velocities measured at several points in the flow. These velocities are normalized by the free stream undisturbed velocity. The turbulence in the flow was inferred from the tuft pictures. In the no crosswind case there is negligible turbulence.

The velocities and turbulence in the wake are used in modeling the spray plumes (see Article III.B). Figure 70b shows the turbulent flow field for the −20 deg crosswind case with the basic truck. The clear background areas indicate turbulent velocities on the order of five percent or less of the free stream velocity (light turbulence). Turbulence levels of 10 percent of the free stream velocity are indicated by the cross-hatched areas (moderate turbulence). High turbulence regions (about 20 percent of the free stream) are shown by the shaded areas. Of the nominal configurations tested (detailed in Ref. 4), the empty flatbed had the lowest average turbulence levels and largest areas of clean flow. The configuration with the next lowest turbulence was the liquid tanker configuration. There were some areas of clean flow for this configuration, a large area of moderate turbulence, and an area of high turbulence from the cab. The 3 axle COE plus 40 ft van configuration fitted with drag shield and Reddaway flaps had the most extensive areas of turbulence. Most of the turbulence greater than the turbulence of the unmodified 3 axle COE plus 40 ft van configuration comes from the cab. There is also an area of clean flow near the front of the van. The (unmodified) basic truck has about average turbulence in the wake area, as shown in Fig. 70b.

Surface pressure measures were made on the basic truck in the GALCIT tests, and the results are given in Ref. 4. These are expressed in terms of pressure coefficients, C_p. In general, for the relative crosswind case the pressure on the windward side of the truck was higher than for no crosswind, as would be expected due to cross flow. It should be noted that

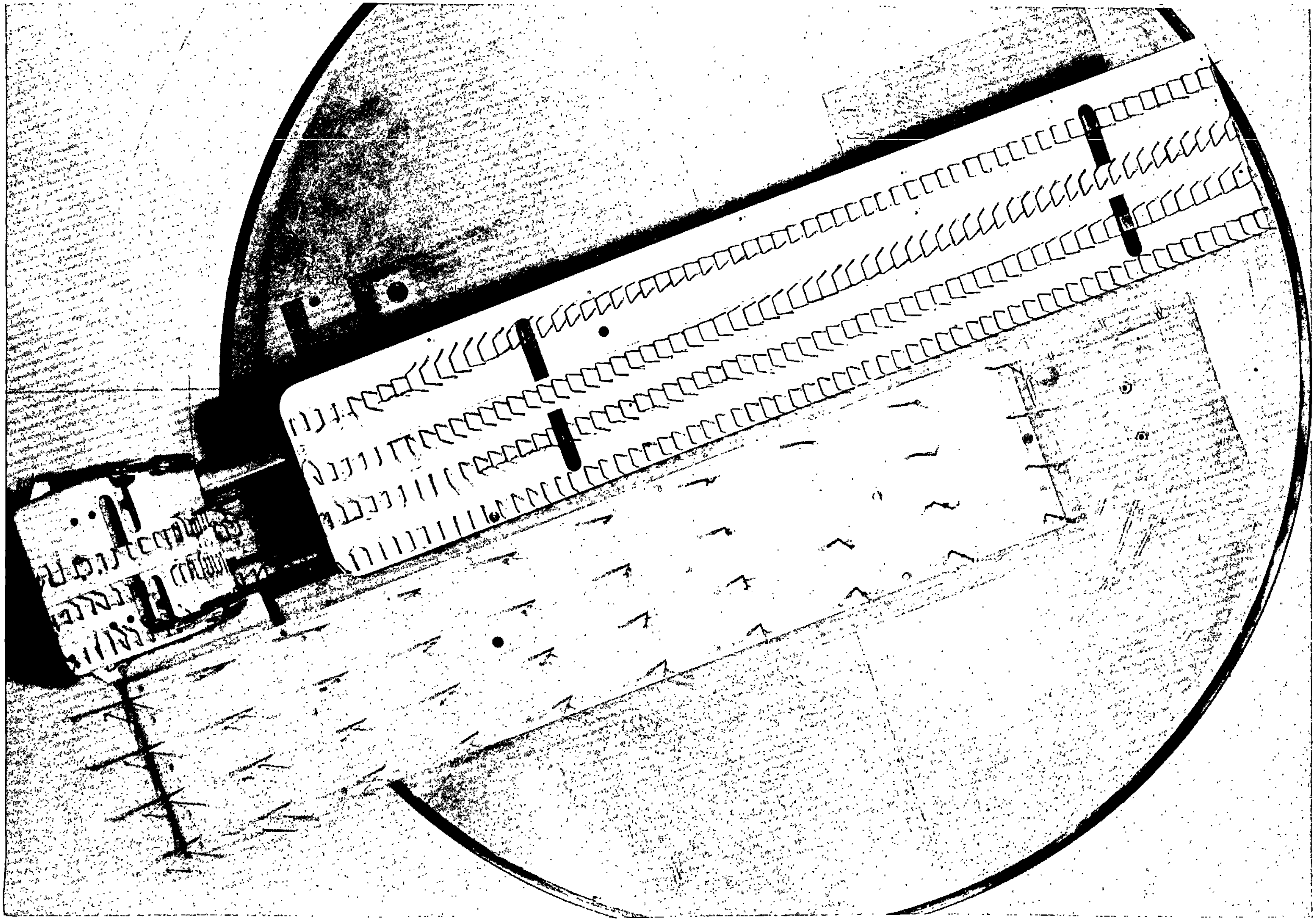

Figure 69. Typical Tuft Photograph, 3 Axle COE Plus 40 ft (12.2 m) Van, $\psi_W = -20$ deg

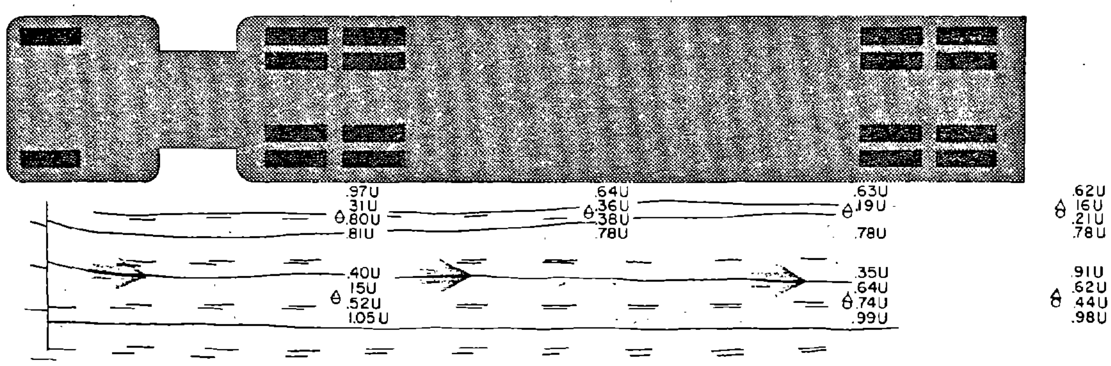

a) No Crosswind

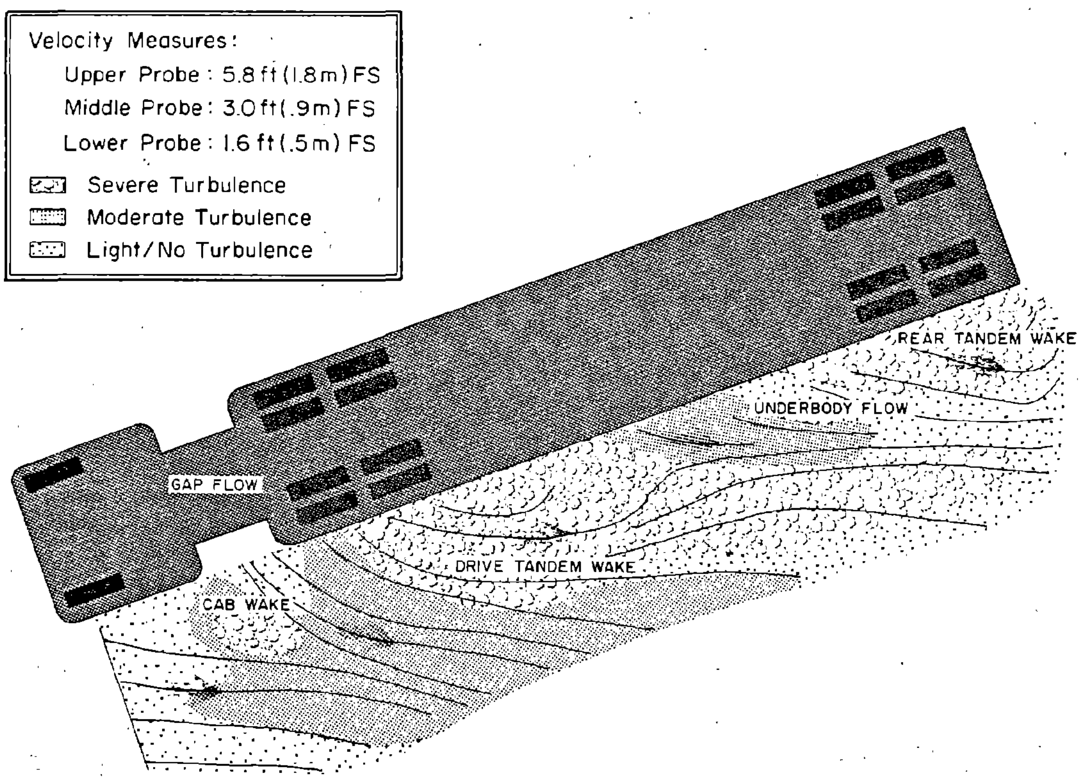

b) -20 deg Relative Crosswind

Figure 70. Streamlines and Turbulence, Basic Truck Configuration

pressure readings made in the separated wake regions cannot be used to determine the surface velocities. Pressure measures in the wake were illustrated in Fig. 68, from Ref. 31.

4. Full Scale Test Results

At the first series of full scale tests at Ft. Stockton, six anemometers were set up near the track to record the wake velocities of the truck. These anemometers were arranged in two rows of three each. Each row was parallel to the test lane, and they were at different distances from the lane. Usually, two anemometers from each row gave useful data. Data for representative truck configurations are given in the AVI report, Ref. 4.

Example results obtained downwind of the basic truck, with a relative crosswind angle (ψ_W) of about −9 deg, are shown in Fig. 71. Here, U_T is the truck ground speed, v_O is the nominal truck airspeed component in the direction of travel, and v/v_O is the wake velocity as a fraction of the nominal truck airspeed. This figure shows the wake velocities as recorded by four of the anemometers, two from each row. The anemometer locations are shown in the figure, with the zero velocity line of the anemometer traces placed at the appropriate distance from the truck. The horizontal axis gives the distance from the front of the truck. The horizontal and vertical scales are not the same, resulting in a distorted representation of the truck shape, but the anemometer traces are in scale to the length of the truck. A broken line is given to mark the leading edge of the wake region.

The data in Ref. 4 show that, by comparison with the basic configuration, the addition of a drag shield and Reddaway flaps caused an increase in the wake velocity deficit near the truck, but a decrease in the deficit away from the truck. The liquid tanker had wake velocities comparable to the basic configuration near the truck, but lower velocities away from the truck. However, the regions of large velocity deficit extended further downstream than in the baseline configuration. The 3 axle COE plus empty flatbed semitrailer had the lowest wake velocities of the four nominal configurations analyzed.

The anemometer data were analyzed to find the maximum wake velocity deficit given by each trace. These data were then plotted against distance

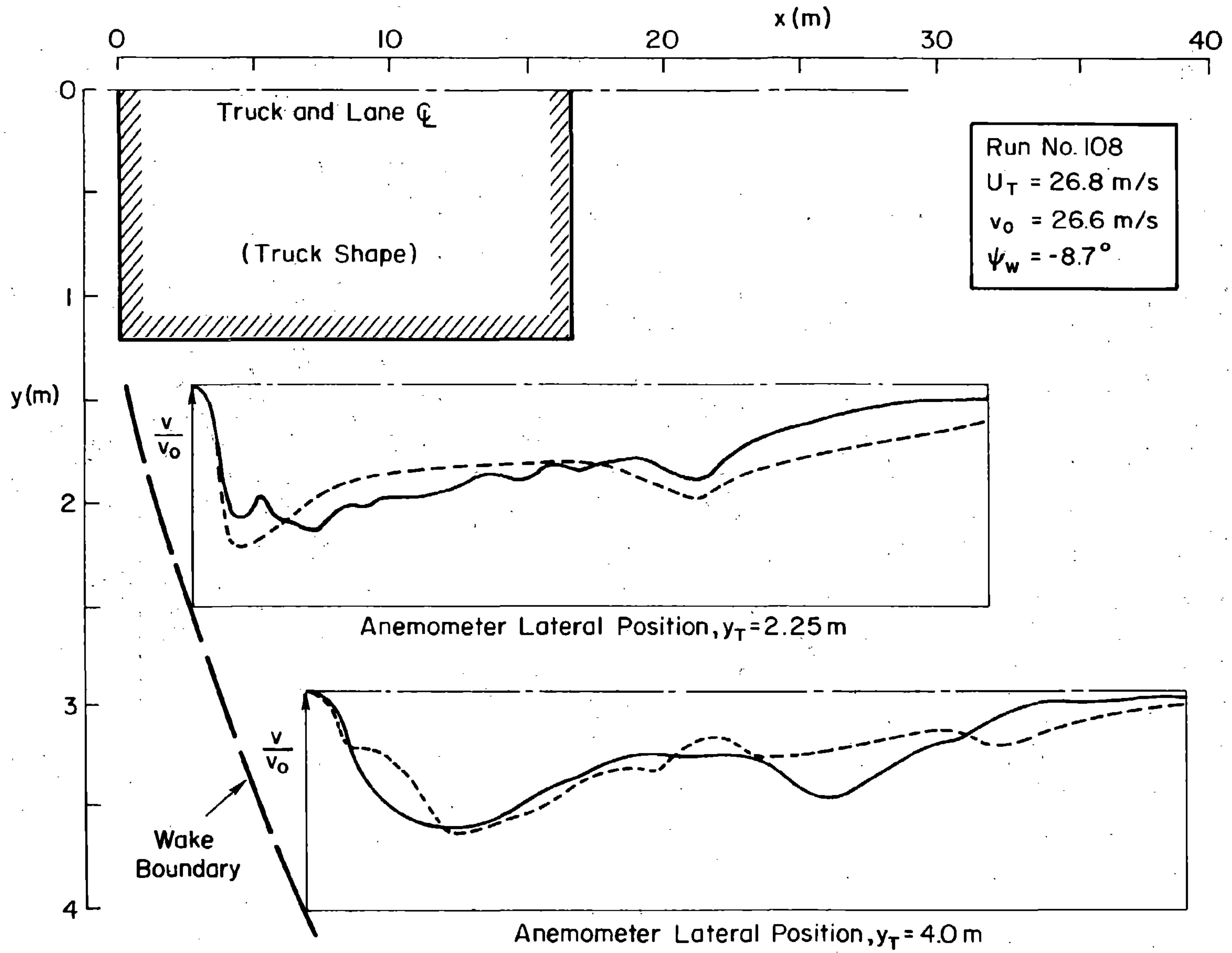

Figure 71. Wake Velocities from Full Scale Anemometers, 3 Axle COE Plus 40 ft Van

from the truck side. The wake velocity deficits for several different configurations are shown in Fig. 72. The wake deficit $(v_o - v)$ is shown normalized by the truck airspeed (v_o). These velocities are as measured by anemometers, so a value of $1 - (v/v_o)$ equal to one indicates the air is moving at the same speed as the truck. This shows very clearly the differences in the wake flows between the various configurations. It can be seen that the drag shield does decrease the wake velocities over the configuration without a drag shield. The flatbed and liquid tanker semitrailers are seen to have lower wake velocities than the 40 ft van. The CBE tractor also has lower wake velocities than the COE tractor.

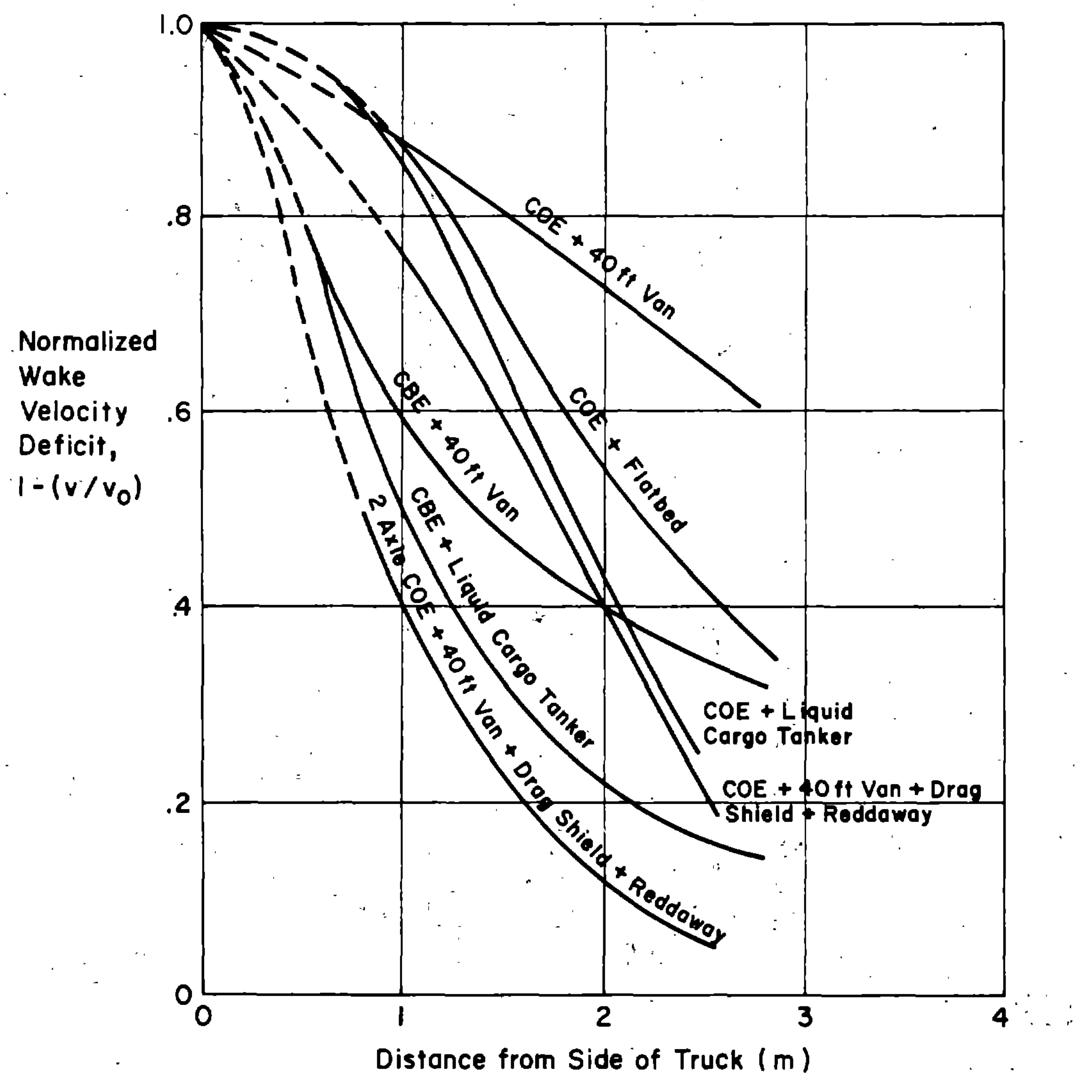

Figure 72. Summary of Full Scale Ground Aneometer Data (Ref. 4)

5. Wake Velocity and Turbulence Parameters

The splash and spray model requires the mean wake velocity (U_1) and turbulence levels (V_T) for plumes starting at the various points on the truck. The former were determined from the GALCIT data and the anemometer data, and the turbulence levels were estimated from the anemometer data and turbulence diagrams. These flow parameters have been determined for three regions of interest: flow from the front wheel area, from the drive tandem wheels, and from the semitrailer rear wheels. These parameters are shown in Table 5 for four nominal configurations at –20 deg relative crosswind angle. The mean wake and turbulence velocity values are averages taken along streamlines over a distance of one truck length. The streamlines in the wake originate at the wheel sets noted, and are assumed to be in the free stream direction. Velocities shown in Table 5 have been normalized by the free stream velocity relative to the truck, v_o.

These mean and turbulence values are generally supported by prior vehicle aerodynamic studies made by STI. Nevertheless, Refs. 2, 3, and 31 show slightly higher turbulence levels along a track parallel to the vehicle direction of travel than are shown in Table 5 as average values along streamlines. Yet, the two sets of results are felt to be compatible, because the averaging process used in the current study gives turbulence levels lower than observed in close proximity to the vehicle but higher than observed one vehicle length downstream.

C. TRUCK FORCE AND MOMENT DATA

Force and moment measures were made on the various truck configurations in the GALCIT tests. From these, drag data have been extracted for use in the cost-effectiveness analyses of Section VII. Pertinent data from the literature were used to confirm the results, and adjustments were made in some cases, in order to obtain representative generic values. Drag estimates were also made for some truck configurations (e.g., triples) and promising device combinations that were not tested.

Drag results for the various truck configurations are presented first, followed by the values for devices. The article concludes with a summary of the other force and moment data.

TABLE 5

MEAN WAKE AND TURBULENCE VELOCITIES (REF. 4)

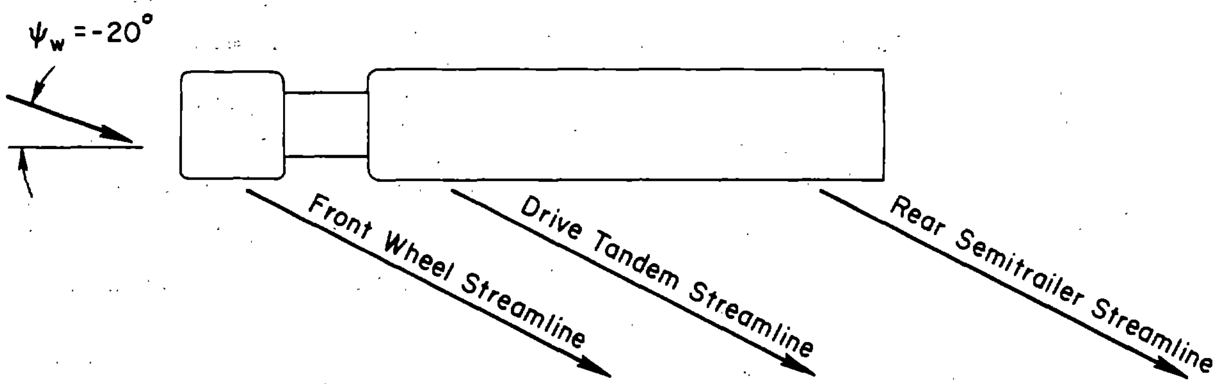

U_1 = Mean wake velocity along streamline averaged over one truck length from GALCIT test data and Ft. Stockton anemometer data

V_T = Turbulence velocity averaged along streamlines over one truck length from Ft. Stockton anemometer data and GALCIT tuft studies

v_o = Wind speed relative to truck

CONFIGURATION	FRONT WHEELS		DRIVE TANDEMS		REAR SEMITRAILER	
	U_1/v_o	V_T/v_o	U_1/v_o	V_T/v_o	U_1/v_o	V_T/v_o
COE + 40 ft van	0.50	0.10	0.60	0.10	0.70	0.10
COE + liquid tanker	0.50	0.15	0.70	0.10	0.80	0.07
COE + flatbed	0.55	0.10	0.65	0.10	0.75	0.05
COE + 40 ft van + drag shield + Reddaway flaps	0.55	0.15	0.70	0.07	0.80	0.10

At GALCIT, the lateral-directional coefficients were obtained by the equations for a right hand system with z down and x forward,

$$C_y = \frac{Y}{qA} \tag{8}$$

$$C_n = \frac{N}{qA\ell} \tag{9}$$

$$C_\ell = \frac{L}{qA\ell} \tag{10}$$

for side force, and yaw and roll moment. The longitudinal coefficients were defined by

$$C_D = \frac{-X}{qA} \tag{11}$$

$$C_L = \frac{-Z}{qA} \tag{12}$$

$$C_m = \frac{M}{qA\ell} \tag{13}$$

for drag, lift, and pitch moment. The dynamic pressure is q, A is the frontal area of the complete truck configuration (including the portions of the semitrailer extending beyond the tractor), and ℓ is the wheelbase, as defined in Article A, above. When devices were added to the basic truck, the reference frontal area was not changed. The moment reference point is at the ground, at midwheelbase, on the centerline.

1. Drag Data for Various Trucks

Truck drag data are available for no crosswind (the usual case) and for a 20 deg relative wind angle. To more readily express and analyze the results for a variety of trucks, the drag is expressed in terms of an effective full scale flat plate area, i.e.,

$$A_{EFF} = C_D A \tag{14}$$

where C_D is the drag coefficient computed from Eq. 11 and A is the reference frontal area for that truck.

The presence of the surface mounted tufts caused a small increment in the drag measures, and this has been removed in the results reported below. In addition, the raw drag coefficient values for the two relative wind angles were compared with data in the literature (e.g., Refs. 21, 23, and 57), and some minor corrections were made, as discussed later. In general, however, the agreement was quite clear.

The effective drag values for various trucks are presented in Table 6, in terms of effective frontal area (1 ft^2 = 0.093 m^2). Those for the first six trucks listed were direct measures, verified as noted above. The remainder were obtained from the literature and data composites, as discussed below. It is interesting to note that the CBE results do not differ

TABLE 6. DRAG VALUES FOR VARIOUS TRUCK CONFIGURATIONS
(1 ft^2 = 0.093 m^2)

CONFIGURATION	$A_{EFF}(0)$ (ft^2)	$A_{EFF}(20)$ (ft^2)
3 axle COE + 40 ft van	85	145
3 axle COE + 40 ft flatbed	70	87
3 axle COE + liquid cargo tanker	71	108
3 axle COE + dry cargo tanker	81	144
3 axle CBE + 40 ft van	85	119
2 axle COE + 27 ft van	81	118
2 axle COE + double 27 ft vans	93	156
2 axle COE + triple 27 ft vans	108	199
2 axle COE + 40 ft van	80	126
2 axle COE + double 40 ft vans	94	178

from those for the COE (with no crosswind), and this is confirmed in the literature (e.g., Ref. 55). Adding trailers to create doubles and triples only has a small effect, relative to the increase in cargo capacity, for no crosswind. The effect in a strong crosswind is more pronounced, as would be expected, but the drag does not increase directly with size or length (see the last two entries, for example).

To estimate the drag values for the combination rigs shown in Table 6, the drag was broken down into components of:

- Form drag, C_{D_P}
- Gap interference drag, C_{D_G}
- Friction drag, C_{D_F}
- Base drag, C_{D_B}
- Induced drag, C_{D_I}

The drag related to the gaps between successive trailers, C_{D_G}, was estimated from wind tunnel measurements by Flynn and Kyropoulos (Ref. 7) for $\psi_W = 0$ and 20 deg. Friction drag was estimated from standard friction curves (C_f vs. Re) and proportioned according to trailer length. Base drag was estimated using the expression in Hoerner (Ref. 58), i.e.,

$$C_{D_B} \doteq .029/\sqrt{C_{f_B}}$$

where the forebody friction drag, C_{f_B}, is proportional to the ratio of the wetted area and the reference area. Thus, C_{D_B} is taken to be inversely proportional to the square root of the trailer length, because the wetted area grows with the length of the trailer. Note that the surfaces assumed to contribute significantly to the wetted area were the two sides and the top of the semitrailer. The underneath and the two ends were omitted, as was the wetted area of the tractor. The values of base drag were confirmed by the University of Maryland wind tunnel tests (Ref. 59) and extended to $\psi_W = 20$ deg by the same tests. The induced drag of the basic truck (single semitrailer) configuration was inferred from this drag breakdown after assuming that the form drag was constant. The induced drag for $\psi_W = 20$ was assumed to be proportional to the total side force and thus the trailer length.

To summarize these points, the components in this drag estimating procedure are tabulated in Table 7. The total drag is given in the first column, C_D. The five components are given next. As noted, the following proportional relations hold:

$$C_{D_G} \sim \text{Number of trailers}$$

$$C_{D_F} \sim \ell/\ell_o$$

$$C_{D_B} \sim \sqrt{\ell_o/\ell}$$

$$C_{D_I} \sim \ell/\ell_o$$

where ℓ_o is the length of the basic single semitrailer, 40 ft (12.2 m). The last column in Table 7 is the incremental drag, ΔC_D, due to adding another trailer, i.e., the difference between the respective C_D values in the first column. As a crosscheck, analogous train data presented by Johansen (Ref. 60) suggest that the drag increment roughly doubles in going from zero crosswind to a 20 deg relative wind angle. Such a large increase is seen by comparing the ΔC_D values for the 20 deg wind case (0.31) and the no crosswind case (0.12) for the double 27 ft vans in Table 7.

The general scatter in absolute drag levels in tests by various experimenters should be noted. For example, for a 3 axle COE sleeper with a gap of about 0.5 of the trailer height, Mason and Beebe (Ref. 55) measured a zero yaw drag coefficient of about 1.0 in wind tunnel tests at a Reynolds number based on effective diameter of 2×10^6. They quote in their paper the result given in Ref. 62 of a drag coefficient of about 0.59 for a similar rig in a wind tunnel test of unknown Reynolds number. In the same volume of proceedings (Ref. 54), Buckley in a discussion of Bearman quotes, for a similar COE rig at similar gap, the drag coefficient of 0.75 obtained both in full scale road tests at a Reynolds number of about 6×10^6 and in wind tunnel tests at a Reynolds number of about 1.2×10^6. In terms of drag coefficient, the Table 7 values indicate a drag coefficient of about

TABLE 7. DRAG COEFFICIENT BREAKDOWN FOR MULTIPLE TRAILER CONFIGURATIONS

CONFIGURATION	ψ_W (deg)	C_D	C_{D_P}	C_{D_G}	C_{D_F}	C_{D_B}	C_{D_I}	ΔC_D
3 axle COE + 40 ft van	0	.84[a]	.56	.14[b]	.04[c]	.10[d]	0	—
2 axle COE + 27 ft van	0	.79[a]	.51	.13	.03	.12	0	—
2 axle COE + double 27	0	.91	.51	.26	.06	.08	0	.12
2 axle COE + triple 27	0	1.06	.51	.39	.09	.07	0	.15
2 axle COE + 40 ft van	0	.78	.51	.13	.04	.10	0	—
2 axle COE + double 40	0	.92	.51	.26	.08	.07	0	.14
3 axle COE + 40 ft van	20	1.43[a]	.56	.24[b]	.04[c]	.25[d]	.34	—
2 axle COE + 27 ft van	20	1.16[a]	.40	.20	.03	.30	.23	—
2 axle COE + double 27	20	1.53	.40	.40	.06	.21	.46	.37
2 axle COE + triple 27	20	1.95	.40	.60	.09	.17	.69	.42
2 axle COE + 40 ft semi	20	1.23	.40	.20	.04	.25	.34	—
2 axle COE + double 40	20	1.74	.40	.40	.08	.18	.68	.51

[a]Present tests. [b]Reference 7. [c]Reference 58. [d]Reference 59.

0.80 for a similar rig, with only a few percent reduction when the tractor is changed to a CBE (conventional) design.

2. Drag Data for Configuration Changes and Devices

Drag values for some variations in the basic truck configuration (3 axle COE plus 40 ft van) are given in Table 8. As with Table 7, the drag is expressed here in terms of the effective frontal area, $A_{EFF} = C_D A$, in square feet (1 ft^2 = .093 m^2). As noted above, the reference frontal area (A) was not changed when a device was added. The three different gap variations (full scale dimensions shown) were all run with 12 in. (0.31 m) radius vertical leading edges on the semitrailer. The 90 in. (2.30 m) gap was standard on the basic truck. The 30 in. (0.76 m) gap was obtained via the gap filler block, effectively simulating a 45 ft (13.7 m) semitrailer. In Table 6 the two axle COE plus 40 ft van gap was set at 44 in. (1.12 m), full scale. The gap between the respective 27 ft vans and the 40 ft vans was set at 46 in. (1.17 m), full scale.

TABLE 8

DRAG VALUES FOR VARIATIONS IN BASIC TRUCK CONFIGURATION
(1 ft^2 = 0.093 m^2)

VARIATION	$A_{EFF}(0)$	$A_{EFF}(20)$
90 in. (2.30 m) gap	85	145
60 in. (1.50 m) gap	85	136
30 in. (0.76 m) gap	82	127
Square corners	91	155
24 in. (0.61 m) corner radii	86	131
Lateral lips on semitrailer	84	139
Deflector foil	87	147

Other investigators (e.g., Mason and Beebe in Ref. 55) have also shown that the drag reduces in the yawed case with rounding of the trailer leading edges. It is interesting to note that Table 8 shows little advantage of minor rounding of the leading edges when there is no cross flow ($\psi_W = 0$).

Drag values for the basic truck with various devices and device combinations are given in Table 9, in terms of the effective area per Eq. 14. Again, note that the reference frontal area (A) was not changed when the devices were added. The wind tunnel configurations in the middle column are keyed to the list in Article A.3, above. The basic truck is the 3 axle COE plus 40 ft van, as usual, and two entries are also given for the CBE tractor. The device configurations in the last column provide a cross reference to the devices listed in Table 3 (Section IV). As discussed, some of the device combinations shown in Table 9 are hybrids, based on a composite of data. The last entry, 3 axle CBE plus 40 ft van plus drag shield, was based in part on the Ref. 23 data. Some of the latter entries in Table 9 do not have a device code associated with them, because they were not run as prototypes in the full scale splash and spray tests.

The drag values for some of the truck plus device combinations were estimated by considering incremental values from the basic measures. The more pertinent of these increments are listed in Table 10, again in terms of effective frontal area. With only one device installed, such as the drag shield, the change is a simple decrement in drag. Most of the increments shown are based on the GALCIT data, and confirmed by the literature. The last crosswind value, longitudinal baffle plus gap splitter panel, was estimated by taking the square root of the sum of the squares of the two contributions. The two together are somewhat better than either alone, but the drag of the truck in the 20 deg relative crosswind is unlikely to be less than the drag of the basic truck with no crosswind. It should be noted that the Reddaway flaps are not treated here as "fenders" in the sense of the DOT or Roberts design, and they have been assumed to not provide the small drag advantage associated with the fender results. Full scale test experience bears this out.

Some of the drag-reducing devices in Table 9 are similar to those in current use on the highway. Typically, these concentrate on flow control

TABLE 9

DRAG VALUES FOR BASIC TRUCK WITH DEVICES
(1 ft^2 = 0.093 m^2)

WIND TUNNEL CONFIGURATION	DEVICE CONFIGURATIONS	$A_{EFF}(0)$	$A_{EFF}(20)$
Basic truck	F1, M1, M2, M3, M4, M5, T	85	145
+ drag shield	D1, F2, MO, M7	68	145
Basic truck + fenders	E1, E2, R1	84	142
+ fenders + drag shield	R2	67	142
Basic truck + longitudinal baffle	L3	84	97
+ longitudinal baffle + gap splitter panel	L2	85	85
+ longitudinal baffle + gap splitter panel + drag shield	L1	68	85
Basic truck + longitudinal baffle + drag shield	F3, L4, M6	68	97
Basic truck + horizontal gap plate	G1, G2	85	139
+ 1/2 horizontal gap plate	P1, P2, P3	85	142
Basic truck + side vanes	V1	105	165
+ side vanes + drag shield	V2	88	165
+ 1/2 side vanes + drag shield	V3, V4	78	155
Basic truck + gap splitter panel		86	109
Basic truck + bumper dam		98	152
Basic truck + lateral lips		84	139
Basic truck + deflector foil		87	147
Basic truck – mud flaps		84	143
3 axle CBE + 40 ft van		85	119
+ drag shield		75	119

TABLE 10. NOMINAL DRAG INCREMENTS FOR VARIOUS DEVICES

CHANGE OR DEVICE	$\Delta A_{EFF}(0)$	$\Delta A_{EFF}(20)$
Drag shield	−17	0
Mud flaps off	− 0.5	− 2
Fenders	− 1	− 3
Longitudinal baffle	− 1	−48
Horizontal gap plate	0	− 6
Angled side vanes	+20	+20
Gap splitter panel	+ 1	−36
Longitudinal baffle + gap splitter panel	0	−60

near the front face of the trailer and in the tractor-trailer gap, and they essentially affect the forebody drag of the rig. For devices mounted on the tractor roof, the basic function is to smoothly deflect the incoming flow so that it does not impinge on the semitrailer face, but strikes approximately at the upper edge of the semitrailer. The device should not be so large that the flow is deflected substantially above the trailer roof, since this will cause drag penalties. By avoiding a stagnation region on the front face of the trailer, not only is the pressure drag on the trailer reduced, but also the vertical downwards flow towards the rear wheels of the tractor. The latter effect has been observed by many other experimenters too (see, e.g., Ref. 55). It can be significant in the dispersion of the spray by this wheel set, by creating a more intense turbulence field near the wheels. Hence, reducing the gap vertical flow by shields should reduce turbulence, as well. On the other hand, in cross flow cases, shield-type devices can produce more intense turbulence fields due to flow through the gap, and (presumably) interactions with separations developed on the lateral edges of the shield. Similarly, a gap sealer or vertical plate between the tractor and semitrailer could produce the same effect of more turbulence at the wheel level in relative crosswind flows due to cross flow over the top and bottom of the plate.

The effect of the gap dimension can be considered in similar terms. While it has some effect on drag in the no yaw case, the effect is more pronounced in the case of cross flows (see Table 10). Thus, gap flow can contribute to the wheel turbulence, and have some influence on splash and spray.

Another forebody parameter previously discussed is the effect of radiusing the vertical leading edges of the semitrailer. This can suppress or delay flow separation from these edges, and the drag effect can be significant. However, for relative crosswind angles of about 10 deg, the flow at the downstream or lee side of the gap is apparently similar to that for sharp edges. Thus, the drag reduction with cross flow is apparently due to effects at the windward leading edge.

3. Effect of Variations in Relative Crosswind Angle

In the preceding results, two values of drag have been given, one for no crosswind angle ($\psi_W = 0°$) and one for a crosswind angle (ψ_W) of 20 deg. There are abundant data in the literature to show how the drag varies for intermediate values of relative flow angle (e.g., Refs. 16, 23, 24, 29, and 61). Based on the results, the functional relation shown in Fig. 73 has been used to define the drag, given the values at 0 and 20 deg relative wind. It has been modeled as if the effective cross sectional area, A_{EFF}, is varying. The expression for the truck drag is

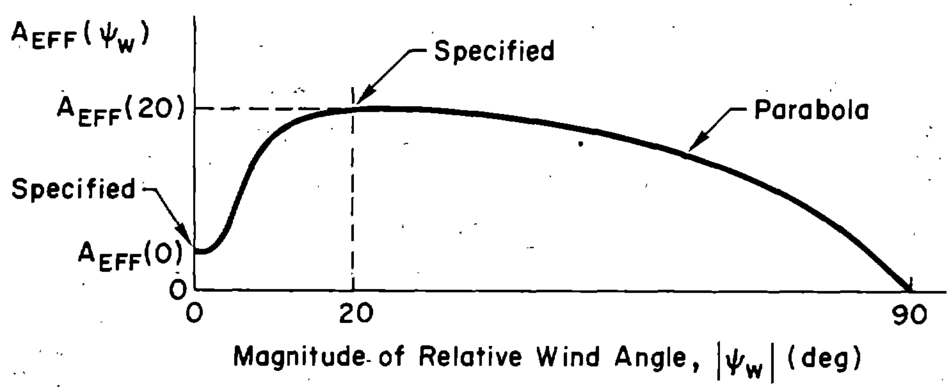

Figure 73. Assumed Variation in Effective Cross Sectional Area with Relative Wind Angle

$$\mathrm{DRAG} = A_{EFF}(\psi_W) \cdot \frac{1}{2} \rho v_o^2 \tag{15}$$

where ρ is the air density, v_o is the total truck velocity relative to wind, and ψ_W is the apparent wind angle relative to the truck centerline. The variation in effective cross sectional area with relative wind angle is given by

$$A_{EFF}(\psi_W) = A_{EFF}(0) + [A_{EFF}(20) - A_{EFF}(0)]f(\psi_W) \tag{16}$$

with the wind angle function being

$$f(\psi_W) = \begin{cases} \left[1 - \left(\frac{|\psi_W|}{20} - 1\right)^{2.8}\right]^2 & ; \quad \text{for } \psi_W \text{ in deg and } |\psi_W| \le 20 \text{ deg} \\ 1 - \left(\frac{\frac{|\psi_W|}{20} - 1}{(90/20) - 1}\right)^2 \left[1 + \frac{A_{EFF}(0)}{A_{EFF}(20) - A_{EFF}(0)}\right] & ; \quad \text{for } \psi_W \text{ in deg and } |\psi_W| > 20 \text{ deg} \end{cases} \tag{17}$$

This is the equation for the curve shown in Fig. 73. Using this relation, the available data were scaled over a range of ambient wind angles and magnitudes in the cost-effectiveness analyses of Section VII. Clearly, relative wind angles in the range ±20 deg involve the least extrapolation of A_{EFF}.

4. Lateral-Directional Data for Various Trucks

At GALCIT, the lateral-directional forces and moments were measured for the various trucks, and for the basic truck with the devices and configuration modifications. The basic aerodynamic coefficients were defined and computed using Eqs. 8-10 for side force, yaw moment, and roll moment, respectively. Note the negative signs in Eqs. 9 and 10. The measurement axis system was at the ground level, midway between the front axle and the center (midpoint) of the trailer tandems. To compute the aerodynamic "derivative" coefficient, the change over 20 deg (0.35 rad) was computed, and the reported value is a nondimensional force or moment per radian of aerodynamic sideslip ($\beta = -\psi_W$). This assumes that the gradient was linear up to 20 degrees of relative crosswind angle. The results are given in Table 11.

In general, for ψ_W positive, the side force was to the right. The yaw moment was tending to weathervane the truck into the wind, unlike a car which is usually tending to blow the nose away. The roll moment was towards the right wheels for $\psi_W +$.

The tuft rake location on the tunnel floor adjacent to the model is indicated in the last column. These locations are defined in Fig. 45 of Article A, above. The location is important because even when it was downwind of the truck it is seen to have a minor influence on the measures. Note also that all the models had surface tufts mounted (see Fig. 69) for these data, except for the one basic truck run so indicated in Table 11. Despite variations the tufts may have introduced, the results are reported here for reference.

The longitudinal baffle is seen to have a very significant effect on the side force ($C_{y_{\psi_W}}$) and roll moment ($C_{\ell_{\psi_W}}$) coefficients, as would be expected. The reason for the change in sign of the roll moment is unclear, and it may reflect an error in the data (which were recorded automatically). The gap splitter panel changes sign of the yaw derivative, although the side force coefficient increases in magnitude only a small amount. This change in the yaw derivative could lead to a more sensitive crosswind gust response, particularly with a lightly loaded truck (neglecting articulation dynamics). The shorter gap (30 in., 0.76 m) resulting from the gap filler block leads to a similar trend. The coefficients vary quite a bit for the other truck configurations, and the differences are what would be expected from overall geometry and shape factors.

TABLE 11. LATERAL-DIRECTIONAL COEFFICIENTS FOR VARIOUS TRUCK CONFIGURATIONS

TRUCK	DEVICE	$C_{y_{\psi_W}}$ (rad^{-1})	$C_{n_{\psi_W}}$ (rad^{-1})	$C_{\ell_{\psi_W}}$ (rad^{-1})	TUFT LOCATION
3 axle COE + 40 ft van	—	6.3	−.54	.99	Forward
	—	6.1	−.49	.97	Aft
	(No tufts)	6.6	−.38	1.09	None
	+ drag shield	6.2	−.49	.99	Forward
	+ fenders	6.2	−.49	.97	Aft
	+ longitudinal baffle	9.0	−.40	−.56	Aft
	+ horizontal gap plate	6.3	−.42	1.00	Forward
	+ angled side vanes	6.0	−.54	.95	Forward
	+ gap splitter panel	7.1	+.10	1.06	Forward
	+ bumper dam	6.2	−.66	.99	Forward
	30 in. (.76 m) gap	6.7	−.02	1.07	Forward
	Square corners	6.1	−.58	.96	Forward
	24 in. (.61 m) corner radii	6.3	−.43	1.03	Forward
	+ lateral lips	5.6	−.42	.83	Forward
	+ deflector foil	6.5	−.66	1.06	Aft
	− mud flaps	6.1	−.44	.96	Aft
3 axle CBE + 40 ft van	—	6.1	−.23	.99	Forward
3 axle COE + dry cargo tanker	—	4.4	−.17	.50	Aft
3 axle + flatbed	—	1.8	−.03	.21	Aft
3 axle COE + liquid cargo tanker	—	3.6	−.19	.36	Aft
2 axle COE + 27 ft van	—	4.5	−.14	1.07	Aft

D. ADJACENT CAR FORCE AND MOMENT DATA

The aerodynamic forces and moments on cars in proximity to commercial vehicles have been studied extensively by STI for the FHWA. Basic results are given in Refs. 2, 3, 29, and 31, and a summary is provided in Ref. 6. Some work on the aerodynamic interaction of road vehicles has been accomplished by others, most notably that of Brown and Seeman (Ref. 30), Beauvais (Ref. 65), Larrabee (Ref. 66), and Romberg, et al. (Ref. 67). Definition of the disturbance situation and example aerodynamic data, full scale results, and performance measures are presented in Article III.C, based on the STI work referenced above.

This article presents additional adjacent car disturbance data obtained in the Northrop low speed tunnel during the current test series. That facility, and the test procedures used, are described in Article A of this section. The article begins with definitions of the forces and moments and a discussion of the data. This is followed by the basic aerodynamic data for the car alone. Then, the main data set for the adjacent car in the presence of various truck configurations is presented.

1. Definitions and Discussion

The lateral-directional forces and moments on the 1972 Chevrolet station wagon model in the Northrop tests were nondimensionalized as follows:

$$C_y = \frac{Y}{qA} \tag{18}$$

$$C_n = \frac{N}{qA\ell} \tag{19}$$

$$C_\ell = \frac{L}{qAt} \tag{20}$$

for side force and yaw and roll moment, respectively. These are similar to the forms used for the truck measures, given in Eqs. 8-10. As before, q is the dynamic pressure, A is the reference frontal area of the car, ℓ is the wheelbase, and t is the mean track. A right-hand axis system is used with y positive to the right, x forward, and z down. The axis system origin was at the ground level at midwheelbase.

The present experiments, and those reported by STI in Refs. 2 and 3, were all accomplished with models stationary relative to one another. Force and moment measures were taken for one relative car-truck orientation (see Figs. 20 and 46), then the wind tunnel was shut down momentarily while the disturbing truck was moved to a new location relative to the metric car model. Our past correlations between these results and dynamic full scale results (see, e.g., Fig. 21) have been good, primarily because the relative speed between the car and truck is relatively slow (2-4 m/s) compared to the time constants associated with any aerodynamic nonstationarities. Comparison of our model scale results with transient measures of others confirm this finding, as illustrated below.

The findings of Brown and Seeman (Ref. 30) from moving model experiments with a car and a bus can be compared to our "static" test data (e.g., from Refs. 2 and 29). Noting that Ref. 30 used a Ford Torino while we used a Chevrolet station wagon model,* and accounting for differences in axis systems and sign conventions, the comparison of nondimensional side force coefficients shown in Fig. 30 obtains. The curves are for no crosswind and an 8 ft (2.44 m) bus-vehicle centerline separation. The Ref. 30 data were obtained from one run under transient (moving model) conditions with the bus model at 70 mph (31 m/s) passing the Torino Model going 50 mph (22 m/s). The STI data were obtained for various relative orientations of the car and bus, one point at a time, as noted. Both sets of data show the bow wave peak near the front of the bus. The first Ref. 30 peak occurs somewhat aft of the STI peak, and this may reflect a true transient phenomenon resulting from the relative motion of the Ref. 30 models. The initial peak is a little higher for Ref. 30 than STI, and this may correspond partly to the 28 percent difference in vehicle-alone side force derivatives noted above. Note that such a shift in the first peak will not affect such overall performance measures as peak lateral deviation ($\hat{y}_I$); it just means that it will occur at a slightly different location relative to the front of the

---

*$C_{y_{W_\psi}}$ was 0.037 deg^{-1} for the Chevrolet wagon and 0.047 deg^{-1} for the Ford Torino.

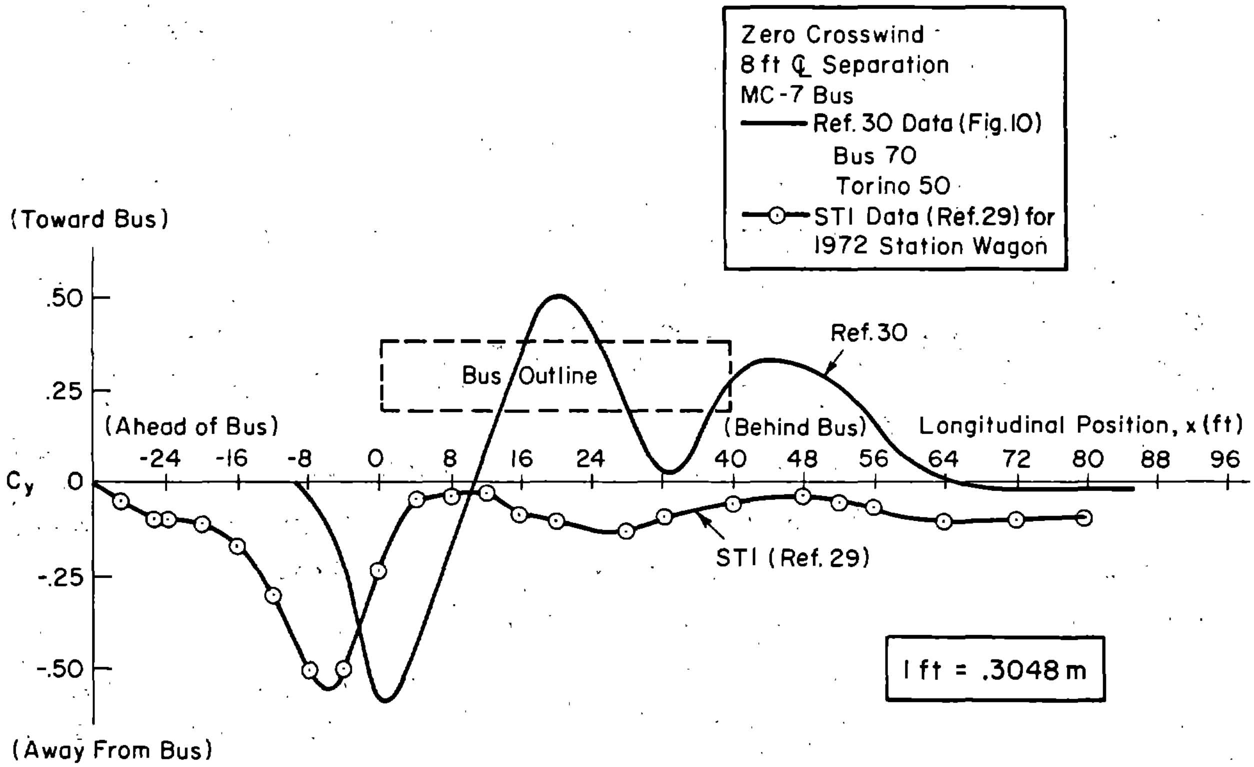

Figure 74. Comparison of Side Force Coefficients, Zero Crosswind (Refs. 29 and 30)

bus. The big difference between the Ref. 29 and Ref. 30 results occurs alongside and to the rear of the bus. The latter shows two large peaks toward the bus, while the STI data show little disturbance aft of the bow wake peak. Informal discussions with the authors of Ref. 30 indicates that these aft peaks are probably due to the closeness of the models with 8 ft (2.44 m) centerline separations, placing the car in the influence of a vortex street shed off the bus and causes the fluctuations. This effect was not readily repeatable (the location of the peaks varies from run to run), and it was strongly Reynolds number sensitive. The STI data, taken at much higher Reynolds number, do not show it. In all likelihood these secondary peaks (alongside the bus and to the rear) in the Ref. 30 data are an experimental artifact, and the real world case is more like the STI result with one dominant disturbance at the front of the commercial vehicle, in the no crosswind case.

Comparisons between Refs. 29 and 30 for the crosswind case give similar agreement, with the Ref. 29 data showing the wake extending somewhat further aft of the bus. Overall, the differences which can be attributed to nonstationary effects are relatively small; and from a driver/vehicle system performance standpoint, they tend to be "filtered out" by the dynamics of the adjacent car. Further discussion of the transient effects of aerodynamics on vehicles is given by Beauvais (Ref. 68) and unpublished work by the Motor Industry Research Association in the U.K. In these studies the relative velocity between the car and the aerodynamic perturbation was high (i.e., on the order of the car's speed).

As a final point, the first order effects of relative speed scaling between truck and car can be accounted for, simply, as shown in Refs. 2 and 3. This is done by using a composite dynamic pressure containing the product of the car and truck airspeeds to compute full scale forces and moments from the model scale data. This scaling relationship is given by the following expressions for the lateral-directional forces and moments:

$$Y(x) = \frac{\rho A U_c U_T}{2} C_y(x) \tag{21}$$

$$N(x) = \frac{\rho A \ell U_c U_T}{2} C_n(x) \tag{22}$$

$$L(x) = \frac{\rho A t U_c U_T}{2} C_\ell(x) \tag{23}$$

where U_c is the airspeed of the car, U_T is the airspeed of the bus, A is the reference frontal area, ℓ is the wheelbase, t is the mean track, and ρ is the air density. With reference to Eqs. 8-13 and 18-20, the dynamic pressure there was $q = (1/2)\rho V_0^2$.

2. Lateral-Directional Data for the Adjacent Car Alone

To establish a basis for interpretation, and to tie-in with prior studies, an initial series of test runs was made at Northrop with the 1972 Chevrolet station wagon alone. The side force and yaw moment results are shown in Fig. 75. Also shown are data from the 1972 tests with the same model in the same facility, taken from Refs. 3 and 29. These data are for the car mounted in the forward tunnel position with the flow probe in front, see Fig. 46. The results show good agreement, as would be expected. Note that the car data shown are typical of sedans with a forward aerodynamic center, and linear and force and moment variations for small angles of aerodynamic yaw (sideslip). The value of $C_{y_{\psi_W}}$ shown is about 2.1 per radian, and $C_{n_{\psi_W}} \doteq 0.63\ \text{rad}^{-1}$.

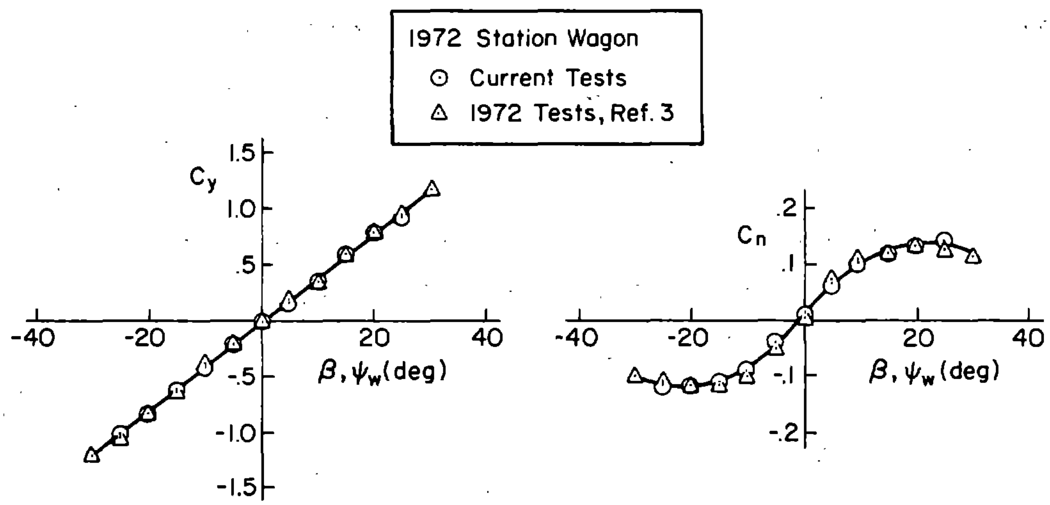

a) Side Force *b) Yaw Moment*

Figure 75. Adjacent Car-Alone Lateral-Directional Data

3. Forces and Moments on the Adjacent Car with Various Truck Configurations

Using the truck-plus-adjacent car test procedure discussed above and in Article A, force and moment data on the car were obtained in the presence of the following truck configurations:

- Basic truck (3 axle COE plus 40 ft van)
- 3 axle COE plus 40 ft flatbed
- 3 axle COE plus liquid cargo tanker
- 3 axle CBE plus 40 ft van
- 3 axle CBE plus dry cargo tanker

- 2 axle COE plus 27 ft van
- 2 axle COE plus double 27 ft vans

The basic truck results, in Fig. 76, are presented for reference and as a base case; and because the 1972 station wagon model had not been tested with it before. The example results in Fig. 20 in Article III.C are for the 1970 station wagon plus basic truck, and there is generally good agreement.

The data for the seven truck configurations listed above are given in Figs. 76-82. In each case, the data are for a car to truck centerline separation of 12 ft (3.7 m), full scale. In Figs. 77-82, two curves appear on each plot. The dashed curves through the plotted points are for the truck type being presented. The solid line (with no data points) is a trace of the basic truck curve from Fig. 76, for comparison purposes. The background line in Fig. 82 is a trace of the 3 axle CBE plus 40 ft van data from Fig. 79.

For some configurations data points were taken only in the region where changes in the truck shape were expected to change the flow, for testing economy. Elsewhere, the data should fair into the basic truck results.

The truck outline at the top of each figure shows its relation to the data. The dashed line parts on these outlines show how the truck type being presented differs from the basic truck or other reference case. More detailed differences, in three views, are shown in Article A, above.

a. <u>Basic Truck</u>

Figure 76 shows the data for the basic truck. With zero crosswind, the disturbance effect is dominated by the bow wave at the front of the truck. A side force and yaw rotation away from the truck result as the car overtakes the tractor. Peak values are not as large as those for the −20 deg crosswind case with the car downwind.

In the latter case (Fig. 76b) the variations are larger and they change more as the car overtakes and passes the truck. As shown in Fig. 20 of

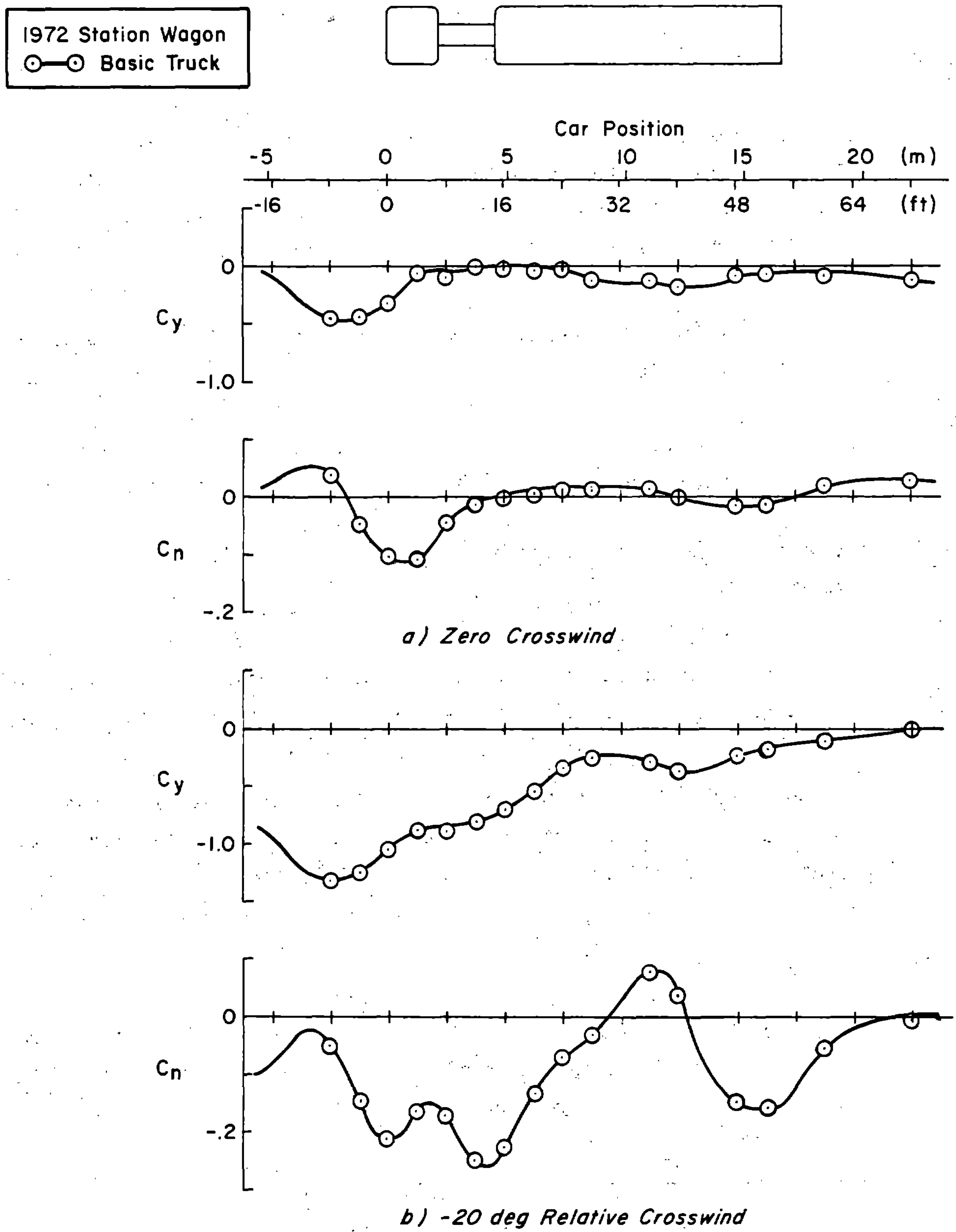

Figure 76. Aerodynamic Disturbance with Basic Truck

Article III.C, the car initially encounters the disturbance two to three vehicle (truck) lengths aft. The side force decreases to the rear of, and alongside the van, and then it increases steadily as the car moves past. The bow wave component is still evident at the front. The steady state side force coefficient for the car in the absence of the truck is about −0.8 for this relative wind angle. The yaw moment is more variable due to such things as the flow under the semitrailer and through the gap, and, alternatively, the blocking effect of the wheels.

b. COE Plus Flatbed

The disturbance effect of the COE plus flatbed is plotted in Fig. 77. The zero crosswind data are quite similar to that for the basic truck, except in the region aft of the tractor where the leading edge of the van is located in the basic truck. Apparently the flow converges behind the tractor with the flatbed, modifying the side force and yaw moment accordingly.

The crosswind data are different alongside the semitrailer as would be expected. Yet the effect is not too large. It appears in the C_y data of Fig. 77b that the presence of the unloaded flatbed semitrailer still causes a shadowing effect, presumably because the top of the bed is nearly as high as the top of the car. The more apparent difference in the C_n data of Fig. 77b is attributable to flow differences resulting from the lack of the semitrailer face and body.

c. COE Plus Liquid Cargo Tanker

Data for the disturbance caused by the tank truck are shown in Fig. 78. The zero crosswind data are quite similar to the basic truck. The crosswind data, with car downwind, in Fig. 78b show some differences in the region around the gap and the tractor tandems. This is probably due to the more open nature of the region around the tandems with the tanker, as opposed to the van whose box sits closely on the top of the wheels.

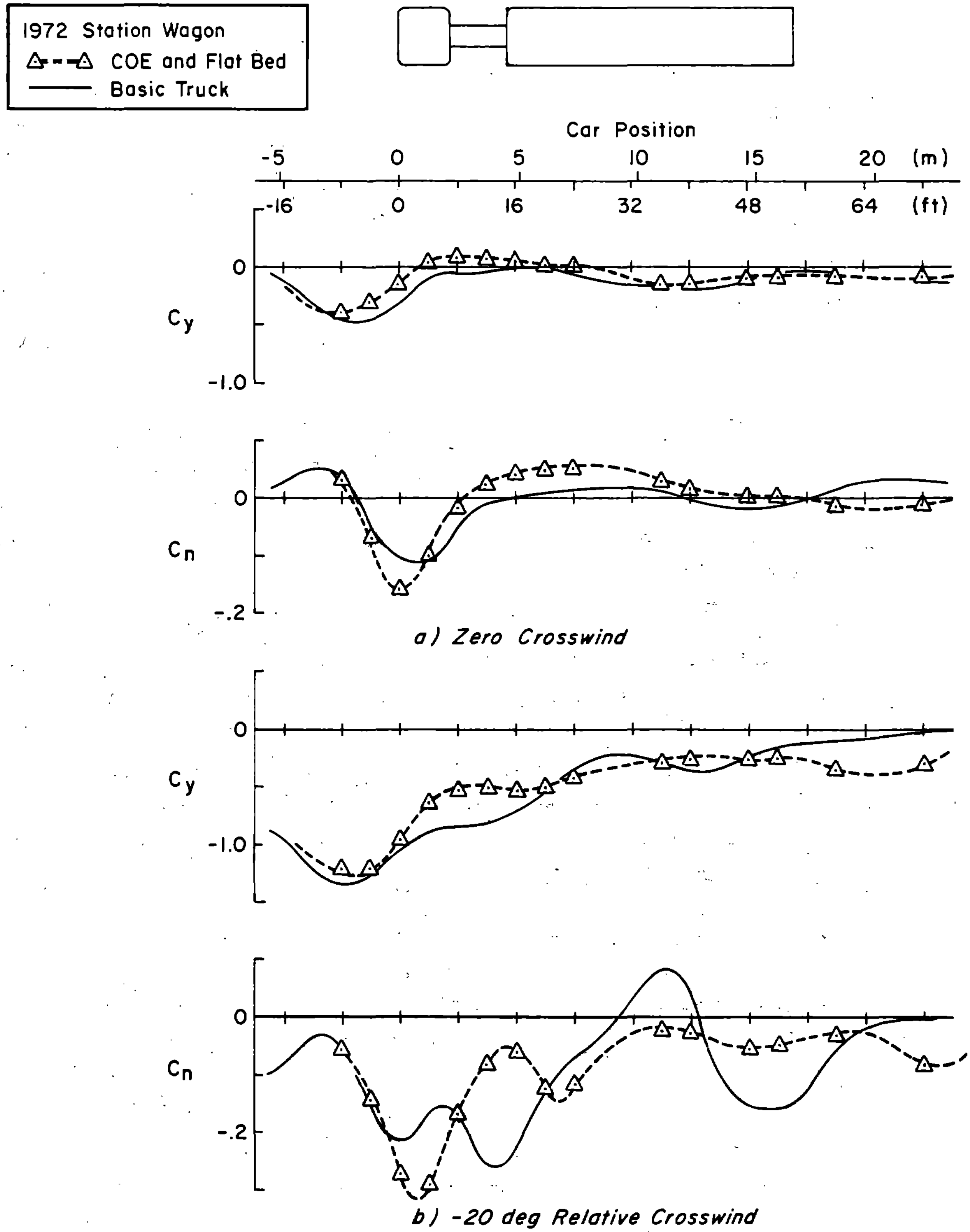

Figure 77. Aerodynamic Disturbance with 3 Axle COE Plus Flatbed

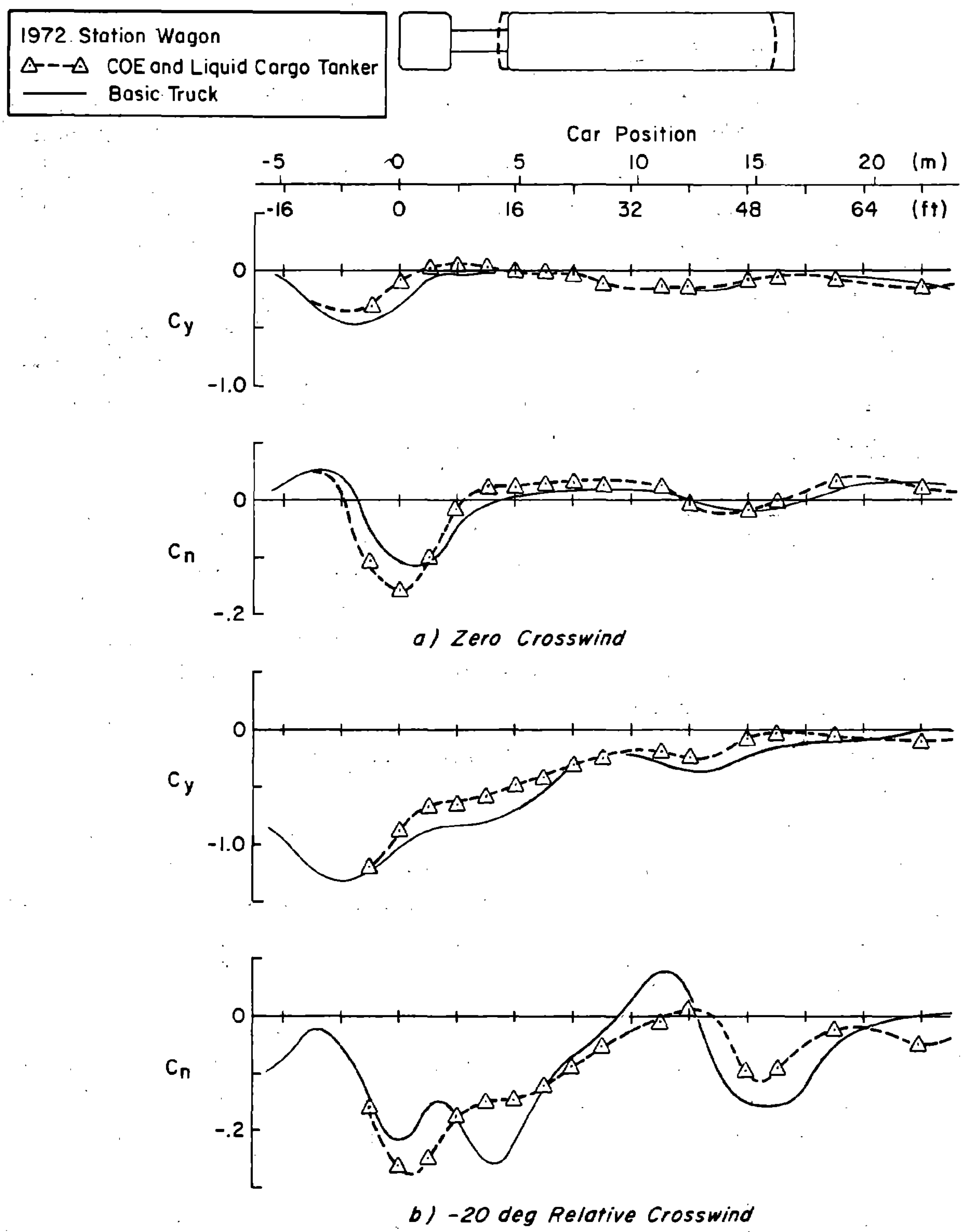

Figure 78. Aerodynamic Disturbance with 3 Axle COE Plus Liquid Cargo Tanker

d. CBE Plus 40 ft Van

Data to show the effect of changing tractor type on the disturbance are given in Fig. 79. With no crosswind, the level of the bow wave effect is reduced, but the distance over which the effect extends is increased. The peak side force change is less than that for the basic truck, but occurs over a greater distance.

For a −20 deg crosswind (Fig. 79b) the side force change is close to that for the basic truck. The peak levels are about the same as is the distance over which the change occurs. The yaw moment variation is smoother alongside the CBE tractor. This difference must be attributable to the longer cab and shorter gap of the CBE relative to the COE.

e. COE Plus 27 ft Van

The disturbance effect of the 2 axle COE plus 27 ft van is shown in Fig. 80. The zero crosswind results appear simply as a foreshortened version of the basic truck data. The side force bow wave effect is about the same, and there is little apparent effect of the reduced tractor and gap lengths with no crossflow.

The crosswind data in Fig. 80b also show this foreshortening effect. The change in side force alongside the truck varies between the same levels but over less distance. The yaw moment curve shows about half the peak to peak variation along the rear part of the semitrailer and reveals a smoother variation along the forward part of the truck. The latter is probably due to the shorter gap and changes in the wheel spacing.

f. COE Plus Double 27 ft Vans

Data for the doubles are shown in Fig. 81, and compared with both the basic truck and the single 27 ft van (Fig. 80) data. Emphasis in this series of runs was on the semitrailer-trailer gap flow. The dashed lines forward of the gap are from Fig. 80, as are the ones aft — suitably shifted.

The results in Fig. 81a show little effect of the presence of the gap in the zero crosswind case. If anything, the car is pushed away slightly from the truck alongside the gap.

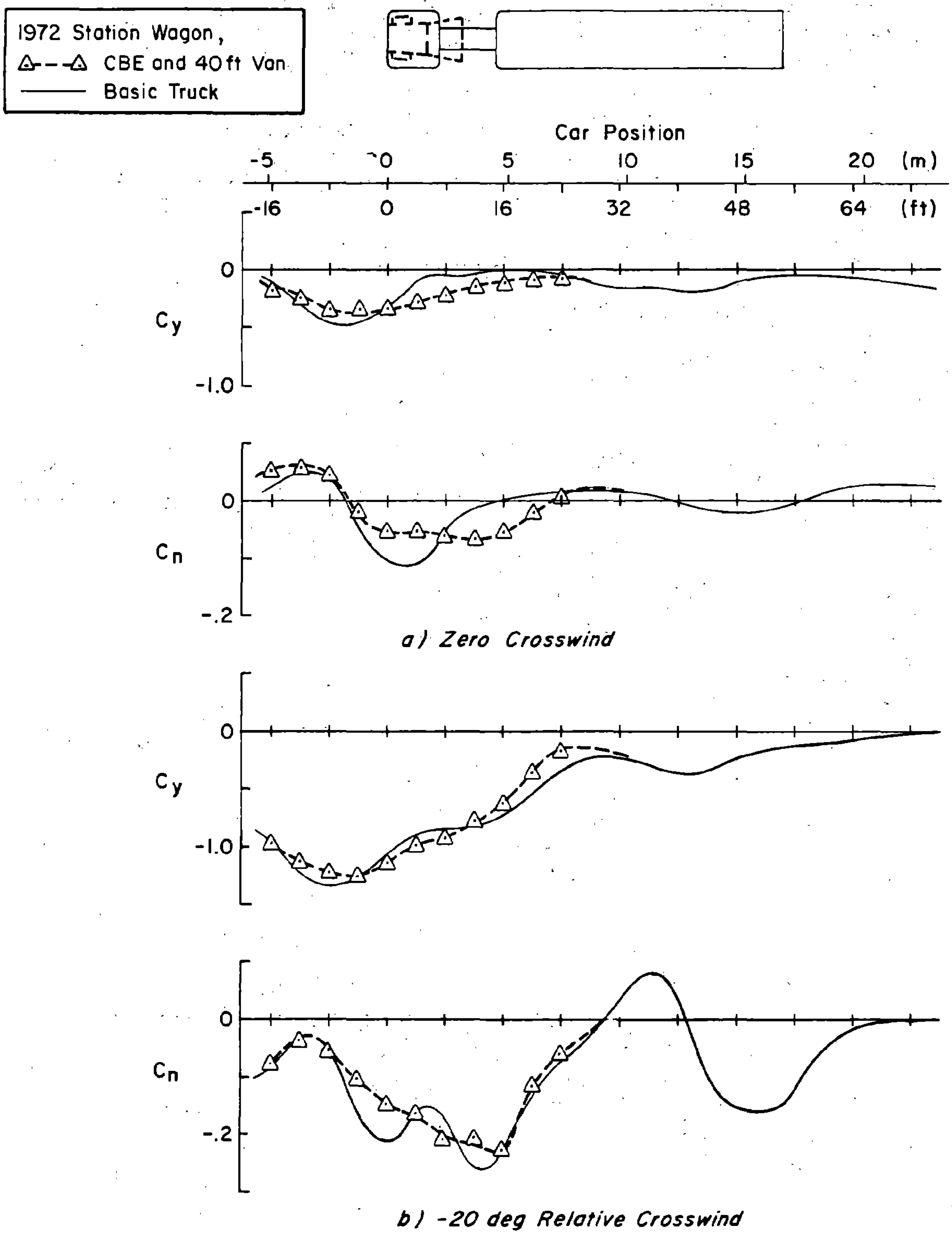

Figure 79. Aerodynamic Disturbance with 3 Axle COE Plus 40 ft Van

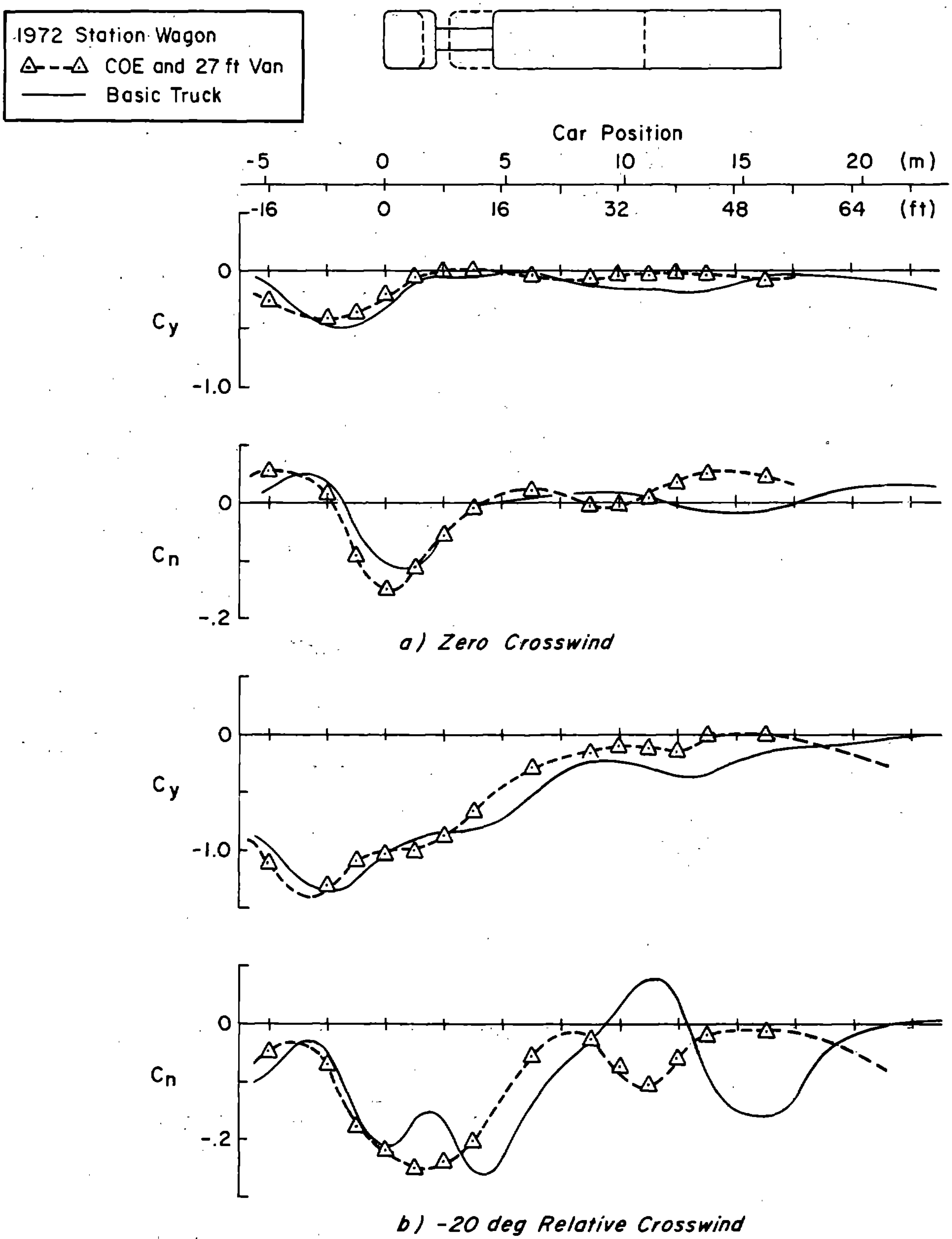

Figure 80. Aerodynamic Disturbance with 2 Axle COE Plus 27 ft Van

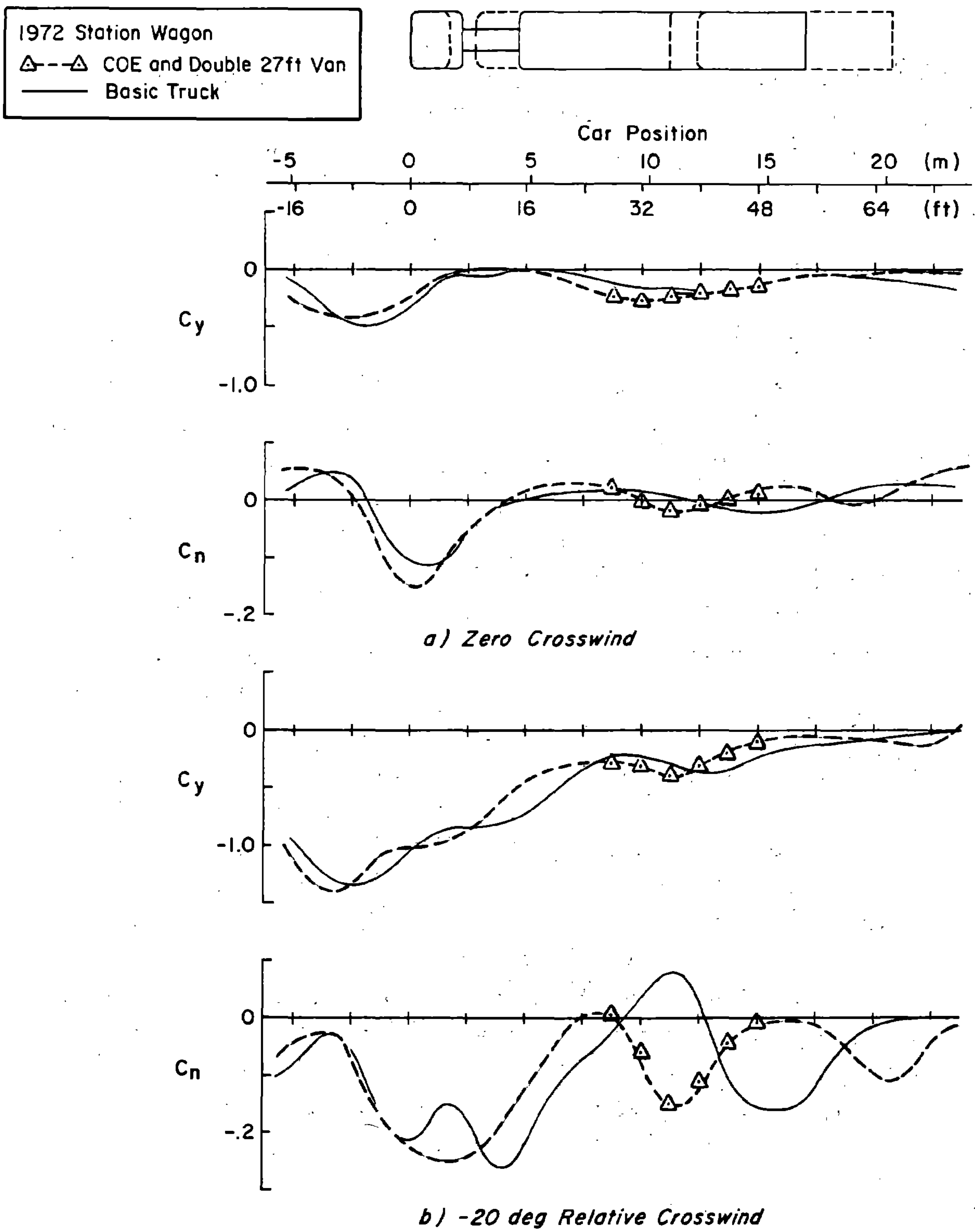

Figure 81. Aerodynamic Disturbance with 2 Axle COE Plus Double 27 ft Vans

With the car downwind in a crosswind (Fig. 81b) the main effect of the doubles rig is the increased overall length. The disturbance at the gap between the trailers (see C_n) is similar to that which occurs at the rear of a van. Then, there is an additional variation due to the second trailer, followed by the wake effect. Considering the phase shift due to the different semitrailer lengths, the peak to peak excursions are about the same as for the basic truck.

g. <u>CBE Plus Dry Cargo Tanker</u>

The combined effect on the adjacent car disturbance of changing the tractor and semitrailer shape is shown in Fig. 82 for the dry cargo tanker rig. The data from the front of the semitrailer forward are essentially the same as seen in Fig. 79 for the CBE plus 40 ft van. Alongside the semitrailer and further aft, the no crosswind data (Fig. 82a) are essentially the same as the basic truck results, despite the shape differences described in Article A, above.

With the car downwind in the crosswind case (Fig. 82b), the close similarity still exists, except for a small shift related to the reduced length of the dry cargo tanker.

Overall, the gross changes in truck configuration considered above result, for the most part, in only detailed changes in the force and moment disturbance of the adjacent car. It is clear that the main disturbance effect is caused simply by the overall size and bulk of the truck. Accordingly, those changes which are most significant result from changing semitrailer length, or adding a second trailer. Based on our prior analytical studies (Refs. 2 and 3), it appears that the detail changes which typify much of this data would not have much effect on overall driver/vehicle system performance. By comparison, fairly major changes in adjacent car performance result from variations in such things as car and truck speed and the relative wind geometry, as discussed in Article III.C, and elsewhere.

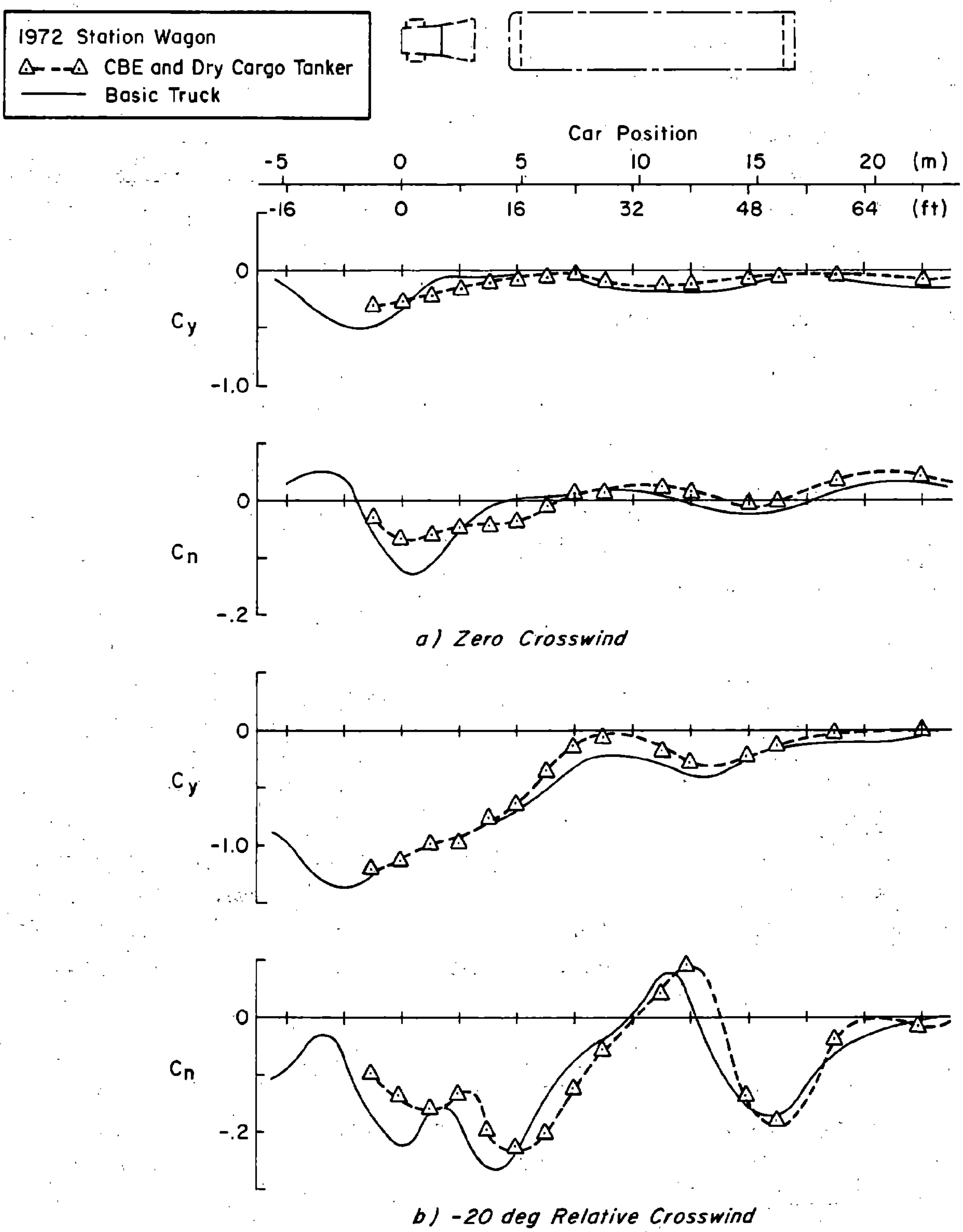

Figure 82. Aerodynamic Disturbance with 3 Axle CBE Plus Dry Cargo Tanker

4. Forces and Moments on the Adjacent Car with Various Truck Plus Device Combinations

A representative set of devices was mounted, one at a time, on the basic truck in the Northrop tests, in order to assess their possible effect on the adjacent car disturbance. Because these devices were mainly aimed at suppressing splash and spray or reducing drag, their study from a disturbance standpoint was aimed mainly at quantifying any potentially harmful (or helpful) side effects.

The data shown here are for those devices which resulted in the larger effects on the disturbance, or which were important for the reasons noted above. Data are shown for

- Drag shield
- Full fenders on tractor
- Longitudinal baffle
- Horizontal gap plate
- Gap splitter panel
- Angled side vanes

all mounted on the basic truck. Again the centerline separation was 12 ft (3.7 m) equivalent full scale, and measures were taken for zero crosswind and for the car downwind in a –20 deg relative flow. The plots follow the same format as for the truck configuration studies, above. The device is sketched on the truck outline. For test economy, data were only taken in the expected region of greatest influence on the adjacent car disturbance.

a. Drag Shield

The effect of adding the drag shield is shown in Fig. 83. For the zero crosswind case, essentially no change in disturbance effect is seen. Although the drag shield is known to alter the flow in the tractor/semitrailer gap, it does not affect the flow around the truck enough to alter the disturbance of the adjacent car (with no crosswind).

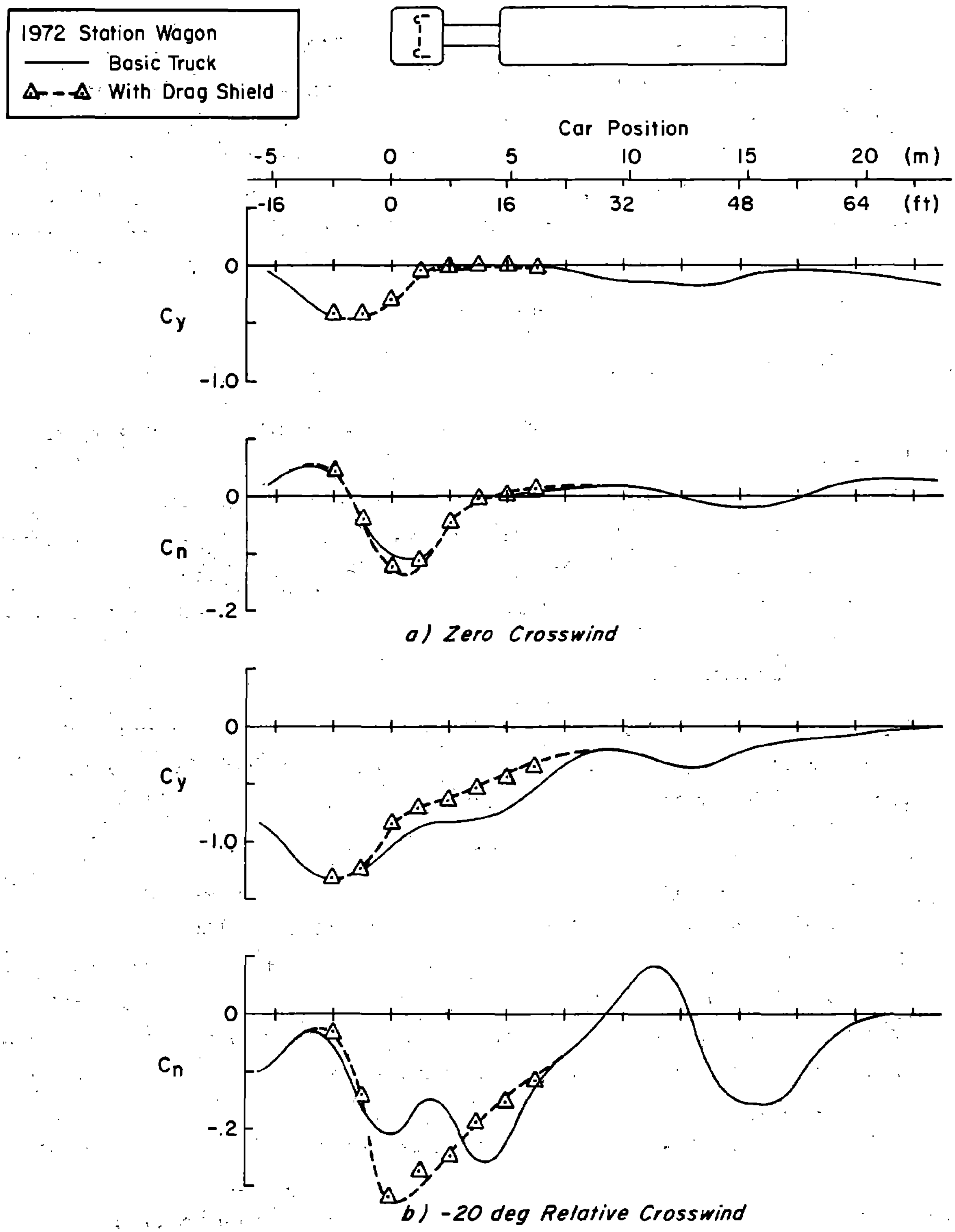

Figure 83. Aerodynamic Disturbance with Drag Shield

The drag shield does have an interesting effect on the disturbance with a crosswind. The side force changes more abruptly alongside the tractor, with a more gradual change near the van. The peak level of C_y attained is about the same, however. The yaw moment changes form, accordingly. These effects are presumably due to the enhanced masking effect of the reduced gap flow, and this is supported, for example, by the data in Fig. 80 for the shorter gap 2 axle COE plus 27 ft van (which are similar to the Fig. 83 results in the gap region).

b. Full Fenders on Tractor

The effect on the disturbance of adding full fenders to the tractor tandem duals is shown in Fig. 84. Little change is seen for either the zero or −20 deg crosswind cases. This is not surprising, since the fenders do not change the basic truck configuration other than to add a small amount of flow blockage around the tractor tandem wheels. With the 40 ft van, of course, the clearance between wheels and semitrailer is already small.

c. Longitudinal Baffle

The change in the adjacent car disturbance due to the longitudinal underbody baffle is shown in Fig. 85. As would be expected due to symmetry, there is no change in the zero crosswind results.

With the car downwind in the crosswind there is a very substantial shadowing effect alongside the semitrailer, and the wake properties aft of the truck are also changed substantially. The large positive side force coefficient (C_y) towards the truck in Fig. 85b may be due to the back flow of vortex flow over the top of the truck which curls down and strikes the adjacent car on the side away from the truck, hence pushing the car inward. This tends to be confirmed by the relatively small effect seen in the yaw moment coefficient (C_n). Typically, with the flow interruptions caused by various regions of the truck, the yaw moment is approximately the derivative of the side force (see the basic truck data, for example). This is not the case in Fig. 85b, suggesting that some other flow phenomenon is dominant.

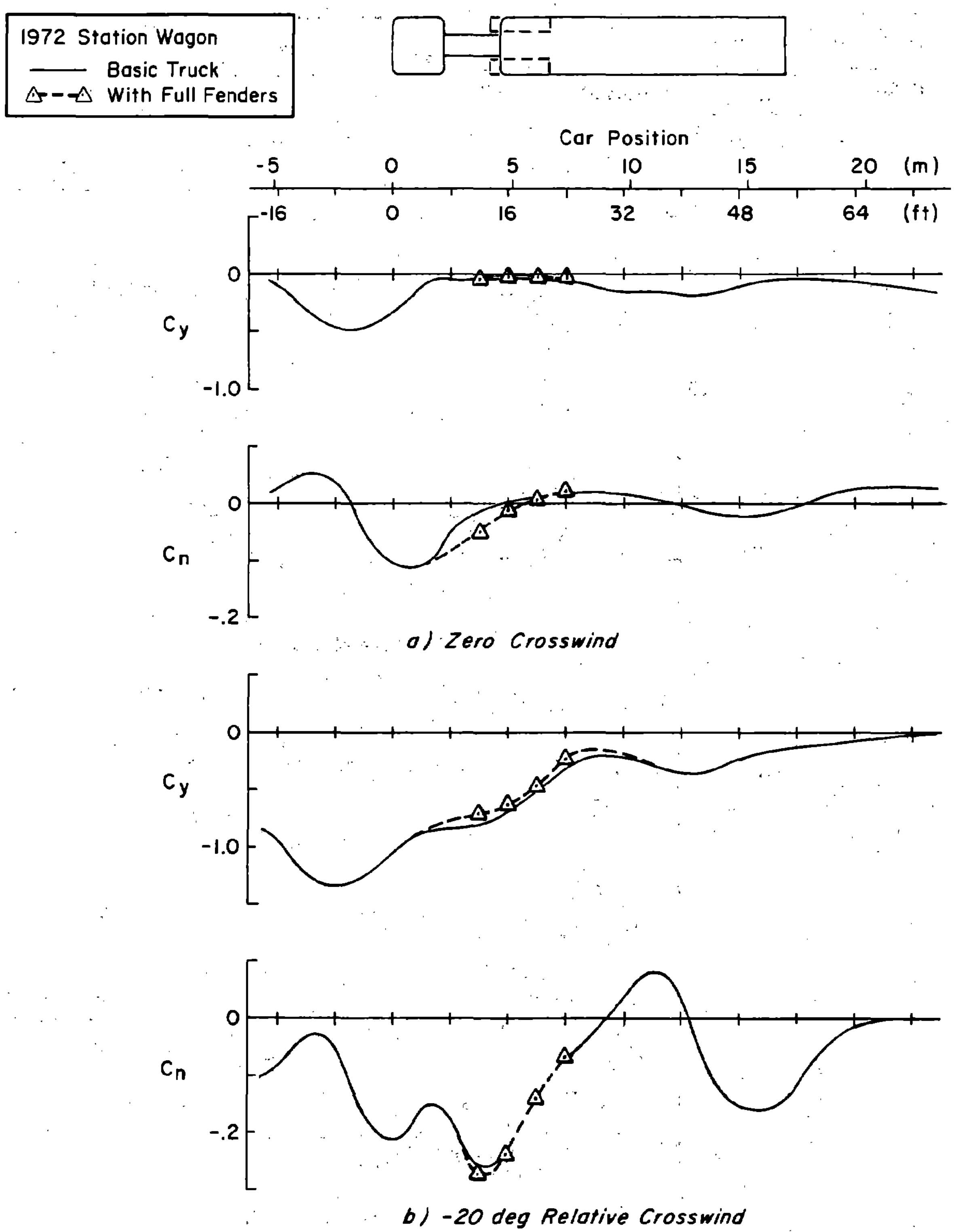

Figure 84. Aerodynamic Disturbance with Full Fenders on Tractor Tandems

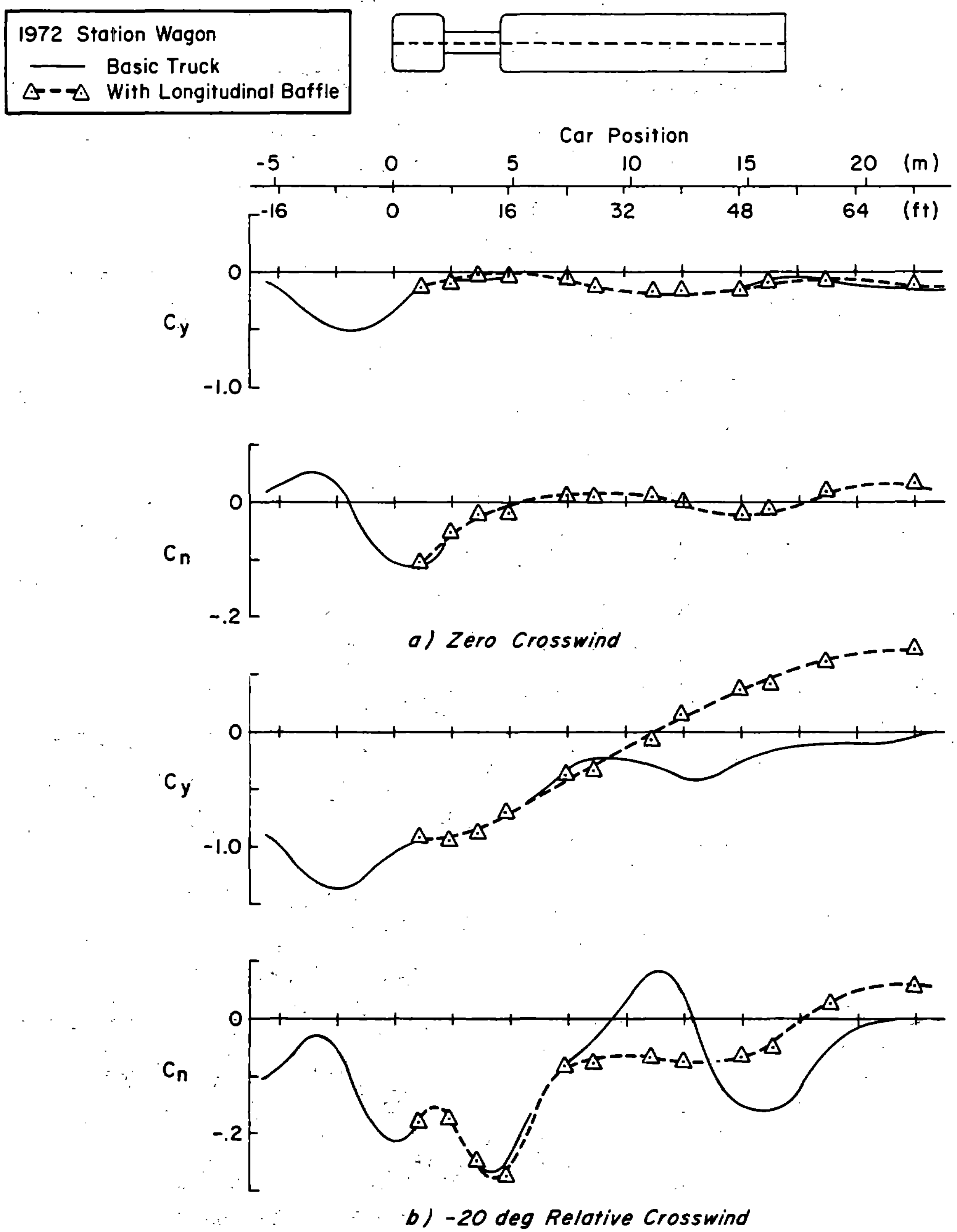

Figure 85. Aerodynamic Disturbance with Longitudinal Underbody Baffle

Interesting, too, in Fig. 85 is the result that the underbody baffle has little effect on the cross flow adjacent to the tractor (even though it is there — see Fig. 62). This suggests that the level of underbody blockage in that region is already high with the basic configuration.

These crosswind results with the baffle have substantial similarities with the basic truck plus van underbody, and the rectangular block data in Refs. 2 and 29, as would be expected.

d. Horizontal Gap Plate

Figure 86 shows the effect of adding the horizontal gap bottom plate. In both the zero and –20 deg crosswind cases essentially no significant alteration of the disturbance is seen. This is not surprising, considering the location of the plate, lying flat across the bottom of the gap. The gap area is not changed significantly, and any wake effects due to the thin plate would be expected to be minimal.

e. Gap Splitter Panel

The vertical gap splitter panel effect is plotted in Fig. 87. Again, no change in the zero crosswind disturbance is seen, due to symmetry.

With the crosswind, the side force on the car is reduced as shown by C_y in Fig. 87b. Yet, the peak, related to the front of the tractor, remains the same. The yaw moment (C_n) trace changes form, reflecting changes in the detail flow above and below the splitter panel in the gap area. Though different in form than the basic truck, the general (spatial) frequency content and the peak amplitude of Fig. 87b suggest that this configuration would have about the same effect on adjacent driver/vehicle system performance. The form of C_y and the peak in C_n in the crosswind case are not unlike that of the drag shield in Fig. 83b, despite the substantial physical differences between these two devices.

f. Angled Side Vanes

The change in the force and moment on the adjacent car due to angled side vanes mounted at 3 places on the forward part of the truck is shown in Fig. 88. There is some variation in the no crosswind case due to the

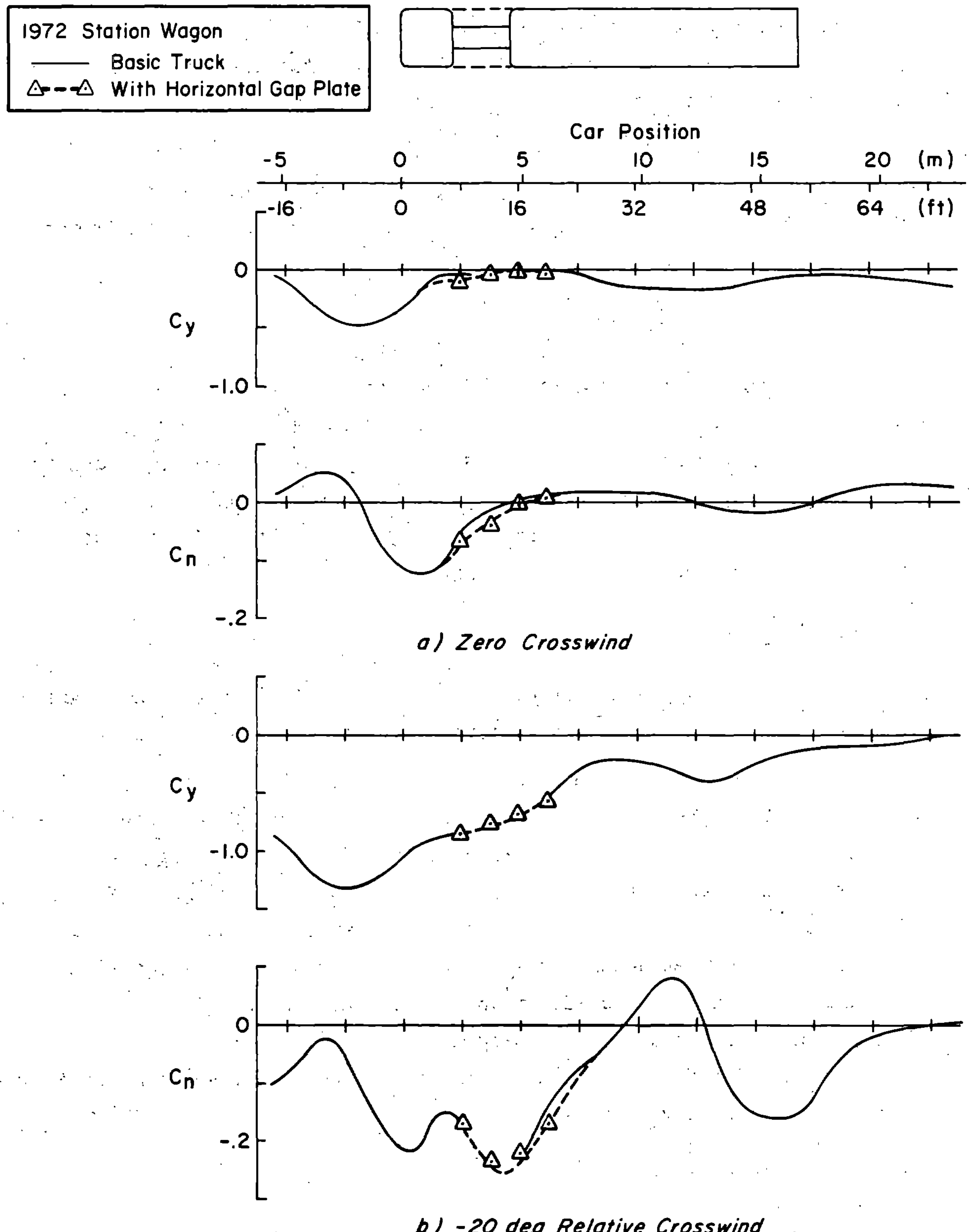

Figure 86. Aerodynamic Disturbance with Horizontal Gap Bottom Plate

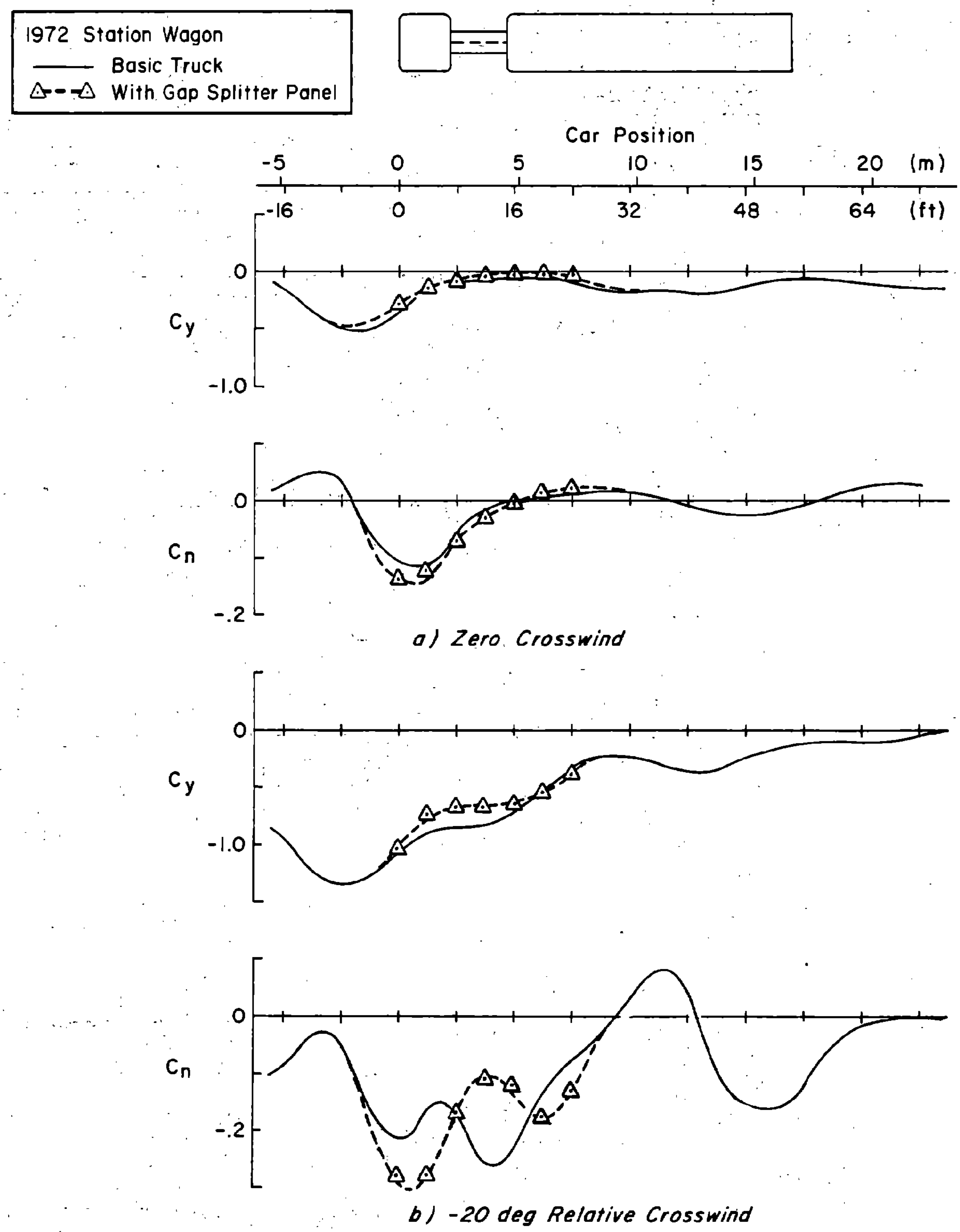

Figure 87. Aerodynamic Disturbance with Vertical Gap Splitter Panel

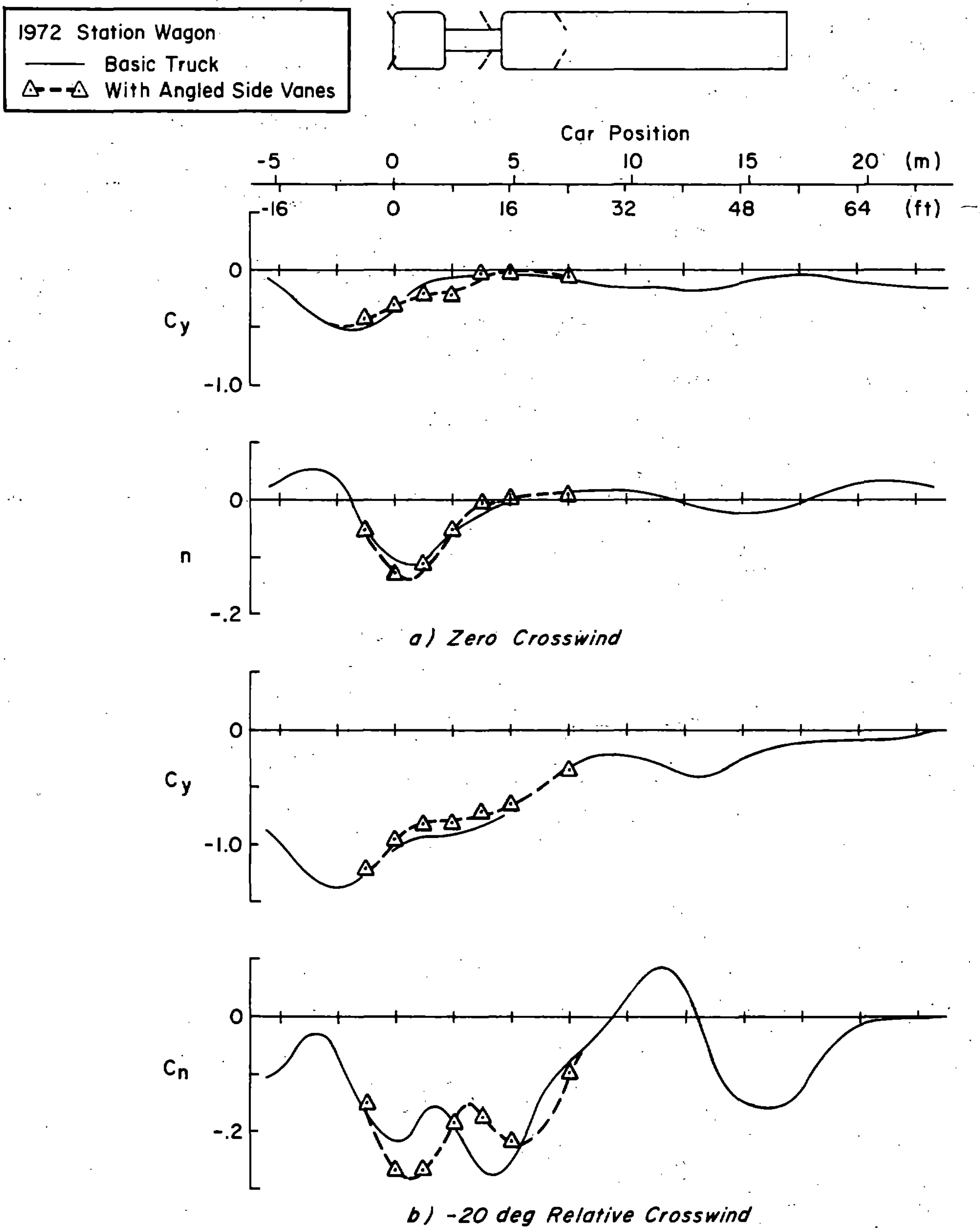

Figure 88. Aerodynamic Disturbance with Angled Side Vanes

resulting flow modification in the vicinity of the gap and the tractor tandems.

In the negative crosswind case, the change is to reduce the side force alongside (see C_y) and this causes corresponding changes in the yaw moment profile as the car moves progressively past. The result is not unlike that of the vertical gap splitter panel (compare C_n in Figs. 87b and 88b). This is curious, because the latter blocks flow through the gap, while the former tends to modify the flow under the tractor and lower down on the truck around the wheels.

Overall, and with the exception of the longitudinal underbody baffle, the changes in the adjacent car disturbance due to the installation of the devices is minimal. This means, in turn, that there will be little change in the truck's influence on the response and performance of the driver/vehicle system.

The longitudinal baffle under the semitrailer does have a substantial effect on the wake flow and the disturbance, in a crosswind with the car in the lee of the truck. This does degrade driver/vehicle performance, and it is closely analogous to the van underbody and rectangular block cases of Refs. 2, 6, and 29. These latter performance effects are analyzed and quantified in detail in those references, and compared to performance in the presence of the basic truck. As a result, there is no need to redo the performance calculations for those cases. At the same time, the potential, adjacent car performance disadvantage due to the longitudinal baffle must be kept in mind when assessing its attributes as an alleviating candidate.

SECTION VI

SPLASH AND SPRAY TESTS AND RESULTS

Full scale field tests were accomplished as a combined effort of STI, WHI, and AVI. These tests involved complete vehicle configurations with various aerodynamic devices under both dry and wet (i.e., splash and spray) conditions. This section describes the experimental procedures and results for the wet splash and spray tests. The dry, aerodynamics alone, tests are described in Article V.B, above.

Two sets of splash and spray tests were carried out. The first was accomplished in June 1977, and emphasized various vehicle types. The second set was performed in November 1977, and focused on splash and spray devices, mounted on the basic truck configuration. Both sets of tests were run at the Firestone Test Center, Ft. Stockton, Texas, under the auspices of the Western Highway Institute. Including preparation, setup, and experiments, each test required about one and a half week's occupancy at the Test Center.

The purpose of the June tests was to quantify splash and spray effects and tie lab and simulator test results and analyses to representative truck types. By studying a variety of truck configurations we were able to define and quantify the splash and spray problem as it existed at the start and verify the descriptive methodology. The truck configurations tested in June began with the basic truck, consisting of the 3 axle COE plus 40 ft van semi-trailer. The tractor was a 1977 Freightliner FLT-8664T and the semitrailer was a Fruehauf Model FB9-F2-40, 1974. Variations on the semitrailer included:

- Liquid cargo tanker, which was a Fruehauf Model TAG-F2-ESF-9200
- Dry cargo tanker, which was a 36 ft (11 m) Feed-liner Model RDM
- Flat bed, which was a 40 ft (12.2 m) Fruehauf.

A 3 axle CBE tractor was also tested with these semitrailers, and that was a 1977 Freightliner FLC-12064T. Other truck variations included a 2 axle COE tractor (1977 Freightliner FLT-7542T) and single, double, and triple 27 ft

(8.2 m) van semitrailers (and dollies). The tires on all the trucks were near new or only partly worn, so the tread depth was ample. Additional details of the selected vehicles are given in Articles II.E and V.A.

Attention in the June tests was directed to the visibility for an adjacent driver, and to the effects of general truck aerodynamic geometry and the potential for improvements with aerodynamic devices. The tests included crosswind effects using natural winds; and the range of that portion of the testing was that which resulted from weather conditions existing during the test period. Another function of the initial wet tests was to further verify and develop instrumentation and test procedures useful for splash and spray measurements, and to relate such measurements to observed visibility. Results from June lead to refinements in procedures which were used in November.

The purpose of the November tests was to quantify splash and spray effects for selected alleviation and aerodynamic devices, mounted on the basic truck configuration. The devices tested included:

- Drag shield
- Longitudinal baffle
- Gap filler panel
- Partial gap panel
- Angled side vanes
- European fender
- Roberts fender
- Reddaway fender
- Fuzzy truck

Detailed descriptions of these devices are given in Section IV. Preliminary tests were also made with the drag shield and Reddaway fender in June.

The next article in this section describes the two sets of tests, including the facilities, procedures, and measures. The following article presents the basic truck results, in order to show the nature of the data, and to illustrate the effect of situational parameters other than truck shape and the presence of devices. Connections and correlations between the various types of measures and ratings are shown next. Results showing the effect of variations in truck type on visibility are presented following that, and the section concludes with data and interpretations showing the effect of various devices on the visibility in the vicinity of the truck.

A. SPLASH AND SPRAY TEST PROCEDURES

This article describes the facilities and instrumentation used in the splash and spray tests. It also defines and discusses the objective and subjective measures, and describes the driver subjects for the truck plus adjacent car runs.

1. Test Facility

The layout of the track at the Firestone Test Center is shown in Fig. 89. The total circuit is about 5 miles (8 km) with loops at each end to permit the test vehicles to maintain their speed while changing direction.

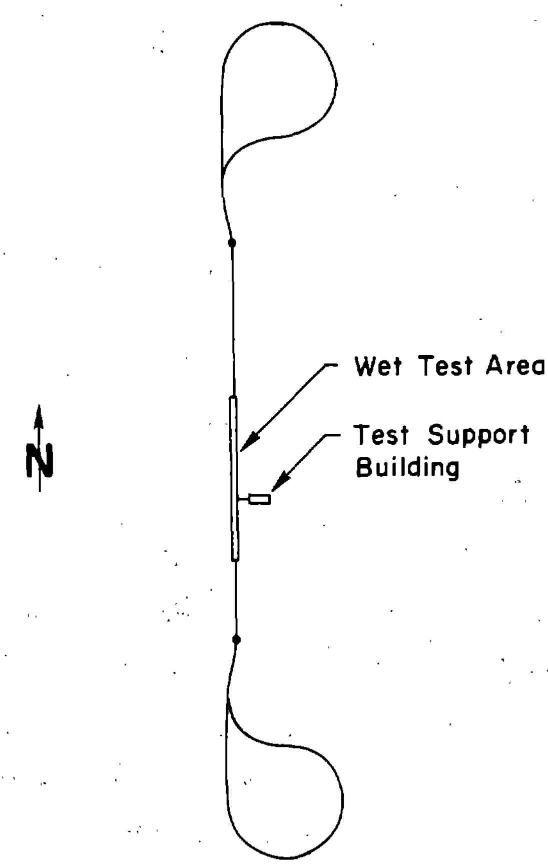

Figure 89. Firestone Test Center Track

The portion of the test track used for the wet tests consisted of a 1000 ft (305 m) long, 30 ft (9.14 m) wide, lane of Type C asphalt, bordered by strips of asphalt, containing light poles and water drains. Additional dry lanes were available on the west side for chase vehicles (see Fig. 90), and they were surfaced with Type D asphalt or concrete. The Type C asphalt was divided into two 15 ft (4.6 m) lanes, using small white dots painted every 25 ft (7.62 m) on the surface. At the ends of the 305 m section were the single lane high-speed turn-around loops shown in Fig. 89. Trucks were run along the Type D asphalt and concrete surfaces for flow visualization runs in June; however, only the Type C asphalt was watered and it served as the main test surface.

Watering was provided by a 1000 ft (305 m) length of perforated irrigation pipe run along the track center edge of the Type C asphalt. The entire 305 m surface was kept continually wet using a high capacity pump. A 1 percent cross slope and a mean texture depth (macrotexture) of 0.036 in. (0.91 mm) provided a consistent uniform flow across the surface. Water depth measures were taken at 10 consecutive 5 ft (1.5 m) increments down the centers of the 4.6 m lanes, near the midpoint of the track. They showed a day to day average variation in depth of 0.055 to 0.059 in. (1.4 to 1.5 mm). The average of all water depth measures taken during the week was 0.057 in. (1.4 mm) during both the June and November tests.

The track layout is in a north-south direction. In June, the ambient wind was usually out of the south or southeast at 0 to 10 mph (4.5 m/sec) in the mornings and 5 to 15 mph (2.2 to 6.7 m/sec) in the afternoons. In November the winds were more variable during the test day. The wind was measured for each test run. The "relative wind" was measured relative to the heading of the truck, zero being for no crosswind component. The "ambient wind" direction was measured in terms of + angles, corresponding to wind from an easterly direction, and – angles, corresponding to wind from a westerly direction, with no wind from the north corresponding to degrees. The direction of test runs was defined as northbound (N) and southbound (S).

Generally, a truck (or pair of trucks) made four consecutive runs, two northbound and two southbound, before test conditions or configuration were changed. Therefore, typically, each configuration for each test condition

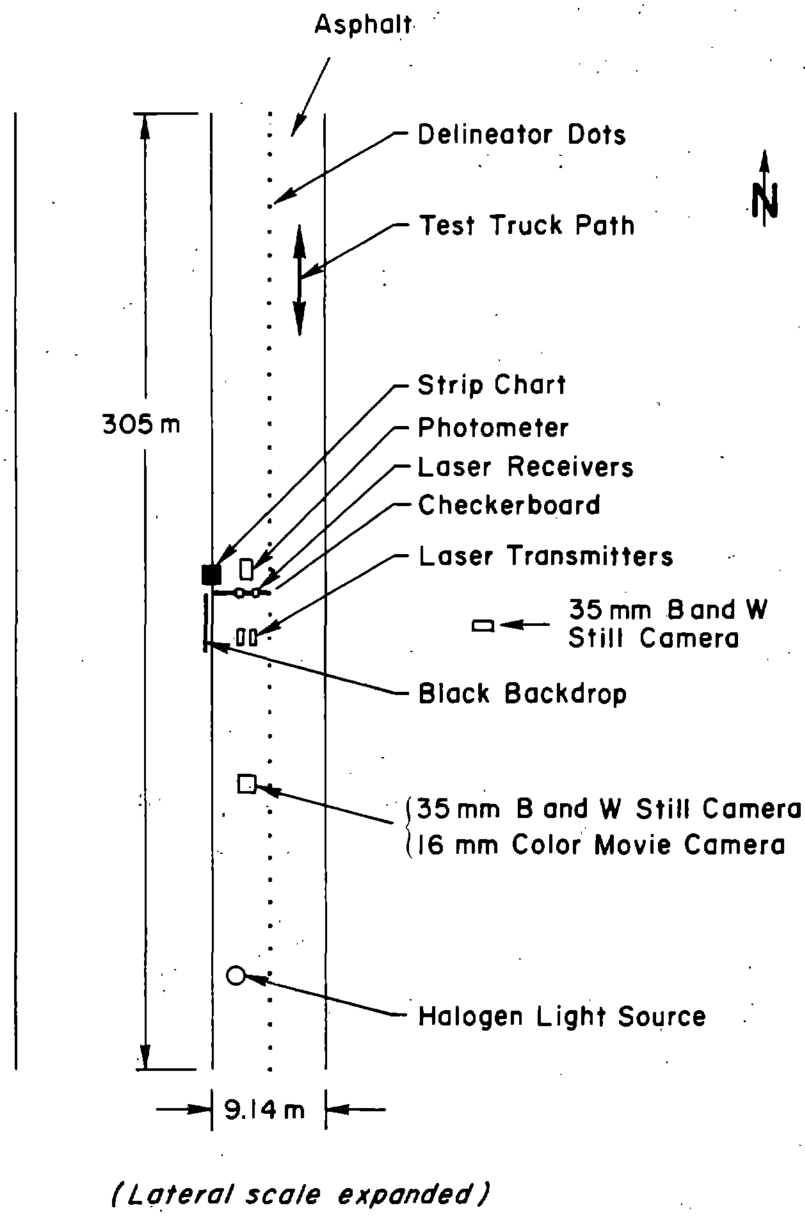

Figure 90. Detail of Wet Test Area

was run with an ambient headwind or crosswind from the left or with an ambient tailwind or crosswind from the right. The left-right symmetry of the truck configurations allowed these results to be readily generalized.

2. Track Instrumentation

For the truck-alone tests, track instrumentation was set up to measure splash and spray properties in terms of adjacent driver visibility and light attenuation. Visibility-related measures were taken with the following ground-based instruments:

- A Pritchard photometer focused on a halogen light source, 400 ft (122 m) away.
- Two laser transmissometers aimed at receiver power meters, 50 ft (15.2 m) away.
- A 35 mm SLR still camera with black and white film and a 250 mm lens, focused on an 8 × 12 ft (2.44 × 3.66 m) black and white checkerboard 200 ft (61 m) away, oriented parallel to the track centerline.
- A 16 mm color motion picture camera located next to the parallel still camera viewing the checkerboard and the test truck.
- A 35 mm SLR still camera with black and white film and a 50 mm lens, oriented perpendicular to the track centerline, 200 ft (61 m) away, viewing a 100 ft (30.5 m) section of test area which included a black backdrop.

The location of these devices on the track is shown in Fig. 90. The location of the devices, looking to the north from the southern part of the wet test area, is shown in Fig. 91. The measurement devices are discussed below, including some minor differences in arrangement between the June and the November tests. Additional details are given in the appendix.

The Pritchard photometer arrangement is shown in Figs. 90 and 91. With a telephoto lens it was possible to reduce the field of view so as to include only the halogen light source, 400 ft (122 m) away. When properly aligned at this condition the light source provided about 75 percent of the recorded light levels on a bright day. Attenuation of the light source by the truck splash and spray provided quantitative data over the 400 ft (12.2 m) test length.

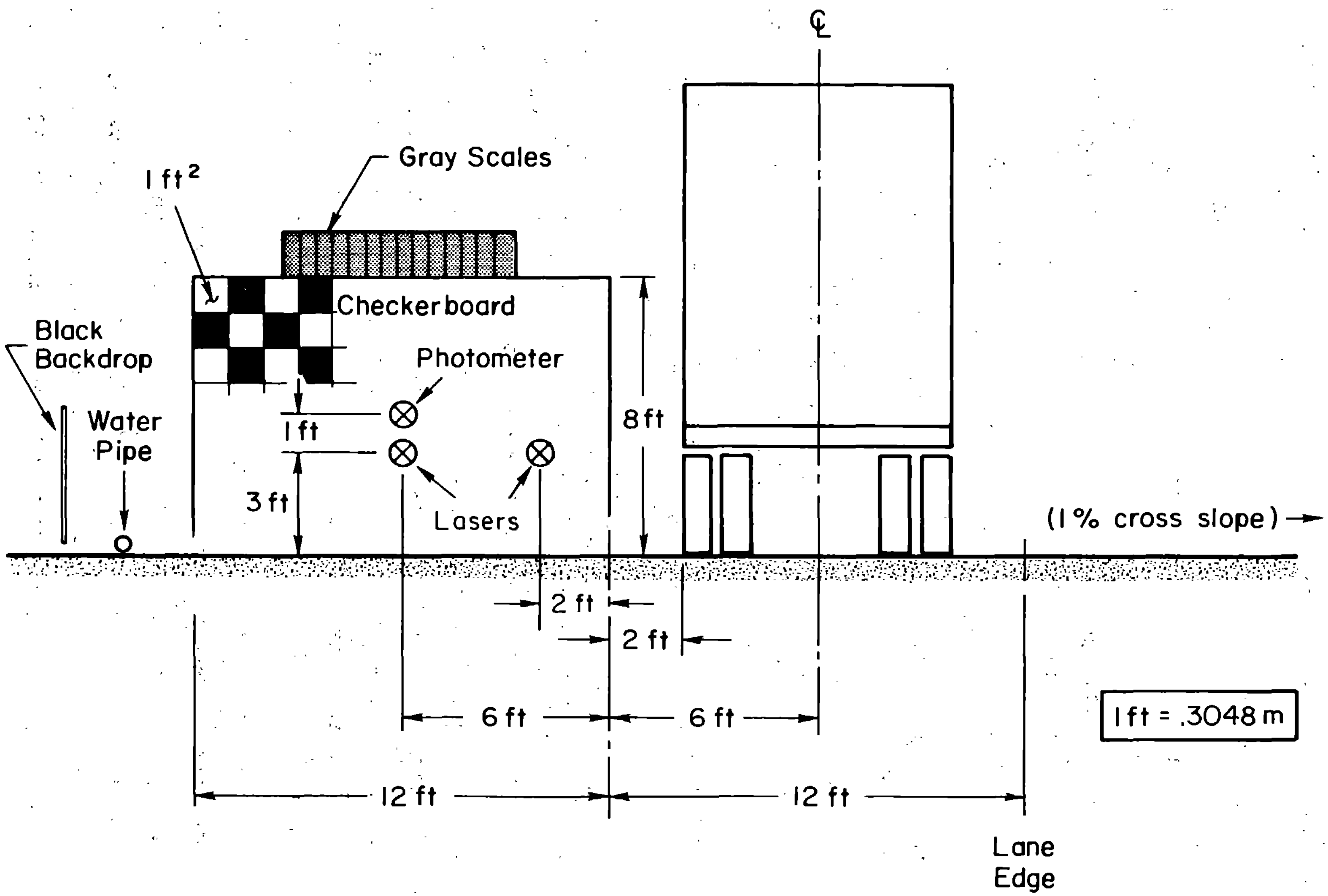

Figure 91. Track Instrumentation for Truck-Alone Tests

The lasers operated over a shorter test length [50 ft (15.2 m)] but provided a more detailed measure of transmissibility through the spray. Since the laser provides collimated light, the receiver readings at 15.2 m were due almost entirely (i.e., 95 percent) to the laser source. In June, the lasers were mounted north of the checkerboard. In November they were moved to the south side, so that they would be measuring in the same test segment as the photometer and the cameras. This is shown in Figs. 90 and 91.

The location and arrangement of the lasers were based on several factors. The heights and lateral location were similar to those used in prior studies (e.g., Ref. 26), as were the distances apart, to provide the potential for data tie-ins. The height of the lasers [3 ft (0.91 m)] is in the region of a slightly depressed driver line of sight. The photometer and laser at 6 ft (1.83 m) were on the centerline of the 12 ft (3.66 m) lane, while the laser at 2 ft (0.61 m) is in the region ahead of and to the right of the car, where the driver looks for information regarding position relative to the truck. Also, the lasers and photometer were positioned in regions of the driver field of view which were expected to be influenced by splash and spray under various conditions, as suggested by past data.

The spray-attenuation signals from the lasers and the photometer were recorded on a strip chart adjacent to the checkerboard. Camera operation was also recorded on the strip chart for data correlation purposes. A track-side anemometer was used to record the ambient wind in the test area on the strip chart. In June, this anemometer was about 30 m east of the test area, in the vicinity of the 35 mm side camera. In November, the anemometer (vector vane) was mounted 13 ft (4 m) above the pavement on a pole atop the checkerboard.

The black and white camera that was focused on the checkerboard obtained a picture of the spray alongside the truck, against the black and white back-ground. This photography was planned so that densitometer measures of the relative luminance could be made from the film. The shades of gray scale at the top of the checkerboard facilitated this. In November, an additional neutral gray square was added to the center of each black and white square, to enhance resolution of spray cloud density in the photographs. The latter squares were 1 ft (0.305 m) on each side, while the gray squares were 0.5 ft (0.15 m) on a side. The checkerboard can be seen in the film data of the appendix and the Fig. 94 example, shown subsequently.

The color motion picture camera aimed at the checkerboard had a larger field of view than the still, and it was run for 10-15 seconds for each run in order to provide an overview record.

The side-looking black and white camera photographed the spray around and beneath the truck against the 65 ft (19.8 m) long by 4 ft (1.2 m) high longitudinal black backdrop, in June. In November, two additional 4 × 8 ft (1.2 × 2.4 m) black sections were constructed, extending the total black backdrop length to 80 ft (24.4 m) which was centered so as to fill the side camera view. Accordingly, the side 35 mm still camera was moved inward to a point 150 ft (46 m) from the track center line, so as to view only the 80 ft (24.4 m) section of the test area.

The two black and white cameras were triggered to fire simultaneously when the truck ran over a pneumatic switch on the track. There were two such switches, for north and south bound, respectively, to provide for proper framing. In June, these switches were 65 ft (19.8 m) apart, with the nearest being 15 ft (4.6 m) from the checkerboard. In November, the south pneumatic camera switch was moved towards the north switch, decreasing their separation to 45 ft (13.7 m). This corresponded to the new location of the side camera.

Other minor changes were made in November which did not influence the data or the measures. The strip chart recorder and camera control box were moved inside the test trailer, located near mid track. Delineation cones were placed on the east side of the track in the area of the checkerboard, as guides, so as to obtain a more consistent truck path and lateral separation from the checkerboard. As discussed later, variations in the lateral position of the truck were accounted for in the data interpretation.

In addition to the track instrumentation, observers at either end of the 305 m wet test section rated the splash and spray visibility conditions. These subjective ratings were a judgment of the visibility through the cloud formed to the side of the trucks. They were based on a scale of 1 (good) to 5 (very bad), using the form shown in Fig. 92. Since these subjective results

TEST OBSERVER'S REPORT

Observer ______________________ Location ______________________

Test No. ______ Visibility Rating No. ______

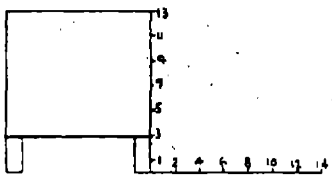

Comments: ______________________

Test No. ______ Visibility Rating No. ______

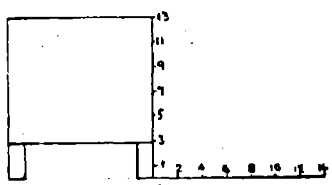

Comments: ______________________

Test No. ______ Visibility Rating No. ______

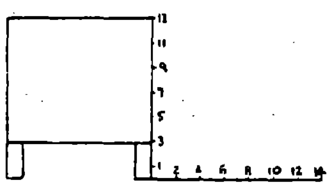

Comments: ______________________

DIRECTIONS

TEST OBSERVER'S REPORT

1. Observer - Name or initials of observer
2. Location - Location of observer during test. (For example, chase car #1, 2 or 3, at end or side of test track, etc.)
3. Test No. - Control number assigned to test.
4. Visibility Rating No. - Use code number shown below which most closely describes the condition encountered by a passing automobile.
   1. GOOD
   2. SATISFACTORY
   3. MARGINAL
   4. POOR
   5. VERY BAD
5. Sketch height, width and shape of general splash and spray pattern.
6. Comments - Any other technical or personal remarks which may assist in evaluating performance.

Figure 92. WHI Test Observer's Report Form

have been shown to correlate well with the objective measures from the lasers and photometer in the June data (as discussed subsequently), observer ratings were not made in November.

3. Vehicle Instrumentation

Adjacent vehicle tests were used to determine the effect of vehicle-induced disturbances and splash and spray on driver/vehicle performance. This was accomplished in the June tests by overtaking and passing the various trucks, using an instrumented 1973 Chevrolet station wagon. These tests were typically run in the afternoon, following the truck-alone tests. The checkerboard and the track instrumentation were removed, so that the adjacent car and the truck could proceed down the parallel lanes through the wet test area.

Driver/vehicle response parameters measured by instrumentation on the station wagon included:

- Driver steering wheel angle (δ_{SW})
- Yaw velocity (r)
- Forward speed (U_o)
- Relative lateral position from the truck as photographed by a down-looking 16 mm motion picture camera mounted 6 ft (1.8 m) over the roof
- Wind magnitude ($|WV|$) measured relative to the car by a Gill vector vane mounted in front of the bumper, on the car centerline
- Wind direction ($\angle WV$) measured relative to the car by the Gill vector vane

All these parameters, except lateral position, were recorded directly by a strip chart in the car. Lateral position was derived manually from the overhead motion picture camera film. Since the truck proceeded in a straight line in its own lane, lateral deviation of the car from the edge of the truck is the same as lateral deviation of the car in its lane, adjusted for the offset. The vector vane was situated at approximately the height of the lasers, and at the equivalent full scale height [34 in. (0.86 m)] of the flow probe in the wind tunnel.

In addition, a 16 mm motion picture camera mounted inside the car was used to record the driver's view through the windshield. Also, a 35 mm still camera, mounted next to the motion picture camera, was used to snap a shot through the windshield, when the front of the car reached the rear of the truck, during each run.

The driver of the car made a subjective rating of the task difficulty and the accident risk encountered during each pass. Each rating was based on a scale of 1 (none) to 5 (extreme), using the adjectival procedure shown in Fig. 93. This form is the same as that used in the driving simulator experiments (see Article III.E). The driver subjects were also common to both the simulator and full scale tests, to minimize the effects of inter-subject variability in the data. As can be seen in Fig. 93, two types of ratings were provided by the driver: accident risk and task difficulty. The latter was intended to be a subjective measure of control workload, while the former was aimed at an assessment of the likelihood of collision with either the truck or an obstacle on the roadway (perhaps obscured by the spray).

To round out the measures centered in the adjacent car, a backseat observer made a visibility rating through the windshield on the 1 (good) to 5 (very bad) scale using the format in Fig. 92.

Rating Instructions

Task Difficulty (Attentional Demand)		Accident Risk	Comments
Condition:			
None	1	None	________
Mild	2	Mild	________
Moderate	3	Moderate	________
Significant	4	Significant	________
Extreme	5	Extreme	________

(Detailed instructions not shown here)

Figure 93. Driver Rating Form

The magnitude and direction of the wind relative to the truck were measured by a propeller anemometer and direction vane mounted on a boom ahead of the tractor. This was used in both the June and November tests, and provided one of the primary measures of the test conditions.

Truck speed was maintained constant, at the prescribed value, by the driver using the tachometer. This was verified on each run by test personnel using a hand-held, calibrated, radar speed sensor. The test speed was recorded in the run log, and it was usually within about 1 mph (1.6 km/h) of the target value.

4. Driver Subjects

Adjacent car tests were run under splash and spray conditions in the June experiments. Four driver subjects were used in the adjacent car. They were all members of the STI engineering team involved in running the experiments. Their ages ranged from 26 to 41, and they were males in good health. They were all experienced drivers, and three of the four had extensive and varied backgrounds as test drivers in other research programs. They were familiar with the goals and measures of this program.

To offset the well known potential drawbacks of using experimenters as subjects, there were several compelling reasons for doing it in this study. First, we were interested in skilled behavior, and the assessment of differential effects in response and performance due to changes in truck configuration or operating condition. Each subject was his own control. Second, it simplified the logistics of remote site operation. An important third point is that it allowed the same drivers to be used as subjects in the driving simulator experiments and the full scale tests, to facilitate data correlation and the examination of other experimental effects. Finally, these drivers were all experienced in giving subjective ratings, and they were familiar with the driving task of interest.

5. Experimental Procedures

To a considerable extent, the test procedures are implicit in the previous discussion of the facilities and instrumentation. Some elaboration is provided here. There were a few differences in procedure between the

June and November tests, mainly reflecting their differing objectives, and these are noted. The details of the tests, run by run, are given in the run logs and detailed data sheets of Appendix B.

Prior to a data run, a number of steps were required — all part of good experimental practice. This included checking and calibrating the instrumentation, briefing the relatively large number of test personnel on the test schedule, defining safety procedures, and establishing the desired truck configurations and test conditions. For the wet tests, the water system was turned on and allowed to stabilize the wetting and water depth. This normally took about 30 to 45 minutes. The trucks were warmed up and inspected.

In the truck-alone tests, the truck circulated around the "dogbone" track shown in Fig. 89. Speeds were specified a priori, and verified by radio link and with the radar gun. The truck passed through the wet test area, past the checkerboard, twice on each lap, once northbound and once southbound. A typical test sequence with a given configuration and condition was two such laps in June. In November, typically, 4 laps were used (4 northbound and 4 southbound passes). The average ambient wind was recorded for the time the truck passed through the wet test area.

In the June truck-alone tests, only one truck ran at a time. Following the sequence, it stopped, and another configuration would start running; or a speed change might be prescribed. The June tests emphasized differences in trucks. A few devices were tested on a preliminary basis. In addition, loads and truck speeds were varied to assess their effect on splash and spray intensity. The test configurations and conditions run in June are summarized in Table 12, based on the detailed run log listing in Appendix B.

In the devices tests in November, two trucks ran simultaneously, in tandem about 1 minute apart. One truck was the basic configuration, "bogey," while the other had a device mounted. This allowed more precise determination of differential visibility effects, under almost identical ambient and test conditions. The 1 minute separation gave ample time for the wetting to become uniform again, and for the experimenters to reset the cameras and instrumentation. The November tests were all run at 60 mph (97 km/h), with empty semitrailers.

TABLE 12. SUMMARY OF SPLASH AND SPRAY TESTS — JUNE 1977

CONFIGURATION			TRUCK-ALONE RUNS						ADJACENT CAR RUNS									
			TRUCK SPEED		SEMITRAILER LOAD				CAR/TRUCK SPEED		SEMITRAILER LOAD				DRIVER SUBJECT			
TRACTOR	SEMITRAILER	DEVICE	50 mph	60 mph	NONE	20 kp	38 kp	MAXIMUM	65/55	55/60	NONE	20 kp	38 kp	MAXIMUM	W	K	F	S
COE	40 ft van	None	×	×		×	×		×			×	×		×	×		
COE	40 ft van	MO	×	×		×			×			×			×			
COE	40 ft van	M1	×	×		×												
COE	40 ft van	M4[a]		×		×												
COE	Flatbed	None	×	×	×				×		×					×		
COE	Liquid cargo tanker	None	×	×	×			×	×					×				×
COE	Dry cargo tanker	None	×	×	×													
Two axle COE	27 ft van	None	×	×	×				×		×				×			
Two axle COE	Double 27 ft vans	None	×	×	×				×		×				×			
Two axle COE	Double 27 ft vans	D1		×	×													
Two axle COE	Triple 27 ft vans	None	×	×	×				×		×				×			
CBE	40 ft van	None	×	×	×				×	×	×				×			
CBE	Flatbed	None		×	×													
CBE	Liquid cargo tanker	None	×	×	×				×	×	×				×			
CBE	Dry cargo tanker	None	×	×	×				×	×	×						×	

Note: 50 mph = 22 m/s; 55 mph = 24.5 m/s; and 60 mph = 27 m/s. 20 kp = 9100 kg; 38 kp = 17,300 kg.
[a]Except Reddaway flaps at rear of van, only.

There were some truck-centered differences in the basic truck (3 axle COE + 40 ft van) runs between June and November. The 3 axle COE tractors were slightly different — a Freightliner was used in June and Peterbilts in November. The cab depths were the same [86 in. (2.2 m)], but the wheelbase was about a foot (0.3 m) longer in June, so the gap was a little larger too. In November, conventional mud flaps were mounted behind the tractor tandems on the basic truck, while in June these flaps were not mounted. In all cases, the semitrailer on the basic truck had conventional mud flaps. The potential effects of these differences are all relatively minor compared to the configuration and devices variations of main interest here. Furthermore, in the November tests, none of these differences were present in the basic vs. device truck comparisons.

The splash and spray tests were conducted in the daytime in dry weather. Hence, the spray built up from zero as the truck entered the wet test section. This buildup required about 200 ft (60 m) typically, so that the spray cloud was stabilized by the time the truck reached the area around the cameras and the lasers. As a result of this relatively rapid establishment of steady spray conditions, "pre-wetting" of the truck was not needed.

The truck drivers were all skilled professionals in the trucking industry. Members of the WHI test team, they were either test engineers or managers whose jobs involve truck operations and safety. Most had prior splash and spray test experience. As a result, they were able to establish and maintain the desired truck speeds and ground tracks with precision, which enhanced the quality and repeatability of the data.

The adjacent car tests were run with the station wagon plus the truck on the track. As noted above, the track instrumentation was moved out of the way. This left the 30 ft (9.1 m) wide wet test area clear, and two adjacent 12 ft (3.7 m) lanes were defined inside the 30 ft (9.1 m). Ordinarily the car overtook and passed the truck. Sometimes the truck passed the car. In order to accomplish this in the wetted section, it was necessary to synchronize the acceleration profile of the passing vehicle (car) with that of the constant speed, overtaken vehicle (truck). Also, it was necessary to stop the car each time in order to photograph the run number and reset things for the next run. During that time, the driver also made his ratings. After passing through the wet section, the car would stop and turn around, and wait for the truck to round the loop. At an appropriate time the car would accelerate and pass the truck in the wetted section. The car always passed on the left side of the truck. In a crosswind, then, both upwind and downwind situations were encountered, as the car and truck alternated directions, north and south bound. The adjacent car test conditions studied are included in Table 12, based on the run log details in Appendix B. Adjacent car tests were not run in November, since the necessary connections between vehicle performance and the track data had been established using the June results.

B. BASIC TRUCK RESULTS

The photographic and strip chart records for each run have been formatted on individual data sheets, and these are included in Appendix B. Two formats are used. An example from the truck-alone tests in June is shown in Fig. 94, and the format used to present the adjacent car test data is illustrated in Fig. 95.

The truck-alone data sheet in Fig. 94 presents both the test conditions and the visibility results. The upper left-hand corner shows that the air was calm, and the truck was proceeding northbound at 48 mph (21.5 m/s). The edge of the truck (van) was 2.3 ft (0.7 m) from the edge of the checkerboard (the lane centerline), as determined by manual reduction from the photographs. The track-side observer ratings were "2," from each end, using the rating scale in Fig. 92. The parallel and perpendicular photos are as defined in Fig. 94. Densitometer analyses of the film were not made, although this could be accomplished at a future time. Darkened (opaque) square counts from the checkerboard photo were used in some of the comparisons. Generally, the laser and photometer data were sufficiently selective and reliable that they could be used as the primary objective measures, and the photographic coverage tended to be supplemental in the data interpretation.

The photometer and laser time responses for the interval of the test run are shown to the right in Fig. 94. In each case, the transmitted light reduces as the truck plus the spray cloud pass through the test area. The measure used is the maximum reduction, R, which is measured as a percentage from the ambient level just prior to the truck entering the wet test area

TRUCK-ALONE TEST

Configuration: *Conventional Tractor plus Dry Cargo Tanker Semitrailer - Empty*

Run: *001* Date: *6 June 77* Time: *10:28AM* Direction: *Northbound*

Ambient Wind: *0/—* Effective 90 deg Crosswind: *0/—* Truck Measured Wind: ______

Truck Speed: *48 mph* Truck Lane Position: *1.9 ft.* Water Depth: 0.057 in.

Visibility Ratings: *2* (From In Front) *2* (From Behind)

16mm Movie Film Comments: ______

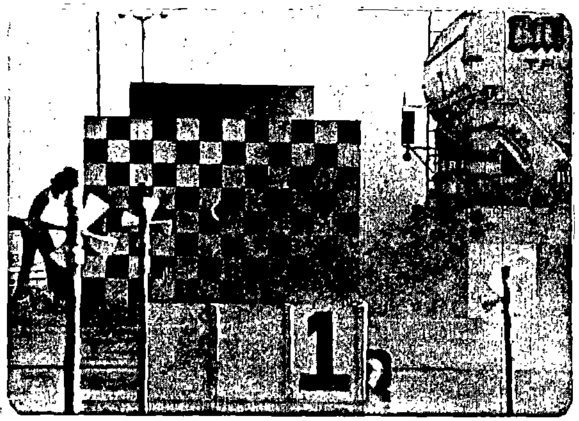

Parallel Photo: 250 mm, f22, 1/500 sec

DENSITOMETER ANALYSIS:

Section Reading

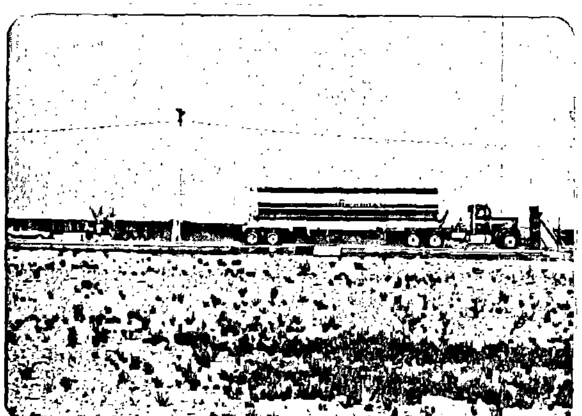

Perpendicular Photo: 50 mm, f9, 1/500 sec

DENSITOMETER ANALYSIS:

Position Reading

Photometer Reading Over 400 ft 6 ft From Track Centerline

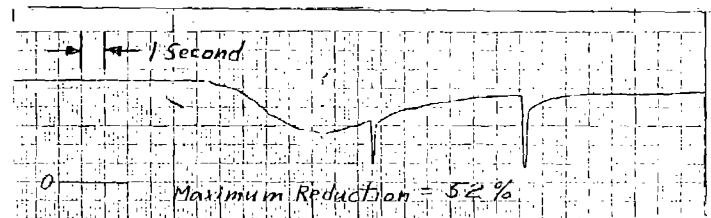

Laser Reading Over 50 ft 6 ft From Track Centerline

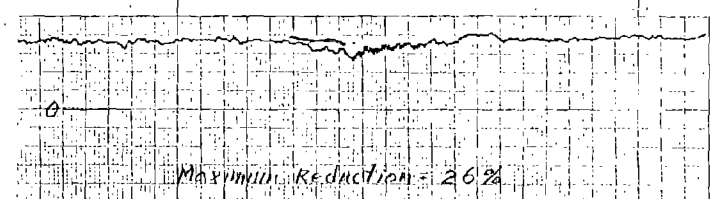

Laser Reading Over 50 ft 2 ft From Track Centerline

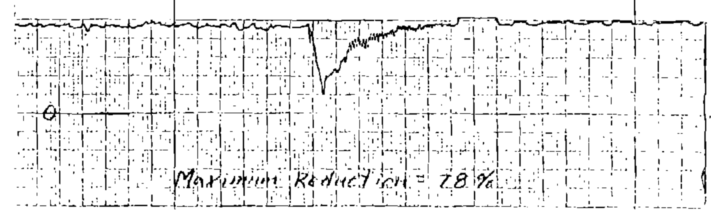

1 ft = .3048 m
1 in. = 25.4 mm
1 mph = 1.61 km/h

Figure 94. Example of Truck-Alone, Track Data Sheet

ADJACENT VEHICLE TEST

Configuration: CONVENTIONAL TRACTOR + DRY CARGO TANKER SEMITRAILER-EMPTY

Run: 031 Date: 6 JUNE 77 Time: 2:54 Direction: NORTHBOUND

Ambient Wind: 5/180 Effective 90 deg Crosswind: 0/— Truck Measured Wind: ______

Truck Speed: 54 MPH Car Speed: 66 MPH Relative Car-Truck Speed: 12 MPH

Water Depth: 0.057 in.

Subjective Ratings:

3 (Task Difficulty) 2.5 (Accident Risk) 2 (Observer Visibility)

16 mm Movie Film Comments: ______

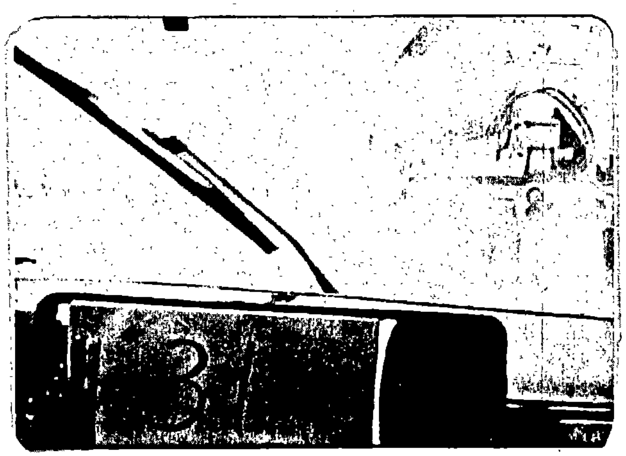

Photo From Car: 50 mm, f11, 1/125 sec

1 ft = .3048 m
1 in. = 25.4 mm
1 mph = 1.61 km/h

Steering Wheel Angle, δ_{sw} (deg)

Relative Wind Magnitude, |VW| (mph)

Relative Wind Direction, ∡WV (deg)

Relative Lateral Position From Truck (ft) and Overhead Camera Frame Count

Yaw Velocity, r (deg/sec)

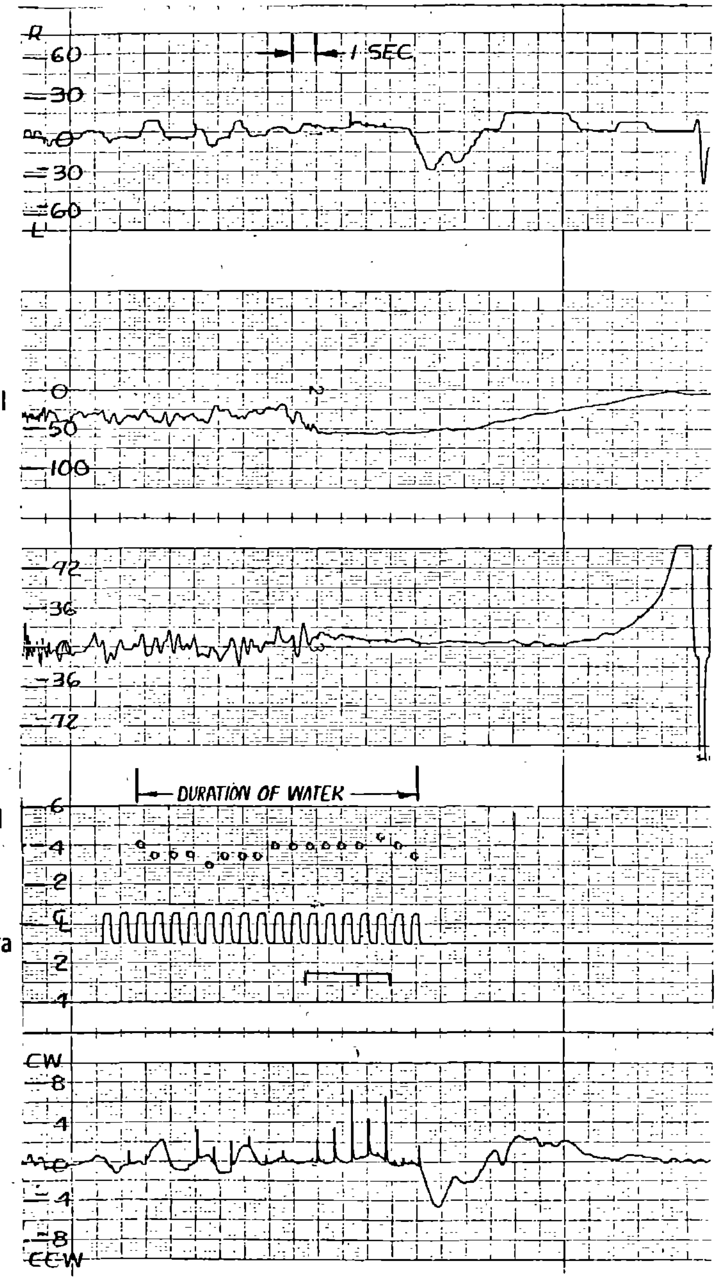

Figure 95. Example of Adjacent Car Data Sheet

of the track. Subsequently, we used a "visibility" measure, which is instead the maximum reduction relative to zero, i.e., the opaque, no light transmitted case. The definition is:

$$\boxed{\text{Visibility} = (1 - R) \text{ in percent}}$$

In the Fig. 94 example, the visibility reading from the photometer was 48 percent; and the visibility values from the lasers at 6 ft and 2 ft (1.83 m and 0.61 m), respectively, were 74 percent and 22 percent. The laser values differ because the latter one is much closer to the truck and hence more fully immersed in the spray cloud. The photometer value differs from the laser at 6 ft because it is higher above the roadway, and due to differences in the spectral characteristics of the light source and the sensitivity properties of the photometer/receiver.

The track data format used in November differs slightly from that shown in Fig. 94. The ambient wind magnitude and direction were recorded on the strip chart in the devices tests, the track side observer ratings were not made, and there were some minor changes in format.

The adjacent car test data sheet example in Fig. 95 shows a similar description of the test conditions in the upper left-hand corner. The speed of both vehicles is shown. The first two ratings (task difficulty and accident risk) were given by the car driver, using the form in Fig. 93. The observer visibility rating was made by an observer in the back seat using the procedure in Fig. 92. The photo from inside the car was taken with a camera on the centerline near the right side of the driver's head.

The onboard data is shown to the right of Fig. 95. In this case there was a light tailwind, and no crosswind component, so the aerodynamic disturbance was relatively small. Variations in the relative wind angle in the vicinity of the truck are due to wake effects. The lateral position of the car relative to the truck was obtained from the camera mounted on the roof of the car. The sawtooth-like signal pulses on that trace indicate each time an overhead picture was taken (approximately 1.5 frames/second).

1. Effect of Truck Load and Speed on Visibility

As shown in Table 12, some runs were made in June to investigate the effect on splash and spray of variations in semitrailer load. Comparison of the visibility values for the 20,000 and 38,000 lb (9100 and 17,300 kg) load cases is shown in Fig. 96. The zero load case is not included here, because it was not run in June. In addition to illustrating this experimental effect, the results show the nature of the raw data.

The photometer and laser results are given in Fig. 96 for the basic truck with the load variation. Each data point is the result for a single truck-alone run. The superimposed bars are the mean values. The flag indicates a northbound run. All the data shown are for the "downwind" case, which means that the wind was blowing from the east and the sensors were in the wake of the truck. As will be detailed shortly, the spray is substantially greater downwind than it is upwind, so it is appropriate to compare the configuration effect under similar conditions.

The data show that the run to run variability for a given measure is quite small, with occasional exceptions. Furthermore, these results indicate that there is not a large effect of changing the load, by comparison with other effects to be shown below. Consequently, most of the runs in the June tests, and all of those in November, were made with no load. This greatly simplified the experimental procedure, since it avoided having to load the trucks, and it saved the running delays connected with longer truck acceleration times on the test course.

The effect of changes in truck speed on the visibility measures is shown in Fig. 97, taken from the experiments in June. Again, these are downwind measures, and the data are for the basic truck with 38,000 lb (17,300 kg) load. Compared to 50 mph (22 m/s), the overall visibility is reduced at 60 mph (27 m/s), with the mean levels decreasing to about half their value at the lower speed. The data are seen to be quite repeatable.

The speed effect can be seen more graphically by comparing the darkened (or opaque) regions of the checkerboard due to the spray cloud, as seen in the longitudinal black and white camera data. This is sketched in Fig. 98. The outlined borders of the opaque region shown represent the average of

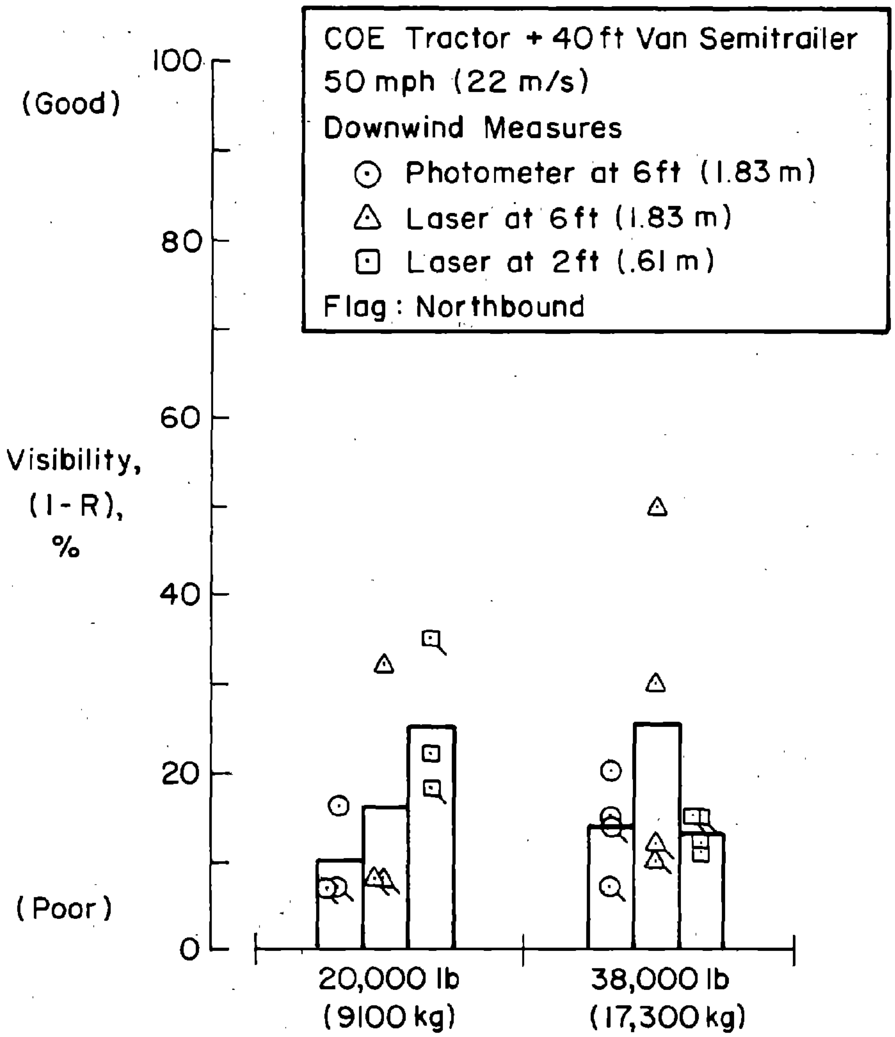

Figure 96. Effect of Semitrailer Load on Visibility Measures

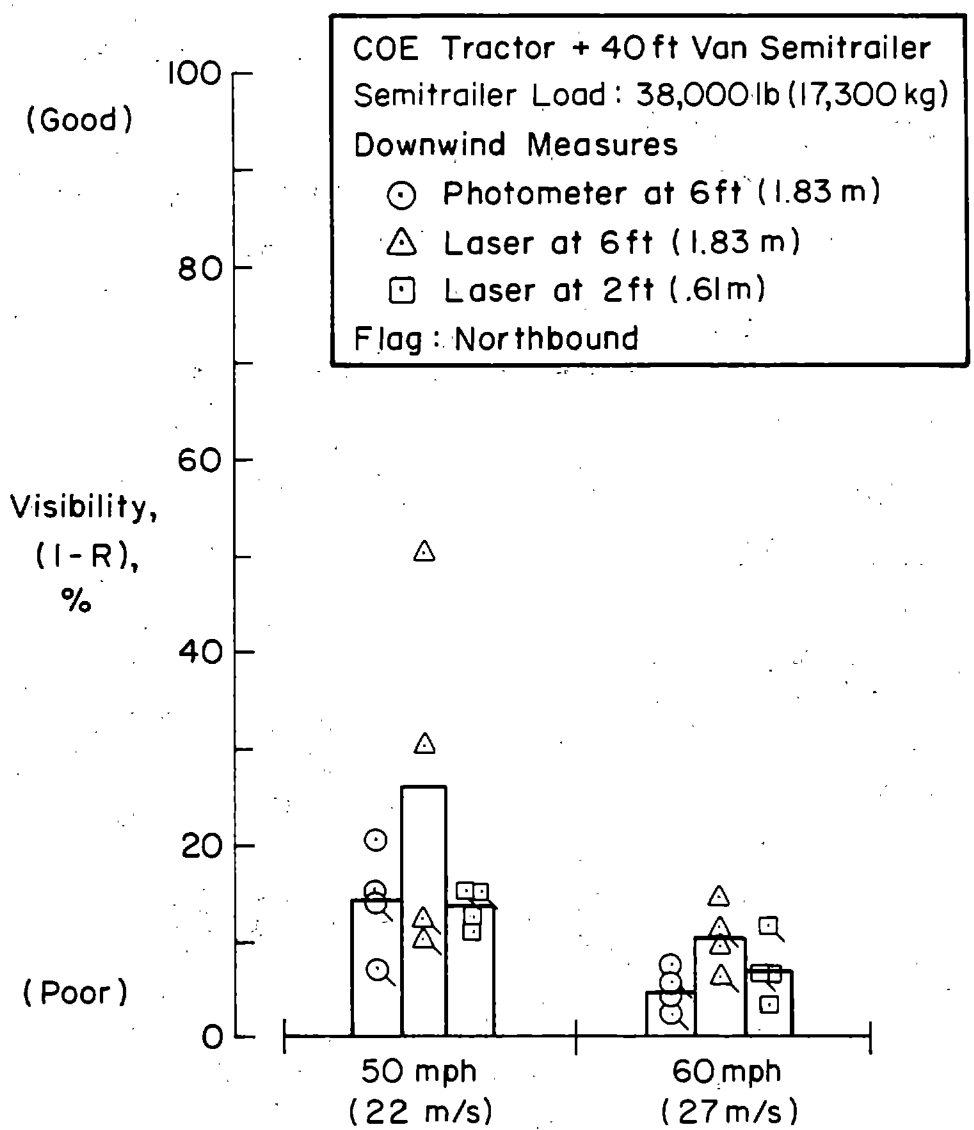

Figure 97. Effect of Truck Speed on Visibility Measures

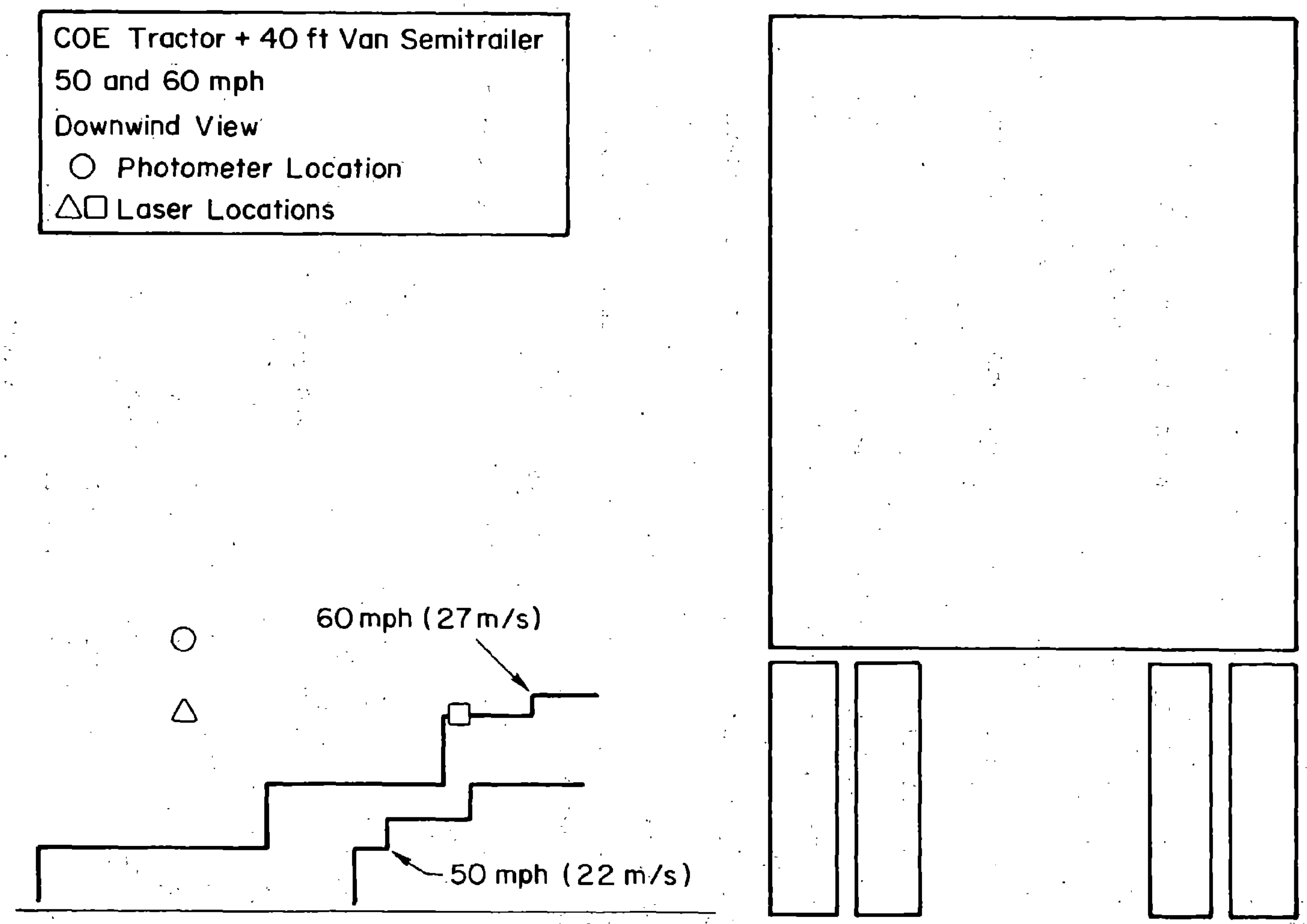

Figure 98. Effect of Truck Speed on Opaque Splash and Spray Cloud Areas

several runs. The semi-opaque portions of the spray cloud are more extensive at the higher speeds, also. The locations of the laser and photometer receivers in the field of view are shown for comparison.

2. Effect of Wind and Truck Position on Visibility

Variations in visibility conditions due to ambient wind are greatly influenced depending on whether the measures are being made upwind or downwind of the truck, and they are also affected by the wind magnitude. The laser and photometer spray measures were also sensitive to the lateral position of the truck relative to the lane centerline, as it passed through the test area. Scaling procedures have been developed to account for these effects in a systematic way, and they are presented below.

The laser and photometer visibility measures obtained in the June and November tests were made under a variety of ambient wind conditions. In addition, the lateral position of the truck varied relative to the test section lane edge and the checkerboard, from run to run. As a result, empirical procedures have been derived to place the results from all the runs on a common basis for comparison. These scaling procedures can also be used in reverse, to adjust the reference visibility values to a range of ambient wind conditions as selected in the cost/benefit analyses. These scaling procedures are based on the laser at 2 ft values, because they were the main measures used in the comparison of trucks and devices (as discussed in Article C, below).

The first step in scaling the $V = (1 - R)$ visibility measures to a common reference was to adjust them to a lateral lane position, y_T, of the truck from the checkerboard of 3.5 ft (1.1 m). The gradient for this was derived from basic truck data from the November tests for winds with no crosswind component (less than ±1 deg relative to the truck), and winds giving a relative wind angle less than −6 deg. These data points are shown in Fig. 99. Scatter aside, the trends show little difference, so they were fit with the single scaling curve marked "Ref," plotted on Fig. 99, which takes into account the data shown as well as other results and engineering considerations. This reference curve indicates a correction of 17 percent visibility per foot, for y_T values greater than 3.5 ft (1.1 m) and no correction for smaller values of y_T.

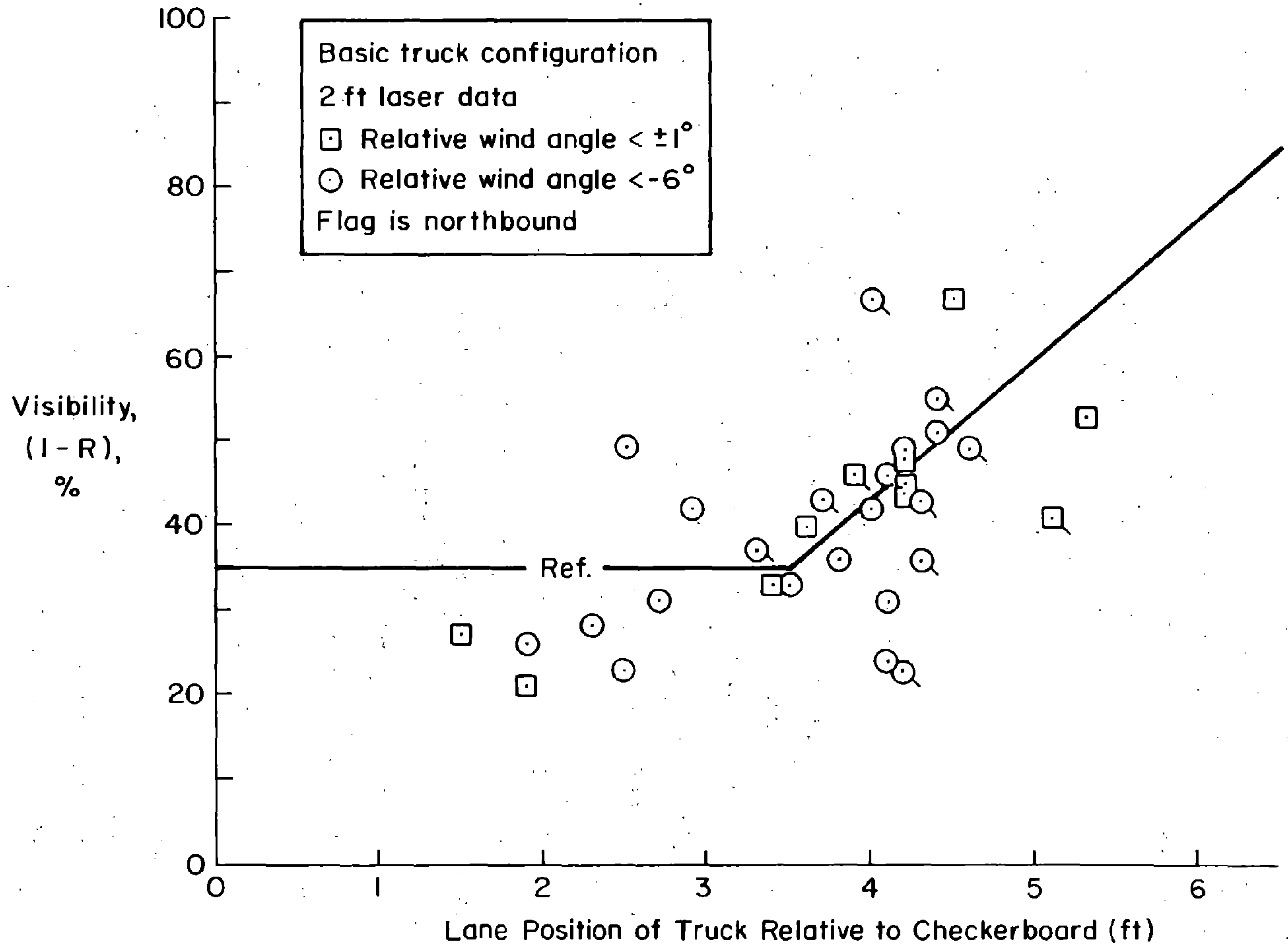

Figure 99. Basis for Truck Lane Position Scaling Factor, 1 ft = 0.3048 m

Next, it was recognized that the ambient wind angle, $\measuredangle W$, variations have a profound effect on the truck spray cloud, as it proceeds north or south bound. To investigate this, selected basic truck visibility data were plotted as a function of ambient angle (relative to north), for three different wind magnitude categories, and for raw values of y_T between 2 and 4 ft. The resulting data points are shown in Fig. 100 (for southbound) and Fig. 101 (for northbound). The wind magnitude, $|W|$, data legend is as follows:

$$\bigcirc \quad 0 \le |W| \le 2.5 \text{ mph } (1 \text{ m/s})$$

$$\square \quad 4 \le |W| \le 7 \text{ mph } (3 \text{ m/s})$$

$$\triangle \quad 9 \le |W| \le 12 \text{ mph } (5 \text{ m/s})$$

The open data points are from the November tests while the filled points are from June. Generally, the June data gave lower raw visibilities, especially for the basic truck runs. This is reflected in the sharp gradients in the angle scaling curves for visibility values below the "Ref" line.

Examination of the results for $|W| \le 2.5$ mph (1 m/s) indicated that they did not vary systematically with ambient wind angle, and that no angle scaling factor was needed.

For the $4 \le |W| \le 7$ points, the variation with angle was faired using the dark line labeled "Ref." Although the curve does not fit all the points in detail, it is a best engineering fit, based on all the data, physical considerations, and the desire to have a simple and conservative scaling procedure. Note that the variations in Figs. 100a and 100b, laid side by side, from −180 deg to +180 deg are the same as the mirror images of Figs. 101a and 101b, from −0 to +0 deg, as they should be.

The higher velocity winds, $9 \le |W| \le 12$, show poorer visibility for strong crosswinds from the east (sensors downwind of the truck), and this was taken into account by the fairings shown. In the absence of data, intuition tells us, also, that the visibility should be a little better when the wind is stronger from the west, and allowance is made for that in the scaling procedure, as shown subsequently.

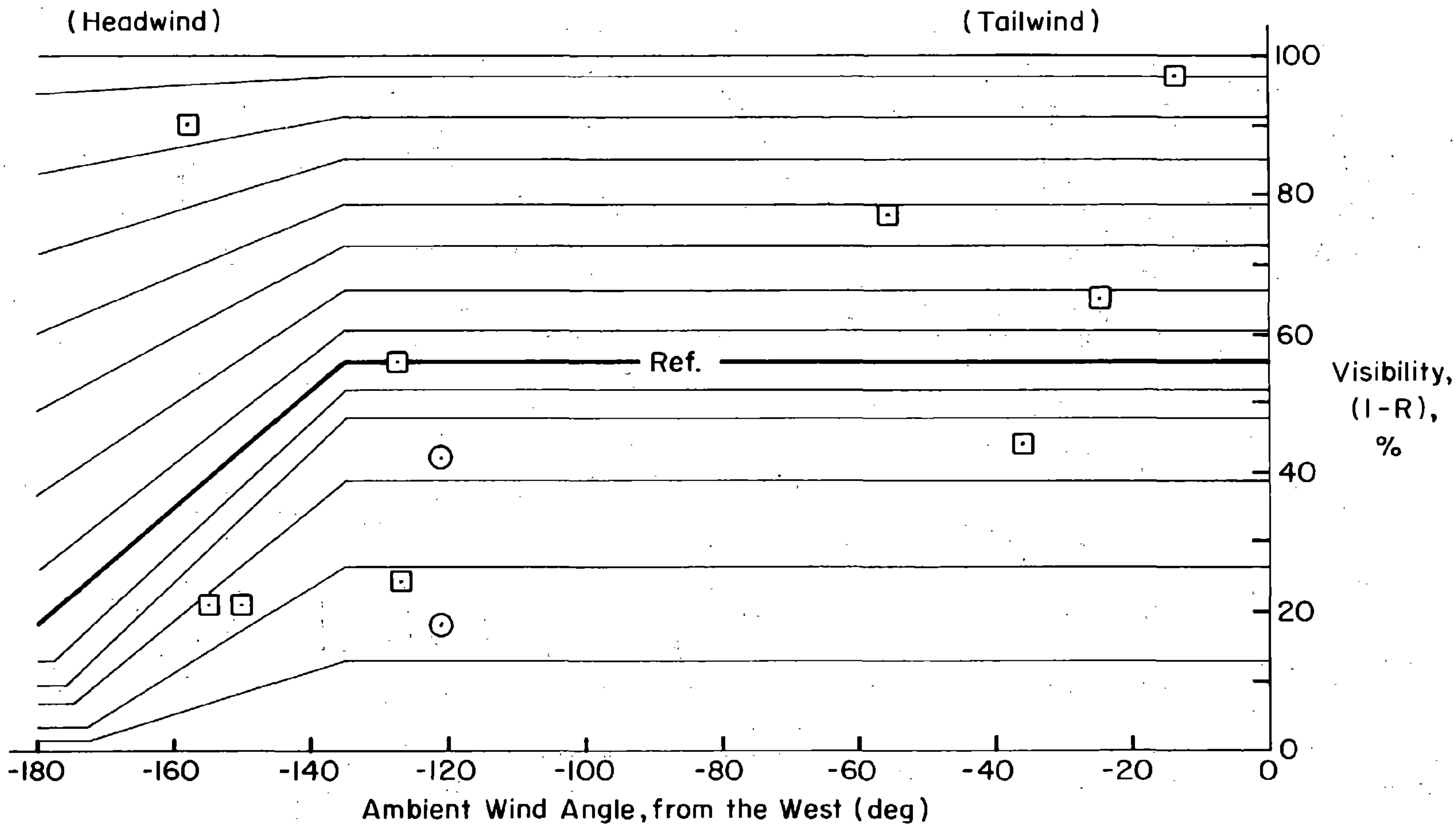

Figure 100a. Ambient Wind Angle Scaling Curve, Southbound

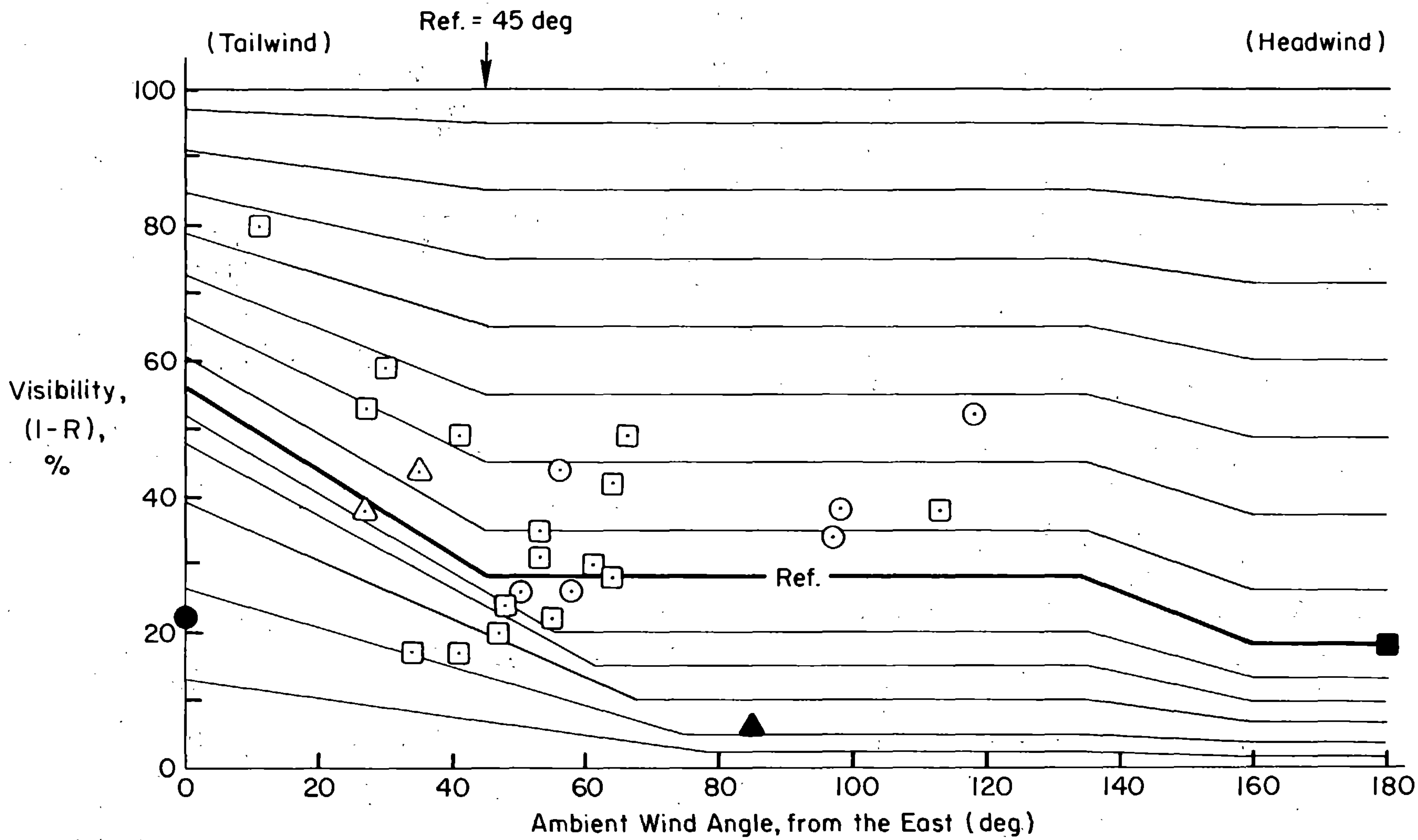

Figure 100b. Ambient Wind Angle Scaling Curve, Southbound

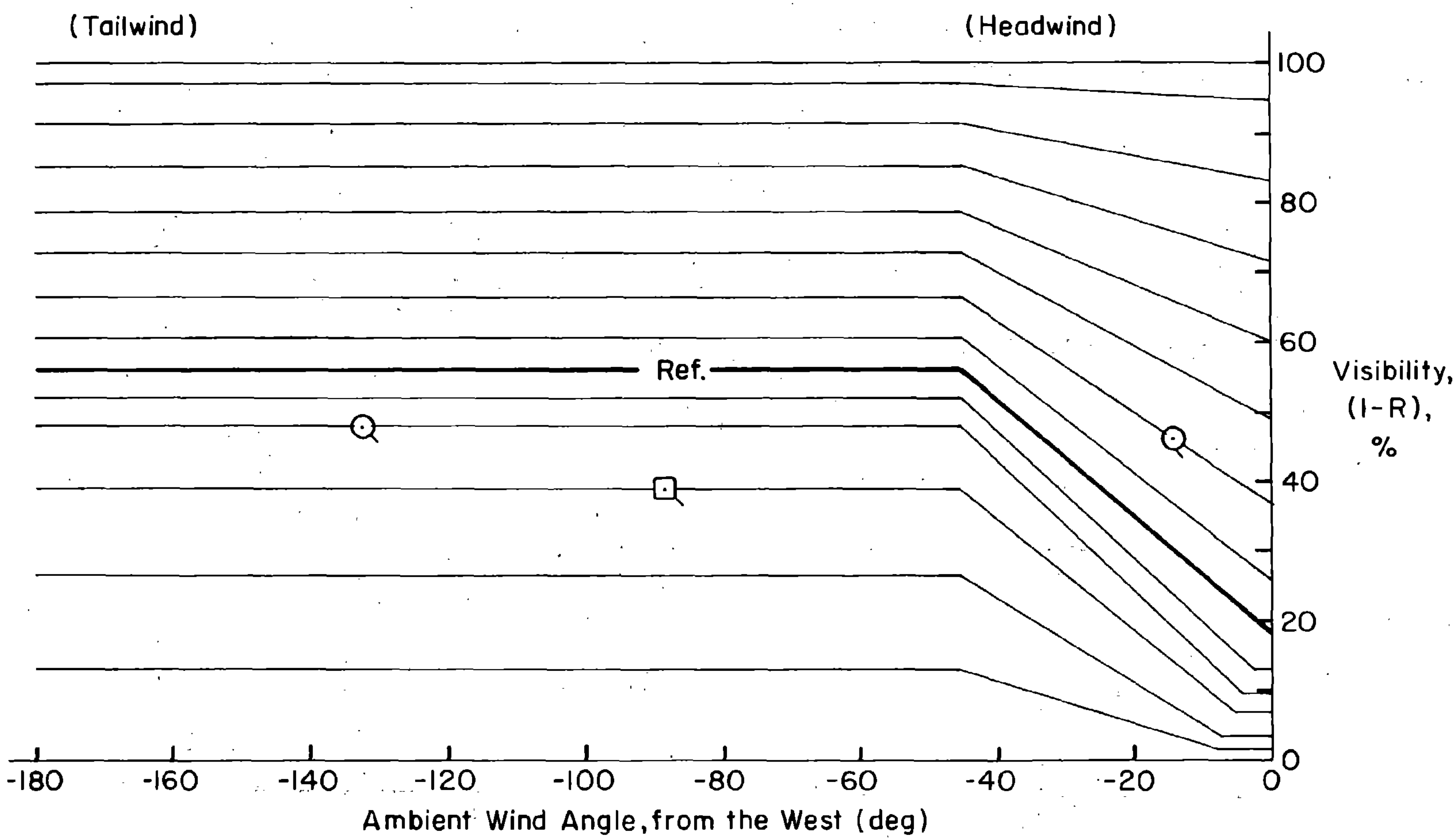

Figure 101a. Ambient Wind Angle Scaling Curve, Northbound

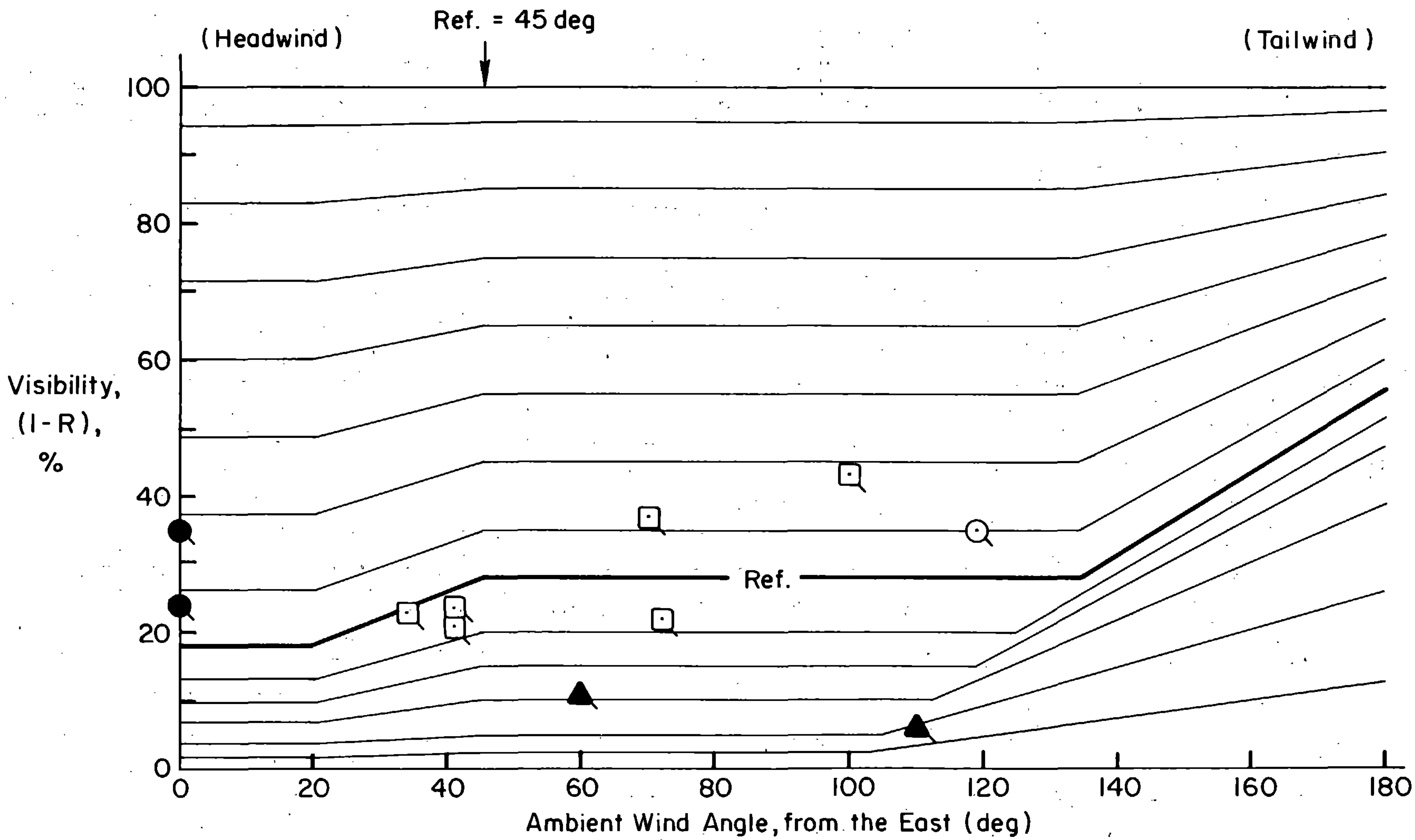

Figure 101b. Ambient Wind Angle Scaling Curve, Northbound

The basis for the "Ref" curve in Figs. 100 and 101 has been noted, above. The additional families of curves shown are needed when the measured visibility, V, is other than the reference value at a given ambient wind angle. As can be seen, these curves were structured in a proportional way, given the Ref curve and the 0 and 100 percent boundaries. Together, the Figs. 100 and 101 sets of curves allow the visibility to be scaled to a common angle value, and 45 deg has been selected for two reasons. First, it typifies the data so that many visibility values require no scaling or manipulation; and second, it is a representative crosswind value from the standpoint of the spray disturbance of the adjacent driver.

Once the wind angle correction has been made to the 45 deg reference value, it remains to scale the visibility to a common ambient wind magnitude, and 5 mph (2 m/s) was selected for this for the reasons noted above. The magnitude correction was contrived on a proportional basis, as follows. The southbound data in the region of 45 deg suggest the visibilities with the basic truck are about:

$$V_0 = 35\% \qquad \text{for } |W| = 0 \text{ mph}$$

$$V_5 = 28\% \qquad \text{for } |W| = 5 \text{ mph } (2 \text{ m/s})$$

So, the concept is that the multiplicative correction factor is 0.8 when $V_0 = 35\%$ and it reduces to 1.0 (no correction) when $V_0 = 100\%$, i.e., when there is no visibility reduction due to the truck. Similarly, for values of $V_0 < 35\%$, the correction factor should vary proportionally from 0.8 at 35% to 1.0 at 0%. Mathematically,

if $V_0 \geq 35\%$

$$V_5 = \frac{72}{65}(V_0 - 35) + 28 \tag{24}$$

if $V_0 < 35\%$

$$V_5 = \frac{28}{35}(V_0 - 35) + 28 \tag{25}$$

This magnitude scaling is to be applied to the visibility reading obtained for either a basic truck or a "devices" truck. A possible exception to the latter might be a device such as the longitudinal baffle, which has the potential of modifying the gross flow around the truck, and hence the wake shape. Devices which simply change spray source strengths, or add or delete sources, should not change the basic spray propagation and extinction properties.

Similarly, when ambient wind magnitude is greater than 7.5 mph (3.4 m/s) (and less than 15 mph, 6.7 m/s), and it is desired to increase the visibility to the 5 mph value, the following empirical relations are deemed to apply.

if $V \geq 14\%$

$$V_5 = \frac{72}{86}(V - 14) + 28 \tag{26}$$

if $V < 14\%$

$$V_5 = \frac{28}{14}(V - 14) + 28 \tag{27}$$

Again, these corrections apply to both the basic and devices truck data.

The scaling procedure outlined above is summarized in flow chart form in Fig. 102. Given the raw visibility readings, this allows them to be placed on a common basis. Then the respective devices truck and basic truck comparisons can be made for back to back runs, and the results will be more readily comparable across devices and the wide range of test conditions which were encountered. As noted, the reference conditions selected were the ones most prevalent in the November data, resulting in the least changes from the raw results, which was felt to be a conservative approach.

3. Scaling Procedure for Cost/Benefit Analysis

As noted earlier, "reversing" the scaling procedure flow charted in Fig. 102 provides a basis for correcting the visibility measures to a range of ambient winds in the cost/benefit computations. The steps to be used are

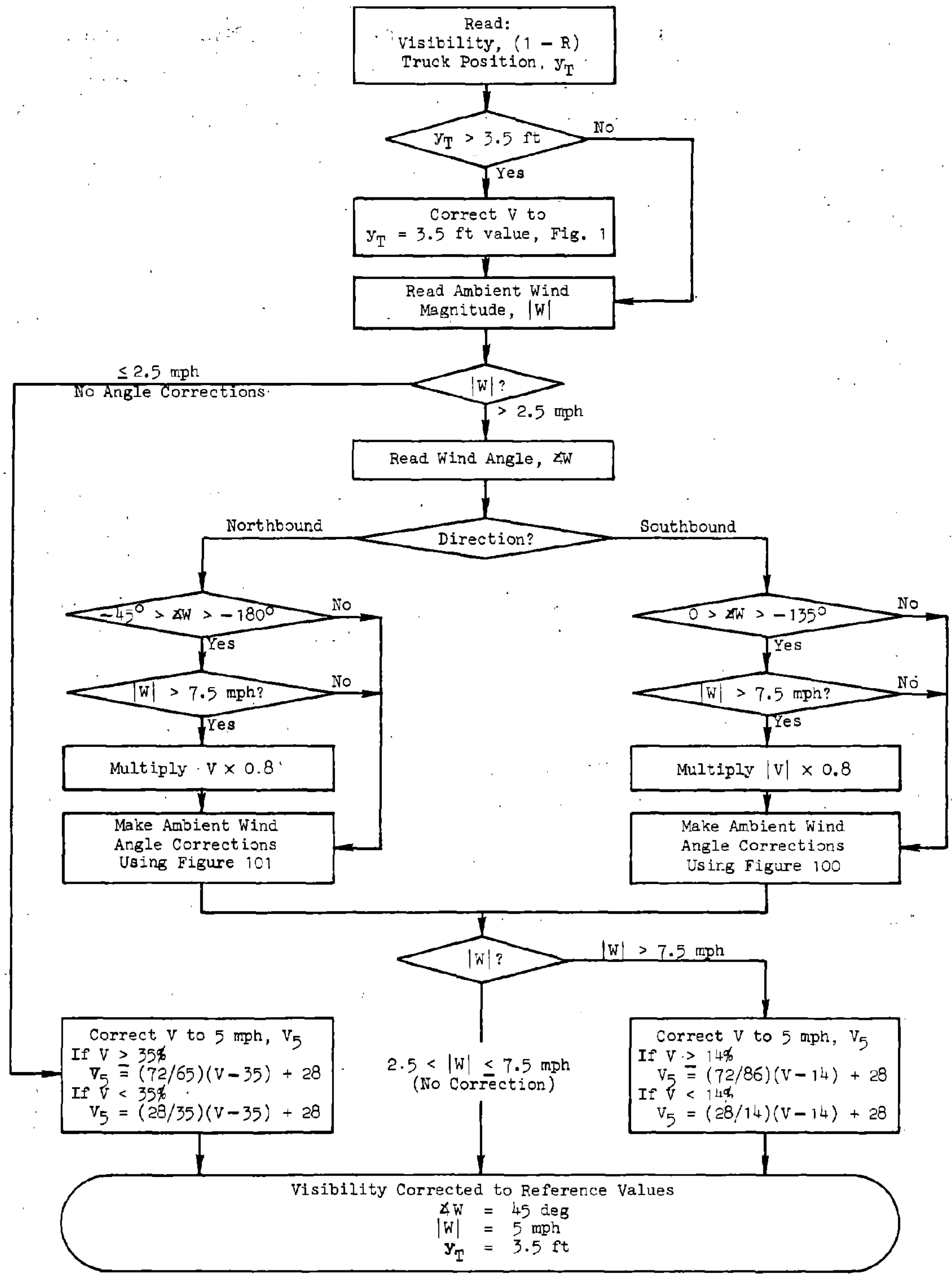

Figure 102. Flow Chart of Visibility Scaling Procedure,
1 ft = 0.3048 m, 1 mph ≐ 0.45 m/s

summarized below, for reference. There are three cases, based on the magnitude of the ambient wind, i.e., $|W|$ less than 2.5 mph (1.1 m/s), between 2.5 and 7.5 mph (1.1 and 3.4 m/s), and between 7.5 and 15 mph (3.4 and 6.7 m/s).

If the ambient wind magnitude is $\leq$ 2.5 mph, then from Eqs. 24 and 25

if $V_5 \geq 28\%$

$$V = \frac{65}{72}(V_5 - 28) + 35 \tag{28}$$

if $V_5 < 28\%$

$$V = \frac{35}{28}(V_5 - 28) + 35 \tag{29}$$

where V_5 is the tabulated, scaled, visibility value. Note that no angle correction is needed when the wind velocity is near zero, i.e., when $|W| \leq 2.5$ mph (1 m/s).

If the ambient magnitude is between 2.5 and 7.5 mph (1.1 and 3.4 m/s), i.e., near the reference value, then no magnitude correction is needed. In that case, define the ambient wind angle as being relative to the truck heading, in which case the truck is always "northbound." Then, the angle scaling can be done using Figs. 101a and 101b. For analysis, the car/driver is assumed to be in the lane to the west.

If the ambient wind is between 7.5 and 15 mph (3.4 and 6.7 m/s), correct the magnitude using Eqs. 26 and 27, i.e.,

if $V_5 \geq 28\%$

$$V = \frac{86}{72}(V_5 - 28) + 14 \tag{30}$$

if $V_5 < 28\%$

$$V = \frac{14}{28}(V_5 - 28) + 14 \tag{31}$$

Then scale the ambient wind angle using Figs. 101a and 101b, as described in the preceding paragraphs. As noted previously, if $-45° > \angle W > -180°$ an additional magnitude correction is needed, multiply V by 1.25.

Note that the lateral position correction factor is not needed in the C-E scaling procedure. The truck is assumed to be proceeding in a straight line in its own lane. Although there can be some car motion alongside the truck due to the aerodynamic force and moment disturbance, the peak variation in lateral position is small, e.g., 1 ft (0.3 m). Random motions of the truck and car about their respective nominal trajectories tend to be small, also, and furthermore their effect on visibility tends to average out. Hence, the overall variations in lane position during the car-truck passing encounter are not large enough to warrant scaling for C-E comparisons.

In doing the C-E analyses the ambient winds selected need not be randomly distributed from all quadrants. Rather, they could emphasize calm air (no ambient wind), headwinds, and winds from ahead and to the side. In other words, the ambient wind angles should be from the two quadrants which are ±90 deg from the direction of travel of truck and car. Winds from the rear quadrants give the same relative effects with diminished amplification factors, and hence are somewhat redundant and less interesting. Note, again, that the reference case for the visibility measures is a 5 mph (2.2 m/s) wind from a relative bearing of 45 deg relative to the truck — such that the car is in the truck's wake. Also, the wind tunnel aerodynamic measures of truck drag and truck-induced car disturbances were made, for wind angles relative to the truck of zero, and ±20 deg. The 20 deg values used in the wind tunnel reflect the fact that the aerodynamic flow transition to a crosswind wake situation occurs at about a 10 deg relative flow angle (Refs. 2 and 6), so a 20 deg relative angle was a fully developed strong crosswind case. Hence, pertinent relative wind angles would seem to be

±10 to 20 deg for aerodynamics

±5 deg for visibility factors

These will result in representative and discriminating crosswind cases, and the least extrapolation of the basic data; and they are also interesting from the standpoint of the resulting performance of the adjacent car/driver system. Finally, ambient wind magnitudes greater than 15 mph (6.7 m/s) need not be considered in the C-E comparisons. Larger values would not change the relative ranking of the effects; they are relatively uncommon, and they would require an unwarranted extrapolation of the bulk of the splash and spray data base.

C. CORRELATIONS BETWEEN THE MEASURES

The available measures related to the visibility and performance of the driver of the adjacent car have been defined and discussed in previous articles. Briefly, these include:

- Laser at 2 ft, transmissivity
- Laser at 6 ft, transmissivity
- Photometer, transmissivity
- Trackside observer ratings
- Driver risk and task difficulty ratings
- Backseat observer ratings
- Lane position of the adjacent car

Car/driver response measures (steer angle and yaw velocity) were also obtained, and they are shown in the data sheets of Volume II, but they were not reduced in detail. The connections and correlations among the measures listed above are the subject of this article. To simplify data interpretation and comparison it has been useful to relate the several measures to one variable which can then provide the basis for analysis of experimental effects. This has been done, and the result is that the visibility transmissivity of the laser at 2 ft provides an index that is selective, representative, and parametrically well behaved, as discussed below.

The first set of correlations shown are among the laser and photometer readings. Then, these measures are related to the trackside observer ratings. Finally, connections are shown between adjacent car driver performance and visibility, and between driver ratings and visibility. In each case, these plots are based on the summary data tables and associated individual run data sheets in Volume II.

1. Relation of Laser and Photometer Measures

The correlation between the visibility values, $1 - R$, for the laser at 6 ft and the laser at 2 ft is shown in Fig. 103. These are raw data, for the basic truck, from June and November, under conditions where the lasers are downwind of the truck. A least squares regression fit to the data gave $\rho = 0.66$ with a standard error (SE) of 18 percent, which confirms that the expected physical relation is present in the data. The regression line does not necessarily have to pass through zero, since it would be possible for the 2 ft laser to be fairly obscured, yet to have the 6 ft laser largely outside the spray cloud. For this downwind case, the data points near zero suggest that the two laser measures do become small simultaneously. This is a result of the diffuse nature of the spray cloud and its being carried downwind, in the truck wake, across the path of the sensors.

The correlation between the photometer and 2 ft laser visibility values is shown in Fig. 104. Again, these are raw data for the basic truck downwind. Generally, the attenuation of the halogen light as seen by the photometer is a much greater percentage of the clear value than is the attenuation of the 2 ft laser. Put another way, in this downwind condition with varying amounts of splash and spray in the adjacent lane, the photometer shows small readings in all cases, while the 2 ft laser has a much larger dynamic range (readings varying from near 0 to near 100 percent).

The correlation between the laser at 6 ft and the laser at 2 ft visibility values for the upwind case is shown in Fig. 105. Now, both the 6 ft and 2 ft laser values tend to be a little higher than in Fig. 103, yet the correlation between the pairs of readings under various test conditions is still strong. The standard error in the linear fit is 11 percent, in terms of the vertical scale. It should be noted that detailed examination of these correlations (for both the upwind and downwind cases) showed no systematic shift in the data due to variations in the lateral lane position of the truck.

The final correlation in this set is between the photometer and the laser at 2 ft, under upwind conditions, shown in Fig. 106. As in Fig. 105, both sets of readings tend to be higher but the relationship is quite evident. A few data points were not shown in this plot, because the lateral position of the truck relative to the sensors was unusually large.

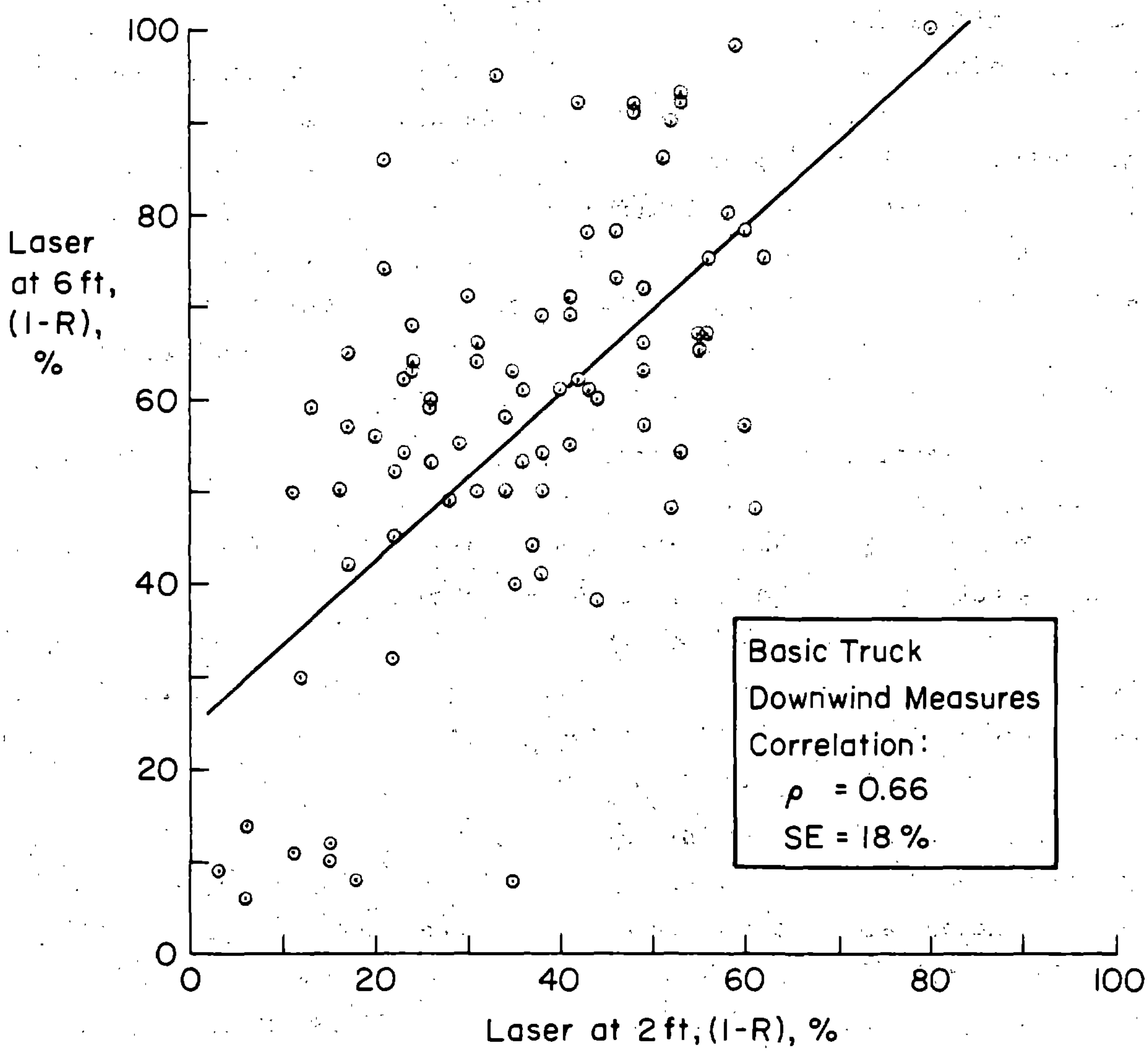

Figure 103. Correlation of Laser Raw Data, Downwind

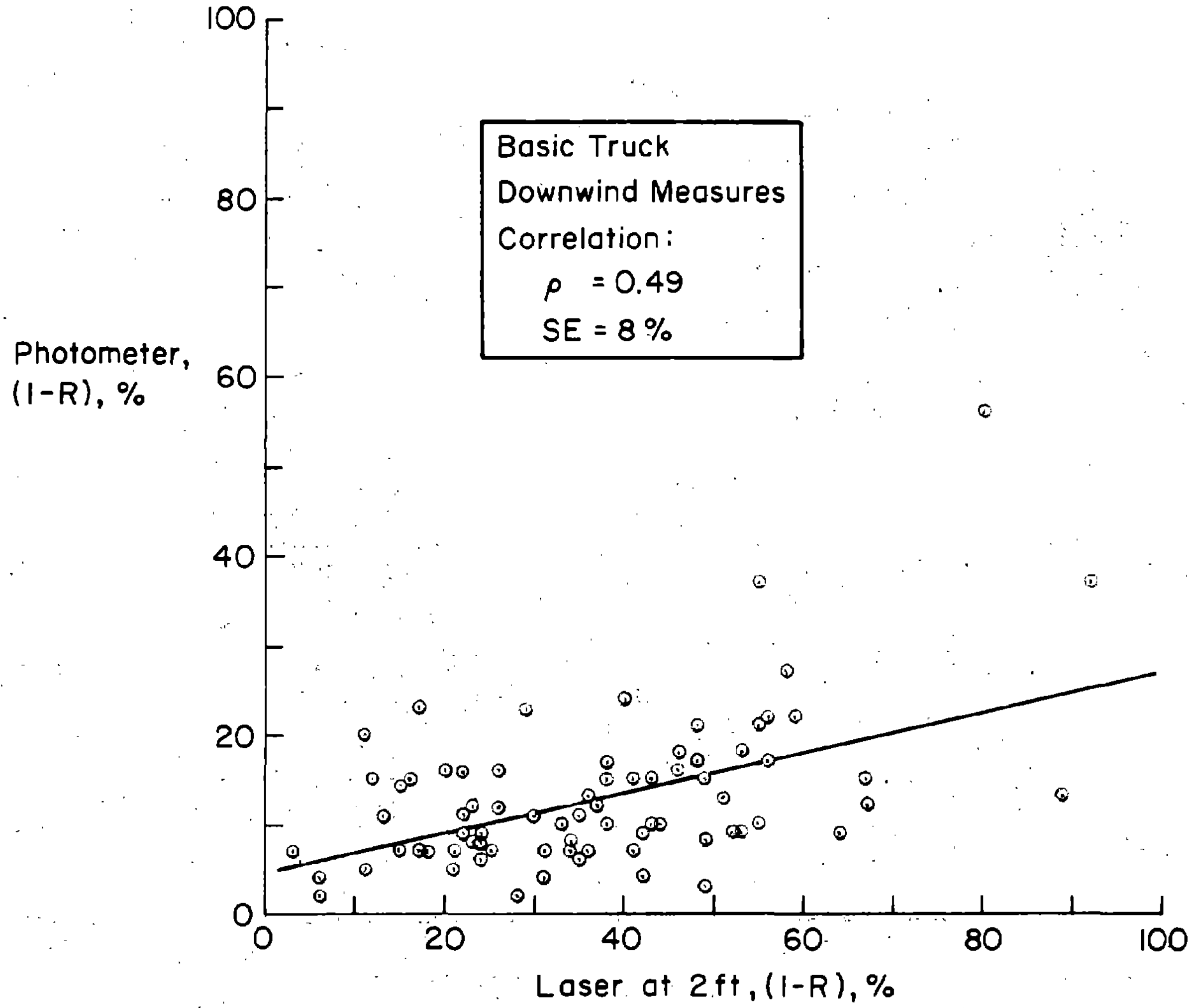

Figure 104. Correlation of Photometer and Laser Raw Data, Downwind

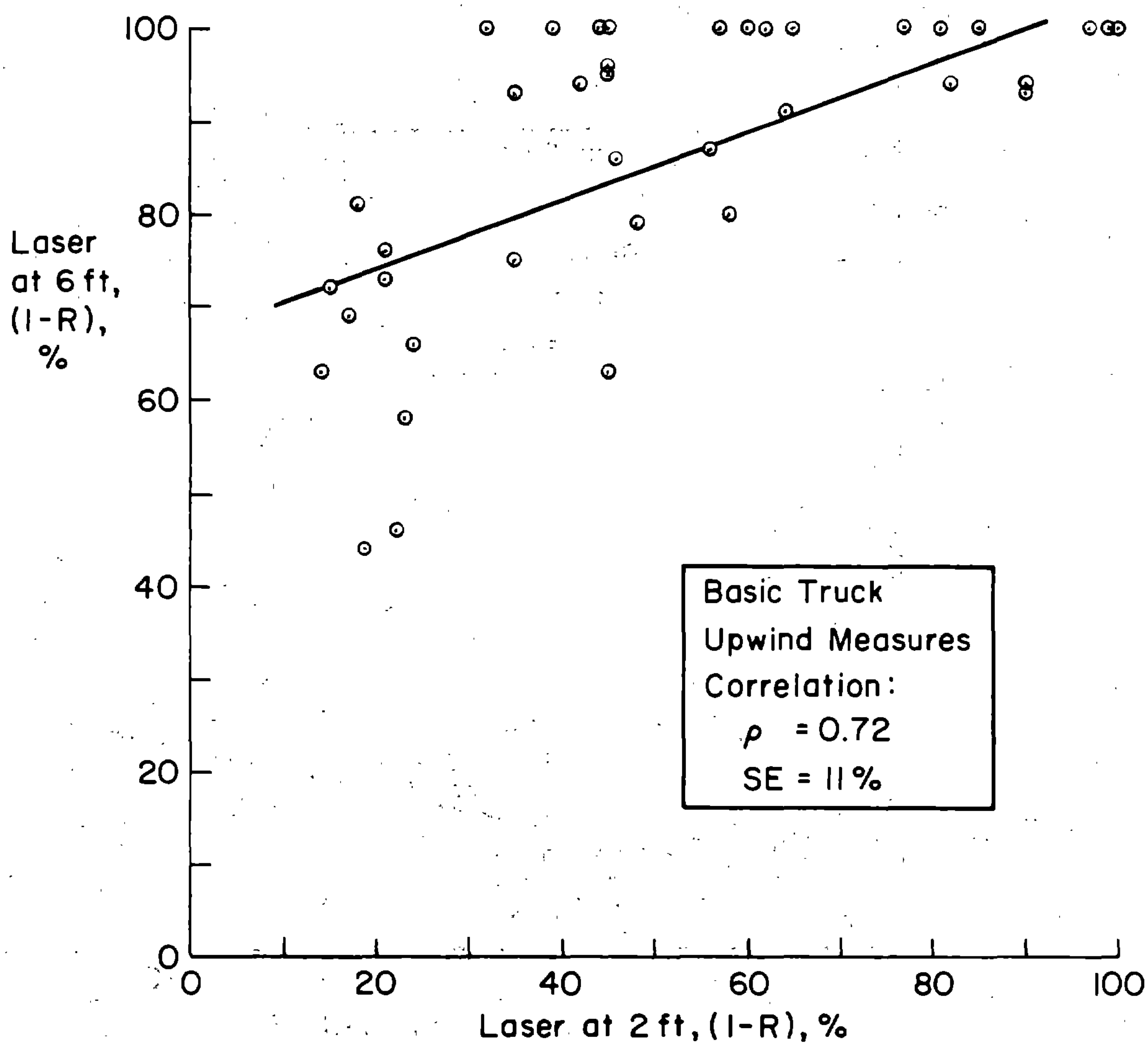

Figure 105. Correlation of Laser Raw Data, Upwind

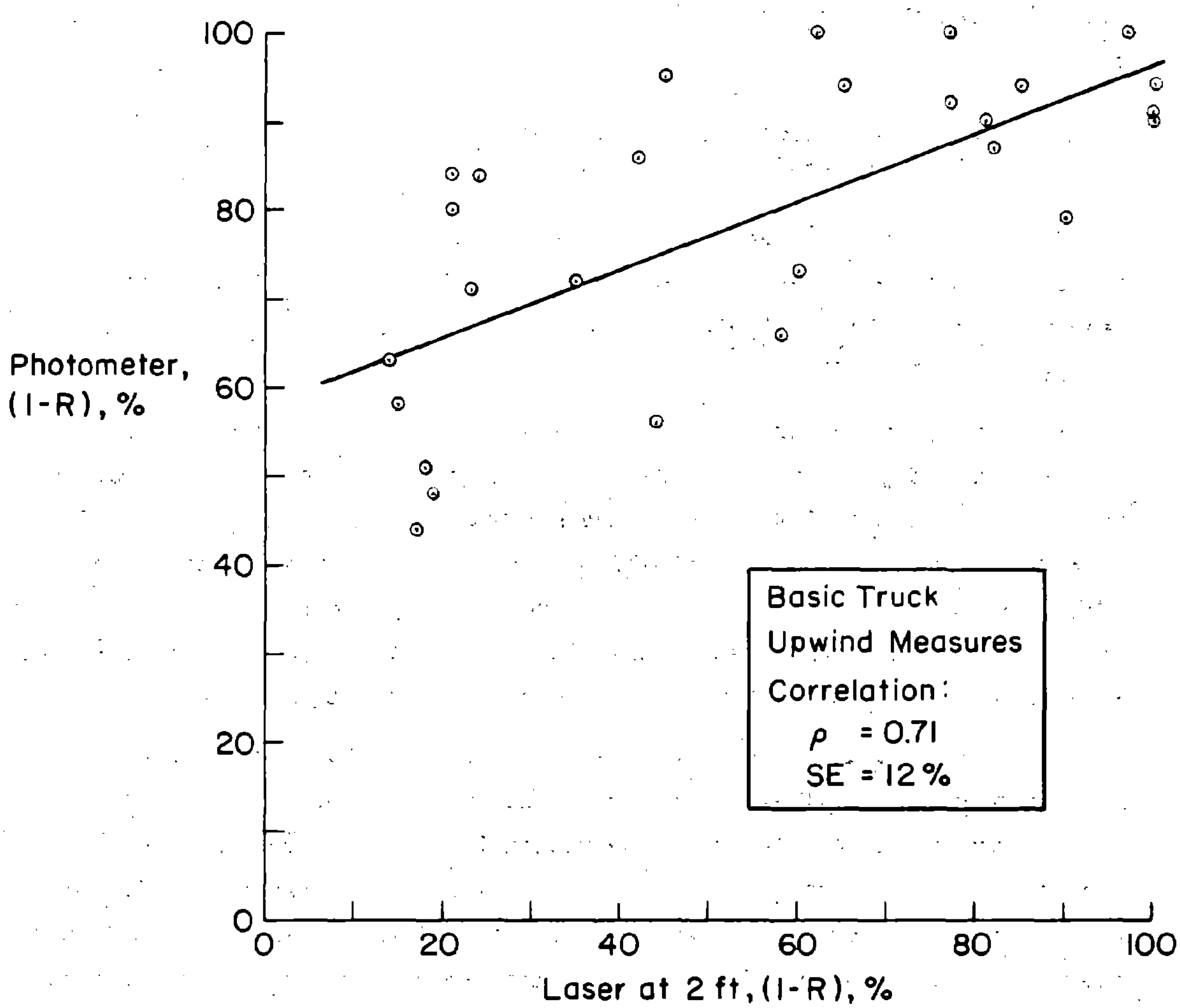

Figure 106. Correlation of Photometer and Laser Raw Data, Upwind

The main result of these figures is that there is a strong correlation in each case. So, given one set of measures and an elementary knowledge of the conditions, we can estimate what the other values would be. Hence, the laser and photometer results are interchangeable, and we can choose one to be a correlating "dependent" variable, based on other considerations. Possibilities for the latter include performance and ratings, as examined below.

2. Relation of Trackside Observer Ratings and Visibility Measures

During the June splash and spray tests, observers were stationed at each end of the wet test area ahead of and behind the trucks. They rated the reduction in visibility through the splash and spray clouds, using the rating form shown in Fig. 92.

These subjective visibility ratings have been plotted versus the quantitative visibility measures of the lasers and the photometer. Each rating was plotted individually against each measure for a given truck run. Of course, the raw (unscaled) visibility measures are used here, since we are interested in the actual conditions present on a given run. For each sensor, there are ratings from ahead (viewing the truck coming towards the observer) and behind (truck going away). The plots are given in Figs. 107-112.

All available data from the June tests were plotted, reflecting the ratings of several different observers and measures for all truck configurations and conditions tested. The visibility ratings were grouped into brackets of 10 percentage points of the visibility measure (e.g., 10 to 20 percent). The mean and standard deviation of the ratings in each grouping were calculated and plotted at the mid percentage point of the group. On the figures, the means have been connected by the solid lines, and the plus and minus one standard deviations are shown by the cross lines.

These plots relate the quantitative measures to the observers' feeling about their visual field of view impairment. In general, the mean visibility ratings are seen to become poorer as the measures of visibility reduce. The 2 ft laser results (Figs. 107 and 108) show, most clearly, a good monotonic variation in the ratings with visibility in the intermediate visibility range

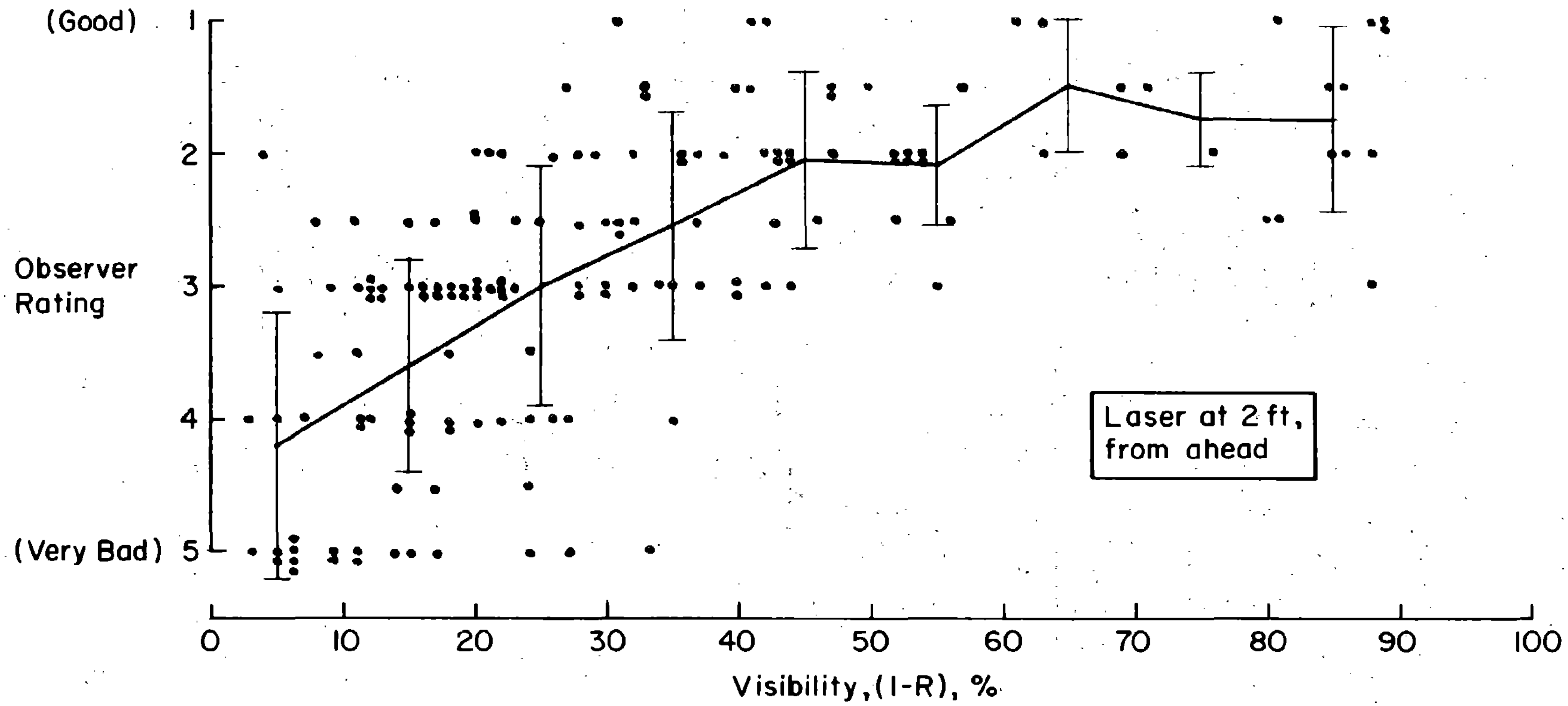

Figure 107. Correlation of Observer Rating from Ahead and Visibility, Laser at 2 ft

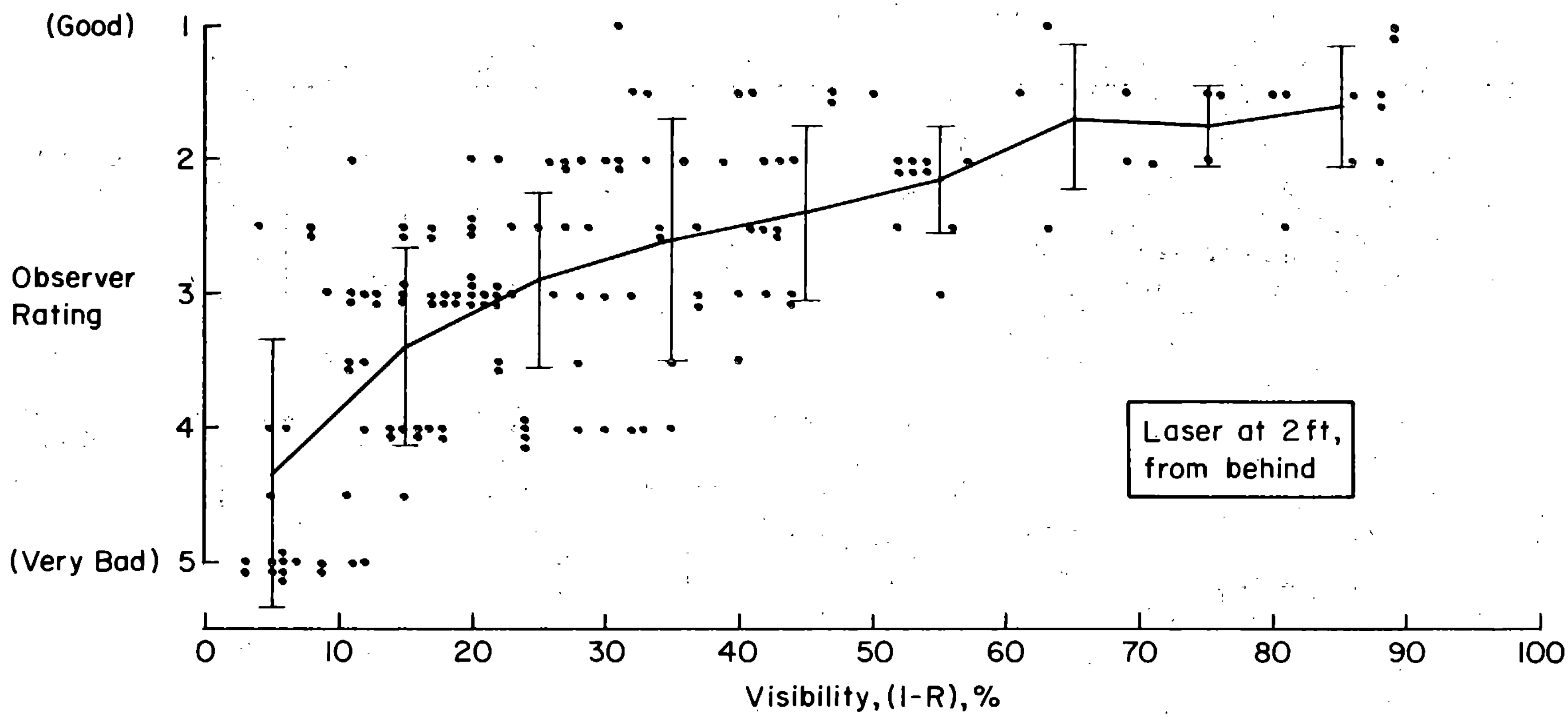

Figure 108. Correlation of Observer Rating from Behind and Visibility, Laser at 2 ft

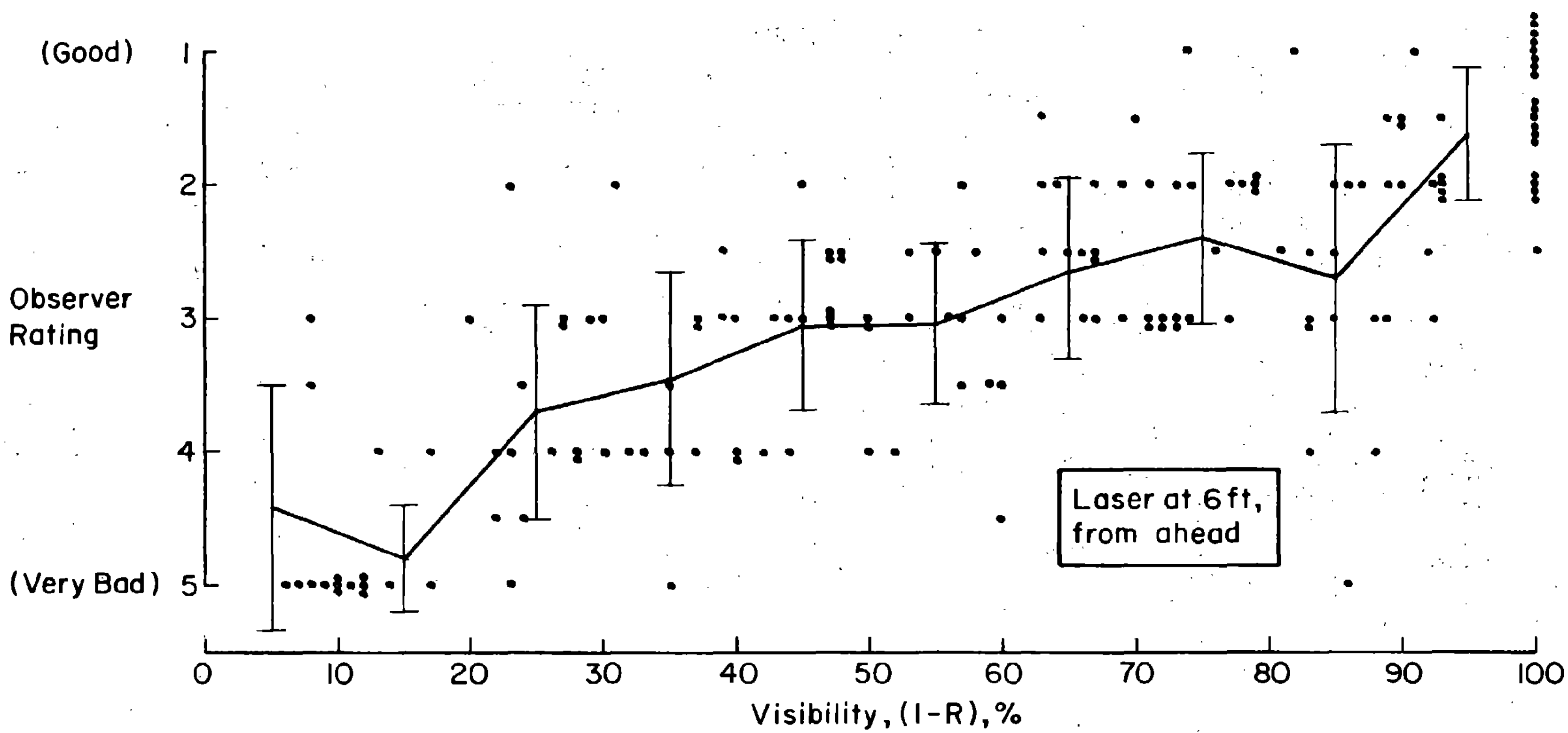

Figure 109. Correlation of Observer Rating from Ahead and Visibility, Laser at 6 ft

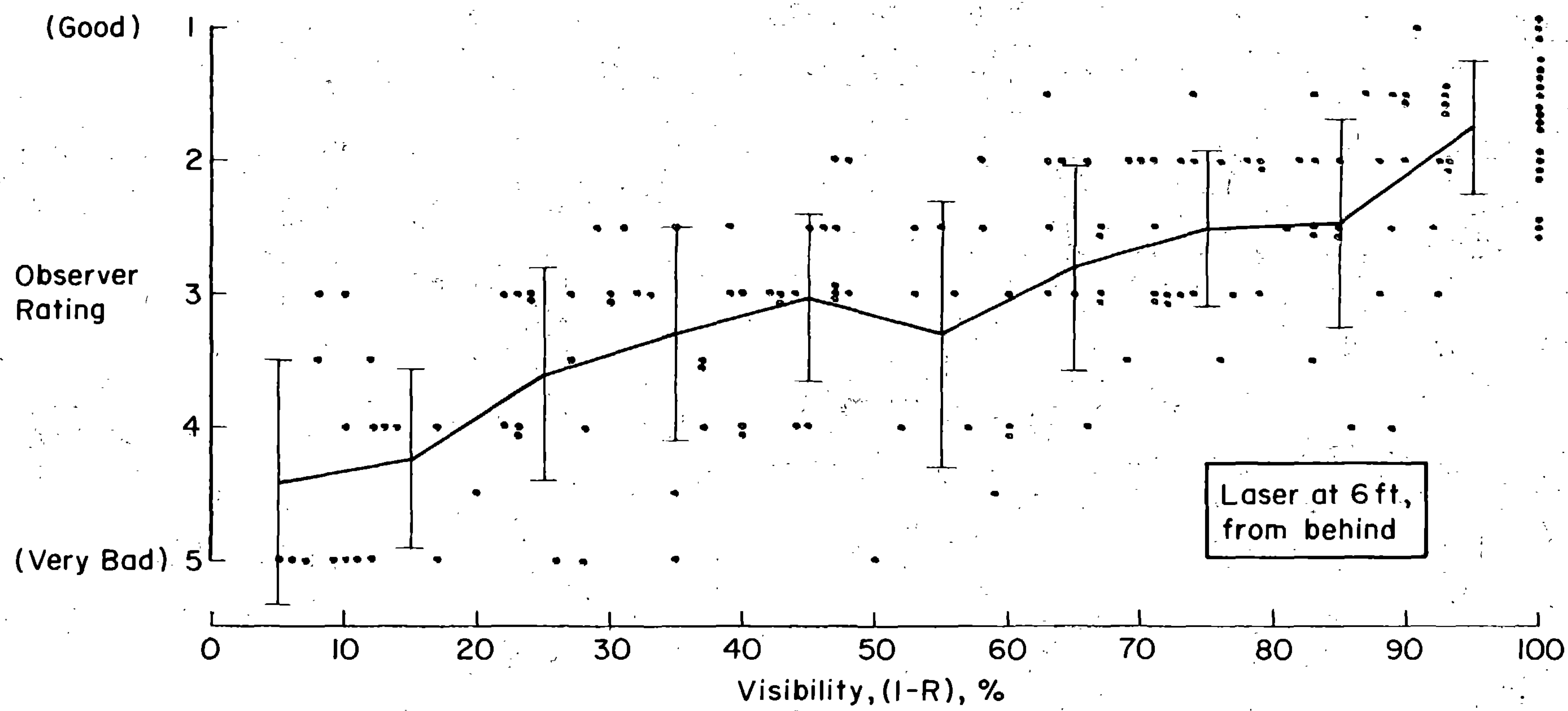

Figure 110. Correlation of Observer Rating from Behind and Visibility, Laser at 6 ft

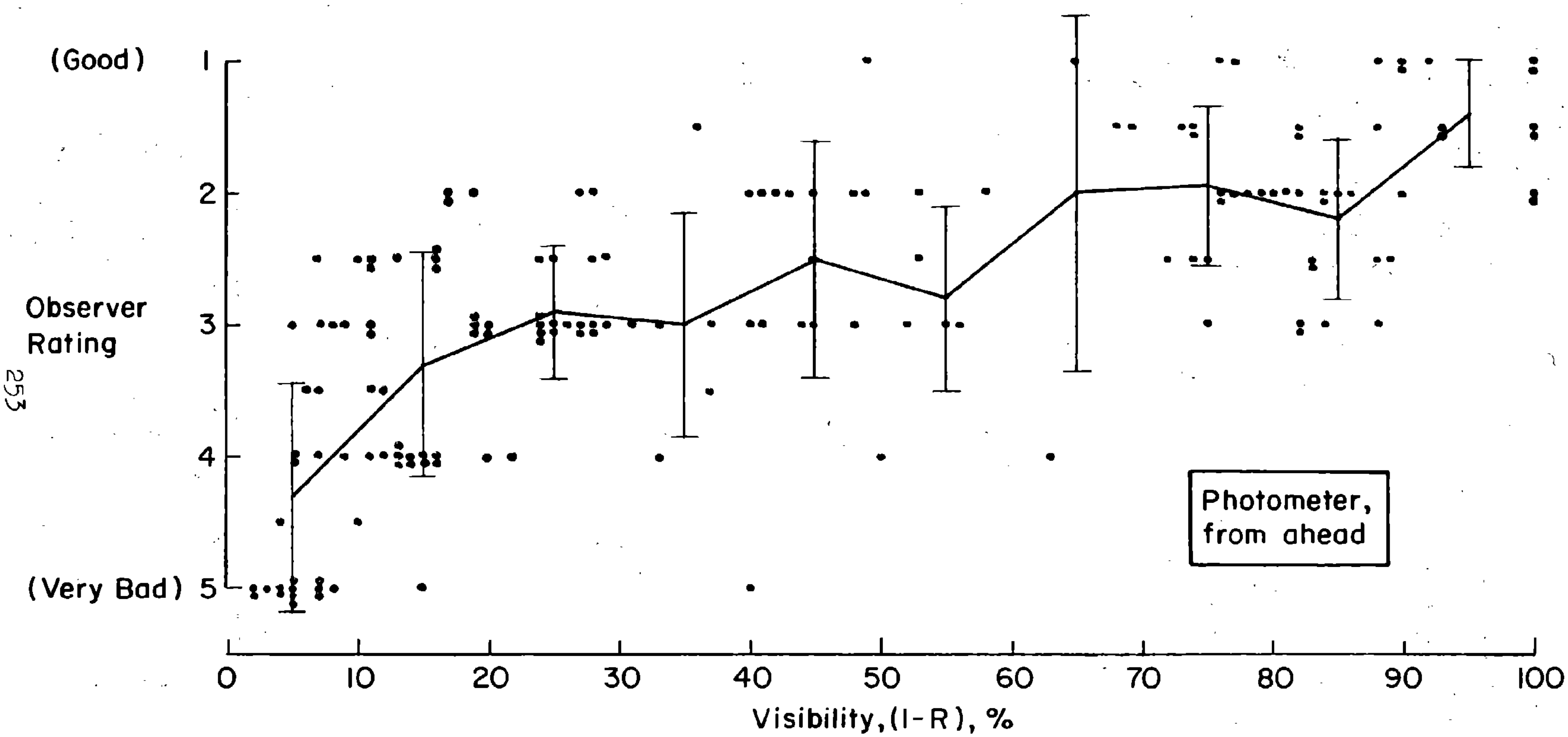

Figure 111. Correlation of Observer Rating from Ahead and Visibility, Photometer

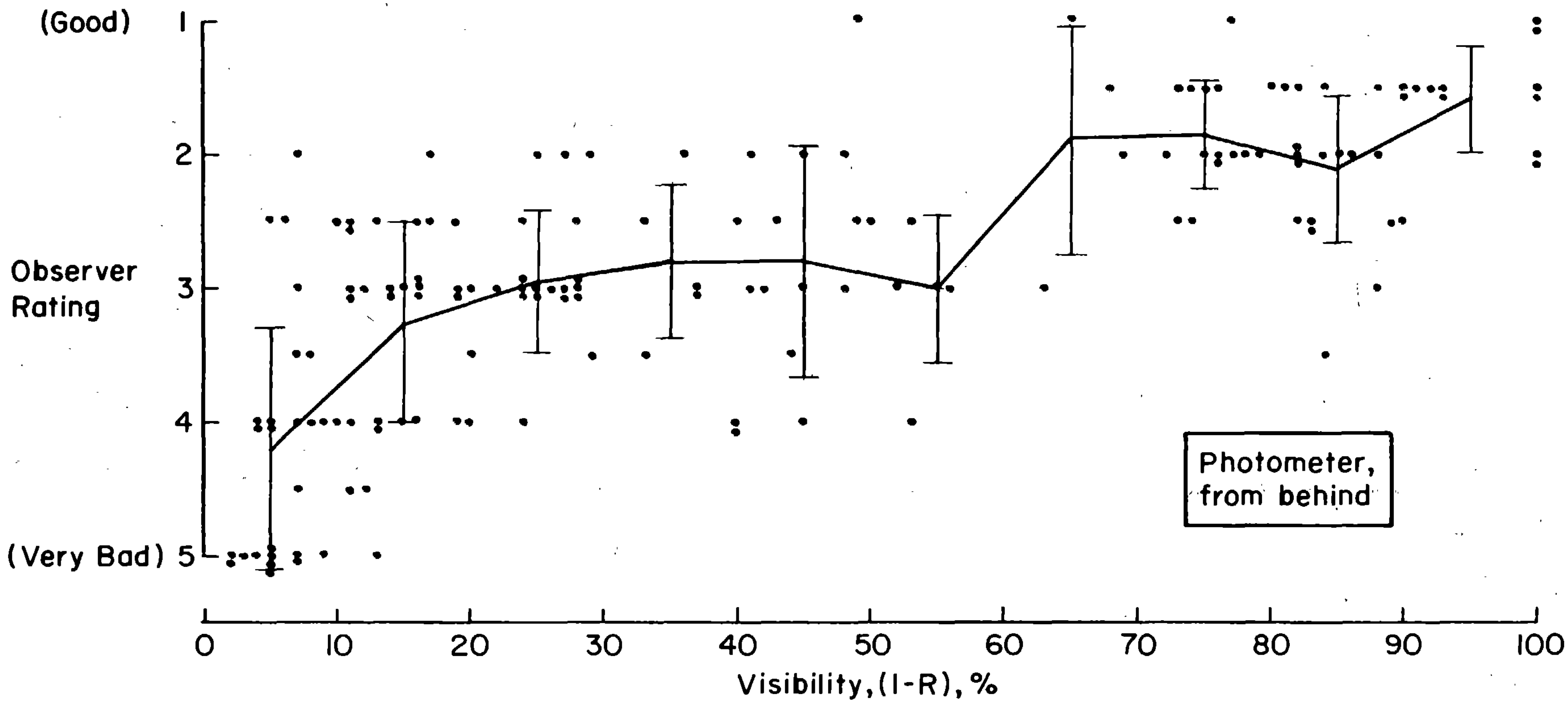

Figure 112. Correlation of Observer Rating from Behind and Visibility, Photometer

(i.e., 5 to 70 percent). The 6 ft laser and photometer correlations (Figs. 109-112) show less sensitivity of ratings to visibility over the intermediate range of most interest. These results suggest that the 2 ft laser is viewing that portion of the lane and the splash and spray cloud to which the observer is most sensitive, and that the 2 ft laser measures should correlate well with driver-perceived visibility properties, also.

In addition, Figs. 107-112 represent "calibrations" of the particular transmissivity measures against subjective visibility. So, given a visibility measure, they could be used to estimate the subjective reduction to be expected. Conversely, subjective measures could be converted to equivalent transmissometer values. For instance, this might allow results from prior studies, where only subjective data were obtained, to be connected to the objective data base derived in the current program.

3. Relations Between Driver Performance, Ratings, and Visibility

Task difficulty and accident risk ratings were obtained from the driver of the adjacent car, using the scales in Fig. 93. Lateral lane position performance measures of the adjacent car, in the vicinity of the truck, were also obtained. These are compared and correlated with the visibility measures, below.

The relation between driver task difficulty rating and visibility is shown in Fig. 113. Data for four driver subjects and a variety of truck configurations from the June tests are shown. The scaled visibility is used for correlation. Direct visibility measures were not made during the adjacent car tests, as noted before, so the visibility was determined given the ambient conditions, using the scaling procedure outlined in Article B.3, above. A clear relation is evident in Fig. 113, with the ratings degraded for values of visibility less than about 40-50 percent. The correlation coefficient was 0.64, based on a least squares fit, with a standard error of 0.9 rating points. Referring back to Figs. 107 and 108, a good similarity is seen to those trends in the trackside observer ratings with visibility (laser at 2 ft).

The relation between driver accident risk rating and visibility is shown in Fig. 114. Again, the data are for four subjects and a variety of June

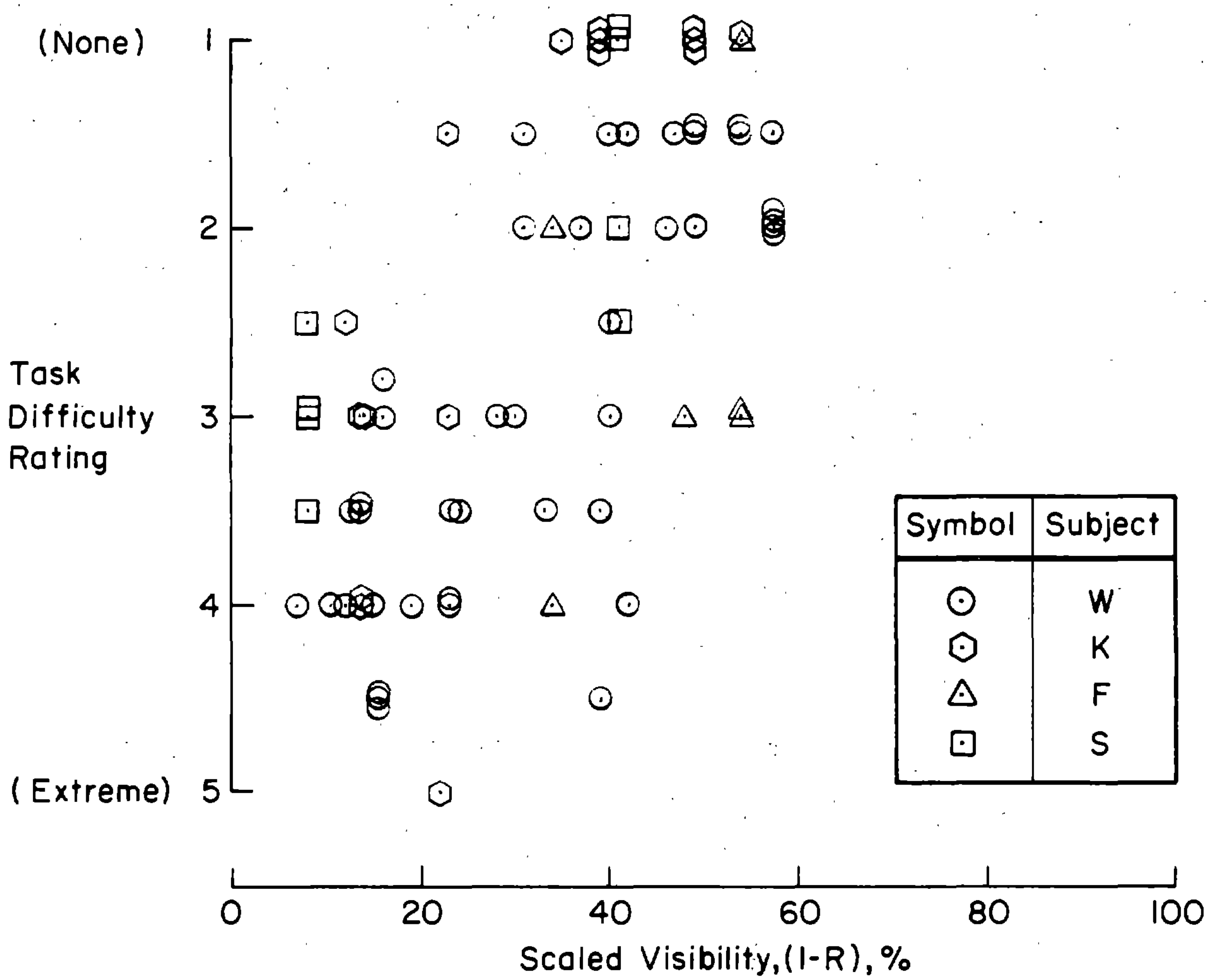

Figure 113. Relation Between Task Difficulty Rating and Visibility

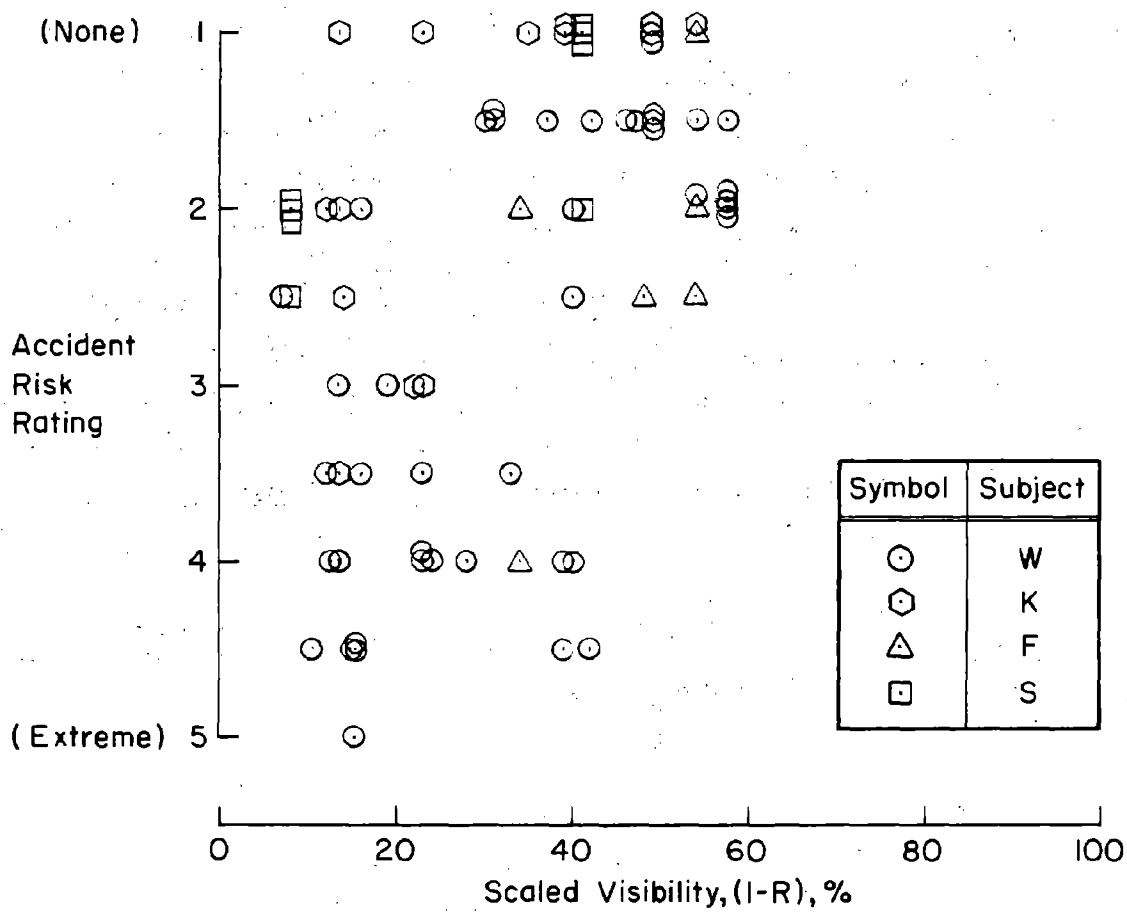

Figure 114. Relation Between Accident Risk Rating and Visibility

configurations. The scaled visibility is based on the ambient conditions. The results are similar to those in Fig. 113, with reduced visibilities associated with higher risk ratings. The correlation coefficient, for a least squares fit, was less at 0.46, however, and the standard error was 1.1 rating points, reflecting the larger amount of scatter.

Together, Figs. 113 and 114 show that the driver ratings are relatable to the 2 ft laser visibility values in a quantifiable way. Alternatively, given a visibility condition inferences can be made regarding the corresponding subjective assessment that would be expected.

The trajectory of the adjacent car in its lane during the splash and spray encounters was obtained from the roof-mounted camera. From these film data, the lateral position of the car in its lane could be obtained at intervals of about 0.7 sec, so that 10-15 samples were available during a pass through the wet test area. These data were only obtained on some runs, as can be seen in the summary data tables of the appendix. The data were lost when the camera system malfunctioned, or when the lens became too wet and dirty. Furthermore, the truck-passes-car data are not included because that scenario involves substantially different factors than the car-passes-truck case.

The adjacent car lane position measures were used to compute the mean square lane position, i.e.,

$$\overline{y_I^2} = \frac{1}{T} \int_0^T (y_I - \overline{y}_I)^2 \, dt \qquad (32)$$

where T is the duration of the data segment, and $\overline{y}_I$ is the mean lateral lane position of the car over the run. Larger values of this measure mean more variation of the car path about a straight line, and poorer performance. The variation of $\overline{y_I^2}$ with scaled visibility for 3 driver Ss is shown in Fig. 115. The data show a definite trend toward improved performance for increased visibility, as indicated by the faired line. This fairing also indicates that the driver is able to maintain performance fairly constant down to a certain level of visibility (about 30-40 percent) and beyond that performance begins to degrade markedly. The data show a little scatter, and

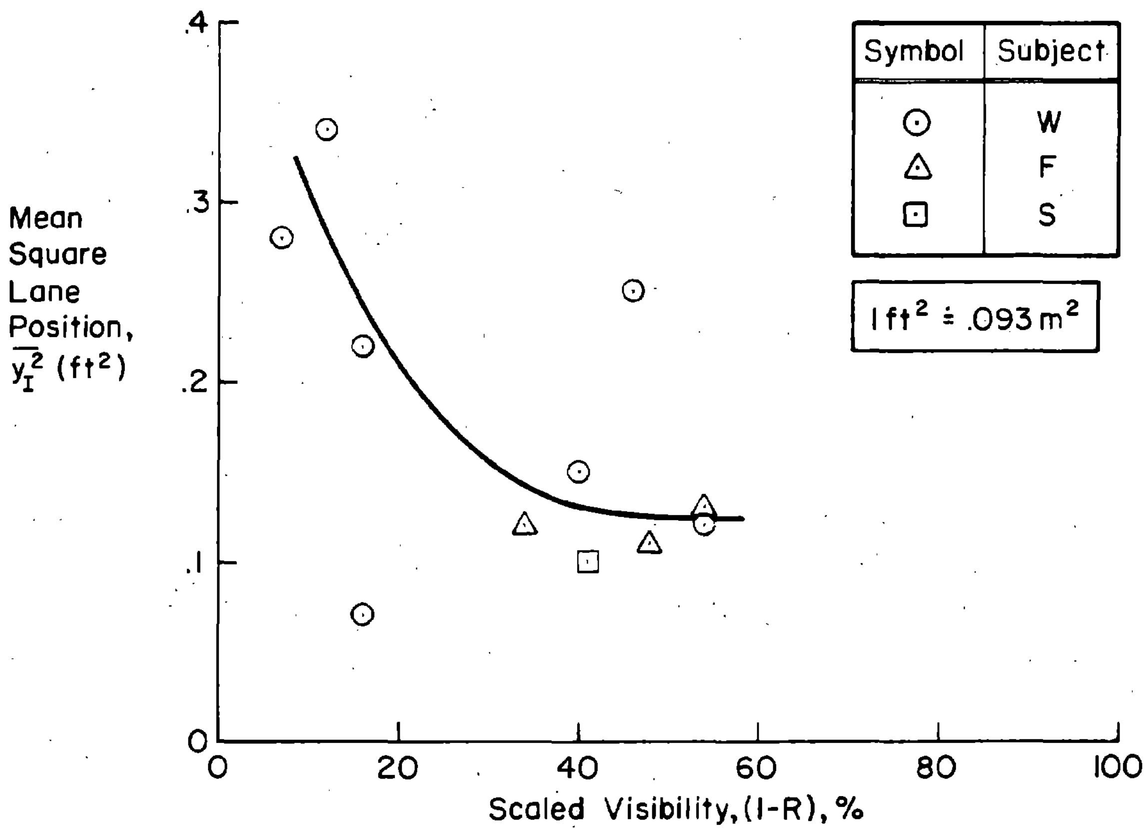

Figure 115. Relation Between Path Performance and Visibility

some of this scatter may be due to the added aerodynamic disturbance from the truck, which can vary with configuration and crosswind conditions (see Section V). For instance, the data point at $\overline{y_I^2} = 0.07$ and V = 18 is for the liquid cargo tanker, which has a smaller aerodynamic disturbance effect than the other rigs (there are no flatbed data in Fig. 115. Nevertheless these data demonstrate that car/driver performance and visibility are related, and that the latter can be used as surrogate for the former in assessing the effect of changing truck configuration or incorporating devices to alleviate splash and spray. Plots of peak lane position deviation vs. visibility, not included here, showed similar results.

Both driver ratings and car/driver performance have been shown to vary systematically with visibility. Of potential interest is the way that rating and performance covary, and this is given in Figs. 116 and 117. These plots combine the data from Fig. 115 with the respective points in Figs. 113 and 114. Where Figs. 113 and 114 suggest a linear trend (scatter aside) between ratings and visibility, the relation in Fig. 115 shows the noted knee in the curve. Their combined effect does not produce any particular trends in either Fig. 116 or 117. Each show some scatter, with a not unexpected overall degradation in rating with degradation in performance.

The fact that performance and rating each vary with visibility, yet do not covary, suggests that their respective variations with visibility relate to different factors or elements in the overall situation. This tends to support the conclusion that visibility values are the pertinent objective figure of merit, as described previously.

D. VISIBILITY VALUES FOR VARIOUS TRUCK CONFIGURATIONS

Results from the June tests can be used to show differences in adjacent car visibility due to changes in truck configuration. This includes the two tractor types (COE and CBE) and four semitrailer types (van, flatbed, liquid cargo tanker, and dry cargo tanker).

This comparison is made for a truck speed of 60 mph (27 m/s). It is a worst case in the sense of being a higher speed, it accentuates the display of differences, and it provides an important connection with the November tests which were all run at this speed.

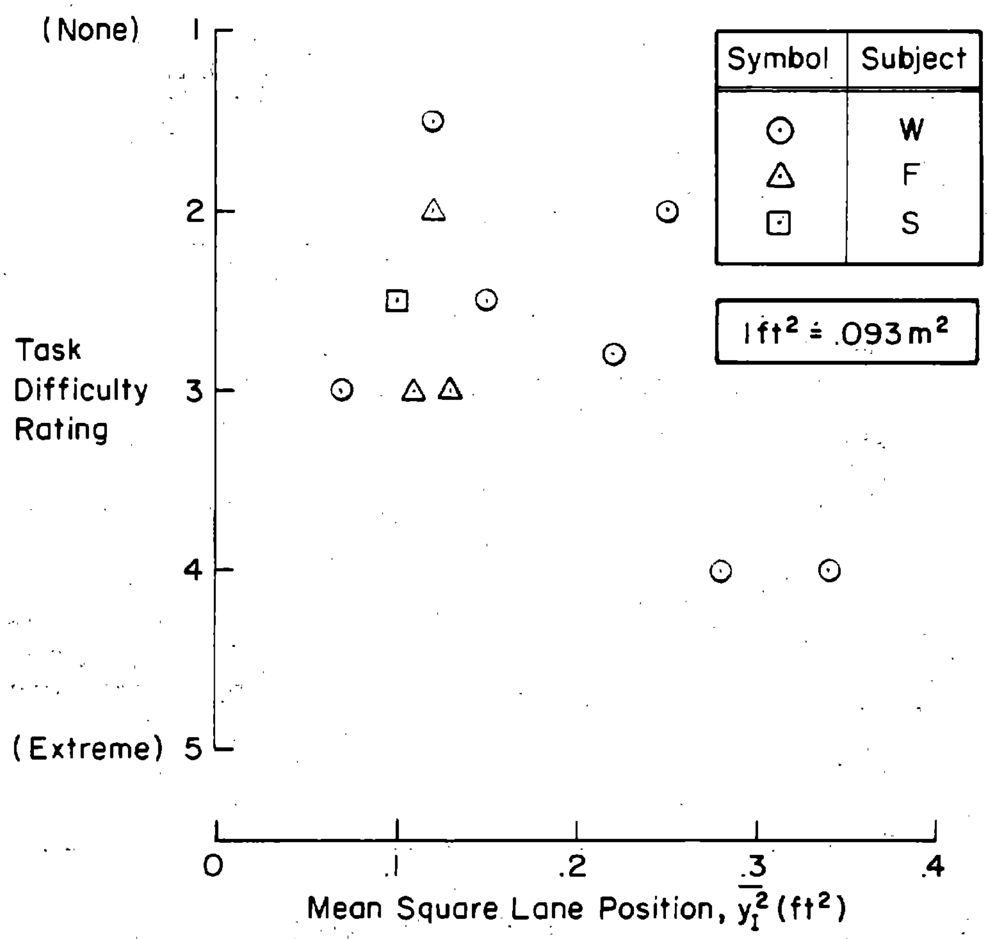

Figure 116. Relation Between Task Difficulty Rating and Path Performance

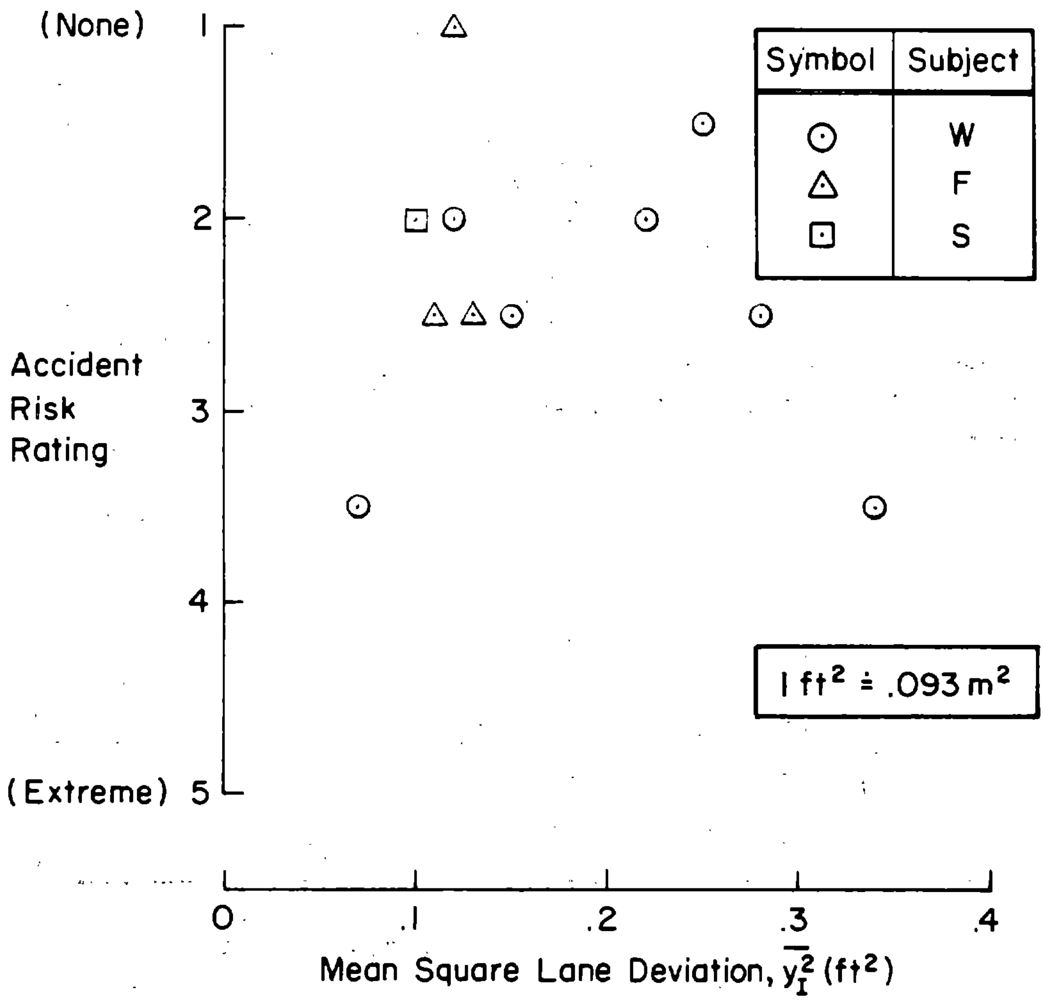

Figure 117. Relation Between Accident Risk Rating and Path Performance

The visibility measure used is the laser at 2 ft, based on the previous discussion. Raw data measures are shown for downwind conditions, as well as scaled values using the procedures presented in Article B, above.

Most of the test runs in June were made with the trucks empty. One exception was the COE plus 40 ft van basic configuration, which was always run with either 20 or 38 thousand lb (9100 or 17,300 kg) loads. This basic configuration was run empty in November. The other exception in June involved occasional loaded runs with the liquid cargo tanker. Also, as described in Article B, above, there were minor differences in gap length and other details between the June and November basic truck configurations.

Raw visibility measures for the several semitrailer types with the COE tractors are shown in Fig. 118, taken from the detailed data in the appendix. Note that the 27 ft vans were pulled by the 2 axle COE tractor. As noted, these data points are all for (sensor) downwind conditions, to make them comparable, and to enhance the subsequent comparison with the scaled values which correspond to that condition, also. The level of scatter inherent in the repeat measures for a given truck is evident. The bars shown are simply the means of the points plotted. The basic configuration is seen to cause the worst visibility conditions, though the others are not much better in most cases. The low values shown for the 40 ft van may be due partly to the fact that it had the 17,300 kg load for the points shown (see Fig. 96 for trends in visibility due to load).

A similar raw visibility data comparison over semitrailer types with the 3 axle CBE tractor is shown in Fig. 119. Here, the 40 ft van was empty, as were the other semitrailers. Again the visibility with the 40 ft van is worse than the others, although the difference is probably not significant considering the spread of the data. Differences due to the COE vs. CBE tractor can be seen by comparing Figs. 118 and 119. These raw downwind measures show that the respective visibility is reduced with the COE for each semitrailer type.

The raw data in Figs. 118 and 119 are taken directly from the data sheets and summary tables in the appendix. The other raw numbers in that appendix show the effects of variations in ambient wind, truck speed, and truck lane position for a given truck configuration. The effects of ambient

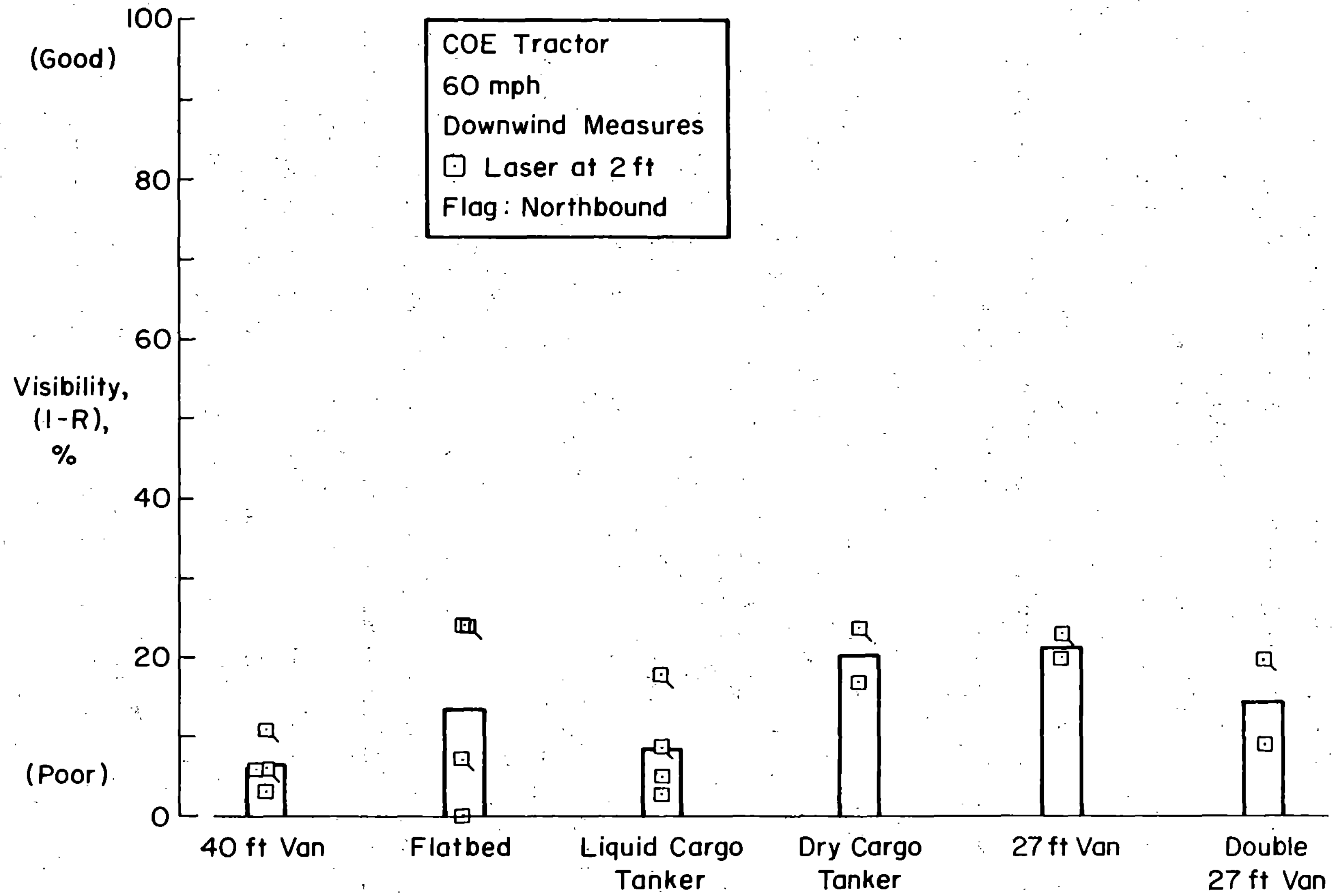

Figure 118. Effect of Semitrailer Type on Raw Visibility Measures, COE, 1 mph = 1.6 km/h, 1 ft = 0.3048 m

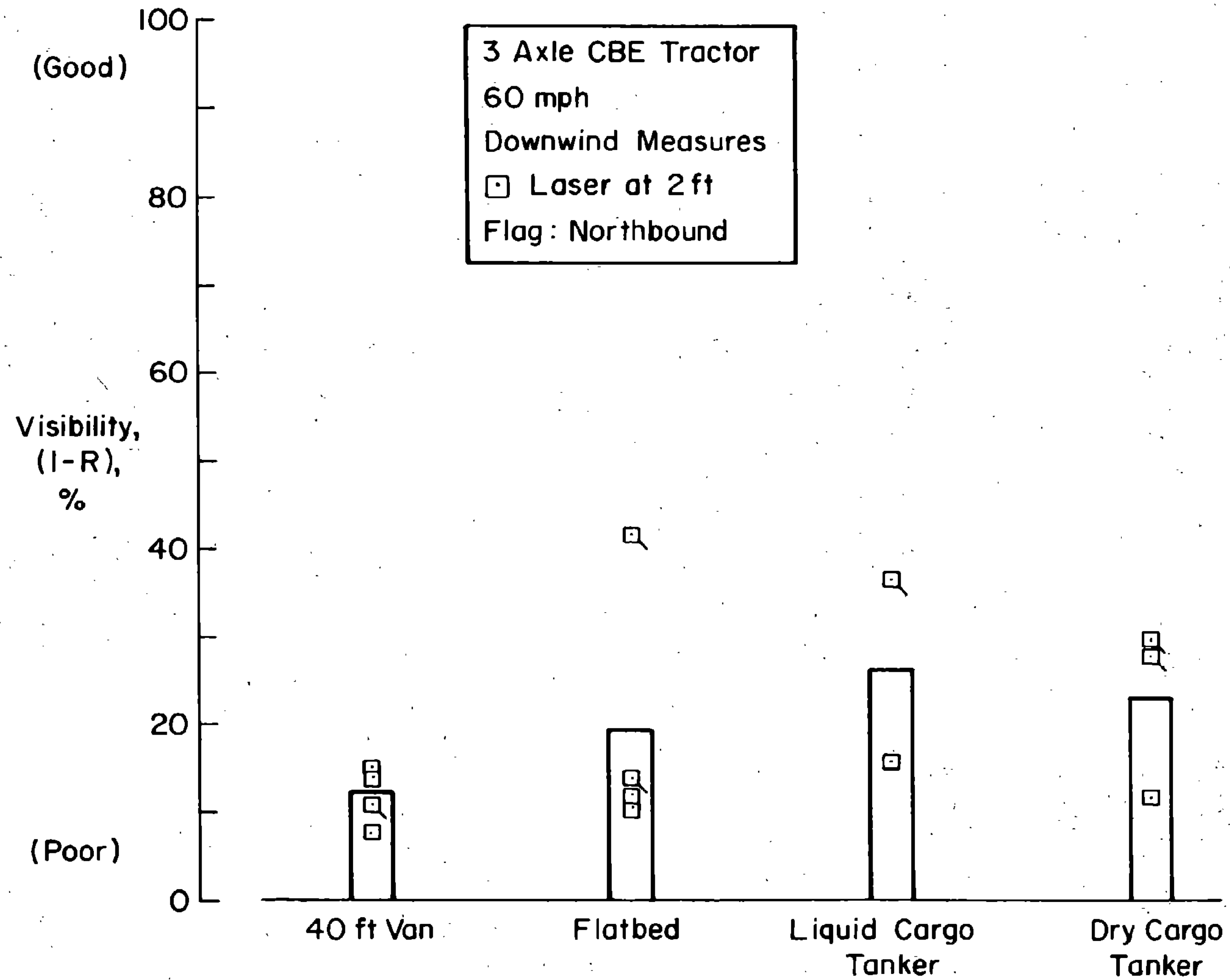

Figure 119. Effect of Semitrailer Type on Raw Visibility Measures, CBE, 1 mph = 1.6 km/h, 1 ft = 0.3048 m

wind and lane position can be accounted for using the scaling procedures of Article B, above, so that more data points can be included in the comparisons. The results are shown below. Recall that the scaled reference condition is for a 5 mph ambient wind from 45 deg, and a truck lane position giving less than 3.5 ft (1.1 m) from the truck edge to the road centerline.

Comparison of the scaled visibility values over the various semitrailers with the COE-type tractor is shown in Fig. 120. Again, the bars denote the mean of the points shown. Nearly all the pertinent points from the June tests have been included. An occasional point has been deleted, where the scaling procedure resulted in a large change which seemed unreasonable and inconsistent with the other points for that configuration. As a consequence, the scaling procedure is conservative, and some of the data points were unchanged from their raw values. Again, the 40 ft van results may reflect some influence of load, while the other rigs were run empty.

The scaled values in Fig. 120 show that the several trucks create similar visibility levels in the adjacent lane, on the average. Considering that downwind, upwind, headwind, etc., points are all combined here, it is evident that (as intended) the scaling has reduced the normalized variability a substantial amount. The resulting spread is on the order of the nominally homogeneous raw downwind measures, as shown in Fig. 118.

Comparison over semitrailer types with the CBE tractor is shown by the scaled visibility values in Fig. 121. As with the COE, the results indicate little difference over configuration, on the whole. In addition, there is less effect due to tractor type, between Figs. 120 and 121, with the exception of the CBE plus 40 ft van which shows lower values than the other rigs.

Overall, the differences between trucks seen in Figs. 120 and 121 are on the order of ±5 visibility percentage points. This seems to represent the order of resolution and accuracy that can be obtained in these measures. At that level, there are not substantial differences across the truck types studied in their current configurations. As will be shown in Article E, below, the improvement in visibility that can be achieved with splash and spray and aerodynamic devices substantially exceeds the level of resolution and accuracy displayed in Figs. 118-121.

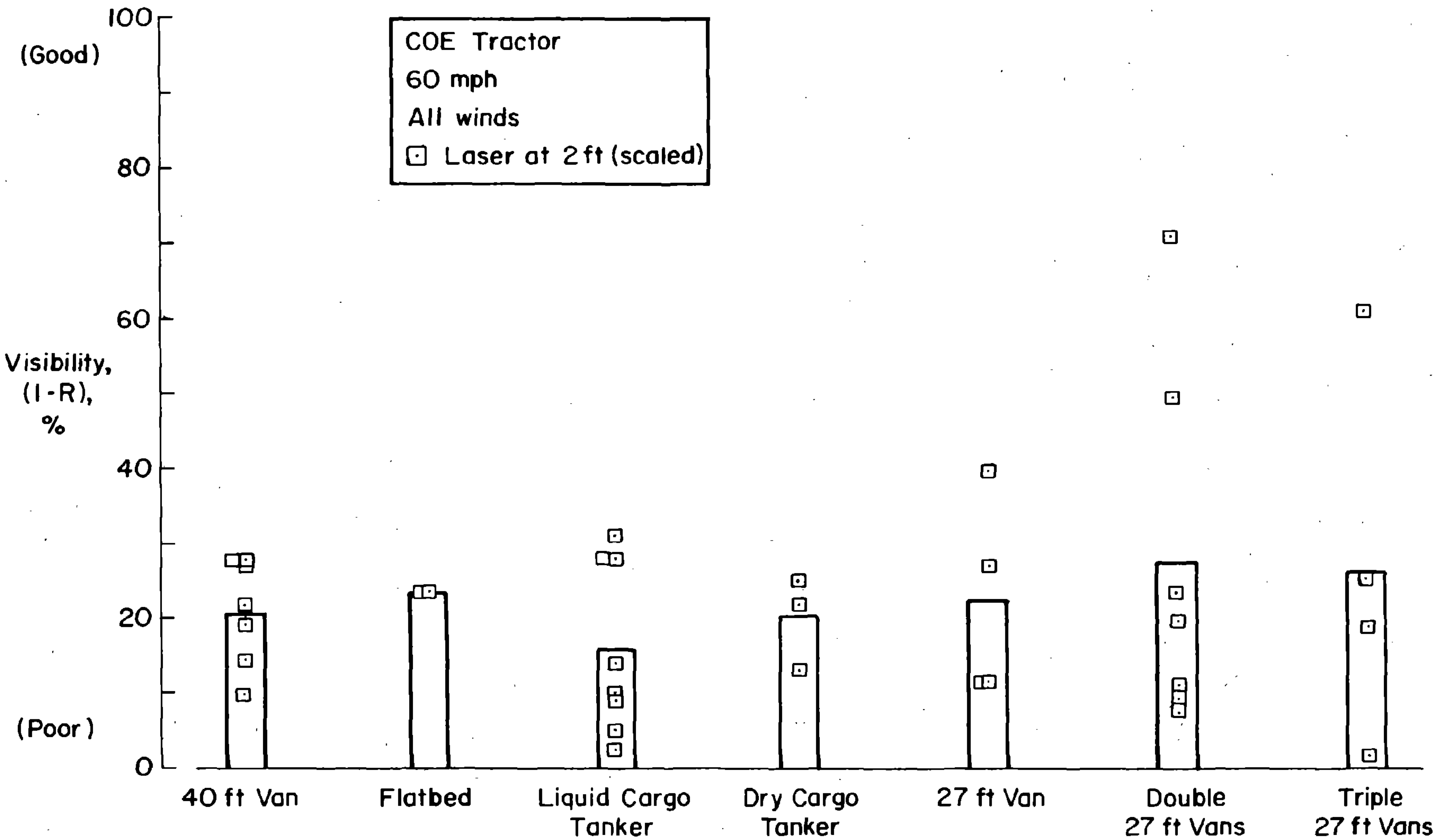

Figure 120. Effect of Semitrailer Type on Scaled Visibility Values, COE, 1 mph = 1.6 km/h, 1 ft = 0.3048 m

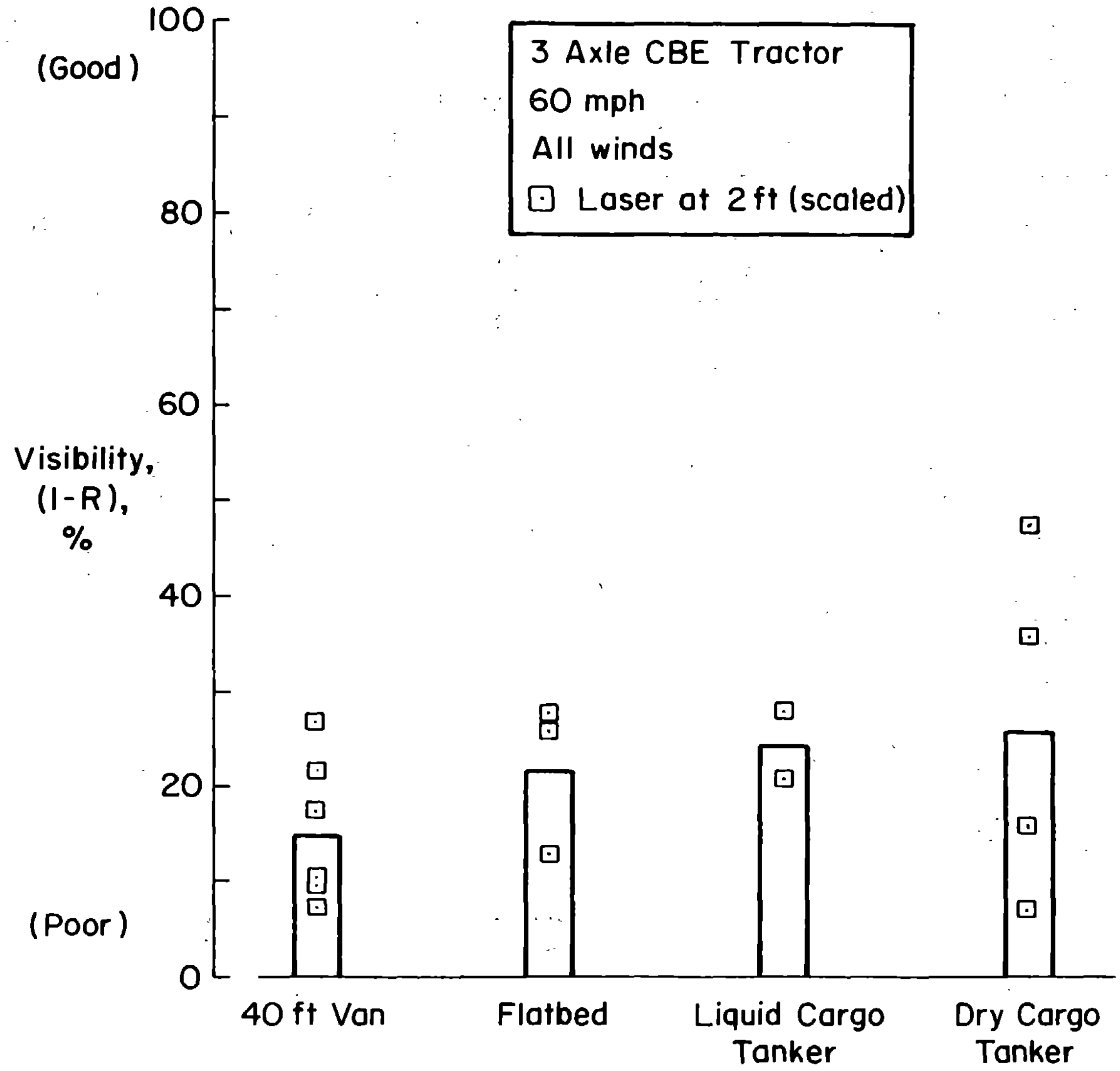

Figure 121. Effects of Semitrailer Type on Scaled Visibility Values, CBE, 1 mph = 1.6 km/h, 1 ft = 0.3048 m

The means of the raw data and scale visibility values shown in Figs. 118 to 121 for the various truck configurations are summarized in Table 13. As described above, these visibility measures are for the laser at 2 ft and truck speed of 60 mph (27 m/s), and they are for the June data. The raw data are for downwind conditions (see Figs. 118 and 119), while the scaled values are for the reference conditions defined in Article VI.B, above. A raw data value is not shown for the triple 27 ft van, because it was not tested under "downwind" conditions. As discussed above, the scaled visibility values show little difference over truck configurations, on the whole. Values for the 40 ft van rigs are lower, and this probably reflects an adverse influence due to the size and shape of the semitrailer, compared to the other types tested.

TABLE 13

SUMMARY OF VISIBILITY VALUES FOR VARIOUS TRUCK CONFIGURATIONS, (1 – R), %

CONFIGURATION	RAW DATA[a]	SCALED VALUES
3 axle COE + 40 ft van	7	21
3 axle COE + flatbed	14	24
3 axle COE + liquid cargo tanker	9	16
3 axle COE + dry cargo tanker	21	21
2 axle COE + 27 ft van	21	23
2 axle COE + double 27 ft vans	15	28
2 axle COE + triple 27 ft vans	—	27
3 axle CBE + 40 ft van	12	15
3 axle CBE + flatbed	19	22
3 axle CBE + liquid cargo tanker	26	25
3 axle CBE + dry cargo tanker	23	27

[a]Downwind measures only.

As shown in the next article, the visibility values obtained for the 40 ft van (basic configuration) were somewhat higher (i.e., 28 percent on the average vs. 21 percent for the COE plus 40 ft van in June). This probably reflects some combination of the differences in configuration previously noted, i.e., 1 ft (0.3 m) longer gap, lack of tractor tandem mud flaps, and semitrailer load in June. It may also be a result of differing ambient conditions in November, where the temperature was cooler, the relative humidity was higher, and the ambient winds were generally less strong (when they blew) than was the case in June. Nevertheless, this June-November difference is still small by comparison with the device effects discussed next.

E. THE EFFECT OF ALLEVIATION DEVICES ON VISIBILITY

The November 1977 splash and spray tests studied aerodynamic and collector devices designed to reduce the effects of splash and spray as they influence the visibility of an adjacent driver. Four nearly identical trucks were used in the November tests, and they were all the basic configuration (3 axle COE plus 40 ft van). This permitted some trucks to be outfitted with devices, while one truck remained unmodified for back to back comparisons on a given run (see test procedures in Article A, above). The speed used was 60 mph (97 km/h). The visibility comparisons have been done with the 2 ft laser values, scaled according to the procedure described in Article B, above. The trucks were empty.

The test procedure used in November was carefully planned to quantify the effect of a given device on spray-related visibility. Two trucks were running on the track at the same time, approximately a minute apart. The lead truck was fitted with a device or set of devices, and the following truck was the unmodified base case. The wetting and ambient conditions had ample time to return to steady state before passage of the second truck. As a result of this procedure, the ambient conditions were nearly identical for the two trucks, and the differences in their visibility values reflect only the effect of the devices to a high degree. Typically, four successive passes were made with the two trucks. As this set of four runs was accomplished in a period of a few minutes, the ambient conditions did not change much over the set. As a result, and because an occasional data point is missing, the visibility differences were computed over the set of four runs, not as paired comparisons from a given pass. Note that there would be no difference algebraically, if the data set were complete. Since conditions did vary from device to device (i.e., between sets of runs) and from day to day, the basic and device truck values were scaled (as with the truck configurations in Article D) so that comparisons could be made across devices under the same ambient conditions.

The devices tested are described in Section IV, where they are listed in Table 3 on page 122, in summary form.

As with the truck configuration results in Article D, it is instructive to look at the raw data for downwind conditions, as well as the scaled results. This is done below.

1. Raw Data for Downwind Conditions

Examples of the applicable raw data for downwind measures are shown for some of the devices in Figs. 122 to 124. In each figure there are several pairs of bar charts and associated data, one for the truck with the device and the other for the basic truck in the same set of runs. Results for five of the Reddaway fender configurations are shown in Fig. 122. The scatter in the raw data, as well as the marked differences in the means for most of these conditions, is evident. There are no basic truck values shown with Configuration MO, because some of the ambient wind measures were lost and some of the 2 ft laser data for the basic truck were not good. Yet the ambient conditions were steady that morning and the basic truck data for other run sets (e.g., M1) give the needed reference. Note that the average of the visibility values for the basic truck points shown in Fig. 122 (under downwind conditions in November) is about 28 percent. This is somewhat higher than the basic truck raw data values from June, as discussed in Article D.

Raw downwind measures for the angled side vanes are compared with each other, and corresponding basic truck values, in Fig. 123. The raw data suggest that Configuration V1 with all the vanes is actually worse than the basic truck, while the ones with the drag shield and without the vanes behind the tractor tandems show some improvement. Again, the scatter shown

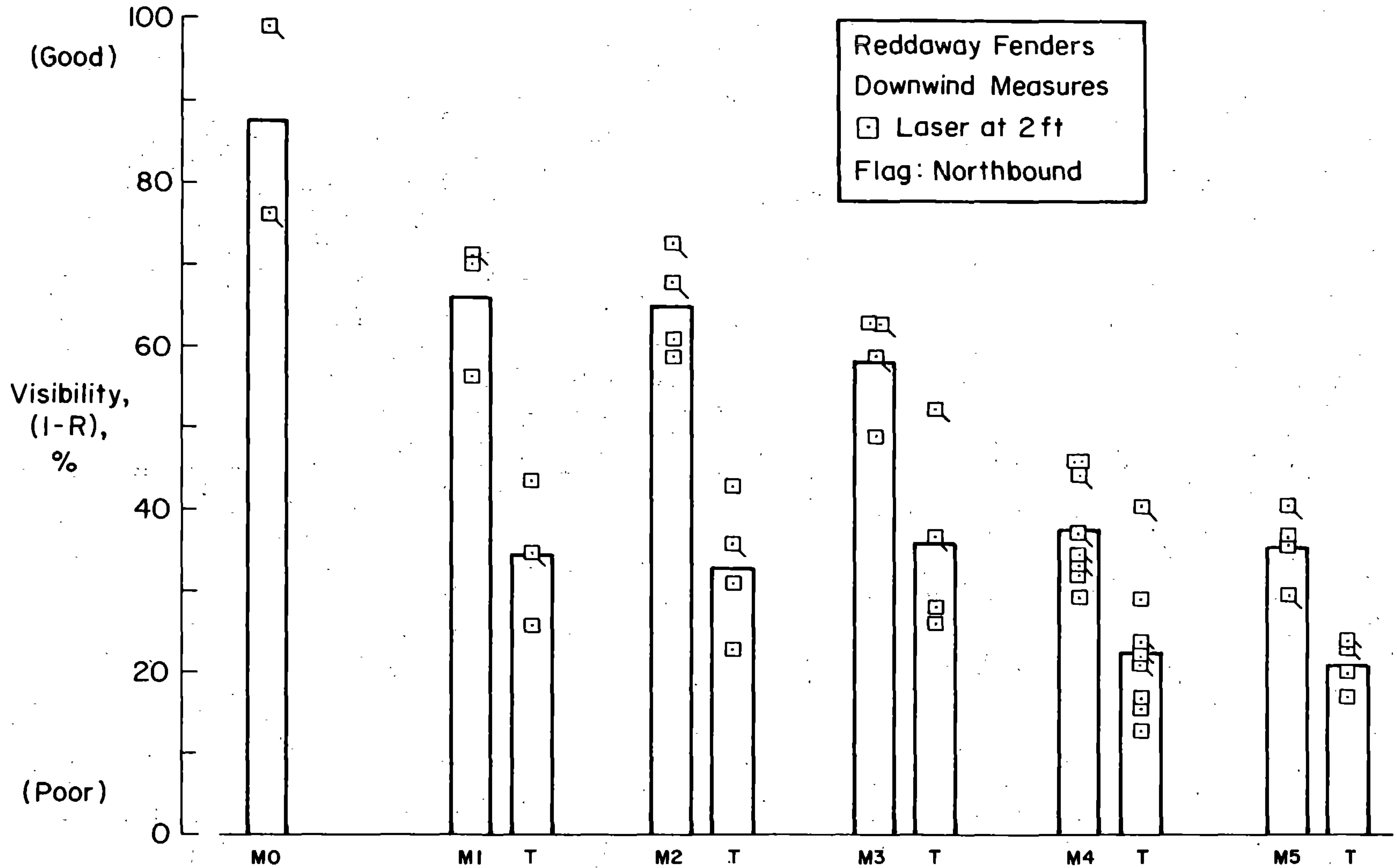

Figure 122. Comparison of Raw Visibility Measures for Reddaway Fenders and Basic Truck

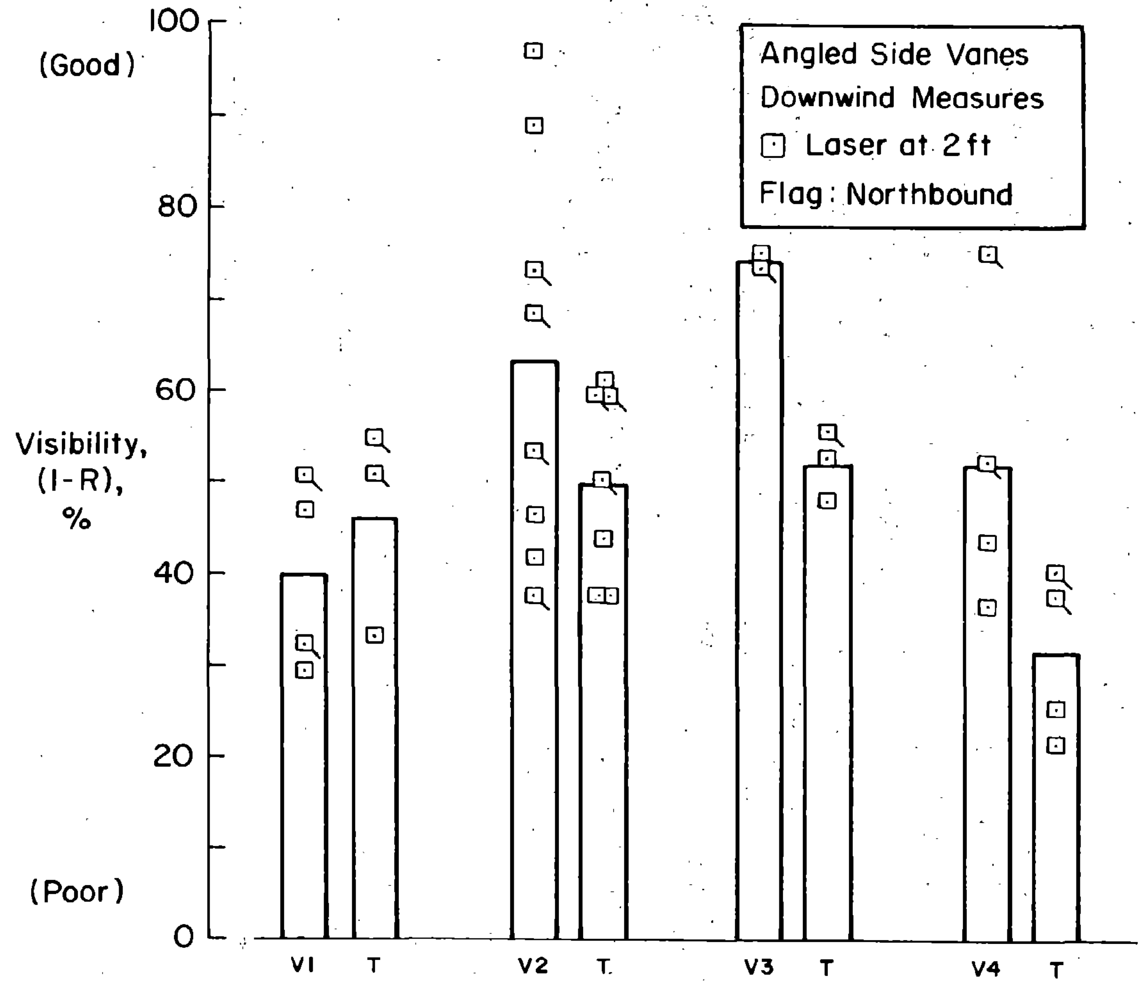

Figure 123. Comparison of Raw Visibility Measures for Angled Side Vanes and Basic Truck

is due in part to variations in ambient wind conditions and truck position, which are normalized in the scaled values to be presented shortly.

Comparison of the raw data measures for the gap filler panel configurations G1 and G2 (top and bottom positions) is shown in Fig. 124. Here, the ambient conditions were such that the basic truck visibility values were relatively high, yet the presence of the gap filler panel still shows some improvement.

These raw data visibility measures are summarized in Table 14, for those cases where pertinent downwind measures were available. The values shown by the bars in Figs. 122-124 are included, and the additional numbers come from the detailed results in Appendix B. Also shown in Table 14 are the corresponding raw "visibility margins," which are the differences between the visibility measures for the device truck and the basic truck in a given set of runs. The Roberts fender data are mixed, with R2 (with the drag shield) being worse than the basic truck. Detailed examination of the film data and the other visibility measures (laser at 6 ft and photometer) lead us to conclude that the raw R2 measures shown here were anomalous, and analysis indicates that the splash and spray suppression properties of a Roberts fender should be largely unaffected by the presence of the drag shield, and that the visibility margin for R2 should be approximately that of R1. Similarly, we would not expect the drag shield to give a large incremental spray suppression benefit to the European fender, since it too can have a forward component (such as a quarter fender) which tends to cover the front of the tractor tandem duals and foil the air moving down in the gap behind the cab.

Some of the raw measures for the partial gap panels (P1 and P2) were worse than with no panel, also. The fuzzy truck (F1 and F2) showed some improvement. Two other types of devices tested, European fender and longitudinal baffle, are not shown in Table 14, because raw data for downwind conditions were not available. Values for these devices are included in the scaled results presented below.

Some "hybrid" devices are also included in the scaled results. These are composites of devices which were not tested, such as L4, the longitudinal baffle plus drag shield, but which the data suggested would be effective. Visibility values for such combinations were estimated using differential effects present in the composite data.

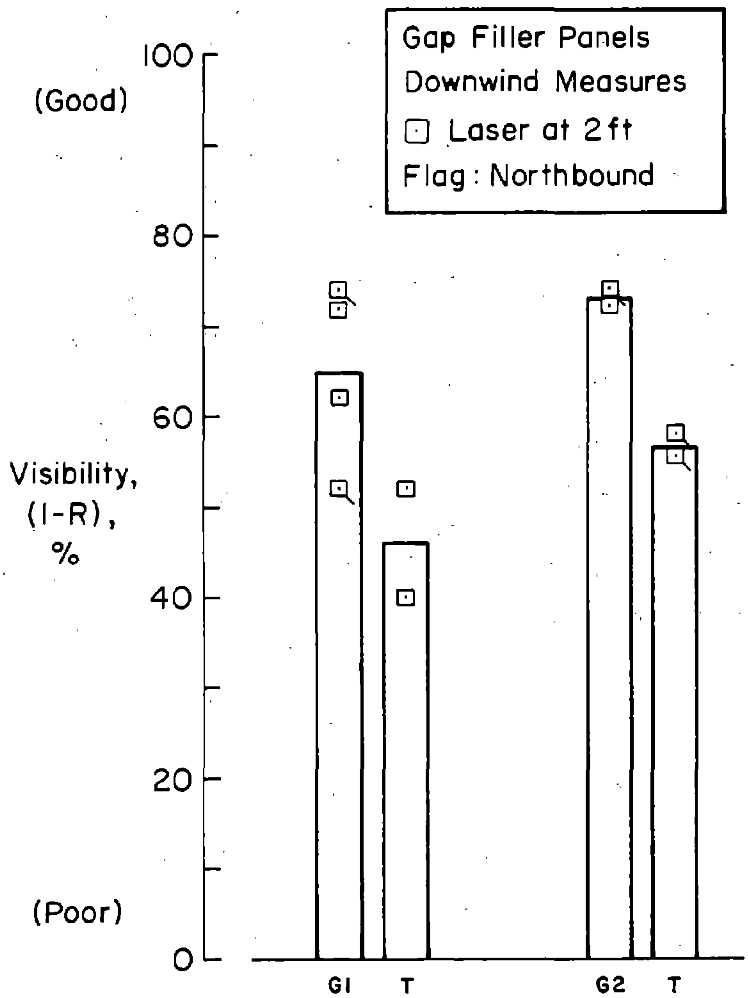

Figure 124. Comparison of Raw Visibility Measures for the Gap Filler Panels and Basic Truck

TABLE 14

SUMMARY OF RAW VISIBILITY MEASURES FOR VARIOUS DEVICES, DOWNWIND CONDITIONS, LASER AT 2 FT

DEVICE	DESCRIPTION	VISIBILITY MEASURE, %	VISIBILITY MARGIN, %
M0	Reddaway system + drag shield	88	NA[a]
M1	Reddaway system	67	32
M2	Like M1, less flaps between the tandems	65	32
M3	Like M1, grass forward only	59	23
M4	Like M2, less side flaps	38	15
M5	Like M4, less rear flaps on tractor	36	15
R1	Roberts fender	49	13
R2	Roberts fender + drag shield	39	− 9
P1	Partial gap panel	34	−16
P2	Partial gap panel + straight end plates	38	− 4
P3	Partial gap panel + angled end plates	78	11
V1	Angled side vanes (basic layout)	40	− 7
V2	Like V1 + drag shield	64	14
V3	Like V2, less vanes behind tractor tandems	75	23
V4	Like V3, less tank vanes and with trailer vane angles reset	53	21
F1	Fuzzy truck	71	7
F2	Fuzzy truck + drag shield	33	4
G1	Gap filler panel in upper position	65	19
G2	Gap filler panel in lower position	73	17

[a]Basic truck comparison not available, downwind.

2. Scaled Results

Examples of the scaled results for several types of devices are shown in Figs. 125 to 128. The scaling procedure used is detailed in Article B, above. The purpose of the scaling was to adjust the results towards a common value for comparison, and to bring more data points to bear in the process.

The Reddaway-type fender scaled values and comparisons with the basic truck are shown in Fig. 125. This is the scaled equivalent of the Fig. 122 raw results. The good suppression properties of most of these Reddaway variations is immediately evident. The complete Reddaway system plus the drag shield (MO) is the best tested. It includes the two sided flaps between the tandems. Configuration M1 is like MO without the drag shield, and there is a substantial drop in the visibility values. Since the drag shield has fuel economy benefits as well, its inclusion with the Reddaway fenders would seem to be highly desirable, as demonstrated in Section VII. M2 is like M1, except that the double sided flaps between the tandems have been deleted, and it seems to have made little difference in these results. M3 is like M1, with the flaps between the tandems, but with grass on the front facing side only. This is not quite as good as M1 or M2, but the difference is small considering the data spread in Fig. 125. Deleting the side flaps gives configuration M4, and the collection properties are now markedly inferior. This design feature of the Reddaway-type fender is clearly essential. M5 is a further strip down, without either side flaps or rear flaps on the tractor tandems, and it shows only a small improvement over the basic truck.

Scaled results for the partial gap panel and corresponding basic truck values are shown in Fig. 126. Configuration P3 with the angled end plates shows a slight improvement, based on only one run. The other configurations, P1 and P2, are actually a little worse than no partial gap panel at all. These are the no end plate, and straight end plate versions, respectively.

The scaled results for the angled side vanes are given in Fig. 127. Configuration V1, with all the vanes and no drag shield, is seen to cause more visibility reducing spray than the basic truck. Adding the drag shield, V2, improves things considerably, albeit with some scatter. Deleting the vanes behind the tractor tandems, V3, stabilizes the spray results, and produces a good improvement over the corresponding basic truck runs. Resetting

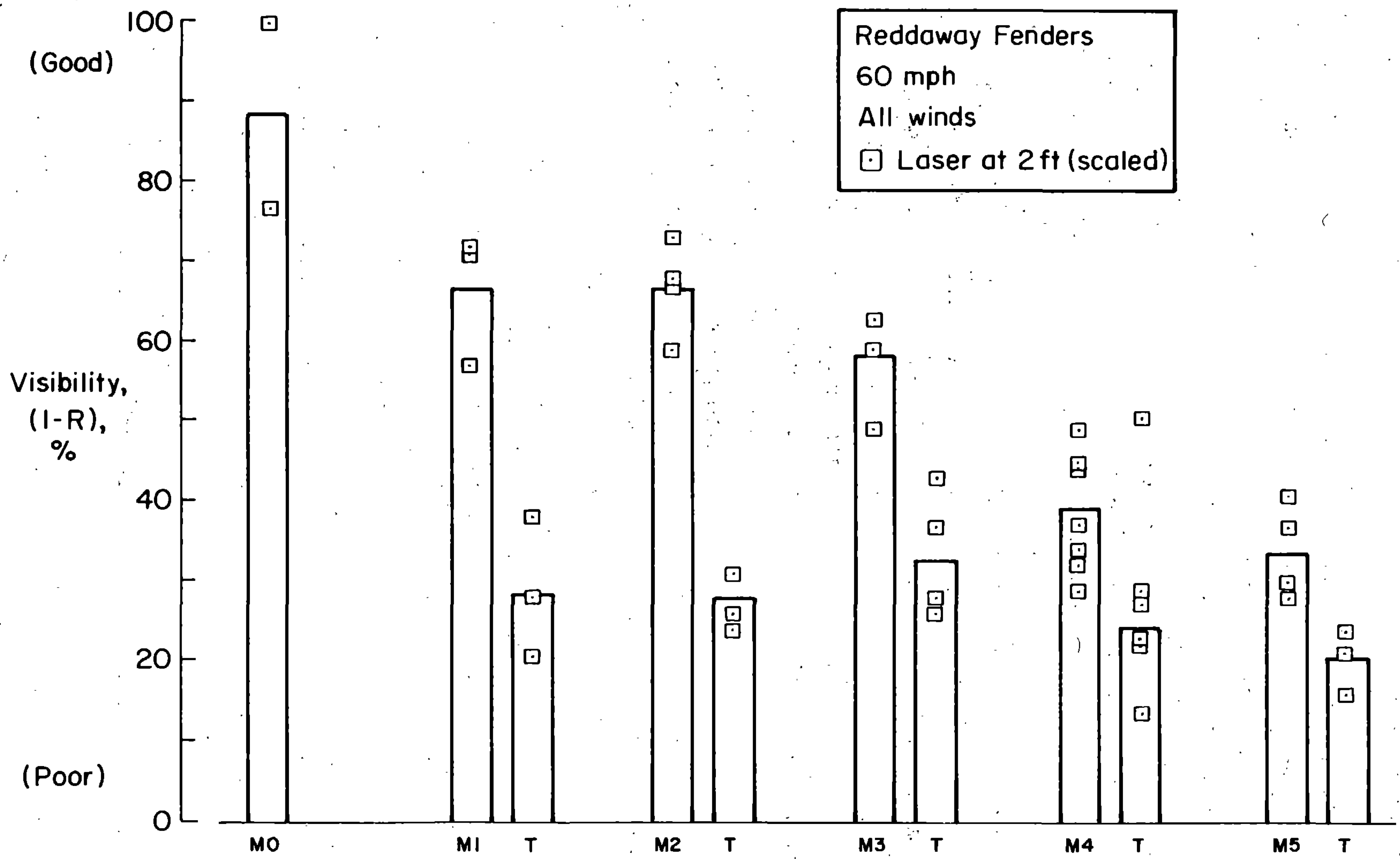

Figure 125. Comparison of Scaled Visibility Values for Reddaway Fenders and Basic Truck, 1 mph = 1.6 km/h, 1 ft = 0.3048 m

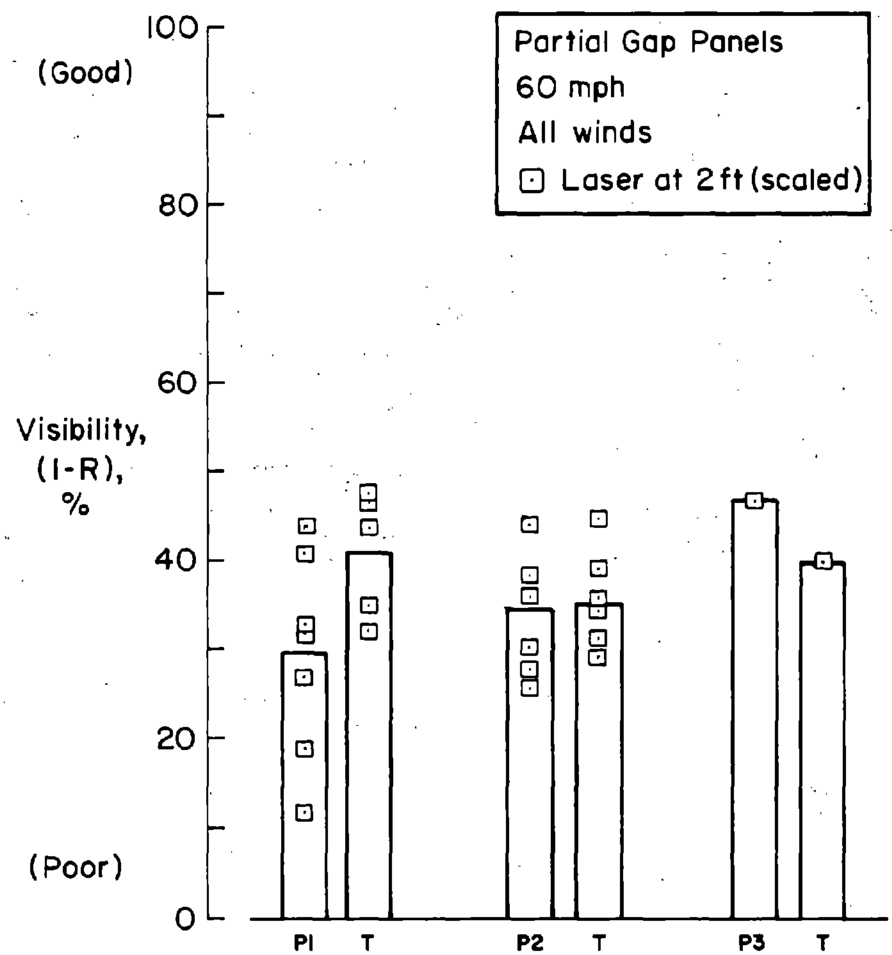

Figure 126. Comparison of Scaled Visibility Values for Partial Gap Panels and Basic Truck, 1 mph = 1.6 km/h, 1 ft = 0.3048 m

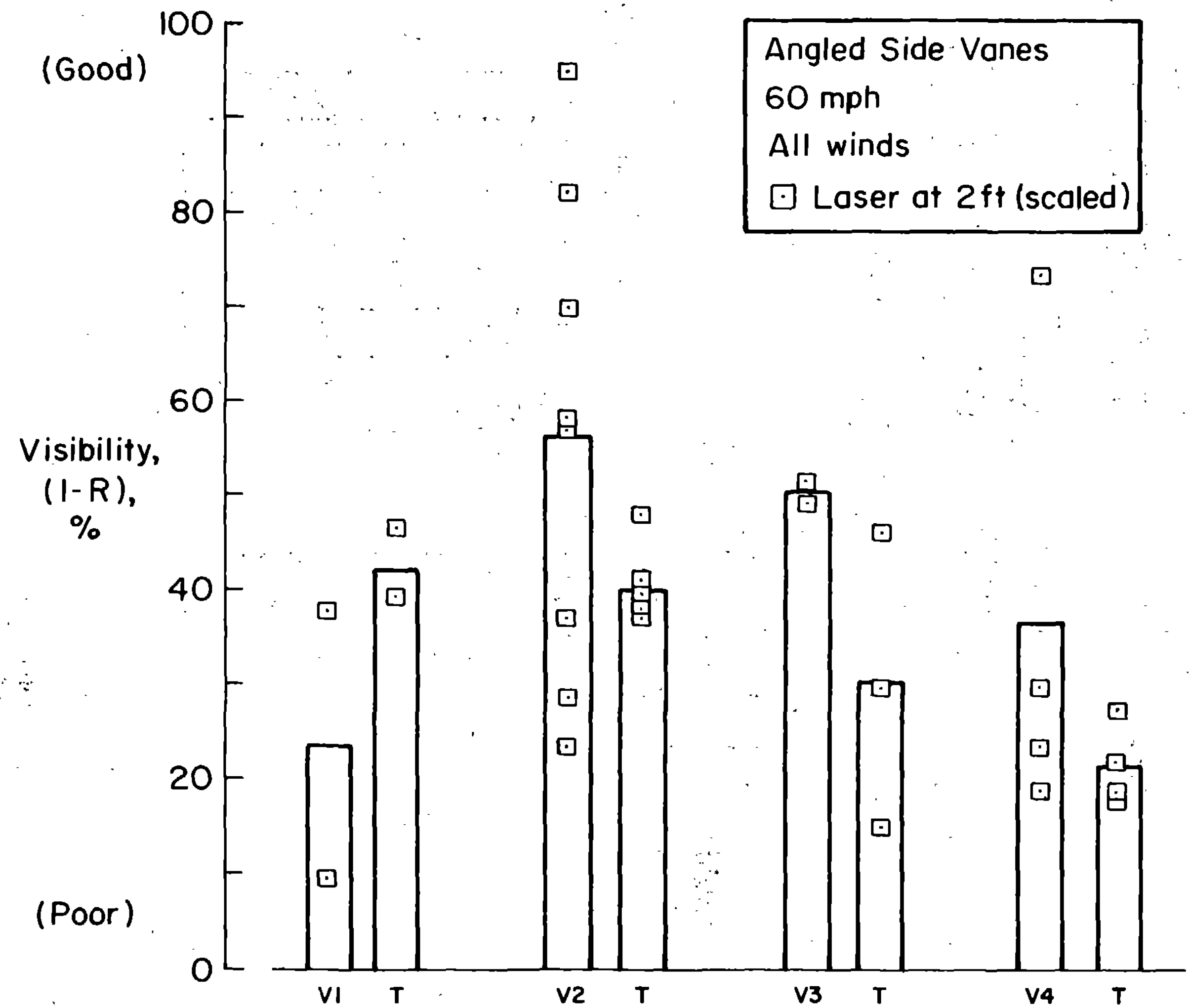

Figure 127. Comparison of Scaled Visibility Values for Angled Side Vanes and Basic Truck, 1 mph = 1.6 km/h, 1 ft = 0.3048 m

the angles of vanes under the semitrailer retained their nominal suppression properties, while reducing their extension beyond the edge of the truck and keeping them within current width restrictions.

The gap filler panel values in Fig. 128 show that both variations are effective in reducing spray. With the panel up near the top of the gap, G1, the improvement is more than in the lower position, G2.

The resulting scaled visibility margins for all the devices studied are summarized in Table 15, in order of size — larger values meaning less splash and spray. Again, the visibility margins shown are the differences in the scaled visibility values, between the devices truck and the basic truck, in a given set of runs. They derive from the 2 ft laser values at a truck speed of 60 mph (97 km/h). The results plotted in Figs. 125 to 128 are included in Table 15. Some of the other results shown are discussed below.

The degree to which the scaling procedure affects the results and the ordering of the effectiveness of the devices are illustrated in Fig. 129. Not all devices are shown, because adequate raw downwind measures were not always available. The trends in Fig. 129 show that the ordering for most of the better devices is largely unaffected by the scaling, and that the scaling procedure is generally conservative as was intended.

The most effective devices are seen in Table 15 to be the Reddaway-type collector fenders with drag shield. Also, in the good region are gap filler panel configuration G1 and angled side vane configurations V2 and V3, already discussed. The longitudinal baffle with the gap splitter panel and drag shield (L1) is also seen to be effective. Adding the longitudinal baffle with the Reddaway fenders (M6) is estimated to have excellent potential as an alternative. The data show that the fuzzy truck with the drag shield (F2) is fairly effective, and it is estimated that adding the longitudinal baffle would give further improvement. The European fender (E2) is competitive with the simpler Reddaway configurations (i.e., without the very important Reddaway side skirts), and with some of the better aerodynamic devices (gap filler panel, angled side vanes, and partial gap panel).

The drag shield, alone, on the basic truck (D1) provides only a small improvement. Yet, when coupled with some of the collector-type devices it

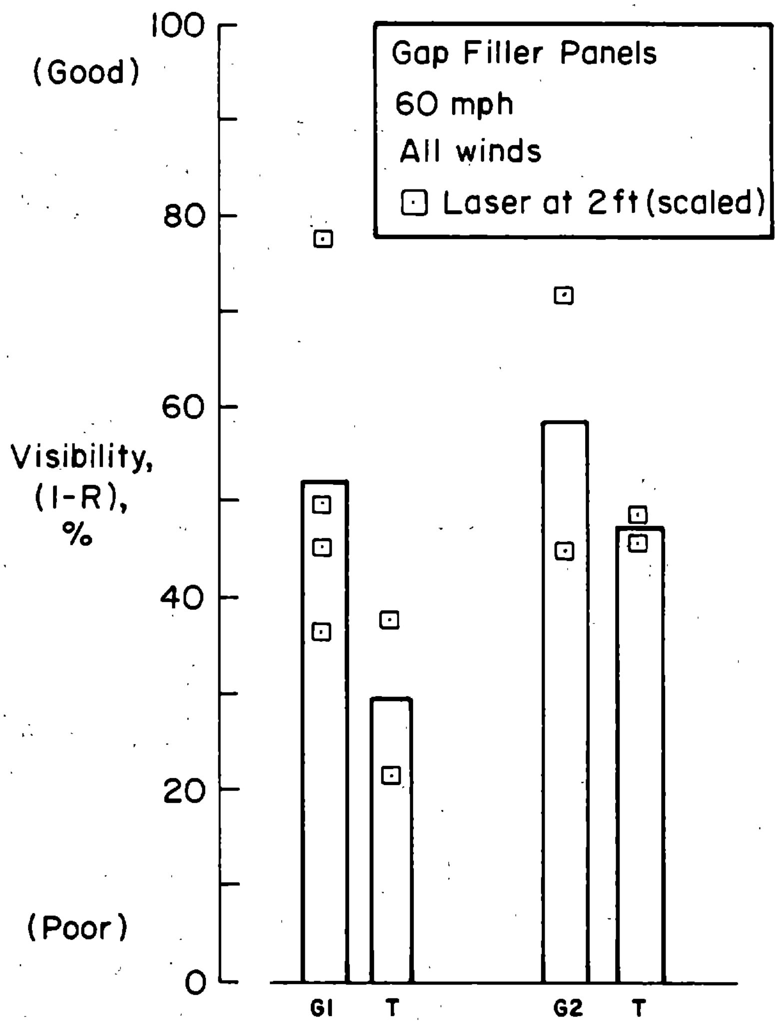

Figure 128. Comparison of Scaled Visibility Values for Gap Filler Panels and Basic Truck, 1 mph = 1.6 km/h, 1 ft = 0.3048 m

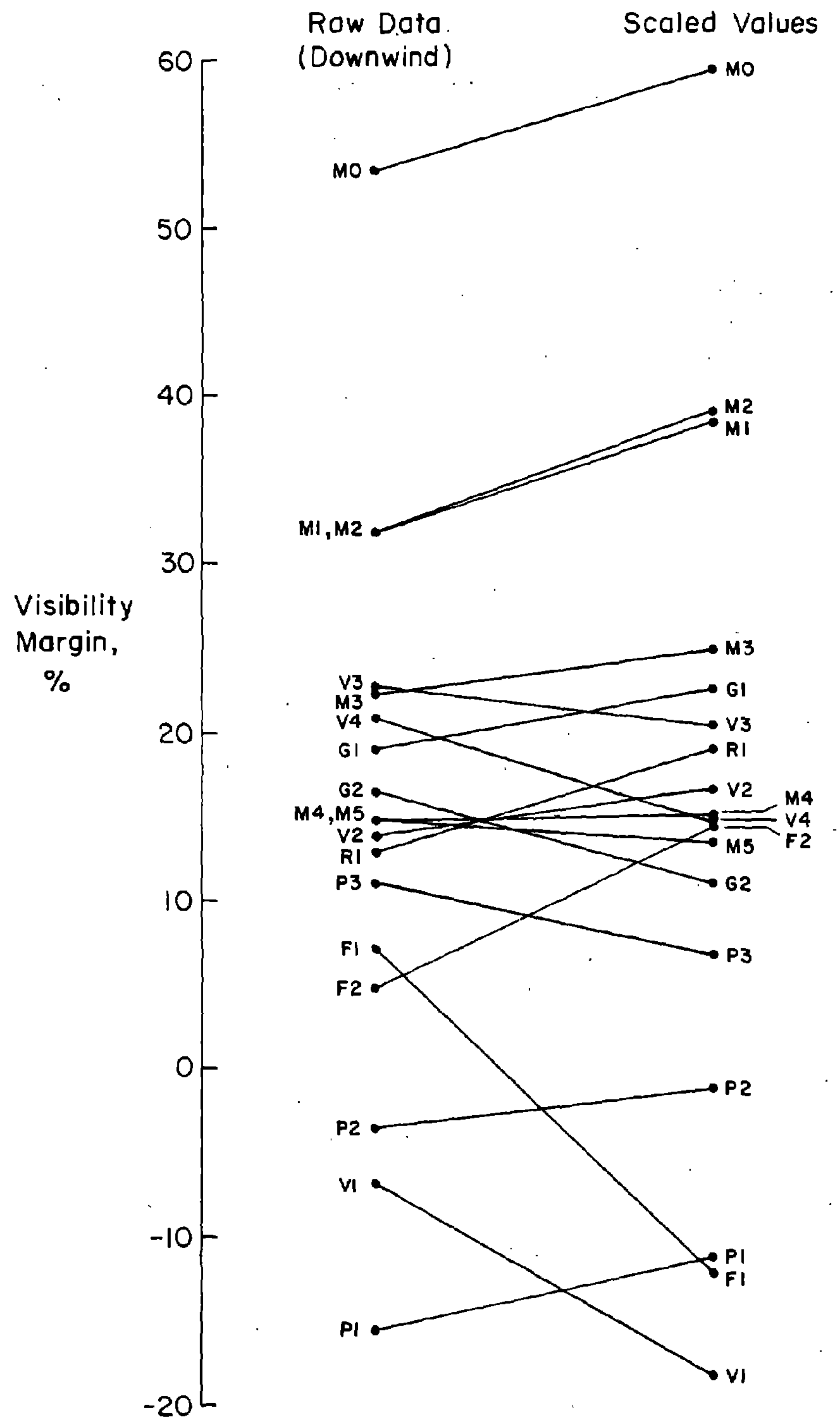

Figure 129. Effect of Scaling Procedures on Visibility Margins

TABLE 15

SUMMARY OF SCALED VISIBILITY MARGINS FOR VARIOUS DEVICES

DEVICE	DESCRIPTION	VISIBILITY MARGIN, %
M0	Reddaway system + drag shield	60
M6	Like M2 + drag shield + longitudinal baffle	59
M7	Like M2 + drag shield	59
M2	Like M1, less flaps between the tandems	39
M1	Reddaway system	38
M3	Like M1, grass forward only	25
L1	Longitudinal baffle + gap splitter panel + drag shield	25
G1	Gap filler panel in upper position	23
V3	Like V2, less vanes behind tractor tandem	20
L2	Longitudinal baffle + gap splitter panel	20
R1, R2	Roberts fender with or without shield	19
F3	Fuzzy truck + drag shield + longitudinal baffle	17
V2	Angled side vanes + drag shield	16
M4	Like M2 less side flaps	15
L4	Longitudinal baffle + drag shield	15
V4	Angled side vanes + drag shield, reset	15
E2	European fender	15
F2	Fuzzy truck + drag shield	14
M5	Like M4, less rear flaps on tractor	14
G2	Gap filler panel in lower position	11
L3	Longitudinal baffle	10
P3	Partial gap panel + angled end plates	7
D1	Basic truck + drag shield	5
T	Basic truck	0
P2	Partial gap panel + straight end plates	−1
P1	Partial gap panel	−11
F1	Fuzzy truck	−12
V1	Angled side vanes (basic layout)	−18

provides a marked increment in the overall reduction, for reasons discussed in Section IV. The drag shield also complements the underbody baffle. It does not help much with other devices that modify the gap flow, such as the gap filler panel, partial gap panel, and quarter fenders at the front of the tractor tandems.

Overall, Table 15 and the supporting development in this section tell us that several different kinds of devices and approaches have good promise for alleviating the effects of splash and spray on the adjacent motorist. At the same time, some ideas were not particularly productive. The positive results shown here have been considered in the cost/benefit analysis presented next in Section VII. They also comprise an important input to our planning for the over-the-road assessments in Phase 2 of this contractual effort.

SECTION VII

COST-EFFECTIVENESS ANALYSIS

The cost-effectiveness (C-E) analyses of potential remedial devices are described, and the results are presented in this section. These C-E analyses were accomplished by subcontractor Alan M. Voorhees and Associates, Inc. (AMV), and further details are given in their basic technical report (Ref. 5). The devices studied are described in Section IV, above. Aerodynamic drag data for the truck and device configurations under various wind conditions were needed, and those results were taken from the STI wind tunnel tests and analyses (Section V). The driver visibility measures for various splash and spray conditions provided the non-economic benefit, and those values are given in Section VI, based on the full scale tests. Several of the candidate devices analyzed were evolved during the course of this program. Others represent prototypes or current practice (e.g., the drag shield) with good alleviation potential. Some of the devices were eliminated from the C-E analysis at the outset, if they compared unfavorably, across the board, with a similar device configuration.

The role and objectives of the C-E analysis in the overall program were to:

- Help identify non-vehicle countermeasures and their advantages and disadvantages
- Formulate representative line-haul truck operating scenarios for evaluation purposes
- Delineate data needs and sources for a C-E study of the aerodynamic and economic performance of reconfigured trucks operating in the representative scenarios
- Help select candidate devices and techniques for detailed C-E analysis
- Conduct the cost-effectiveness evaluation of line-haul tractor plus semitrailer trucks equipped with the candidate devices

Results of the first objective, the identification of non-vehicle countermeasures, are included in Section II. Although some preliminary planning and preparation were done early in the project, the second and third objectives were not fully attained until the wind tunnel and full scale field testing by STI had confirmed the choice of appropriate truck plus device configurations and experimental operating conditions. The last AMV objective, the actual cost-effectiveness evaluation, could begin only after all effectiveness data were available in a final form from the field testing.

This section begins with a further overview of the AMV approach, Article A. This is followed by descriptions of the AMV cost-effectiveness and fuel consumption computer programs, Articles B and C. The cost-effectiveness analyses and results are then described. This starts with a summary of the input data and scenarios, Article D, and concludes with the C-E findings in Article E. In each case, additional detail is presented in the AMV source document from which this material and summary have been taken, Ref. 5.

A. OVERVIEW OF C-E APPROACH

The AMV approach to the definition of operating scenarios, identification of data types and sources, and the C-E evaluation is introduced below.

1. Selection of Operating Scenarios

An operating scenario was defined as a combination of ambient wind condition, truck loading, and severity of terrain to be traversed. Wind condition is specified by an absolute wind direction relative to the centerline of the roadway and an absolute wind speed relative to the ground. Ambient wind is an important variable since it affects two major parts of the benefit/cost computation: both the visibility experienced by the adjacent driver (the benefit) and aerodynamic drag (in terms of fuel consumption, a cost) vary according to wind direction and speed.

On the other hand, truck loading and terrain are considered to affect only operating costs. Three "benchmark" values are chosen for each variable to represent fundamentally different conditions: empty, "cubed out," and "weighted out" truck loadings; and flat, rolling, and mountainous terrains. Terrain effects on operating costs are fairly evident. However, certain aspects of the truck loading assumptions are more subtle, and they have been overlooked in other evaluations. In addition to ensuring a wide range of gross vehicle weights (and absolute fuel consumption rates), loadings were chosen to evaluate the effects of tare weight changes due to the extra weight of the add-on devices, themselves. For instance, if an unmodified truck is carrying a cargo type that causes it to load to maximum legal gross weight (i.e., weighted out), any extra tare weight means that less cargo can be moved per trip. Over a period of time, more trips will be required to transport a given tonnage. A premise of this study was that the operating costs of any additional trips (or a prorated share of one additional trip) should be distributed across all trips made by the reconfigured truck. Note that for a loaded truck operating at less than maximum legal gross weight (cubed out), typical device weights may change the rate of fuel consumption slightly, but they do not decrease the cargo capacity of the truck. Economic variables were not directly incorporated in the definition of an operating scenario. However, unit costs for fuel and travel time are certainly variables of interest. As will be explained later, these two variables were considered along with estimates of the capital and maintenance costs of the add-on devices to constitute an economic condition.

2. Data Types and Sources

The data required for the cost-effectiveness analyses were of four main types:

- Feasible aerodynamic and splash and spray add-on devices
- For proof-of-concept devices, not yet commercially available, estimates of device weight, initial cost, service life, and maintenance requirements
- Aerodynamic drag properties of reconfigured trucks, expressed in terms of effective cross-sectional area
- Visibility margins or differentials between the unmodified (or basic) truck and each reconfigured truck, for a standardized (reference) ambient wind condition

Cost and service data for commercially available devices were obtained from several sources, as discussed subsequently and in Ref. 5. Information on truck performance and fuel consumption was obtained from the Cummins Engine Company and other sources in the literature.

3. Approach to the Cost-Effectiveness Evaluation

Having identified a large number of relevant variables, it was decided at an early stage to develop a computer program to simulate line-haul truck operations. This program has some basic features in common with other deterministic transportation simulation models, especially those used in logistical studies. A network of origins, destinations, and intervening roadway links must first be defined. In this case, the program is limited to three contiguous links or trip legs, where each leg is uniquely defined by a set of geometric and ambient wind characteristics (details are given in Article D and Ref. 5).

Secondly, the truck plus device configurations were described. A list of up to 25 reconfigured truck types was identified in terms of cargo capacity, aerodynamic drag, splash and spray suppression properties, power train specifications, and a variety of economic data related to the add-on devices. In addition, a transportation requirement was quantified to cause the vehicles to move along the legs of the network. In this program, a different cargo tonnage and density can be specified on each leg (i.e., terminals are assumed to exist at each node).

Selected performance data are output to indicate such things as the number of trips made by each vehicle type of each leg, the costs incurred, and other variables of interest. This program determines only marginal costs and marginal benefits related to the presence of the add-on devices. Marginal cost categories include fuel, capital cost of the add-on device, associated special operating and maintenance costs (due to the device itself or the extra trips required in a weighted out case), and the cost of any travel time differential. The marginal costs are then totaled and expressed in terms of a cost per ton·mile (kg·m). At the same time, a subroutine develops a marginal visibility benefit scaled for the wind condition on each leg, divides benefit by cost, and ranks the various truck/device configurations on a leg-specific basis according to their respective benefit/cost ratios. Article B describes the assumptions and computational procedures of the main cost-effectiveness program and the benefit/cost subroutine. Article C discusses the subroutine used to estimate fuel consumption and travel time differentials.

B. COST-EFFECTIVENESS PROGRAM

As discussed above, a computer program was used by AMV in order to efficiently evaluate the marginal benefits and costs of numerous add-on devices for reducing the adverse aerodynamic effects of large trucks. The overall structure of the truck simulation program, called TRKSIM in Ref. 5, is shown in Fig. 130. Input data describe the characteristics of either the scenario or the alternative equipment configurations operating in that scenario. Once the model is primed with such data, the movement requirement is processed by determining the physically and legally permissible truck loadings and the consequent number of trips required to move a given tonnage. This loading process is repeated for each truck/device combination, where only the device type is varied, since each device will define a unique volume and/or weight capacity for the combination. The priming of the model and the processing of the movement requirement are discussed more fully in Chapter II of Ref. 5.

1. Marginal Costs

Once the input data have been entered, sufficient information is available with which to estimate the fuel requirements, travel time, and cost characteristics of the simulated movements. A subroutine named CONSUM computes fuel and travel time consumption for individual truck trips, and the main program (TRKSIM) produces aggregate statistics for all trips by leg. Once each truck/device combination has been run through all of the above claculations, fuel consumption differentials are determined between each combination and the basic (unmodified) truck.

TRKSIM then computes, by leg, the following cost components on a per-trip basis:

- Marginal fuel cost or saving (using a separately input unit fuel cost)
- Capital cost of add-on device or devices (prorated according to length of evaluation period and proportion of distance traveled on each leg of simulation)

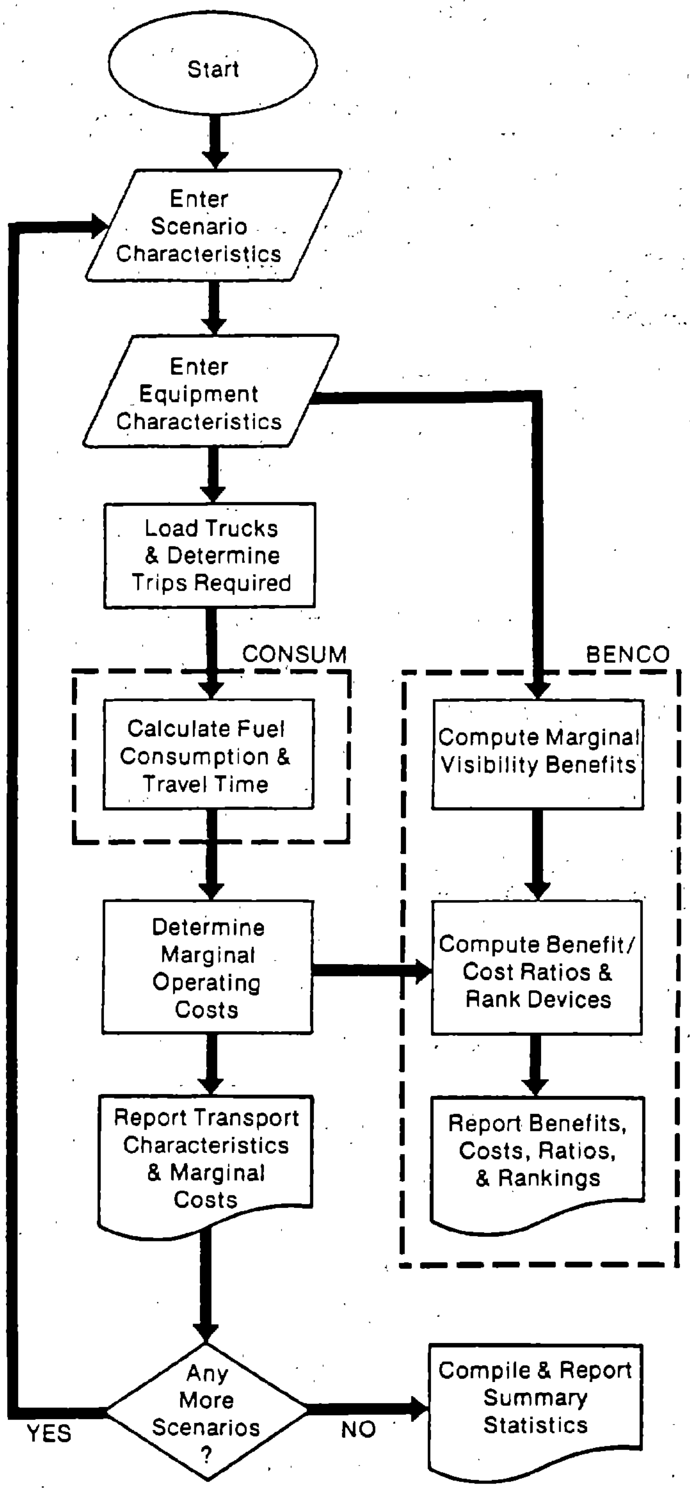

Figure 130. Macro Flow Chart of TRKSIM Program

- Marginal operating and maintenance costs; operating portion related to any extra trips needed because of reduction in truck's cargo weight capacity, and maintenance portion to cover any additional shop costs attributable to add-on device(s)

- Travel time cost or saving; due to changes in road speed with changes in aerodynamic drag, or to additional roadside stopped time needed to service add-on device(s)

The method of determining these costs is discussed in detail in Ref. 5. The results are presented in Article E. The CONSUM subroutine is the subject of the next article.

2. Benefits vs. Cost

Another subroutine, named BENCO, processes (visibility) benefit data, computes benefit/cost ratios, and ranks the alternative truck/device combinations on the basis of these ratios. The first step is to scale the visibility values, given for the reference ambient wind of 5 mph (8 km/h) from 45 deg to the right of head on, to the wind speed and direction specified for a particular trip leg. This scaling is accomplished using the procedure given in Article VI.B.3.

The second major step within BENCO is to combine the scaled benefits computed above with the marginal operating costs determined in the main program. Prior to actually calculating benefit/cost ratios for ranking purposes, however, a constant (the integer 4) is added to the cost values in order to avoid negative and indeterminate ratios. Lastly, relative cost-effectiveness is highlighted through a ranking based on these normalized benefit/cost ratios.

3. Output Reports

TRKSIM prints three different output reports. The first, "Transport Characteristics and Marginal Operating Costs," lists selected scenario characteristics; truck loading and gross vehicle weight; over-the-road speed, drag, and fuel use; marginal costs of the four types enumerated above; and total marginal cost per trip, per evaluation period, and per ton·mile (kg·m). Secondly, subroutine BENCO (see Fig. 130) summarizes benefits and costs by listing for each truck/device combination the visibility improvement scaled for the wind condition on each leg, the adjusted or normalized value of marginal cost per ton·mile (kg·m), the benefit/cost ratio, and the benefit/cost ranking by leg of the scenario. These first two reports include all truck/device combinations for a particular operating scenario. When all desired scenarios have been processed, a final summary report is written to give overall benefit/cost rankings and to identify those scenarios and legs where each device was most and least cost-effective. Examples of these reports are given subsequently, in Article E.

C. FUEL CONSUMPTION PROGRAM

The fuel consumption program has been formulated to be sensitive to basic truck and roadway characteristics and wind conditions. The major variables that can be examined for their effect on fuel consumption are truck horsepower, speed, gross vehicle weight, effective cross-sectional area, type of terrain, trip length, and wind speed and direction. For validation, the grade ability and the fuel consumption predicted by the program have been compared with previously published material (see Ref. 5). This yielded quite satisfactory results. Yet, it is important to bear in mind that the model's primary purpose was not to produce a consumption rate per se, but rather, an estimate of consumption changes due to aerodynamic modifications to large trucks operating under a variety of loading, terrain, and ambient wind conditions.

1. Computational Procedure

The calculation of fuel consumption and travel time are dependent on the dynamic values of vehicle speed, air resistance, rolling resistance, and static values describing the gross vehicle weight, engine power, route followed by the truck, and other constants. The dynamic values used in the equation are determined computationally through a repetitive procedure which finds the equilibrium point in the truck-wind-route system.

At equilibrium, the truck is moving at the maximum speed allowed by the various physical constraints. At this speed, the horsepower of the engine output equals the horsepower required to overcome the grade resistance, air resistance, rolling resistance, and chassis friction losses which oppose truck motion. This crawl speed is the maximum uniform speed the truck can maintain on a particular constant grade. The maximum grade that the truck can negotiate at a constant speed is known as the grade ability of the truck. At equilibrium, the grade ability of the truck equals the grade of the route and the speed of the truck equals the crawl speed.

An overall flow chart of the fuel consumption program (named CONSUM) is shown in Fig. 131. The procedure is divided into four major steps:

- Entry of basic characteristics
- Computation of aerodynamic factors
- Determination and testing of grade ability
- Calculation of fuel consumption and travel time

Basic characteristics which describe the truck, the cargo, the route, and the wind conditions are transferred to CONSUM from the main program. The aerodynamic factors used to determine the horsepower required to overcome air resistance, and which influence fuel consumption, are then computed for an assumed truck speed. The grade ability of the truck is calculated based on the procedure in Ref. 69. If the grade ability of the truck is less than the grade of the road, the program reduces truck speed and iterates through the computation of aerodynamic factors and grade ability until the grade ability test is satisfied. Fuel consumption and travel time are then determined using the equations developed by Sawhill and Firey (Ref. 70). These equations were modified to increase their sensitivity to changes in the aerodynamic characteristics. A more detailed description of the computational process is included in Ref. 5. Each step is further illustrated by a flow chart showing its major operations and decision.

2. Illustrative Results

Example results for two truck/device rigs, produced by the combined cost-effectiveness algorithm, can be reviewed to illustrate the effects of the aerodynamic modifications on fuel consumption and travel time. This is done with a comparison of the basic truck to a truck (MO) equipped with

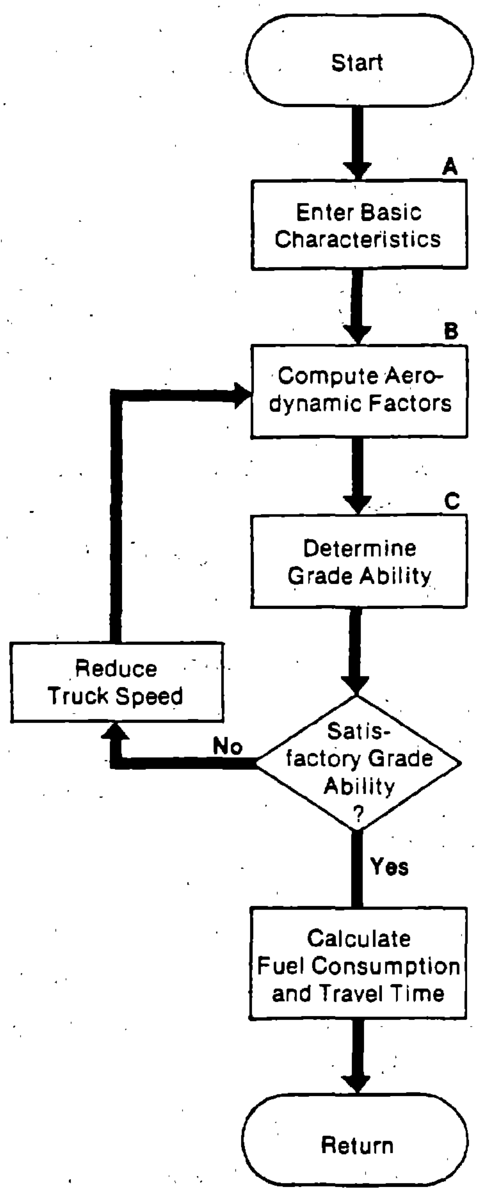

Figure 131. Flow Chart of CONSUM Program

Reddaway flaps and a drag shield (designated MO). The following results were obtained, summarized in Table 16:

- The average improvement in fuel economy for the fully loaded case is less than 5 percent
- The improvement is greatest on level terrain and declines as the design upgrade increases
- The difference in fuel consumption decreases as wind speed increases, except for the pure headwind condition
- A marginal reduction in travel time is obtained on rolling terrain

These illustrative findings are discussed in greater detail in the following paragraphs. It should be emphasized that the overall cost-effectiveness results are given in Article E, subsequently. This discussion is mainly to illustrate the methodology.

The average improvement in fuel economy for the fully loaded case is less than 5 percent on level terrain, less than 2 percent on rolling terrain, and is negligible on mountainous terrain. This is based on the example comparison of the basic truck to a truck equipped with Reddaway flaps and a drag shield (MO). Although the modified truck has 20 percent less effective cross-sectional area at a zero degree relative crosswind angle, it has an effective area equal to that of the basic truck at a 20 deg relative crosswind angle (see Table 9 in Section V). Thus, as the relative wind direction and angle increase, the difference between the effective cross-sectional areas (and the power required to overcome air resistance) decreases.

Table 16 shows that the percentage fuel savings for the empty truck case are predicted to be roughly twice those of fully loaded trucks. Also, some degree of saving is possible for empty trucks on all types of terrain.

Fuel economy improvements for the modified truck decrease as the severity of the terrain increases. This difference would be less than shown in Table 16 for many flat terrain conditions if the vehicles were not constrained to operate at a maximum speed of 60 mph (97 km/h), as they were in this analysis. If speed were not limited by the analyst, the modified truck would reach equilibrium at a higher speed than the basic truck,

TABLE 16. PERCENTAGE IMPROVEMENTS IN FUEL ECONOMY FOR MO SYSTEM[1]

Absolute Wind Direction W.R.T. Truck Axis	Absolute Wind Speed (mph)	Nominal GVW (lb)[2] / Terrain Code[3]	25,000 (Empty) 1.0	25,000 (Empty) 2.0	25,000 (Empty) 3.0	80,000 ("Weighted Out") 1.0	80,000 ("Weighted Out") 2.0	80,000 ("Weighted Out") 3.0
270°	9.5		3.7			2.4		
300°	9.5		6.0			(1.0) 2.2		
330°	9.5		12.4			6.9		
360° or 0°	0		17.6	6.5	3.4	8.1	(0.5) 3.0	(0.9) 0.3
	5		18.5			8.9		
	9.5		19.1	8.1	4.4	9.6	(1.0) 3.1	1.3
	15		19.6			10.6		
30°	5		15.7			7.8		
	9.5		12.4	5.8	(0.5) 2.3	6.9	(0.6) 2.1	0.5
	15		8.8			(2.0) 2.0		
60°	5		12.0			6.1		
	9.5		6.0			(1.0) 2.2		
	15		2.1			(1.0) -0.3		
90°	9.5		3.7	1.8	(0.5) 0.0	2.4	0.5	0.0
180°	5		16.7			7.0		
	9.5		15.6	4.9	2.2	6.2	(1.0) 1.7	0.3
	15		14.2			5.3		
Avg.[4]	9.5		8.0	3.4	1.7	4.2	1.5	0.0

[1]X.X (in each cell) = Percent increase in distance traveled per unit of fuel; (Y.Y) = Absolute increase in average speed due to reduced drag, in mph (1 mph = 1.61 km/h ; 1 lb = .454 kg)

[2]Excluding net additional weight of add-on devices, estimated to be 230 lb. (105 kg).

[3]1.0 = Flat, 2.0 = Rolling, and 3.0 = Mountainous

[4]Values were obtained for a 9.5 mph (15.3 km/h) absolute wind speed by calculating effective cross-sectional area and relative wind speed at every degree of absolute wind direction between 0° and 180°, and then averaging these latter two values across all 181 wind directions. Maximum truck speed was limited to 60 mph (97 km/h) on flat and rolling terrain and 55 mph (89 km/h) on mountainous terrain.

and the potential fuel savings would be reduced. This phenomenon was evident to some degree in several of the examples of loaded trucks operating on rolling terrain, where an increase in vehicle speed was indicated.

The improvements in fuel economy on mountainous terrain were minimal. This is principally accounted for by the relatively low speeds at which trucks climb the upgrade. At these speeds, air resistance is relatively small, and the difference in the power required to overcome this air resistance is insignificant.

For all ambient wind directions, other than a pure headwind, increasing wind speed decreases the difference in the fuel economy between the basic and modified truck. For a given ambient wind direction, other than 0 or 180 deg, higher wind speeds produce greater relative wind angles and a decrease in the difference between the effective cross-sectional areas. Depending on the particular angle and initial wind speed, this may be accompanied by an increase in the relative wind speed. However, assuming that the basic truck and modified truck are operating at the same speed, these relative wind speeds will be equivalent and, therefore, it is the effective cross-sectional area that controls the magnitude of the power required to overcome air resistance.

For a wind angle of 0 deg (i.e., a pure headwind), the relative wind angle does not change as the speed of the wind increases. The increase in the speed of the wind relative to the truck amplifies the difference between the effective cross-sectional areas, the air resistance, and the fuel consumption of the basic and modified trucks. Alternatively, in the case of the pure ambient tailwind condition, the relative wind again remains at 0 deg, but the speed of the wind relative to the truck decreases as the wind speed increases. This results in a reduced difference in fuel economy for stronger tailwinds.

In these computations the maximum speed of the truck was limited to 60 mph (97 km/h) on flat and rolling terrains and 55 mph (89 km/h) on mountainous terrain. This ceiling on speeds readily reveals differences in fuel consumption, but it does not allow the truck to reach its equilibrium point in most of the computations. Changes in vehicle speed were noted most frequently in the rolling terrain cases. These range from 0.4 to 1.1 mph (0.6 to 1.8 km/h), approximately equivalent to a 1 to 2 percent reduction in travel time.

D. INPUT DATA AND SCENARIOS

The truck equipment and the conditions under which it is assumed to operate comprise the input used by AMV for evaluation. These are detailed in Chapter IV of Ref. 5 and summarized below. Topics of interest include:

- Definition of add-on devices
- Visibility and drag effects of devices
- Economic characteristics of devices
- Weight and power characteristics of basic truck
- Line-haul operating scenarios
- Economic conditions for evaluation

The devices are described in Section IV.

1. Device Performance Data

The AMV cost-effectiveness program requires two basic types of input data on the performance of each truck/device combination. The first is the visibility margin for the reference ambient wind conditions (see Section VI). This has been called "baseline marginal visibility" in the C-E analyses, as a benefit, by analogy with "marginal cost." The second type of input data is the aerodynamic drag, quantified in terms of the effective area (see Section V). These visibility and drag values are summarized for reference in Table 17 for the truck/device combinations studied, based on Tables 9 and 15. The definition of the system codes is given in Table 3 of Section IV. Some truck/device combinations are not listed, and these were deleted by inspection, e.g., if they had the same performance characteristics as another less expensive combination. Note, too, that the "yaw angle" in Table 17 is the relative crosswind angle.

TABLE 17. PERFORMANCE CHARACTERISTICS

System	Scaled Visibility Margin (%)	Aerodynamic Drag[1] (Effective Frontal Area, ft^2)	
		at 0° Yaw Angle[2]	at 20° Yaw Angle[2]
T	0	85	145
DI	5	68	145
M0	60	68	145
M1	38	85	145
M2	39	85	145
M4	15	85	145
M5	14	85	145
M6	59	68	97
M7	59	68	145
E2	15	84	142
R1	19	84	142
R2	19	67	142
P2	0	85	142
P3	7	85	142
G1	23	85	139
G2	11	85	139
L1	25	68	85
L2	20	85	85
L3	10	84	97
L4	15	68	97
V2	16	88	165
V3	20	78	155
V4	15	78	155
F2	14	68	145
F3	17	68	97

[1] Source: Section V
Note: $1 ft^2 = 0.093 m^2$

[2] Relative crosswind

2. Device Economic Data

In addition to the effect of aerodynamic drag on fuel costs, three other categories of input data influence the economics of line-haul truck operation:

- Installed weight of add-on device(s)
- Capital cost elements
- Travel time and maintenance impacts

The ways in which these items affect operating costs were discussed above, and Table 18 is a summary listing of these data. The following paragraphs briefly describe the related AMV tables and data sources in Ref. 5.

a. Installed Weight

The extra weight of an add-on device is of interest because it is a non-revenue producing "dead" weight which can penalize both the fuel economy and cargo-carrying capacity of a truck. In this study weight estimates were made for all devices evaluated — both the prototype designs and those already in limited over-the-road use.

b. Capital Cost Elements

As shown in the headings of Table 18, capital cost elements include initial cost, service life, and salvage value. The table presents these data in the form of ranges in most cases. Such ranges are based on low and high unit cost assumptions for materials, and not on alternative designs for a given system. Although they are not listed here, midpoint (or average) values for the ranges were also computed for the analysis.

c. Travel Time and Maintenance Impacts

Assumptions regarding likely travel time and maintenance impacts are summarized in Table 18 in the form of numerical ranges. The bases for these ranges are presented in some detail in Table B-6 of Ref. 5, which outlines minimum and maximum shop-performed maintenance actions and their associated costs, assuming a total (direct and indirect) labor cost of $17.00/hour.

TABLE 18. SUMMARY OF ECONOMIC CHARACTERISTICS FOR INPUT TO C-E ANALYSIS

System	Installed Weight (lb)[1]	Initial Cost Range ($)[2]	Service Life (Yrs) (A-B)	Salvage Value ($) After Period (A-B)[3]	Extra Shop-Performed Maintenance ($/Yr)[4]	Extra Road-Side Stopped Time (Hrs./ 1000 mi.)[4]
T *	30	50-60	5-10	0-0	0	0
DI	120	470-480	5-10	180-0	0	0
MO	260	930-1,090	3-5	360-260	0-70	0
M1	170	510-670	3-5	110-80	0-70	0
M2	100	270-360	3-5	40-30	0-40	0
M4	60	180-230	3-5	40-30	0-40	0
M5	50	140-180	3-5	40-30	0-30	0
M6	380	1,260-1,350	3	280	70-180	0.5-1.0
M7	190	690-770	3-5	280-200	0-40	0
E2	170	230-290	2	0	0	0
R1	120	340-440	1-3	0-0	140-270	0-0.5
R2	210	760-860	1-3	310-240	140-270	0-0.5
P2 *	90	290-300	5	0	0	0
P3	90	290-300	5	0	0	0
G1	60	240-280	1	20	70-140	0.5-1.0
G2	60	240-280	1	20	70-140	0.5-1.0
L1 *	340	1,230-1,270	1	540	140-270	1.0-2.0
L2	250	810-850	1	230	140-270	1.0-2.0
L3	220	620-630	3	10	70-140	0.5-1.0
L4	310	1,040-1,050	3	250	70-140	0.5-1.0
V2	290	1,080-1,210	3	240	0-70	0.5-1.0
V3	220	860-940	3	240	0-50	0.3-0.6
V4	190	750-810	3-5	240-180	0-30	0
F2	180	660	5	180	0-140	0
F3	370	1,230	3	240	70-270	0.5-1.0

Notes: * Means all systems in box include conventional mud flaps (00).
All costs rounded to nearest $10; 1 mi. = 1.61 km & 1 lb = 0.45 kg

[1] Weights derived in Table A-5 and A-6 of Ref. 5.
All weights rounded to nearest 10 lb (4.5 kg) for this table.

[2] See Tables A-1 and A-2 in Ref. 5

[3] See Table A-3 in Ref. 5 for derivation of non-zero salvage values.

[4] See Table A-4 in Ref. 5

Also outlined are minimum and maximum actions which might be required by the driver in order to activate, deactivate, or service the add-on device(s). These costs are expressed in terms of hours per 1000 mi (hrs per km) traveled. Several of the estimates used in Ref. 5 were recommended by STI and the Oregon State Highway Division. Others are AMV estimates. In any case, it is important to stress their very tentative nature.

3. Characteristics of Basic Truck

While the visibility and aerodynamic properties of the basic truck have already been presented, two other major categories of characteristic data are also required by the simulation. These are cargo capacity and power train factors.

a. Cargo Capacity

The basic truck is a 3 axle tractor pulling a 40 ft (12.2 m) semitrailer van. This is the most common large truck on the highways today. The van has a cubic capacity of 2150 ft^3 (60.9 m^3). Since the tare weight of this rig averages about 25,000 lb (11,360 kg) and since a maximum legal GVW of 80,000 lb (36,360 kg) has been assumed, the weight capacity of the unmodified van is assumed to be 55,000 lb (25,000 kg).

b. Power Train Factors

As required by the AMV fuel consumption program CONSUM, representative input values were selected for output power of the tractor engine at a specified number of revolutions per minute, and for total gear reduction of the drive train. Various industry sources were consulted to determine the range of common values for these factors. From this range, it appeared reasonable to adopt a tractor with 350 hp (261 kW) at 2100 rpm, plus a total gear reduction of 3.9.

4. Operating Scenarios and Economic Conditions

In the AMV C-E analyses an operating scenario was a set of line-haul truck operating conditions uniquely defined by the direction and magnitude of the ambient wind, truck loading, severity of terrain, and length of trip leg. In this study, both "prototypical" and "real world" scenarios were developed. The former were used for sensitivity analysis and are characterized by incremental wind conditions and truck loadings. They also featured standard lengths of trip leg representing one and one-and-a-half days of travel. Selected real-world scenarios, on the other hand, are rough approximations of actual U.S. trucking circuits. Their purpose is primarily to link findings obtained from the more abstract "prototypical" framework to operations more familiar to truck owners and operators. For each scenario considered, a set of economic conditions was also defined. These include unit costs for fuel and travel time, plus an assumption of either low-, medium-, or high-cost equipment (see cost ranges in Table 18).

a. Prototypical Scenarios

Table 19 is a matrix showing key physical characteristics of the trip legs in the prototypical operating scenarios. As noted earlier, the TRKSIM model accommodates from one to four trip legs in a single scenario. For simplicity, then, the 81 bulleted cells (i.e., legs) of Table 19 were represented by 27 three-leg scenarios. The names of these scenarios used by AMV are given in Appendix C of Ref. 5.

Reference 5 also indicates that while truck operations in all cells were simulated over a 500 mi (805 km) trip leg, 18 cells representing common headwind and tailwind conditions were replicated using a 750 mi (1208 km) leg. These 18 additional legs were grouped into six scenarios, bringing the totals to 99 legs and 33 scenarios. A 500 mi (805 km) leg was chosen for the general case because this is the maximum trip length FHWA considers capable of completion in a 24 hr period without violating speed limits or hours of service restrictions (Ref. 71).

Ambient Winds. The wind directions chosen emphasize winds from ahead and to the side of the truck, or those in Quadrants 1 and 4 (i.e., 0-90 deg

TABLE 19. KEY PHYSICAL CHARACTERISTICS OF PROTOTYPICAL OPERATING SCENARIOS

Ambient Wind Direction	Wind Speed (mph)	Truck Loading	Empty			"Cubed Out"			"Weighted Out"		
		Terrain Code[1]	1.0	2.0	3.0	1.0	2.0	3.0	1.0	2.0	3.0
270°	9.5		●			●			●		
300°	9.5		●			●			●		
330°	9.5		●			●			●		
360° or 0°	0		●	●	●	●	●	●	●	●	●
	5		●			●			●		
	9.5		●	●	●	●	●	●	●	●	●
	15		●			●			●		
30°	5		●			●			●		
	9.5		●	●	●	●	●	●	●	●	●
	15		●			●			●		
60°	5		●			●			●		
	9.5		●			●			●		
	15		●			●			●		
90°	9.5		●	●	●	●	●	●	●	●	●
180°	5		●			●			●		
	9.5		●	●	●	●	●	●	●	●	●
	15		●			●			●		

[1]1.0 = Flat, 2.0 = Rolling, 3.0 = Mountainous
Note: 1 mph = 1.61 km/h

and 270-360 deg). These directions — especially those in Quadrant 1 — provide the most critical, most sensitive effects in terms of differences in aerodynamic drag (translatable to marginal cost) and visibility for the passing motorist (benefit). They are also the directions for which the most reliable experimental drag and visibility data were available (see Sections V and VI).

The matrix emphasizes the national average wind speed of 9.5 mph (15.3 km/h). Less consideration is given to a zero wind and to the bracketing wind speeds of 5 mph (8 km/h) and 15 mph (24.2 km/h).

Truck Loading. Three different truck loading conditions are represented due to marginal cost effects. If a cargo is sufficiently dense to cause the gross vehicle weight (GVW) to reach the legal maximum before a truck's cubic capacity is reached (i.e., the truck is weighted out), any additional tare weight associated with an add-on device will mean that more trips are required to move a given tonnage of cargo over the evaluation period. However, if a less dense cargo causes cubic capacity to be filled first, device weight will probably not change the number of required trips. The only weight effect in this cubed out case is to reduce the fuel economy slightly as a function of the modified GVW. Lastly, to investigate marginal costs for deadheading (empty) trucks, a zero tonnage is specified on some legs of the various operating scenario circuits.

Terrain. The truck speed and fuel consumption effects of terrain are introduced through a terrain code:

Terrain Code 1: Flat road, 0% upgrade

Terrain Code 2: Rolling terrain, 1.5% design upgrade

Terrain Code 3: Mountainous terrain, 4% design upgrade

For computational purposes, the upgrade portions were assumed to have the constant slopes (design upgrades) shown. Each trip segment has level, upgrade and downgrade portions. Design upgrades for other terrain codes between 1.0 and 3.0 were obtained by interpolation. Terrain is a factor in terms of both the potential energy to be expended in climbing grades and the engine's operating efficiency as a function of elevation.

In summary, the conditions selected in Table 19 mean that the influence of varying wind direction was studied primarily on flat terrain, and the effect of varying terrain was analyzed primarily at the national average wind speed of 9.5 mph (15.3 km/h).

b. "Real World" Scenarios

Five so-called "real world" operating circuits or scenarios were defined by AMV. These three- and four-legged circuits are geographically and climatically dispersed, as shown in Fig. 132. Both freeway and non-freeway facilities are represented. Table 20 more fully describes these scenarios in terms compatible with the TRKSIM analysis program. The "real world" scenarios were evaluated using the average annual wind speed and an assumption that such an average wind prevails from the west.

c. Economic Conditions

All combinations of aerodynamic configuration and operating scenario were processed for each of six economic conditions. An economic condition was defined by AMV to be a particular combination of hardware/maintenance cost (low, average, or high) and unit fuel cost, $0.50 or $1.00/gal ($0.13 or $0.26/L), as shown in Table 21. A unit time cost of $10.00/hour was used for all six cells of the matrix.

A "low" hardware/maintenance cost was associated with the lowest estimated initial add-on hardware cost, the longest service life, the salvage value at that service life, and the lowest additional maintenance and travel time costs. By reviewing the estimated ranges for these cost components for each aerodynamic configuration, the "average" and "high" cost combinations were similarly identified for input to the program.

E. COST-EFFECTIVENESS FINDINGS

Presented in this article are selected results from the AMV cost-effectiveness computations. The word "selected" is emphasized, since it is impossible to develop a unique, universally applicable solution to the countermeasure selection problem. (This is common to most cost-effectiveness

TABLE 20. GEOGRAPHIC VARIATIONS AMONG SELECTED "REAL WORLD" OPERATING SCENARIOS

Circuit	Leg No.	Length (mi.)	Terrain Code	Average Elevation (ft.)	Truck Azimuth (°)	Ambient Wind Direction		Average Wind Speed (mph)	Precipitation	
						Azimuth (°)	Quadrant[1]		Days	Inches
National (NA)	1	2,550	2.2	2,700	265	5	1	9.5	76	29
	2	380	1.5	1,200	330	300	4	9.0	48	16
	3	2,850	2.0	2,700	85	185	3*	10.3	92	30
	4	390	2.0	200	190	80	1	8.8	114	43
		6,170								
North Central (NC)	1	860	1.5	1,800	275	355	4	9.5	97	28
	2	1,000	1.1	2,100	80	190	3*	10.1	102	25
	3	290	1.2	600	200	70	1	10.0	113	34
		2,150								
Southeast (SE)	1	345	1.7	200	290	340	4	8.3	112	52
	2	170	1.7	300	210	60	1	8.6	115	60
	3	410	1.5	100	85	185	3*	9.1	120	61
		925								
Southwest (SW)	1	400	3.0	3,900	300	330	4	7.8	40	8
	2	385	3.0	4,600	90	180	3*	7.4	46	8
	3	190	3.0	4,600	190	80	1	9.4	51	8
		975								
Intrastate (IS)	1	45	1.8	150	25	245	3	7.7	153	37
	2	115	2.3	2,600	130	140	2	7.7	100	25
	3	45	2.0	2,500	190	80	1	7.7	50	12
	4	130	2.7	3,200	305	325	4	7.7	125	30
		335								

[1] * means approximate tail wind

Note: 1 mi. = 1.61 km, 1 ft. = 0.305 m, and 1 inch = 25.4 mm

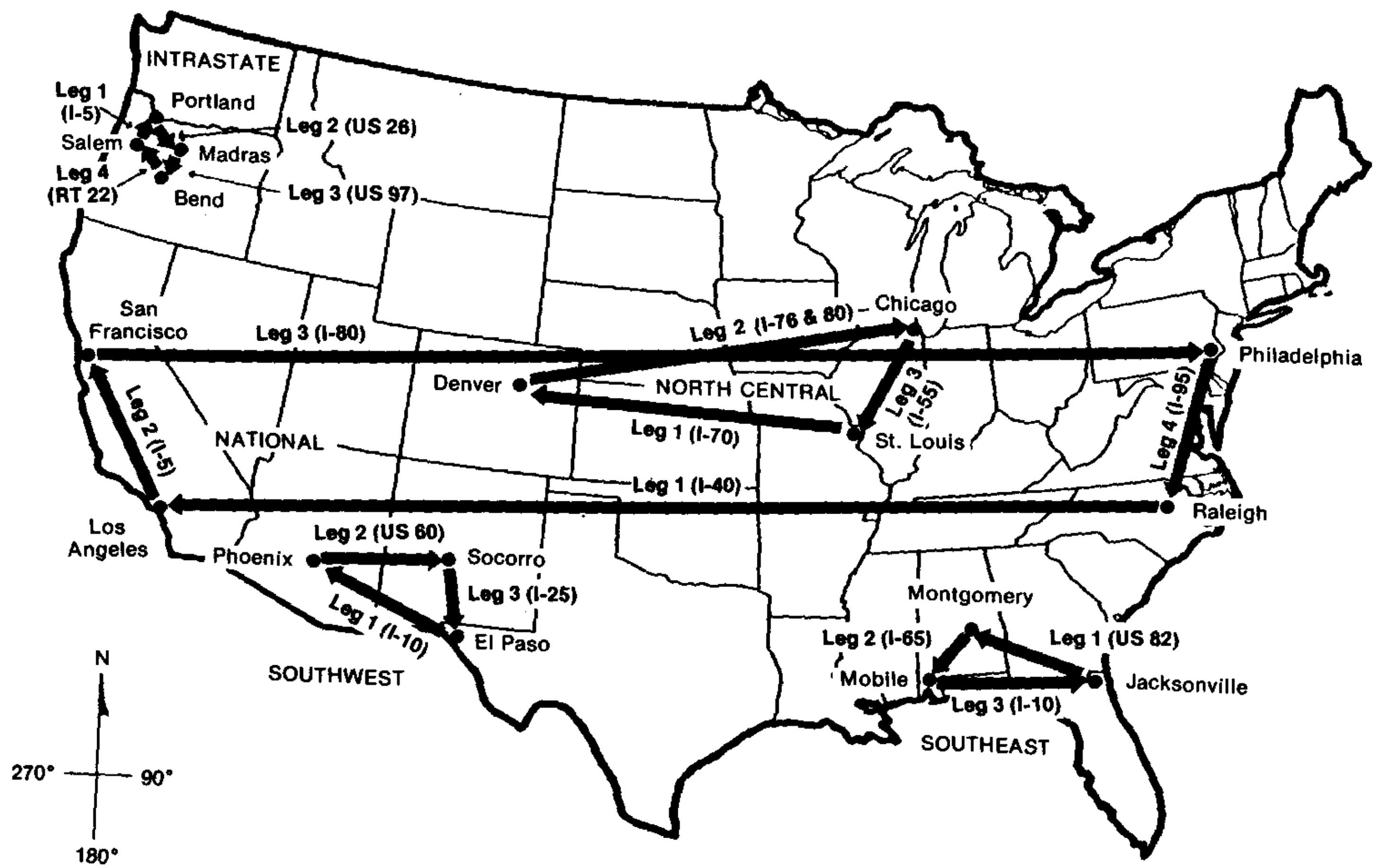

Figure 132. Selected "Real World" Circuits

TABLE 21. MATRIX OF ECONOMIC CONDITIONS

Unit Fuel Cost	Cost of Hardware and Maintenance		
	Low	Average	High
Low ($0.50/gal.)	1	2	3
High ($1.00/gal.)	4	5	6

Note: 1 gal = 3.8 L

studies.) Rather, patterns of effectiveness and cost are described, and alternative rankings are derived on the basis of overall relative cost-effectiveness, capital cost within ranges of objective effectiveness, and fuel savings within these ranges.

1. Overall Cost Effectiveness

Presented here are cost-effectiveness results averaged across all 99 prototypical trip legs described in the preceding article.

a. Rankings

Table 22 lists the overall average benefit/cost rankings for the 25 truck/device systems evaluated by AMV. Highlights of this table are as follows:

- Economic condition has relatively minor influence on the rankings. Seventeen of the 25 systems maintained the same rankings across all six economic cells, and the rankings of the other eight systems varied by no

TABLE 22. AVERAGE BENEFIT/COST RANKINGS FOR DIFFERING ECONOMIC ASSUMPTIONS

System	Unit Fuel Cost / Cost of Hardware & Maintenance	Low ($0.50/gal.) C1* Low	Low ($0.50/gal.) C2 Average	Low ($0.50/gal.) C3 High	High ($1.00/gal.) C4 Low	High ($1.00/gal.) C5 Average	High ($1.00/gal.) C6 High	Overall Rank
T		25	25	25	25	25	25	24
D1		23	23	23	23	23	23	23
M0		2	2	2	2	2	2	2
M1		5	5	5	5	5	5	5
M2		4	4	4	4	4	4	4
M4		13	13	13	13	13	13	13
M5		19	19	19	19	19	19	19
M6		3	3	3	3	3	3	3
M7		1	2	2	2	1	1	1
E2		17	14	14	18	16	16	16
R1		11	10	10	11	11	11	11
R2		9	9	9	9	9	9	9
P2		25	25	25	25	25	25	25
P3		22	22	22	22	22	22	22
G1		7	7	7	7	7	7	7
G2		20	20	20	20	20	20	20
L1		6	6	6	6	6	6	6
L2		10	11	11	10	10	10	10
L3		21	21	21	21	21	21	21
L4		15	18	18	14	14	15	15
V2		14	16	17	16	18	18	17
V3		8	8	8	8	8	8	8
V4		18	17	16	17	17	17	18
F2		16	15	15	15	15	14	14
F3		12	12	12	12	12	12	12

*Cell 1 Note: 1 gal. = 3.79 L

more than one to four places. The higher ranked systems generally had a much lower degree of ranking variation.

- The Reddaway (M Series) systems ranked very highly except where no side flaps were used (i.e., M4 and M5). The top five systems in terms of overall cost-effectiveness are M7, M0, M6, M2, and M1, respectively.

- Systems with overall rankings between 6 and 10 are distributed among four other of the system categories suggested by the horizontal lines in Table 22. These include L1 (ranking 6, in the longitudinal baffle category); G1 (ranking 7, one of our candidate gap panels); V3 (ranking 8, angled vanes); R2 (ranking 9, one of three fender systems); and L2 (ranking 10, also a longitudinal baffle system).

b. Average Values of B/(C + 4)

Table 23 lists the overall average values of the mixed unit benefit/cost ratio denoted B/(C + 4). Although the ratio is structured to be especially sensitive to changes in benefit B (i.e., marginal visibility), some variation is evident across the six economic conditions. Points of interest include:

- Systems utilizing a drag shield generally have higher ratios with higher unit fuel costs because fuel savings decrease the value of C. These systems include D1, M0, M6, M7, R2, L1, L4, F2, and F3. Exceptions to this trend are V2, V3, and V4, where the drag shield is apparently unable to overcome the drag penalty of the vanes under an average set of operating conditions. Other marginal costs are considered, of course, but the one related to fuel appears to be most significant.

- Some of the differences cited above are due in part to the presence of the longitudinal baffle under the semitrailer. This becomes evident upon examination of the ratios for systems utilizing this baffle but no drag shield, i.e., L2, and L3.

To avoid making economic assumptions regarding unit fuel cost or the cost of hardware and maintenance, the ratios in Table 23 can be assumed to occur with equal probability. In that case, they can be averaged with the same weight given to each, as was done in the last column of Table 23. These average values can then be reviewed in graphic form (see Fig. 133). Most

TABLE 23. AVERAGE VALUES OF B/(C + 4) FOR DIFFERING ECONOMIC ASSUMPTIONS

System	Unit Fuel Cost	Low ($0.50/gal.)			High ($1.00/gal.)			Overall Average $\frac{B}{C+4}$
	Cost of Hardware & Maintenance	C1* Low	C2 Average	C3 High	C4 Low	C5 Average	C6 High	
T		0.0	0.0	0.0	0.0	0.0	0.0	0.0
DI		1.3	1.3	1.3	1.4	1.4	1.4	1.3
M0		15.8	15.8	15.7	16.7	16.6	16.4	16.2
M1		9.5	9.4	9.4	9.4	9.4	9.4	9.4
M2		9.8	9.8	9.8	9.8	9.8	9.8	9.8
M4		3.6	3.6	3.6	3.6	3.6	3.6	3.6
M5		3.2	3.1	3.1	3.2	3.1	3.1	3.1
M6		15.3	14.9	14 6	17.2	16.6	16.0	15.8
M7		15.8	15.8	15.7	16.7	16.6	16.5	16.2
E2		3.5	3.5	3.5	3.5	3.5	3.5	3.5
R1		4.6	4.5	4.3	4.6	4.5	4.3	4.5
R2		4.8	4.6	4.4	5.0	4.8	4.6	4.7
P2		0.0	0.0	0.0	0.0	0.0	0.0	0.0
P3		1.7	1.7	1.7	1.7	1.7	1.7	1.7
G1		5.3	5.2	5.1	5.3	5.2	5.1	5.2
G2		2.4	2.4	2 3	2.4	2.4	2.3	2.4
L1		5.9	5.7	5.5	6.8	6.3	6.0	6.0
L2		4.5	4.4	4.2	4.9	4.7	4.5	4.5
L3		2.3	2.2	2.2	2.4	2.4	2.3	2.3
L4		3.6	3.5	3.5	4.1	3.9	3.8	3.7
V2		3.6	3.5	3.5	3.5	3.5	3.4	3.5
V3		4.8	4.7	4.7	4.8	4.8	4.7	4.8
V4		3.5	3.5	3.5	3.5	3.5	3.5	3.5
F2		3.5	3.5	3.5	3.7	3.7	3.7	3.6
F3		4.1	4.0	3.9	4.6	4.5	4.3	4.2

*Cell 1 Note: 1 gal. = 3.79 L

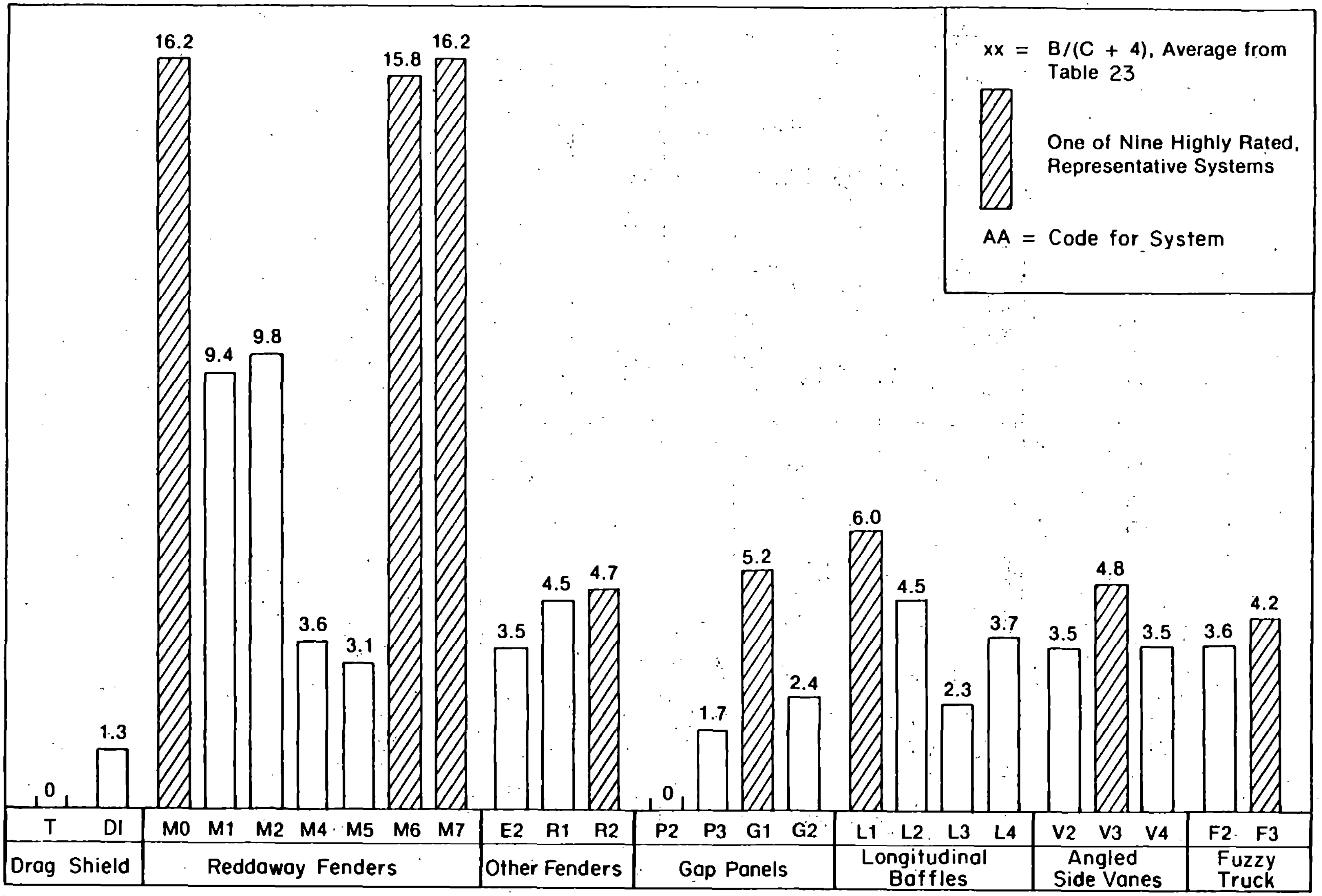

Figure 133. Relative Cost-Effectiveness by B/(C + 4) Ratio

evident in the figure are the substantial superiority of the top five Reddaway systems and the existence of a viable alternative in each of the other system categories.

2. Marginal Visibility

As discussed earlier, the baseline marginal visibility values (visibility margins) were scaled for the various ambient wind condition represented in the operating scenarios. This section presents the results of the scaling and averaging and draws conclusions concerning the maximum and minimum effectiveness of the 25 systems evaluated.

a. Maxima and Minima

Table 24 shows the scaled marginal visibility values under the 17 wind conditions present in the prototypical operating scenarios described in Article D. Cells containing the maximum value for each system are dotted.

Not surprisingly, the maximum visibility benefit generally occurs under 60-90 deg crosswind cases. The few exceptions include M0, M6, and M7, but here the difference between the crosswind and headwind cases is only 3 percentage points on an absolute basis or an insignificant 4 percent on a relative basis.

Cells with minimum values of marginal visibility are not highlighted in Table 24, but they invariably include the 5 mph (8 km/h) tailwind case. A review of the table shows that the minimum value for a given system is always roughly one-half the associated maximum value.

As shown in Fig. 134, for the fairly typical conditions stated below the figure, it can be seen that air resistance horsepower is maximum at an ambient wind angle of approximately 60 deg, and a minimum at 180 deg (i.e., a tailwind). To the extent that marginal cost varies with absolute fuel consumption, then, one might anticipate the most sensitive marginal cost for a 15 mph (24 km/h) ambient crosswind at 60 deg, and the least sensitive marginal cost for the 5 mph (8 km/h) tailwind. Hence, these two wind conditions are good candidates for investigating cost-effectiveness

TABLE 24. MARGINAL VISIBILITY FOR PROTOTYPICAL WIND CONDITIONS (%)

Ambient Wind Direction	Wind Speed (mph)	Truck / Device System											
		T	DI	M0	M1	M2	M4	M5	M6	M7	E2	R1	R2
270°	9.5	0	**7**	57	36	37	16	14	57	57	16	20	20
300°	9.5	0	**7**	57	36	37	16	14	57	57	16	20	20
330°	9.5	0	6	57	36	37	14	13	56	56	14	18	18
360° or 0°	0	0	5	54	34	35	14	12	53	53	14	17	17
	5	0	6	68	43	44	17	15	67	67	17	22	22
	9.5	0	4	**74**	44	45	13	11	**73**	**73**	13	19	19
	15	0	4	**74**	44	45	13	11	**73**	**73**	13	19	19
30°	5	0	5	65	41	42	16	14	64	64	16	21	21
	9.5	0	5	72	44	**46**	15	13	72	72	15	20	20
	15	0	5	72	44	**46**	15	13	72	72	15	20	20
60°	5	0	5	60	38	39	15	13	59	59	15	19	19
	9.5	0	6	71	**45**	**46**	**18**	**16**	70	70	**18**	**23**	**23**
	15	0	6	71	**45**	**46**	**18**	**16**	70	70	**18**	**23**	**23**
90°	9.5	0	6	71	**45**	**46**	**18**	**16**	70	70	**18**	**23**	**23**
180°	5	0	4	37	23	24	10	9	37	37	10	12	12
	9.5	0	6	46	29	30	13	11	45	45	13	16	16
	15	0	6	46	29	30	13	11	45	45	13	16	16

Maximum; 1 mph = 1.61 km/h

TABLE 24. (Concluded)

Ambient Wind Direction	Wind Speed (mph)	Truck / Device System												
		P2	P3	G1	G2	L1	L2	L3	L4	V2	V3	V4	F2	F3
270°	9.5	0	9	23	12	25	21	11	16	17	21	16	15	18
300°	9.5	0	9	23	12	25	21	11	16	17	21	16	15	18
330°	9.5	0	7	21	11	23	19	10	14	16	19	14	14	16
360° or 0°	0	0	6	20	10	23	18	9	14	15	18	13	13	15
	5	0	8	26	13	29	23	11	17	18	23	17	16	19
	9.5	0	5	23	8	26	20	7	13	15	20	13	12	16
	15	0	5	23	8	26	20	7	13	15	20	13	12	16
30°	5	0	8	24	12	27	22	11	16	18	22	16	15	18
	9.5	0	6	25	10	28	21	9	15	17	22	15	14	18
	15	0	6	25	10	28	21	9	15	17	22	15	14	18
60°	5	0	7	23	11	25	20	10	15	16	20	15	14	17
	9.5	0	8	27	13	30	24	12	18	20	24	18	17	20
	15	0	8	27	13	30	24	12	18	20	24	18	17	20
90°	9.5	0	8	27	13	30	24	12	18	20	24	18	17	20
180°	5	0	5	14	7	16	13	7	10	11	13	10	9	11
	9.5	0	7	18	9	20	16	9	13	14	17	12	12	14
	15	0	7	18	9	20	16	9	13	14	17	12	12	14

Maximum; 1 mph = 1.61 km/h

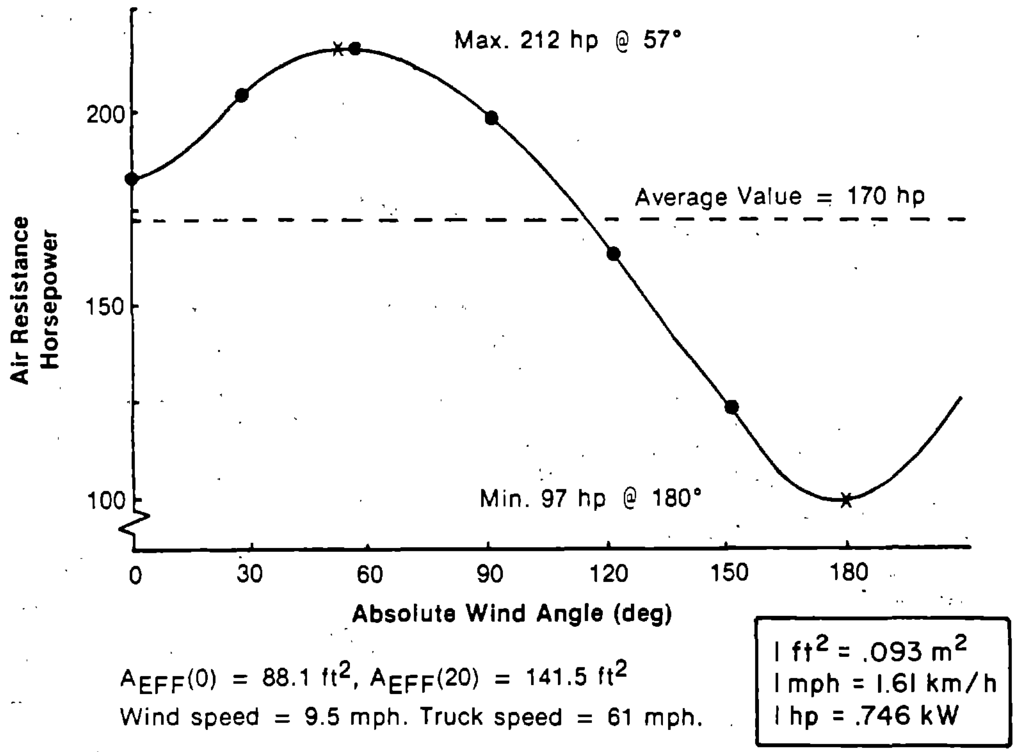

Figure 134. Air Resistance Horsepower Versus Absolute Wind Angle

in greater detail. They should approximate the more interesting bounds of the problem for systems shown to reduce aerodynamic drag:

- Crosswind Case — Maximum visibility effectiveness with substantial fuel savings (and quite possibly minimal marginal cost).

- Tailwind Case — Minimum visibility effectiveness with little, if any, fuel savings (hence, maximum marginal cost).

b. Overall Average Marginal Visibility

Figure 135 shows the marginal visibility of each system averaged across all 17 prototypical wind conditions. Interestingly, the values are little different than the baseline (reference) values for the 5 mph (8 km/h), 45 deg ambient wind most common in the full scale tests.

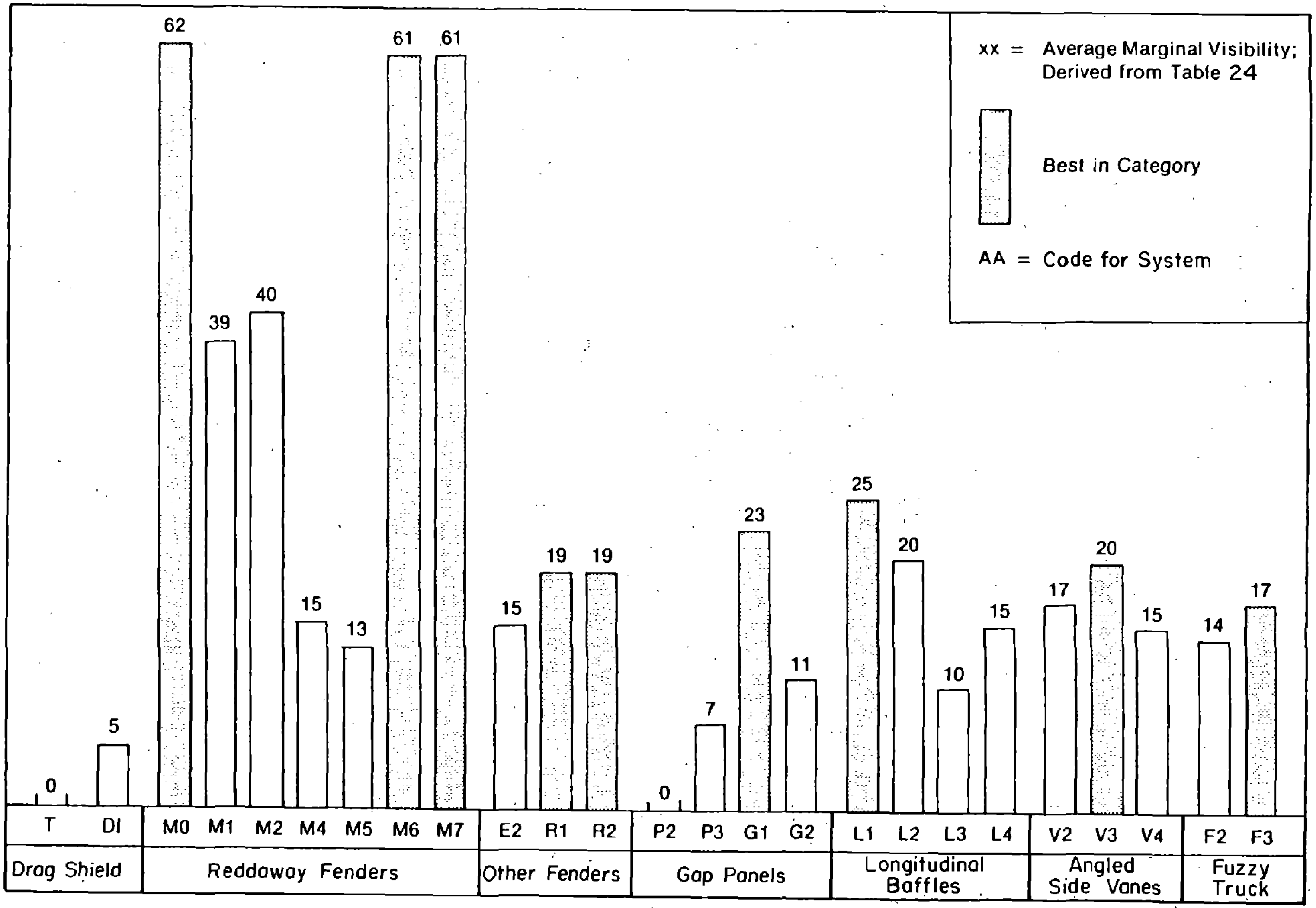

Figure 135. Average Marginal Visibility over 17 Prototypical Wind Conditions

3. Marginal Costs

Three aspects of marginal costs are considered below, i.e.,

- Costs associated with maximum and minimum visibility effectiveness
- Capital cost as a ranking criterion
- Fuel savings as a ranking criterion

Typical marginal cost components are presented and discussed in conjunction with this last item.

a. Costs Associated with Maximum and Minimum Visibility Effectiveness

Table 25 lists marginal visibility for a 60 deg, 15 mph (24 km/h) ambient wind and for a 180 deg, 5 mph (8 km/h) ambient wind. As shown in the preceding discussion, these generally correspond to maximum and minimum marginal visibility, respectively.

Also shown in Table 25 are selected marginal costs associated with the visibility extremes. To roughly approximate greatest cost-effectiveness, the lowest marginal cost associated with the maximum marginal visibility is listed for two unit fuel costs. Similarly, the least cost-effectiveness is approximated by listing the maximum marginal cost associated with the lowest marginal visibility. Average hardware and maintenance costs were used in developing the table (i.e., data from economic cells 2 and 5 in Table 21).

It should be noted that the costs shown are only for a cubed out truck operating on flat terrain. All cubed out trucks in the simulation were loaded with 30,000 lb (13,640 kg) of cargo such that the gross vehicle weight, excluding the weight of add-on devices, was nominally 55,000 lb (25,000 kg). Flat terrain was chosen here in order to provide the most sensitive evaluation of marginal costs as they are affected by aerodynamic drag and fuel consumption related thereto.

A final feature of Table 25 is the two columns listing marginal cost as a percent of total operating cost. These percentages are based on a typical total cost of truck operation of 5 mills/ton mile (3.4 mills/kg·m).

TABLE 25. APPROXIMATE RANGE OF SYSTEM BENEFITS AND ASSOCIATED COSTS

System	Cross-Wind Case[1]				Tail-Wind Case[2]			
	Maximum Marginal Visibility (%)	Marginal Cost[3] (Mills/Ton-Mile)		Percent of Total Operating Cost[4] (Range)	Minimum Marginal Visibility (%)	Marginal Cost[3] (Mills/Ton-Mile)		Percent of Total Operating Cost[4] (Range)
		Fuel at \$0.50/gal.	Fuel at \$1/gal.			Fuel at \$0.50/gal.	Fuel at \$1/gal.	
T	0	0.0	0.0	0 - 0	0	0.0	0.0	0 - 0
DI	6	-.126	-.113	<3 - 2>	4	-.404	-.862	<8 - 17>
M0	71	.006	.029	0 - 1	37	-.272	-.720	<5 - 14>
M1	45	.128	.137	3 - 3	23	.128	.137	3 - 3
M2	46	.066	.071	1 - 1	24	.067	.071	1 - 1
M4	18	.038	.040	1 - 1	10	.038	.040	1 - 1
M5	16	.027	.028	1 - 1	9	.027	.028	1 - 1
M6	70	-1.005	-2.456	<20 - 49>	37	.388	-.051	8 - <1>
M7	70	-.055	-.037	<1 - 1>	37	-.332	-.786	<7 - 16>
E2	18	-.047	.002	<1> - 0	10	.080	.062	2 - 1
R1	23	.249	.300	5 - 6	12	.376	.360	8 - 7
R2	23	.184	.101	4 - 2	12	-.013	-.487	<0 - 10>
P2	0	-.098	-.046	<2 - 1>	0	.048	.053	1 - 1
P3	8	-.098	-.046	<2 - 1>	5	.048	.053	1 - 1
G1	27	.420	.371	8 - 7	14	.666	.668	13 - 13
G2	13	.420	.371	8 - 7	7	.666	.668	13 - 13
L1	30	-.717	-2.577	<14 - 52>	16	1.082	.639	22 - 13
L2	24	-.659	-2.374	<13 - 47>	13	1.452	1.468	29 - 29
L3	12	-1.005	-2.325	<20 - 46>	7	.683	.669	14 - 13
L4	18	-1.078	-2.534	<22 - 51>	10	.315	-.129	6 - <3>
V2	20	1.527	1.902	31 - 38	11	.843	.943	17 - 19
V3	24	.817	.955	16 - 19	13	.300	.122	6 - 2
V4	18	.465	.601	9 - 12	10	-.052	-.232	<1 - 5>
F2	17	-.051	-.033	<1 - 1>	9	-.328	-.782	<7 - 16>
F3	20	-.996	-2.448	<20 - 49>	11	.398	-.043	8 - <1>

[1] Approximated by "cubed-out" truck operating on flat terrain with a 15 mph (24 km/h) ambient wind 60° to the right of head-on.

[2] Approximated by "cubed-out" truck operating on flat terrain with a 5 mph (8 km/h) ambient tail wind

[3] Assumes average costs for hardware and maintenance (i.e., cells 2 and 5). See tables in Ref. 5 for other economic conditions.

[4] Assumes 5 mills/ton-mile, shown by Ref. 72 to be typical.

Note: 1 mill/ton-mile = 0.685 mill/kg·m and 1 gal. = 3.79L ; < > means negative.

This base cost was derived from 1976 data published in Carrier Reports — Financial Reports on the Nation's Leading Carriers (Ref. 72) and plotted in Fig. 136. As can be seen on the figure, the chosen unit cost is representative of operations by fleet owners incurring total annual costs of about $10,000,000.

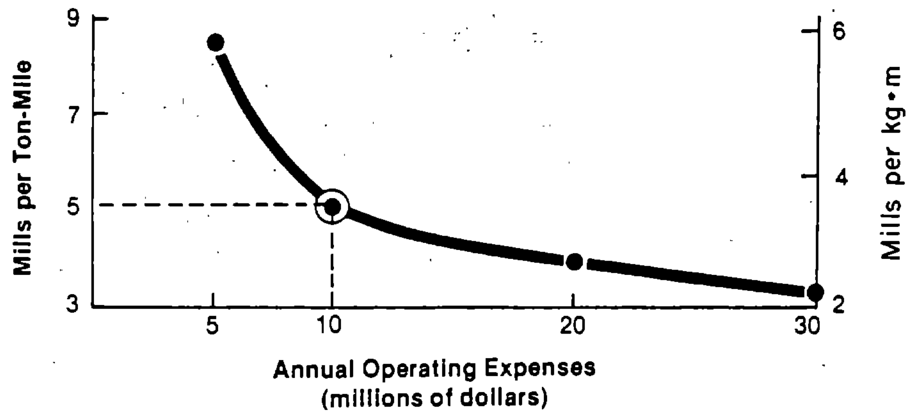

Figure 136. Total Operating Cost as a Function of Feet Size (Ref. 72)

b. Capital Cost as a Ranking Criterion

The benefit/cost rankings and ratios presented in Tables 22 and 23 are quite informative and useful in suggesting aerodynamic and splash and spray systems worthy of further consideration. However, operators will want to consider other basic economic factors before selecting one or more systems for installation. One important factor of this type is the absolute level of capital cost, and these values are summarized in Table 26. In Table 27 the 25 systems analyzed by AMV are grouped according to various levels of marginal visibility (taken from Fig. 135). Within each group, the systems are then listed in ascending order of capital cost. The results clearly show the advantage of the assumed Reddaway system relative to this criterion.

c. Fuel Savings as a Ranking Criterion

Still another economic consideration — one given increased emphasis since 1974 — is fuel consumption. Given a reasonably high benefit/cost ranking, an acceptably low capital cost, and a minimum marginal visibility advantage, the next most conspicuous selection factor is probably the degree

TABLE 26. AVERAGE CAPITAL COSTS

System	Average Initial Cost[1] ($)	Capital Cost		
		Per Year ($)	Per Day[2] ($)	Per Vehicle-Mile[3] (mills)
T	55	11	0.04	0.08
DI	475	79	0.26	0.52
M0	1,010	236	0.79	1.58
M1	590	157	0.52	1.04
M2	315	87	0.29	0.58
M4	205	54	0.18	0.36
M5	160	41	0.13	0.26
M6	1,305	420	1.40	2.80
M7	730	167	0.56	1.12
E2	260	146	0.49	0.98
R1	390	219	0.73	1.46
R2	810	322	1.07	2.14
P2	295	74	0.25	0.50
P3	295	74	0.25	0.50
G1	260	260	0.87	1.74
G2	260	260	0.87	1.74
L1	1,250	810	2.69	5.38
L2	830	666	2.22	4.44
L3	625	239	0.80	1.60
L4	1.045	328	1.09	2.18
V2	1,145	370	1.23	2.46
V3	900	275	0.92	1.84
V4	780	189	0.63	1.26
F2	660	135	0.45	0.90
F3	1,230	403	1.34	2.68

[1] Midpoints of ranges given earlier in Table 24.

[2] Assumes truck is operated 6 days a week, 50 weeks a year.

[3] Assumes daily travel of 500 miles (805 km), or annual travel of 150,000 miles (241,500 km).

TABLE 27. CAPITAL COST AS A RANKING CRITERION

	Minimum Standard for Average Marginal Visibility					
	≥5%	≥10%	≥15%	≥20%	≥30%	≥50%
Increasing Annual Capital Cost ↓	M5 M4 P3 DI M2* F2 E2 M1 M7* V4 R1 M0* L3 G1* G2 V3* R2* L4 V2 F3* M6* L2 L1*	M5 M4 M2* F2 E2 M1 M7* V4 R1 M0* L3 G1* G2 V3* R2* L4 V2 F3* M6* L2 L1*	M4 M2* E2 M1 M7* V4 R1 M0* G1* V3* R2* L4 V2 F3* M6* L2 L1*	M2* M1 M7* M0* G1* V3* M6* L2 L1*	M2* M1 M7* M0* M6*	M7* M0* M6*
Cost Range	$41-810	$41-810	$54-810	$87-810	$87-420	$167-420

* As shown on Figure 133, one of the 10 most cost-effective systems.

of fuel savings offered under various operating conditions. One problem in assessing this factor, however, is the degree of variation across these different conditions. Several aspects are explored below.

Representative Marginal Fuel Costs. In order to highlight the key points, the fuel and other components of marginal cost* can be considered under a rather limited but representative set of wind, load, and terrain conditions:

- A cubed out truck operating on flat terrain with no wind, an average headwind, and an average 90 deg ambient crosswind (see summary in Table 28).
- An empty truck operating on flat, rolling, and mountainous terrain, with an average 90 deg ambient crosswind in each case (see Table 29).
- A weighted out truck operating on flat, rolling, and mountainous terrain, with an average 90 deg ambient crosswind in each case (see Table 30).

As can be seen in the three tables, only nine systems are listed. These systems correspond largely to those shown in Fig. 133 to have the highest benefit/cost ratios. The one exception to this statement is system M1, which has been deleted from consideration at this point because it has the same performance characteristics as M2 at a slightly higher capital cost.

Assumptions or conditions beyond those footnoted on the several tables include:

- Average hardware and maintenance costs and a unit fuel cost of $0.50/gallon ($0.13/L), i.e., economic condition Cell 2. (Fuel savings would, of course, increase proportionally with increases in unit fuel cost.)
- Maximum truck speeds of 60 mph (97 km/h) on flat and rolling terrain and 55 mph (89 km/h) on mountainous terrain.

Equilibrium truck speeds in the simulation were often lower than these maximums on rolling and mountainous terrains. Average road speeds and other data describing the movements are given in Appendix E of Ref. 5. Those AMV computer written tables also provide cost data on the balance of the 25 systems.

*Marginal cost is the cost difference between the basic truck and a modified truck.

TABLE 28. DAILY MARGINAL COST COMPONENTS AS A FUNCTION OF AMBIENT WIND FOR 9 MOST COST-EFFECTIVE SYSTEMS[1]

System	Zero Wind				Average Head Wind[2]		Average Cross Wind[2]	
	Oper. & Maint.	Travel Time	Fuel	Total[3]	Fuel	Total[3,4]	Fuel	Total[3,4]
M0	$0.57	$0.00	-$4.02	-$2.66	-$5.44	-$4.08	-$1.32	$0.04
M2	0.21	0.00	+0.04	0.53	+0.04	0.53	+0.04	0.53
M6	1.11	3.74	-3.96	2.29	-5.38	0.87	-9.18	-2.93
M7	0.39	0.00	-4.05	-3.12	-5.48	-4.54	-1.36	-0.42
R2	1.18	1.25	-4.26	-0.76	-5.76	-2.26	-1.89	1.60
G1	0.41	3.74	+0.02	5.03	+0.02	5.03	-0.97	4.04
L1	1.30	7.48	-3.98	7.48	-5.40	6.07	-11.18	0.29
V3	0.46	2.24	-1.61	2.01	-2.19	1.43	+1.16	4.78
F3	1.24	3.74	-3.97	2.35	-5.38	0.94	-9.18	-2.86

1 Cubed-out truck on flat road (i.e., 55,000 lb. or 25,000 kg, excluding weight of add-on devices). Assumes 500 mi. (805 km) of travel per day.
2 Wind velocity equal to national annual average of 9.5 mph (15.3 km/h).
3 Daily capital cost also included in total; see values in Table 26
4 Non-fuel marginal cost components same as for zero-wind case.

TABLE 29. DAILY MARGINAL COST COMPONENTS FOR EMPTY TRUCK AS A FUNCTION OF TERRAIN FOR 9 MOST COST-EFFECTIVE SYSTEMS[1].

System	Flat Terrain				Rolling Terrain		Mountainous	
	Oper. & Maint.	Travel Time	Fuel	Total[2]	Fuel	Total[2,3]	Fuel	Total[2,3]
M0	$0.46	$0.00	-$1.32	-$0.08	-$0.76	$0.49	+$0.04	$0.45*
M2	0.17	0.00	+0.04	0.50	+0.03	0.50	+0.04	0.50
M6	0.94	3.74	-9.18	-3.11	-5.45	0.62	-3.12	2.11*
M7	0.31	0.00	-1.36	-0.50	-0.79	0.07	+0.01	0.03*
R2	1.06	1.25	-1.89	1.48	-1.10	2.28	-0.17	2.36*
G1	0.39	3.74	-0.97	4.03	-0.58	4.42	-0.02	4.15*
L1	1.14	7.48	-11.18	0.13	-6.66	4.65	-3.95	6.52*
V3	0.37	2.24	+1.16	4.68	0.72	4.25	+0.59	4.11
F3	1.07	3.74	-9.18	-3.03	-5.46	0.69	-3.13	2.18*

1 90°, 9.5-mph (15.3-km/h) cross wind assumed; empty GVW nominally 25,000 lb (11,360 kg), excluding weight of add-on devices. Assumes 500 mi (805 km) of travel per day.
2 Daily capital cost also included in total; see values in Table 26
3 Non-fuel marginal cost components same as for flat-terrain case, except starred (*) totals refect a lower marginal travel time cost due to higher speed.

TABLE 30

DAILY MARGINAL COST COMPONENTS FOR WEIGHTED OUT TRUCK AS A FUNCTION OF TERRAIN FOR NINE MOST COST-EFFECTIVE SYSTEMS[1]

System	Flat Terrain				Rolling Terrain		Mountainous	
	Oper. & Maint.	Travel Time	Fuel	Total[2]	Fuel	Total[2,3]	Fuel	Total[2,3]
M0	$1.76	$0.00	-$1.15	$1.38	-$0.16	$2.38	+$0.28	$2.81
M2	0.57	0.00	+0.08	0.93	+0.08	0.93	+0.08	0.94
M6	2.92	3.70	-6.85	-0.85	-3.12	2.14*	-0.82	7.18
M7	1.21	0.00	-1.24	0.52	-0.24	1.52	+0.19	1.95
R2	2.46	1.23	-1.70	3.05	-0.40	4.35	+0.22	4.98
G1	0.56	3.68	-0.94	4.15	-0.45	4.64	-0.12	4.97
L1	2.90	7.39	-10.86	2.10	-3.93	5.45*	-1.18	11.77
V3	1.44	2.21	+1.27	5.83	+0.85	5.41	+049	5.05
F3	3.0	3.70	-8.86	-0.84	-3.13	2.15*	-0.84	7.19

[1] 90°, 9.5-mph (15.3 km/h) cross wind assumed; "weighted-out" GVW is 80,000 lb (36,360 kg), including weight of add-on devices. Assumes 500 mi (805 km)/day.

[2] Daily capital cost also included in total; see values in Table 26.

[3] Non-fuel marginal cost components same as for flat-terrain case, except starred (*) totals reflect a lower marginal travel time cost due to higher speed.

Changes in Fuel Economy. Table 31 presents percentage changes in total fuel consumption for the nine systems favored across all categories in Fig. 133. The conditions represented correspond directly with those used in Tables 28-30, above. Taken together, Tables 28-31 show that:

- Systems employing both a drag shield and a longitudinal baffle (i.e., M6, L1, and F3) show excellent fuel savings under all conditions examined. These range from about 3 percent for a heavy truck on mountainous terrain to over 40 percent for an empty truck on flat terrain (average ambient crosswind in both cases). In terms of dollar savings, this corresponds to a range of about $1-10/day.

- Systems employing a drag shield but no longitudinal baffle (i.e., M0, M7, R2, and V3) perform best with no wind or a headwind. With the exception of V3, typical fuel economy improvements range as high as 12 percent, equivalent to a saving of $5-6/day.

TABLE 31

PERCENTAGE IMPROVEMENTS IN FUEL ECONOMY FOR 9 MOST COST-EFFECTIVE SYSTEMS[1]

System	By Ambient Wind[2]			By Terrain, Empty[3]			By Terrain, Weighted[3]		
	Zero	Head Wind	Cross Wind	Flat	Rolling	Mtns.	Flat	Rolling	Mtns.
M0	10.3	12.0	2.1	3.0	1.8	-0.0	0.0	0.0	-0.0
M2	-0.0	-0.0	-0.0	-0.0	-0.0	-0.0	-0.0	-0.0	-0.0
M6	10.3	12.0	21.3	32.8	14.5	7.8	15.8	5.3	2.7
M7	10.3	12.0	2.1	3.0	1.8	-0.0	0.0	0.0	-0.0
R2	12.1	12.0	4.3	4.5	3.6	2.0	2.6	0.0	-0.0
G1	-0.0	-0.0	2.1	3.0	1.8	0.0	0.0	0.0	0.0
L1	10.3	12.0	25.5	41.8	18.2	9.8	18.4	7.9	2.7
V3	3.4	4.0	-2.1	-3.0	-1.8	-0.0	-2.6	-0.0	-0.0
F3	10.3	12.0	21.3	32.8	14.5	7.8	15.8	5.3	2.7

1 "+" is an improvement and "–" is a degradation in fuel economy; signs apply even to "0.0," since this value is less than ± 0.5.

2 "Cubed out" modified truck on flat highway.

3 90 deg, 9.5 mph (15.3 km/h) crosswind assumed.

- Systems employing neither a drag shield nor a longitudinal baffle (i.e., M2 and G1) show very little, if any, fuel savings. Only G1 demonstrated a small saving, and only under a crosswind condition on flat or rolling terrain (2-3 percent, or \$0.50-1.00/day).

Ranking by Dollar Fuel Savings. The nine cost-effective systems (from Fig. 133) are ranked in Table 32 in a manner similar to that described in the preceding section on capital costs. All nine systems provide a marginal visibility of at least 15 percent under the average headwind and crosswind cases used. Within each of the four columns, representing alternative levels of marginal visibility, the systems are listed in order of decreasing dollar fuel savings under the stated ambient wind condition.

TABLE 32. FUEL SAVINGS AS A RANKING CRITERION

Wind	Marginal Visibility Level			
	≥15%	≥20%	≥30%	≥50%
9.5-mph Head Wind	R2 M7 M0 L1 F3 M6 V3 G1 M2	M7 M0 L1 M6 V3 G1 M2	M7 M0 M6 M2	M7 M0 M6
9.5-mph Cross Wind[1]	L1 F3 M6 R2 M7 M0 G1 M2 V3	L1 F3 M6 R2 M7 M0 G1 M2 V3	L1 M6 M7 M0 M2	M6 M7 M0

Decreasing Fuel Savings[2] ↓

[1] i.e., Absolute wind direction of 90°
Note: 1 mph = 1.61 km/h.

[2] Based on "cubed-out" truck operating on flat terrain; see Table 28.

4. Illustrative Results for Real-World Scenarios

As discussed in Article C.4, above, five so-called real-world scenarios were developed to allow the estimation of benefits and costs over trucking circuits between actual U.S. cities. These circuits were described geographically in Fig. 132 and Table 26. The truck loading assumed by trip leg is further detailed by AMV in Appendix C of Ref. 5, which is also useful in correlating prototypical and "real world" results on the basis of similar trip leg characteristics.

Overall Results. Table 33 shows some illustrative results of the cost-effectiveness simulation for the "real world" scenarios. The three aerodynamic and splash and spray systems chosen for this presentation are:

TABLE 33

ILLUSTRATIVE RESULTS FOR "REAL WORLD" SCENARIOS[1,2]

Scenario	Geographical End Points of Trip Leg (See Fig. 132)	Distance Traveled (Miles)	M2 ($315 Init. Cost) Marginal Visibility (%)	M2 ($315 Init. Cost) Total Marginal Cost ($/Trip)[3]	M7 ($730 Init. Cost) Marginal Visibility (%)	M7 ($730 Init. Cost) Total Marginal Cost ($/Trip)[3]	M6 ($1,305 Init. Cost) Marginal Visibility (%)	M6 ($1,305 Init. Cost) Total Marginal Cost ($/Trip)[3]
National (NA)	Raleigh, N.C. → Los Angeles	2,550	45	8.47	73	-9.02	73	17.54
	Los Angeles → San Francisco	380	37	0.70	57	0.02	57	0.23
	San Francisco → Philadelphia	2,850	37	5.17	57	2.47	57	38.27
	Philadelphia → Raleigh, N.C.	390	46	0.72	70	1.01	70	1.55
	Full Circuit (& Avg. Mar. Vis.)	6,170	41	15.06	64	-5.52	64	57.59[4]
North Central (NC)	St. Louis → Denver	860	47	0.88	73	-6.16	73	2.79
	Denver → Chicago	1,000	37	1.20	57	-2.90	57	7.00
	Chicago → St. Louis	290	46	0.54	70	-0.04	70	-0.79
	Full Circuit (& Avg. Mar. Vis.)	2,150	42	2.62	65	-9.10[5]	65	9.00
South-East (SE)	Jacksonville → Montgomery	345	41	0.64	63	-0.87	63	2.63
	Montgomery → Mobile	170	46	0.31	70	-0.03	70	0.56
	Mobile → Jacksonville	410	37	0.42	57	-1.17	57	3.13
	Full Circuit (& Avg. Mar. Vis.)	925	40	1.37	62	-2.07	62	6.32
South-West (SW)	El Paso, TX → Phoenix	400	37	0.44	56	0.54	56	4.26
	Phoenix → Socorro, NM	385	24	0.72	37	1.31	37	6.28
	Socorro, NM → El Paso TX	190	46	0.35	70	0.58	70	1.90
	Full Circuit (& Avg. Mar. Vis.)	975	34	1.51	51	2.43	51	12.44
Intra-State (IS)	Salem, OR → Portland	45	37	0.10	57	0.11	57	0.31
	Portland → Madras, OR	115	37	0.17	60	0.18	60	1.09
	Madras, OR → Bend, OR	45	46	0.06	70	0.02	70	0.25
	Bend, OR → Salem, OR	130	34	0.18	52	0.00	52	0.94
	Full Circuit (& Avg. Mar. Vis.)	335	37	0.51	58	0.31	58	2.59

1 Source data in Appendix G of Ref. 5. Note: 1 mile = 1.61 km.

2 Positive figures indicate additional marginal trip costs and negative figures indicate a marginal trip cost savings.

3 Assumed fuel cost is $.50/gal ($.13/l).

4 If fuel cost is $1.00/gal ($.26/l), the marginal trip cost would be reduced by $24.07 to $33.52.

5 If fuel cost is $1.00/gal ($.26/l), the marginal trip cost would be reduced by $11.15 to a trip savings of $20.24.

- Among the four most cost-effective systems on an overall basis (refer to Table 22).
- Among the five systems providing an average marginal visibility of 30 percent or greater (see Tables 27 and 32).
- Potential extensions of the basic M2 Reddaway flap system, i.e., M7 adds a drag shield to M2 and M6 adds both a drag shield and a longitudinal baffle. Hence, they represent a good range of both drag/fuel consumption effects (refer to discussion in preceding article) and initial (or threshold) costs (see Tables 18 and 26 for more detailed data).

The full set of "real world" simulation results is presented by AMV in Appendix G of Ref. 5. These printouts describe in detail the operating conditions, truck loading, and marginal costs and benefits for all 25 evaluated systems. Average hardware and maintenance costs were assumed for all runs, as was a unit fuel cost of $0.50/gallon ($0.13/L), i.e., Cell 2 economic conditions.

The results are discussed by scenario in the following paragraphs.

National. The three systems yielded a wide range of marginal costs, with M7 clearly the best due to fuel savings on the westbound (headwind) leg. If initial system installation cost were a concern for a large fleet, however, M2 would be a close second with a relatively modest marginal cost of $15 for over 6000 miles (9700 km) of travel.

Since many cross-country trucks are already equipped with drag shields, the addition of the Reddaway flaps of the M2 configuration (net initial cost of $415) would yield System M7. Providing a very substantial marginal visibility of 64 percent, this would be an attractive option for national service.

North Central. On this mid-range circuit of 2150 miles (3460 km), all three systems would provide good service at a reasonable cost. Although M7 and M2 still rank better than M6, the latter would be a good option if normal operations in the plains states also involve a significant amount of north-south (crosswind) travel.

Southeast. On a marginal cost basis, these results are quite similar to those for the longer North Central scenario. However, Table 20 shows significantly heavier rainfall in the Gulf Coast states. Therefore, serious consideration should be given to using M7 or M6 with their superior marginal visibility. For trucks operating up and down the Florida peninsula or Atlantic seaboard, where a crosswind prevails much of the time, M6 might be preferred because of the significant potential fuel savings.

Southwest. In contrast, the Southwest scenario is characterized by mountainous terrain and much lower rainfall. All three systems were found to have positive marginal costs, due to the fact that the drag reduction effects of the add-on devices are less consequential in a situation where grade resistance is such a large fuel consumption factor. System M2 would probably be preferred for trucks limited to this operating environment.

Intrastate. Since the intrastate route chosen in Oregon incurs very frequent rain to the west of the Cascade Mountains, M7 or M1 would be strongly preferred over M2. Also, for trucks operating primarily in the crosswinds of the Willamette Valley (I-5), System M6 with its longitudinal baffle would offer substantial potential fuel savings.

SECTION VIII

CONCLUSIONS AND RECOMMENDATIONS

The overall objective of this program has been to develop methods to minimize the adverse effects of truck aerodynamics and splash and spray. These adverse effects include those related to truck operations, such as economy; and to the influence of the truck on an adjacent motorist, passing or operating in the vicinity. As detailed in prior sections, our approach in Phase 1 has been to better understand the problem by a combination of analyses and experiments, and then to interpret the results in terms of vehicular operations on the highway. As a result, methods have been identified and studied which have the potential to reduce significantly the presence and influence of the adverse effects of said aerodynamic, splash, and spray factors.

The results and interpretations of those analyses and experiments are summarized in this section to form the conclusions and recommendations for Phase 1. The discussion is organized in accordance with the preceding sections, to present conclusions with respect to the following:

- Aerodynamics
- Splash and spray
- Driver/vehicle performance
- Cost-effectiveness

The contractually required "list of probable techniques" is also included, together with recommendations for over the road evaluation in Phase 2.

A. AERODYNAMIC EFFECTS

Aerodynamic factors can be divided into two categories for convenience of discussion, those related to truck operations, mainly drag, and those involving the force and moment disturbance of the adjacent car.

1. Truck Alone

Most tractor plus semitrailer combinations are similar in overall size and shape, since they are legally constrained. As a result, aerodynamic differences which can occur tend to be small. An understanding of the gross flow properties can help to interpret the aerodynamic results and conclusions, as noted below.

Due to the boxy, bulky shape of the typical semitrailer, for zero crosswind there is always a typical subsonic base separation region at the rear face. Whether the flow is separated along the sides depends upon the length of the trailer, and on the details of the corners of the front face, as well as whether devices have been installed on the tractor or semitrailer.

The flow around the front of the truck varies somewhat depending upon the design of the tractor. A significant flow aspect from the points of view of aerodynamics and splash and spray is the pronounced downard flow through the gap between the tractor and semitrailer. This flow generally increases with increase in gap distance. Drag reducing shields mounted on the semitrailer roof can significantly alter this flow, also, and can eliminate the downward vertical component if the shield is appropriately sized for the proportions of both the gap and the step height. The latter is the difference in height between the tractor and semitrailer roofs.

Considering the flow streamlines for the case of a crosswind, a distinctly different aerodynamic situation occurs. At angles exceeding about a 10 deg relative crosswind there is massive separation not only at the base and behind the tractor, but also on the lee sides of both the tractor and the semitrailer. Although the flow is very complicated, and specific details vary for different geometries, the important result is that in all cases near the wheels, on the lee side there is a major volume of separated flow. Variables which change this significantly include the size of the gap and any gap sealing devices, the rounding of the side edges of the van semitrailer, changes in semitrailer type (e.g., van vs. tanker), the effects of a drag-reducing shield on the tractor, and the mounting of an underbody baffle. Although it does affect the flow around the tractor tandems, removing the gap, either by moving the tractor close to the semitrailer face, or by adding a gap splitter panel as a gap sealer, does not greatly affect the large turbulent separated area in the lee of the semitrailer in a crosswind. This is largely because of the strong three-dimensional effects on the separated flow moving over the top and bottom of the rig.

Drag data for the various types of trucks were presented in Section V, and the highlights can be summarized as follows. The CBE results did not differ particularly from those for the COE, with no crosswind, and this is confirmed in the literature. Adding trailers to create double and triple combinations adds a relatively small drag effect in comparison to the increase in cargo capacity, for the no crosswind case. The drag effect of longer combinations in a strong crosswind is more pronounced, as would be expected, but the drag still does not increase in direct proportion to size or length. Upon shortening the gap between tractor and semitrailer, the drag with no crosswind was essentially unchanged, while with a relative crosswind the shorter gap resulted in a reduced effective drag. Rounding the leading edges of the semitrailer decreased the drag slightly with no crosswind, and produced a reduction in the drag in the crosswind case of nearly 20 percent. The addition of a tractor-mounted drag shield reduced the drag by about 20 percent in the no wind or headwind condition. The drag shield is relatively ineffective with a crosswind condition, however. In general, for the basic truck the aerodynamic drag increased substantially for relative crosswind angles of about 20 deg or greater. The increase can be about as much as 70 percent for such a crosswind. Of all the devices tested, the longitudinal baffle under the semitrailer or the longitudinal baffle plus the gap splitter panel were the only ones to show a significant reduction in the crosswind drag. With both devices mounted, the drag in the 20 deg crosswind reduced to the value of the basic truck in the no crosswind case. With only the longitudinal baffle under the semitrailer, the drag increase in the 20 deg crosswind was only about 15 percent, instead of the 70 percent increase noted above for the basic truck. The wind tunnel results showed that the angled side vanes around the wheels (designed to reduce splash and spray) could actually increase the drag significantly, if they were not mounted and adjusted in an appropriate way.

Other forces and moments were measured on the truck models as a function of relative crosswind angle. Of most interest were the side force, and yaw and roll moments. The longitudinal baffle had a very significant effect on the side force ($C_{y_{\psi_W}}$) and roll moment ($C_{\ell_{\psi_W}}$) coefficients, as would be expected. The gap splitter panel changed the sign of the yaw derivative, although the side force coefficient increased in magnitude only a small amount. This change in the yaw derivative could lead to a more sensitive crosswind gust response, particularly with a lightly loaded truck (neglecting articulation dynamics). The shorter gap (30 in., 0.76 m) resulting from the gap filler block lead to a similar trend. The coefficients vary quite a bit for the other truck configurations, and the differences are what would be expected from overall geometry and shape factors.

2. Adjacent Car Disturbance

The force and moment data on the adjacent car were measured for various truck configurations. In general the data had a similar form to that resulting from flow around the basic truck, as measured in prior studies. The more interesting variations which did occur are discussed below.

With the tractor plus flatbed combination the data differ in the region of the semitrailer as would be expected. With the flatbed and no crosswind, the flow converges behind the tractor, modifying the side force and yawing moment on the car, by comparison to the basic truck case. The crosswind data are different alongside the semitrailer, but the effect is not large. The presence of the unloaded flatbed still causes a shadowing effect, probably because the top of the truck bed is nearly as high as the top of the car.

Comparison between the basic truck and the liquid cargo tanker, in terms of the force and moments on the adjacent car, showed that the disturbance effect was quite similar in the no crosswind case. With a crosswind, there were some differences in the region around the gap and the tractor tandems, probably due to the more open nature of this part of the tanker semitrailer. The basic truck with its box type van sits more closely on the top of the wheels.

Comparing the CBE (conventional) and COE tractors shows that the level of the bow wave is reduced with the former. In a crosswind there are minor differences alongside the CBE tractor which are attributable to the longer cab and shorter gap with the conventional configuration. Overall, however, the differences in the adjacent car disturbance between the CBE and COE are minor.

Contrasting the 3 axle COE plus 40 ft (12.2 m) van, the basic truck, with the 2 axle COE plus 27 ft (8.2 m) van, the basic effect in the data is the expected foreshortening. The variation in the side forces alongside the truck have similar form and magnitudes but they occur over the corresponding shorter distance. The yaw moment curve shows about half the peak to peak variation along the rear part of the semitrailer, and gives a smoother variation along the forward part of the truck, also. This reduction in disturbance is probably due to the shorter gap and changes in the wheel spacing.

In the 2 axle COE plus double van combination, there is little effect of the presence of the semitrailer-trailer gap in the no crosswind case. With a crosswind, the disturbance at the gap between the trailers is similar to that which occurs at the rear of the tractor. The overall wake effect, then, occurs at the rear of the second semitrailer. Considering the change in form due to the different semitrailer lengths, the peak to peak adjacent car excursions with the doubles rig are about the same as for the basic truck.

Comparing the dry cargo tanker with the basic truck, there is little difference in the no crosswind case. With the car downwind in the crosswind case, the differences are still minor except for a small shift related to the reduced length of the example dry cargo tanker, compared to the basic semitrailer.

The forces and moments on the adjacent car in the presence of the basic truck outfitted with various devices were also studied. With the exception of the longitudinal baffle, the changes in the adjacent car disturbance due to the devides were minimal. The longitudinal baffle did have a substantial effect on the wake flow and hence on the disturbance in a crosswind, with the car in the lee of the truck. Correlations with prior results indicate that this would degrade driver/vehicle performance in the crosswind case. The result is not unlike that which occurs with a "moving van" underbody on the semitrailer, which drops closer to the ground and causes more crossflow shadowing.

Overall, fairly large changes in truck configuration resulted in only detailed variations in the force and moment disturbance of the adjacent car. It is clear that the main disturbance effect is caused simply by the overall size and bulk of the truck. As a result, the most significant effects result from changes in semitrailer length or adding additional trailers. The results of prior studies indicate that the detailed changes which occurred would not have much effect on overall driver/vehicle system performance. By comparison, fairly major changes in adjacent car performance result from variations in such things as car and truck speed and the relative wind geometry, as discussed in Section III.

B. SPLASH AND SPRAY EFFECTS

The process of spray formation is discussed in Section III based on the detailed development in Ref. 4. The discussion shows that there are four primary mechanisms for water ejection by a tire. These include the bow and side splash waves, tread pickup, and capillary adhesion. All four are functions of tire speed, road water depth, and tire tread depth. Based on the qualitative results available, a simple model was constructed to describe splash and spray generation by a single wheel. In this model the bow wave accounted for about 10 percent of the water mass flow, and each side wave accounted for about 45 percent of the water mass flow, or roughly half the remaining. Capillary adhesion comprised only about 1 percent of the tread pickup.

The single wheel model results, together with the data from the full scale laboratory tests, were used to estimate water flow and dispersion for the complete truck. The results are given in Section III, and they show that about 75 percent of the water encountered by the steered wheels is transported into the tractor tandem duals as tread throw, and this is combined with the additional water flow into the other tire of the duals. Most of the water flowing into the tractor tandem duals is dispersed by them, either as side wave or tread throw, and only about 10 percent of the water encountered by the tractor tandem wheels carries back into the tandem duals of the semitrailer. This further confirms the importance of the tractor axles, in particular the leading axle of the tractor tandem duals, as a major source of splash and spray.

To complete the analytical understanding, these spray stream mass flows were used by AVI as the source strengths for the spray dispersion analysis. It was based on the Pasqual-Gifford diffusion relations, with the mean and turbulent wake flow velocities and spray source strengths estimated on the basis of analysis and the full scale data. The resulting model was used to compute spray droplet behavior and dispersion in the plumes downstream of the spray sources on the truck. The results were presented graphically for various locations around the truck and various ambient wind conditions in Ref. 4, and examples are given in Section III. In general, these analytical results were in good agreement with the spray-related visibility measures obtained during the June and November full scale tests. The resulting procedure is a tool that can be used to make initial estimates of changes in the spray patterns due to the installation of devices which could either change the source strength or modify the mean wake flow properties.

From the standpoint of the adjacent driver, splash and spray has been quantified and interpreted in terms of its effect on visibility. Based on results of the June tests, the several different tractor/semitrailer configurations were shown to create similar visibility levels in the adjacent lane on the average. This was true for both the raw downwind laser data and for the scaled visibility values, considering all the available results. In the raw data with the car downwind, the visibility with the CBE (conventional) tractor was somewhat better on the average than that for the COE tractor, for a given semitrailer configuration. The scaled results showed less difference due to tractor type. Overall, the differences between the different truck configurations were on the order of 5 visibility percentage points. Since this is about the resolution accuracy that can be obtained with such visibility measures, it can be concluded that there were not substantial differences across the truck types in their current configurations. Put another way, the improvement in visibility that was achieved with various splash and spray and aerodynamic devices was substantially greater than the variations seen among the different basic truck configurations. As an exception to this general finding, the basic truck consisting of the 3 axle COE plus the 40 ft (12.2 m) van generally showed somewhat lower visibility values. This probably does reflect an adverse influence due to the size and shape of that semitrailer compared to the other configurations tested.

Visibility results were shown in Section VI in terms of both the raw data (with the sensors downwind) and the scaled visibility values. These raw and scaled results are generally in good agreement. This demonstrates, first, that most of the data were obtained for conditions nearer the reference scaled values and, second, that the scaling procedure is a relatively conservative one. In general, the ranking for most of the better devices was largely unaffected by the scaling process.

Overall, the visibility results showed that the most effective devices are the Reddaway collector fenders with the drag shield (M0 and M7). The Reddaway system plus the drag shield plus the longitudinal baffle (M6) was equally effective. Somewhat less effective were the Reddaway fender systems without the drag shield (M1 and M2). Of the other systems tested, the following showed substantial improvement over the basic truck, but not as much as the Reddaway system:

- Roberts fender (R2)
- Gap filler panel in the upper position (G1)
- Longitudinal baffle, with either or both of the gap splitter panel or drag shield (L1, L2, or L4)
- Angled side vanes (V3 or V4)
- Fuzzy truck with either the drag shield or the longitudinal baffle (F2 or F3)

Adding the longitudinal baffle to the Reddaway fenders was estimated to have excellent potential as an alternative. The data show that the fuzzy truck with the drag shield is fairly effective, and the results suggest that adding the longitudinal baffle would give further improvement. The European fender was shown to be competitive with the simpler Reddaway configurations, that is, the ones without the very important Reddaway side skirt. The European fender was similar in visibility performance to some of the better aerodynamic devices such as the gap filler panel, the angled side vanes, and the partial gap panel.

The drag shield alone on the basic truck provided only a small improvement. Yet, when coupled with some of the collector-type devices it gave a marked improvement in the overall visibility, for reasons discussed in Section IV. The drag shield also complemented the underbody baffle. It did not help much with other devices that tend to modify the gap flow, such as the gap filler panel, partial gap panel, and quarter fenders at the front of the tractor tandems.

Overall, the visibility results in Section VI showed that several kinds of devices and approaches have good promise for alleviating the effects of splash and spray on the adjacent motorist. At the same time, some of the ideas were not particularly useful, and even resulted in greater amounts of spray than the basic truck. The visibility results presented in Section VI were a primary input to the cost-effectiveness analyses in Section VII, and they also comprise an important input to planning for the over the road assessments in Phase 2, as noted subsequently.

C. PERFORMANCE OF ADJACENT DRIVER/VEHICLE

Variations in adjacent driver/vehicle system performance with changes in the commercial vehicle configuration, and the geometry of the situation, have been studied in detail in past research studies, as discussed in Section III. The results given there show that good correspondence can be achieved between empirically based analytical calculations and corresponding full scale vehicle response and performance data. In general, the situations can be divided into: 1) zero crosswind cases; and 2) those cases involving a substantial relative crosswind with the disturbed car downwind of the truck or other commercial vehicle. The consequences of these two situations are summarized below.

1. Zero Crosswind Case

With zero crosswind the principal disturbance results from the flow around the bluff front of the truck. Typically, that disturbance results in a small deviation of the driver-controlled adjacent car, typically about 1 ft (0.3 m) peak value. Gross changes in truck shape, including streamlining of the tractor, have a relatively minor influence on adjacent car performance. On the other hand, changes in car and truck speed can have a large effect due to the increase in the aerodynamic forces and moments resulting from the higher dynamic pressure, q. Variations in the lateral separation of the car and truck can also change the magnitude of the performance deviation, with closer clearances resulting in a larger displacement of the car in the direction away from the truck.

As would be expected, large, low density passenger vehicles such as vans and campers are more affected by the truck disturbance than conventional sedan configurations. Cars towing trailers are particularly susceptible to the truck-induced aerodynamic disturbance. The resulting response and performance of these types of vehicles are influenced by both their aerodynamic properties and their directional handling properties.

2. Crosswind Case

In the crosswind case, with the car downwind of the truck, the ambient wind is shadowed and blocked by the presence of the truck as the car passes alongside. This can result in a larger peak lateral position excursion. Typical peak magnitudes can be as much as 2 to 3 ft (0.6 to 0.9 m) towards the truck, as shown in Refs. 2 and 3. Changes to the truck configuration which cause more crossflow blockage, such as with a moving van underbody or the incorporation of a longitudinal baffle, can increase the peak deviation of the car/driver system even more.

Results in Ref. 3 obtained with both a rectangular block (no underbody clearance), and representations of the truck with van underbodies extending nearly to the ground show peak deviations of about 4.5 ft (1.5 m). The longitudinal baffle aerodynamic data are closely analogous to the moving van underbody results previously obtained in Ref. 2. The adjacent car response in the crosswind is dominated by the wake effect which results from the truck blocking the flow. The main disturbance is large and of lower frequency, and this causes the greater path deviation.

Variations in car-truck centerline separation have less effect on the disturbance magnitude with a crosswind than they do in the zero crosswind case. The magnitude of the relative wind angle is also important. For relative angles less than about 5 deg the behavior is close to that of the zero crosswind case. As the relative angle increases above about 10 deg with the car downwind, then the flow transitions to the dominant crosswind case. In addition, varying the relative speed of the car and the truck can have a substantial effect on performance with the worst results obtaining for both vehicles traveling at high speeds with a relative velocity difference on the order of 5 mph (2 m/s).

3. Car and Truck Oncoming

With the car and truck oncoming, the disturbance on the total car is somewhat less than for the crosswind case. This is because the relative speed is very high, and the resulting aerodynamic disturbance, although an intense pulse, has a short duration. This, in turn, results in a relatively small lateral deviation. As noted in Section III, the median on most modern highways further increases the separation and reduces the disturbance effect due to oncoming vehicles.

4. Preliminary Simulator Results

Tests were run on the STI Driving Simulator early in the program to make a preliminary study of the effects of visibility changes on driver performance, and to gain a further understanding of the important visual cues. Related to this was an interest in trying to identify important spray cloud shapes and patterns and to further develop potential visibility and performance measures for use in the full scale splash and spray experiments.

Overall, the driving simulator results showed that system performance, as measured by the lateral lane position, was not significantly impaired under the combinations of visibility and aerodynamic disturbance conditions would could be used. The response variables of yaw velocity and lateral acceleration did show minor effects resulting from changes in the aerodynamic disturbance amplitude, as would be expected.

The driver evaluations of accident risk showed that a large aft cloud, which obscured visibility before the driver encountered the truck, did result in substantially poorer ratings. The ratings were also quite sensitive to the aerodynamic disturbance magnitudes, and this tended to accentuate visibility differences in an interactive sense. Task difficulty ratings showed similar results. Overall, the subjective ratings were more sensitive to changes in the visibility and disturbance conditions than were the objective performance results.

The simulator results showed that spray cloud length behind the truck had a significant visibility effect. This helped to focus attention on means to minimize the spray cloud length in the adjacent lane. The measured interaction between visibility effects and the aerodynamic disturbance level also underscored the importance of minimizing the aerodynamic disturbance, particularly in the crosswind cases.

5. Connections Between the Measures

To codify splash and spray data interpretation and comparison, it was useful to relate the several measures available to one variable, which could then provide the basis for analysis of experimental effects. This was done, and the result was that the visibility transmissivity of the laser at 2 ft (0.6 m) provides an index that is selective, representative, and parametrically well behaved, as detailed in Section VI.

Specifically, there was a strong correlation between measures made by the laser at 2 ft (0.6 m) and the laser at 6 ft (1.8 m), and between the laser at 2 ft and the photometer, for both upwind and downwind conditions. Hence, the laser and photometer results were shown to be relatable, and we could choose the laser at 2 ft to be a correlating dependent variable, for convenience.

The laser and photometer results were also correlated with the performance of the adjacent car/driver, and with the trackside observer and adjacent driver ratings. These correlations suggest that the 2 ft laser is viewing that portion of the lane, and the splash and spray cloud, to which the observer is most sensitive; and that the 2 ft laser measures correlate well with driver perceived highway visibility properties also. The path performance of the adjacent car also correlates with the visibility in an inverse way, with reduced visibility resulting in poorer performance, as reflected in larger mean square lane deviations. Interesting, too, is the fact that the driver performance remains fairly constant until the visibility reduces to about 30 percent, as measured by the 2 ft (0.6 m) laser values. Then the performance began to degrade markedly. By contrast, the driving simulator results did not show a degradation in performance, suggesting that perhaps the visibility conditions, coupled with the total task scenario in the simulator, were not as severe as the more critical cases encountered in the full scale tests.

Overall, the results demonstrate that adjacent driver/vehicle performance and visibility are related, and that the latter can be used as a surrogate for the former in assessing the effect of changing the effect of truck configuration or incorporating devices to alleviate splash and spray. It is also shown in Section VI that, while performance and rating each vary with visibility, they do not covary. This suggests that their respective variations with visibility relate to different factors or elements in the overall situation, which further supports the conclusion that visibility values are the pertinent objective figures of merit.

D. COST-EFFECTIVENESS

Operating scenarios have been defined as a combination of ambient wind condition, truck loading, and severity of terrain. Using these scenarios, the various truck plus device configurations have been evaluated in terms of their cost and their potential for alleviating the adverse visibility effects of splash and spray. The results are summarized in Section VII, based on the detail in Ref. 5.

The cost-effectiveness analysis considered marginal costs and benefits related to the presence of the add-on devices. Included in the marginal costs were fuel, the capital costs of the add-on device, associated special operating and maintenance costs, and the cost of any travel time differential. These marginal costs were totaled and expressed in terms of a cost per ton mile. The marginal benefits were quantified in terms of the change in visibility or the visibility margin attributable to a given device, as determined in the full scale splash and spray tests and the subsequent data interpretation. This marginal visibility benefit was scaled for the wind conditions and the truck speed.

Truck weight was an important factor in this evaluation, also. This included not only the weight of the cargo, and considerations of cargo volume, but also the incremental weight change due to the presence of the add-on devices.

1. Overall Results

The overall benefit to cost rankings for the truck plus device configurations analyzed by AMV were presented in Table 22 of Section VII. The results shown there can be highlighted as follows:

- The Reddaway systems and their variations ranked the highest. Note that the Reddaway systems without the side flaps were ranked relatively low, due to a combination of visibility and marginal cost factors.
- Systems with intermediate overall rankings were distributed among four other truck plus device categories. These include the longitudinal baffle, the gap filler panel in the upper position, the angled side vanes, and the Roberts fender.
- Economic condition had a relatively minor influence on the rankings. Seventeen of the 25 systems analyzed maintained the same rankings across all six economic cells, despite variations in assumed cost and fuel prices. The rankings of the other eight systems varied by no more than 1 to 4 places. The highest ranked systems were generally least affected by variations in the economic assumptions.

These ranking results were generally borne out and elaborated by the cost-effectiveness values discussed below.

The overall average values of the mixed unit benefit to cost ratios were presented in Table 23 of Section VII. Highlights include:

- Systems using a drag shield generally had higher B/C ratios with higher unit fuel costs, because of the resulting fuel savings. This included the Reddaway systems, the longitudinal baffle, the Roberts fender, and the fuzzy truck when run with the drag shield. This was not true with the angled side vanes where the drag shield is apparently unable to offset the drag penalty due to the presence of the side vanes. Although other marginal costs were considered, the one related to fuel appeared to be the most significant in these comparisons.

- Some of the differences which were seen in the average benefit/cost values were due to the presence of the longitudinal baffle under the semitrailer. This comparison was particularly evident for the cases with the longitudinal baffle and no drag shield, where the predominance of a crosswind component in the scenario is offset by the drag reduction provided by the baffle in a crosswind.

Although the benefit to cost ratio was structured to be especially sensitive to changes in benefit (visibility margin), some variation was evident across the six economic conditions, as noted. To minimize the possible influence of economic assumptions relating to fuel costs or the cost of hardware and maintenance, the benefit to cost ratios were averaged over the various economic conditions. The results were presented graphically in Fig. 133 of Section VII. That presentation confirmed the substantial superiority of the better Reddaway systems while at the same time demonstrating that viable alternatives exist in several of the other truck plus device categories.

2. Aerodynamic Factors

An interesting result of the truck aerodynamic measures and the subsequent analyses is that the air resistance power (drag) is a maximum for an ambient wind angle of approximately 60 deg and speed of about 10 mph (3 m/s). This fact is not generally recognized. When coupled with the result that the drag shield is relatively ineffective in such an ambient crosswind, one concludes that conventional solutions to the drag problem may not be as effective as they could be. This further suggests that the longitudinal baffle and gap splitter panel concepts should bear further investigation for their potential economic advantage, splash and spray aside. It should also provide some impetus for additional investigations of devices which might reduce the aerodynamic drag of the truck in typical crosswind conditions.

At the same time, cost-benefit analyses reflect the advantage of the longitudinal baffle in reducing the splash and spray for the motorist passing downwind of the truck. This combined effect would be even more dramatic except for the fact that the crosswind is often from the same side of the truck that the motorist is on, in which case the calculation shows only the reduction in the cost due to reduced drag and not the corresponding visibility benefit. A caveat here, of course, is the fact that the blocking of the flow under the semitrailer can worsen the force and moment disturbance of the adjacent car, as discussed above and in Section V.

The previous comments related to truck drag and fuel economy warrant some elaboration. Those systems which employ both a drag shield and the longitudinal baffle, such as M6, L1, and F3, show good fuel savings under all conditions examined. The least savings occurred with a heavy truck on mountainous terrain due to the low speeds involved, while the greatest improvement occurred with empty or lightly loaded trucks on flat terrain. Those combinations which used a drag shield but no longitudinal baffle, such as M7, R2, and V3, gave the best results with no wind or only a headwind. Fuel economy improvements in those cases were as high as 12 percent with typical loads and flat terrain, which is substantially less than the 40 percent which occurred with the lightly loaded truck on flat terrain. With neither a drag shield nor a longitudinal baffle mounted, the fuel savings due to other variations in drag were negligible. The gap filler panel did show a small savings under crosswind conditions on flat or rolling terrain.

Further appreciation for the aerodynamic effects on cost can be obtained by comparing the basic truck to one of the more effective aerodynamic and splash and spray configurations (M0). First, the average improvement in fuel economy due to the drag shield for the fully loaded case is less than 5 percent on level terrain. Further, it is less than 2 percent on rolling terrain and is negligible on mountainous terrain. This is due to the fact that the grades slow down the truck, which reduces the airspeed, and the fact that the drag shield is not effective in the 20 deg relative crosswind which is typical of the wind conditions resulting from the assumed scenarios and in the real world. Second, the difference in fuel consumption decreases as the wind speed increases with the exception of the pure headwind or no wind conditions. This is because the total fuel consumption goes up and the percentage improvement is less. Third, with the drag shield a marginal reduction in travel time is obtained on rolling terrain. The percentage savings in fuel consumption is increased for empty trucks with the drag shield, but that is the less typical case. Typically the travel time did not improve more than 1 or 2 percent with the drag shield, because the maximum speed of the truck was limited to 60 mph (97 km/h) on flat and rolling terrains, and to 55 mph (89 km/h) on mountainous terrain, in the calculations.

3. List of Probable Techniques

On the whole, the cost-benefit results and the supporting data suggest that the following truck device configurations warrant further development and possible over the road evaluation.

- M7 — Reddaway fender system, less flaps between the tandems, plus drag shield
- L1 — Longitudinal baffle + gap splitter panel + drag shield
- G1 — Gap filler panel in upper position
- V3 — Angled side vanes, less vanes behind the tractor tandems, or V4 with the trailer vane angles reset
- R2 — Roberts fender + drag shield
- F2 — Fuzzy truck + drag shield, or F3 which is the fuzzy truck + drag shield + longitudinal baffle

Although several other versions of the Reddaway system were superior to the other device approaches noted, only the one candidate, M7, has been listed here as representative of its design.

Other potential device combinations are considered in Sections IV through VII. The following points are pertinent to show some of the factors involved in selecting and assessing device combinations.

In combination L1, listed above, the gap splitter panel does not reduce the crosswind drag as much as the longitudinal baffle under the semitrailer, and the gap splitter panel does not contribute much to the visibility when the drag shield is present. As a result the gap splitter panel is the least important element of this configuration and it could be considered for deletion.

Regarding a possible Reddaway plus longitudinal baffle plus drag shield combination (M6), the first and last components have a big impact on the visibility, while the baffle and the drag shield have a big effect in reducing drag. Furthermore, the longitudinal baffle also helps the visibility. As a result, that complete combination would be attractive in a benefit-cost sense. However, to be conservative, the visibility estimate for M6 was assumed to be the same as M7, implying that the longitudinal baffle would probably have a negligible incremental effect on the already good visibility present in the Reddaway system plus the drag shield.

Alternatively, the fuzzy truck, plus the longitudinal baffle, plus the drag shield would have the same advantages noted for the Reddaway system, and it might be simpler to fabricate, install, and maintain. Again, the visibility value used for F3 was derived from a composite standpoint, as a conservative combination of the values from the fuzzy truck, plus the drag shield, plus the baffle data.

Although the presence of the drag shield on the Reddaway system showed a fairly dramatic increase in the visibility (20 percentage points), this improvement may be too optimistic for anything but such a flap system, where the source strength is sharply reduced by the presence of the collector fenders. For this reason, the presence of the drag shield on the basic truck was assumed to contribute a more conservative improvement of 5 percentage points in the visibility, reflecting the fact that the source strength can still be high when only the drag shield is added to the basic truck.

The attributes of the collector devices are discussed in Section IV. Based on the observations during the experiments in this study and their general design characteristics, the following additional comments can be made.

On the European fender the lips along the inside and outside edges extend down only about 80 mm. This may limit their effectiveness in trapping the side spray from the top of the tires. In addition, the water dripping off the underside of these fenders tends to recycle into the spray source. The clearance with the European fenders will ordinarily vary with load and suspension deflection.

The Roberts fenders have some disadvantages related to trapping side spray and the installation of chains. They are also reported to be susceptible to clogging by mud, snow, and ice under adverse conditions. Although not easily installed on the 40 ft (12.2 m) van semitrailer, they may be well suited to installation on more open designs such as liquid cargo tankers. For these latter kinds of trucks, special fenders are normally fabricated by the manufacturer, and these could be modified to provide some sort of water collector design such as the Roberts principle.

The Reddaway fender has been tested in various configurations and discussed at some length. One additional pointed noted in Section IV is that it may be desirable to extend the side flap downwards in the area between the tandems, perhaps a triangular shaped extension. This would tend to offset any possible effect of the lack of a double-sided flap between the tandems, and trap residual side spray between those wheels. The Reddaway fenders are well suited to mounting on box-like van bodies. They are rugged and flexible and do not interfere with either brake cooling or the installation of chains. They also do not appear particularly susceptible to clogging by ice, snow, and slush.

The fuzzy truck is still in the conceptual stage, but it would appear to have most of the performance features of the Reddaway type fender with additional practical advantages. By mounting directly to the underbody and components of the truck it does not interfere with access to the wheels, brake cooling air flow, and so forth. It would not modify the basic appearance or shape of the truck, which may be an important factor in obtaining owner and operator acceptance. Suitably designed it could be replaced periodically as it wears.

4. Regional Factors

Using selected real world scenarios, the cost-effectiveness study in Section VII considered regional effects across the national range of operating conditions. Using the Reddaway system plus drag shield as an example, the following regional results were observed:

- Nationally, the system showed good fuel savings on westbound legs (with predominant headwinds). Since many cross country trucks are already equipped with drag shields, the addition of the Reddaway flaps at a relatively nominal cost could provide a substantial increase in the cost-benefit from a splash and spray standpoint.

- In the North Central region the Reddaway system plus drag shield is estimated to provide good service at a reasonable cost. If normal operations in the plains states involved a significant amount of north-south (crosswind) travel then the addition of the longitudinal baffle to the basic Reddaway plus drag shield system could show further benefit.

- Results for the Southeast are similar to those for the longer North Central scenario. However, since there is significantly more rainfall in the Gulf Coast states, systems which show the greatest visibility improvement would tend to be favored, and the Reddaway version M7 falls in this category.

- In the Southwest the scenario is characterized by mountainous terrain and relatively little rainfall. As a result, the marginal cost differentials due to reduced drag are somewhat less because of the lower speeds in mountainous regions. At the same time, potential benefits due to splash and spray devices are less because of the reduced precipitation. Hence, both elements of the benefit to cost ratio tend to decrease. This suggests that the capital and maintenance costs would play a larger role, which should favor the simpler, more durable systems.

- In the assumed intra-state route, in Oregon, the Reddaway system plus drag shield (M7) is very favorable because the terrain is relatively flat and there is frequent rainfall in the area to the west of the Cascade Mountains.

In the regional investigation it was interesting to note that the best ranked systems were almost universally appropriate.

5. Recommendations for Phase 2

The work described in this report comprised Phase 1 of the subject contract, and it was the major effort. Nominal funds were available for a Phase 2, to involve field evaluation of the most promising devices and techniques.

It is recommended that the devices for evaluation in Phase 2 be drawn from the list in Article 3, above, with possible variations as suggested by the supporting discussion and data.

It should be recognized that the device concept found to be most promising from our studies, the Reddaway fender, is currently undergoing active development and promotion by the manufacturer. Systems have already been installed on hundreds of trucks. Drag shields are also relatively commonplace, and the results of this study should further encourage their use. So, in these regards, an effective approach to evaluation is simply to monitor ongoing operational activity, and collect related economic and operational data. It does not appear necessary to mount a separate field evaluation test program.

Some of the other possible devices require further prototype development and testing. Such activity is beyond the scope of Phase 2, for the most part. Rather, an effective course of action would appear to be to encourage truck and equipment manufacturers to undertake their own development programs, in view of the potential safety, public relations, and economic gains for the operators and the industry.

REFERENCES

1. "Reduction of Adverse Aerodynamic Effects of Large Trucks," Federal Highway Administration Contract DOT-FH-11-9165, Nov. 1976.

2. Weir, David H., Robert F. Ringland, Robert K. Heffley, and Irving L. Ashkenas, An Experimental and Analytical Investigation of the Effect of Truck-Induced Aerodynamic Disturbances on Passenger Car Control and Performance, FHWA-RD-71-3, Oct. 1971.

3. Weir, David H., Roger H. Hoh, Robert K. Heffley, and Gary L. Teper, An Experimental and Analytical Investigation of the Effect of Bus Induced Aerodynamic Disturbances on Adjacent Vehicle Control and Performance, Systems Technology, Inc., TR-1016-1, Nov. 1972.

4. Lissaman, P. B. S., et al., Methods of Reducing the Splash and Spray Hazard of Large Trucks, Final Report and Appendices (2 vols), AeroVironment, Inc., Rept. AVFR7149, 31 Mar. 1978.

5. Stimpson, William A., and Steven R. Shapiro, A Cost-Effectiveness Evaluation of Devices for Reducing the Adverse Aerodynamic Effects of Large Trucks, Alan M. Voorhees and Associates, Final Report on Subcontract S-1093-2 to Contract DOT-FH-11-9165, Aug. 1978.

6. Weir, David H., Roger H. Hoh, and Gary L. Teper, "Driver/Vehicle Control and Performance in the Presence of Aerodynamic Disturbances from Large Commercial Vehicles," Transportation Research Record, No. 520, Jan. 1974.

7. Flynn, Harold, and Peter Kyropolous, "Truck Aerodynamics," 1961 SAE Congress, Preprint 284A, Jan. 1961.

8. Kamm, Irmin O., et al., The Formation of Truck Spray on Wet Roads, Stevens Inst. of Technology, Davidson Lab Rept. R-1431, Apr. 1970.

9. Kamm, Irmin O., and Gilbert A. Wray, "Suppression of Water Spray on Wet Roads," SAE Transactions, Vol. 80, 1971, pp. 412-422.

10. "Stopping Splash and Spray," Heavy Duty Trucking, Nov. 1972.

11. Splash and Spray Characteristics of Trucks and Truck Combinations, Western Highway Inst., Research Committee Rept. No. 5, 1 May 1973.

12. Sherard, Thurman D., "Suppression of Vehicle Splash and Spray," SAE Paper 730718, Aug 1973.

13. Palmer, George M., and James B. Amy, "Model Tests of Drag and Spray Effects of Aerodynamic Modifications to Present Vehicles," Proc. of the NSF/DOT Conf. on Reduction of the Aerodynamic Drag of Trucks, NSF Rept. NSF-RA-N-74-191, Oct. 1974.

14. Kirsch, Jeffrey W., and William H. Bettes, "Feasibility Study of the S3 Air Vane and Other Truck Drag Reduction Devices," Proc. of the NSF/DOT Conf. on Reduction of the Aerodynamic Drag of Trucks, NSF Rept. NSF-RA-N-74-191, Oct. 1974.

15. Lissaman, P. B. S., and J. H. Lambie, "Reduction of Aerodynamic Drag of Large Highway Trucks," Proc. of the NSF/DOT Conf. on Reduction of the Aerodynamic Drag of Trucks, NSF Rept. NSF-RA-N-74-191, Oct. 1974.

16. Steers, L. L., et al., "Aerodynamic Drag Reduction Tests on a Full-Scale Tractor-Trailer Combination and a Representative Box-Shaped Ground Vehicle," SAE Paper 750703, West Coast Meeting, Seattle, Aug. 1975.

17. Brunow, C. L., An Evaluation of Truck Aerodynamic Drag Reduction Devices and Tests, Innocept, Inc., Dallas, Texas, June 1975.

18. Buckley, F. T., and W. S. Sekscienski, "Comparisons of Effectiveness of Commercially Available Devices for the Reduction of Aerodynamic Drag on Tractor-Trailers," SAE Paper No. 750704, Aug. 1975.

19. Lissaman, P. B. S., "Development of Devices to Reduce the Aerodynamic Resistance of Trucks," SAE Preprint 750702, Aug. 1975.

20. Buckley, F. T., C. H. Marks, and W. H. Walston, "Analysis of Coast-Down to Assess Aerodynamic Drag Reduction on Full-Scale Tractor-Trailer Trucks in Windy Environments," SAE Paper 760850, 1976 SAE Truck Meeting, Nov. 1976.

21. Marks, C. H., F. T. Buckley, and W. H. Walston, "An Evaluation of the Aerodynamic Drag Reductions Produced by Various Cab Roof Fairings and a Gap Seal on Tractor-Trailer Trucks," SAE Paper 760105, 1976 SAE Automotive Engineering Congress, Feb. 1976.

22. Daggerhart, J. A., An Evaluation of Several Techniques of Aerodynamic Drag Reduction for Tractor-Trailer Trucks, North Carolina State Univ., Dept. of Mech. and Aero. Engr., Aug. 1976.

23. Cooper, K. R., "A Wind Tunnel Investigation into the Fuel Savings Available from the Aerodynamic Drag Reduction of Trucks," DME/NAE Quar. Bull. No. 3, Ottawa, Oct. 1976, pp. 31-86.

24. Steers, L. L., and E. J. Saltzman, "Reduced Truck Fuel Consumption Through Aerodynamic Design," AIAA J. Energy, Vol. 1, No. 5, Sept.-Oct. 1977, pp. 312-318.

25. Maycock, G., The Problem of Water Thrown Up by Vehicles on Wet Roads, Transportation and Road Research Lab., TRRL Rept. No. 4, 1966.

26. Ritter, Thomas E., Truck Splash and Spray Tests at Madras, Oregon, Southwest Research Inst., Rept. AR-955, Oct. 1974.

27. Sandberg, U., National Swedish Road and Traffic Research Inst., Linkoping, Sweden, Unpublished communication to D. H. Weir, May 1978.

28. Highway and Vehicle Safety Report, Vol. 4, No. 12, Stamler Pub. Co., 13 Mar. 1978.

29. Heffley, Robert K., "Aerodynamics of Passenger Vehicles in Close Proximity to Trucks and Buses," SAE Paper 730235, Intl. Auto. Eng. Congress, Detroit, 8-12 Jan. 1973.

30. Brown, G. J., and Gerald Seeman, An Experimental Investigation of the Unsteady Aerodynamics of Passing Highway Vehicles, NHTSA Rept. DOT HS-800 671, May 1972 (see also SAE Paper 730234).

31. Johnson, Walter A., and David H. Weir, Flow Field Properties in the Vicinity of a Tractor/Semitrailer Truck, and Correlations with the Aerodynamic Disturbance of an Adjacent Vehicle, Systems Technology, Inc., TR-1016-3, Oct. 1972.

32. "Aerodynamics Disturbance Test Procedure Development," National Highway Traffic Safety Admin. Contract DOT-HS-7-01716, Sept. 1977.

33. Braun, Horst, More Recent Knowledge About Wheel Covers, Technical Univ. Braunshweig, Inst. for Vehicle Technology, Rept. 223, 1972.

34. Trott, M. W., The Suppression of Spray from Aircraft Wheels on Flooded Runways, British Defense Research Information Center, Rept. DRICBR-46379, 1975.

35. Pasquill, F., "The Estimation of the Dispersion of Windborne Material," Meteorology Mag., Vol. 90, 1961, pp. 33-49.

36. Gifford, F. A., "Use of Routine Meteorological Observations for Estimating Atmospheric Diffusion," Nuclear Safety, Vol. 2, No. 4, 1961.

37. Weir, David H., and Duane T. McRuer, "A Theory for Driver Steering Control of Motor Vehicles," Highway Research Record, No. 247, 1968, pp. 7-28.

38. Weir, David H., Fredrick R. Alex, and Robert F. Ringland, Driver Control During Overtaking and Passing Under Adverse Conditions, Systems Technology, Inc., TR-174-1, 1969.

39. McRuer, Duane T., and David H. Weir, "Theory of Manual Vehicular Control," Ergonomics, Vol. 12, No. 4, 1969, pp. 599-633.

40. Weir, David H., and Duane T. McRuer, "Dynamics of Driver/Vehicle Steering Control," Automatica, Vol. 6, No. 1, 1970, pp. 87-98.

41. Weir, David H., and Duane T. McRuer, "Measurement and Interpretation of Driver Steering Behavior and Performance," SAE Paper 730098, Jan. 1973.

42. McRuer, Duane T., and Ezra S. Krendel, Mathematical Models of Human Pilot Behavior, AGARD-AG-188, Jan. 1974.

43. McRuer, Duane T., and Richard H. Klein, Automobile Controllability — Driver/Vehicle Response for Steering Control. Vol. I: Summary Report. Vol. II: Supporting Experimental Results, NHTSA Repts. DOT HS-801 407 and HS-801 406, respectively, Feb. 1975.

44. McRuer, Duane T., R. Wade Allen, David H. Weir, and Richard H. Klein, "New Results in Driver Steering Control Models," Human Factors, Vol. 19, No. 4, Aug. 1977, pp. 381-397.

45. Weir, David H., Richard J. DiMarco, and Duane T. McRuer, Evaluation and Correlation of Driver/Vehicle Data. Vol. II: Technical Report, NHTSA Rept. DOT HS-803 246, Apr. 1977. Also, David H. Weir and Richard J. DiMarco, "Correlation and Evaluation of Driver/Vehicle Directional Handling Data," SAE Paper 780010, SAE Congress and Exposition, Detroit, Feb. 1978.

46. Weir, David H., Charles P. Shortwell, and Walter A. Johnson, Dynamics of the Automobile Related to Driver Control, Systems Technology, Inc., TR-157-1, July 1966; also SAE Paper 680194, Feb. 1967.

47. McHenry, Raymond R., and Norman J. DeLeys, Vehicle Dynamics in Single Vehicle Accidents — Validation and Extensions of a Computer Simulation, Cornell Aero. Lab., Inc., CAL No. VJ-2251-V-3, Dec. 1968.

48. Bohn, Paul F., et al., Hybrid Computer Vehicle Handling Program, Johns Hopkins Univ., APL/JHU CP049, Sept. 1977.

49. Allen, R. Wade, James F. O'Hanlon, Duane T. McRuer, et al., Drivers' Visibility Requirements for Roadway Delineation. Vol. I: Effects on Driver Performance and Behavior, Systems Technology, Inc., TR-1065-1, Nov. 1977.

50. Allen, R. Wade, Jeffrey R. Hogge, and Stephen H. Schwartz, "A Simulator for Research in Driver, Vehicle and Environment Interaction," presented at the 56th Annual Meeting of the Transportation Research Board, Jan. 1977.

51. White, R. G. S., An Experimental Survey of Vehicle Aerodynamic Characteristics (Second Report), Motor Industry Research Assoc., Rept. 1964/4, Dec. 1963.

52. The DOT/SAE Truck and Bus Fuel Economy Measurement Conference Report SAE P-59, Apr. 1975.

53. Bettes, W. H., "Aerodynamic Testing of High Performance Land-Borne Vehicles — A Critical Review," in E. Pershing, ed., Proceedings of the AIAA Symposium on the Aerodynamics of Sports and Competition Automobiles, North Hollywood, Calif., Western Periodicals Co., 1969, pp. 87-115.

54. Sovran, Gino, Thomas Morel, and William T. Mason, Jr., eds., Aerodynamic Drag Mechanisms of Bluff Bodies and Road Vehicles, New York, Plenum Press, 1978.

55. Mason, W. T., Jr., and P. S. Beebe, "The Drag Related Flow Field Characteristics of Trucks and Buses," in Gino Sovran, et al., eds., Aerodynamic Drag Mechanisms of Bluff Bodies and Road Vehicles, New York, Plenum Press, 1978.

56. Nakaguchi, H., "Recent Japanese Research on Three Dimensional Bluff Body Flows Relevant to Automobile Aerodynamics," in Gino Sovran, ed., Aerodynamic Drag Mechanisms of Bluff Bodies and Road Vehicles, New York, Plenum Press, 1978.

57. Montoya, Lawrence C., and Louis L. Steers, Aerodynamic Drag Reduction Tests on a Full Scale Tractor-Trailer Combination with Several Add-On Devices, NASA TM X-56028, Dec. 1974.

58. Hoerner, S. F., Fluid Dynamic Drag, published by author, 1958.

59. Marks, C. H., et al., "A Study of the Base Drag of Tractor-Trailer Trucks," ASME 77-WA/FE-18, Winter Annual Meeting, 1977.

60. Johansen, F. C., "The Air Resistance of Passenger Trains," IME Proc., Vol. 134, Nov. 1936.

61. Cooper, Kevin R., "Wind Tunnel Investigations of Eight Commercially Available Devices for the Reduction of the Aerodynamic Drag of Trucks," presented at the Roads and Transportation Association of Canada National Conference, Quebec City, Sept. 1976.

62. Bauer, Paul T., and Ronald A. Servais, "An Experimental and Analytical Investigation of Truck Aerodynamics," Reduction of the Aerodynamic Drag of Trucks, Proc. of the conference workshop at Caltech, Oct. 1974.

63. Carr, G. W., The Aerodynamics of Basic Shapes for Road Vehicles. Part 2: Saloon Car Bodies, Motor Industry Research Assoc., Rept. 1968/9, May 1968.

64. Walston, W. H., F. T. Buckley, and C. H. Marks, "Test Procedures for the Evaluation of Aerodynamic Drag on Full Scale Vehicles in Windy Environments," SAE Preprint 760106, 1976.

65. Beauvais, F. N., "Aerodynamic Inputs to a Parked Vehicle Caused by a Passing Bus," SAE Paper 700037, Automotive Engineering Congress, Detroit, Jan. 1970.

66. Larrabee, E. Eugene, "Small Scale Research in Automobile Aerodynamics," SAE Paper 660384, Mid-Year Meeting, Detroit, June 1966.

67. Romberg, G. F., F. Chianese, Jr., and R. G. Lajoie, "Aerodynamics of Race Cars in Drafting and Passing Situations," SAE Paper 710213, Automotive Engineering Congress, Detroit, Jan. 1971.

68. Beauvais, F. N., "Transient Nature of Wind Gust Effects on an Automobile," SAE Paper 670608, Detroit Section Junior Activity, Feb. 1967.

69. "Truck Ability Prediction Procedure — SAE J688," SAE Handbook, procedure approved Oct. 1951 and last revised May 1968.

70. Sawhill, R. B., and J. C. Fiery, "Predicting Fuel Consumption and Travel Time of Motor Transport Vehicles," HRB Bulletin, No. 334, Jan. 1962.

71. Adkins, W. G., A. W. Ward, and W. F. McFarland, "Values of Time Savings of Commercial Vehicles," NCHRP Report, No. 33, 1967.

72. Carrier Reports — Financial Reports on the Nation's Leading Carriers, Vol. 17, No. 1, Whole Number 65 Issued by "Carrier Reports," July 1976.

73. Fogg, A., and J. S. Brown, Some Experiments on Scale-Model Vehicles with Particular Reference to Dust Entry, Motor Industry Research Assoc., Rept. 1948/1, Apr. 1948.